Student Poster Session

2018 IEEE PES General Meeting

Portland, OR USA
August 5-9, 2018

Poster Categories:

- Advanced Computational Methods for Power System Planning, Operation, and Control
- Asset Management
- Cyber and Physical Security of the Smart Grid
- Dynamic Performance and Control of Power Systems
- Electric Machines and Drives
- Emerging Software Needs for the Restructured Grid
- Flexible AC Transmission Systems
- Integrating Renewable Energy into the Grid
- Intelligent Monitoring and Outage Management
- Market Interactions in Power Systems
- Power System Modeling and Simulation
- Smart Cities
- Smart Grid Technology
- Smart Sensors, Communication and Control in Energy Systems
- Substation and Distribution Automation
- System-Wide Events and Analysis Methods

IEEE PES Student Activities Subcommittee
Dr. Aaron St. Leger, Dr. Valentina Cecchi, Dr. Sridhar Chouhan, Dr. Anthony Deese

Advanced Computational Methods for Power System Planning, Operation, and Control

No.	Poster Title	Student Name (Last First)	UG/Grad
18STUGM001	Identifying Long Term Voltage Stability Caused by Distribution Systems vs Transmission Systems	Amarsagar Reddy	GRAD
18STUGM002	Probabilistic Power Flow Analysis based on theAdaptive Polynomial Chaos-ANOVA Method	Yijun Xu	GRAD
18STUGM003	Exploring Power System Problems with the Technique behind AI AlphaGo	Du Yan	GRAD
18STUGM004	Economic Dispatch Considering Risk Using Zig-zag Search Method With Adaptive Step-size	zhang qiwei	GRAD
18STUGM005	Improvement to the Prediction of Fuel Cost Distributions Using ARIMA Model	Zhao Zhongyang	GRAD
18STUGM006	CIM/E Oriented Graph Database Model Architecture and Parallel Network Topology Processing	Zhou Zhangxin	GRAD
18STUGM007	Chance Constrained Optimal Reactive Power Dispatch	Geng Xinbo	GRAD
18STUGM008	Security-Constrained Transmission Expansion Planning with Risk Index of N-1 Security Obtained from PMU Data	Mehrtash Mahdi	GRAD
18STUGM009	An Integrated Distributed Economic Dispatch-Droop Control Architecture for Distribution System Operation	Wang Shengyi	GRAD
18STUGM010	Flexible Long Term Planning Cooptimization Method Comparison and Validation	Maloney Patrick	GRAD
18STUGM011	Voltage and Thermal Concerns during Geomagnetic Disturbance Corrective Measures	Klauber Cecilia	GRAD
18STUGM012	DC Catenary Line Modeling of Subway Systems	Sezgin Mustafa Erdem	GRAD
18STUGM013	Volt-Var Optimization Algorithm Utilizing Custormer- and Utility-Owned Distributed Resources	David J Mulcahy	GRAD
18STUGM014	Cloud Computing Based Real-Time Energy Management System with RNN-LSTM Wind Forecasting	Azimian Behrouz	GRAD
18STUGM015	Progressive Hedging Algorithm in two stage stochastic optimization of look-ahead unit commitment	Saleh Mehdi	GRAD
18STUGM016	Robust Unit Commitment Considering the Temporal and Spatial Correlations of Wind Farms Using a Data-Adaptive Approach	Yipu Zhang	GRAD
18STUGM017	SDP Based ACOPF and Network Reconfiguraiton for Three-phase Distribution System	Li Yikui	GRAD
18STUGM018	Finite-Difference Relaxation for Parallel Compution of Ionized Field of HVDC Lines	Liu Peng	GRAD
18STUGM019	PV Extreme Capacity Factor Analysis	Tang Zefan	GRAD
18STUGM020	Robust Koopman Operator-based Kalman Filter for Power Systems Dynamic State Estimation	Netto Marcos	GRAD
18STUGM021	Information Transfer Based Modal Analysis in Power System	Sharma Pranav	GRAD
18STUGM022	Horizontal Decomposition-Coordination Strategy for Power System Scheduling with Overlapping Intervals	Farnaz Safdarian	GRAD

Asset Management

No.	Poster Title	Student Name (Last First)	UG/Grad
18STUGM023	Flexibility Scheduling for Large Customers	Angizeh Farhad	GRAD
18STUGM024	Analysis of Vibration Signal for Power Transformer On-Load Tap Changer (OLTC) Condition Monitoring	Seo Junhyuck	GRAD

Cyber and Physical Security of the Smart Grid

No.	Poster Title	Student Name (Last First)	UG/Grad
18STUGM025	On False Data Injection in Wide Area Protection Schemes	Khalaf Mohsen	GRAD
18STUGM026	Reliability and Vulnerability Assessment of Interconnected ICT and Power Networks Using Complex Network Theory	Zhu Wentao	GRAD
18STUGM027	Load Redistribution Attack Detection using Machine Learning: A Data-Driven Approach	Pinceti Andrea	GRAD
18STUGM028	A Coordinated Cyber Attack Detection System (CCADS) for Multiple Substations	Sun Chih-Che	GRAD
18STUGM029	Distribution System Hardening against Natural Disasters	Tan Yushi	GRAD
18STUGM030	Embedding Cyber-Physical Resiliency in Synchrophasor-based Remedial Action Schemes	Nie Zhijie	GRAD
18STUGM031	Decentralized Power System Integrity Protection Schemes based on MAS: Anomaly Detection and Self-Adaptive Load Shedding	Pengyuan Wang	GRAD
18STUGM032	Data Analytics for Cyber-Physical Security of Transmission Protection System	Foroutan Sayedeh Armina	GRAD
18STUGM033	Impact of Communication Failures on Solar Generation Forecasting	Heidari Kapourchali Mohammad	GRAD
18STUGM034	Real-time Cyber Physical Test-bed for validation of Automated Failure Diagnosis in Transmission Network	Gholami Amir	GRAD
18STUGM035	Content Development of IoT for Grid Modernization - a Two Class Series for the Future Power Engineer	Crystal R Eppinger	GRAD
18STUGM036	Federation based Testbed Implementation of Anomaly Detection for Wide Area Protection Scheme in Power System	Singh Vivek Kumar	GRAD
18STUGM037	False Data Injection Attacks in Electric Energy Markets	Kaviani Ramin	UG
18STUGM038	CP-SAM Cyber-Physical Security Assessment Metric	Venkataramanan Venkatesh	GRAD

Dynamic Performance and Control of Power Systems

No.	Poster Title	Student Name (Last First)	UG/Grad
18STUGM039	Calculation of Critical Oscillation Modes for Large Delayed Cyber-Physical Power System Using Pseudo-Spectral Discretization of Solution Operator	Qianying Mou	GRAD
18STUGM040	VSC-HVDC for enhancing power system stability in the load restoration stage of black start	Feng Wei	GRAD
18STUGM041	Optimal Damping Actuator Selection Through Oscillation Energy Sensitivity Analysis	Silva-Saravia Horacio	GRAD
18STUGM042	Practical Modeling of Flywheel Energy Storage for Primary Frequency Control in Power Grids	Dario Peralta	GRAD
18STUGM043	Location and Migration Laws of Out-of-Step Center under Multi-Frequency Oscillation Based on Voltage Phase Angle Trajectory	Liu Jiale	GRAD
18STUGM044	Development and Frequency Application of an European Low Voltage Microgrid Network	Ayaz Melike Selcen	GRAD
18STUGM045	Provision for Guaranteed Inertial Response in Diesel-Wind Systems via Model Reference Control	Zhang Yichen	GRAD
18STUGM046	Tube-Based Model Predictive Control of Energy Storage Units for Improving Transient Stability of Power Systems	Kiaei Iman	GRAD
18STUGM047	Probabilistic Transient Stability Assessment of Renewable Generation Integrated Power System	Wang Yingying	GRAD

18STUGM048	New Optimization-Based Algorithms for a Substation Voltage Controller Using Local Synchrophasor Measurements	Amelian Sayed Mohammad	GRAD
18STUGM049	Optimal Design of Virtual Inertia and Damping Coefficients for Virtual Synchronous Machines	Ademola-Idowu Atinuke	GRAD
18STUGM050	A N4SID based estimator for identifying the parameters and sources of forced oscillations	Mansouri Habibabadi Mohammad	GRAD
18STUGM051	Towards the New Low-Order System Frequency Response Model of Power Systems with High Penetration of Variable-Speed Wind Turbine Generators	Krpan Matej	GRAD
18STUGM052	Oscillation Monitoring and Control of the RTE Power System Using Synchrophasors	Farrokhifard Mohammadreza	UG
18STUGM053	ADAPTIVE ADJUSTMENT OF NOISE COVARIANCE	Akhlaghi Shahrokh	GRAD
18STUGM054	Probabilistic Transient Stability Assessment of Renewable Generation Integrated Power System	Wang Yingying	GRAD
18STUGM055	Decreasing the Ice Storm Risk on Power Conductors by DSRs and Dispatch Adjustment	Lashkarbolooki Sahar	GRAD
18STUGM056	Fractional Order PI Control for Microgrid Application	abdulkader rasheed	GRAD
18STUGM057	Parameter Space and Rotor Angle Stability Control of Virtual Synchronous Machine	Qi Chen	GRAD

Electric Machine and Drives

No.	Poster Title	Student Name (Last First)	UG/Grad
18STUGM058	Design of a Supercapacitor Energy Storage System for Marine Turbines Utilizing Advanced Control	Aaronson Hannah	GRAD
18STUGM059	Fault Ride Through Analysis of Grid Connected Doubly Fed Induction Generator Based Wind System	Vishwanath Gururaj	GRAD
18STUGM060	Design and Performance Analysis of Low Cost Acoustic Chamber for Electric Machines	Pindoriya Rajesh	GRAD
18STUGM061	Demagnetization Fault Detection and Analysis for a Permanent Magnet Synchronous Machine	Usman Adil	GRAD
18STUGM062	Behavioral Device-Level Modeling of Modular Multi-Level Converters in Real-Time for Variable Speed Drive Applications	Lin Ning	GRAD
18STUGM063	Harmonic Mitigation and a Practical Study of Torque Harmonics in Induction Motor Startup	Khaledian Parviz	GRAD

Emerging Software Needs for the Restructured Grid

No.	Poster Title	Student Name (Last First)	UG/Grad
18STUGM064	Dynamic Modeling in OpenDSS: An Implementation Sequence for Object Pascal	Andres Arguello	GRAD

Flexible AC Transmission Systems

No.	Poster Title	Student Name (Last First)	UG/Grad
18STUGM065	Analyzing Mutual Influences of Conventional and Distributed FACTS via Stochastic Co-optimization	Yuanrui Sang	GRAD
18STUGM066	Analysis of Transient Stability According to Initial Operating Condition of STATCOM	Hyeokjin Noh	GRAD
18STUGM067	Rotor Angle Stability of MMC Based HVDC Transmission Under DC Short-Circuit Fault	Wang Peng	GRAD

Integrating Renewable Energy into the Grid

No.	Poster Title	Student Name (Last First)	UG/Grad
18STUGM068	Calculation of Fault Level in Power Systems with High Penetration of Renewable Energy Resources	Aljarrah Rafat	GRAD
18STUGM069	Stability Analysis of Microgrids under Disturbances via Reachable Sets	Li Yan	GRAD
18STUGM070	An in-depth analysis of grid-connected solar plant feasibility and technology selection	Stephens Greg	GRAD
18STUGM071	An LMI Based Stability Margin Analysis for Active PV Power Control of Distribution Networks with Time-Invariant Delays	Fu Chang	GRAD
18STUGM072	A Framework to Utilize DERs' VAR Resources to Support the Grid in an Integrated T-D System	Singhal Ankit	GRAD
18STUGM073	Quantitative Control Approach for Wind Turbine Generators to Provide Fast Frequency Response With Guaranteed Rotor Security	Wang Siqi	GRAD
18STUGM074	Optimal Corrective Control for Bipolar Multi-terminal HVDC Grid	Jiahong Li	GRAD
18STUGM075	Bi-Level Arbitrage Potential Evaluation for Grid-Scale Energy Storage Considering Wind Power and LMP Smoothing Effect	Cui Hantao	GRAD
18STUGM076	State Space Model of Electric Vehicle Aggregator for Frequency Control	Wang Mingshen	GRAD
18STUGM077	Stochastic market clearing for integrated energy systems considering CHP and power to gas technology	Wang Haibing	GRAD
18STUGM078	Optimal Placement of Grid-connected Solar Generation using Geographical Information System	Ospina Ana	GRAD
18STUGM079	Frequency Support of DFIG by Using Improved Inertial Control	Gucheng Xiao	GRAD
18STUGM080	Combined Heat and Power Dispatch Based on Integrated Demand Response and Heat Transmission for Wind Power Accommodation	Xu Yeyan	GRAD
18STUGM081	VSG Control for DFIG-based Islanded Wind Farm with LCC-HVDC Integration	Xiuqiang He	GRAD
18STUGM082	Voltage Sensitivity Matrix-Based Volt-Var Control for Unbalanced Distribution Systems using DERs	McEntee Catie	GRAD
18STUGM083	Minimizing Curtailments due to Voltage Stability Using Security Constrained OPF	Nycander Elis	GRAD
18STUGM084	The Value of Reactive Power for Voltage Control in Lossy Networks	Deakin Matthew	GRAD
18STUGM085	Study and Comparison of Wind Power Correlation Using Two Types of Dataset	Yannan Luo	GRAD
18STUGM086	Application of Solid State Transformers in Hybrid Residential Energy Delivery	Maharjan Manisha	GRAD
18STUGM087	Comparing Capacity Value Metrics of Energy-Limited Resources	Awara Sarah	GRAD
18STUGM088	Energy Storage Integration in an Islanded Wave Energy System	Wu Eric	GRAD
18STUGM089	Life Cycle Testing of Vanadium Redox Flow Battery and Lithium Ion Energy Storage Systems	Rashid Muhammad	GRAD
18STUGM090	modeling and control of an integrated wind power generation and modular multilevel converter with energy storage system	Kang Jaesik	GRAD
18STUGM091	Indirect Mechanism Design for Efficient and Stable Renewable Energy Aggregation	Khazaei Hossein	GRAD
18STUGM092	Power-frequency Response Model Identification for Adaptive Virtual Inertia Algorithms	Tamrakar Ujjwol	GRAD
18STUGM093	Enhancement of Grid Connected PV Arrays Fault Ride Through and Post Fault Recovery Performance	Mojallal Aslan	GRAD
18STUGM094	Real-Time Modeling and Battery-in-the-Loop Characterization of an Energy Storage System	Arzani Ali	GRAD
18STUGM095	Robust Microgrid Economic Dispatch Considering Renewable Uncertainty using Interval Optimization	Rooks Cody	GRAD
18STUGM096	Benefits of Short-term PV Forecasting in a Remote Area Standalone Off-grid Power Supply System	Jamal Taskin	GRAD

18STUGM097	A Comparison Study of Dispatching Various Battery Technologies in a Hybrid PV and Wind Power Plant	Yang Yuqing	GRAD

Intelligent Monitoring and Outage Management

No.	Poster Title	Student Name (Last First)	UG/Grad
18STUGM098	Monitoring the Voltage Stability Margin Using Norton Current Distribution Relationship	Wang Qi	GRAD
18STUGM099	Fault Classification and Location Identification in a Smart Distribution Network Using ANN	Usman Muhammad Usama	GRAD
18STUGM100	Sub-Synchronous Resonance Detection in Series Compensated DFIG-Based Windfarms	Bo Gao	GRAD
18STUGM101	An Distributed Event Diagnosis Solution for Protection Operation in IEC 61850	Touhiduzzaman Md	GRAD
18STUGM102	Toward a Synthetic Model for Distribution System Restoration and Crew Dispatch	Zhigang Ye	GRAD
18STUGM103	Enabling Resiliency Through Outage Management and Real Time Data-Driven Aggregated DERs	Menazzi Matteo	GRAD

Market Interactions in Power Systems

No.	Poster Title	Student Name (Last First)	UG/Grad
18STUGM104	Building Energy Scheduling with Transactive Approach Having Autonomous Temperature Setting	Basnet Ashim	GRAD
18STUGM105	Cooperative Game Theory for Allocating Cost Savings from Coalitional Energy Management	Han Liyang	GRAD
18STUGM106	Game-theory-based Real-Time Inter-Microgrid Market Design Using Hierarchical Optimization Algorithm	Mahmoudian Esfahani Mohammad	GRAD
18STUGM107	Reference Bus Independent Components of LMP through a Non-Marginal Choice of its Energy Component	Kiran Deep	GRAD
18STUGM108	Who has an incentive to improve the renewable day-ahead forecast?	Spyrou Evangelia	GRAD
18STUGM109	A Bi-Level Optimization Formulation of Priority Service Pricing	Mou Yuting	GRAD
18STUGM110	Transactive Energy Based Multi-microgrids System Operation	Pathiravasam Chirath	GRAD
18STUGM111	Generator contingency modelling in ISOs: Pricing Implications	Saikumar Karthik	GRAD
18STUGM112	Optimal Energy Management for the Integrated Power and Gas Systems via Real-time Pricing	Shu Kangan	GRAD
18STUGM104	Building Energy Scheduling with Transactive Approach Having Autonomous Temperature Setting	Basnet Ashim	GRAD
18STUGM105	Cooperative Game Theory for Allocating Cost Savings from Coalitional Energy Management	Han Liyang	GRAD
18STUGM106	Game-theory-based Real-Time Inter-Microgrid Market Design Using Hierarchical Optimization Algorithm	Mahmoudian Esfahani Mohammad	GRAD
18STUGM107	Reference Bus Independent Components of LMP through a Non-Marginal Choice of its Energy Component	Kiran Deep	GRAD
18STUGM108	Who has an incentive to improve the renewable day-ahead forecast?	Spyrou Evangelia	GRAD
18STUGM109	A Bi-Level Optimization Formulation of Priority Service Pricing	Mou Yuting	GRAD
18STUGM110	Transactive Energy Based Multi-microgrids System Operation	Pathiravasam Chirath	GRAD
18STUGM111	Generator contingency modelling in ISOs: Pricing Implications	Saikumar Karthik	GRAD
18STUGM112	Optimal Energy Management for the Integrated Power and Gas Systems via Real-time Pricing	Shu Kangan	GRAD

Power System Modeling and Simulation

No.	Poster Title	Student Name (Last First)	UG/Grad
18STUGM113	Cost Benefit Analysis of Technology Options for Enabling High PV Penetration	Sun Lisha	GRAD
18STUGM114	Transmission Constrained Economic Dispatch via Interval Optimization Considering Wind Uncertainty	Kou Xiao	GRAD
18STUGM115	Analytical method to aggregate multi-machine SFR model with applications in power system dynamic studies	Shi Qingxin	GRAD
18STUGM116	Matlab Simulation Framework for Integration of Battery Storage and Solar Generation in Distribution Systems	Soleimani Milad	GRAD
18STUGM117	Global Sensitivity Analysis of Islanded Microgrid Power Flow	He Kun	UG
18STUGM118	Simultaneous Global Identification of Dynamic and Network Parameters in Transient Stability Studies	Francis Benjamin	GRAD
18STUGM119	Comparative Analysis of Hybrid Bipolar HVDC and FACTS Performance for Improving Commutation Failure Immunity	Zicong Zhang	GRAD
18STUGM120	Impact of Dynamic Load Model on Short-Term Voltage Stability of Korea Power System	Jaemin Moon	GRAD
18STUGM121	Impact of Load Step Change on Thermal and Voltage Stability Limits of Overhead Transmission Lines	Rahman Mahbubur	GRAD
18STUGM122	A Dynamic Inverse-Time Overcurrent Relay Model for Overload Analysis with Varying Overcurrents	Liu Jianan	GRAD
18STUGM123	A Novel MILP-Based Method of Optimal Energy Flow in Gas-electricity System	Liu Tianhao	GRAD
18STUGM124	Modeling of Geomagnetically Induced Currents in the Power Grid Using Time-Domain Simulation	Vemprala Hemanth Kumar	GRAD
18STUGM125	Optimization of Electric Vehicle Aggregation in Energy and Balancing Markets in the Nordics	Herre Lars	GRAD
18STUGM126	Building Very Large Synthetic Power Grids	Birchfield Adam	GRAD
18STUGM127	Initial Work on Formalizing the Multiple-Time Scale Structure of Power System Models	Hin Matthew	GRAD
18STUGM128	Convex Relaxations and Approximations of Chance-Constrained AC-OPF Problems	Lejla Halilbasic	GRAD
18STUGM129	Analysis of Transformers Thermal Response to Geomagnetic Disturbances	Dehghanian Pooria	GRAD
18STUGM130	A Hybrid Simulator for the Study of EP Project Multi-Terminal DC in South Korea Gird	Lee Jeehoon	GRAD
18STUGM131	Design of Scalable and Flexible Distributed Islanded Microgrid for Rural Electrification	Khan Rabia	GRAD
18STUGM132	Synthetic Residential Load Models for Analysis of Energy Management Impact on Smart Cities	Bereta dos Reis Fernando	GRAD
18STUGM133	Finite Element Analysis of Transformers in Subterranean Vaults	Kolln Jaime	UG
18STUGM134	An Object Oriented Matlab Toolbox for Power Distribution System Analysis	Dharmawardena Hasala	GRAD
18STUGM135	Big Data: Application to Transmission and Distribution Co-Simulation for the Future Grid	Velaga Yaswanth Nag	GRAD
18STUGM136	Interdependent Electric and Water Infrastructure Modeling	Zuloaga	GRAD
18STUGM137	Online Identification of Generator Participation Factors using Cellular Computational Networks	Abu Umar	GRAD
18STUGM138	A Real-Time Hardware-in-the-Loop Simulation of Sampled Value based Differential Protection	Yellajosula Jaya Raghavendra Arun Kumar	GRAD
18STUGM113	Cost Benefit Analysis of Technology Options for Enabling High PV Penetration	Sun Lisha	GRAD
18STUGM114	Transmission Constrained Economic Dispatch via Interval Optimization Considering Wind Uncertainty	Kou Xiao	GRAD
18STUGM115	Analytical method to aggregate multi-machine SFR model with applications in power system dynamic studies	Shi Qingxin	GRAD

18STUGM116	Matlab Simulation Framework for Integration of Battery Storage and Solar Generation in Distribution Systems	Soleimani Milad	GRAD
18STUGM117	Global Sensitivity Analysis of Islanded Microgrid Power Flow	He Kun	UG
18STUGM118	Simultaneous Global Identification of Dynamic and Network Parameters in Transient Stability Studies	Francis Benjamin	GRAD
18STUGM119	Comparative Analysis of Hybrid Bipolar HVDC and FACTS Performance for Improving Commutation Failure Immunity	Zicong Zhang	GRAD
18STUGM120	Impact of Dynamic Load Model on Short-Term Voltage Stability of Korea Power System	Jaemin Moon	GRAD
18STUGM121	Impact of Load Step Change on Thermal and Voltage Stability Limits of Overhead Transmission Lines	Rahman Mahbubur	GRAD
18STUGM122	A Dynamic Inverse-Time Overcurrent Relay Model for Overload Analysis with Varying Overcurrents	Liu Jianan	GRAD
18STUGM123	A Novel MILP-Based Method of Optimal Energy Flow in Gas-electricity System	Liu Tianhao	GRAD
18STUGM124	Modeling of Geomagnetically Induced Currents in the Power Grid Using Time-Domain Simulation	Vemprala Hemanth Kumar	GRAD
18STUGM125	Optimization of Electric Vehicle Aggregation in Energy and Balancing Markets in the Nordics	Herre Lars	GRAD
18STUGM126	Building Very Large Synthetic Power Grids	Birchfield Adam	GRAD
18STUGM127	Initial Work on Formalizing the Multiple-Time Scale Structure of Power System Models	Hin Matthew	GRAD
18STUGM128	Convex Relaxations and Approximations of Chance-Constrained AC-OPF Problems	Lejla Halilbasic	GRAD
18STUGM129	Analysis of Transformers Thermal Response to Geomagnetic Disturbances	Dehghanian Pooria	GRAD
18STUGM130	A Hybrid Simulator for the Study of EP Project Multi-Terminal DC in South Korea Gird	Lee Jeehoon	GRAD
18STUGM131	Design of Scalable and Flexible Distributed Islanded Microgrid for Rural Electrification	Khan Rabia	GRAD
18STUGM132	Synthetic Residential Load Models for Analysis of Energy Management Impact on Smart Cities	Bereta dos Reis Fernando	GRAD
18STUGM133	Finite Element Analysis of Transformers in Subterranean Vaults	Kolln Jaime	UG
18STUGM134	An Object Oriented Matlab Toolbox for Power Distribution System Analysis	Dharmawardena Hasala	GRAD
18STUGM135	Big Data: Application to Transmission and Distribution Co-Simulation for the Future Grid	Velaga Yaswanth Nag	GRAD
18STUGM136	Interdependent Electric and Water Infrastructure Modeling	Zuloaga	GRAD
18STUGM137	Online Identification of Generator Participation Factors using Cellular Computational Networks	Abu Umar	GRAD
18STUGM138	A Real-Time Hardware-in-the-Loop Simulation of Sampled Value based Differential Protection	Yellajosula Jaya Raghavendra Arun Kumar	GRAD

Smart Cities

No.	Poster Title	Student Name (Last First)	UG/Grad
18STUGM139	Optimal Routing and Charging of an Electric Vehicle Fleet for High-Efficiency Dynamic Transit Systems	Chen Tao	GRAD
18STUGM140	Analysis of “8•15” Blackout in Taiwan and the Improvement Method of Contingency Reserve Capacity Through Direct Load Control	Hui Hongxun	GRAD
18STUGM141	A Hierarchical Control Structure for Residential Community Energy Optimization	Paudyal Priti	GRAD
18STUGM142	Home Energy Management System in Co-Simulation Framework	Munankarmi Prateek	GRAD
18STUGM143	Distributed Locational Marginal Pricing based of Smart Home Management	Mohsenzadeh Amin	GRAD

Smart Grid Technology

No.	Poster Title	Student Name (Last First)	UG/Grad
18STUGM144	Impacts of Smart Inverters on Microgrids' Controls and Protections	Samkari Husam	GRAD
18STUGM145	Multi-parameter Intelligent Energy Forecasting: From Insight to Impact	Sakib Nazmus	GRAD
18STUGM146	Adaptive Phasor Estimation Algorithm Using Improved KFs under Steady-State/Dynamic Conditions	Wang Yinfeng	GRAD
18STUGM147	Robust Unit Commitment and Dispatch Considering with Atmospheric Pollutant Concentration Constraints	Wang Yongcan	GRAD
18STUGM148	Coordinated Power Allocation and Robust DC Voltage Control of UPQC with Energy Storage Unit During Source Voltage Sag	Liu Ziwen	GRAD
18STUGM149	Distributed Voltage Control for Demand Response	Guo Jinrui	GRAD
18STUGM150	Progressive Time-differentiated Peak Pricing (PTPP) for Aggregated Air-conditioning Load in Demand Response Programs	Shen Yunwei	GRAD
18STUGM151	A Multilevel Dual Converter fed Open end Transformer Configuration for Hybrid AC-DC Microgrid	Bandla Krishna	GRAD
18STUGM152	Reactive Power Support from EVs for Distribution Grid Voltage Management	Wang Jingyuan	GRAD
18STUGM153	Joint Planning of BESS and DR for industrial consumers participating in peak-shaving	Hu Xiao	GRAD
18STUGM154	Stochastic Optimal Transmission Switching Considering N-1 Security Constraints	Zhang Heng	GRAD
18STUGM155	Peak Energy Management using Renewable Integrated DC Microgrid	Pannala Sanjeev	GRAD
18STUGM156	A Two-Step Load Disaggregation Algorithm for Quasi-static Time-series Analysis on Actual Distribution Feeders	Wang Jiyu	GRAD
18STUGM157	Optimal Water-Power Flow Problem: Formulation and Distributed Optimal Solution	Zamzam Ahmed	GRAD
18STUGM158	Real Time Tool to Characterize Power System Communication Delays	Lackner Christoph	GRAD
18STUGM159	Diagonal Quadratic Approximation for Decentralized Collaborative TSO DSO Optimal Power Flow	Mohammadi Ali	GRAD
18STUGM160	A Data-driven Voltage Control Framework for Power Distribution Systems	Xu Hanchen	GRAD
18STUGM161	A Machine Learning Approach for Residential Load Extraction using Low-resolution Smart Meter Data	Meng Yao	GRAD
18STUGM162	Nonparametric User Behavior Prediction for Distributed EV Charging Scheduling	Khaki Behnam	GRAD
18STUGM163	Detection of PMU Time Error Sources Using Phase Angle Measurement Data	Idehen Ikponmwosa	GRAD
18STUGM164	Stability Robustness for Secondary Voltage Control in Autonomous Microgrids With Consideration of Communication Delays	Lou Guannan	GRAD
18STUGM165	A Novel Consensus-based Distributed Algorithm for Economic Dispatch Based on Local Estimation of Power Mismatch	Pourbabak Hajir	GRAD
18STUGM166	Automated Distribution System Restoration with the Multiagent Q-Learning Based Algorithm	Alvarez Fernandez Inalvis	UG
18STUGM167	Modelling and evaluation of flexible multi-energy systems for low carbon environment	Holjevac Ninoslav	GRAD
18STUGM168	Adoption of IoT framework for DER aggregation and control	Slay Tylor	GRAD
18STUGM169	A Distributed Energy Resource Aggregated System for Providing Ancillary Services	Marnell Kevin	GRAD
18STUGM170	Online Identification of Power System Electromechanical Modes	Arunagirinatthan Paranietharan	GRAD

Smart Sensors, Communication and Control in Energy Systems

No.	Poster Title	Student Name (Last First)	UG/Grad
18STUGM171	A Power Waveform Classification Method for Adaptive Synchrophasor Estimation	QIAN Cheng	GRAD
18STUGM172	Non-Invasive System Impedance Estimation Based on Data Selection	Zhang Ori	GRAD
18STUGM173	An advanced maximum power point capturing technique with supercapacitor for PV system	Zhang Lijun	GRAD
18STUGM174	Comparative Analysis of Demand Response and Load Management Algorithms	Vedullapalli Divya	GRAD
18STUGM175	A Non-Contact Method for Real-Time Monitoring of Conductor Sag	Mukherjee Monish	GRAD

Substation and Distribution Automation

No.	Poster Title	Student Name (Last First)	UG/Grad
18STUGM176	Smart Grid-enabled CVR: An advanced application for Distribution Management System	Singh Shailendra	GRAD

System-Wide Events and Analysis Methods

No.	Poster Title	Student Name (Last First)	UG/Grad
18STUGM177	D2NDZ: Evaluating Unintentional Islanding Risks in Distribution Grids with Deep Integration of Distributed Energy Resources	Li Yan	GRAD
18STUGM178	Real-time Operation Pattern Detection using Measurements from a Network of PMUs	Liang Ming	GRAD
18STUGM179	Nonlinear Dynamics Based On-line Detection of Oscillation Using Power System Measurement Data	Cho Hwanhee	GRAD
18STUGM180	Frequency Response Estimation Following Large Disturbances using Synchrophasors	Fernandes Lucas	GRAD
18STUGM181	A Hybrid Approach towards Event Detection in Multi-machine Power Systems	Banerjee Abhishek	GRAD
18STUGM182	Security versus Computation Time in IV-ACOPF with SOCP Initialization	Sadat Sayed Abdullah	GRAD
18STUGM183	Advanced Situational Awareness: Identification of Localized and Widespread Events	Chatterjee Paroma	GRAD
18STUGM184	Measurement-Based Voltage Stability Indicator for Voltage Dependent and Induction Motor Loads	Kamel Mariana	GRAD
18STUGM185	Advanced Situational Awareness: Identification of Localized and Widespread Events	Chatterjee Paroma	GRAD

Identifying Long Term Voltage Stability Caused by Distribution Systems vs Transmission Systems

Amarsagar Reddy Ramapuram M.
Department of Electrical and Computer Engineering
Iowa State University, Ames, IA,
amar@iastate.edu

Ankit Singhal
Department of Electrical and Computer Engineering
Iowa State University, Ames, IA,
ankit@iastate.edu

Venkataramana Ajjarapu
Department of Electrical and Computer Engineering
Iowa State University, Ames, IA,
vajjarapu@iastate.edu

***Abstract* — Monitoring the long term voltage stability of the power grid is necessary to ensure its secure operation. This paper presents a new phasor based methodology that distinguishes between long term voltage stability caused by distribution systems versus transmission systems. From a conceptual understanding of a simplified system, a Transmission-Distribution Distinguishing Index (TDDI) is proposed to distinguish between the two scenarios. A methodology to calculate the TDDI for multi-bus systems using quasi-steady state phasor measurements is described and validating results are presented for the IEEE 9 Bus system with a load replaced by various distribution feeders. The results verify that the TDDI can indeed be used to distinguish between transmission limited and distribution limited systems. This information can be utilized by the operator to effectively choose controls in distribution and transmission systems to improve the system margin.**

Keywords — Long Term Voltage Stability, Transmission vs Distribution, Thevenin Index, Phasor Measurement Units.

I. INTRODUCTION

There is increasing pressure on power system operators and on electric utilities to utilize the existing grid infrastructure to the maximum extent possible and this mode of operation can lead to long term voltage stability problems. To handle this, operators are adopting real-time tools using Wide-Area measurements (WAMS) and Phasor Measurement Units (PMUs) that are providing them with better situational awareness. The increasing number of PMUs in the grid have led to various online Voltage Stability Indices (VSI) being proposed in recent times to monitor the grid in real time [1].

Traditionally, the VSI's were calculated at a bus by estimating the Thevenin Equivalent using local PMU Voltage and Current measurements at a Bus [2-6]. However, all these methods assume an aggregated load at the transmission level and do not consider the sub-transmission system or the distribution system where the loads are actually present. Ignoring the distribution feeder network and the distribution of loads in the sub-transmission/ distribution network will lead to an error in the voltage stability assessment.

Furthermore, as the distribution systems are often operated close to their limits (for economic reasons), considering their topology and loads into the voltage stability assessment might provide insights to operators and planners on how to improve the system behavior. In fact, voltage collapse in distribution feeders has been identified as a critical issue for some time [7] and a major blackout in 1997 in the S/SE Brazilian system is attributed to a voltage instability problem in one of the distribution feeders that spread to the transmission grid [8].

Recently, techniques incorporating the distribution system in the transmission system analysis have been proposed [9] and have been utilized to verify how the increase in Distributed Generation (DG) can improve both the overall system margin [10] and the distribution system margin [11]. However, as far as the authors know, none of the existing methods distinguish between the voltage stability caused by distribution system versus transmission systems. Our previous paper [12] describes a method to determine if the voltage stability limit is due to the distribution system or the transmission system. This method performs a continuation power flow [13] and compares the resultant nose point with a predetermined hypersurface based on the distribution topology. The methodology requires a full-fledged CPF routine along with the calculation of the hyper surfaces, making it time consuming for power system operations and so an online methodology would be preferred.

In this paper we address this issue by presenting a technique based on phasor measurements to estimate the voltage stability and to also determine if the limit is due to the transmission or distribution systems. This information will be useful for operators, especially as the control of DG devices in distribution limited systems can lead to a larger percentage increase in the margin [12] and a load shedding action on the distribution limited systems will lead to a larger improvement in system margin [12]. Thus, determination of the limiting system can be used to improve voltage stability with minimum control. This paper starts by describing a conceptual understanding of the methodology on a simple system (Section II), presents a technique to estimate the parameters of the equivalent circuit for multi-bus systems (Section III), describes how the method works on a test-system and compares it to existing results (Section IV) and finally concludes in Section V.

II. CONCEPTUAL UNDERSTANDING OF METHOD

A block diagram of the conventional power system is shown in Fig. 1, with the various generation, transmission and distribution circuits. The loads are in the distribution feeders and vary based on time of day, etc.

Probabilistic Power Flow Analysis based on the Adaptive Polynomial Chaos-ANOVA Method

Yijun Xu, *Student Member, IEEE,* Lamine Mili, *Life Fellow, IEEE*

***Abstract*—While the conventional generalized polynomial chaos method exhibits excellent computational efficiency and accuracy in the probabilistic power flow calculations applied to medium-size power systems, it suffers from the curse of dimensionality when applied to large-scale systems and is limited to standard probability distributions assumed for the input variables. In this paper, we propose to adaptively reduce the dimension and thereby, to significantly speed up the calculations of the generalized polynomial chaos method via the ANOVA decomposition. We also propose to make use of the Steltijes' procedure so that any probability distribution may be assumed for the input random variables.**

***Keywords*—Probabilistic Power Flow, Generalized Polynomial Chaos (gPC), Analysis-of-Variance (ANOVA).**

I. Introduction

CURRENTLY, two traditional techniques have been utilized to account for power system model uncertainties, namely, the Monte Carlo (MC) method and the analytical Method. It turns out that the former is too time-consuming for large-scale power systems while the latter method can bring some inaccuracy in the results. To overcome these weaknesses, the generalized Polynomial Chaos (gPC) method that was initiated by Wiener and further developed by Xiu and Karniadakis has been recently used for probabilistic power flow calculations. While the gPC method shows great accuracy and efficiency when the number of the input random variables are not large, it suffers from the curse of dimensionality. It turns out that the ANOVA decomposition can help polynomial chaos based method to identify the main coupling effects while ignoring the others. This property will allow us to greatly alleviate the curse of dimensionality in the gPC method.

II. Theoretical Background

A. The Generalized Polynomial Chaos

In the gPC method, the stochastic outputs are represented as a weighted sum of a set of orthogonal polynomial chaos basis functions constructed from the probability distribution of the input random variables.

$$z = \sum_{i=0}^{N_P} a_i \phi_i(\boldsymbol{\xi}), \tag{1}$$

Y. Xu, and L. Mili are with the Bradley Department of Electrical and Computer Engineering, Virginia Polytechnic Institute and State University, Northern Virginia Center, Falls Church, VA 22043, USA, (e-mail:yijunxu@vt.edu;lmili@vt.edu;).

where $N_P = \frac{(N+P)!}{N!P!} - 1$. From the polynomial chaos coefficients, the sample mean, μ, and the sample variance, σ^2, of the output z can be determined as follows:

$$\mu = a_0, \tag{2}$$

$$\sigma^2 = \sum_{i=1}^{N_P} a_i^2 E[\phi_i^2], \tag{3}$$

B. The ANOVA Decomposition

The ANOVA expansion represents a function f with N random variable in the form of

$$f(\xi_1, \ldots, \xi_N) = f_0 + \sum_{1 \le j_1 \le N} f_{j_1}(\xi_{j_1}) + \sum_{1 \le j_1 < j_2 \le N} f_{j_1,j_2}(\xi_{j_1}, \xi_{j_2}) + \ldots + f_{1,2,\ldots,N}. \tag{4}$$

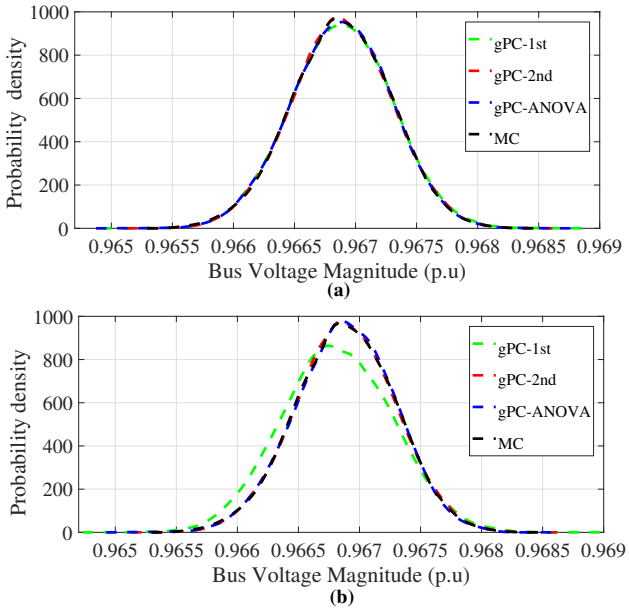

Fig. 1. Plots for probability distribution function of voltage magnitude

TABLE I. Average CPU Times of the gPC 2nd-order, gPC-ANOVA, and MC Methods

Method	gPC(P=2)	gPC-A(0.96)	gPC-A(0.98)	MC
CPU time	4.4955 s	1.6772 s	1.8228 s	2028.5 s

Exploring Power System Problems with the Technique behind AI AlphaGo

Yan Du
Dept. of EECS, UTK
Knoxville, TN, USA

Fangxing Li
Dept. of EECS, UTK
Knoxville, TN, USA

***Abstract*—In this work, a data-driven method for power flow calculation is proposed as opposed to the traditional model-based method with computation burden. The main idea is to apply the technique behind the heated AI-led computer program AlphaGo, the deep convolutional neural network (CNN), to establish the mathematical formulation between bus power injection and voltage, which is a regression process. The neural network is constructed via both training stage and testing stage based on a large data set of existing power flow results. The obtained deep CNN is further implemented on a series of standard IEEE systems to verify its accuracy. The proposed study may inspire some new directions for applying deep learning related techniques in future power system researches.**

***Index Terms*—AlphaGo, convolutional neural network, data-driven, deep learning, power flow**

I. Introduction

The computer program AlphaGo marks the beginning of the development of modern AI technologies. Nowadays, the AI technology has made tremendous progresses in a wide variety of domains including image recognition, speech identification, natural language processing. However, there's still little application of AI in the field of power system. One basic problem in the power system is the calculation of power flow. In this work, we propose a data-driven method to solve the power flow problems. Deep convolutional neural network (CNN), which is the main magic behind AlphaGo, is adopted as a tool to identify the mathematical formulation between system decision variables and state variables, and dense computation is avoided. The performance and accuracy of deep CNN is also validated on standard IEEE test cases.

II. Deep CNN-based Power Flow Calculation

The main reason of applying deep CNN to power flow calculation is that power system has a grid-like structure similar to image data, and can be described by square matrix, i.e. nodal admittance matrix. We can treat the topology of power system as two $n\times n$ matrices, i.e. the conductance matrix and the susceptance matrix, where n is the number of buses. For the output, two $1\times n$ vectors can be built for bus voltage magnitude and voltage angle. The advantage of applying the above matrix representation is that they can be adapted to power system with different scales by simply increasing the dimension of the matrix. Fig. 1. demonstrates how to map power system data to CNN training data with matrix structure. The CNN structure for training is shown in Fig. 2.

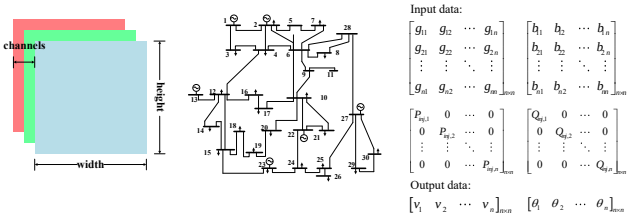

(a) Image parameter (b) Power system topology (c) Matrix representation of poser system

Fig. 1. Mapping power system data to CNN training data

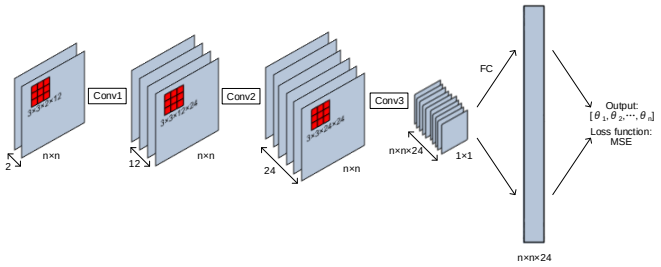

Fig. 2. CNN structure for voltage training

III. Case Study

The data set for training the above CNN is generated via a Monte Carlo simulation, where active and reactive bus power injection varies within a normally distributed range [-0.01, 0.01]. The simulation results are demonstrated in TABLE I. The errors of θ and v are in per unit mean absolute value. As can be observed from the table, the simulation results from CNN possess considerable accuracy.

TABLE I Power Flow Results of CNN Simulation

Case	Errors		Time(s)	
	θ	v	θ	v
5	4.7e-4	8.4e-5	8.4	11.4
9	1.7e-3	2.6e-4	8.8	11.5
14	8.4e-4	1.3e-4	9.4	12.8
30	5.3e-4	8.6e-5	22.3	33.1
57	1.9e-3	2.4e-4	77.1	127.9
118	2.0e-3	9.6e-4	333.9	203.3
145	4.7e-2	2.5e-4	508.9	499.3
181	2.0e-2	1.2e-3	906.9	1401.0

IV. Conclusions

This work proposes a CNN-based approach to solve power flow problem. Simulation results on standard IEEE test cases verifies the computation performance of the proposed data-driven method, which indicates the promising potentials of applying CNN and related deep learning techniques to power system studies.

Economic Dispatch Considering Risk Using Zig-zag Search Method With Adaptive Step-size

Qiwei Zhang, *Student Member, IEEE, Fangxing Li, Fellow, IEEE*

***Abstract*—Major advantages brought by high wind power penetration are low operation cost and significant reduction of detrimental gases. However, it also brings uncertainty and randomness into power system. Therefore, how to evaluate its influence in the economic dispatch has been a huge challenge for future integration of large amount of wind power. Conditional value at risk (CVaR) is a concept has been widely used in risk management field and recently has been introduced to power system. In this paper, a multi-objective economic dispatch problem considering conditional value at risk (CVaR) with high wind power penetration is proposed and a modified version of classic zig-zag search method (zig-zag AS) is proposed to solve it.**

***Index Terms*—Weibull distribution, conditional value at risk, economic dispatch, multi-objective optimization, zig-zag search algorithm.**

I. PROBLEM FORMULATION

A. *Objective Functions*

➢ Minimization of fuel costs

$$F = \sum_{i=1}^{N} F_i(P_{G_i}) \tag{8}$$

Typically, $F_i(P_{Gi})$ is represented by quadratic functions:

$$F_i(P_{G_i}) = c_i + b_i P_{G_i} + a_i P_{G_i}^{\ 2} \tag{9}$$

where a_i, b_i , and c_i are fuel cost coefficients of the generator i.

➢ Minimization of CVaR

Under wind power uncertainty, the evaluation of CVaR can be formulated in equation (10) (11).

$$F_\beta(P_G,\alpha) = \alpha + \frac{1}{q(1-\beta)} \sum_{k=1}^{q} [f(P_G,P_W) - \alpha] \tag{10}$$

$$f(P_G,P_W) = \begin{cases} \rho^1 \times (P_{W,i}^{\ k} - P_{W,i}^{\ s}) & P_{W,i}^{\ k} - P_{W,i}^{\ s} \geq 0 \\ \rho^2 \times (P_{W,i}^{\ s} - P_{W,i}^{\ k}) & P_{W,i}^{\ s} - P_{W,i}^{\ k} < 0 \end{cases} \tag{11}$$

B. *Technical Constraints*

➢ Power balance

$$\sum_{i=1}^{N} P_{G_i} + \sum_{i=1}^{NW} P_{W_i}^{\ s} = \sum_{i=1}^{NL} P_{L_i} \tag{12}$$

➢ Generation limits

$$P_{G_i}^{\ \text{Min}} \leq P_{G_i} \leq P_{G_i}^{\ \text{Max}} \quad ,\forall i \in N \tag{13}$$

$P_{G_i}^{Min}$ and $P_{G_i}^{Max}$ are the minimum and maximum value for power output respectively.

➢ Wind power forecast constraint

$$P_{W,i}^{\ \min} \leq P^s_{\ W,i} \leq P_{W,i}^{\ \max}, \forall i \in NW \tag{14}$$

II. MAIN METHODOLOGY

A. *Classic Approach*

The classic zig-zag search method consists of two parts: Find the First Pareto optimal (FFPO) search and a loop of zig-zag search.

$$g^1 = g_2(x) - \langle g_1(x), g_2(x) \rangle \times g_1(x) \tag{15}$$

$$g^2 = g_1(x) - \langle g_1(x), g_2(x) \rangle \times g_2(x) \tag{16}$$

where <, > is the vector dot production, $g_1(x)$ is the gradient of $f1$, and $g_2(x)$ is the gradient of $f2$.

B. *Zig-zag Search With Optimal Step Size*

The step-size for classic zig-zag search method is firstly defined by user. Here, zig-zag search with adaptive step size is proposed to determine the step size automatically.

$$\varepsilon^s < \left| f_1(X_{n+1}) - f_1(X_n) \right| < \varepsilon^u \tag{19}$$

$$\min \ f(x^k + \lambda d^k) \tag{20}$$

Replacing d^k with g^2, solving equation (21) (22) will generate the step-size. Then, the step size configuration is completed.

$$\min \ f_2(x^k + \lambda g^k) \tag{21}$$

$$\varepsilon^s < \left| f_1(x^k + \lambda g^k) - f_1(x^k) \right| < \varepsilon^u \tag{22}$$

III. CASE STUDY

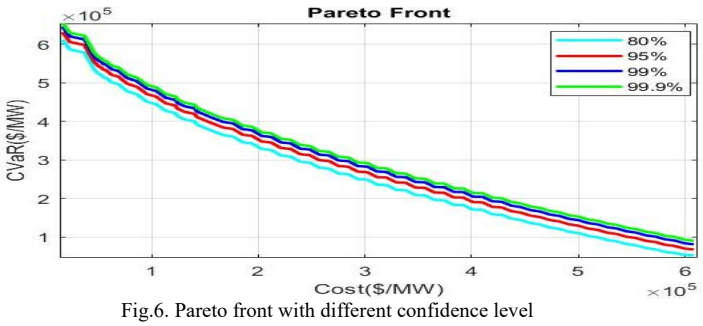

Fig.6. Pareto front with different confidence level

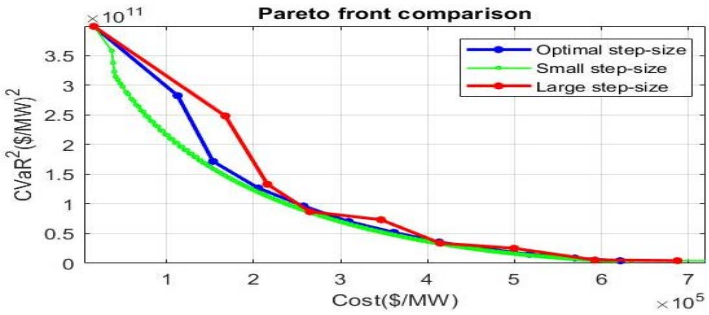

Fig.7. Pareto front comparison

Improvement to the Prediction of Fuel Cost Distributions Using ARIMA Model

Zhongyang Zhao, *Student Member, IEEE,* Chang Fu, *Student Member, IEEE*, Caisheng Wang, *Senior Member, IEEE*
Department of Electrical and Computer Engineering, Wayne State University, Detroit, USA
Carol J. Miller
Department of Civil and Environmental Engineering, Wayne State University, Detroit, USA

***Abstract*—This paper uses an autoregressive integrated moving average (ARIMA) model with historical fuel cost data in development of a three-step-ahead fuel cost distribution prediction. First, the data features of Form EIA-923 are explored and the natural gas fuel costs of Texas generating facilities are used to develop and validate the forecasting algorithm for the Texas example. Furthermore, the spot price associated with the natural gas hub in Texas is utilized to enhance the fuel cost prediction. The forecasted data is fit to a normal distribution and the Kullback-Leibler divergence is employed to evaluate the difference between the real fuel cost distributions and the estimated distributions. The comparative evaluation suggests the proposed forecasting algorithm is effective in general and is worth pursuing further.**

Keywords—ARIMA model; fuel cost; natural gas; price prediction; distribution estimation;

I. Introduction

The fuel cost distributions can be used to generate large and realistic power system network models without compromising the confidentiality of the utilities. However, the EIA-923 form updates the fuel cost data with a three-month delay. Due to the three months update lagging of the form, the most current data is not available for the study. Hence, the motivation of this paper is to develop a forecasting algorithm to provide more accurate FC characterization and distribution estimation instead of relying on the data with a three-month delay.

II. Key Equations

In this paper, the public fuel cost data extracted from Form EIA-923 are analyzed and utilized for achieving more accurate probability density estimation using ARIMA model forecasting.

A. Natural Gas Fuel Cost Processing

$$\Delta FC_t^{'} = FC_t^{'} - FC_t^{hub}, \qquad t = 1,2,\dots \tag{1}$$

B. ARIMA Model

$$\phi_p(B)\nabla^d y_t = \mu + \theta_q(B)\varepsilon_t, \qquad t = 1,2,\dots \tag{2}$$

C. Normal Distribution Fitting

$$F(X) = \frac{1}{\sigma\sqrt{2\pi}} e^{-\frac{(x-\mu)^2}{2\sigma^2}} \tag{3}$$

D. Kullback-Leibler Divergence of Normal Distributions

$$KL(p||q) = log\frac{\sigma_2}{\sigma_1} + \frac{\sigma_1^2 + (\mu_1 - \mu_2)^2}{2\sigma_2^2} - \frac{1}{2} \tag{4}$$

III. Forecasting Process

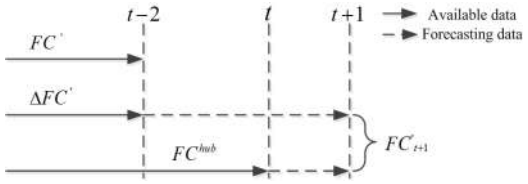

Fig. 1. *Fuel cost* forecasting process diagram.

IV. Prediction Performance

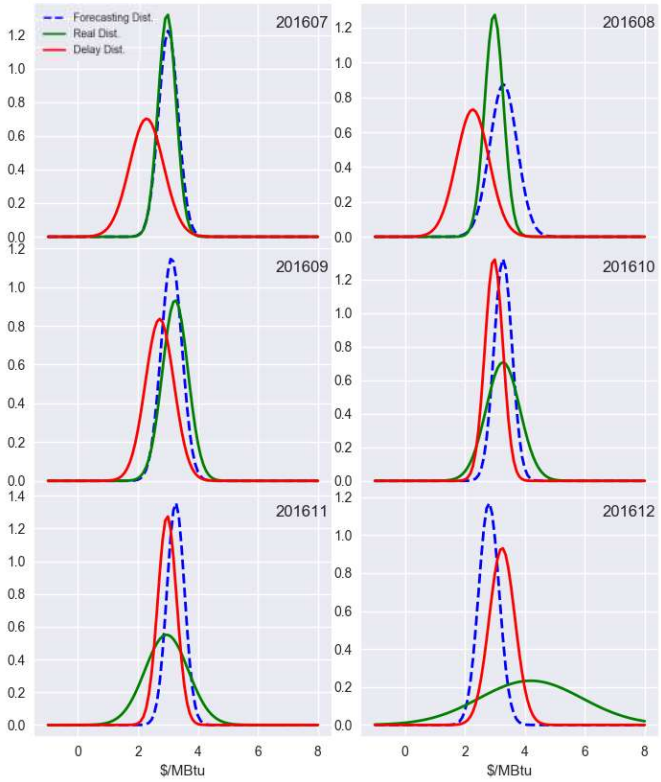

Fig. 2. Fitted Normal Distributions for three-month delay fuel costs, forecasting fuel costs and real fuel costs.

V. Conclusion

The results show the proposed forecasting algorithm has a superior performance over the method that uses the three-month delayed data. The results also indicate the good capability of the method in handling the prediction after the turning point. The proposed algorithm is able to be extended and implemented in other states when there are sufficient data.

CIM/E Oriented Graph Database Model Architecture and Parallel Network Topology Processing

Zhangxin Zhou[a, b], Chen Yuan[a], Ziyan Yao[a], Jiangpeng Dai[a], Guangyi Liu[a],
Renchang Dai[a], Zhiwei Wang[a], and Garng M. Huang[b]
[a] GEIRI North America, San Jose, CA, USA
[b] Texas A&M University, College Station, TX, USA

***Abstract*—CIM/E is an easy and efficient electric power model exchange standard between different Energy Management System vendors. With the rapid growth of data size and system complexity, the traditional relational database is not the best option to store and process the data. In contrast, the graph database and graph computation show their potential advantages to handle the power system data and perform real-time data analytics and computation. The graph concept fits power grid data naturally because of the fundamental structure similarity. Vertex and edge in the graph database can act as both a parallel storage unit and a computation unit. In this paper, the CIM/E data is modeled into the graph database. Based on this model, the parallel network topology processing algorithm is established and conducted by applying graph computation. The modeling and parallel network topology processing have been demonstrated in the modified IEEE test cases and practical Sichuan power network. The processing efficiency is greatly improved using the proposed method.**

Keywords—CIM/E, Graph Database, Graph Computation, Parallel Network Topology Processing

I. Introduction

To design next-generation Energy Management System software with graph computation technique, the most fundamental step is to model the power grid data into the graph database. In power grid control center, two basic configurations are used to describe the power system models: node breaker model and bus branch model. Through network topology processing, a node breaker model is mapped to a bus branch model.

The CIM/E is an efficient electric grid model exchange standard format developed by State Grid Corporation of China (SGCC). The CIM/E model simplifies CIM/XML model by ignoring terminal without compromising information to process network topology. This paper firstly models the CIM/E standard data into graph database and implements parallel topology processing algorithm using graph computation, which greatly reduces the network topology processing time.

II. CIM/E Model and Parallel Processing

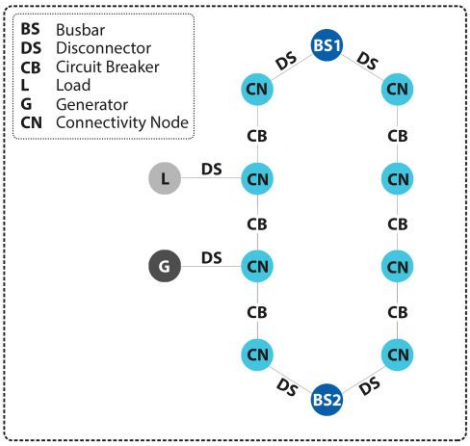

Fig. 1. Substation Modeling in CIMGDB

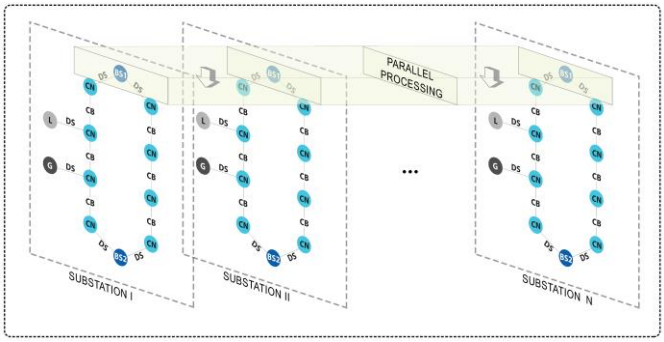

Fig. 2 Parallel Network Topology Processing

III. Case Study and Results

TABLE I. NTP Query Results for Sichuan Network

Sichuan Network	Total Vertices in Graph Database	Total Edges in Graph Database	NTP Execution Time (ms)
Modelling objects using vertices	78411	75277	150
Modelling objects using vertices and edges	48118	44984	100

This work was supported by State Grid Corporation of China technology project SGSHXT00JFJSI700138.

Chance Constrained Optimal Reactive Power Dispatch

Xinbo Geng, *Student Member, IEEE,* Le Xie, *Senior Member, IEEE,* and Diran Obadina, *Member, IEEE*

***Abstract*—The uncertainties from deepening penetration of renewable energy resources have already shown to impact not only the market operations, but also the physical operations in large power systems. It is demonstrated that deterministic modeling of wind would lead to voltage insecurity in the reality where wind fluctuates. This could render deterministic control of reactive power ineffective. As an alternative, we propose a chance-constrained formulation of optimal reactive power dispatch which considers the uncertainties from both renewables and contingencies. This formulation of a chance constrained optimal reactive power dispatch (cc-ORPD) offers system operators an effective tool to schedule voltage support devices such that the system voltage security can be ensured with quantifiable level of risk. The cc-ORPD problem is a Mixed-Integer Non-Linear Programming (MINLP) problem with a joint chance constraint and is extremely challenging to solve. Using the Big-M approach and linearized power flow equations, the original cc-ORPD problem is approximated as a Mixed-Integer Linear Programming (MILP) problem, which is efficiently solvable. Case studies are conducted on a modified IEEE 24-bus system to investigate the optimal operating schedule under uncertainties and the out-of-sample violation probability.**

I. Introduction

The high variability and limited predictability of renewables impose new challenges on the secure and reliable operation of power systems. There has been a substantial amount of literatures showing that deep penetration of renewables could jeopardize the security and reliability of power systems. For example, the rapid increase and stochastic nature of renewables might lead to voltage issues, which could be severe when a stressed system is lack of reactive support. An Optimal Reactive Power Dispatch (ORPD) problem is often formulated for better voltage profiles. The ORPD problem aims at finding optimal settings of current installed Reactive Power Support Devices (RPSDs) such as SVCs and Capacitor Banks to ensure system voltage constraints. Although numerous papers have studied the ORPD problem, most of them adopt a deterministic formulation and uncertainties from wind are ignored.

II. Chance-constrained Optimal Reactive Power Dispatch (cc-ORPD)

In this paper, we propose a framework for optimal reactive power dispatch considering joint uncertainties from wind uncertainties $\xi \in \Xi$ and contingencies $c \in \mathcal{C}$. The proposed framework is built upon chance-constrained programming, which is a natural and efficient tool for decision making in an uncertain environment.

A. Problem Formulation

$$\min \quad h_B(Q_B) + h_C(Q_C) + \lambda \mathbb{E}_{\mathcal{C}\times\Xi}\big[P_L(c,\xi)\big] \tag{1a}$$

$$\text{s.t. } P = A_G(c)P_G - A_G(c)\eta(c)P_\delta^c - A_D P_D + A_W \text{diag}(P_W)(1+\xi) \tag{1b}$$

$$Q = A_G(c)Q_G + A_C Q_C + A_B Q_B - A_D Q_D + A_W \text{diag}(Q_W)(1+\xi) \tag{1c}$$

$$P_i^c = \sum_{j=1}^{n_b} |V_i^c||V_j^c||Y_{ij}|\cos(\theta_i^c - \theta_j^c - \phi_{ij}), \forall c, i \tag{1d}$$

$$Q_i^c = \sum_{j=1}^{n_b} |V_i^c||V_j^c||Y_{ij}|\sin(\theta_i^c - \theta_j^c - \phi_{ij}), \forall c, i \tag{1e}$$

$$P_L^c = \sum_{l=1,l:i\sim j}^{n_l} g_l\big(|V_i|^2 + |V_j|^2 - 2|V_i||V_j|\cos(\theta_i - \theta_j)\big), \forall c \tag{1f}$$

$$\mathbb{P}_{\mathcal{C}\times\Xi}\Big(|V(c)|^- \le |V(c,\xi)| \le |V(c)|^+ \text{ for PQ buses and } Q_G^- \le Q_G(c,\xi) \le Q_G^+\Big) \ge 1-\epsilon \tag{1g}$$

$$|V(c)|^- \le |V| \le |V(c)|^+ \text{ for PV buses} \tag{1h}$$

$$Q_B \in \{0, Q_B^+\}, \quad Q_C^- \le Q_C \le Q_C^+ \tag{1i}$$

$$i,j = 1,2,\cdots,n_b, \quad c = 0,1,2,\cdots,n_c$$

The cc-ORPD problem is a two-stage chance-constrained programming problem. The *first-stage* variables are the operating states of RPSDs (Q_B and Q_C) and the voltage set points of generators (i.e. voltage magnitudes of PV buses). The *second-stage* variables include the nodal injection (P and Q), power imbalance P_δ, total line losses P_L, reactive generation Q_G, as well as the voltage magnitudes and angles of PQ buses ($|V|$ and θ). Since the parameters A_G^c and η^c depend on the contingency c, we change the notation to $A_G(c)$ and $\eta(c)$ for better understanding.

B. Solving cc-ORPD

The cc-ORPD problem is very challenging to solve for the following three reasons: (1) some decision variables are binary, thus the feasible region of cc-ORPD is naturally non-convex; (2) the power flow equations are non-linear equations, which further increase the difficulty of solving cc-ORPD; and (3) the chance constraint Eqn. (1g) induces computationally intractable issues. Difficulty (3) is solved via sample average approximation technique; difficulty (2) is handled by linearizing the AC power flow equation using Jacobian matrix. The cc-ORPD problem is converted to a Mixed Integer Linear Program (MILP) and solved using GUROBI.

Xinbo Geng and Le Xie are with the Department of Electrical and Computer Engineering, Texas A&M University, College Station, TX, 77840. Email: xbgeng@tamu.edu, le.xie@tamu.edu. Diran Obadina is with Electric Reliability Council of Texas (ERCOT). Email: Diran.Obadina@ercot.com.
This work is supported in part by the ERCOT, and in part by NSF ECCS-1150944 and ECCS-1546682.

Distributed Transmission Expansion Planning with Analytical Target Cascading

Mahdi Mehrtash, *Student Member*, *IEEE,* Amin Kargarian, *Member, IEEE,* Ali Mohammadi, *Student Member, IEEE*

***Abstract*—In this research a distributed collaborative transmission expansion planning (TEP) algorithm for interconnected multi-regional power systems has been studied. A local TEP is formulated for each region with respect to the region's local characteristic and interactions (i.e., tie-line flows) with its neighbors. Nodal power balances at border buses are modified to model the interactions. Realistic planning constraints and objectives, such as budget constraints, operational costs, and N-1 security criterion, are modeled in the local TEPs. The information privacy is respected as each local planner needs to share only limited information related to cross-border tie-lines with other planners. To coordinate the local planners, a two-level distributed algorithm is proposed based on the concept of analytical target cascading (ATC) for multidisciplinary optimization. While the upper-level solves the local TEPs in parallel, the lower-level seeks to coordinate neighboring regions. The lower-level problem is further replaced in the upper-level optimization by KKT conditions to relax the need for any form of central coordinator. This makes the proposed ATC-based TEP a fully parallelized distributed algorithm that is potentially less vulnerable to cyber-attacks and communication failures than the distributed methods utilizing a coordinator. An initialization strategy is suggested to enhance the performance of the distributed TEP.**

***Index Terms*—Collaborative transmission expansion planning, analytical target cascading, distributed optimization, information privacy, *N*-1 security criterion.**

I. Introduction

In electric power industries, transmission networks must have adequate capacity and appropriate design for reliable, secure, and fair power transmission. TEP is a more challenging problem in interconnected multi-regional power systems including several independent networks. Each power system could have its own local transmission planner. If the planners separately solve their TEP problem, the grid topology might not be optimal from the perspective of the whole grid. This separate planning imposes unnecessary investment costs and reduces the social advantage welfare. This study contributes to the literature by presenting an ATC-based distributed transmission expansion planning (DTEP) algorithm for interconnected multi-regional power systems in a collaborative framework taking into account N-1 security criterion for each region. Each region has its independent planning entity. Interactions (i.e., power exchange) between the regions through tie-lines is modeled by a set of pseudo generations and a set of pseudo loads, and the power balance equation at border buses are modified accordingly.

The authors are with the Department of Electrical and Computer Engineering, Louisiana State University, Baton Rouge, LA 70803 USA (e-mail: mmehrt3@lsu.edu, kargarian@lsu.edu, amoha39@lsu.edu.)

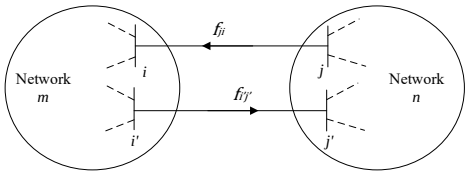

Fig. 1. Two interconnected networks.

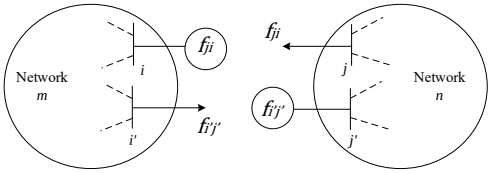

Fig. 2. Modeling power exchange between interconnected networks *m* and *n*.

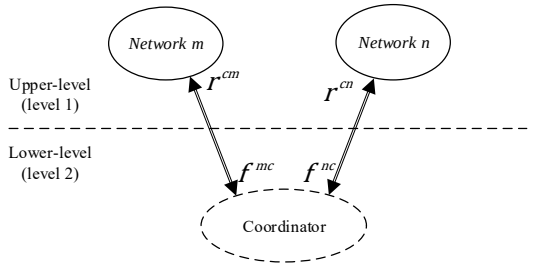

Fig. 3. Bi-level ATC structure for networks *m* and *n*.

Algorithm 1. The proposed parallel ATC-based coordination strategy with no coordinator for decentralized TEP implementation

Initialize coupling variables, α, β, and set λ, $k = 0$
While {not converged} **do**
  $k = k + 1$
  Solve (12) for all regions in parallel and determine the optimal values of coupling variables
  Exchange the values of coupling variables between neighboring regions
  Update $\alpha^k = \alpha^{k-1} + 2(\beta^{k-1})^2(r^{k-1} - f^{k-1})$
  Update $\beta^k = \lambda.\beta^{k-1}$
  If $\{\ |f_{mn}^k - f_{nm}^k| \le \epsilon_1$ and $\frac{|F^{m,k}(\Gamma) - F^{m,k-1}(\Gamma)|}{F^{m,k}(\Gamma)} \le \epsilon_2\ \}$ **then**
    Declare convergence
  End if
End while

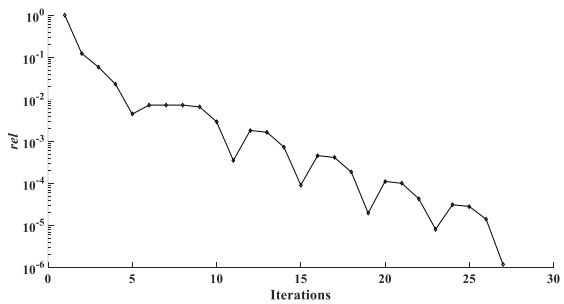

Fig. 4. The rel index (relative error) obtained by DTEP for 24-bus system.

An Integrated Distributed Economic Dispatch-Droop Control Architecture for Distribution System Operation

Shengyi Wang, Jie Li, and Lei Wu
Department of Electrical and Computer Engineering
Clarkson University
Potsdam, NY, USA

***Abstract*—With a proliferation of distributed energy resources integrated into electric distribution systems, secure and economic operation of distribution systems becomes more challenges, while conventional distribution system control architecture is expected to experience a transformation. In this paper, a bi-layer control architecture is proposed, in which the upper layer executes a distributed economic dispatch (ED) and the lower layer conducts individual DERs' droop control. Specifically, minimum generation cost is pursued through incremental cost (IC) consensus among all DERs, and an efficient update law is explored to guarantee convergence of the consensus algorithm. Furthermore, optimal ED decisions are dynamically incorporated into individual DERs' droop controllers by setting primary frequency control references. A bi-layer ED-droop co-simulation framework is developed to verify the proposed control scheme. A 4-bus medium-voltage primary distribution system is built in PSCAD, and the IC consensus based economic dispatch model is implemented in MATLAB. Furthermore, sensitivity analysis is conducted to explore optimal coordination between the two layers for the best tradeoff between power output tracking and total system generation cost.**

***Index Terms*—Distributed control, economic dispatch, incremental cost consensus algorithm**

I INTRODUCTION

In this paper, a bi-layer control architecture is proposed, in which the upper layer executes a distributed ED and the lower layer conducts individual DERs' droop control. Generation cost is minimized through IC consensus among all DERs. The major contributions of this paper are summarized as follows:

1. The proposed ED based droop control obviates the requirement for a central controller and thus the reliability and flexibility of the control are strengthened significantly.
2. ED decisions are dynamically incorporated into DERs' droop controllers by setting primary frequency control references for better tracking optimal power outputs.
3. A bi-layer ED-droop co-simulation framework is developed to mimic coordination between economic operation and droop frequency control to verify the effectiveness of the proposed control scheme.

II INTEGRATED ED-DROOP CONTROL

The relationship between real power and frequency can be expressed as:

$$\omega_i = \omega_{0i} - m_{P_i} P_i \tag{1}$$

Mathematical formulation of an integrated ED-droop control can be expressed as follows:

$$w_{0i} = w_{0i}^* + \delta w_{0i} \tag{2}$$

$$\delta w_{0i} = K_p (P_{Gi} - P_i) + K_i \int (P_{Gi} - P_i)\, dt \tag{3}$$

Substituting (2) into (1), we can derive the following equation:

$$w_i = w_{0i}^* + \delta w_{0i} - m_{P_i} P_i \tag{4}$$

III ALGORITHM DESIGN FOR IC CA BASED ED

The detailed pseudocode of proposed IC CA based ED is shown in Table I.

TABLE I IC CA AT THE i^{th} AGENT

Initialization: $P_{Gi}[0] = 0, \alpha_i, \beta_i, \lambda_i[0] = \beta_i, d_{ij}, K, \varepsilon, k = 0, DR_i, UR_i$.

Input: $P_{Di}[0], P_{Gi}^0$

while $k < K$

[1] Transmit $\lambda_i[k]$ and receive $\lambda_j[k]$ from $j \in N_i$.

[2] Compute $\lambda_i[k+1]$ using (27).

[3] Compute $P_{Gi}[k+1]$ using (28).

if $P_{Gi}[k+1] < Max\{P_{Gi,\min}, P_{Gi}^0 - DR_i\}$

$P_{Gi}[k+1] = Max\{P_{Gi,\min}, P_{Gi}^0 - DR_i\}$;

end if

if $P_{Gi}[k+1] > Min\{P_{Gi,\max}, P_{Gi}^0 + UR_i\}$

$P_{Gi}[k+1] = Min\{P_{Gi,\max}, P_{Gi}^0 + UR_i\}$;

end if

[4] Transmit $P_{Di}[k], P_{Gi}[k]$ and $P_{Gi}[k+1]$ and receive $P_{Dj}[k], P_{Gj}[k]$ and $P_{Gj}[k+1]$ from $j \in N_i$.

[5] Compute $P_{Di}[k+1]$ using (29).

[6] Update $k = k+1$.

end while

Output: $P_{Gi}[K]$

IV CASE STUDY

The effectiveness of the proposed distributed ED-droop control architecture is verified via a bi-layer co-simulation framework as shown in Fig. 1.

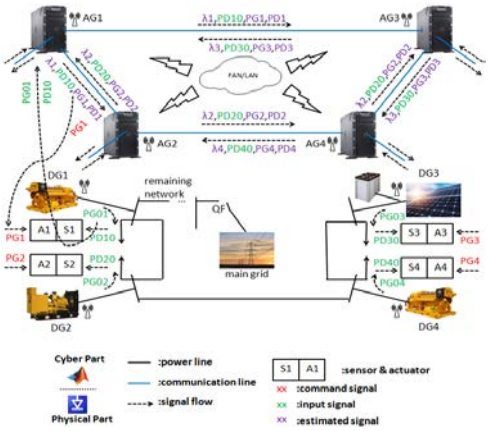

Fig. 1. A bi-layer ED-droop co-simulation framework

Flexible Long Term Planning Cooptimization Method Comparison and Validation

Patrick Maloney, Ping Liu, James McCalley

***Abstract*—This work compares and evaluates two different methods for long term planning under uncertainty on a 312 bus representation of the Western Interconnection (WI). The first, called stochastic programming (SP), is widely used throughout industry and specializes at finding flexible investments for the present. The second, called adaptation, takes an alternative approach and attempts to find a flexible trajectory through all time. This work provides a overview of the differences between the two methods and compares their performance within a Monte Carlo based validation methodology**

I. Model and Simulation Setup

The long term planning algorithms are run over an ∼20 year planning horizon on a 312 bus representation of the WI with emphasis on the Bonneville Power Administration's operational area (Figure 1).

Fig. 1. WI system Map. Green circles represent BPA buses and pink squares represent buses outside of BPA area.

Generic SP and adaptation formulations for expansion planning are given by equations (1)-(4)) and (5)-(9). Conceptual diagrams of the investment space are given in Figure 2.

II. Stochastic Programming Formulation

$$\min_{Cap,\triangle Cap} I_{1,c} \triangle Cap_{1,c} + \sum_{t>d,s} P_s(I_{t,s} \triangle Cap_{t,s} + OC_{t,s}) \tag{1}$$

Non-anticipative consts. $(e.g.\ \triangle Cap_{1,s} = \triangle Cap_{1,c})$ (2)

$$Cap_{t,s} = Cap_{t-d,s} + \triangle Cap_{t-d,s}\ \forall\ t > d, s \tag{3}$$

Operational constraints for each scenario s. (4)

III. Adaptive Programming Formulation

$$\min_{Cap,\triangle Cap} \sum_{t} I_{t,c} \triangle Cap_{t,c} + \sum_{t>d,s} P_s(I_{t,s}\beta \triangle Cap'_{t,s} + OC_{t,s}) \tag{5}$$

Non-anticipative constraints (Implicit) (6)

$$Cap_{t,c} = Cap_{t-d,c} + \triangle Cap_{t-d,c}\ \forall\ t \tag{7}$$

$$Cap_{t,s} = Cap_{t,c} + \triangle Cap'_{t-d,s}\ \forall\ t > d, s \tag{8}$$

Operational consts for each scenario s. (9)

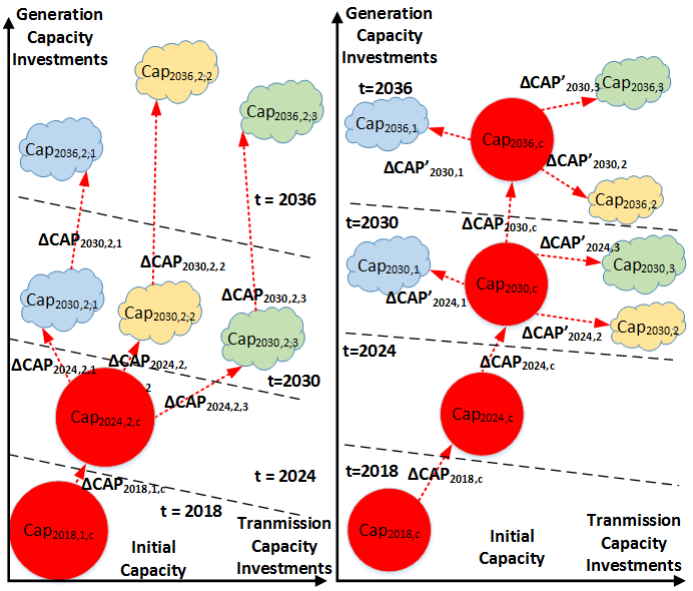

Fig. 2. Red arrows to red dots and clouds indicate "here and now" and "wait and see" investments respectively in the stochastic programming investment decision space on the left. The same nomenclature applies to the adaptive program on the right, however, the analogous "here and now" investments (or investments common to all scenarios) span multiple time periods forming a flexible trajectory through time.

IV. Validation

Investment plans from each programming methodology are compared in a Monte Carlo based folding horizon simulation. The comparison exposes the scenario based trajectories from SP and the core trajectory from adaptation to out of sample parameter values developed using Markov Chains. The differences in the two approaches are evaluated for both the initial time period and for the full planning horizon.

Voltage and Thermal Concerns during Geomagnetic Disturbance Corrective Measures

Cecilia Klauber, *Student Member, IEEE* and Thomas Overbye, *Fellow, IEEE*
Department of Electrical and Computer Engineering, Texas A&M University, College Station, Texas 77843
Email: cklauber@tamu.edu, overbye@tamu.edu

***Abstract*—Geomagnetic disturbances caused by solar activity can induce quasi-dc geomagnetically induced current (GIC) flows in the power grid. These currents lead to half cycle saturation of high voltage transformers, resulting in heating, damage, reactive power losses and ultimately voltage stability issues. Previous work has sought to mitigate these damages through topology control algorithms, but these operational actions can lead to unintended consequences, if not considered. In this work, GIC distribution factors and reactive power distribution factors are used to quickly generate the potential voltage deviation due to various corrective actions to inform operators making such decisions. The computational benefits of these linear methods enables quick results for even large systems. Furthermore, the resulting approximate redirected GIC flows are fed to a transformer heating model to quickly provide insight as to the effects of the corrective measures on thermal aspects that can lead to transformer damage.**

I. Introduction

The operation of the electric power system can be severely impacted by geomagnetic disturbances (GMD) and the changes in the earth's magnetic and electric fields therein. The currents induced by these fields flow in the earth's crust as well as conductors such as the electric transmission system, leading to half-cycle saturation of transformers and resulting in reactive power losses, voltage drop, and transformer heating and damage. GIC mitigation schemes, namely line switching, previously sought to minimize reactive power losses. A comprehensive scheme will consider the ac effects on the grid, in addition to the quasi-dc currents induced during a GMD, as well as the thermal state of the transformers. The development of GIC line outage distribution factors (GLODFs) greatly aids this analysis by providing a quick means of finding the redistribution of GICs during line switching. In conjunction with reactive power distribution factors or as an input to a transformer heating model, the expected voltage deviation at a bus or the change in transformer temperature can be evaluated as a function of the current state and impending change without having to re-solve the full ac power flow, or even the GIC dc network.

II. Topology Control Algorithm and Resulting Considerations

The localized nature of GICs and the GLODFs are leveraged to formulate a mixed-integer programming (MIP) problem, efficiently solvable by commercial solvers, to select the best sets of candidate switching lines for certain objectives, such as minimum reactive power losses. To address voltage and thermal concerns, only those line switching schemes deemed among the best need to be analyzed. The GLODFs are again invoked to estimate the resulting redistribution of GICs flowing in the system. Then the expected voltage deviation can be estimated as a linear combination of the pre-switching states and the redistributed GICs. The new flows also serve as the input to the transformer heating model and produce the expected transformer temperature across the system. These calculations can be programmed in parallel, quickly providing comprehensive considerations for an operator during an event.

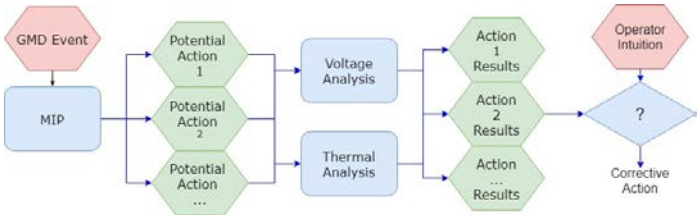

Fig. 1. Flow chart of topology control with voltage and thermal considerations

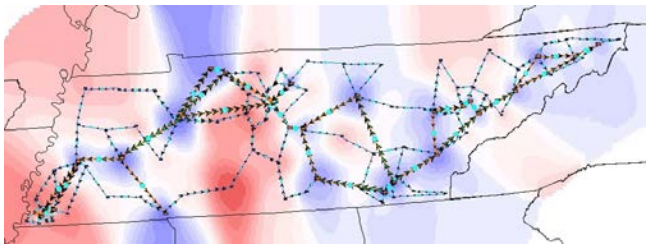

Fig. 2. Voltage contour over the UIUC 150-bus system

III. Conclusion

The proposed methodology is applied during simulated disturbances over the UIUC 150-bus case (Fig. 2). The output, a list of potential topology control actions and the consequential voltage and thermal effects, is efficiently calculated for a given storm. These results provide system operators with valuable information in the event of geomagnetic disturbances, which in tandem with operators' expertise and intuition can ensure the reliable operation of the electric power grid. The results are also scaled to the Texas 2000-bus synthetic case.

Acknowledgment

This work was supported in part by the National Science Foundation under a Graduate Research Fellowship and the Award EAR 15-20864.

DC Catenary Line Modeling of Subway Systems

Mustafa Erdem SEZGİN, *Student Member, IEEE,* Murat GÖL, *Senior Member, IEEE*
Department of Electrical and Electronics Engineering
Middle East Technical University
Ankara Turkey
erdems@metu.edu.tr, mgol@metu.edu.tr

***Abstract*— Today's technology and trend for clean energy, made electrified traction systems more and more popular around the world. As number and capacities of those systems increase, electrical modeling of those systems became a must for power quality studies and dynamic distribution system analysis. However, those models have inaccuracies due to electrical parameters and high computational burden. This paper proposes a linearized DC catenary line model for real subway systems, which has a little computational burden. Moreover, the parameter approximations employed by the method provides more accurate results. The proposed method is validated using real measurement data.**

***Keywords*— DC Catenary Line, DC Voltage Variation, Distributed Parameters, DC System Analysis, Electrical FEM Analysis.**

I. Introduction

In this paper, a linearized dynamic voltage model is developed for the DC catenary line. Due to the movement of the train along the rails, DC voltage at the catenary line has a time and position dependent characteristic, which causes both accuracy and computational burden problems. The developed model is generalized to reflect the real behavior of a subway system, such that operations of multiple trains are considered. Validation of the method is realized with real field data.

II. Electrical Parameters

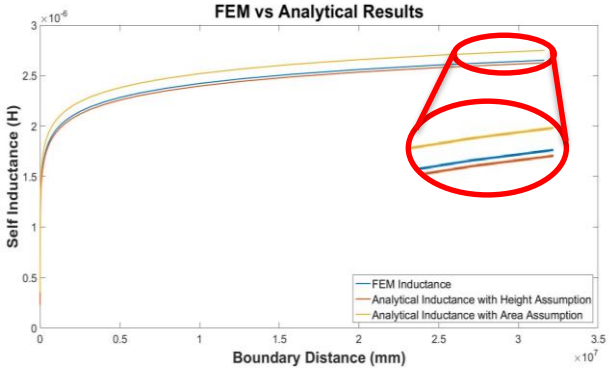

Fig. 1. Comparison between radius assumptions

$$r_{eq,conventional} = \sqrt{\frac{A}{\pi}} \tag{1}$$

$$r_{eq,proposed} = \frac{h_R}{2} \tag{2}$$

III. System Modeling

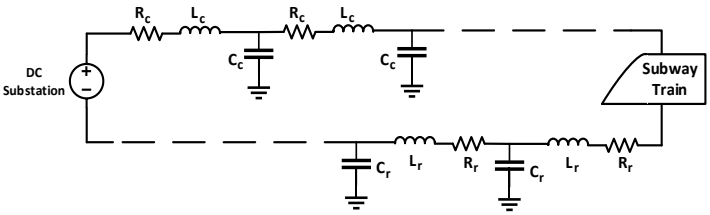

Fig. 2. System configuration for distributed parameter model.

$$\frac{dV}{dx} = RI + L\frac{dI}{dx}\frac{dx}{dt} \tag{3}$$

$$\frac{dI}{dx} = C\frac{dV}{dx}\frac{dx}{dt} \tag{4}$$

By solving (3) and (4);

$$I(x) = C_1 e^{\frac{RCv}{1-LCv^2}x} \tag{5}$$

$$V(x) = \left(C_1\frac{1-LCv^2}{Cv} + LC_1\right)e^{\frac{RCv}{1-LCv^2}x} + V_1 \tag{6}$$

Boundary conditions can be written as;

$$V_C(x=l) = V_{source} \tag{7}$$

$$P = [V_C(x=0) - V_R(x=0)] \times I_C(x=0) \tag{8}$$

$$V_R(x=l) = 0 \tag{9}$$

$$I_C(x=0) = I_R(x=0) \tag{10}$$

IV. Validation of the Method

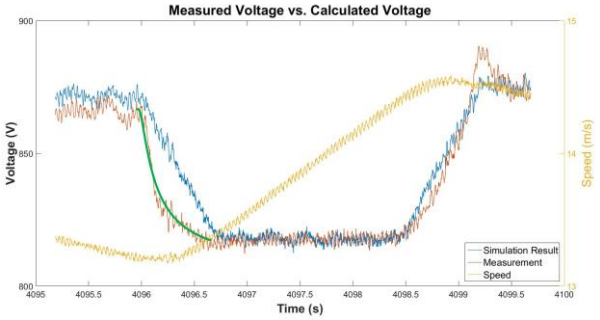

Fig. 8: Simulation result and measurement of the voltage

Volt-Var Optimization Algorithm Utilizing Custormer- and Utility-Owned Distributed Resources

David Mulcahy, Catie McEntee, Jiyu Wang, Ning Lu

Department of Electrical and Computer Engineering

North Carolina State University, Raleigh, NC, USA

djmulcah@ncsu.edu

Keywords— Volt-Var Optimization, Mixed-Integer Nonlinear Programs, Distributed Energy Resources, OpenDSS, Photovoltaics

I. INTRODUCTION

Rooftop photovoltaic (PV) systems and utility-scale PV farms have proliferated rapidly in recent years as utilities and customers have moved toward low-cost, low-emission electricity generation. High penetration of solar generation on distribution circuits can cause violations of voltage standards, larger voltage fluctuations, and increased operation of utility-owned device. In these circuits, voltage control is increasingly difficult while relaying solely on traditional voltage control devices like capacitors, on-load tap changers (LTC) and line voltage regulators. There is a significant need for voltage control methods that can maintain voltage limits and coordinate all available resources to manage voltage in real time.

While the integration of PV can worsen these voltage issues, the PV inverters and the integration of smart controls for customer loads can provide better voltage control than conventional resources. When voltages are high, customers with smart inverters and/or controllable loads can increase load, curtail PV, or absorb reactive power to reduce voltages. When voltages on the feeder are low, reducing load, or injecting reactive power can increase voltages. These resources can operate in conjunction with traditional methods of discrete switching of capacitors or changing regulator taps. However, combining all these resources effectively requires new algorithms for voltage control and distribution circuit operation.

This research proposes a mixed-integer nonlinear program (MINLP) to schedule the dispatch of distribution resources. The algorithm incorporates the controls of photovoltaic (PV) smart inverters (reactive power and PV curtailment), controllable load, voltage regulators, and capacitors to maintain voltage across the feeder.

II. METHODOLOGY

The optimization utilizes a voltage sensitivity matrix for all resources based on [1] using an OpenDSS model of a feeder and approximates the voltage across the circuit after control actions (eqn. 2) The objective function (1) minimizes the cost of control actions (eqn. 1) which include PV curtailment, reactive power injection/absorption, capacitor switching, and regulator tap changes (ΔP_i^{PV}, ΔQ_i^{PV}, ΔP_i^{Load},ΔS_i, and ΔT, respectively). Additionally, (1) minimizes the change in voltage between time periods while maintaining voltage within limits (eqn. (3)). Individual loads (increase and decrease) have a quadratic price while PV curtailment has a linear price based on opportunity cost of PV production. Discrete actions from regulators and capacitor switching have a fixed price per switching operation.

$$\min \sum_{i=1}^{n} \left[C_i^{Load+}\left(\Delta P_i^{Load+}\right) + C_i^{Load-}\left(\Delta P_i^{Load-}\right)\right] + \sum_{i=1}^{n} C^{PV}\left(\Delta P_i^{PV}\right) + \sum_{i=1}^{m} C^{cap}\left(\Delta S_i\right) + C^{LTC}\left(\Delta T^{+}\right) + C^{LTC}\left(\Delta T^{-}\right) + \sum_{i=1}^{n} V_{cost} \times \left[V_i^{prev} - V_i\right]^2$$

s.t.

$$V_i(\cdot) = V_i^{Base} + \sum_{j=1}^{n} VSM_{i,j}^{P} \times \left(\Delta P_j^{Load} + \Delta P_j^{PV}\right) + \sum_{j=1}^{n} VSM_{i,j}^{Q} \times \Delta Q_{i,j} + \sum_{j=1}^{m} VSM_{i,j}^{Qcap} \times \Delta S_i \times Q_{cap} + \Delta T \times VSM_m^{LTC+} \quad (2)$$

$$V_{\min} \leq V_i \leq V_{max} \quad (3)$$

III. CASE STUDY

A case study for one day (5-min resoltuion load and PV profiles) was performed on a rural, distribution feeder with 371 load nodes and 75 PV systems (20% penetration). The

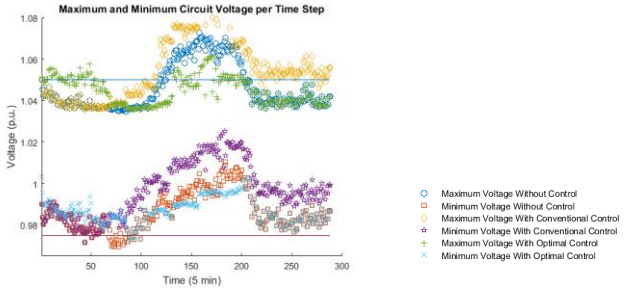

voltage results across the feeder are shown in figure 1

Figure 1. Max and Min Votlage across circuit by control method

compared to the system without voltage control, with conventional control, and with our VSM-based MINLP control. The results show how the diurnal maximum votlage and minimum voltage stay within the ANSI voltage limits more frequently and with less deviation than the other control methods.

IV. REFERENCES

[1]Zhu, Xiangqi, Jiyu Wang, David Mulcahy, David L. Lubkeman, Ning Lu, Nader Samaan, and Renke Huang. "Voltage-Load Sensitivity Matrix Based Demand Response for Voltage Control in High Solar Penetration Distribution Feeder." 2017 IEEE Power & Energy Society General Meeting. IEEE, 2017

Cloud Computing Based Real-Time Energy Management System with RNN-LSTM Wind Forecasting

Behrouz Azimian
Inamori School of Engineering
Alfred University
Alfred, USA
mr.behrouz.azimian@ieee.org

Dan Lu
Inamori School of Engineering
Alfred University
Alfred, USA
lu@alfred.edu

Xingwu Wang
Inamori School of Engineering
Alfred University
Alfred, USA
fwangx@alfred.edu

***Abstract*—With wind and solar resources, power generation facilities can be close to the loads via distributed networks. It is possible to isolate local renewable power generations in the extreme weather events, if energy storages are included in the islanding operations. Since wind speeds randomly vary, it is critical to predict the power generations based on the historical data and minute-ahead data. With Internet of Things (IoT) and Real-Time Hardware-in-Loop (RT-HIL), one can monitor and control power flows. Using machine learning and cloud computing, one may be able to predict wind power generation 10 minutes ahead of the actual events. In this study, Recurrent Neural Networks (RNN) with Long Short-Term Memory (LSTM) method is used for "10-minute-ahead wind power forecasting." A real-time simulation is carried out in a distribution network via OPAL RT-HIL. Results will be presented, along with observations.**

Keywords—recurrent neural networks; wind power; forecasting; hardware-in-loop; real-time simulaiton

I. INTRODUCTION

By 2030, the renewable energy penetration level in New York State's electric power generation will be 50%. New wind farms are being proposed, planned and installed in upstate New York, including southern tier and western New York, where electrical loads near the new wind farms are relatively low. Local consumptions with energy storages such as batteries can be formed in distribution network; one can envision a resilient power network to resist power outages due to extreme weather and other unexpected events. Forming a community power island may be beneficial. Thus, it is critical to develop a predictive methodology based on the historical data and existing data. In this study, our model is based on electrical power grid in Alfred, NY; the wind power generation data are from a system of 100 kW located on Alfred State College campus. Our ultimate goal for the project is to design a real-time energy management system with live data from wind turbines nearby, harvested via IoT data acquisitions systems. We'll use an IEEE 33 bus system as an example of distribution network because this benchmark is similar to Alfred power grid. With OPAL-RT simulations, we can study the effectiveness of forecasting schemes.

II. METHODOLOGY

A. Wind power forecasting

Among different methodologies, RNN with LSTM provides suitable performance in terms of accuracy and computation time. The LSTM structure is depicted in Fig. 1 where X_t is the real time wind power generation acquired from IoT data acquisition system, h_t is the hidden state which can be represented by the previous state h_{t-1} and the current input X_t under a control of a set of weight coefficient (stored as the short-term memory), and C_t is the cell state which keeps long short-term memory (seasonal or monthly information of historical data) and C_{t-1} will be trained along with h_{t-1} to the updated C_t.

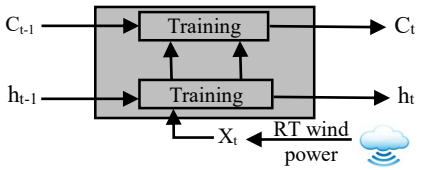

Fig.1. LSTM structure for 10 minutes ahead wind power forecasting

Figure 2 shows the forecasted wind power and actual data gathered. After initial "machine learning," the predication yields close resemblance of actual data, however, with a latency. Such time delay can be corrected by systematically shifting the time. It takes 20 seconds to forecast the next 10 minutes' wind speed, indicating a promising methodology for real-time operation.

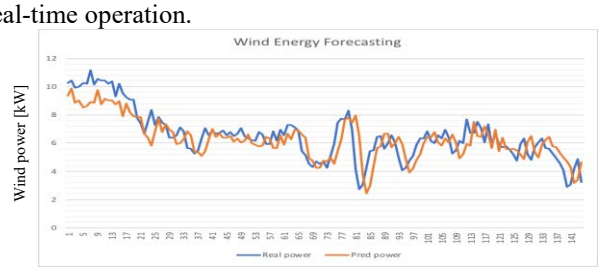

Fig. 2. Forecasted and actual wind power generation

B. HIL power system simulation

The predicted output is sent to simulated renewable energy integrated power system (OPAL-RT), and real time response of the entire system is monitored to ensure system security constraint compliances by generating correction control signals. For example, wind power spillage can be managed to meet the optimum operation condition of the system. The whole RT-HIL system is depicted in Fig. 3.

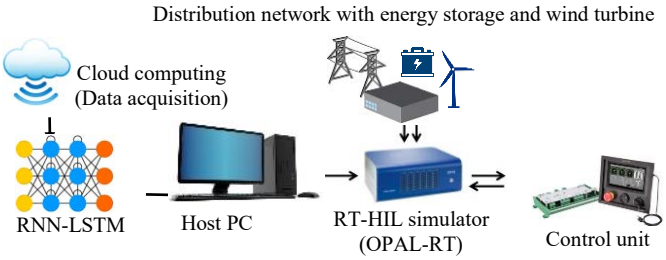

Fig. 3. Real-time simulation of distribution network

Progressive Hedging Algorithm in Two Stage Stochastic Optimization of Look-Ahead Unit Commitment (SLAC)

Mehdi Saleh
School of Computing, Informatics, Decision Systems Engineering
Arizona State University
Tempe, AZ, USA
mehdi.saleh@asu.edu

Kory Hedman
Department of Electrical Engineering
Arizona State University
Tempe, AZ, USA

kory.hedman@asu.edu

***Abstract*— Modeling uncertainties coming from renewable sources and generator outages in the unit commitment framework add a great deal of complexity to the model. With today's computational capabilities for mixed integer programming problems, solving multiple renewable scenarios and generator contingencies could be time inefficient. Progressive Hedging (PH) is a scenario-based decomposition method to solve stochastic model in a time efficient manner. Dealing with large scale MIP problems could arise some issues that is application dependent. In the paper, we propose PH heuristics such as scenario bundling, forcing solutions, and slamming to obtain a solution in a desired timeframe.**

Keywords—Unit commitment, Progressive Hedging, mixed integer programming, stochastic optimization.

I. INTRODUCTION (*HEADING 1*)

The industry is in the process of moving towards technologies like SLAC. This SLAC is a tool that will sit right in front of the decision-making process where SCED resides, which is in the real-time operations and market environments. The SLAC will sit at an hour-ahead time stage. Note that the technology that we are developing will also be deployed within real-time SCED tools in the future as well as within day-ahead security-constrained unit commitment (SCUC) and day-ahead residual unit commitment (RUC) tools. Progressive Hedging (PH) is a scenario-based decomposition method to solve stochastic model in a time efficient manner. Dealing with large scale MIP problems could arise some issues that is application dependent. In this paper, we propose PH heuristics such as scenario bundling, forcing solutions, and slamming to obtain a solution in a desired timeframe for an hour ahead unit commitment model.

II. METHODOLOGY

A horizontal decomposition method is applied to the extensive form of the SLAC model (Fig 1) where each subproblem is consisted of a single renewable scenario and a generator contingency. Before creating the subproblem and invoking PH algorithm, data is preprocessed and the network topology is built.

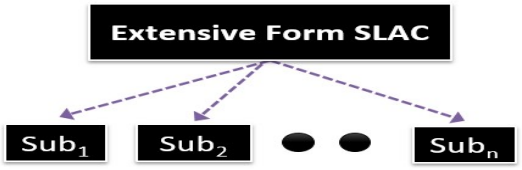

Figure 1. Horizontal decomposition of extensive form

After processing the data, subproblem is solved and the solution is passed to deliverability test stage. If there are no violations is reported the final solution is handed over to PH server to obtain convergence among different solutions of subproblems. Figure 2 summarizes the flowchart of a single scenario and a single generator contingency subproblem.

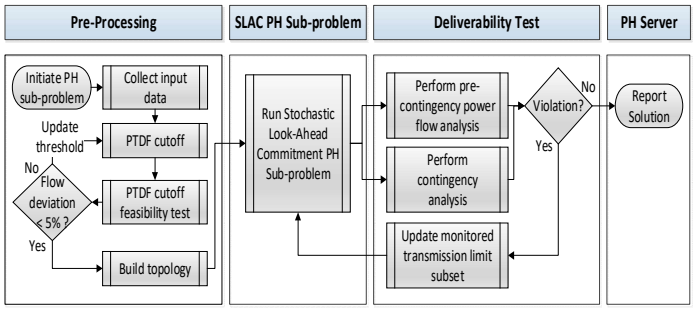

Figure 2. Subproblem flowchart

III. REFERENCES

[1] Watson, Jean-Paul, and David L. Woodruff. "Progressive hedging innovations for a class of stochastic mixed-integer resource allocation problems." *Computational Management Science* 8.4 (2011): 355-370.

[2] Gade, Dinakar, et al. "Obtaining lower bounds from the progressive hedging algorithm for stochastic mixed-integer programs." *Mathematical Programming* 157.1 (2016): 47-67.

Robust Unit Commitment Considering the Temporal and Spatial Correlations of Wind Farms Using a Data-Adaptive Approach

Yipu Zhang, Xiaomeng Ai, Jinyu Wen
Huazhong University of Science and Technology, Wuhan, China

Jiakun Fang
Aalborg University
Aalborg, Denmark

Cheng Luo
Northern Indiana Public Service Company
Merrillville, USA

***Abstract*—In robust optimization problems, building a proper uncertainty set for the stochastic variables plays an important role. Due to the restricted mathematical formulations of the uncertainty sets, the results derived from conventional two-stage robust optimization are usually over conservative. In this paper, a novel data-adaptive robust optimization method for the unit commitment is proposed for the power system with wind farms integrated. The extreme scenario extraction and the two-stage robust optimization are combined in the proposed method. The data-adaptive set consisting of a few extreme scenarios is derived to reduce the conservativeness by considering the temporal and spatial correlations of multiple wind farms. Numerical results demonstrate that the proposed data-adaptive robust optimization algorithm is less conservative than the current two-stage optimization approaches while maintains the same level of robustness of the solution.**

***Index Terms*—Unit commitment, two-stage robust optimization, temporal and spatial correlations, data-adaptive uncertainty set, extreme-scenario**

I. KEY EQUATIONS

A data-adaptive robust optimization (DARO) method is proposed in this section. The proposed method considers the correlation of the wind farms by building a data-adaptive set as shown in (1).

$$\boldsymbol{\omega} \in \Re_3 = \left\{ \boldsymbol{\omega} \in \boldsymbol{R}^n \left| \begin{array}{l} \boldsymbol{\omega} = \sum_{i=1}^{N_e} p_i \boldsymbol{\omega}_{e,i} \\ \sum_{i=1}^{N_e} p_i = 1,\ p_i \geq 0 \end{array} \right. \right\} \tag{1}$$

The approach is divided into 3 steps in detail. Firstly, the MVEE algorithm is used to determine the approximate region of the historical scenarios. Then the extreme scenarios and the data-adaptive set is obtained by the algorithms from linear algebra. Finally, the two-stage robust optimization is adopted to solve the robust UC problem.

II. KEY RESULTS

A. System description

To validate the effectiveness of the proposed algorithm, a 6-bus distribution network is used as the test system. The topology is shown in Fig. 2.

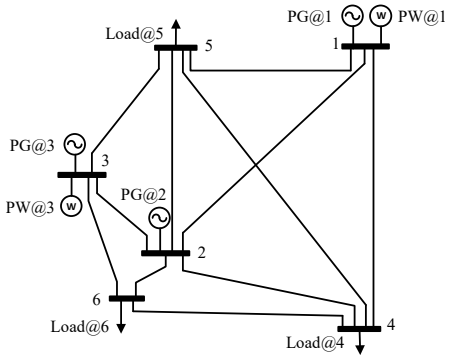

Fig. 2. 6-bus System topology

B. Comparative study on DARO and conventional TRO

TABLE I. THE COMPARISON RESULTS

Method	Traditional robust optimization	DARO
α_{RO}	100%	100%
UCt (h)	41	37
OUC (MWh)	7150	6380
Operation cost in the worst scenarios (CNY)	61910.23	52102.15
Operation cost in the forecasted scenarios (CNY)	52099.94	51314.07
Operation cost in the historical scenarios S^H1(CNY)	51987.97	51206.66
Operation cost in the historical scenarios S^H2 (CNY)	52329.76	51513.51
Operation cost in the historical scenarios S^H3 (CNY)	52098.94	51310.09
Calculating time (s)	104.99	28.53

III. CONCLUSION

In this paper, a robust unit commitment model considering the temporal and spatial correlation of wind farms is proposed. Combining the advances of scenario-generation algorithms and two-stage robust optimization, the proposed data-adaptive robust method can make full use of the empirical knowledge obtained from the historical data. Case studies show that the proposed algorithm improves the utilization rate of the online unit capability significantly and reduces the operation cost while guarantees the robustness of the system. This leads to the improved economy of the decision with uncompromised security. In addition, the computational efficiency is significantly improved so that the proposed method is applicable to large systems.

SDP Based ACOPF and Network Reconfiguration for Three-phase Distribution System

Yikui Li, Jie Li, and Lei Wu
Department of Electrical and Computer Engineering
Clarkson University
Potsdam, NY, USA
Email: {yikliu, jieli, lwu}@clarkson.edu

***Abstract*—In emerging distribution systems with a proliferation of distributed energy resources (DER) and flexible demand assets, operation characters of the unbalanced network and voltage regulation devices need to be accurately addressed for ensuring the secure and economic operation. This poster introduces an AC optimal power flow model and a network reconfiguration model, both of which are based on semidefinite programming (SDP). Numerical studies illustrate effects of the proposed approach.**

Keywords—Distribution systems; AC Optimal power flow; Distribution network reconfiguration; Semidefinite programming

I. Introduction

Distributed energy resources (DER) present unique advantages in providing clean and cheap energy locally, reducing active power losses, and enhancing energy resiliency in distribution systems. Motivated by these incentives, existing distribution systems are experiencing new changes by including a deeper penetration of DERs. However, as another side of a coin, the proliferation of DERs in distribution systems also brings new challenges. Specifically, distribution lines have compatible resistance and reactance, which makes voltage magnitudes also sensitive to active power injections from DERs. Thus, voltage fluctuation caused by intermittent power outputs of DERs, such as voltage sag and voltage swell, is one of the prominent problems in emerging distribution systems. It could degrade power quality and cause damages to electrical equipment. Particularly, voltage swell issues could more likely emerge in distribution feeders with excessive DERs. Furthermore, bidirectional power flows induced by proliferated DERs in distribution systems, by contrast with past unidirectional power flows, could cause potential risk of line congestion and require reconfiguration of protection systems.

II. Distribution System ACOPF Model [1]

This section focuses on the modeling and solution approach of AC optimal power flow (ACOPF) problems for unbalanced three-phase distribution systems with DERs and voltage regulators (VR). ACOPF problem is essentially nonlinear and nonconvex because of the quadratic relationship among phase voltages and complex power injections. Challenges of nonlinearity and non-convexity are further deteriorated by unique characteristics of unsymmetrical distribution systems. The ACOPF problem is formulated as a chordal relaxation based SDP model, and a tighter convexification model of VRs is proposed to mitigate solution inexactness. Analytical conditions are presented and proved to determine whether global optimal solution to the original ACOPF problem can be retrieved from solutions of the chordal relaxation based SDP model.

This work was supported in part by the U.S. National Science Foundation grants PFI:BIC-1534035, CNS-1647135, and ECCS-1653179.

III. Distribution System Reconfiguration Model [2]

Distribution network reconfiguration has long been used by distribution system operators to achieve certain operation objectives, such as reducing system losses or regulating bus voltages. Co-optimizing network topology and DERs' dispatches could further enhance such operational benefits. Thus, this section focuses on the optimal network reconfiguration problem of distribution systems under an unbalanced ACOPF framework, which rigorously addresses operation characters of unbalanced network, DERs, and VRs. Two VR models with continuous and discrete tap ratios are studied and compared. The proposed co-optimization problem is formulated as a mixed-integer semidefinite programming (MISDP) model with binary variables indicating line-switching statuses and tap positions. Several acceleration strategies by studying the structure of distribution networks are explored for reducing the number of binary variables and enhancing the computational performance.

IV. Case Studies

Numerical case studies are conducted on modified IEEE 34-bus and 8500-node distribution systems. Numerical studies illustrate effects of the proposed approaches. Computational performances of the proposed ACOPF and network reconfiguration models are discussed.

References

[1] Y. Liu, J. Li, L. Wu and T. Ortmeyer, "Chordal relaxation based ACOPF for unbalanced three-phase distribution system with DERs and voltage regulation transformers", *IEEE Trans. Power Syst.*, vol. 33, no. 1, pp. 970–984, Jan. 2018.

[2] Y. Liu, J. Li, and L. Wu, "Coordinated optimal network reconfiguration and voltage regulator/der control for unbalanced distribution systems," *IEEE Trans. Smart Grid*, (Early Access).

Finite-Difference Relaxation for Parallel Computation of Ionized Field of HVDC Lines

Peng Liu, *Dept. of Electrical and Computer Engineering*
University of Alberta
Edmonton, Canada
pliu3@ualberta.ca
Venkata Dinavahi, *Dept. of Electrical and Computer Engineering*
University of Alberta
Edmonton, Canada
dinavahi@ualberta.ca

Abstract

Ionized field calculations for high-voltage direct current (HVDC) transmission line is a computationally demanding problem, which can benefit from the application of massively parallel high-performance compute architectures. The finite element method (FEM) commonly employed to solve this problem is both memory and execution time intensive. In this paper, a finite-difference relaxation (FDR) method is proposed to solve a unipolar and a bipolar ionized field problem in an HVDC line. The novel FDR method has several advantages over FEM. First, the scheme is suitable for massively parallel computation and runs much faster: Compared with the commercial FEM software Comsol Multiphysics, the speed-up is more than 14 times in CPU parallelization and 35 times in graphics processor parallel implementation, while providing high accuracy. Moreover, the set of equations in FDR need not be assembled; instead, it is solved by a relaxation scheme and requires much less memory than FEM. Additionally, differentiated grid size with interpolation techniques is proposed to improve the flexibility of FDR for problem domain containing irregular geometries or disproportional sizes.

Index Terms

Finite-difference method, graphics processors, HVDC lines, ionized field, Jacobi method, multi-core, many-core, parallel algorithms, relaxation.

PV Extreme Capacity Factor Analysis

Zefan Tang[1], Peng Zhang[1], Jaemo Yang[2], Kunihiro Muto[1], Marina Astitha[2], Joseph N. Debs[3], David A. Ferrante[3], Devon Marcaurele[3], Isabelle M. Hazlewood[4], Dale Hedman[4]

***Abstract*—Spatiotemporally analyzing the extreme photovoltaic (PV) capacity factor is of great importance for system planning and protection. However, due to the scarce number of the extreme data, the traditional extreme value analysis (EVA) could not be directly applicable. This paper addresses this challenge by combining data from multiple PV sites. The k-means clustering method is developed to spatiotemporally divide the utility service territory into k clusters, such that PV systems in each cluster will have similar behaviors in terms of the extreme capacity factor (ECF). The value of k is determined by using the Silhouette Value, and the extreme data of each PV site are selected by setting a threshold. Specifically, the effects of different k and thresholds are evaluated. The results illustrate that different k and thresholds can have different return levels with great dissimilarity.**

I. Main Results

In this paper, k-means clustering is utilized to spatiotemporally divide the utility service territory into k clusters based on five meteorological variables: solar irradiance, humidity, temperature, wind speed, and cloud coverage. The objective is to combine more extreme data from multiple PV systems with the similar behaviors in terms of ECFs.

EVA is subsequently applied to evaluate the probability distributions of ECFs. It uses the extreme data selected through a threshold from each PV system in the same cluster. The effects of different k and thresholds are both evaluated.

Key conclusions: 1) different k and thresholds can lead to different return levels with great dissimilarity; 2) the higher threshold, the higher return levels; and 3) the value of k can be determined through Silhouette Value.

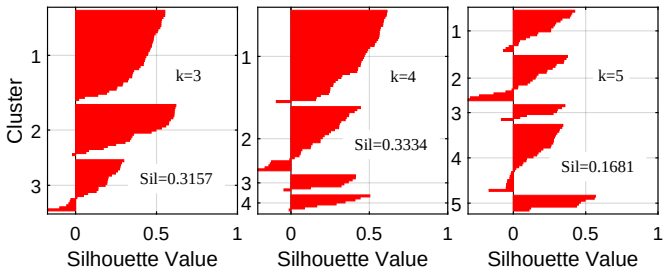

Fig. 1. Comparison results of the Silhouette Value for different k in February.

This material is based upon work supported by Eversource Energy Center under Grant No. 6200980 and 6200990, National Science Foundation US Ignite under Award No. 1647209, and UConn Academic Plan Level 1 under Award No. 2806600.

[1]Dept. of Electrical and Computer Engineering, University of Connecticut, Storrs, CT 06269
[2]Dept. of Civil and Environmental Engineering, University of Connecticut, Storrs, CT 06269
[3]Eversource Energy, Berlin, CT 06037
[4]Connecticut Green Bank, Rocky Hill, CT 06067

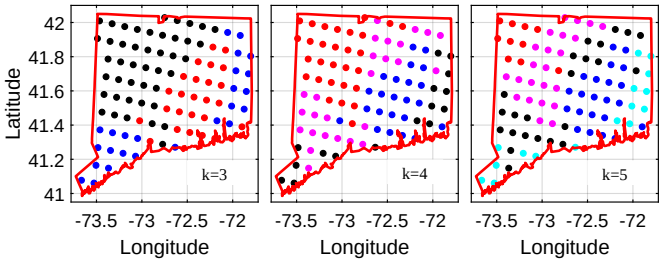

Fig. 2. Comparison results of the clustering for different k in February. Each dot represents each weather site. Different colors mean different clusters.

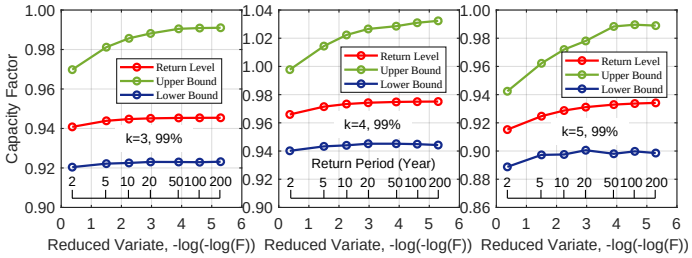

Fig. 3. Comparison results of the return levels for different k in February when the threshold is 99%. The upper and lower bounds are the 95% confidence intervals.

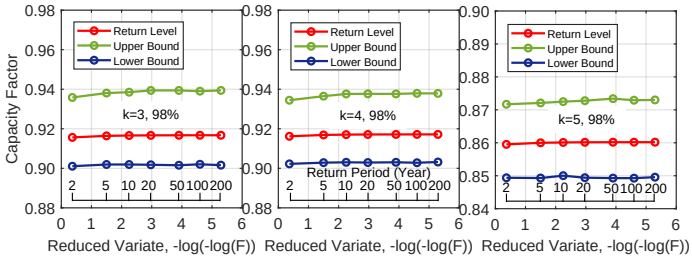

Fig. 4. Comparison results of the return levels for different k in February when the threshold is 98%. The upper and lower bounds are the 95% confidence intervals.

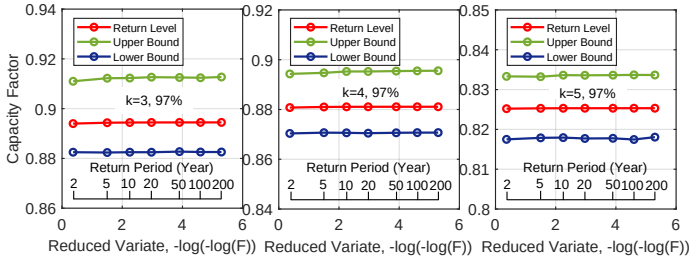

Fig. 5. Comparison results of the return levels for different k in February when the threshold is 97%. The upper and lower bounds are the 95% confidence intervals. With a low threshold, the return level is almost constant for different return periods.

Robust Koopman Operator-based Kalman Filter for Power Systems Dynamic State Estimation

Marcos Netto, *Student Member, IEEE,* and Lamine Mili, *Life Fellow, IEEE*
Virginia Polytechnic Institute and State University

***Abstract*—We develop a robust Koopman Kalman filter (GM-KKF) to estimate the rotor angle of synchronous generators. The approach is data-driven and model independent. The design phase is carried out offline and requires estimates of the generators' rotor angle and active/reactive power; in real-time, only measurements of active/reactive power at the terminal of the generators are assumed. We investigate the probability distribution of the transformed state variables by means of Q-Q plots and verify that they follow a Student's t-distribution with 20 degrees of freedom when the initial state vector is normally distributed. Our filter presents high statistical efficiency under this assumption. We carry out numerical simulations on the IEEE 39-bus system. They reveal that the GM-KKF has a faster convergence rate than the non-robust Koopman Kalman filter. They also show that the computing time of the GM-KKF is roughly reduced by one-third as compared to the one taken by our previously developed robust GM-extended Kalman filter.**

I. Key Equations

Consider an autonomous discrete time nonlinear system

$$\bar{\boldsymbol{x}}_k = \boldsymbol{f}(\bar{\boldsymbol{x}}_{k-1}), \qquad \bar{\boldsymbol{y}}_k = \boldsymbol{h}(\bar{\boldsymbol{x}}_k). \tag{1}$$

A. Design of Nonlinear Observers

One design approach is to seek a nonlinear transformation

$$\boldsymbol{x} = \mathcal{X}(\bar{\boldsymbol{x}}), \qquad \boldsymbol{y} = \mathcal{Y}(\bar{\boldsymbol{y}}), \tag{2}$$

such that (1) can be converted into a canonical observer form,

$$\boldsymbol{x}_k = \boldsymbol{F}_{k-1}\boldsymbol{x}_{k-1} + \alpha(\bar{\boldsymbol{y}}_k), \qquad \boldsymbol{y}_k = \boldsymbol{H}_k\boldsymbol{x}_k + \beta(\bar{\boldsymbol{y}}_k). \tag{3}$$

B. Generalized maximum-likelihood Koopman Kalman filter

Interestingly, the Koopman canonical transformation does not yield output injection terms. Therefore, we neglect them. Instead, we include additive error terms in (3),

$$\boldsymbol{x}_k = \boldsymbol{F}_{k-1}\boldsymbol{x}_{k-1} + \boldsymbol{w}_{k-1}, \qquad \boldsymbol{y}_k = \boldsymbol{H}_k\boldsymbol{x}_{k-1} + \boldsymbol{e}_k. \tag{4}$$

Let $\mathcal{F}^p = \text{span}\{\phi_i\}_{i=1}^p$ be a subset of Koopman eigenfunctions (KEFs) of (1), with $\boldsymbol{h}(\boldsymbol{x})$, $\boldsymbol{x} \in \mathcal{F}^p$. Then,

$$\bar{\boldsymbol{x}} = \sum_{i=1}^{p} \phi_i(\bar{\boldsymbol{x}})\boldsymbol{v}_i^x, \qquad \boldsymbol{h}(\bar{\boldsymbol{x}}) = \sum_{i=1}^{p} \phi_i(\bar{\boldsymbol{x}})\boldsymbol{v}_i^h. \tag{5}$$

Define $\mathcal{T}_{\mathcal{U}}(\bar{\boldsymbol{x}}) = \left[\hat{\phi}_1(\bar{\boldsymbol{x}}), ..., \hat{\phi}_p(\bar{\boldsymbol{x}})\right]^\top$, where

$$\begin{cases} \hat{\phi}_i = \phi_i, \text{ if the } i\text{-th KEF is real, and} \\ \hat{\phi}_i = 2\Re(\phi_i) \text{ and } \hat{\phi}_{i+1} = -2\Im(\phi_i), \text{if } i \text{ and } (i+1)\text{-th} \\ \quad \text{KEFs form a complex conjugate pair.} \end{cases}$$

The nonlinear change of coordinates is given by the KEFs. If the i-th KEF is real, the block diagonal $A_{i,i} = \lambda_i$ and the columns of $\boldsymbol{C}^x$ and $\boldsymbol{C}^h$ are, respectively, defined as $\boldsymbol{C}^x_{:,i} = \boldsymbol{v}_i^x$ and $\boldsymbol{C}^h_{:,i} = \boldsymbol{v}_i^h$. If the KEFs form a complex conjugate pair,

$$\begin{bmatrix} A_{i,i} & A_{i,i+1} \\ A_{i+1,i} & A_{i+1,i+1} \end{bmatrix} = |\lambda| \begin{bmatrix} \cos(\arg\lambda) & \sin(\arg\lambda) \\ -\sin(\arg\lambda) & \cos(\arg\lambda) \end{bmatrix},$$

$\boldsymbol{C}^x_{:,i} = \Re\{\boldsymbol{v}_i^x\}$, $\boldsymbol{C}^x_{:,i+1} = \Im\{\boldsymbol{v}_i^x\}$, $\boldsymbol{C}^h_{:,i} = \Re\{\boldsymbol{v}_i^h\}$, and $\boldsymbol{C}^h_{:,i+1} = \Im\{\boldsymbol{v}_i^h\}$. Finally, we have

$$\boldsymbol{x}_k = \boldsymbol{A}\boldsymbol{x}_{k-1}, \quad \boldsymbol{h}(\bar{\boldsymbol{x}}_k) = \boldsymbol{C}^h\boldsymbol{x}_k, \quad \bar{\boldsymbol{x}}_k = \boldsymbol{C}^x\boldsymbol{x}_k. \tag{6}$$

The GM-KKF is a robust estimator of (6).

II. Numerical Results

TABLE I. Computation time per discrete-time step.

	KKF	GM-EKF	GM-KKF
Time (milliseconds)	10.6395	220.1923	83.3937

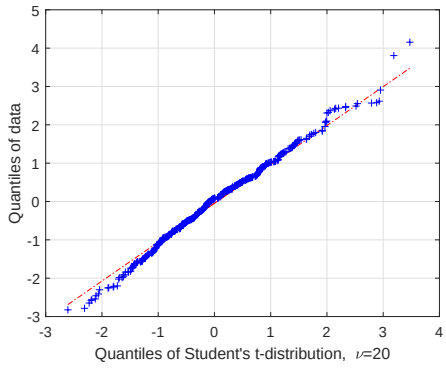

Fig. 1. The Q-Q plot of the transformed state variables, $\mathcal{T}_{\mathcal{U}}(\bar{\boldsymbol{x}})$, indicates that they roughly follow a Student's t-distribution with 20 degrees of freedom.

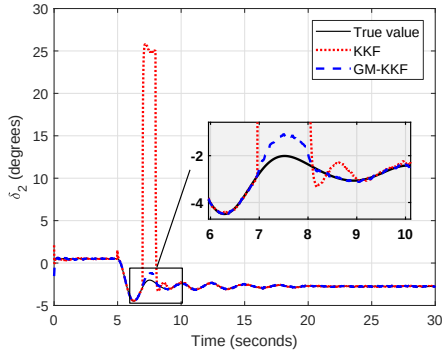

Fig. 2. Comparison between the KKF and the proposed GM-KKF. Multiple outliers placed from $t = 7$ to $t = 8$ seconds.

Information Transfer Based Modal Analysis in Power System

Pranav Sharma, Subhrajit Sinha, Umesh Vaidya, Venkatramana Ajjarapu
Department of Electrical and Computer Engineering, Iowa State University, Ames, Iowa, USA
Email: spranav@iastate.edu

***Abstract*—Information theory has been used for influence characterization in a network, having application in biology, finance and physical infrastructure from a long time. Recent work on information transfer theory extends the concept to characterize influence in a dynamical system. This poster present a case for information transfer for small signal analysis in power system. A comparative study of information transfer based modal analysis and known technique of participation factor is presented, demonstrating advantage over the later methodology.**

I. Key Concepts

Information transfer is based on the notion of uncertainty propagation which gives a physical meaning to interaction of dynamic states. The information transfer from a state x to state y ($T_{x\to y}$), as the dynamical system $z(t+1) = S(z(t)) + \xi(t)$ evolves from time step t to time step $t+1$ is defined as

$$T_{x\to y} = H(y(t+1)|y(t)) - H_{\not x}(y(t+1)|y(t)) \tag{1}$$

where $z = \begin{pmatrix} x & y \end{pmatrix}^\top$, $H(y(t+1)|y(t))$ is the entropy of y at time $t+1$ conditioned on $y(t)$ and $H_{\not x}(y(t+1)|y(t))$ is the conditional entropy of $y(t+1)$, conditioned on $y(t)$, when x is absent from the dynamics.

A. Information transfer in linear systems

Information transfer can be understand analytically for a linear system. Considering a discrete linear model with an additive Gaussian noise into the system, we can define information transfer for linear system(2).

$$x_{t+1} = Ax_t + \sigma\xi_t \tag{2}$$

$$\Sigma(t+1) = A\Sigma(t)A^T + (\sigma\xi_t)^2 I \tag{3}$$

Where (3) is the covariance matrix defined on the system. This covariance matrix essentially captures the propagation of uncertainty in system dynamics introduced by the noise. The information transfer from subspace x_i to x_j {where $x_i, x_j \in x$ is given by 4. Here $\Sigma^s_{x_j}$ is the Schur complement of Σ_{x_j} in Σ_t.

$$T_{x_i\to x_j} = \frac{1}{2}\log\frac{|A_{x_jx_i}\Sigma^s_{x_i}A^\top_{x_jx_i} + \sigma^2 I|}{\sigma^2} \tag{4}$$

The key contribution of information transfer based modal analysis are as follow:

- Address the issue related to uncertainty in initial condition, where participation factor fails to capture the correct system behavior[1].
- Quantify the contribution of collection of states (subspace) in modes, thereby extracting meaningful information about physical nature of the system[2].

II. Results

Here IEEE 9 bus system is considered with 4^{th} order generator dynamic model[3]. We compute information transfer from generator subspace to critical mode, thus identifying influential generator in the system. Further we quanitfy influence of individual states on system mode, thus validting with known phenomena of *participation factor*

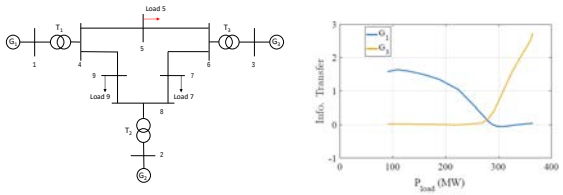

(a) (b)

Fig. 1. (a) IEEE 9 bus system. (b) Information transfer from generator state cluster to critical mode.

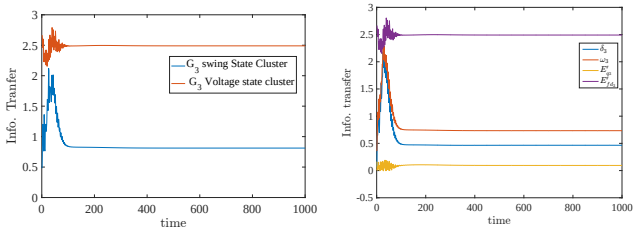

(a) (b)

Fig. 2. (a) Information transfer from state cluster in G_3 near SNB. (b) Information transfer from individual states of G_3 to critical mode

References

[1] E. H. Abed, M. A. Hassouneh, and W. A. Hashlamoun, "Modal participation factors revisited: One definition replaced by two," in *American Control Conference, 2009. ACC'09.*, pp. 1140–1145, IEEE, 2009.

[2] J. Van Ness and F. Dean, "Interaction between subsystems of a power system," in *American Control Conference, 1994*, vol. 2, pp. 1553–1557, IEEE, 1994.

[3] P. W. Sauer and M. Pai, "Power system dynamics and stability," *Urbana*, 1998.

Horizontal Decomposition-Coordination Strategy for Power System Scheduling with Overlapping Intervals

Farnaz Safdarian, *Student Member, IEEE,* and Amin Kargarian, *Member, IEEE*

***Abstract*—This paper presents a horizontal time decomposition and coordination strategy to reduce the computational complexity of power system multi-interval operation problems with the main focus on dynamic security-constrained economic dispatch (SCED). The considered scheduling horizon is decomposed into multiple smaller sub-horizons. The concept of overlapping time intervals is introduced to model ramp constraints of generating units for transition from one sub-horizon to another sub-horizon. A sub-horizon includes n internal intervals and one or two overlapping time intervals. The overlapping intervals are modeled with shared variables that interconnect the consecutive sub-horizons, and a local ramp-constrained SCED subproblem is formulated for each sub-horizon. To find the optimal solution for the whole operation horizon, a distributed coordination strategy is developed to coordinate the SCED solutions obtained in the sub-horizons. The coordination algorithm is based on auxiliary problem principle (APP). Furthermore, we present an accelerated APP and an initialization strategy to enhance the convergence performance of the coordination strategy. The proposed algorithm is applied to solve a week-ahead SCED on the IEEE 118-bus system and a 472-bus system, and promising results are obtained.**

***Index Terms*— Time decomposition, distributed optimization, security-constrained economic dispatch, accelerated auxiliary problem principle, overlapping time intervals.**

I. Introduction

The larger the system is, the more the number of variables and constraints is, and consequently the larger the size of the optimization problem will be. Computational burden and costs increase with growing the system size. Centralized algorithms may not be able to handle such large optimization problems within an acceptable time. Most techniques presented in the literature to solve ED in a distributed manner implement a geographical decomposition to divide the power system into several smaller subsystems. Since subsystems are coupled physically through cross-border tie-lines, any decisions made in one subsystem affects decisions made in other subsystems. The intertemporal constraints or consistency constraints, which originate from limits of ramping capabilities of generating units, interconnect decisions made in a time interval to decisions made in other intervals and increase complexity of the decision-making. Another factor that increases the size and computational complexity of the ED problem is N-1 security criteria. The ED problem with N-1 security criteria is called security-constrained economic dispatch (SCED).

II. The Proposed Time Decomposition Strategy

To handle coupling intertemporal constraints, we present the concept of overlapping (or coupling) time intervals between the consecutive sub-horizons as illustrated in Fig. a. We duplicate the first interval of each sub-horizon N and consider that as interval $n+1$ of sub-horizon $N\_$. We separate the sub-horizons and duplicate the overlapping time intervals in each sub-horizon as shown in Fig. b

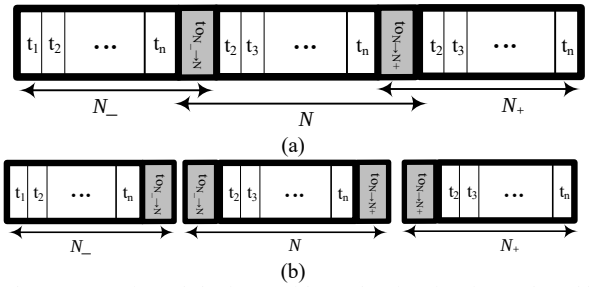

Fig. a) Three consecutive sub-horizons with overlapping time intervals and b) sub-horizons decomposition with overlapping time intervals.

III. Case Study

The proposed algorithm is applied to IEEE 118-bus system. The operation horizon is divided into seven sub-horizons, each including 24 intervals.

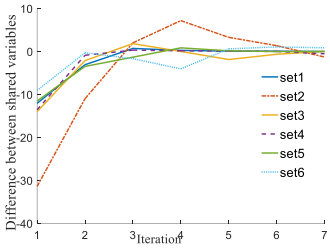

Fig. Difference between shared variables of unit 25 as an example.

We apply the proposed algorithm on a larger system with 472 buses.

TABLE I RESULTS

Algorithm	Iteration	rel	Time (s)
Centralized	-	-	2399
Normal distributed	2+1	1e-08	147
Accelerated distributed	2+1	1e-08	147

Afterwards, we manipulate the standard ramping of some units to make sure that ramping of several generating units are heavily binded in some hours and some consistency constraints are active.

TABLE II RESULTS WITH MANIPULATED RAMPINGS

Algorithm	Iteration	rel	Time (s)
Centralized	-	-	1900
Normal distributed	9+1	1e-06	532
Accelerated distributed	9+1	1e-07	532

Even in this case, the distributed method decreases the time.

IV. Conclusion

The simulation results showed that the proposed method reduced the computational time of SCED for the IEEE 118-bus system from 45% to 400% depending on the problem. We then applied the proposed method to a 472-bus system as a larger system and observed that as the size of the problem (that depends on the size of the system and the number of contingencies) increases, the distributed algorithms show better performance compared to the conventional centralized SCED.

Flexibility Scheduling for Large Customers

Farhad Angizeh, *Student Member, IEEE*, Masood Parvania, *Member, IEEE*,
Mahmud Fotuhi-Firuzabad, *Fellow, IEEE*, and Abbas Rajabi-Ghahnavieh, *Member, IEEE*

***Abstract*—In this poster, we will present a decision-making tool for enabling large customers to determine how they adjust their electricity usage from normal consumption patterns in expectation of gaining profit in response to changes in prices and incentive payments offered by the system operators. We first define customers' flexibility options which includes any onsite activities making net change in the energy supplied by the grid. Then, we propose our model which simultaneously determines the optimal integration of the potential flexibility options comprising flexible loads rescheduling, utilizing onsite generation (OG) and energy storage system (ESS), along with energy procurement from the grid that allows the large customers to optimize their energy portfolio from different sources including bilateral contracts and the energy market. The characteristics of the proposed integrated flexibility scheduling and energy procurement model and its benefits are investigated through several case studies conducted on a test large industrial load.**

I. Introduction and Methodology

Customers play an effective role in today's competitive electricity markets where they would be able to save money by strategically scheduling their various onsite energy solutions. Thus, a savvy customer can optimize its energy consumption profile by intelligently modifying and thence procuring it from available resources so that its total electricity cost is minimized. In this work, we introduce customers' *flexibility option* including flexible loads and production processes rescheduling, utilizing energy storage system (ESS), and operating distributed generation (DG) units. Then, we argue that although the individual flexibility options would equip customers to participate in the DR program, the three options could be integrated to capture the interdependencies and the relative costs and benefits among the options, delivering additional flexibility at lower costs. The integrated model intends to combine the three models into a unified flexibility scheduling model where the power generation by OG and/or energy stored in ESS are utilized in order to compensate some or all of the curtailed flexible loads and/or supplying inflexible parts of customer's demand. The proposed integrated model, formulated as a mixed-integer linear programming problem, simultaneously optimizes the integrated flexibility of the customers for hourly load reductions in the system, as well as energy portfolio procurement from different sources including bilateral contracts and the market (See Fig. 1).

II. Results

Here we adapt the proposed integrated model to solve the flexibility scheduling and energy procurement for a sample large industrial manufacturer over a one-week period. The simulation results reveal that optimal scheduling of the flexibility options, which is illustrated in Fig. 2, helps customers to reduce the energy procurement costs by being flexible to modify demand and prevent buying energy at the more expensive hours. Fig. 3 demonstrates the stemmed modified demand for a one-week horizon.

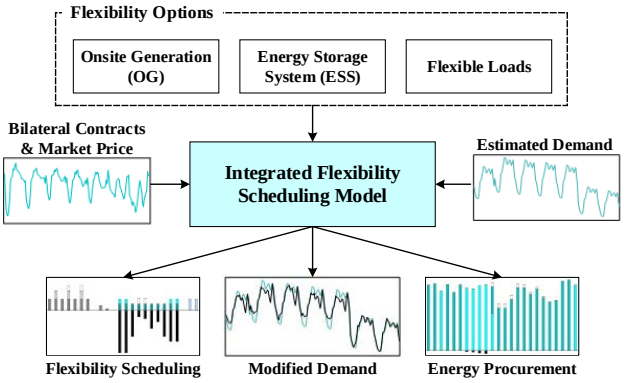

Fig. 1. Customer's Integrated Flexibility Scheduling Framework

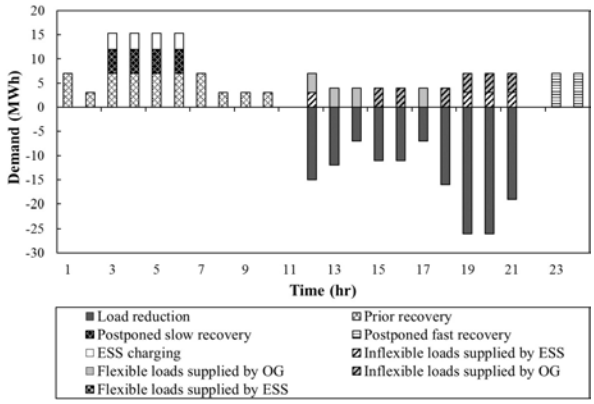

Fig. 2. Optimal hourly load reductions and scheduled flexibility options during 4^{th} working day

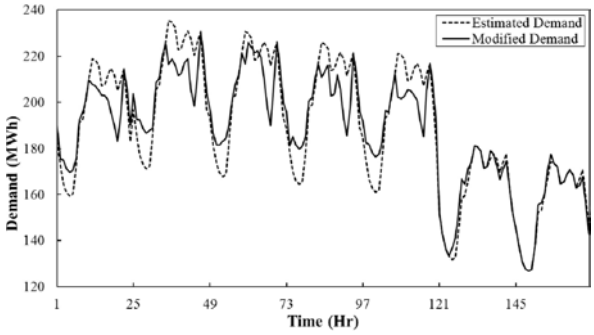

Fig. 3. Estimated and modified demands of the customer

Analysis of Vibration Signal for Power Transformer On-Load Tap Changer (OLTC) Condition Monitoring

Junhyuck Seo, *Student Member* IEEE, Hui Ma, *Member* IEEE, Tapan K. Saha, *Senior Member* IEEE
The University of Queensland, Brisbane, Australia

***Abstract*—Vibration measurement has been used for power transformer's On-Load Tap Changer (OLTC) condition monitoring. In this paper, a signal processing method based on Savitzky-Golay filter is developed. The proposed method is applied to process a series of vibration signals measured from an OLTC when the OLTC operates throughout a number of its tap positions and subsequently evaluate the condition of these tap positions. The Savitzky-Golay filter extracts the information embedded in the originally measured signal without latency. As such, it transforms effectively complicate feature of vibration signal into a simplified form of envelope curve. After being processed by the Savitzky-Golay filter, the vibration signals corresponding to different tap positions are compared. The comparison results help to understand the characteristics of vibration signals for monitoring the mechanical condition change in OLTC.**

***Index Terms*— Condition assessment, On-Load Tap Changer (OLTC), power transformer, Savitzky-Golay filter, vibration.**

I. Methodology & Key Equations

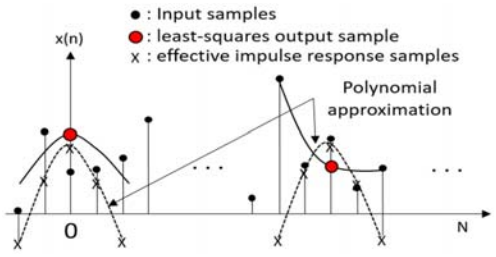

Fig. 1 Graph illustration of Savitzky-Golay filter.

$$p(n) = \sum_{k=0}^{N} a_k n^k \quad (1)$$

The above polynomial should satisfy the requirement of a minimum mean-squared error ϵ_N as

$$\sum_{n=-M}^{M}(p(n) - x[n])^2 = \sum_{n=-M}^{M}(\sum_{k=0}^{N} a_k n^k - x[n])^2 \quad (2)$$

$$\frac{\partial \epsilon_N}{\partial a_i} = \sum_{n=-M}^{M} 2n^i \,(\sum_{k=0}^{N} a_k n^k - x[n]) = 0 \quad (3)$$

$$\sum_{k=0}^{N}(\sum_{n=-M}^{M} n^{i+k})\, a_k = \sum_{n=-M}^{M} n^i x[n], \quad i = 0, 1, \ldots, N \quad (4)$$

$$CC = \frac{\sum_{i=0}^{N-1}(Y(i)-\overline{Y})(R(i)-\overline{R})}{\sqrt{\sum_{i=0}^{N-1}(Y(i)-\overline{Y})^2 \sum_{i=0}^{N-1}(R(i)-\overline{R})^2}} \quad (5)$$

Among a number of filters in Fig. 2, the adopted Savitzky-Golay shows superior performance in 1) depicting well the overall feature of vibro-acoustic signals; 2) causing no time delay in the filtration process; and 3) achieving high resolution of output.

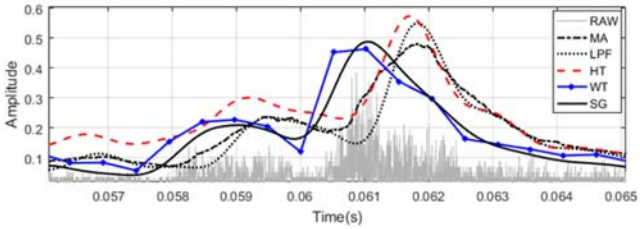

Fig. 2 Comparison of the time shifts in outputs of moving average (MA), Low-pass filter (LPF), Hilbert transform (HT), wavelet transform (WT)'s approximation, and Savitzky-Golay (SG) filter.

II. Results & Analysis

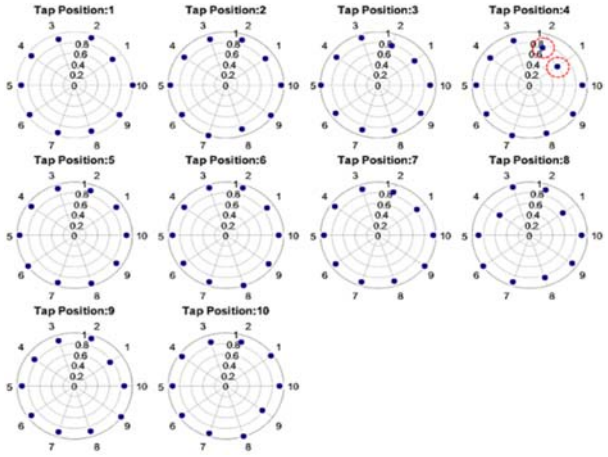

Fig. 3. The result of correlation coefficients of ten trials at each tap position. Labels along theta direction indicate the number of trial and labels in radius axis show the correlation coefficient.

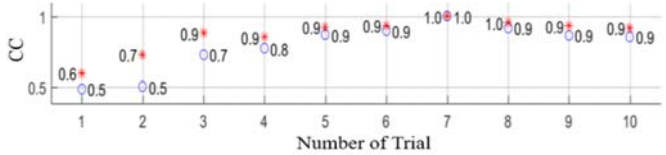

Fig. 4. The result of the similarity coefficients at 4th tap position. The value at circle is a correlation coefficient before waveform alignment and the value at asterisk shows a coefficient after the adjustment.

The proposed method integrates Savitzky-Golay filter, waveform comparison and waveform alignment methods. The case studies demonstrated it could be used for effectively comparing vibration signal from OLTC and identifying a mechanical condition change of OLTC.

On False Data Injection in Wide Area Protection Schemes

Mohsen Khalaf
ECE Department
University of Waterloo
Waterloo, Ontario, Canada
Email: m.khalaf@uwaterloo.ca

Ali Hooshyar
EECS
Lassonde School of Engineering
York University, Toronto, Ontario, Canada
Email: hooshyar@cse.yorku.ca

Ehab El-Saadany
ECE Department
University of Waterloo
Waterloo, Ontario, Canada
On leave with Khalifa University, PI, UAE
Email: ehab@uwaterloo.ca

***Abstract*—Maintaining power system stability and normal operation are the most important roles of the protection system. Recently, wide-area protection (WAP) makes use of the wide system information and sends specific data to specific local locations to help them make their own decisions. This paper investigates, for the first time, the problem of false data injection (FDI) in WAP schemes. The problem is general in all WAP schemes. To perform this investigation, the underfrequency load shedding (UFLS) is considered as the case under study throughout this work. To show the generality of the problem in UFLS schemes, three different UFLS schemes are simulated using PSCAD and applied to the IEEE 39-bus system. The results show the FDI attacks affect the operation of the UFLS schemes and hence, affect the grid stability and operation.**

I. Introduction

In wide area UFLS protection schemes, the values of the frequency and/or ROCOF are sent from the local SCADA systems to the control center, and consequently, the control center sends control actions to different areas in the system. These control actions include shedding loads in one or more area from the system. Manipulation of frequency signals affects the output of these schemes such that they shed a higher amount of load or disconnect a complete area while no need to this. At the same time, the attacker can block the real values of the system frequency, in the case of real system disturbances, such that everything appears to be normal. This latter action can lead to blackouts and a system equipment damage.

II. Important Equations

$$\frac{2H_i}{f_n}\frac{df_i}{dt} = P_{m_i} - P_{e_i} = \Delta P_i \tag{1}$$

$$\Delta P = \sum_{i=1}^{N} \Delta P_i = \frac{2\sum_{i=1}^{N} H_i}{f_n}\frac{df_c}{dt} \tag{2}$$

where

$$f_c = \frac{\sum_{i=1}^{N} H_i f_i}{\sum_{i=1}^{N} H_i} \tag{3}$$

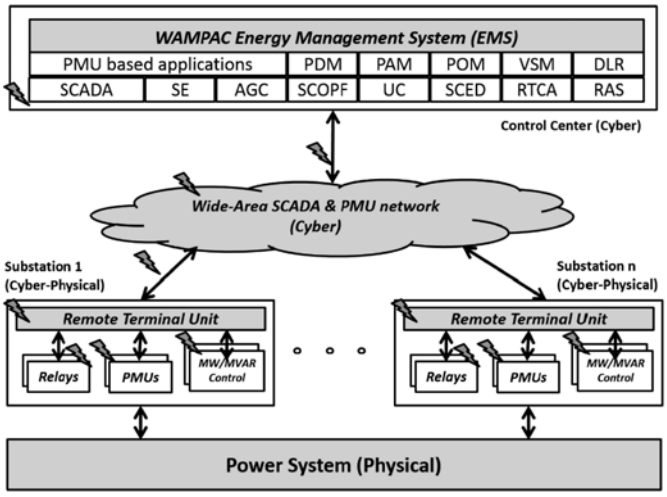

Fig. 1: High-level schematic of the WAMPAC

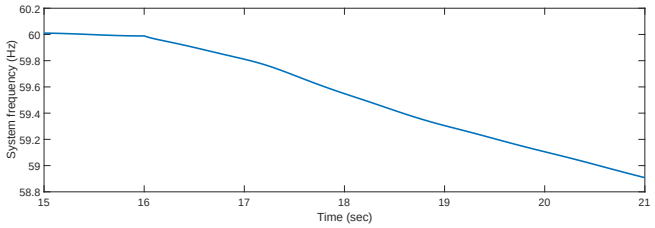

(a) System frequency with attack

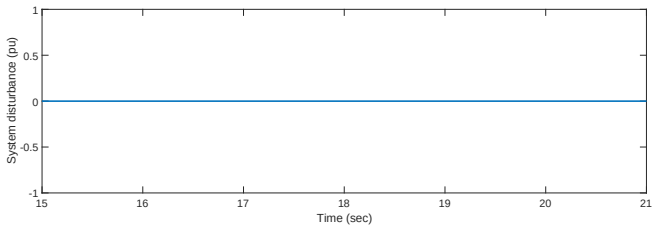

(b) The amount of disturbance (swing equation output) with attack

Fig. 2: UFLS scheme performance with coordinated attack

Reliability and Vulnerability Assessment of Interconnected ICT and Power Networks Using Complex Network Theory

Wentao Zhu, *Student Member IEEE,* Mathaios Panteli, *Member IEEE*, and J. V. Milanović, *Fellow IEEE*

***Abstract*—The increasing reliance of power systems on Information and Communication Technologies (ICTs) places higher requirements on the reliable and secure operation of ICT networks. This paper proposes an approach to measure the effect of failure/misoperation of ICT network components on the reliability of power grid. A new vulnerability index, namely the system security index (SSI), based on Complex Network Theory (CNT), is derived for this purpose. The vulnerability of each ICT network component is quantified based on the influence of its failure/misoperation on the probability of the failure/misoperation of the power system. The proposed approach is demonstrated on a real UK's power station intertrip scheme and compared with the conventional fault-tree analysis.**

***Index Terms*—Information and Communication Technology (ICT), Complex Network Theory (CNT), reliability, vulnerability**

I. Introduction

Interactions between physical power system and Information and Communication Technology (ICT) network should not be ignored and new understanding and methods for assessing the dependability and reliability of this interconnected system must be developed.

A framework based on Complex Network Theory (CNT) has been proposed in this paper to study the reliability of interconnected ICT and power systems, as shown in Fig. 1.

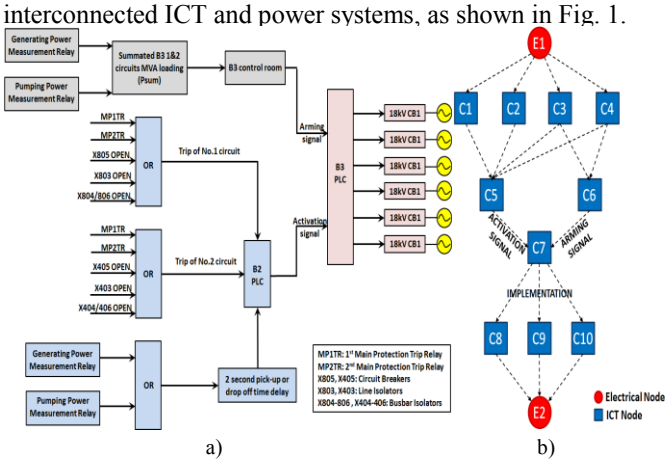

Fig. 1. a) Operating logic of intertrip scheme b) Complex network model of intertrip scheme

II. Methodology

A System Security Index (SSI) is introduced to assess the security level of the interconnected system.

$$SSI = \frac{1}{n_e n_c} \sum_{i \in V_c \cap V_{es}, j \in V_{et}, i \neq j} R_{ij} \quad (1)$$

where n_e and n_c are the number of EP system nodes and ICT network nodes respectively. R_{ij} is the reliability of the most reliable path between i and j, which is calculated as

$$R_{ij} = \prod_{c \in V_c} (1 - P_c(SBM)) \quad (2)$$

where $P_c(SBM)$ is the probability of security-based misoperation of ICT network component c within the most reliable path between i and j.

The ICT component vulnerability V(C) is therefore analyzed by comparing the SSI and SSI*, where SSI* is the System Security Index when the probability of security-based misoperation of the analyzed ICT element is set to zero.

$$V(C) = \left| \frac{SSI - SSI*}{SSI} \right| \quad (3)$$

III. Key Results and Conclusions

The results of vulnerabilities of the most critical ICT network components are presented in Fig. 2.

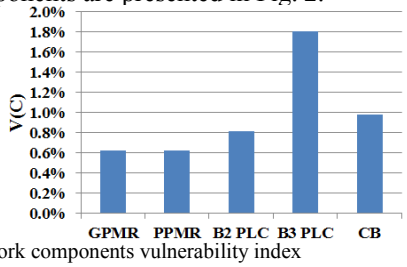

Fig. 2. ICT network components vulnerability index

The results of the analysis using the newly proposed approach confirm the findings of the past, conventional, fault-tree analysis; however the complex network model is found to be more scalable and easy-to-implement. The proposed methodology can be easily extended by including more logic relationships to facilitate analysis of large interconnected systems.

Load Redistribution Attack Detection using Machine Learning: A Data-Driven Approach

Andrea Pinceti, Lalitha Sankar, and Oliver Kosut
School of Electrical, Computer and Energy Engineering
Arizona State University
Tempe, AZ, 85287

***Abstract*—Three detection techniques are presented against a wide class of cyber-attacks that maliciously redistribute loads by modifying measurements. The detectors use different anomaly detection algorithms based on machine learning techniques: nearest neighbor method, support vector machines, and replicator neural networks. The detectors are tested using a data-driven approach on a realistic dataset comprised of real historical load data in the form of publicly available PJM zonal data mapped to the IEEE 30-bus system. The results show all three detectors to be very accurate, with the nearest neighbor algorithm being the most computational efficient.**

***Index Terms*—machine learning, neural network, false data injection (FDI) attack, load redistribution attack, cybersecurity**

I. Introduction

The state estimators (SE) employed by the majority of system operators as part of their energy management systems (EMS) are vulnerable to false data injection (FDI) attacks. By intelligently modifying some system measurements, an attacker can create an erroneous representation of the state of the system. This leads the EMS to redispatch generation in such a way that it will create line overloads in the physical system. This type of threat belongs to a broad class of attacks called *load redistribution attacks*.

In this work, we develop countermeasures against load redistribution attacks in the form of detectors that analyze the measured loads, before they are used to perform economic dispatch, and determine if they represent a realistic state of the system or if they have been maliciously engineered. Our approach exploits the fact that system operators have access to historical load data which can be used to learn patterns in an offline manner and design machine learning algorithms that can check load consistency in real time scenarios. We use *nearest neighbor algorithm*, *support vector machines* (SVM) and *replicator neural networks* to design three different detectors which are tested on realistic historical load data created for the IEEE 30-bus system. To design a detector that works for any possible load pattern that might occur, we exploit publicly available PJM zonal data [1] to create realistic load data for multiple years for the IEEE 30-bus system.

II. Detection Algorithms

The three detectors proposed analyze the measured loads of a power system during any hour of the day and determine if they are normal loads or if they have been maliciously modified through a cyber-attack. The measured load configuration to be tested is given as input to the detector, which generates a scalar value based on a metric specific to the machine learning technique used: *minimum distance* for nearest neighbor, *confidence score* for SVM, and *replication error* for replicator neural network. This value is compared against a predetermined threshold to label the loads as *normal* or *attacked*. Figure 1 and Table I show the performance of the three techniques against attacks of varying magnitude.

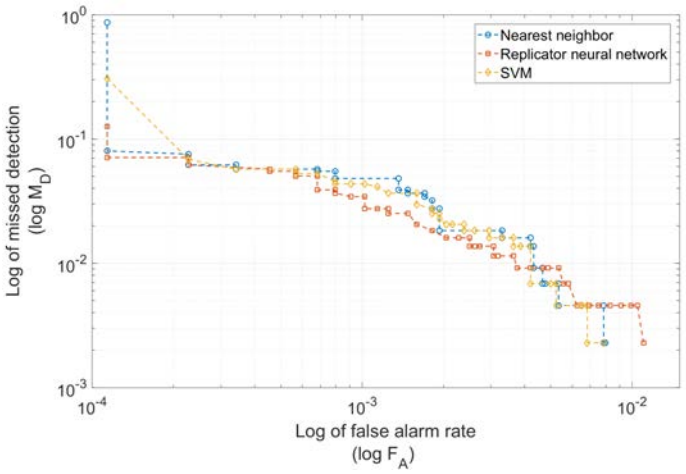

Fig. 1. Receiver operating characteristic of the three detectors with 10% load shift attacks.

TABLE I
Performance of the detectors with 15% LS attacks

Detector	M_D	F_A	# of false alarms
Nearest neighbor	0.2192	0	0
	0	1.138×10^{-4}	1
SVM	0.0021	1.138×10^{-4}	1
	0	2.277×10^{-4}	2
Replicator Neural Network	0.0125	0	0
	0	1.138×10^{-4}	1

References

[1] PJM. (11 Nov 2017). PJM Metered Load Data [Online]. Available: https://www.pjm.com/markets-and-operations/ops-analysis/historical-load-data.aspx.

A Coordinated Cyber Attack Detection System (CCADS) for Multiple Substations

Chih-Che Sun
Energy Systems Innovation Center
Washington State University
Pullman WA, USA
chih-che.sun@wsu.edu

Chen-Ching Liu
Energy Systems Innovation Center
Washington State University
Pullman WA, USA
liu@wsu.edu

***Abstract*— Since cyber attacks have become a major threat in smart grids, various detection algorithms have been developed to protect cyber-power systems. However, most of existing cyber security solutions still lack the capability to handle coordinated cyber attacks. In this research, a cyber protection system is proposed to detect coordinated cyber attacks by inspecting relations among abnormal events in substations. The techniques of Fuzzy Cognitive Map (FCM) and Time Failure Propagation Graph (TFPG) are used for detection algorithms to generate attack index numbers, representing the likelihood of coordinated cyber attacks. This work has been simulated and validated by the Smart City Testbed (SCT) at Washington State University (WSU).**

Keywords—Cyber security, coordinated cyber attacks, intrusion detection system, smart grid

I. Introduction

In large scale coordinated cyber attack events, attacker(s) have a well-organized plan to launch an attack. The attack actions have some logic relations among one another. This kind of attacks can make a greater impact on the power systems than a single or a multiple attack. Currently, IDS is regarded as a important line of defense against cyber intruder(s), installed on different power system facilities. Nonetheless, most of the intrusion detection algorithms only cope with a single or a multiple cyber attack event. In this research, the proposed CCADS [1] is an on-line detection system, capable of detecting coordinated cyber attacks by identifying the relations based on detected anomaly events and security logs at multiple substations. Based on FCM, Relation Algorithm (RA) is developed as a detection algorithm. RA correlates the detection log files from IDSs in [1], and generate a state value for each defined relation based on the concept of FCM model. The state value is the indicator of the strength of relations between attack actions. The Correlation System collects the highest state values from each relation and generates the state value for identification of coordinated attacks. When the state value exceeds a user defined threshold value, the detected event is considered to be a coordinated cyber attack. Fig. 1 shows the structure of the proposed CCADS.

SCT is a hardware-in-a-loop cyber-physical system testbed at WSU. DIgSILENT PowerFactory is used as a power system simulation tool. The simulation functions include time domain simulation, dynamic analysis, state estimation, and optimal power flow. With the OPC communication, PowerFactory can be connected with the cyber module to provide a simulation environment for cyber system events.

This research is supported by U.S. National Science Foundation under the award number ECCS-1824577 and ECCS-1711048.

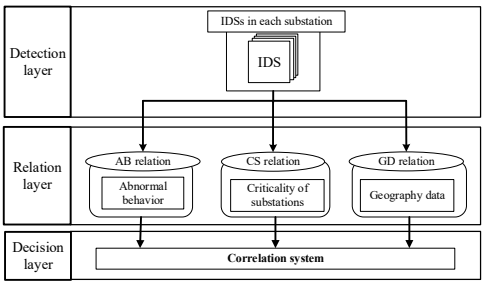

Fig. 1. Structure of CCADS.

II. Test Cases

In the test attack scenario, attackers successfully compromised four critical substations in the IEEE 39 bus system. Since the relation correlation system reports a high similarity index, CCADS triggers an alarm to notify an attack event. Fig. 3 shows the simulation results.

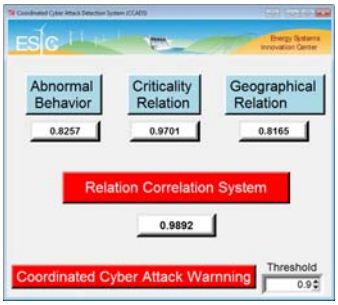

Fig. 2. Coordinated cyber attack event is detected.

References

[1] C. C. Sun, J. Hong, and C. C. Liu, "A Coordinated Cyber Attack Detection System (CCADS) for Multiple Substations," in *2016 Power Syst. Computation Conf. (PSCC)*, Genoa, IT, 2016, pp. 1-7.

J. Hong, C.-C. Liu, and M. Govindarasu, "Integrated Anomaly Detection for Cyber Security of the Substations," IEEE Trans. Smart Grid, vol. 5, no. 4, pp. 1643–1653, Jul. 2014.

Distribution Systems Hardening against Disasters

Yushi Tan, *Student Member, IEEE* Arindam K. Das, *Member, IEEE*, Payman Arabshahi, *Senior Member, IEEE*, and Daniel S. Kirschen, *Fellow, IEEE*

***Abstract*—Distribution systems are often crippled by catastrophic damage caused by natural disasters. Well-designed hardening can significantly speed-up the post-disaster restoration process. This performance is quantified by a resilience measure associated with the operability trajectory. The distribution system hardening problem can be formulated as a two-stage stochastic problem, where the inner operational problem addresses the proper scheduling of post-disaster repairs and the outer problem the judicious selection of components to harden. We propose a deterministic single crew approximation with two solution methods, an MILP formulation and a heuristic approach. We provide computational evidence based on several IEEE test feeders, which demonstrates that the heuristic approach provides near-optimal hardening solutions in a computationall efficient manner.**

I. Introduction

NATURAL disasters have caused major damage to electricity distribution networks and deprived homes and businesses of electricity for prolonged periods. Kwasinski et al. [1] reported that facilities, which had been hardened in Christchurch at a cost of $5 million, remained serviceable immediately after the September 2010 earthquake and saved approximately $30 to $50 million in subsequent repairs. Hardening minimizes the potential damages caused by disruptions, thereby facilitating restoration and recovery efforts [2]. However, as indicated in [3], it is difficult to quantify a priori what the expected performance improvement might be. Hence the need for a systematic decision process balancing cost versus potential future benefit.

In civil engineering, resilience is illustrated using the "operability trajectory" $Q(t)$ [4], which shows the increase in infrastructure functionality over time and provides an effective visual representation of the 'goodness of the restoration process'. Letting T be some restoration time horizon, a resilience measure, R, can be defined as $R = \int_0^T Q(t)dt$.

To the best of our knowledge, this research is the first to consider the restoration process in conjunction with hardening. Our approach is formulated as a two-stage stochastic optimization problem. The first stage selects from the set of hardening choices and determines the extent of hardening to maximize the expected resilience measure, while the second stage solves the operational problem for each scenario by optimizing the scheduling of post-disaster repairs in distribution network with parallel repair crews. Since an ideal formulation of the problem is hard to solve and also turns out to be impractical, we developed a deterministic single crew approximation with an MILP formulation and a heuristic approach to solve the hardening problem.

II. Key Results

We varied the hardening budget from 0 to 50 on the IEEE 13 node test feeder. Fig. 1 shows the aggregate harm as a function of the budget for one repair crew. The MILP and the heuristic approaches produced almost identical results under the $f(\mathbb{E}[\cdot])$ measure so that their plots almost overlap. The plots corresponding to the $\mathbb{E}[f(\cdot)]$ measure are also very close.

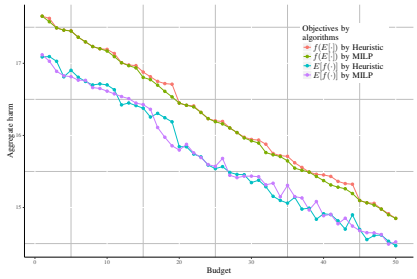

Fig. 1: Aggregate harm vs. hardening budget for the IEEE 13 node test feeder.

Even if hardening decisions at the planning stage are made based on a single crew operational schedule, the resilience of the system would still improve if multiple crews are deployed at the operational stage. To demonstarte this point, Fig. 2 shows the normalized improvement in harm $\beta(m) := \frac{H^m - H_A^m}{H^m}$ for different numbers of crews. We can observe that the normalized improvement in harm due to hardening remains above 8%.

Fig. 2: Normalized improvement in harm as a function of the number of repair crews, m, for the IEEE 8500 node test feeder.

References

[1] A. Kwasinski, J. Eidinger, A. Tang, and C. Tudo-Bornarel, "Performance of electric power systems in the 2010 - 2011 Christchurch, New Zealand, Earthquake Sequence," *Earthquake Spectra*, vol. 30, no. 1, pp. 205–230, 2014.

[2] M. Omer, *The Resilience of Networked Infrastructure Systems: Analysis and Measurement*, vol. 3. World Scientific, 2013.

[3] M. Rollins, "The hardening of utilitiy lines-implications for utility pole design and use." http://woodpoles.org/portals/2/documents/TB_HardeningUtilityLines.pdf, 2007. [Online; accessed 25-March-2018].

[4] D. A. Reed, K. C. Kapur, and R. D. Christie, "Methodology for Assessing the Resilience of Networked Infrastructure," *IEEE Systems Journal*, vol. 3, pp. 174–180, June 2009.

Embedding Cyber-Physical Resiliency in Synchrophasor-based Remedial Action Schemes

Zhijie Nie, Jing Xie, Anurag K. Srivastava
School of Electrical Engineering and Computer Science
Washington State University
Pullman, WA, U.S.A.
{zhijie.nie, jing.xie6, anurag.k.srivastava}@wsu.edu

***Abstract*—Emerging technology in decentralized computing infrastructure provides new opportunities for real-time data-driven analytics used in smart grid applications. Remedial action scheme (RAS), designed to protect the system under predetermined operating conditions, relies on the network communication in the wide-area measurement system (WAMS). In order to improve the resiliency of network environment and to secure the data transmission, the Resilient Information Architecture Platform for Smart Grid (RIAPS) has been developed for the use of power system analytics. In this poster, two typical remedial action schemes, wind farm generation curtailment and under-frequency load shedding are presented. Experiments based on RIAPS are conducted under a hardware-in-the-loop (HIL) cyber-physical testbed using a modified IEEE 14-bus system.**

***Index Terms*—remedial action scheme, cyber-physical system, phasor measurement unit, decentralized computing**

I. Introduction

Due to an increasing number of installations of phasor measurement units (PMUs), the resiliency and security of network communication becomes new requirements of the modern power system. In [1], a data transmission platform called RIAPS (Resilient Information Architecture Platform for Decentralized Smart Systems) is developed to improve the resiliency and security for power system analytics. With a resilient and secure data platform established, many of real-time analytics in power systems become realizable, for example, state estimation. Based on the previous work, the analytic of distributed linear state estimation (DLSE) has been developed [2] and latter implemented on the RIAPS platform. And in this paper, the authors utilize the distributive simplex method to distribute the computation in both state estimation and DCOPF-formulated optimal wind curtailment problem. This poster is going to present the analytics development using RIAPS platform, and to demonstrate the hardware-in-the-loop (HIL) cyber-physical testbed for two RAS applications, which are wind curtailment and under-frequency load shedding (UFLS).

II. Description of HIL Cyber-Physical Testbed

Fig. 1 demonstrates our proposed hardware-in-the-loop cyber-physical testbed. Real-Time Digital Simulator (RTDS) is used to simulate the power system in a real-time manner. A modified IEEE 14-bus system is considered and divided into three groups. With one installed SEL hardware PMU and eight GTNET software PMUs, the measurements from the RTDS are captured ans transmitted under C37.118.1-2011 synchrophasor data protocols.

The implementation of the distributed computational blocks (controllers) is carried out by using BeagleBone Blacks (BBBs), where the RIAPS platform is established. The wind curtailment RAS setup uses three BBBs to solve the optimal wind curtailment, and to transmit control action commands to each wind farm. The BBBs are connected to RTDS and the PMUs using Ethernet cables. Control commands of optimal solution are sent back to RTDS in text strings over its listening port-interface using standard TCP sockets.

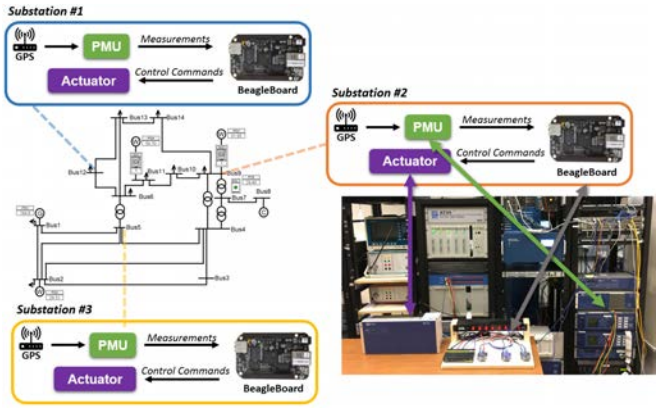

Fig. 1. HIL cyber-physical testbed for RAS applications.

Acknowledgment

The authors would like to thank Advanced Research Projects Agency-Energy (ARPA-E) and Power Systems Engineering Research Center (PSERC) for the technical and financial supports in this work.

References

[1] S. Eisele, I. Mardari, A. Dubey, and G. Karsai, "Riaps: resilient information architecture platform for decentralized smart systems," in *Real-Time Distributed Computing (ISORC), 2017 IEEE 20th International Symposium on*. IEEE, 2017, pp. 125–132.

[2] R. Liu, A. K. Srivastava, D. E. Bakken, A. Askerman, and P. Panciatici, "Decentralized state estimation and remedial control action for minimum wind curtailment using distributed computing platform," *IEEE Transactions on Industry Applications*, vol. 53, no. 6, pp. 5915–5926, Nov 2017.

Decentralized Power System Integrity Protection Schemes based on MAS: Anomaly Detection and Self-Adaptive Load Shedding

Pengyuan Wang
Department of Electrical and Computer Engineering
Iowa State University
Ames, IA. USA.
pywang@iastate.edu

Manimaran Govindarasu
Department of Electrical and Computer Engineering
Iowa State University
Ames, IA. USA.

Abstract—**With the wide application of the communication and information technologies in modern power system, malicious cyber attacks have become great concerns, especially for the wide area protection and control schemes. Traditional cyber security technologies can be applied to alleviate the situation, but the problem will not get solved by merely securing the periphery of schemes. To make the critical functions per se situation-aware and attack-resilient is a promising path. This paper presents a peer-to-peer multi-agent architecture for power system integrity protection and control schemes (SIPS), which provides an alternative implementation for the non-resilient legacy SIPS and the centralized ones. Every agent within the architecture is embedded into one substation/power plant, and it collects local data as well as information from its community. All the agents possess the similar level of intelligence and interact in a peer-to-peer manner. To verify the validity of the proposed SIPS architecture, coordinated anomaly detection and situation adaptive optimal load shedding are further investigated as two sub-problems. Anomaly detection takes place within each intelligent agent based on the local data but the final detection conclusion will be achieved by the consensus of interconnected agents. A data-driven algorithm named as Support Vector Machine embedded Layered Decision Tree (SVMLDT) is proposed for the anomaly detection. Global data propagation lays the foundation for the situation adaptive load shedding such that a protocol is proposed to facilitate the data propagation. Dynamic programming is utilized to get the remedial actions for each agent. A load rejection SIPS adopted in reality is mapped onto IEEE 39 bus system as a study case. Via evaluation, it shows that the proposed decentralized SIPS attains better attack resiliency than the centralized solution under Denial of Service (DoS) attack and when part of the decentralized SIPS gets compromised, the rest of it can still deliver the remedial actions desired.**

Keywords—SIPS decentralization; cyber attack resilience; Multi-Agent System; anomaly detection; optimal load shedding.

I. AGENTS INTERACTION PROTOCOL

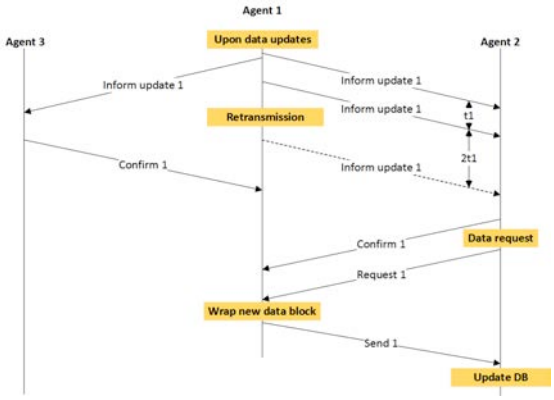

Fig. 1 Agents interaction flow

II. MAIN EVALUATION RESULTS

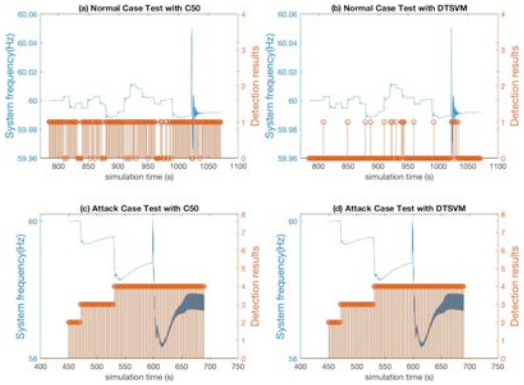

Fig. 2 On-line Anomaly Detection Resutls

Data Analytics for Cyber-Physical Security of Transmission Protection System

S. Armina Foroutan, Anurag Srivastava
School of Electrical Engineering and Computer Science
Washington State University
Pullman, Washington
s.foroutan@wsu.edu

Sindhu Suresh

Siemens Corporate Research
Princeton, New Jersey

***Abstract*—The transmission protection system is critical for normal operation of power systems and mis-operation of them can cause cascade failures. Failure diagnosis of these mis-operations which can be caused by either physical malfunction of protection relay or cyber intrusion to the relay, usually become very complex. Therefore, a systematic approach seems to be necessary to determine the root cause of the mis-operation as well as a framework to collect data, test and study the proposed approach. In this paper we first introduce a framework to model the mis-operation of protection relays using Real Time Digital Simulator (RTDS) and then a data analytic tool is proposed using data provided by Phasor Measurement Unit (PMU)s to detect malfunctions and identify whether they are cyber or physical. Simulation results using IEEE 14 bus system are also presented showing how the framework and tool confirm the actual incident.**

***Index Terms*—Transmission Protection, Distance relay, RTDS, Data analytic, Failure diagnosis, Phasor measurement unit, Relay malfunction, Hardware-in-the-loop**

I. Introduction

In power systems, protection system mis-operations often lead to cascading effects and system wide failures. Distance protection relays have been known to incorrectly initiate tripping signal due to apparent impedances that fall into zone settings of line relays or malicious intrusion to the relays. However, failure diagnosis of protection system usually become very complex due to high number protection relays, available information and level of expertise of the protection engineer. This Poster address this issue by introducing a framework to collect relevant cyber data as well as minimizing the number of PMU measurements need to be taken from the system. Then a data analytic tool is proposed to identify cyber/physical anomalies in Transmission system. At last, RTDS simulation results are presented based on HIL validation.

II. Methodology and Testbed

After the occurrence of a fault in the system, the protection relays at the end-point of the line should trips and isolate the fault. However, sometimes one of these relays is malfunctioned and stays close. In this case, the relevant relays on the adjacent lines trip to isolate the fault. In such cases, if the status of the breakers on the lines connected to the bus that malfunctioned relay resides, is symmetric, then all lines with at least one tripped relay can be candidates of location of the fault. Figure 1 shows a test case of such conditions. In order to identify the root causes of the failure, first all lines and buses adjacent to tripped relays are selected as so called ProNet and corresponding PMU measurements are collected. Then, corresponding scenarios related to the situation are produced and cyber data corresponding to suspicious relays are also collected. Then all these data can be fed to the analytic tool to pinpoint the location of fault and malfunctioned relays.

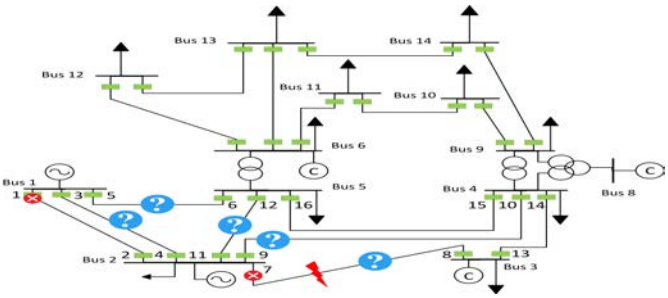

Fig. 1. A test case of relay malfunctions

III. Simulation Testbed

We simulate this scenario in RSCAD utilizing a distance protection relay as HIL with RTDS. RSCAD sends out the simulated voltage and current signals via GTAO card to the hardware relay. Then the output dry contacts of relay are connected to digital interface panel of RTDS to communicate breaker commands. In our simulations all relays simulated by RTDS except one which is replaced by hardware relay. We also consider two possible scenario to validate our assumptions; normal operation where all relays react normally to the fault and ProNet scenario where two relays misoperate; a simulated relay malfunction due to physical incident and a hardware relay misoperation due to cyber intrusion to the relay. Cyber intrusion is also modelled by emailing BlackEnergy3 to the operator and gaining access to the victim's PC as well as the relay and finally reconfiguring the relay setting.

IV. Acknowledgements

We would like to show our gratitude to Bo Cui, Arman Ahmed and Mohammad Touhiduzzaman for assistance with data analytics and cyber intrusion.

Impact of Communication Failures on Solar Generation Forecasting

Mohammad Heidari Kapourchali, *Student Member, IEEE*, Mojtaba Sepehry, *Student Member, IEEE*, and Visvakumar Aravinthan, *Senior Member, IEEE*

***Abstract*—The power from solar resources has reached grid parity and must be predicted based on real-time observations available up to the current time step to ensure efficient power systems operation. However, solar data in the form of time series generated by a network of sensors are not always available. Communication failure leaves the energy management data acquisition system with incomplete solar time series, thus leading to inaccurate forecasts. This poster addresses the impact of partially observable measurements on short-term solar power prediction.**

***Index Terms*— Communication failure, spatio-temporal solar prediction, missing data**

I. Problem Definition

Fig. 1 shows an abstract view of solar PV sites with a communication infrastructure for real-time measurements of solar generation data.

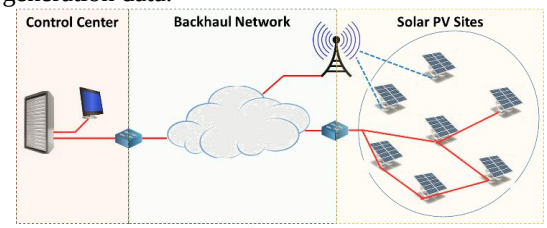

Fig. 1. Communication network for real-time measurements of PV plants

Solar forecasting in a partially observable environment is a data analytics problem that includes both pattern completion and prediction.

Photovoltaic power generation varies with geographical and meteorological factors.

$$P_{PV} = [P_{PV,STC} \times \frac{G_T}{1000} \times [1 - \gamma \times (T_j - 25)]] \times N_{PVs} \times N_{PVp} \quad (1)$$

II. Partially Observable Solar PV Measurements

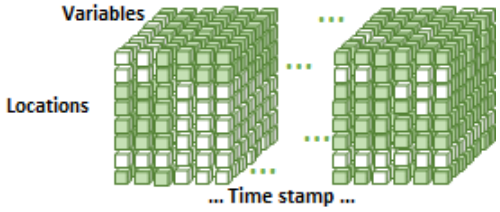

Fig. 2. Representation of higher dimensional data

This work was supported by the Power Systems Engineering Research Center (www.pserc.org), Project No: T-53.

M. H. Kapourchali is with the Department of Electrical Engineering and Computer Science, Wichita State University, Wichita, KS 67260 USA (e-mail: mxheidarikapourchali@shockers.wichita.edu)

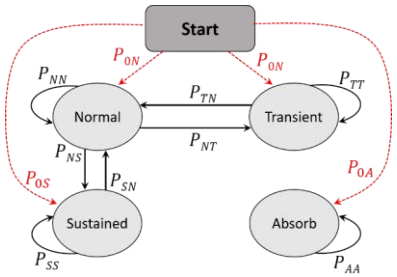

Fig. 3. State-space diagram for two-node connection between typical solar site and control center

III. Results

The publicly available NREL solar and meteorological data within the state of Kansas are used in this work.

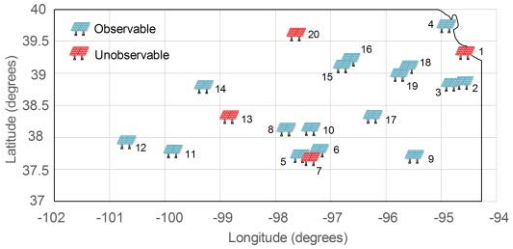

Fig. 4. Solar PV sites in the state of Kansas

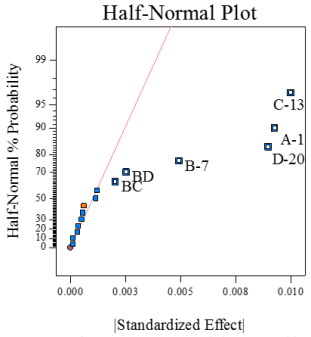

Fig. 5. Half-normal plot of factor effects

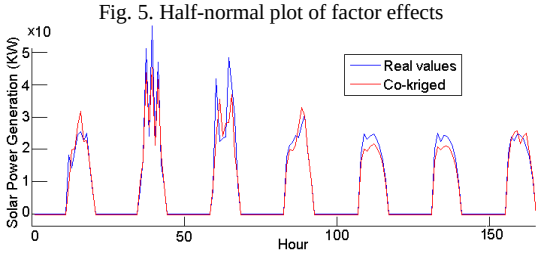

Fig.6. Visual comparison for sustained failure lasting for seven consecutive days

IV. Conclusion

This work is the first step towards more efficiently and systematically designing renewable forecasting algorithms. It gives insight on how to design communication infrastructures for PV fleets, and whether or not to install the measurement requirements for PV sites.

Real-time Cyber Physical Test-bed for validation of Automated Failure Diagnosis in Transmission Network

Amir Gholami, Anurag Srivastava
School of Electrical Engineering and Computer Science, Washington state University
Email: amir.gholami@wsu.edu

***Abstract*—Protection part of the transmission system in power grid plays a significant role in detection and isolation of the faulty part of the grid. Also it might be useful in finding the location of the fault. In the case of contingency, it is very important for the relays to be properly working and accomplishing the isolation process. Otherwise, the fault will be spread into the other parts of the grid. In addition, it is of high importance to differentiate between a cyber-attack and physical malfunctioning. In worst case scenario, it is also possible to be attacked by a Cyber hacker at the same time of a physical malfunctioning of the relays. In this poster, two different cases have been studied and validated using real-time monitoring of the system in OPAL-RT. Malfunctioning Case Studies have been developed and actual and possible scenarios have been extracted. Then the case studies have been analyzed in OPAL-RT real-time simulation and then, using the 5-digit algorithm (proposed by [1]), the system has been validated.**

I. Introduction

Generally speaking, the distance protection of the transmission lines is a set of current and voltage transformers, protective relays, circuit breakers, and batteries. Any type of fault in any of the aforementioned components may lead to the propagation of the fault to the other parts of the system, as a result of which it may ends up with a black-out, which is kind of disaster as far as the damage to the system and the restoration effort and money are concerned.

In order to address this issue, in this work two standard power transmission systems have been studied, which are IEEE 68-bus system and WECC 179-bus system accordingly.

Firstly, the 68-bus system is to be examined in terms of the relay malfunctioning situations. To do so, some case studies of combinations of relay malfunctioning is developed and the actual and possible scenarios have been theoretically investigated. As it can be seen from Fig. 1, in case of two relays malfunctioning (relay r2 and r6) the fault current will not be disrupted on the fault line (line 3-4), but rather it will be propagated to the adjacent lines as well. (lines 4-5 and 4-14 and then lines 5-8 and 5-6)

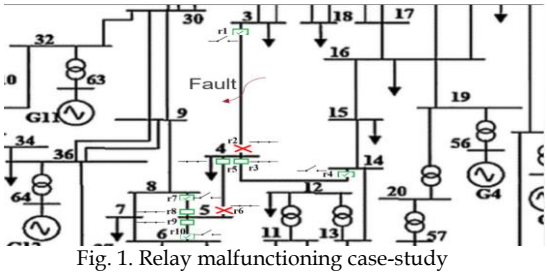

Fig. 1. Relay malfunctioning case-study

In the next step, in order for the analysis to be completed in real time, the model of the system has been built-up in Hypersim (Fig. 2) and the developed case studies for relays malfunctioning has been implemented in the model. Then using the OPAL-RT real time simulation, the cases have been implemented and the real time results have been extracted.

As the final step of this work, the acquired data from the phasor measurement units (PMUs) of the system have been analyzed using the 5-digit algorithm and as a result of which, the actual and possible scenarios, and also physical and cyber-attacks have been differentiated.

Parallel to this work, to implement a more sophisticated test cases in a bigger standard power transmission system, the WECC 179-bus system is chosen and modeled in OPAL-RT. (Fig. 3) Using the real time simulation, some more complex test cases have been implemented in this system and the resiliency of the system have been examined.

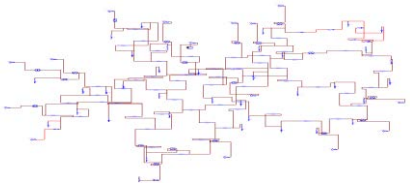

Fig. 2. OPAL-RT model of the 68-bus system

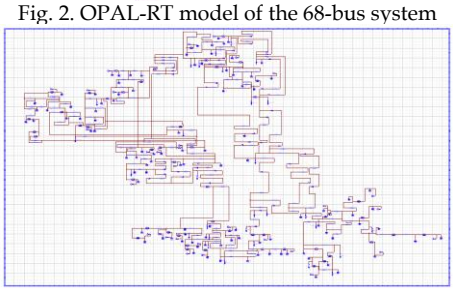

Fig. 3. OPAL-RT model of the 179-bus system

ACKNOWLEGMENT

This research is supported by National Science Foundation (NSF). We also thank Dr. Bo Cui who put his efforts in this project and provided us with assistance on the way to achieve the goals of this project.

References

[1] B. Cui, A. Srivastava and P. Banerjee, "Automated Failure Diagnosis in Transmission Network Protection System Using Synchrophasors," in *IEEE Transactions on Power*

Content Development of IoT for Grid Modernization - a Two Class Series for the Future Power Engineer

1st C. Eppinger
Dept. of Electrical and Computer Engineering
Portland State University
Portland, OR, USA
crystal.eppinger@pdx.edu

2nd Robert B. Bass
Dept. of Electrical and Computer Engineering
Portland State University
Portland, OR, USA
robert.bass@pdx.edu

***Index Terms*—Internet of Things, Demand Response, Energy Management Systems, Distributed Management Systems**

I. Introduction

The grid modernization initiative is transforming our aging grid infrastructure into a grid that both communicates and makes fast, intelligent decisions. The sought-after engineer will be equipped with power systems knowledge and computer science (CS) expertise. This two class series bridges the gap between power engineering and CS by introducing students to the Internet of Things (IoT) as it pertains to the grid modernization effort. Grid modernization requires interaction and control of energy used and produced by millions of devices at the power distribution level. Transactive power along with communication data model standards are being developed and deployed. Additionally, connecting all of the smart devices using internet protocols places significant emphasis on cyber-security.

II. Key Components

Each 1 hour and 50 minute class session will be split into 2, 25-30 minute mini-lectures followed by 15 minutes of discussion and activity. The mini-lectures will be separated by a 10 minute break. Every class session will end with at least 10 minutes of time for questions, clarification and assistance with the assignments and the project.

Class I

The first class will offer an introduction to the elements of the modern grid, such as distributed energy resources (DER) control and transactive power principles. It will lightly touch on communication protocols to familiarize students with the terms required for an in-depth study in the second class of the series.

The first class series project is intended to familiarize students with the open-source, IoT framework. The students will create a free standing manual that offers step-by-step instructions on software installation, bash scripting and interface development.

This project utilizes active learning techniques, such as ”doing” and ”teaching”, in an effort to maximize the students information retention.

Class II

The second class will place emphasis on a project to explore advanced topics relating to IoT-based grid applications. This class teaches standard communication data models, and introduces relevant cyber security techniques. Class lectures will be divided into two parts, one on course content and the other for the students to present project deliverables.

The second class project will involve a class collaborative effort to network the distributed energy resources (DERs) of a fictional building. The students must use an existing energy management system (EMS) template to control the DERs to manage building demand while minimizing total cost. The project encourages time management, interdepartmental collaboration and communication, and the creation of standards and protocols.

Fig. 1. Second Class Series Project Diagram

Federation based Testbed Implementation of Anomaly Detection for Wide Area Protection Scheme in Power System

Vivek Kumar Singh, Manimaran Govindarasu
Department of Electrical & Computer Engineering
Iowa State University, Ames, IA, USA
vsingh@iastate.edu, gmani@iastate.edu

Donald Porschet, Morris Berman, Edward Shaffer
US Army Research Laboratory
Adelphi, MD, USA

***Abstract*—Today's smart grid consists of numerous, geographically distributed systems which are controlled by interconnected, high-speed communication and data processing devices. Significant advances in synchrophasors such as phasor measurement units (PMUs) in smart grid are providing real-time monitoring to protect the grid health at the micro level. However, as PMU technology evolves, so does the potential for increased vulnerability to cyber physical attacks. Synchrophasor based Wide Area Protection Schemes (WAPS) rely on PMUs to detect abnormal conditions, both natural and malicious, and to provide predetermined corrective actions through the wide area communication network to maximize grid stability. The existing multitude of vulnerabilities in the communication and phasor devices make them particularly susceptible to be compromised through the advanced persistent threat (APT). This poster presents our current approach in developing a federation based testbed using Iowa State University's Power Cyber and the US Army Research Laboratory's resources to detect coordinated cyber-attacks targeting the centralized WAPS. The implemented network topology and experimental architecture are based on the modified IEEE 39 bus system which is simulated concurrently on two, separate OPAL-RT, real time digital simulator (RTDS). Initially, we will demonstrate the stealthy, coordinated attacks on the simulated generator and line while disguising the attacks as benign anomalies. Machine learning based random forest classifier algorithm will be adopted to detect the multi-class of attack vectors. Future evaluations will determine how data transmission latency in real-world scenarios affect the federation's anomaly detection performance during communications delays and measurement uncertainty.**

False Data Injection Attacts in Electric Energy Markets

Ramin Kaviani
Arizona State University, Tempe, AZ

Kory W. Hedman
Arizona State University, Tempe, AZ

***Abstract*— Monitoring and controlling an extremely huge system like an electric power system is very complicated and becomes more challenging with the threat of cyber-attacks. While the cyber layer enables many advanced features and provides benefits to operations,, it may put the physical part under many risks and attacks. One way of performing a cyber-attack is to change the real data with fake data, which is called a false data injection (FDI) attack. The goal of a FDI attack could be either financial or physical damage. In this paper the financial side as a result of FDI attacks in electricity market is investigated. Without the presence of a detection mechanism there could be irrecoverable damages in system. Therefore, nowadays, all energy management systems include bad data detectors in order to detect errors. In this research, we propose a detection mechanism using the electric power grid's natural features, along with the use of duality theory from linear optimization theory, to detect FDI attacks in energy markets.**

Keywords—cyber attacks; false data injection attack; cyber attack detection

I. INTRODUCTION

By emerging the concept of cyber physical systems many researches are conducted in this field, among which the paper by Liu, et al [1] is one of the first researches about the so-called FDI attack. They addressed the condition which need to be satisfied by attacker to result an undetectable attack. In [2], the authors investigated physical consequences of an unobservable FDI attack on AC SE on physical system. In [3] as the first paper which tried to evaluated financial damages of FDI attack, the authors showed how the attacker is able to gain profit in electricity markets by bidding into the day-ahead market as a virtual bidder.

II. DUALITY THEORY

In linear optimization, there is a primal problem, which is reflective of the mathematical program that is being solved. Each primal problem then has a dual; together, they form a primal-dual pair. The dual problem describes the relationship for all of the dual variables of the corresponding primal constraints. Those dual variables are the shadow prices on the various constraints within the primal, also known as Lagrange multipliers, which are the settlement prices used for LMPs, flowgate marginal prices, and other prices used to settle the electric energy markets. A simplified DCOPF (the primal formulation) along with its dual is presented below. For this work, we will derive the dual formulation for the electric energy market problem and show how the information in the dual can be used to improve the ability to detect an attack.

Primal Problem:

Minimize: $\sum_{g} c_g P_g$

s.t.

$$\sum_{\forall k(n,.)} P_k - \sum_{\forall k(.,n)} P_k + \sum_{\forall g(n)} P_g = d_n, \forall n \qquad (LMP_n)$$

$$-P_k \geq -P_k^{\max}, \forall k \qquad (F^+_k)$$

$$P_k \geq -P_k^{\max}, \forall k \qquad (F^-_k)$$

$$B_k(\theta_n - \theta_m) - P_k = 0, \forall k \qquad (S_k)$$

$$-P_g \geq -P_g^{\max}, \forall g \qquad (\alpha_g)$$

$$P_g \geq 0;\ \theta_n,\ P_k \text{ free}$$

Dual Problem:

Maximize: $\sum_{n} d_n LMP_n - \sum_{k} P_k^{\max}\left(F_k^+ + F_k^-\right) - \sum_{g} P_g^{\max}\alpha_g$

s.t.

$$LMP_n - LMP_m - F_k^+ + F_k^- - S_k = 0, \forall k \qquad (P_k)$$

$$LMP_n - \alpha_g \leq c_g, \forall g \qquad (P_g)$$

$$\sum_{k(n,.)} B_k S_k - \sum_{k(.,n)} B_k S_k = 0, \forall n \qquad (\theta_n)$$

$$F^+_k,\ F^-_k,\ \alpha_g \geq 0;\ LMP_n,\ S_k \text{ free}$$

III. CONCLUSION

While the auction formulations for electric energy markets are reflective of the power grid, the market participants, security criteria, etc., the mathematical program has a corresponding dual that describes the interaction of prices across the system. This work demonstrates how duality theory can be used to help detect FDI attacks by evaluating the impact of the attack on the dual formulation, to be able to predict what measurements an attacker may modify in order to make a higher profit.

REFERENCES

[1] Y. Liu, P. Ning, and M. K. Reiter, "False data injection attacks against state estimation in electric power grids," in Proceedings of the 16th ACM Conference on Computer and Communications Security, ser. CCS '09. New York, NY, USA: ACM, 2009, pp. 21–32.

[2] J. Liang, L. Sankar, and O. Kosut, "Vulnerability analysis and consequences of false data injection attack on power system state estimation," IEEE Transactions on Power Systems, vol. 31, no. 5, pp. 3864–3872, 2016.

[3] L. Xie, Y. Mo, and B. Sinopoli, "Integrity data attacks in power market operations," IEEE Transactions on Smart Grid, vol. 2, no. 4, pp. 659–666, 2011.

CP-SAM: Cyber-Physical Security Assessment Metric for Microgrid Resiliency

V. Venkataramanan, *Student Member, IEEE,* S. Zonouz, *Member, IEEE,* A. Hahn, *Member, IEEE,* and A. Srivastava, *Senior Member, IEEE*

***Abstract*—Trustworthy and secure operation of the cyber-physical power-grid infrastructures calls for resilience against malicious and accidental failures. The objective is to recover the safe (partially degraded) operation of the system to supply critical loads despite multiple contingencies in the system. To take timely actions, we need to continuously measure the cyber-physical security of the system. We propose a cyber-physical security assessment metric (CP-SAM) based on quantitative factors affecting resiliency and utilizing concepts from graph theoretic analysis, probabilistic model of availability, Markov decision process, cryptographic solutions, message-authentication, controllers and algorithmic trust management embedded across different layers of the microgrid system. These factors are combined into a single metric using analytic network process to compute CP-SAM. The metric will be a valuable asset for *i)* comparing the power-grid architectures during the offline design process; and *ii)* online decision-making to select optimal proactive countermeasure strategies to drive the power grid towards states that can tolerate upcoming adverse events more effectively. We will implement and demonstrate the application of our proposed CP-SAM in a real-world power-grid test-bed for off-line decision process and on-line decision making to enable the resiliency.**

I. Introduction

The objective of this paper is to define a cyber-physical security assessment metric (CP-SAM) that can be used to assess the cyber physical security to enable the microgrid resiliency. In power system, performance of the system can be measured using different metrics. Table I shows the definitions used in this paper for the terms resiliency, reliability, and security. The objective of a secure cyber physical microgrid system is to make sure that the critical loads of the microgrids are supplied even with extreme adverse events. These critical loads are identified in advance, and CP-SAM is used to asses the ability of the microgrid to supply these loads after disturbances.

II. Case Studies

The microgrid operator can obtain a better understanding of the state of the system by using metrics such as CP-SAM. Various case studies are considered to better understand the usefulness of the proposed metric. Fault trees are developed for each these scenarios to identify the key interdependencies between the various factors for that particular scenario.

III. Summary

This paper proposes a novel methodology of assessing the cyber-physical security to enable microgrid resiliency. A cyber-physical security assessment metric (CP-SAM) is obtained by resiliency oriented modeling of all the cyber-physical layers in the microgrid and considering the factors affecting the microgrid resiliency. Various factors across different layers in the microgrid including physical, communication, security, and device level factors. CP-SAM for the microgrid resiliency is derived using fuzzy Choquet Integral for easy interpretation. The various steps in the fuzzy Choquet Integral are also explained, including the steps to determine the interaction index, and determining the fuzzy weights using various game theoretic techniques. Fault trees are also provided that help decide on the factors that contribute to each scenario. Various scenarios including loss of node, loss of link, and a Netflix inspired Chaos Monkey type attack in which a random set of nodes is removed are studied. CP-SAM can be used by system operators to quickly judge the security of the microgrid in extreme contingencies, and decide on control actions.

TABLE I: Definitions of System Performance Metrics

Metric	Definitions
Reliability	Ability of the system to supply all its connected loads (e.g. SAIFI, SAIDI).
Physical Security	Ability of the system to supply all the connected load under contingencies (e.g. 'N-1' or 'N-x') achieved through contingencies screening and detail contingencies analysis.
Cyber Security	Protection of systems from compromise and disruption based on Confidentiality, Integrity and Availability (CIA) concepts (e.g. encryption, firewalls).
Cyber-Physical Security	Ability of the cyber-physical system to supply the loads under contingencies or to meet the requirements specified by the system operators (generally without the self-healing considerations).
Resiliency	Ability of the system to self-adapt and reconfigure its topology dynamically to tolerate multiple contingencies and supply critical load. Our proposed metric can indicate cyber-physical security measures embedded in the system to enable resiliency.

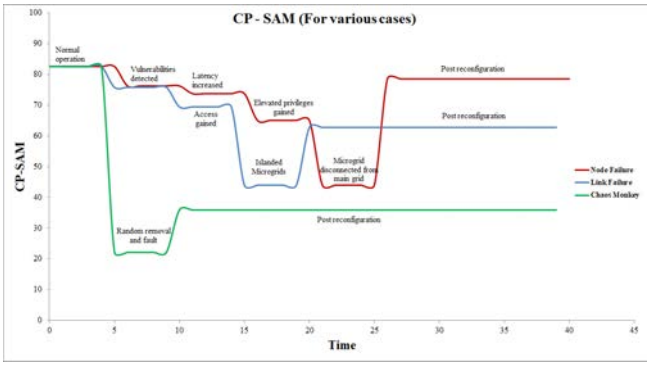

Fig. 1: CP-SAM for Various Cases

V. Venkataramanan, A. Hahn, and A. Srivastava are with Washington State University, Pullman, WA 99163 USA. (E-mail: asrivast@eecs.wsu.edu)

S. Zonouz is with Rutgers University, New Jersey, 08854 USA (E-mail: saman.zonouz@rutgers.edu).

Calculation of Critical Oscillation Modes for Large Delayed Cyber-Physical Power System Using Pseudo-Spectral Discretization of Solution Operator

Qianying Mou, *Student Member, IEEE,* Hua Ye, *Member, IEEE,* and Yutian Liu, *Senior Member, IEEE*

***Abstract*— In eigen-analysis of large delayed cyber-physical power system (DCPPS), power engineers are interested in critical electromechanical oscillation modes with damping ratios less than a specified threshold. To efficiently compute these modes, a method based on pseudo-spectral discretization of the solution operator of DCPPS (SOD-PS) is presented in this paper. First, the unique spectral mapping properties of solution operator are analyzed. The largest eigenvalues in moduli of the operator correspond to the ones of DCPPS with the largest real parts. Second, a rotation-and-multiplication preconditioning technique is presented to enhance the dispersion among eigenvalues of the solution operator's discretized matrix. Third, critical electromechanical oscillation modes of DCPPS with the least damping ratios are captured with priority and an accelerated convergence rate by the implicitly restarted Arnoldi algorithm (IRA). Subsequently, the small signal stability of DCPPS can be readily and reliably determined. In SOD-PS, the unique property of Kronecker product and the inherent sparsity in augmented system matrices are fully exploited to guarantee efficiency and scalability. The accuracy and efficiency of the presented method are intensively studied and thoroughly validated on the 16-generator 68-bus test system and a real-life large transmission grid.**

***Index Terms*— Cyber-physical power system, delay differential equation, eigen-analysis, small signal stability, solution operator, spectral discretization, spectral transformation, time delay, wide-area measurement system.**

I. Key Techniques

By utilizing the properties of the solution operator, efficient stability determination and eigenvalue analysis of DCPPS can be achieved. *1) Reliable Stability Determination.* The stability of DCPPS can be directly determined by the largest modulus $|\mu_1|$. If $|\mu_1|>1$, the system is unstable. If $|\mu_1|<1$, the system is asymptotically stable. $|\mu_1|=1$ denotes that the system is critical. *2) Critical Eigenvalue Computation.* The rightmost eigenvalues λ of DCPPS, i.e., those with the largest real parts, can be recovered from μ with maximum moduli, for further stability analysis and controller design.

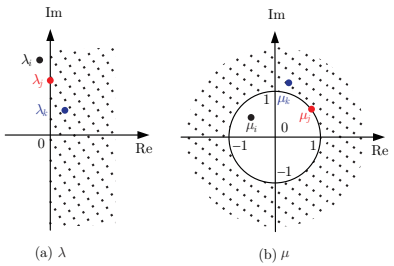

Fig. 1. Spectral mapping of the solution operator. (a) Eigenvalue of DCPPS λ; (b) Eigenvalue μ of the solution operator $\boldsymbol{\mathcal{T}}(h)$. λ relates to μ by $\lambda=\frac{1}{h}\ln\mu$.

The authors are with Key Laboratory of Power System Intelligent Dispatch and Control of Ministry of Education (Shandong University), 17923 Jingshi Road, Ji'nan 250061, China (e-mail: muqy@mail.sdu.edu.cn).

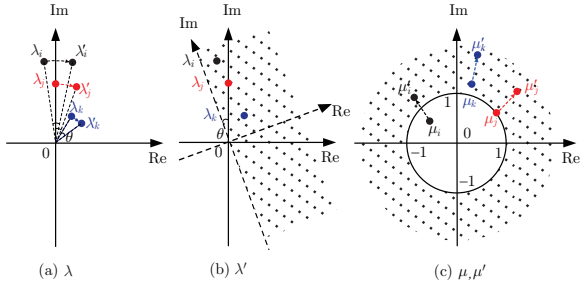

Fig. 2. Spectral mapping of the solution operator with coordinate rotation preconditioning. (a) λ' is achieved by clockwise rotating λ about the origin θ radian, i.e., $\lambda'=\lambda e^{-j\theta}$. (b) The effect of eigenvalue rotation is equivalent to anticlockwise rotate the coordinate about the origin θ radian. (c) The eigenvalues λ of DCPPS with damping ratios less than ζ $(=\sin(\theta))$ are transformed into those μ' of the preconditioned solution operator and located outside the unitary circle. λ relates to μ' as $\lambda=\lambda' e^{j\theta}=\frac{1}{h}e^{j\theta}\ln\mu'$. Conversely, $\mu'=e^{\lambda' h}=e^{\lambda e^{-j\theta}h}$.

II. Key Results

The real-life large DCPPS includes 516 buses, 936 transformer branches and transmission lines, 114 generators, 299 loads and two wide-area damping controllers. The dimension of state variable vector is $n=1128$ and the dimension of algebra variable vector of the system is $l=4637$. The time delays of two wide-area damping control channels are $\tau_1=0.09$ s and $\tau_2=0.10$ s. The dimension of $\boldsymbol{T}_{M,N}$ is 34968. When 100 and 120 eigenvalues are computed by SOD-PS, the computational time is 423.79 s and 435.82 s, respectively.

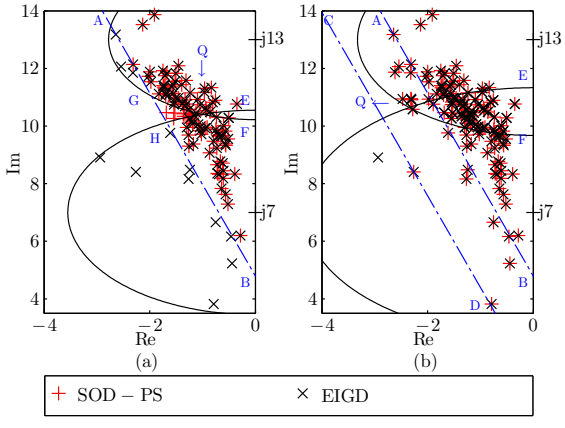

Fig. 3. Eigenvalues computed by SOD-PS with $\theta=17.46°$ and by EIGD around two shift points $s=$ j7 and j13. (a) 100 eigenvalues obtained by SOD-PS and two sets of 50 eigenvalues obtained by EIGD; (b) 120 eigenvalues obtained by SOD-PS and two sets of 80 eigenvalues obtained by EIGD.

VSC-HVDC for enhancing power system stability in the load restoration stage of black start

Wei Feng, Fangxing Li
Department of Electrical Engineering and Computer Science
The University of Tennessee, Knoxville
Knoxville, TN 37996, USA
{wfeng4, fli6}@vols.utk.edu

***Abstract*— In the load restoration stage of power system black start, it is very important to enhance the restoration stability. For a good black start system, it is important to avoid transient voltage and inrush current and frequency variation. However, tradition methods cannot perform well in this. This course project presents Voltage Source Converter based HVDC (VSC-HVDC) used as black start source. The physical model of AC system and VSC-HVDC is founded and analyzed. Based on the simulation software PSCAD/EMTDC, a coordinated control method of VSC-HVDC and generator is presented to improve stability of AC/DC hybrid system. Simulation results show that the coordinated control method has excellent dynamic characteristic such as controlling active quickly, avoid inrush current and transient over voltage, and improving the frequency stability of AC system.**

Keywords— black start, VSC-HVDC, Load restoration, Governor, Frequency stability

I. INTRODUCTION

The tradition definition of 'black start' emphasize self-recovery, shows that the process of restoring an electric power station or a part of an electric grid to operation without relying on the external transmission network. Normally, there are two common methods for black start, hydropower units and gas turbine generator. As for traditional black start, there are a lot of problems to be considered in the restoration of power system after black out, such as: generator's self-excitation; continuing fundamental frequency over voltage, switching surge and resonant over voltage while switching on a long no-load line; ferromagnetic resonance while charging transformers; the stability of voltage and frequency and so on.

The development of VSC-HVDC gives a new method for 'black start'. Unlike self-recovery, VSC-HVDC depends on the large-scale interconnected of model grid. When a blackout occurs in one system, the VSC station can firstly be a firewall to stop the blackout spreading to another system. And then, the neighboring working system can be treated as a power supply via VSC. The basic reason is that VSC-HVDC is a passive inverter that can work without supply of inactive power and voltage from AC system, moreover, within the capacity, it can supply power back to the system.

II. MODEL AND CONTROL STRATEGY

A. Physical model of VSC-HVDC

Firstly, modeling a VSC-HVDC to connect two AC system. In this model, power could transfer two-way and operate in different voltage and capacity.

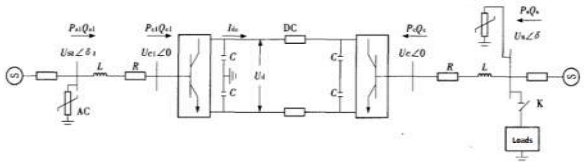

Fig.1 Physical model of VSC-HVDC system

B. Control strategy

When a blackout happens, measuring devices in station could detect rapidly and cut off the fault side. Then, switch to 'power' model to support the blackout area.

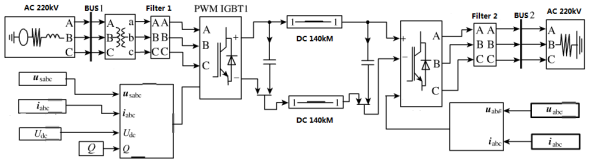

Fig.2 Simulink model of test system

III. SIMULATION RESULTS

The physical model and control strategy are applied in a mixed system with two AC system and test the ability of recovery after blackout. Compared results of hydro-power, gas turbine and VSC-HVDC are given as below.

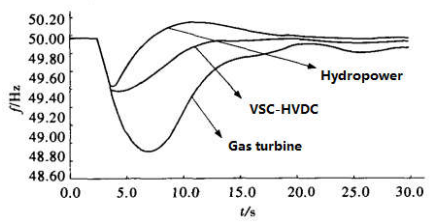

Fig.3 Frequency response of different methods

Optimal Damping Actuator Selection Through Oscillation Energy Sensitivity Analysis

Horacio Silva-Saravia, Yajun Wang, Héctor Pulgar-Painemal, Kevin Tomsovic
Department of Electrical Engineering and Computer Science
University of Tennessee, Knoxville, TN, 37996

***Abstract*—This paper proposes a new method to analyze and select damping control actuators in stressed systems with high penetration of renewable energy. Traditional single dominant mode analysis fails to provide effective control actions when several modes have similar low damping ratios. This work addresses this problem by considering all modes in the formulation of the system kinetic oscillation energy. The integral of energy over time defines the total action as a measure of dynamic performance, and its sensitivity allows comparing the performance of different actuators in the system to select the most effective actuator to damp the oscillation energy. The concept is explained in the single-machine infinite bus (SMIB) system. Time domain simulations are performed in the Western Electricity Coordinating Council (WECC) system to validate the contribution of this work.**

I. Introduction

Traditional analysis of power system oscillations focuses on critical eigenvalues. However, systems with several critical eigenvalues lack a general dynamic performance index to analyze the problem. The method described in this paper provides a solution to this problem. Consider a SMIB system with a damping torque coefficient K_d. As the damping torque is reduced, the stability is compromised and the dynamic performance is worsened as shown in Figure 1.

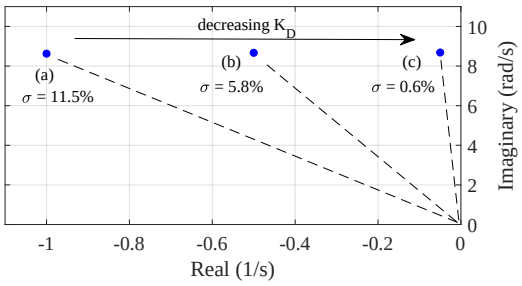

Fig. 1: Eigenvalue plot of SMIB system.

The dynamic performance can be assessed by calculating the area S^0 of the oscillation energy in Figure 2. Thus, the final value of S^0 (total action) works as a tool to compare different actuators.

This material is based on work supported by the National Science Foundation under Grant No. 1509114. This work is also supported by the Engineering Research Center Program of the National Science Foundation and the Department of Energy under NSF Award No. EEC-1041877 and the CURENT Industry Partnership Program.

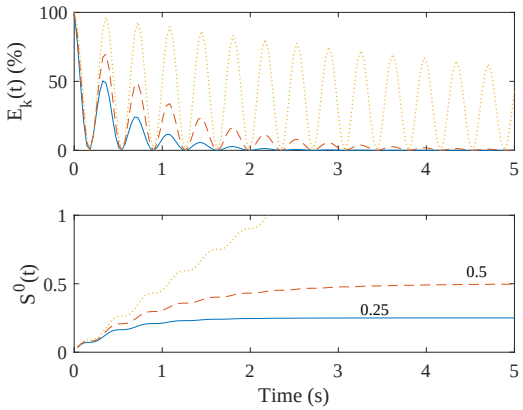

Fig. 2: Oscillation energy and total action of SMIB system.

II. Research Impact

The analytical calculation of the total action sensitivity with respect to different actuators can provide a valuable tool to enhance power system dynamics, specially when high penetration of renewable energy pushes several modes to have critical damping ratios. Applications can be developed for planning considering dynamic strengthening and also for on-line control allocation. Figure 3 shows the oscillation energy and machine speed deviation after applying on-line selection of actuators in the WECC system.

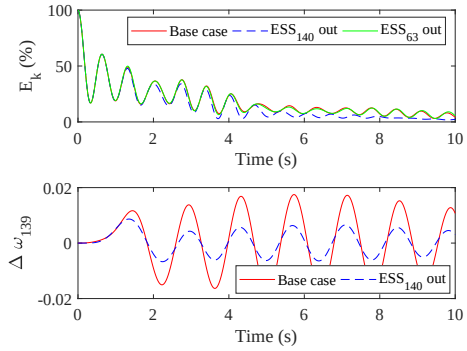

Fig. 3: Kinetic energy of WECC system for disturbance at SG29.

The sensitivities point out that ESS_{140} must be disconnected to achieve an optimal performance for the post-fault condition.

Practical Modeling of Flywheel Energy Storage for Primary Frequency Control in Power Grids

Dario Peralta, *Student Member, IEEE*, Claudio Cañizares, *Fellow, IEEE*, and Kankar Bhattacharya, *Fellow, IEEE*
Department of Electrical and Computer Engineering
University of Waterloo
Waterloo, Ontario, Canada
{d2peralt, ccanizar, kankar}@uwaterloo.ca

***Abstract*—This poster presents the development of a dynamic model for frequency regulation studies, practical and useful for system operators, of a Flywheel energy storage (FES) system connected to a power system to provide Primary Frequency Control (PFC), and study its effects on system stability. The proposed practical model is tested using a commercial simulation package, and compared with respect to a previously reported test system equipped with a high-capacity wind generator, which creates significant frequency and voltage fluctuations, demonstrating its application for solving PFC problems in power networks.**

***Index Terms*—Flywheel energy storage, frequency control, frequency stability, modeling, power system stability, simulation.**

I. Introduction

The development and design of a Flywheel energy storage (FES) model to study the provision of primary frequency control (PFC) is presented in this paper. The FES system comprises of an induction generator/motor, a flywheel represented as a High inertia mass constant (H), and two bi-directional voltage source converters (VSCs), and is modeled in DSATools®. The base system used here is extracted from [1], as shown in Fig. 1.

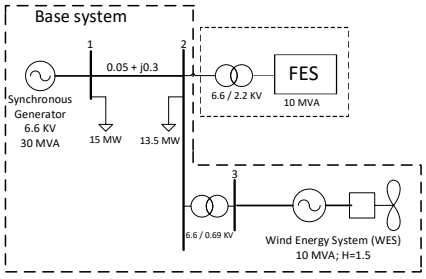

Fig. 1: Test system configuration.

II. FES Speed/Frequency Control

This control determines the active power reference P_{ref}, i.e., in the active power control of the flywheel-side VSC, to be injected to/from the FES, responding to the frequency deviations detected at the terminal of the system. To prevent either the shortage or the surplus of energy stored in the FES, a speed limiter is included, as shown in Fig. 2.

This work has been supported by NSERC Energy Storage Technology (NEST) Network, Canada, http://www.ryerson.ca/nestnet/

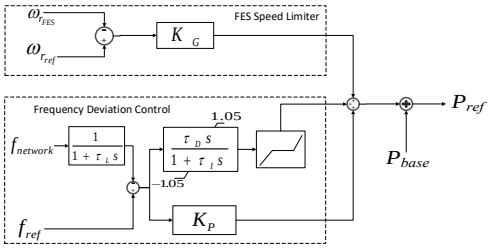

Fig. 2: FES Speed/Frequency Control.

III. Results

There is a significant improvement in the frequency response of the FES system as compared to the Base system, as shown in Fig 3, ensuring frequency stability of the system. Also, the voltage fluctuations are reduced, and the voltage level is increased to its nominal value. Finally, the mechanical torque of the synchronous generator varies considerably in the Base system, while its variation is reduced with the FES, due to the contribution of the FES active power to frequency contro

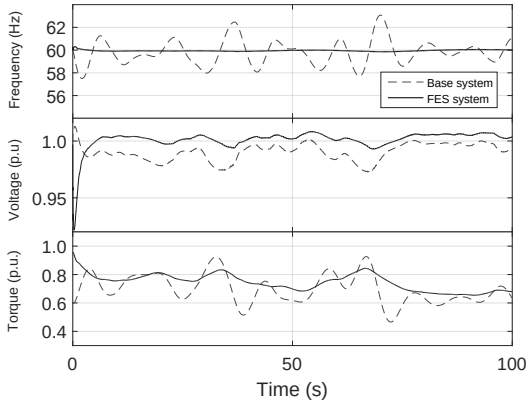

Fig. 3: System response without and with FES.

References

[1] R. Takahashi and J. Tamura, "Frequency stabilization of small power system with wind farm by using flywheel energy storage system," in *Proc. IEEE International Symposium on Diagnostics for Electric Machines, Power Electronics and Drives*, Sept 2007, pp. 393–398.

Location and Migration Laws of Out-of-Step Center under Multi-Frequency Oscillation Based on Voltage Phase Angle Trajectory

Fei Tang[1], Jiale Liu[1], Qingfen Liao[1], Yu Liu[2], Gucheng Xiao[1] and Chenxu Wang[1]
(1. School of Electrical Engineering, Wuhan University, Wuhan, 430072, Hubei Province, China;
2. School of Foreign Languages, South-Central University for Nationalities, Wuhan, 430074, Hubei Province, China)
liujiale@whu.edu.cn

***Abstract*—With the rapid development of ultra-high voltage AC/DC hybrid power grid projects and the large-scale of renewable energy integration, it puts high demand for safety and stability control of the power system. Splitting control (or islanding control) is the last resort to preserve the power system from severe blackouts. In China, the out-of-step center (i.e. the physical point of an oscillating system where the voltage is near to zero) is applied to determining the splitting locations. However, the increasingly complicated power system might oscillate in multi-frequency after large disturbance, which thus leads to dynamic migration of out-of-step centers. To address this issue, this paper derives the migration function of the out-of-step center in three equivalent machines system, based on which the migration laws are analyzed. Accordingly, the voltage angle trajectories method is employed to determine the time and location of splitting control in advance, which could guarantee the real-time implementation of islanding control. Finally, IEEE 9-bus and IEEE 39-bus test systems in PSS/E verify the effectiveness of the proposed method.**

Keywords—multi-frequency oscillation; out of step; voltage phase angle trajectory; oscillation center; positioning

I. INTRODUCTION

With the rapid development of UHV AC/DC projects, the power system is vulnerable to instability of multi-group modes. As a result, it is urgent to research the migration rule of the out-of-step center (OSC) in multi-frequency oscillations.

II. METHODOLOGY

Based on theoretical derivation of the oscillation center location in IEEE9-bus system with three generators, the migration rules of the oscillation center in multi-frequency conditions are proposed as follows:

$$c_i = \begin{cases} \dfrac{m_i^2 + n_i^2 - m_i}{1 - 2m_i + m_i^2 + n_i^2}, & m_i < m_i^2 + n_i^2 \\ 0, & m_i \geq m_i^2 + n_i^2 \end{cases} \quad (1)$$

A case study of line E_1—E_O is analyzed to illustrate the distribution position of the oscillation center (OC), which is shown in Fig.1. When δ_2=δ_3, the value of c_1 reaches maximum (c_{1max}), denoting the OC migrates to the point farthest away from the central point. When $\delta_2 \neq \delta_3$, c_1 varies between zero and c_{1max}. The migration distance is positively correlated to the coherence between generator2 and generator3. The condition for existence of OSC are expressed as Eq.(2).

$$\tan(\delta_{io}) = -n_i / m_i = 0, \ \cos(\delta_{io}) = m_i / \sqrt{m_i^2 + n_i^2} < 0 \quad (2)$$

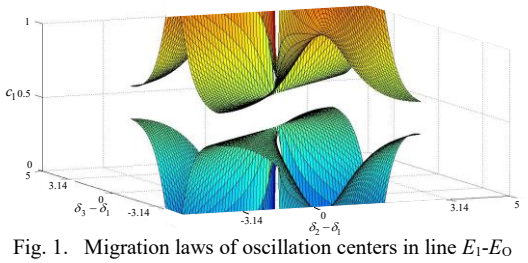

Fig. 1. Migration laws of oscillation centers in line E_1-E_O

Eq. (2) can be further transformed into the constraint condition which the voltage angle need satisfy, as is shown In Fig. 2. The phase angle trajectory, denoted by the gray curve, starts from the point *A* to B to C. The point *C* on the red curve satisfies the condition of appearance of OSC. Accordingly the occurrence time and location of OSC are access to be predicted in advance based on Eq.(2) and Fig.2.

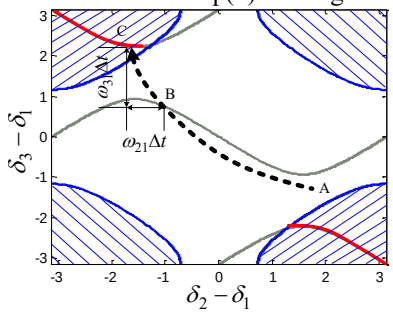

Fig. 2. Voltage phase angle trajectory for locating out-of-step center

III. APPLICATION FOR SIMULATING POWER SYSTEM

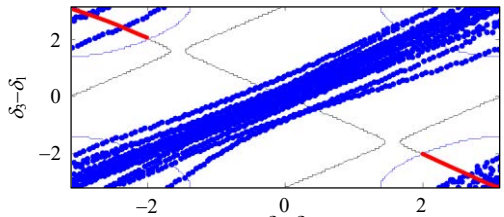

Fig. 3. Voltage phase angle trajectories of line E_1—E_O during 1.5s - 4.5s

Focused on the line E_1—E_O, the simulation study in PSS/E obtains the voltage phase angle trajectories composed by blue dots in Fig.3. During 1.5~4.5s, the intersection of the phase angle trajectory with the red curve illustrates that the OSC occurs in the line E_1—E_O. The validity and reliability of the theory are well tested since the characteristics of phase angle trajectories confirm to the voltage frequency results. In addition, prediction of the OSC position provides enough time for splitting measures.

Development and Frequency Application of an European Low Voltage Microgrid Network

Melike Selcen Ayaz, R. Azizipanah-Abarghooee, *Student Member, IEEE* and Vladimir Terzija, *Fellow, IEEE,* University of Manchester,UK

***Abstract*—A new practical microgrid benchmark system based on Europeian CIGRE data is developed in this paper to investigate distribution based power system dynamics. This test system is modeified to integrate Distributed Energy Resources (DERs). The dynamic frequency studies are applied on this modified low voltage CIGRE benchmark model to demonstrate the frequency nadir improvement in the microgrid system with the increased renewable energy penetration. Two gas turbines, two battery energy storage, two wind turbines and four photovoltaic power plants are appended into the proposed microgrid system. The PV units have a total power of 210 kVA, two WTs are Type 4 direct drive permanent magnet synchronous generator (PMSG) (power of 500 kVA) and the batteries are respectively rated to 35 kVA and 25 kVA with power factor equal to 0.85. The DIgSILENT Power Factory software is deployed to simulate all the case studies. Simulation results evaluate the dynamic performance of all resources as well as the system in terms of the power outputs of the DERs. Furthermore, the frequency response and Rate of Change of Frequency (RoCoF) criterion under a load event, and different penetration level of renewable energy sources are explored. The derived model will enable the researchers to both working with a real network model and designing a flexible microgrid studies and applying the sensitivity analysis for future distribution network studies.**

Keywords—DERs; DIgSILENT; Microgrids; Penetration of renewables; Frequency response

I. INTRODUCTION

The system frequency stability depends on the system inertia, which is the kinetic energy of rotating masses of synchronous machines connected to grid. The power electronic interfaces considered in Distributed energy sources (DERs) decouple the inertia from the system, which can lead to the power system instability. Thus, the microgrid systems are under risk of large frequency oscillations in case of future low and variable inertia system especially in distribution networks. Integrating the battery storage systems (BESSs) in order to contribute to the primary frequency response is a primitive solution to solve the issues mentioned, in realistic dynamic test system including DERs such as photovoltaic (PV) power plant, wind turbines (WTs). The location of the DERs and BESSs are selected according to the sensitivity analysis to provide system frequency stability. After the placement procedure, the modeled LV distribution model based on European CIGRE information is considered as the microgrid.

II. PROPOSED EUROPEAN LV MICROGRID MODEL

This benchmark model provides a high variety of testing for integration of DERs. The network consists of 37 nodes with the combination of residential, industrial and commercial subnetworks, comprising of 6 residential, 8 commercial loads and industrial load connected by underground and overhead line topologies [1] portrayed in Fig. 1. The proposed network is a good candidate for testing discrepant solutions in the areas of microgrids in terms of power system frequency, stability, dynamics and smart grid analysis.

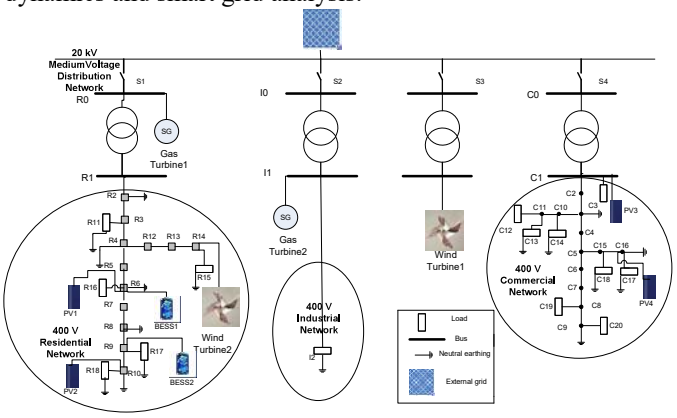

Fig. 1. Modified benchmark model- LV practical test system with DERs

III. SIMULATION RESULTS

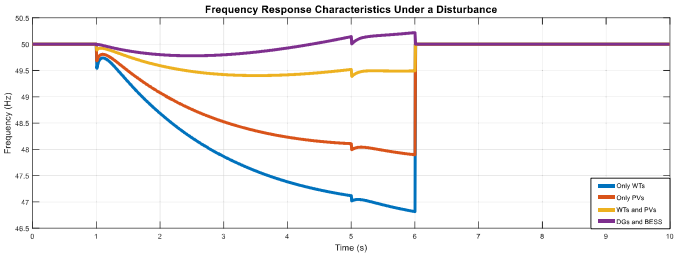

Fig 2.Comparison Results of Frequency Response Characteristics Under a Disturbance

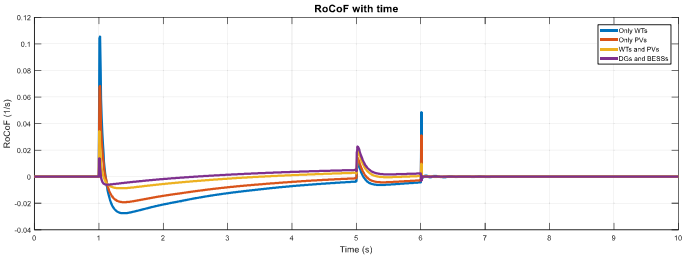

Fig 3. Comparison results of RoCoF Characteristics Under a Disturbance

IV. CONCLUSIONS

The significance of a practical microgrid system is to meet the needs of the researchers for power system dynamic analysis. Simulation results show that increase of WTs and PVs affect the frequency regulation; however, the use of GTs and BESSs can regulate the frequency without a massive frequency drop.

[1] CIGRE, *Benchmark Systems for Network Integration of Renewable and Distributed Energy Resources*, April. 2014.

Provision for Guaranteed Inertial Response in Diesel-Wind Systems via Model Reference Control

Yichen Zhang, *Student Member, IEEE,* Alexander M. Melin,, *Member, IEEE,* Seddik M. Djouadi, *Member, IEEE,* Mohammed M. Olama, *Member, IEEE,* Kevin Tomsovic, *Fellow, IEEE*

***Abstract*—Frequency performance has been a crucial issue for islanded microgrids. On the one hand, most distributed energy resources (DER) are converter-interfaced and do not inherently respond to frequency variations. On the other hand, current inertia emulation approach cannot provide guaranteed response. In this paper, a model reference control based inertia emulation strategy is proposed for diesel-wind systems. Desired inertia can be precisely emulated through the proposed strategy. A typical frequency response model with parametric inertia is set to be the reference model. A measurement at a specific location delivers the information about the disturbance acting on the diesel-wind system to the reference model. The objective is for the speed of the diesel generator to track the reference so that the desired inertial response is realized. The controller is implemented in a nonlinear three-phase diesel-wind system fed microgrid using the Simulink software platform. The results show that exact synthetic inertia can be emulated and adequate frequency response is achieved.**

***Index Terms*—Inertia emulation, low-inertia microgrid, diesel-wind system, model reference control, polytopic uncertainty.**

I. Motivation

Inertia emulation functionality has been widely integrated within wind turbine generators (WTGs) to improve the frequency response by coupling the kinetic energy stored in WTGs in proportion to the rate-of-change of frequency (RoCoF). This configuration, however, is difficult to assess and control how much synthetic inertia can be provided since the emulated inertia is time-varying. In this work, a novel inertia emulation strategy is proposed for diesel-wind systems, through which desired inertia can be precisely emulated.

II. Model Reference Control-based Inertia Emulation

Fig. 1 illustrates the MRC-based inertia emulation on a diesel-wind system. It consists of a parameterized reference model and a physical plant. A reference model similar to the frequency response model will be chosen with desired inertia $\hat{H}$. The physical plant is the diesel-wind unit.

The idea to achieve near-ideal synthetic inertial response of WTGs can be recast as a tracking problem. As illustrated in Fig. 1, let $2\hat{H}s\Delta\omega$ and $2H_Ds\Delta\omega_d$ be the inertial response of the reference model and DSG, respectively, where $\hat{H}$ is the desired inertia constant and $\hat{H} - H_D = H_{\text{ie}} > 0$. Once subjected to a same disturbance ΔP_{pom}, the power balance condition holds as

$$\Delta P_{\text{pom}} = 2\hat{H}s\Delta\omega = 2H_Ds\Delta\omega_d + \Delta P_g \tag{1}$$

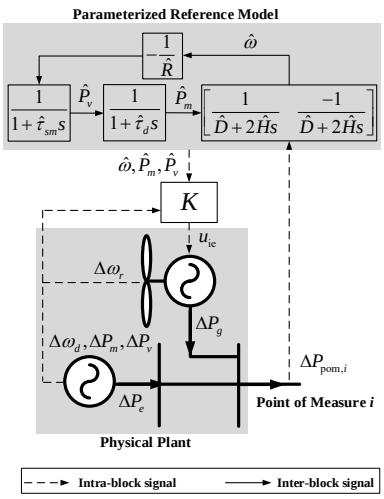

Fig. 1. Realization of MRC on one diesel-wind system.

If the speed of DSG can track the speed of reference model with the support of WTG, that is, $\Delta\omega = \Delta\omega_d$, then the following relation holds

$$\Delta P_g = 2\hat{H}s\Delta\omega - 2H_Ds\Delta\omega = 2H_{\text{ie}}s\Delta\omega \tag{2}$$

Therefore, exact synthetic inertial response $2H_{\text{ie}}s\Delta\omega$ is emulated by the WTG. Finally, the MRC approach is employed to realize the tracking objective. This reference tracking can be realized by means of feedback control. The preliminary result is shown in Fig. 2.

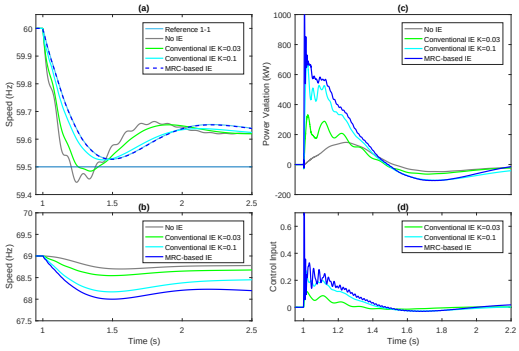

Fig. 2. Performance under conventional and MRC-based inertia emulation with Config. 1. (a) Speeds of DSG and reference model. (b) WTG speed. (c) WTG active power variation. (d) Control input.

Tube-Based Model Predictive Control of Energy Storage Units for Improving Transient Stability of Power Systems

Iman Kiaei, *Student Member, IEEE*, and Saeed Lotfifard, *Member, IEEE*
School of Electrical Engineering and Computer Science, Washington State University, Pullman, WA 99164 USA
E-mail: iman.kiaei@wsu.edu; s.lotfifard@wsu.edu

***Abstract*—In smart grids energy storage units are installed at different locations of the network. This work proposes a method based on model predictive control (MPC) for enhancing the transient stability of power systems by controlling the charging and discharging state of superconducting magnetic energy storage (SMES) systems installed throughout power systems. To enhance the performance of the controller in presence of exogenous disturbances and modelling uncertainty a controller based on tube-based MPC is developed. The proposed controller determines output active and reactive powers of SMES units at each time instance to improve the selected transient stability index defined based on the distance of the rotor angles of generators and the center of inertia of the power system.**

I. Introduction

Transient stability is the ability of a power system to withstand large disturbances. When a contingency occurs in power systems the power balance between generation and load is disturbed. In this condition, unstable generators should be disconnected from the grid and the system operator should execute emergency control actions to balance out the generation and load. In this work, to enhance the transient stability of the power system, a coordinated control system for managing output active and reactive power of SMES units installed throughout power systems is proposed. This coordinated control is based on the tube-based model predictive control which consists of two MPCs, inner and outer MPCs.

II. Proposed Tube-based Model Predictive Controller

The objective function of the Tube-based MPC is as follows:

$$\min \quad \sum_{i=1}^{NG}\left(\theta_i(t)-\theta_{COI}(t)\right)^2+\sum_{j=1}^{NS}\lambda_j\left(\Delta U_j(t)\right)^2 \tag{1}$$

The device constraints, SMES output power bounds, and the system wide constraint, voltage limit are considered as follows:

$$\dot{\theta}_i(t)=\omega_i(t)-\omega_s \tag{2}$$

$$\dot{\omega}_i(t)=\frac{\omega_s}{2H_i}\left(P_{mi}-P_{ei}-D_i(\omega_i(t)-\omega_s)\right) \tag{3}$$

$$P_{ei}=\sum_{j=1}^{n}|V_i||V_j||Y_{ij}|\cos\left(\angle Y_{ij}+\theta_j-\theta_i\right) \tag{4}$$

$$Q_{ei}=-\sum_{j=1}^{n}|V_i||V_j||Y_{ij}|\sin\left(\angle Y_{ij}+\theta_j-\theta_i\right) \tag{5}$$

$$P_{SMES}(output)=\frac{K_s}{1+T_s\times s}U_{\Pr ef} \tag{6}$$

$$Q_{SMES}(output)=\frac{K_s}{1+T_s\times s}U_{Qref} \tag{7}$$

$$\left|V_{LowerLimit}\right|\le\left|V_{SMES}\right|\le\left|V_{UpperLimit}\right| \tag{8}$$

$$P_{\min}\le P_{SMES}\le P_{\max} \tag{9}$$

$$Q_{\min}\le Q_{SMES}\le Q_{\max} \tag{10}$$

III. Simulation Results

The proposed control strategy is applied to a 3 machine system. A three-phase short circuit fault occurs on the line between buses 4 and 9 at 0.1 seconds and is cleared at 1.1 seconds by tripping the faulted line. The proposed controller based on tube-based MPC determines the output active and reactive powers of SMES units.

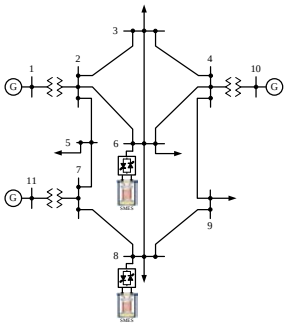

Fig. 1. Schematic of the simulated power system

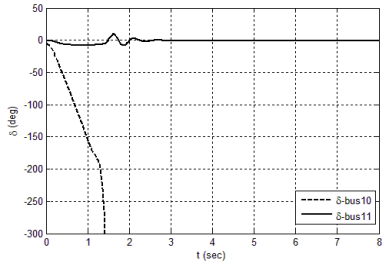

Fig. 2. Relative rotor angles of the generators at buses 10 & 11 for the fault at 0.1 sec.

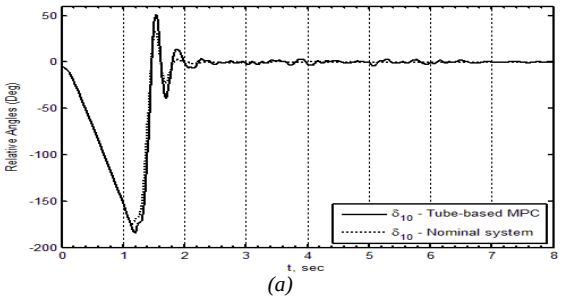

(a)

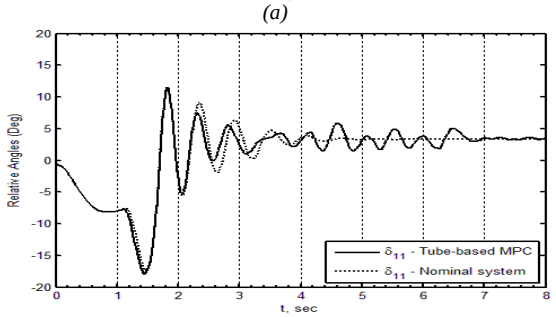

(b)

Fig.3. Trajectories of the rotor angle for MPC#1 and MPC#2 of the tube-based MPC (a) generator at bus#10. (b) generator at bus#11.

Probabilistic Transient Stability Assessment of Renewable Generation Integrated Power System

Yingying Wang, *Student Member*, *IEEE*, Mojdeh Khorsand, *Member*, *IEEE*, and Vijay Vital, *Fellow*, *IEEE*
School of Electrical, Computer and Energy Engineering, Arizona State University, Tempe, AZ, USA
ywang935@asu.edu, Mojdeh.Khorsand@asu.edu, and Vijay.Vittal@asu.edu

***Abstract*—The stochastic characteristic of wind power has introduced challenges to traditional deterministic dynamic security assessment of power systems. A probabilistic approach based on Monte-Carlo simulation (MCS) is proposed in this work to integrate wind power uncertainty and variability into transient stability analysis of power grids. Fault probability including fault rate, fault type and fault location are taken into consideration in the transient stability assessment. System stability is evaluated in term of loss of load to maintain stability after the disturbance and its probability. A synthetic 36-bus test system is utilized to verify the proposed approach. The simulation results show the effectiveness of the proposed approach for incorporating wind power uncertainty and variability into transient stability assessment, as well as identifying critical contingencies that affect system stability.**

***Index Terms*-- Monte Carlo simulation, wind power uncertainty and variability, transient stability.**

I. Introduction

Integration of renewable resources introduces new complexities to the stability assessment of power systems. The main sources of the complexity stem from the uncertain nature of the renewable sources like wind and solar generation, the equipment failure characteristics and the altered inertia in the system due to the power electronics interface to the grid. It is recognized that the traditional deterministic methods to incorporate the increased sources of uncertainty are not adequate and hence comprehensive evaluation methods need to be developed. Moreover, deterministic approaches may not be capable of considering factors like the variability of energy resources and changing equipment characteristics due to increasing use of power electronics. To integrate new characteristics brought by connected wind power, probabilistic stability assessment methods are needed.

II. Methodology, Model and Initial Results

As a probabilistic approach, Monte-Carlo simulation is widely used as the method of selecting system states. It is the most widely application in power systems is generation adequacy assessment. Monte-Carlo simulation includes non-sequential MCS via states sampling and sequential MCS based on states duration time sampling.

In this work, sequential MCS is used to generate the chronological status of wind power, while non-sequential MCS method is used for contingency selection. The overall approach is show in Fig. 1.

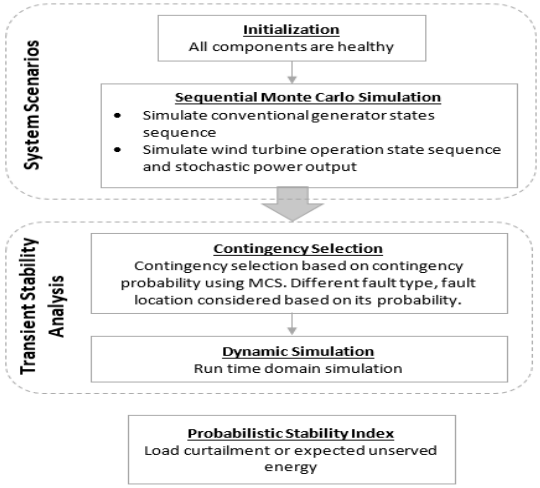

Fig. 1 Probabilitstic stability assesement procedure

Based on the stochastic model, wind turbine output scenarios can be generated as sequential processes. Some initial simulation results are given in Fig. 2 and Fig.3.

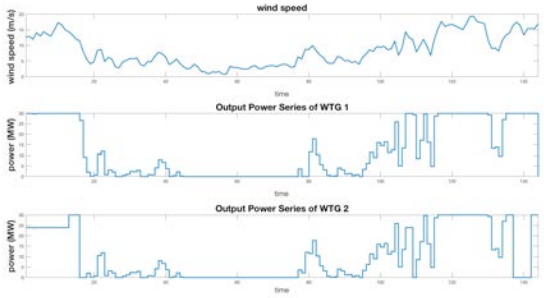

Fig. 2 Stochastic wind power output

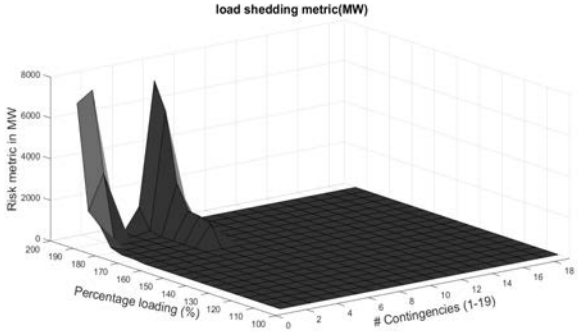

Fig. 3 System risk based on time domain simulation results

New Optimization-Based Algorithms for a Substation Voltage Controller Using Local Synchrophasor Measurements

S. Mohammad Amelian, V. "Mani" Venkatasubramanian
School of Electrical Engineering and Computer Science
Washington State University
Pullman, WA
s.amelian@wsu.edu

Noah Badayos, Farrokh Habibi-Ashrafi,
Armando Salazar, and Backer Abu-Jaradeh
Southern California Edison
Westminster, CA
noah.badayos@sce.com

***Abstract*— This poster presents a substation local voltage controller (SLVC) with available phasor measurement unit (PMU), via optimal usage of its reactive control resources, i.e., shunt reactive devices and transformer taps. Two optimization formulations with different objectives are introduced based on various operating criteria in electric utilities. The first approach aims to minimize the required reactive power injection such that it corrects the substation bus voltages between the determined limits and as close as possible to the optimal values. The second one minimizes number of switching actions, that correct the voltages in the same way mentioned above. Genetic algorithm (GA) is used for solving these discrete optimization problems. Performance of the proposed formulations is tested and analyzed through simulations for a typical substation in Southern California transmission network. Finally, comparison of the obtained results from the two approaches are discussed.**

Keywords—Volt-VAr control, synchrophasor measurement, , local voltage control, optimization, genetic algorithm.

I. Introduction

This poster presents the improved version of an SLVC introduced in [1], using optimization approaches, towards finding the best local control actions within a substation. SLVC uses local PMU measurements and network topology, to predict the local bus voltages after each of the possible control (switching) actions. This prediction is carried out using a Local Voltage Estimator (LVE) which uses linearized reactive power flow equations to estimate the post-switching voltages. Next, two optimization formulations (briefly described above) are solved to bring a deviated bus voltage back within the pre-determined limits and as close as possible to its optimal value. As a result, reactive power reserves of a substation in terms of available MVAr would be maximized, as one of the main performance objectives in power system operation. The two discrete formulations easily fit in as Integer Non-Linear Programming problems. In order to solve this discrete optimization problem, genetic algorithm (GA) is selected, which is capable of handling discrete optimization problems and is proved to be effective in power systems [2]. Since we are solving a relatively small-scale optimization problem, typical speed or convergence issues with GA in dealing with large-scale problems will not be problematic here.

II. Key Results

Simulation results of the proposed formulations (F1 & F2) for a typical 3-level substation in Southern California transmission network, shown in fig. 1, are presented in Table I. They represent the optimal switching combinations of the available reactive control devices in response to voltage deviations for six study cases, and the resulting voltages. Comparing the results with the optimal ones from exhaustive search, it was seen that the proposed formulations overcome the bus voltage deviations and take the corresponding optimal control action to modify the bus voltages.

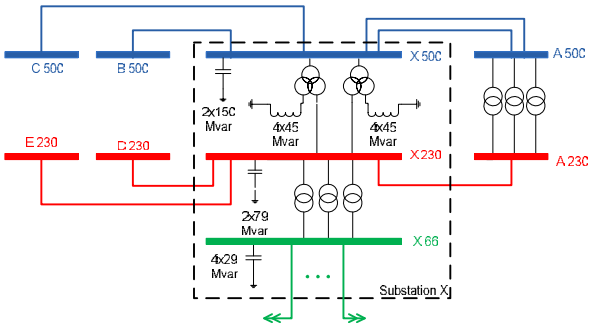

Fig. 1. Diagram of the substation under study.

TABLE I. Resulting voltages and optimal reactive controls for different cases: Formulation 1&2

Device/Bus	Case 1		Case 2		Case 3		Case 4		Case 5		Case 6	
	F1	F2	F1	F2	F1	F2	F1	F2	F1	F2	F1	F2
Reactive injections (MVAr) and tap changings												
X500 Cap.	0	0	0	0	0	1	1	2	2	2	-2	-2
X230 Cap.	0	0	0	0	2	0	2	0	2	2	0	0
X66 Cap.	-1	0	-2	-1	0	0	0	0	0	0	-1	-1
X13.8-Reac1	0	0	0	1	0	0	0	0	0	0	2	1
X13.8-Reac2	0	1	1	1	0	0	0	0	0	0	1	2
Tap_230/66	0	0	0	0	0	0	0	0	0	0	0	0
Tap_500/230	0	0	0	0	0	1	1	1	0	0	0	0
Resulting Voltages (pu)												
X500	1.060		1.060		1.050		1.049		1.051		1.060	
X230	1.009		1.007		1.002		1.000		1.001		1.006	
X66	1.030		1.023		1.023		1.032		1.020		1.030	

References

[1] V. Venkatasubramanian, et al. "Hierarchical two-level voltage controller for large power systems," *IEEE Trans. Power Syst*, vol. 31, no. 1, 2016.

[2] M. Amelian, et al. "Novel Optimization-Based Algorithms for a Substation Voltage Controller Using Local PMU Measurements," *In Proc. of the 51st Hawaii Int'l. Conf. on System Sciences*, *2018*.

Optimal Design of Virtual Inertia and Damping Coefficients for Virtual Synchronous Machines

Atinuke Ademola-Idowu, Baosen Zhang
Electrical Engineering Department,
University of Washington, Seattle, WA 98195
Email: {aidowu, zhangbao}@uw.edu

***Abstract*—Increased penetration of inverter-connected renewable energy sources (RES) in the power system has resulted in a decrease in available rotational inertia which serves as an immediate response to frequency deviation due to disturbances. The concept of virtual inertia has been proposed to combat this decrease by enabling the inverters to produce active power in response to a frequency deviation like a synchronous generator. In this paper, we present an algorithm to optimally design the inertia and damping coefficient required for an inverter-based virtual synchronous machine (VSM) to participate efficiently in the inertia response portion of primary frequency control. We design the objective function to explicitly trade-off between competing objectives such as the damping rate the the frequency nadir. Specifically, we formulate the design problem as a constrained and regularized H2 norm minimization problem, and develop an efficient gradient algorithm for this non-convex problem. This proposed algorithm is applied to a test case to demonstrate its performance against existing methods.**

I. Problem Statement

As the electric power grid transitions from the traditional state only conventional generators to a mix of conventional generators and inverter-connected RES, the immediate response capability by the synchronous machine in the event of a power imbalance to reduce the rate of frequency decline is reduced. This results in an increased rate of change of frequency (ROCOF) and consequently, a higher frequency deviation which results in a low frequency nadir, that is, the maximum frequency deviation. The ROCOF, frequency nadir and settling time/frequency are important frequency response metrics in the power systems network.

II. Proposed Method

To solve this problem, we design an optimal virtual and damping coefficient for a VSM to emulate the inertial response of synchronous machine a based on the ROCOF and frequency deviation. The dynamics of the power system network suitable for analyzing the response of the generators when subjected to disturbances can be represented in first order state space form as in (1):

$$\begin{bmatrix} \dot{\triangle\delta} \\ \dot{\triangle\omega} \end{bmatrix} = \underbrace{\begin{bmatrix} 0 & I \\ -M^{-1}L & -M^{-1}D \end{bmatrix}}_{=A} \begin{bmatrix} \triangle\delta \\ \triangle\omega \end{bmatrix} + \underbrace{\begin{bmatrix} 0 \\ M^{-1} \end{bmatrix}}_{=B} \triangle P \quad (1)$$

where the M and D are the inertia and damping coefficient matrix respectively whose parameters are the inertia and damping values of the individual generators and the virtual inertia and damping parameters of the VSM to be designed.

An augmented $\mathcal{H}_2$ norm is chosen as the objective function for this optimization problem which captures the required frequency response metrics. The optimization problem is then formulated as (2) and computed using using (3):

$$\begin{aligned}
\underset{\mathbf{m},\mathbf{d}}{\text{minimize}} \quad & J_T(\mathbf{m},\mathbf{d}) = \left\|G(\mathbf{m},\mathbf{d})\right\|_2^2 + \beta\|\mathbf{m}\|_2^2 && \text{(2a)}\\
\text{subject to} \quad & \underline{\mathbf{m}} \le \mathbf{m} \le \overline{\mathbf{m}} && \text{(2b)}\\
& \underline{\mathbf{d}} \le \mathbf{d} \le \overline{\mathbf{d}} && \text{(2c)}\\
& A(\mathbf{m},\mathbf{d})P + PA(\mathbf{m},\mathbf{d})^T + B(\mathbf{m})B(\mathbf{m})^T = 0 && \text{(2d)}\\
& A^T(\mathbf{m},\mathbf{d})Q + QA(\mathbf{m},\mathbf{d})^T + C(\mathbf{m})^T C(\mathbf{m}) = 0 && \text{(2e)}\\
& P \succ 0; \quad Q \succ 0 && \text{(2f)}
\end{aligned}$$

where $\left\|G(\mathbf{m},\mathbf{d})\right\|_2^2 = \mathrm{Tr}(B(\mathbf{m})^T Q(\mathbf{m},\mathbf{d})B(\mathbf{m}))$

$$\alpha^{k+1} = \mathrm{Proj}_{\mathcal{C}}[\alpha^k - \gamma \bigtriangledown J(\alpha^k)] \quad (3)$$

where $\alpha = [\mathbf{m}\ \mathbf{d}]^T$ and $\mathcal{C}$ is the set of feasible m and d values. The gradient is derived as in (4):

$$\frac{\partial J}{\partial \alpha} = 2\mathrm{Tr}\left(\frac{\partial A}{\partial \alpha}PQ\right) + \mathrm{Tr}\left(\frac{\partial (BB^T)}{\partial \alpha}Q\right) + \mathrm{Tr}\left(P\frac{\partial (C^TC)}{\partial \alpha}\right) \quad (4)$$

The gradient of $\beta\|\mathbf{m}\|_2^2$ is given as $2\beta\mathbf{m}$.

III. Key Results

The optimization problem in (2) is implemented on a modified 12 bus three-area test case with a disturbance step input applied to one of the nodes, in this case, node 6.

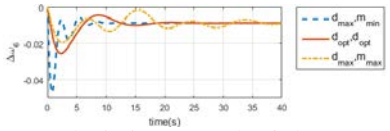

Fig. 1: Frequency deviation at node 6 due to step input. The optimal response balances between a fast and slow ROCOF to give smoother response

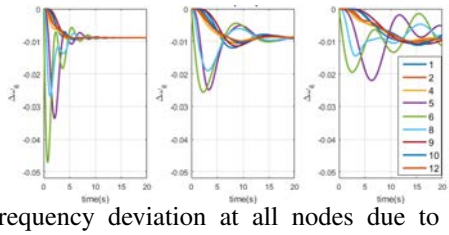

Fig. 2: Frequency deviation at all nodes due to step input in node 6. It shows how the optimal coefficients results in a balanced smoother response in all the nodes. *LHS*: combination of $d_{max}m_{min}$, *MID*: combination of $d_{opt}m_{opt}$, [*RHS*]: combination of $d_{max}m_{max}$.

A N4SID based estimator for identifying the parameters and sources of forced oscillations

Mohammad Mansouri and Andrew M Knight
Department of Electrical and Computer Engineering, University of Calgary, Calgary, Canada

***Abstract*—A blind identification method based on Subspace State Space System IDentification (N4SID) is proposed to identify the sources and parameters of the Forced Oscillations (FOs) in a power system. The proposed method has some advantages such as simplicity, robustness, and being on-line.**

I. Introduction

In power system operation, reliable delivery of electrical power is of paramount concern. Nonetheless, reliability faces various challenges such as electromechanical modes and Forced Oscillations (FOs). Although electromechanical modes and FOs occur in the same frequency range, they are fundamentally different. Electromechanical modes are properties of the power systems dynamics that are typically excited by load variations, whereas FOs are caused by a rogue inputs driving the system. FOs limit inter-area electric power capability, negatively affect the estimation accuracy of natural modes, and seriously threaten the security and stability of power systems. Hence, conducting studies on FOs is of great importance. In this paper, a measurement-based method called N4SID and categorized as a blind identification method, is proposed.

II. Proposed Method

Voltages, currents, electromechanical modes, and FOs are measured by PMUs installed on buses in power system. Considering these measurements as system's outputs, we will have a blind identification problem. Therefore, we can employ N4SID, which categorized as a blind identification, to identify the sources and parameters of FOs. We can also recognize FOs from Electromechanical oscillation because system dynamic is identified, too. The N4SID algorithm can be organized in the following steps:

1) The measured data is formed in a Hankel matrix format, divided in two parts:past data and future data, and the projection of future data on past data is calculated. The singular value decomposition of the projection is extracted as USV, and non-zero part of U and S are called U_1 and S_1.
2) Determine $\hat{X}_i$ and $\hat{X}_{i+1}$ as:

$$\hat{X}_i = \Gamma_i^{\dagger} \varrho_i \quad , \quad \hat{X}_{i+1} = \Gamma_{i-1}^{\dagger} \varrho_{i-1} \tag{1}$$

where

$$\Gamma_i = U_1 S_1^{1/2} \quad , \quad \Gamma_{i-1} = \underline{\Gamma_i} \tag{2}$$

3) Solve the set of linear equation for A and C:

$$\begin{bmatrix} \hat{X}_{i+1} \\ Y_{i|i} \end{bmatrix} = \begin{bmatrix} A \\ C \end{bmatrix} \begin{bmatrix} \hat{X}_i \end{bmatrix} + \begin{bmatrix} \rho_w \\ \rho_v \end{bmatrix} \tag{3}$$

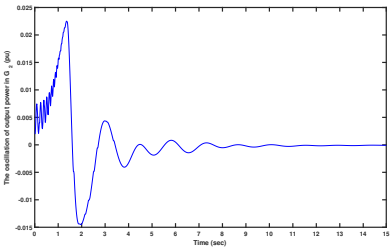

Figure 1. The oscillation of the output power on G_2 after load change

4) Determine Q, S, and R from:

$$\begin{bmatrix} Q & S \\ S^T & R \end{bmatrix} = \frac{1}{j} [\begin{bmatrix} \rho_w \\ \rho_v \end{bmatrix} . \begin{bmatrix} \rho_w & \rho_v \end{bmatrix}] \tag{4}$$

5) Determine Σ^s, G, and Λ_0 from:

$$\begin{aligned} \Sigma^s &= A\Sigma^s A^T + Q \quad solve\ for\ \Sigma^s \\ G &= A\Sigma^s C^T + S \quad solve\ for\ G \\ \Lambda_0 &= C\Sigma^s C^T + R \quad solve\ for\ \Lambda_0 \end{aligned} \tag{5}$$

6) Determine P AND K^f by solving the Riccati equation:

$$\begin{aligned} P &= APA^T + (G - APC^T)* \\ &\quad (\Lambda_0 - CPC^T)^{-1}(G - APC^T)^T \\ K^f &= (G - APC^T)(\Lambda_0 - CPC^T)^{-1} \end{aligned} \tag{6}$$

7) Finally, the identified forward innovation model is:

$$\begin{aligned} x_{k+1}^f &= Ax_k^f + K^f e_k^f \\ y_k &= Cx_k^f + e_k^f \end{aligned} \tag{7}$$

III. Case Study: Four-Machine, Two-Area System

The case study to demonstrate the effectiveness of the N4SID strategy is based on the well-known four-machine, two-area system. The dynamic performance of G_2 under a disturbance is shown in Fig. 1. Using the proposed method, the forward innovation model of the system is identified. The dominant mode, whose frequency and damping are 0.55Hz and 0.08, respectively, can easily be extracted from the identified system. The analysis of the identified system can also help us to distinguish between the FOs and electromechanical modes.

IV. Conclusion

This paper presents a measurement-based strategy for identifying the parameters and sources of FOs that have a ability to distinguish between FOs and electromechanical modes. The simulation confirms the effectiveness of the proposed method.

Towards the New Low-Order System Frequency Response Model of Power Systems with High Penetration of Variable-Speed Wind Turbine Generators

Matej Krpan
Faculty of Electrical Engineering and Computing
University of Zagreb
Zagreb, Croatia
Email: matej.krpan@fer.hr

Igor Kuzle
Faculty of Electrical Engineering and Computing
University of Zagreb
Zagreb, Croatia
Email: igor.kuzle@fer.hr

***Abstract*—In the recent years, frequency support from converter-connected wind power generation has been a hot topic in the field of power system dynamics and control. At the same time, the share of wind generation in the power systems worldwide has significantly risen. Therefore, it is necessary to update existing low-order system frequency response (SFR) models of power systems. In this paper, an approach to low-order SFR modelling of a power system with significant penetration of wind power generation is proposed by taking into account the different operating regimes of variable-speed wind turbine generators (VSWTGs). The results are compared to the nonlinear transient stability dynamic models to show that the low-order model adequately describes the nonlinear model. The proposed model can be used (e.g. by researchers, students or power system engineers) to qualitatively simulate single-area power system frequency behaviour for different operating scenarios.**

I. Introduction

As the share of VSWTGs and other converter-connected generation in the power systems worldwide is exponentially increasing, coupled with the introduction of virtual inertia and power electronics control for frequency support, the paradigm of what is a power system is changing. Low-order SFR models provide a simple platform for studying power system frequency changes by taking into account only the most significant system dynamics in the time scale of interest which is $\leq$ 30 s. Thus, it is necessary to step towards new low-order model of a power system by taking into account the impact of converter-connected generation with frequency support capabilities on the system frequency behaviour. In this paper, the discussion on different operating regimes of VSWTGs is presented alongside with how those regimes are reflected to the SFR model of a power system through the low-order models of VSWTGs. An approach to linearizing VSWTGs by taking into account different operating regimes is presented.

II. Summary of Results

- Zone I: low wind speeds, VSWTGs do not participate in frequency support, system inertia reduction;
- Zone II/III: medium wind speeds, VSWTGs can participate in frequency support, rotor speed control only;
- Zone IV: high wind speeds, VSWTGs can participate in frequency support, pitch angle control active.

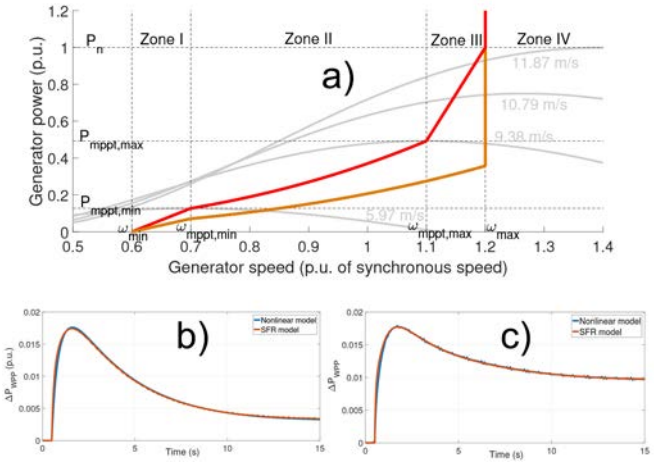

Fig. 1. Operating zones of a VSWTG (a); comparison of SFR model to nonlinear model for zones II/III (b) and IV (c)

A. Key equations

Low order-models for zones II/III (1) and IV (2),(3):

$$\frac{N(s)}{D(s)} = \frac{2H\omega_0 s - (k_{del}\omega_0^2 + a_1\omega_0)}{2H\omega_0 s - \omega_0(a_1 - 2k_{del}\omega_0)}. \tag{1}$$

$$N(s) = 2HT_s s^3 + (2H - a_{11}T_s - \frac{T_{e,0}}{\omega_0}T_s)s^2 - \\ - (a_{11} + a_{13}K_p + \frac{T_{e,0}}{\omega_0})s - a_{13}K_i, \tag{2}$$

$$D(s) = 2HT_s s^3 + (2H - a_{11}T_s)s^2 - \\ - (a_{11} + a_{13}K_p)s - a_{13}K_i. \tag{3}$$

Oscillation Monitoring and Control of the RTE Power System Using Synchrophasors

M.farrokhifard, V. "Mani" Venkatasubramanian
School of Electrical Engineering and Computer Science
Washington State University
Pullman, WA
M.maddipourfarrokhi@wsu.edu@wsu.edu

***Abstract*— This poster will carry out a study of modes' characteristics by available PMU data in RTE portion of European power grid. Frequency Domain Decomposition (FDD) and Stochastic Subspace Identification (SSI) methods are used for modes identification. Analysis of oscillation phenomena in the RTE portion of the European power grid by Implementation of WSU oscillation analysis tools is another aim of this poster. The effectiveness of the oscillation algorithms by using simulated PMU data from dynamic models of the RTE system wherein the expected answers are known from small-signal analysis of the dynamic models is tested. Furthermore, appropriate control algorithms will be proposed in collaboration with RTE to address the oscillation issues in RTE system.**

Keywords— Frequency Domain Decomposition, Synchrophasor Measurement, Stochastic Subspace Identification, Power System Oscillation

I. INTRODUCTION

Recent advances in design of fast oscillation monitoring algorithms have paved the way for real-time detection and analysis of electromechanical oscillations from wide-area synchrophasor measurements in large power interconnections. The oscillations if left unmitigated can lead to unwanted tripping of transmission lines and generators that could cascade into devastating blackouts. Oscillation monitoring algorithms developed at Washington State University have previously been implemented and tested in North American power grid and in India. In this poster, we will study oscillation phenomena in the RTE portion of the European power grid by using available synchrophasor data. Suitability of ambient versus ringdown analysis algorithms for analyzing recent oscillation events in RTE will be investigated. Oscillation analysis results using transmission level PMUs will be compared with corresponding results using distribution level Phasor Measurement Units (PMUs). The effectiveness of the oscillation algorithms will be tested and improved by using simulated PMU data from dynamic models of the RTE system wherein the expected answers are known from small-signal analysis of the dynamic models. New oscillation analysis and control algorithms will be developed in collaboration with RTE to address the oscillation issues in RTE.

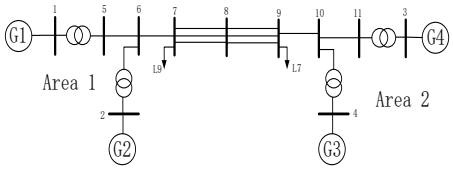

Fig. 1. Kundur two area test system

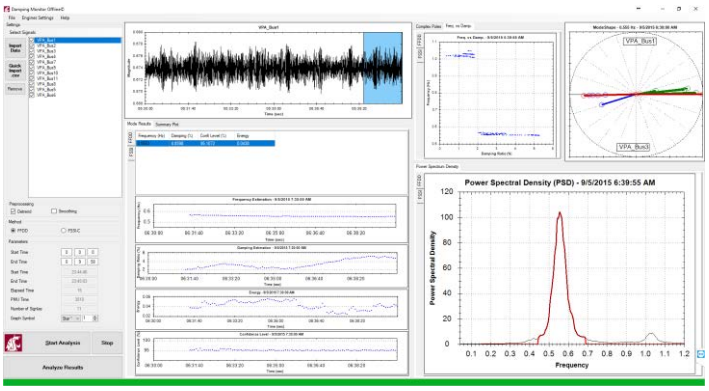

Fig. 2. A view of WSU DMO analyzing simulated PMU data

II. KEY RESULTS

Since RTE PMU data and results cannot be shown now in this abstract, we show a case study in which PMU simulated data of Kundur two area test system, shown in Fig. 1, is imported in WSU Damping Monitor Offline (DMO) tool. This system has an inter area mode with frequency of 0.56 Hz and damping ratio of 4 percent and a local mode with frequency of 1.02 Hz and damping ratio of 1.5 percent, as shown in Fig. 2.

REFERENCES

[1] Guoping Liu, J. Quintero and V. M. Venkatasubramanian, "Oscillation monitoring system based on wide area synchrophasors in power systems," *2007 iREP Symposium - Bulk Power System Dynamics and Control - VII. Revitalizing Operational Reliability*, Charleston, SC, 2007, pp. 1-13

[2] S. A. Nezam Sarmadi, and V. Venkatasubramanian, "Electromechanical mode estimation using recursive adaptive Stochastic Subspace Identification", *IEEE Trans. Power Syst.*, vol.29, pp. 349–358, Jan. 2014.

Adaptive Adjustment of Noise Covariance in Kalman Filter for Dynamic State Estimation

Shahrokh Akhlaghi, *Student Member, IEEE,* Ning Zhou, *Senior Member, IEEE,* Zhenyu Huang, *Senior Member, IEEE*

***Abstract*—It is well known that the covariance matrixes of process noise (*Q*) and measurement noise (*R*) have a significant impact on the Kalman filter's performance in estimating dynamic states. To address this problem, this paper proposes an adaptive filtering approach to adaptively estimate *Q* and *R* based on *innovation* and *residual* to improve the dynamic state estimation accuracy of the extended Kalman filter (EKF). It is shown through the simulation on the two-area model that the proposed estimation method is more robust against the initial errors in *Q* and *R* than the conventional method in estimating the dynamic states of a synchronous machine.**

I. Introduction

Timely and accurately estimating the dynamic states of a synchronous machine (e.g., rotor angle and rotor speed) is important for monitoring and controlling the transient stability of a power system over wide areas [1]. [2] proposed the unscented Kalman filtering to estimate power system dynamic states. Akhlaghi, Zhou and Huang [3] proposed an adaptive interpolation approach to mitigate the impact of non-linearity in dynamic state estimation (DSE). These studies have laid a solid ground for estimating the dynamic states of a power system and also revealed some needs for further studies.

One important problem that needs to be addressed in using the KF is how to properly set up the covariance matrixes of process noise (i.e., *Q*) and measurement noise (i.e., *R*). Note that the performance of the KF is highly affected by *Q* and *R* [5]. Improper choice of *Q* and *R* may significantly degrade the KF's performance and even make the filter diverge. To address this challenge, this paper proposes an estimation approach to adaptively adjust *Q* and *R* at each step of the EKF to improve DSE accuracy. An *innovation*-based method is used to adaptively adjust *Q*. A *residual*-based method is used to adaptively adjust the *R*. A simple example is used to evaluate the impact of *Q* and *R* on the performance of EKF. Then, performance of the proposed approach is evaluated using a two-area model [1].

II. Dynamic State Estimation Model

$$\begin{cases} \dfrac{d\delta}{dt} = \omega_0 \Delta\omega_r & (1.a) \\ \dfrac{d\Delta\omega_r}{dt} = \dfrac{1}{2H}\left(T_m - T_e - K_D\Delta\omega_r\right) & (1.b) \\ \dfrac{de'_q}{dt} = \dfrac{1}{T'_{d0}}\left(E_{fd} - e'_q - (x_d - x'_d)i_d\right) & (1.c) \\ \dfrac{de'_d}{dt} = \dfrac{1}{T'_{q0}}\left(-e'_d + (x_q - x'_q)i_q\right) & (1.d) \end{cases}$$

A. Adaptive Extended Kalman Filter (AEKF)

$$\bar{S}_k = E\left[\varepsilon_k\varepsilon_k^T\right] = E\left[\nu_k\nu_k^T\right] - H_k^{[1]}P_k^- H_k^{[1]T}$$
$$R_k = E\left[\varepsilon_k\varepsilon_k^T\right] + H_k^{[1]}P_k^- H_k^{[1]T} \quad (2)$$

1) Innovation Based Adaptive estimation of Q

$$Q_k = \alpha Q_{k-1} + (1-\alpha)(\bar{K}_k d_k d_k^T \bar{K}_k^T) \quad (3)$$

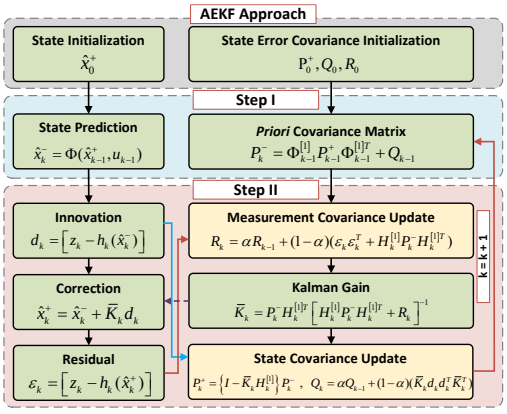

Fig. 1. Implementation flowchart of the proposed AEKF

TABLE I. MSEs of the Estimated Position from the **CEKF**

MSE	**0.01 Q_{true}**	**0.1 Q_{true}**	**Q_{true}**	**10 Q_{true}**	**100 Q_{true}**
0.01 R_{true}	0.051	0.083	0.0984	0.0987	0.0988
0.1 R_{true}	0.219	0.051	0.083	0.0984	0.0988
R_{true}	3.54	0.219	0.051	0.083	0.098
10 R_{true}	27.28	3.54	0.219	0.051	0.083
100 R_{true}	41.40	27.28	3.54	0.219	0.051

TABLE II. MSE of the Estimated Position from the **AEKF**

MSE	**0.01 Q_{true}**	**0.1 Q_{true}**	**Q_{true}**	**10 Q_{true}**	**100 Q_{true}**
0.01 R_{true}	0.0714	0.0787	0.0788	0.0788	0.0789
0.1 R_{true}	0.09	0.076	0.0783	0.0786	0.0787
R_{true}	0.12	0.089	0.072	0.073	0.0736
10 R_{true}	0.13	0.089	0.087	0.076	0.076
100 R_{true}	0.17	0.089	0.081	0.078	0.074

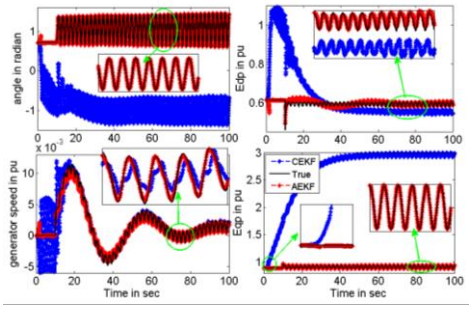

Fig. 2. Comparison of AEKF and CEKF when the initial *Q* is set to be relatively less than the proper value.

References

[1] P. Kundur, *Power System Stability and Control*. New York, NY, USA: McGraw-Hill, 1994.

[2] H. G. Aghamolki, Z. Miao, L. Fan, W. Jiang, D. Manjure, "Identification of synchronous generator model with frequency control using unscented Kalman filter," *Electric Power Systems Research*, vol. 126, pp. 45-55, Sep. 2015.

[3] S. Akhlaghi, N. Zhou, Z. Huang, "A Multi-Step Adaptive Interpolation Approach to Mitigating the Impact of Nonlinearity on Dynamic State Estimation," in Proc. *IEEE Transaction on Smart Grid*.

[4] N. Zhou, D. Meng, Z. Huang, G. Welch, "Dynamic state estimation using PMU Data: a comparative study," *IEEE Trans. Smart Grid*, vol. 6, no. 1, pp. 450-460, Jan. 2015.

[5] A. H. Mohamed and K. P. Schwarz, "Adaptive Kalman filtering f or INS/GPS," *J. Geodesy*, vol. 73, no. 4, pp. 193-203, 1999.

Probabilistic Transient Stability Assessment of Renewable Generation Integrated Power System

Yingying Wang, *Student Member*, *IEEE*, Mojdeh Khorsand, *Member*, *IEEE*, and Vijay Vital, *Fellow*, *IEEE*
School of Electrical, Computer and Energy Engineering, Arizona State University, Tempe, AZ, USA
ywang935@asu.edu, Mojdeh.Khorsand@asu.edu, and Vijay.Vittal@asu.edu

***Abstract*—The stochastic characteristic of wind power has introduced challenges to traditional deterministic dynamic security assessment of power systems. A probabilistic approach based on Monte-Carlo simulation (MCS) is proposed in this work to integrate wind power uncertainty and variability into transient stability analysis of power grids. Fault probability including fault rate, fault type and fault location are taken into consideration in the transient stability assessment. System stability is evaluated in term of loss of load to maintain stability after the disturbance and its probability. A synthetic 36-bus test system is utilized to verify the proposed approach. The simulation results show the effectiveness of the proposed approach for incorporating wind power uncertainty and variability into transient stability assessment, as well as identifying critical contingencies that affect system stability.**

***Index Terms*-- Monte Carlo simulation, wind power uncertainty and variability, transient stability.**

I. Introduction

Integration of renewable resources introduces new complexities to the stability assessment of power systems. The main sources of the complexity stem from the uncertain nature of the renewable sources like wind and solar generation, the equipment failure characteristics and the altered inertia in the system due to the power electronics interface to the grid. It is recognized that the traditional deterministic methods to incorporate the increased sources of uncertainty are not adequate and hence comprehensive evaluation methods need to be developed. Moreover, deterministic approaches may not be capable of considering factors like the variability of energy resources and changing equipment characteristics due to increasing use of power electronics. To integrate new characteristics brought by connected wind power, probabilistic stability assessment methods are needed.

II. Methodology, Model and Initial Results

As a probabilistic approach, Monte-Carlo simulation is widely used as the method of selecting system states. It is the most widely application in power systems is generation adequacy assessment. Monte-Carlo simulation includes non-sequential MCS via states sampling and sequential MCS based on states duration time sampling.

In this work, sequential MCS is used to generate the chronological status of wind power, while non-sequential MCS method is used for contingency selection. The overall approach is show in Fig. 1.

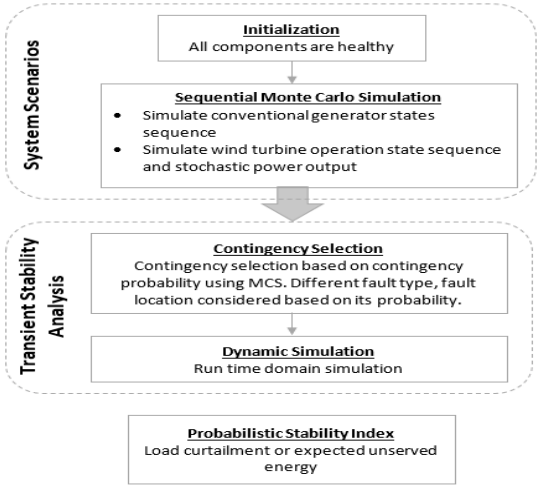

Fig. 1 Probabilitstic stability assesement procedure

Based on the stochastic model, wind turbine output scenarios can be generated as sequential processes. Some initial simulation results are given in Fig. 2 and Fig.3.

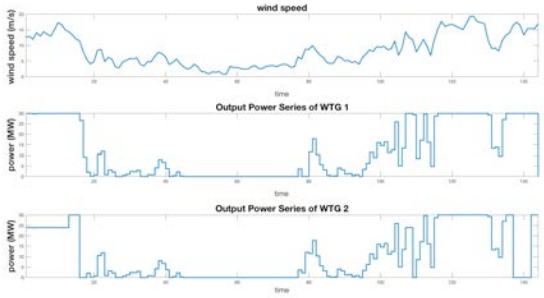

Fig. 2 Stochastic wind power output

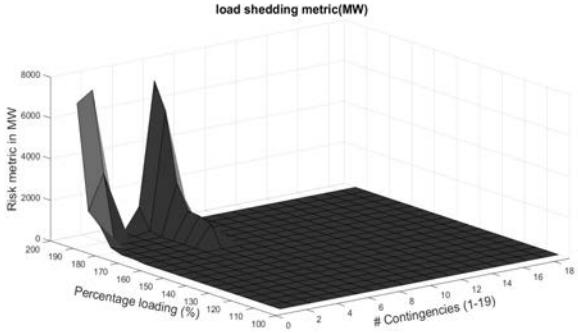

Fig. 3 System risk based on time domain simulation results

Decreasing the Ice Storm Risk on Power Conductors by DSRs and Dispatch Adjustment

Sahar Lashkarbolooki, Anil Pahwa
Department of Electrical and Computer Engineering
Kansas State University
Manhattan, Kansas
lashkarb@ksu.edu, pahwa@ksu.edu

Al Tamimi, Ryan Yokley
Sunflower Electric Power Corporation
Hays, Kansas
atamimi@sunflower.net, ryokley@sunflower.net

***Abstract*— This poster presents an approach for leveraging distributed series reactance (DSR) and generation dispatch adjustment to prevent ice buildup on power conductors during ice storm. DSRs are deployed to increase current on at-risk lines by blocking the power flow on parallel routes. Also, shifting some of the wind turbine generations to non-wind ones during the storm reduces the risk of huge power flow fluctuation on power lines which occurs due to wind turbine shutoffs under heavy winds. These approaches are implemented hourly based on the sensitivity of power flow on the at-risk lines with respect to impedance changes due to DSRs and generation dispatch adjustment. The dispatch adjustment could be limited by non-wind generation ramp rates and the wind generations capacity during storm. In addition, the DSRs can be limited by voltage stability issues and their technical specifications. Leveraging both methods simultaneously is helpful to cover their limitations to determine a suitable solution.**

Keywords—DSRs; dispatch; sensitivity; ice-storm;

I. KEY EQUATIONS

A. Sensitivity calculation with respect to impedance changes:

DC power flow:

$$\begin{bmatrix} B_{11} & B_{12} & \cdots & B_{1N} \\ B_{21} & B_{22} & \cdots & B_{2N} \\ \vdots & \vdots & \vdots & \vdots \\ B_{N1} & B_{N2} & \cdots & B_{NN} \end{bmatrix} \begin{bmatrix} \delta_1 \\ \delta_2 \\ \vdots \\ \delta_N \end{bmatrix} = \begin{bmatrix} P_1 \\ P_2 \\ \vdots \\ P_N \end{bmatrix} \tag{1}$$

$$B_{11}\delta_1 + B_{12}\delta_2 + \cdots + B_{1m}\delta_m + B_{1n}\delta_n + \cdots + B_{1N}\delta_N = P_1$$

$$B_{k1}\delta_1 + B_{k2}\delta_2 + \cdots + B_{km}\delta_m + B_{kn}\delta_n + \cdots + B_{kN}\delta_N = P_k$$

$$\begin{bmatrix} B_{11} & B_{12} & \cdots & \cdots & \cdots & \cdots & B_{1N} \\ B_{21} & B_{22} & \cdots & \cdots & \cdots & \cdots & B_{2N} \\ \vdots & \vdots & \vdots & \vdots & \vdots & \vdots & \vdots \\ B_{m1} & B_{m2} & \cdots & B_{mm} & B_{mn} & \cdots & B_{mN} \\ B_{n1} & B_{n2} & \cdots & B_{nn} & B_{nm} & \cdots & B_{nN} \\ \vdots & \vdots & \vdots & \vdots & \vdots & \vdots & \vdots \\ B_{N1} & B_{N2} & \cdots & \cdots & \cdots & \cdots & B_{NN} \end{bmatrix} \begin{bmatrix} \frac{\partial \delta_1}{\partial X_{mn}} \\ \frac{\partial \delta_2}{\partial X_{mn}} \\ \vdots \\ \frac{\partial \delta_m}{\partial X_{mn}} \\ \frac{\partial \delta_n}{\partial X_{mn}} \\ \vdots \\ \frac{\partial \delta_N}{\partial X_{mn}} \end{bmatrix} = \begin{bmatrix} 0 \\ 0 \\ \vdots \\ \frac{1}{X_{mn}^2}\delta_m - \frac{1}{X_{mn}^2}\delta_n \\ \frac{1}{X_{mn}^2}\delta_n - \frac{1}{X_{mn}^2}\delta_m \\ \vdots \\ 0 \end{bmatrix} \tag{2}$$

$$\frac{\partial f_{mn}}{\partial X_{mn}} = \frac{1}{X_{mn}}\left(\frac{\partial \delta_m}{\partial X_{mn}} - \frac{\partial \delta_n}{\partial X_{mn}}\right) - \frac{1}{X_{mn}^2}(\delta_m - \delta_n) \tag{3}$$

B. Sensitivity calculation with respect to dispatch adjustments

$$[B][\delta] = [P], \Delta P = \begin{bmatrix} 0 \\ 0 \\ +\Delta P_m \\ 0 \\ 0 \\ -\Delta P_m \\ 0 \\ 0 \end{bmatrix}, \left[\frac{\partial \delta}{\partial P_m}\right] = [B]^{-1} \begin{bmatrix} 0 \\ 0 \\ +1 \leftarrow m \\ 0 \\ 0 \\ -1 \leftarrow n \\ 0 \\ 0 \end{bmatrix}, \begin{bmatrix} \frac{\partial \delta_1}{\partial P_m} \\ \vdots \\ \vdots \\ \vdots \\ \vdots \\ \vdots \\ \frac{\partial \delta_N}{\partial P_m} \end{bmatrix} = [B]^{-1} \begin{bmatrix} 0 \\ 0 \\ +1 \\ 0 \\ 0 \\ -1 \\ 0 \\ 0 \end{bmatrix} \tag{4}$$

$$f_{12} = \frac{\delta_1 - \delta_2}{X_{12}} \Rightarrow \frac{\partial f_{12}}{\partial P_m} = \frac{1}{X_{12}}\left(\frac{\partial \delta_1}{\partial P_m} - \frac{\partial \delta_2}{\partial P_m}\right) \tag{5}$$

$$f_{new} = f_{old} + \frac{\partial f}{\partial P_m} * \Delta P_m \tag{6}$$

C. Net effect of DSRs by sensitivity calculation

$$sum_m = \frac{\partial f_{203}}{\partial x_m} * \Delta x_m + \frac{\partial f_{220}}{\partial x_m} * \Delta x_m + \frac{\partial f_{227}}{\partial x_m} * \Delta x_m + \frac{\partial f_{229}}{\partial x_m} * \Delta x_m \tag{7}$$

D. Net effect of dispatch adjustments by sensitivity calculation

$$sum_m = \frac{\partial f_{203}}{\partial P_m} * \Delta P_m + \frac{\partial f_{220}}{\partial P_m} * \Delta P_m + \frac{\partial f_{227}}{\partial P_m} * \Delta P_m + \frac{\partial f_{229}}{\partial P_m} * \Delta P_m \tag{8}$$

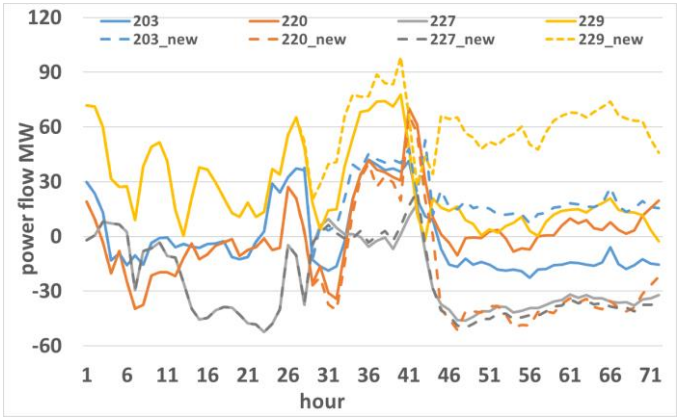

Fig. 1. Power flow results.The solid lines are the initial power flows and the dashed lines are updated ones in presence of DSRs and dispatch adjustment.

Fractional Order PI Control for Microgrid Application

Rasheed Abdulkader
Electrical Engineering Dept.
University of Arkansas
Fayetteville, AR USA
rabdulka@uark.edu

Roy McCann
Electrical Engineering Dept.
University of Arkansas
Fayetteville, AR USA
rmccann@uark.edu

***Abstract*— The increasing use of distributed energy resources has motivated the development of microgrid structures to improve reliability of electric power distribution systems. However, as microgrids become more complex, there is an increased occurrence for instabilities. This research investigates fractional order proportional--derivative (FOPI) control technique which is implemented in a decentralized manner to stabilize the voltage levels throughout a microgrid structure; hence, the algorithm would be synchronized into a grid system forming a smart grid. A method for analyzing three parallel-connected inverters based upon distributed generation is presented. To validate the proposed control algorithm, Matlab simulation is used and FOPI is compared to conventional control methods such as PI and PID. The proposed control algorithm demonstrates an improved performance response to regulate the system analyzed.**

Keywords—Microgrid, FOPID, transient stability, distributed generation.

I. INTRODUCTION

In recent years, the deployment of renewable resources at the distribution level has acquired an increasing attention to utilities around the world. Thus, it can be a promising solution to the issue of increasing fossil fuel cost. While the formation of microgrids from distributed generation systems plays a critical role in efficient utilization of energy, resources and can contribute heavily to the stability of the public power grid [1]. This trend has many advantages and numerous distributed generation poses many challenges that should be eliminated. Thus, regulation and stability of the system is of a great concern and it is the objective of this proposal.

While different topologies are being proposed for interfacing microgrids with the national grid, still the use of interconnected power electronic converts can make instability of the power flow in a system [2]. Hence integrating distributed generators into the power grid might introduces a bidirectional power flow with the resulting system which changes the whole power flow pattern of the existing system and generates concern for its stability [3].

In this paper, the problem of FOPI controller design strategy is examined, consequently the proposed algorithm [allows the integration of the fractional order scheme into existing PI/PID control loop which would result in enhanced performance of the control loop. The system analyzed and the transfer function is derived for each source based on [4].

Factional order control has acquired an increasing attention recently in the control community due to their better control performance when compared to traditional integer order controllers Fractional order calculus dates to three centuries back, hence it would provide a novel modeling approach for systems with extraordinary dynamical properties by introducing a non- integer fractional order system [5]. While there is a variety of control regulation methods applied to microgrids such PI/PID control for their simplicity, whereas they lack robust voltage regulation and have limited capabilities when applied to complex systems [6].

RESULTS

To achieve preliminary results a fractional FOPID controller is applied using Matlab by evaluating a step response to the system. Simulation results demonstrates improved that FOPI leads to improved stability margins and system performance as compared to classical PI.

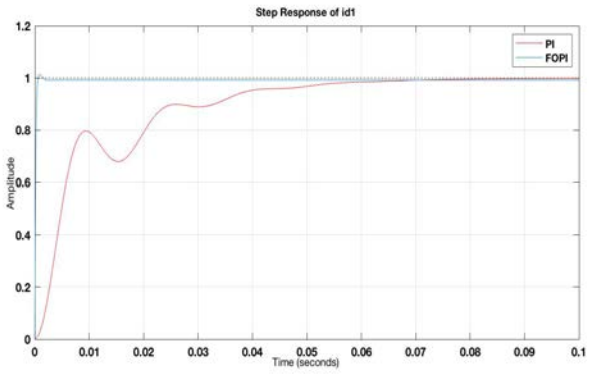

Fig1. Step response PID/FOPID

REFRENCES

[1]X. Tang, W. Deng, and Z. Qi, “Investigation of the Dynamic stability of microgrid,” *IEEE Trans. Power Syst.*, vol. 29,no.2, pp. 698−706, Mar. 2014.

[2] M. Reza, D. Sudarmadi, F.A. Viawan, W.L. Kling, and L. Van Der Sluis, "Dynamic Stability of Power Systems with Power Electronic Interfaced DG," in *Power Systems Conference and Exposition*, 2006, Atlanta, 2006, pp. 1423−1428.

[3] A. B. M. Nasiruzzaman and H. R. Pota, "A new model of centrality measure based on bidirectional power flow for smart and bulk power transmission grid" in *EEEIC* 2012., May. 2012, pp.1−6.

[4 M. Naderi, Y. Khayat, Y. Batmani, H. Bevrani," Robust Multivariable Microrid Control Synthesis and Analysis", In 3rd International conference on power and Energy Systems Engineering, CPESE 2016, 8-12 September 2016, Kitakyushu, Japan.

[5] Tepljakov, Aleksei . Fractional-order Modeling and Control ofmDynamic Systems. Springer International Publishing AG 2017.

[6] M. Mahmoud, N. Alyazidi, M. Abouheaf, Adaptive intelligent techniques for microgrid control systems: A survey, In *Electrical Power and Energy Systems* Volume 90, March 2017, 292-305.

Parameter Space and Rotor Angle Stability Control of Virtual Synchronous Machine

Chen Qi, *Student Member, IEEE*, Keyou Wang, *Member, IEEE* and Guojie Li, *Senior Member, IEEE*
MOE Key Lab of Power Transmission and Power Conversion and Control
Shanghai Jiao Tong University
Shanghai, China 200240
Emails: ee.qichen@sjtu.edu.cn; wangkeyou@sjtu.edu.cn; liguojie@sjtu.edu.cn

***Abstract*—The virtual synchronous machine (VSM) technology is able to control the inverter to mimic the behaviors of the traditional synchronous generator. In this paper, the rotor angle stability of VSM is thoroughly analyzed under the classic second-order dynamic model in a single machine (inverter) infinite bus system. Possible situations covering the global parameter space are presented, analyzed and verified through simulations. Furthermore, the idea of global bifurcation structure shaping (GBSS) control is proposed, which can eliminate the attractor that causes the rotor angle instability under emergency and thus guarantee the stability.**

I. System Model

The VSM dynamics are analyzed based on its normalized second-order model, which can be expressed as

$$\frac{d\delta}{d\tau} = z \tag{1}$$

$$\frac{dz}{d\tau} = -\alpha z - \sin\delta + \beta \tag{2}$$

II. Parameter Space

For the studied system, a parameter space is proposed, which is shown in Fig. 1.

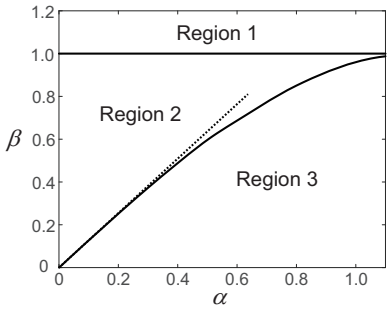

Fig. 1. Parameter space of the normalized VSM dynamic model.

According to Fig. 1, the system stability properties can be expressed as:

1) Region1: when $\beta > 1$, there is only one attractor for the system in the cylinder coordinate, which is the periodic solution. All system trajectories are attracted by this periodic solution. Therefore, the system definitely loses stability.
2) Region2: when $\beta < 1$ and $\alpha < \alpha^*(\beta)$, there are two attractors for the system in the cylinder coordinate, which are the SEP solution and the periodic solution. System trajectories are attracted be either one of the attractors. When the trajectory is attracted by the SEP solution, the system is stable, otherwise the system loses stability.
3) Region3: when $\beta < 1$ and $\alpha > \alpha^*(\beta)$, there is only one attractor in the cylinder coordinate, which is the SEP solution. All system trajectories are attracted by this SEP solution. Therefore, the system is always stable.

III. VSM Validation

The proposed parameter space is validated using the VSM simulations performed in Matlab/Simulink. The dynamic behaviors of the system in region 2 and 3 are shown in Fig. 2 respectively.

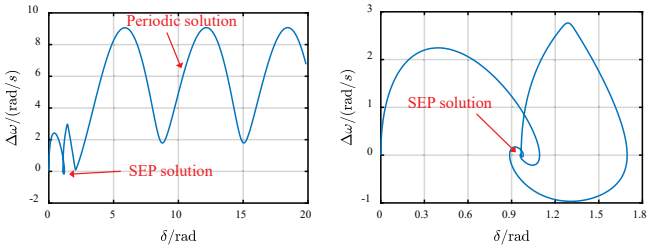

(a) (b)

Fig. 2. System state trajectories $(\delta, \Delta\omega)$ when the VSM operates in (a) region 2 (may lose stability) and (b) region 3 (always keeps stability).

IV. GBSS Control

The GBSS control is proposed to actively move the operating point of the VSM into the region 3 during emergency, which eliminates the periodic solution that causes the instability and shapes the system trajectories to keep the stability. The control diagram and the simulation result are shown in Fig. 3, where the unstable scenario in Fig. 2(a) can be controlled to be stable with the GBSS technique.

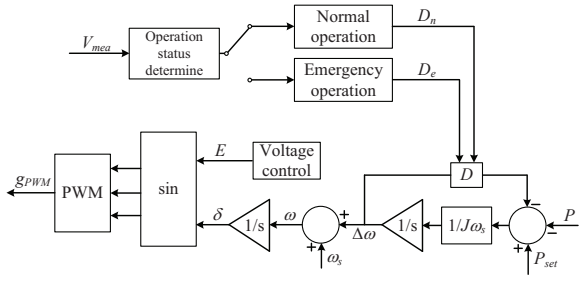

(a)

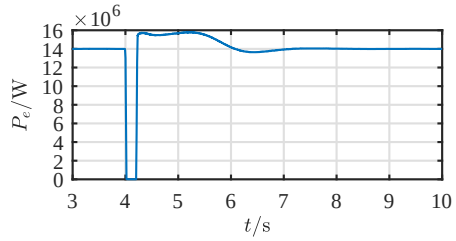

(b)

Fig. 3. GBSS control diagram and the simulation result.

Design of a Supercapacitor Energy Storage System for Marine Turbines Utilizing Advanced Control

Hannah Aaronson[1], Brian Polagye[1], Robert Cavagnaro[2]
1. Department of Mechanical Engineering, University of Washington
2. Advanced Physics Laboratory, University of Washington
Seattle, WA, USA
haarons@uw.edu

***Abstract*— Previous studies optimizing control strategies for cross-flow (i.e., "vertical axis") marine turbines found that sinusoidally varying rotor speed within a single rotation can increase mechanical power output by up to 50%. However, this control strategy, known as intracycle control, also comes with a cost: power output is estimated to fluctuate between *producing* 22 kW and *drawing* 15 kW twice per two second rotation of a two-bladed turbine. This power quality is incompatible with direct use. Here, we describe an energy storage system that smooths the power output from a peak to average ratio of 8.8 to 1.4 without introducing energy losses that offset the efficiency gains from this control strategy.**

Keywords— Marine turbines; marine renewable energy; energy storage system, supercapacitors, simulation

I. System Design

The design objectives of the proposed energy storage system (ESS) are to eliminate power draw from the grid, minimize the peak to average ratio of the output power, and minimize energy losses internal to the ESS. The proposed ESS has two parts, as highlighted on the DC bus between the turbine and grid in Fig. 1. Part I, inspired by research on regenerative braking for electric vehicles, uses a supercapacitor to eliminate the need for the turbine to draw from the grid. This power draw normally occurs when the turbine is commanded to accelerate during some phases of intracycle control. The capacitor charges when the turbine produces power (and vice versa), with excess power available to the grid once the capacitor is fully charged. Part II includes a supercapacitor and a bi-directional DC-DC converter. This uses a PI controller to maintain constant power delivery to the grid by requiring the supercapacitor to charge when instantaneous power is greater than the average power per cycle, and discharge when it is less than the average power per cycle.

II. Simulation Results

The proposed system is modeled in Matlab Simulink, and representative results are shown in Fig. 2. The original power delivered to the grid is in blue, highlighting the large power fluctuations over a short time period. After adding ESS Part I, turbine power draw from the grid is eliminated. When both ESS Part I and ESS Part II are used, the peak to average ratio of the power delivered to the grid is reduced from 8.8 to 1.4. The ESS introduces energy losses between 6 to 8%, due to the internal resistance of the capacitors and switches. The ESS appears to smooth power to an acceptable degree and is feasible to implement on a turbine in terms of its complexity, size, and efficiency. The next step of this research project is to validate the simulation results experimentally, using lab-scale hardware.

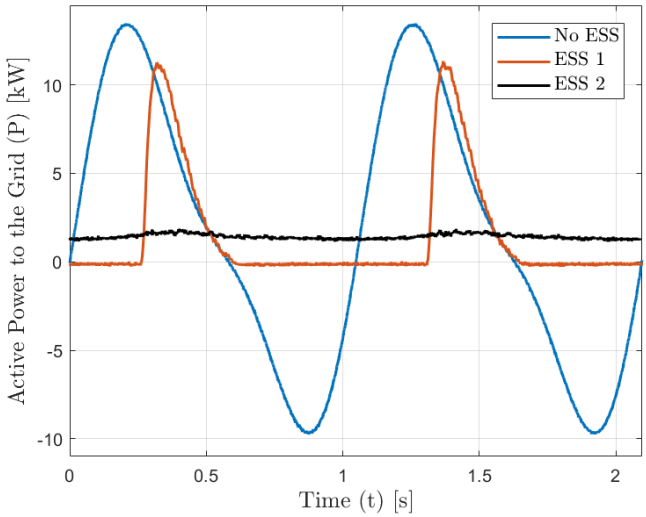

Fig. 2. Simulation results of power delivered to the grid using the energy storage system.

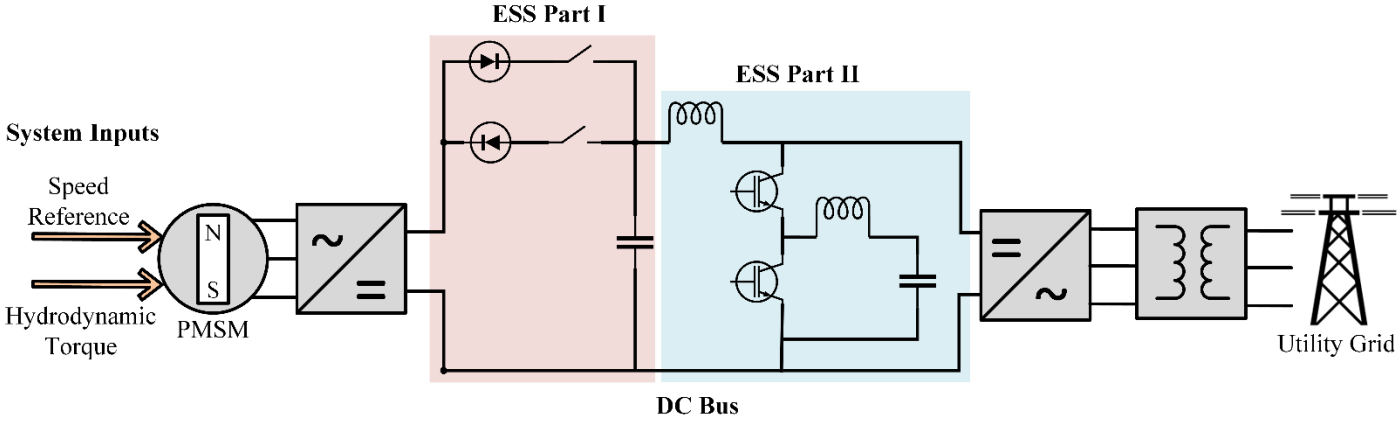

Fig. 1. Simplified simulation layout of the proposed two-part energy storage system, with Part I highlighted in red and Part II highlighted in blue.

Fault Ride Through Analysis of Grid Connected Doubly Fed Induction Generator Based Wind System

M V Gururaj, Student Member IEEE, Narayana Prasad Padhy, Senior Member IEEE
Department of Electrical Engineering, Indian Institute of Technology Roorkee, India

***Abstract*— The world is slowly moving towards renewable based power generation to avoid the demerits associated with the conventional generation mainly global warming. Further, the increased depletion rate of fossil fuels over the years has enhanced the research investments on the renewables like photovoltaic (PV), Wind etc. Among variable speed wind generators, doubly fed induction generators (DFIG) based wind plants has gained more popularity over their counterparts. In this paper, the operation of DFIG based wind system in the grid connected mode is studied along with fault analysis.**

Index Terms-- DFIG, fault Ride Through, Grid side converter (GSC), Rotor side converter (RSC), Wind energy.

I. Introduction

In this paper, the theoretical analysis of the DFIG based wind system during the fault is presented. Further, in order to study the practical behavior of the DFIG system, a 2.2 KW rated DFIG machine is connected to the programmable voltage source. The performance of the system is analyzed during normal and fault operation. During normal operating conditions the machine is controlled to exchange power with the grid at UPF with the help of RSC. A three phase to ground fault is introduced for a duration of 150ms to test the robustness/stability of the controller. The experimental results are in match with the theoretical analysis during FRT. This study helps to develop fault ride through improvement techniques for the DFIG system in future.

II. Fault Analysis of DFIG

When fault occurs, the grid voltages drops. The voltage of the DFIG stator (v_s^s) before and after fault is given below.

$$v_s^s = \begin{cases} V_{pre}\, e^{j\omega_s t}, & t < 0 \\ (1-p)V_{pre}\, e^{j\omega_s t}, & t \geq 0 \end{cases} \quad (1)$$

The expression of the stator flux during fault conditions is given below.

$$\psi_s^s = \frac{pV_{pre}}{j\omega_s} e^{-t/\tau_s} + \frac{(1-p)V_{pre}}{j\omega_s} e^{j\omega_s t} \quad (2)$$

Further, each component of the flux induces emf in the rotor, e_r^r as shown below.

$$e_r^r = \frac{L_m}{L_s} V_{pre} \left(s(1-p)e^{j\omega_r t} - (1-s)pe^{-j\omega_m t} e^{-\frac{t}{\tau_s}} \right) (3)$$

III. Key Hardware Results

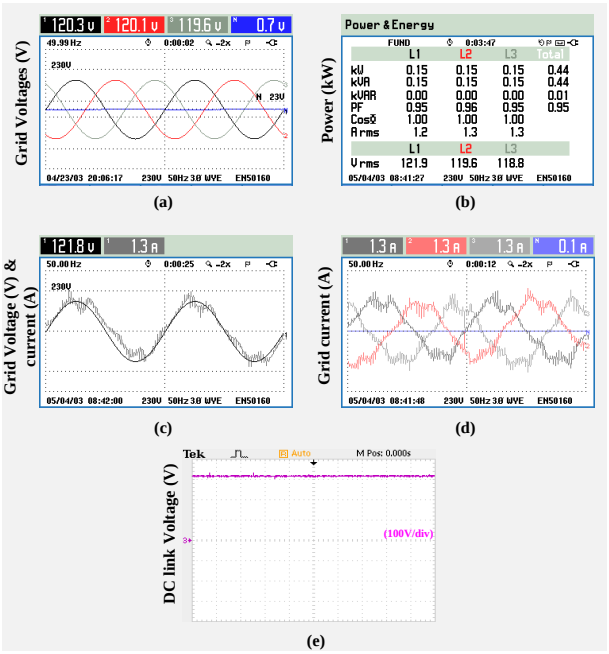

Fig 1: Normal operation: (a) Grid voltages (b) power flow to the grid (c) Grid voltage, current of phase A. (d) Three phase grid currents (e) DC link voltage.

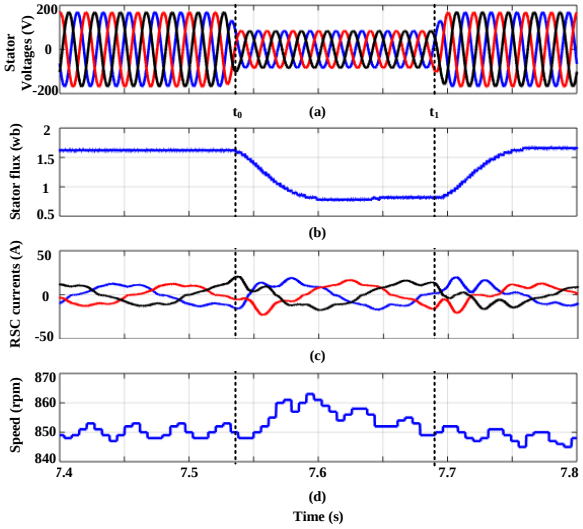

Fig 2: Experimental results during fault (a) Stator voltages (b) stator flux (c) RSC currents. (d) Rotor speed in rpm

Design and Performance Analysis of Low Cost Acoustic Chamber for Electric Machines

R. M. Pindoriya, *Student Member, IEEE*, B. S. Rajpurohit, *Senior Member, IEEE* and R. Kumar
Indian Institute of Technology Mandi, Himachal Pradesh, India
pindoriya_rajesh@students.iitmandi.ac.in

***Abstract*—This work discusses the design, and performance analysis of low cost acoustic chamber for measurement of acoustic noise and vibration of electric machines. The purpose of this paper is to calculate acoustic transfer function, reverberation time, sound power level and cut-off frequency. To obtain the transfer function of the acoustic chamber, a pair of microphones and amplifier as a source of sound have been used. Noise measurements are conducted in both an ordinary environment (laboratory) and acoustic chamber and validated through Inverse Squared Law. The results obtained are found to be helpful in understanding the physical features and characteristics of the acoustic chamber.**

I. Introduction

Nowadays consumers demand more smooth and silent devices, whether it is a computer, vacuum cleaner, electrical drives or washing machine. The free-field enclosure required to test electrical devices. The free-field enclosure may be anechoic chamber, semi-anechoic chamber or acoustic chamber. Organizations like International Organization for Standardization (ISO), International Electrotechnical Commission (IEC), IEEE etc. provide suitable guidelines regarding to the construction and testing for the chamber [1].

An Acoustic Chamber (AC) has been designed and assembled at IIT Mandi, as shown in Figs. 1-2, to perform suitable studies on vibration and acoustic noise of electric machines/drives. Fig. 1 shows the schematic of AC with sensor placements and broad dimensions. A wooden ply of thickness of 12 mm is used for making walls of AC with egg shape wedge acoustic foam (density 32 kg/m^3) attached at both sides with sound barrier sheet made up of polymer vinyl sheet (density 1.07 mg/m^2).

The general expression for the Sound Pressure Level (SPL) difference as a function of acoustic transfer functions can be obtained as [1]:

$$D = L_S - L_R = 10log\left[\frac{\int_{-\infty}^{\infty}|H_S(f)|^2\,df}{\int_{-\infty}^{\infty}|H_R(f)|^2\,df}\right] \quad (1)$$

where L_S and L_R is the SPL measured by sensors in the source room and in the receiving room (cabin) in dB, respectively. $H_S(f)$ and $H_R(f)$ are the forward and reverse acoustic transfer function, respectively, between certain microphone and sound source position in the source room and the receiving room, respectively. An experimental setup for characterization and performance analysis of AC is shown in Fig. 2. An amplified sound signal of 60 dB and 6000 Hz from an external amplifier has been generated and recorded by two microphones i.e. one placed inside the AC and another outside of it.

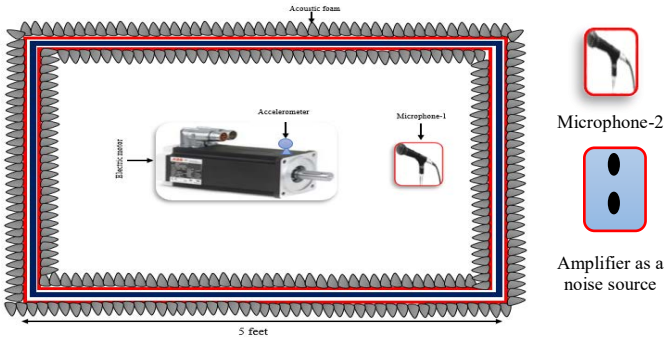

Fig. 1. Schematic layout of acoustic chamber.

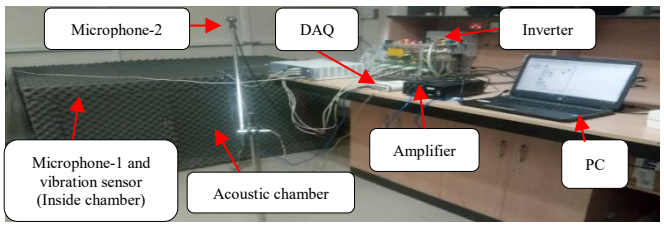

Fig. 2. An experimental setup for characterize of acoustic chamber.

Transfer function plot of forward transfer function ($H_S(f)$) on a semi-log scale is plotted in Fig. 3. It is found that the cut-off frequency of AC is 40 Hz. Fig. 4 shows the noise spectrum record by microphone-1, which is placed inside the AC, with highest noise of around 1.2*e^{-3} Pa (approximate 40 dB).

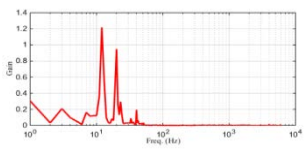

Fig. 3. Bode plot of forward transfer function $H_S(f)$.

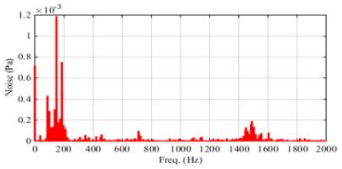

Fig. 4. Noise spectrum of acoustic chamber.

So, based on above results we conclude that this AC is provide free-field environment to measure acoustic noise and vibration of electric machines.

Reference

[1] A. C. Binojkumar, B. Saritha, and G. Narayanan, "Acoustic Noise Characterization of Space-Vector Modulated Induction Motor Drives—An Experimental Approach," *IEEE Trans. Ind. Electron*., vol. 62, no. 6, pp. 3362–3371, Jun. 2015.

Demagnetization Fault Detection and Analysis for a Permanent Magnet Synchronous Machine

Adil Usman, *Student Member, IEEE* and Bharat S. Rajpurohit, *Senior Member, IEEE*
School of Computing and Electrical Engineering
Indian Institute of Technology Mandi
Mandi, Himachal Pradesh, India
adilusman@ieee.org

***Abstract*—** This poster will present the results of a demagnetization effect [1] [2] on the Permanent Magnet Synchronous Machine (PMSM). A PMSM model for both for healthy and faulty conditions [3] has been developed using a Finite Element Modeling Method (FEMM) tool [4]. The model of a faulty machine can be developed by changing one or more parameters of the Permanent Magnet (PM) in the rotor of a PMSM in order to incorporate a demagnetization fault in the machine.

This paper compares and focuses on the demagnetization fault in PMSM by changing two parameters of the Permanent Magnet. One of which is changing the ***magnetic coercivity (H_C)*** parameter of a PM while the other is changing the ***length of a PM*** which signifies a broken magnet, in the rotor of the machine. The change in coercivity parameter and magnet length is used as the demagnetization factor which changes the machine parameters such as flux linkage and current in the coil. Since currently our research is focused on observing only the effect of change in *magnetic flux density (BM) (which is directly proportional to the back emf of the machine)* against the *angular displacement of the rotor (Θ)* for a healthy and faulty PMSM. Therefore any deviation observed in magnetic flux density (B_M) identifies the demagnetization fault in PMSM. In order to know the cause of demagnetization which could be either due to change in coercivity or change in magnet dimensions (length), the simulation results obtained distinguishes them from each other.

The results clearly detect the demagnetization effect in PM of a PMSM along with identifying the cause of it. Secondly the change in coercivity (H_C) which causes an equivalent change in magnetic flux density (B_M), validates the direct relation of H_C with B_M in a liner magnetic circuit. This work is an elaboration to the existing research work done on modeling demagnetization faults in Permanent Magnet Direct Current (PMDC) Motors which is accepted for presentation in IEEE PES GM 2018.

***Index Terms*—Demagnetization Faults, Finite Element Modeling Method (FEMM), Permanent Magnet DC Motor (PMDC), Permanent Magnet Synchronous Motor (PMSM).**

DEMAGNETIZATION RESULTS

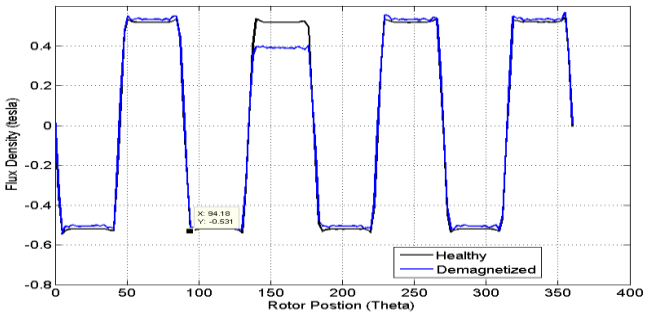

Fig.1 Demagnetization effect of a PMSM due to change in coercivity factor. Number of Poles=8, Pole Angle=2°, $H_{c\ healthy}$= 979000 A/m, **k (coercivity factor) =0.8**, $H_{c\ faulty}$= 783200A/m

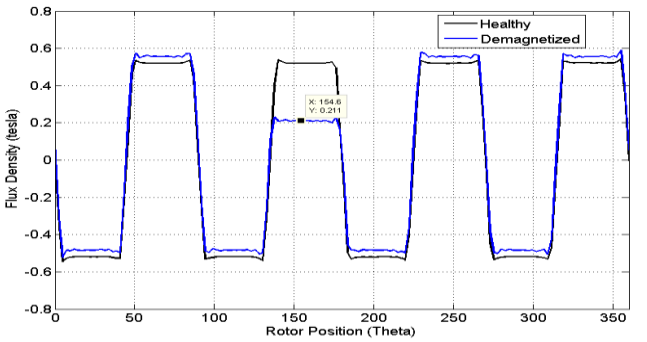

Fig.2 Demagnetization effect of a PMSM due to change in coercivity factor. Number of Poles=8, Pole Angle=2°, $H_{c\ healthy}$= 979000 A/m, **k (coercivity factor) =**0.5, **$H_{c\ faulty}$=** 489500A/m.

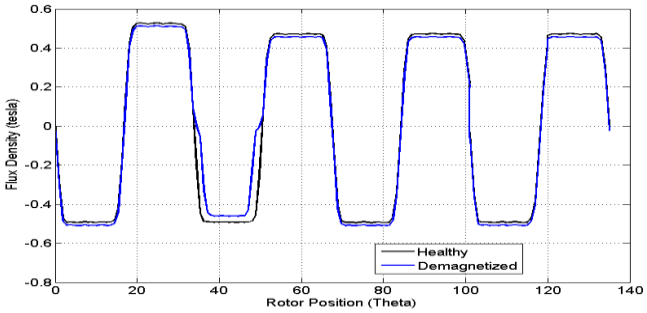

Fig.3 Demagnetization effect of a PMSM due to the ***change in magnet length*** of a PM in PMSM. Number of Poles=8, Pole Angle=2°, $H_{c\ healthy}$= 979000 A/m, **k (coercivity factor) =** 1

CONCLUSION

The flux density plots obtained from the FEMM modeling can be further utilized in analyzing the performance of the machine.

REFERENCES

1. P. C. Krause, O. Wasynczuk, S. D. Sudhoff, Analysis of Electric Machinery, New York:IEEE Press, 1994.
2. J. Faiz and H. Nejadi-Koti, "Demagnetization Fault Indexes in Permanent Magnet Synchronous Motors—An Overview," in *IEEE Transactions on Magnetics*, vol. 52, no. 4, pp. 1-11, April 2016.
3. J. Hong *et al*., "Detection and Classification of Rotor Demagnetization and Eccentricity Faults for PM Synchronous Motors," in *IEEE Transactions on Industry Applications*, vol. 48, no. 3, pp. 923-932, May-June 2012.
4. www.femm.info

Behavioral Device-Level Modeling of Modular Multi-level Converters in Real-Time for Variable Speed Drive Applications

Ning Lin, *Dept. of Electrical and Computer Engineering*
University of Alberta
Edmonton, Canada
ning3@ualberta.ca
Venkata Dinavahi, *Dept. of Electrical and Computer Engineering*
University of Alberta
Edmonton, Canada
dinavahi@ualberta.ca

Abstract

This paper presents the real-time hardware-in-the-loop (HIL) emulation of an induction machine (IM) driven by a modular multi-level converter (MMC) on the field-programmable gate array (FPGA). The insulated gate bipolar transistors (IGBTs) and anti-parallel diodes of the MMC are modeled with nonlinear static and dynamic characteristics to provide not only accurate system-level performance of the converter but also an insight into the power losses under different operation conditions. Due to the large network size of the MMC, its solution in conjunction with the induction machine fifth-order model proved to be a significant computational challenge. Therefore, circuit partitioning based on the transmission line modeling (TLM) is proposed, which introduced an interface to the electrical network for the IM as well as split the multi-loop MMC into several smaller sub-circuits in terms of matrix size, and consequently enabled a fully parallel implementation on the FPGA. Control strategies for the MMC and IM are also emulated in hardware, and due to the large latency difference between sub-circuits and controllers, the overall system hardware design is divided into several layers, each having an independent time-step ranging from 500 ns to 4 μs so as to attain the goal of real-time execution. Comparison of transient and steady-state results from the HIL emulation and off-line simulation tools shows high accuracy of the modeling approach as well as the efficacy of proposed multiple time-steps in achieving real-time.

Index Terms

Field-programmable gate array (FPGA), induction machine, modular multi-level converter (MMC), parallel processing, partitioning algorithms, real-time systems

Harmonic Mitigation and a Practical Study of Torque Harmonics in Induction Motor Startup

Parviz Khaledian, Brian K Johnson, Saied Hemati
Dept. of Electrical and Computer Engineering,
University of Idaho
Moscow, USA

***Abstract*—In this paper, the nature of harmonics due to the operation of nonlinear power system components, the effects of harmonics and methods to eliminate the harmonics will be discussed briefly. Therefore, it helps to compare the compensation methods and choose the best one based on the application. Harmonics are the major source power quality problems for power systems. Therefore, harmonic mitigation techniques are inevitable in power systems and sometimes in the power converters themselves. This paper reviews the common harmonic mitigation techniques. Further, it includes a case study that introduces a different approach to practically mitigate the unwanted harmonics in a 12000 hp synchronous motor that failed to start up with a soft starter.**

***Index Terms*—Active filter, harmonic mitigation, power converter, power quality, torque harmonics.**

I. The Proposed Method in The Case Study

We take three steps: describe the issue, determine its causes, and present a practical mitigation technique.

1: *The problem:* A 12000 hp synchronous motor failed to start up with a soft starter.

2: The causes: The SCRs elements of the starter introduce harmonics to the system. Therefore, the resultant rotating flux consists of the odd harmonics in addition to the fundamental frequency. The fundamental wave revolves synchronously at synchronous speed Ns, whereas 5th harmonics revolve with Ns/5 backward and the 7th harmonics with Ns/7 in forward direction. The harmonic torques result in vibrations, and noise. This phenomenon is known as crawling. There are several torque dips on the resultant motor torque T (Fig. 1).

If the torque dip is lower than the T_{load}, the motor will not have enough torque to start successfully. That is happening around 1/7 of the synchronous speed.

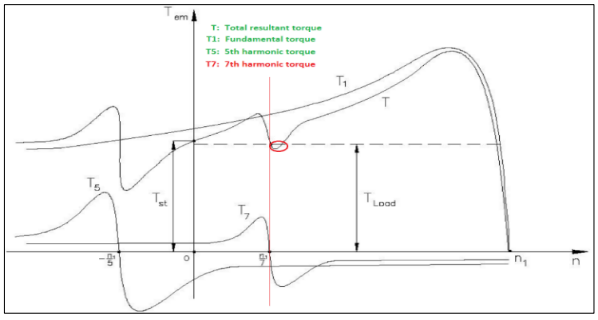

Figure 1. Torque characteristics considering space harmonics.

3: *Practical mitigation technique:* In our case, the remedy is by modifying the startup procedure.

The torque harmonics generated based on input voltage harmonics can be distinguished as following:

$$T_{6k+1} = A_{6k+1}\cos(6k\omega_s t + \theta_{6k+1}) = \Psi_{m(6k+1)} I'_{r1}\cos(6k\omega_s t) - \Psi_{m1} I'_{r(6k+1)}\sin(6k\omega_s t) \quad (1)$$

To diminish the impact of T_7 (T_{6k+1} for k=1) on the resultant torque T (Eq. 1), we decrease the I'_{r1}. It is done by a new start up procedure (Fig. 2 and 3). We have different SCR phases ranging from 70% to 100%.

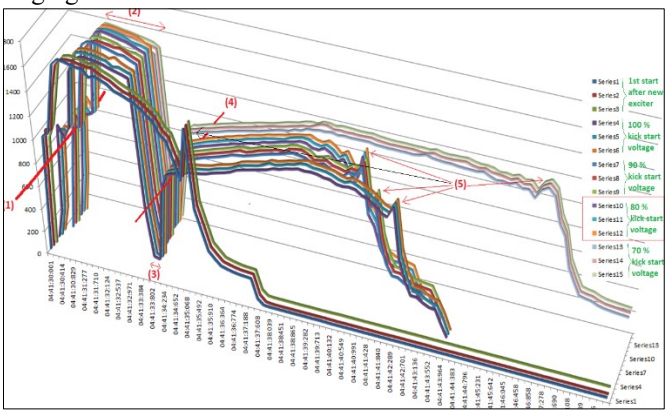

Fig. 2. Five series of startup current measurements for different SCR phases

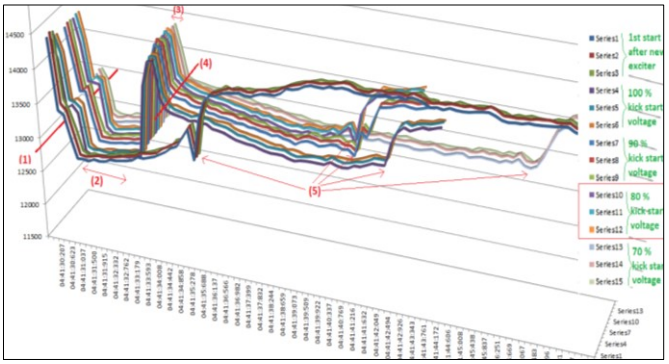

Fig. 3. Five series of startup voltage measurements for different SCR phases

The procedure is as follows: (1) Initially, SCRs start at 60% voltage. Then SCRs ramp up to full voltage in one second, where the starter doesn't contain a high degree of harmonic current. (2) The bypass contactor would then close approximately three seconds later, bringing the motor across the line. (3) The SCRs are off for about one second. (4) SCRs are back on at about 50% voltage and ramp up. (5) The motor gets synchronized.

As soon as we pass the 1/7th of the synchronous speed the harmonic torques are not an issue for startup, because the torque is more than the load torque.

II. Conclusions

Various harmonic sources and several strategies to eliminate or compensate their effects have been discussed. At the end, a case study with actual measurements and its practical remedy is presented. By considering several alternative methods to mitigate harmonics, the decision will be based on the objectives for facility power quality and the budget available.

Dynamic Modeling in OpenDSS: An Implementation Sequence for Object Pascal

Andrés Argüello, Weld L. Cunha, Tiago R. Ricciardi, Ricardo Torquato and Walmir Freitas
Department of Systems and Energy, University of Campinas, Campinas, SP, Brazil
andresag@dsee.fee.unicamp.br

***Abstract*—This paper presents a procedure to implement user-written models in OpenDSS for dynamic simulations using its predefined generator element and the software's original source code in Object Pascal. The implications on the coding of a dynamic model, the internal structure and the solving algorithm sequence are addressed in order to guide the user through such process. The aforementioned is illustrated by implementing a fourth order synchronous machine as generator model and a second order hydro turbine as shaft model.**

***Index Terms*—Distribution networks, Dynamic modeling, Hydraulic turbine, Object Pascal, OpenDSS, Synchronous machine, User-written model**

I. Introduction

The integration of more controllable distributed energy resources such as energy storage and distributed generation brings together the necessity of specialized studies at MV and LV level, such as dynamic performance evaluation. While dynamics study at the transmission level well consolidated in power engineering, it presents novel challenges in distribution.

OpenDSS is a script-driven simulation engine for distribution networks, widely used for power flow analysis, harmonic power flows and short circuit studies, yet it is not limited to these features since EPRI encourages users to contribute to its continuous development. A characteristic of OpenDSS that remains relatively unexplored is its capability to run dynamic simulations. Nevertheless, it only includes a classic synchronous machine model in the generator element to study its swings during disturbances and an induction machine.

II. Dynamic Simulation in OpenDSS, Small Hydro Generator Coding in Object Pascal

The main contribution of this paper consists of a step-by-step procedure in Pascal to understand the use and implementation of user-written *dll*s in OpenDSS for dynamic analysis, with examples of a fourth order *dq* synchronous machine and a non-linear second order hydro turbine based shaft model.

```
new generator.Gen bus1=b2 kVnom=13.8
~ kVAnom=5000 UserModel=SyncGen model=6
~ UserData=(kVnom=13.8 kVAnom=5000
  Phases=3 H=3 D=1 Rs=0.001 Xd=1.5 Xld=0.2
  Xq=1.5 Xlq=0.2 Tld0=3.0 Tlq0=0.0081
  kWsp=0.2 efd=1.0) ShaftModel=HydroTurb
~ ShaftData=(ref=0.2 Tw=3 T1=1)
```

$$\dot{U} = T_W^{-1}\left(H - H_0\right) \qquad \dot{G} = T_1^{-1}\left(g_{ref} - g\right)$$

$$H = \left(U/G\right)^2 \qquad T_W = LU_r\left(a_g H_r\right)^{-1}$$

$$g = G\left(g_{FL} - g_{NL}\right) \qquad P_m = \left(U - U_{NL}\right)H \tag{1}$$

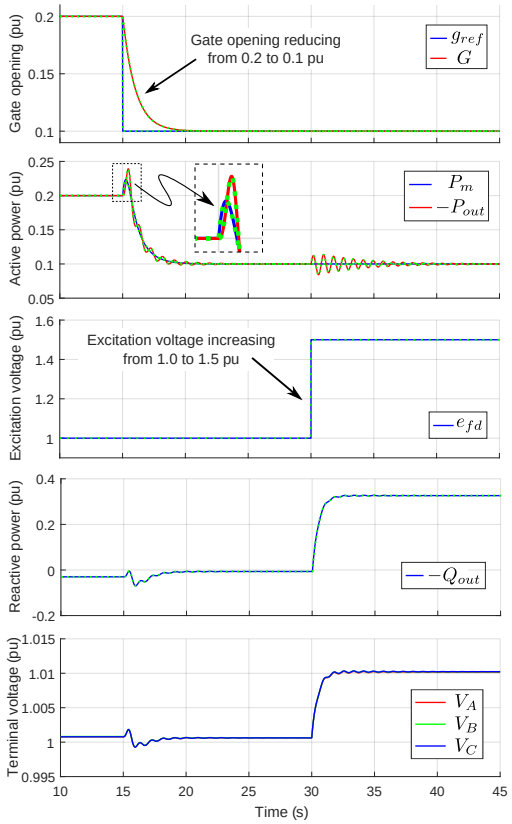

Fig. 1. Model response to turbine gate and excitation voltage steps.

$$\dot{\delta} = \omega_0\left(\omega - 1\right) \qquad \dot{\omega} = \left(2H\right)^{-1}\left(T_m - T_{el} - D\left(\omega - 1\right)\right)$$

$$\dot{e'_d} = \left(T'_{q0}\right)^{-1}\left(-e_{ld} + \left(X_q - X'_q\right)i_q\right)$$

$$\dot{e'_q} = \left(T'_{d0}\right)^{-1}\left(e_{fd} - e'_q - \left(X_d - X'_d\right)i_d\right)$$

$$T_m = P_m/\omega \qquad T_{el} = e'_d i_d + e'_q i_q + \left(X'_q - X'_d\right)i_d i_q$$

$$\begin{pmatrix} i_d \\ i_q \end{pmatrix} = \frac{1}{{R_s}^2 + X'_d X'_q}\begin{pmatrix} R_s & X'_q \\ -X'_d & R_s \end{pmatrix}\begin{pmatrix} e'_d - v_d \\ e'_q - v_q \end{pmatrix} \tag{2}$$

III. Conclusions

The authors are currently working in the implementation of a Python-based platform and a dynamic model library, with storage systems, static converters, protection and control devices, prime sources (wind turbines and PV panels), and higher order machines. These models are expected to widen the analysis capabilities of OpenDSS, as an additional tool for educational, research and industry purposes.

Analyzing Mutual Influences of Conventional and Distributed FACTS via Stochastic Co-optimization

Yuanrui Sang and Mostafa Sahraei-Ardakani
Department of Electrical and Computer Engineering
University of Utah
Salt Lake City, USA
{yuanrui.sang, mostafa.ardakani}@utah.edu

***Abstract*—Distributed flexible AC transmission systems (D-FACTS) is an attractive power flow control technology, featuring low cost and flexibility for re-deployment. Optimal allocation of D-FACTS and the mutual influence between existing FACTS and newly planned D-FACTS are challenging but important issues that need to be addressed. This paper proposes a co-optimization model of FACTS and D-FACTS based on stochastic optimization, considering the uncertainties caused by fluctuating load and renewable energy generation. Using this model, the location and set points of FACTS and D-FACTS can be co-optimized; in a system with existing FACTS, the locations of FACTS can be pre-determined and the locations of D-FACTS can be optimized. The study shows that existing FACTS affects the optimal locations of D-FACTS and adding D-FACTS into the system affects the optimal set points of existing FACTS. Thus, it is essential to co-optimize the two technologies to maximize their economic benefits.**

Keywords—distributed flexible AC transmission systems (D-FACTS), flexible AC transmission systems (FACTS), optimal allocation, power system economics, stochastic optimization

I. Introduction

In recent years, distributed flexible AC transmission systems (D-FACTS) have become an increasingly popular power flow control technique, with the successful deployment of its commercial version, Smart Wires, in many transmission systems [1]. D-FACTS is a light-weight version of conventional flexible AC transmission systems (FACTS), which can be attached to transmission line conductors or towers in a relatively large quantity to achieve a desired power flow control capability [2]. An issue that arises from the increasing popularity of D-FACTS is its co-optimization with other power flow control technologies, such as TCSC. This paper aims at filling this gap by proposing a computationally efficient co-optimization model of FACTS and D-FACTS considering uncertainties in the network and study the mutual influence of the two technologies when D-FACTS are allocated in a system with existing FACTS, such as the influence of FACTS on the optimal locations of D-FACTS, and the influence of D-FACTS on optimal FACTS set points. Simulations were carried out on a modified RTS-96 test system; uncertainties of renewable generation and load fluctuation were both considered. Results do not only prove that D-FACTS is a more economic option than FACTS, but also show the mutual influences between the two technologies need to be considered in order to maximize the economic benefits when allocating D-FACTS in a system with existing FACTS.

II. Key Results

TABLE I. Expected Dispatch and Wind Curtailment Savings

FACTS locations	Maximum investment ($/h)	D-FACTS not co-optimized with FACTS		D-FACTS co-optimized with FACTS	
		Expected dispatch cost savings	Expected wind curtailment savings	Expected dispatch cost savings	Expected wind curtailment savings
22	10	4.07%	23.17%	4.01%	21.63%
	20	4.57%	24.42%	4.57%	24.42%
	30	4.73%	24.93%	5.20%	27.92%
22,23	10	5.31%	30.21%	5.31%	30.21%
	20	5.78%	29.84%	5.78%	29.84%
	30	5.97%	31.53%	6.16%	32.07%
19,22,23	10	5.91%	31.00%	5.94%	34.21%
	20	6.24%	32.83%	6.26%	35.79%
	30	6.55%	33.74%	6.60%	33.79%

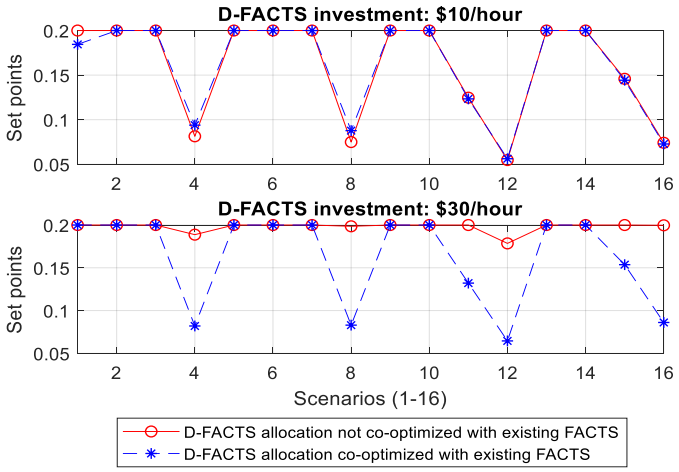

Fig. 1. FACTS set point comparison when D-FACTS locations were co-optimized and not co-optimized with existing FACTS in the system

References

[1] Smart Wires Press Release (2017, November). Smart Wires' Millennium Milestone. Smart Wires, Union City, CA. [Online]. Available: https://www.smartwires.com/2017/11/27/smart-wires-millennium-milestone/

[2] D. Divan and H. Johal, "Distributed FACTS—A New Concept for Realizing Grid Power Flow Control," *IEEE Trans. Power Electron.*, vol. 22, no. 6, pp. 2253-2260, Nov. 2007.

Analysis of Transient Stability According to Initial Operating Condition of STATCOM

Hyeokjin Noh and Byongjun Lee*
School of Electric Engineering
Korea University
Seoul, Republic of Korea
leeb@korea.ac.kr

Seungryul Lee
Smart Power Grid Research Center
Korea Electrotechnology Research Institute
Uiwang, Republic of Korea
srlee@keri.re.kr

***Abstract*—In spite of the continuous increase of electric power demand, the Korean power system is difficult to construct additional transmission facilities due to social acceptability problem. Therefore, FACTS is considered for ensuring transient and voltage stability due to large disturbance such as double fault in 765kV transmission line. In addition, as the proportion of renewable energy including wind power is expanded, it is necessary to introduce a FACTS that can flexibly cope with unstable renewable energy output changes. In order to effectively increase the flexibility of the existing system, there is a need for efficient configuration and operation of the FACTS in a situation where the power grid acceptability is limited. In the case of STATCOM, it is possible to control to output a certain reactive power initially according to the system condition. In case of a large-scale assumption failure, it is necessary to provide inductive output for securing reactive power reserve. When disturbance occurs at this time, the reactive power output changes to the voltage control mode out of the predetermined range. If the reactive power output does not recover within the control range after a fault, there is also a Slow Reset Control controller which arbitrarily lowers the scheduled voltage value and brings in the reactive power output value within a given range. Thus various studies have been conducted to utilize the reactive power control mode of STATCOM. In this paper, we analyze the transient stability according to the initial reactive power output value of STATCOM.**

Keywords—STATCOM; Transient Stability; Initial Operating Point

I. KEY FIGURES

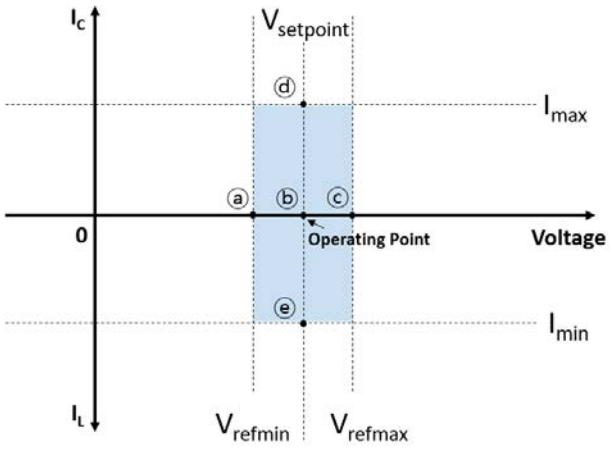

Fig. 1. Steady State Powerflow Boundary Conditions (STATCOM)

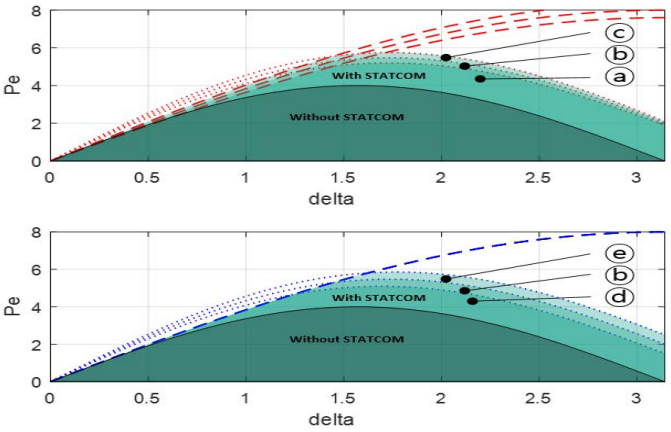

Fig. 2. Corresponding Power-Angle Representation of Voltage and Reactive Power

II. KEY RESULTS

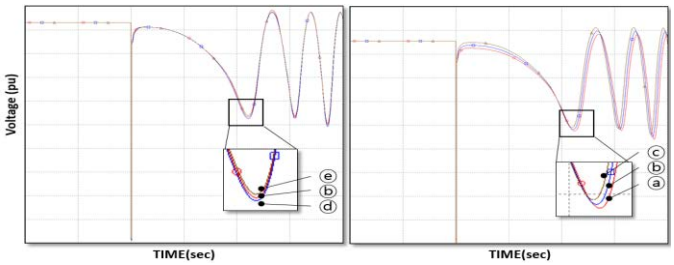

Fig. 3. Transient Stability Results According to Voltage and Reactive Power

III. CONCLUSION

Various control schemes are being studied for efficient operation of STATCOM. In this paper, the initial operating point of STATCOM is classified into voltage and reactive power output magnitude, and its influence is analyzed. In conclusion, we confirmed that the higher the voltage command value of the STATCOM and the larger the inductive reactive power output, the more the transient stability is secured.

REFERENCES

[1] M. H. Haque, "Improvement of First Swing Stability Limit by Utilizing Full Benefit of Shunt FACTS Devices" IEEE Trans. Power Syst., vol. 19, no. 4, pp. 1894–1902, Nov. 2004.

[2] Narain G. Hingorani, "Understanding FACTS", IEEE PRESS, pp. 135-207, 1999

Rotor Angle Stability of MMC Based HVDC Transmission Under DC Short-Circuit Fault

Peng Wang, Maren Kuschke, and Kai Strunz
Sustainable Electric Networks and Sources of Energy (SENSE) Lab, Technische Universität Berlin , Germany

***Abstract*—The modular multilevel converter (MMC) has become a prominent topology for high-voltage direct-current (HVDC) applications. The DC short-circuit fault is the most severe condition, which is a challenge for the HVDC transmission. Under the DC short-circuit fault, the synchronous generator may encounter rotor-angle instability. This transient characteristic is analyzed with equal-area criterion. To quantify the transient stability, the critical mechanical power $P_{\mathrm{m,critical}}$ is defined. A single-machine infinite bus AC-DC transmission system is applied in PSCAD/EMTDC to verify the transient stability characteristics.**

***Index Terms*—bipolar HVDC, DC short circuit, equal-area criterion, MMC, transient stability.**

I. DC Short-Circuit Fault Process

The single-machine infinite bus AC-DC transmission system is shown in Fig. 1. The generator is connected to an infinite bus through a bipolar MMC-HVDC and an AC corridor. The half bridge submodule (HBSM) topology is used. The HBSM has the advantages of low losses and high scalability [1]. A pole-to-ground fault happens at one pole, while the other healthy pole continues to transmit power.

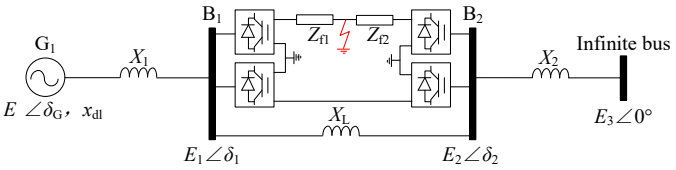

Fig. 1 Single-machine infinite bus AC-DC power system.

The DC short-circuit fault goes through the following process. The inserted capacitors begin to discharge through the upper arm, the lower arm, and the DC link short-circuit path at the fault instant. The IGBTs are blocked for self-protection when the overcurrent is detected. With the IGBTs blocked, the fault current in the arm flows through the freewheeling diodes. At the same time, the capacitors are bypassed and stop discharging. With the capacitors bypassed and the arms conducting, the AC grid suffers from symmetrical three-phase short-circuit fault. At the first zero-crossing point of the arm current, the arm gets into non-conducting state. The AC grid currents then feed into the DC grid. At last, the AC circuit breaker opens to isolate the DC fault.

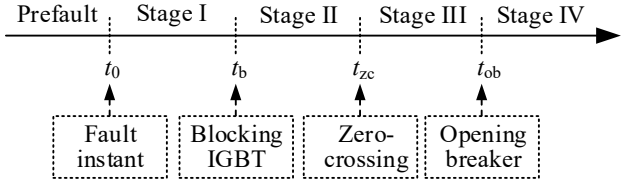

Fig. 2 Four stages of pole-to-pole fault process.

Regardless of the fault location, the fault process is separated into four stages, as shown in Fig. 2. Those are the capacitor discharging stage, the diode freewheeling stage, the AC current feeding stage, and the AC circuit open stage. As the impedances in the arms and the DC link short-circuit path are small, the active power in the faulty pole can be regarded as zero.

II. Rotor Angle Stability Analysis

At the short-circuit fault, the active power $0.5P_{\mathrm{dc0}}$ of the faulty pole is interrupted. The disturbed equilibrium between the mechanical and electrical torques results in the acceleration or deceleration of the rotor [2]. Based on the equal-area criterion, the transient stability is analyzed, as shown in Fig. 3.

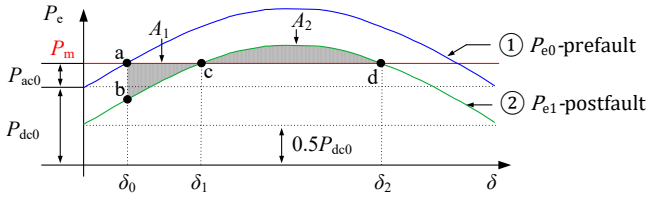

Fig. 3 Power-angle characteristics under DC short-circuit fault.

The system is stable under the condition that

$$A_1 \leq A_2. \tag{4}$$

The critical mechanical power $P_{\mathrm{m,critical}}$ can be obtained from (4). With $P_{\mathrm{m}} > P_{\mathrm{m,critical}}$, the system is unstable at the DC fault.

III. Case Study

The critical mechanical power for the transmission system in Fig. 1 is $P_{\mathrm{m,critical}} = 0.815$ p. u.. The simulation results for two different P_{m} are given in Fig. 4.

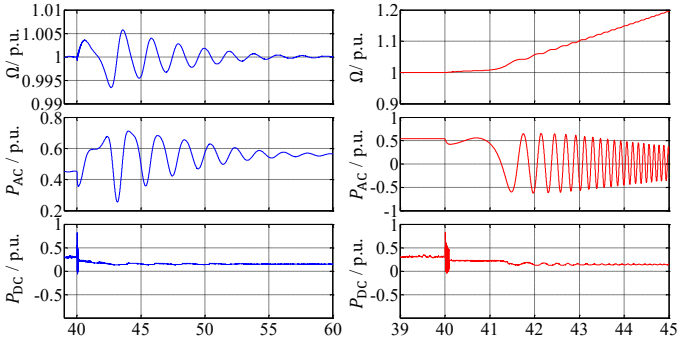

Fig. 4 Stable and unstable operation with $P_{\mathrm{m}} = 0.75$ p. u. and $P_{\mathrm{m}} = 0.85$ p. u..

References

[1] Debnath, Suman, et al. "Operation, control, and applications of the modular multilevel converter: A review." *IEEE Trans. Power Electron.,* vol. 30, no. 1, pp. 37-53, Jan. 2015.
[2] Kundur, Prabha, Neal J. Balu, and Mark G. Lauby. Power system stability and control. Vol. 7. New York: McGraw-hill, 1994.

Calculation of Fault Level in Power Systems with High Penetration of Renewable Energy Sources

Rafat Aljarrah, *Student Member, IEEE*, Hesamoddin Marzooghi, *Member, IEEE*, and Vladimir Terzija, *Fellow, IEEE*

***Abstract*— This paper investigates the changing fault level in systems with high penetration of renewable energy sources (RESs). It aims to evaluate the steady state fault calculation methods which are traditionally used in conventional power systems. Simulation results include fault level calculation using the available calculation methods\standards for various penetrations of RESs are obtained in the 2-area test system. The calculation results are validated against the dynamic simulation results obtained from using DIgSILENT PowerFactory.**

***Index Terms*— Dynamic simulation, fault level calculation, renewable energy sources, steady state calculation.**

I. Introduction

FAULT level is an important parameter usually used to reflect the system strength at a faulty point. In conventional power systems, fault level has had relatively high values due to very high fault level contribution from synchronous generators (SGs) [1]. This contribution can be easily calculated by modeling the SG as a voltage behind a reactance. However, with the increasing penetration of renewable energy sources (RESs, fault level calculation might become more challenging. This is due to the different characteristics of the short circuit currents might be supplied from the RESs which mainly utilize fully rated converters (FRCs), so their contribution to the system fault level is dependent on the converter interfaces [2, 3]. This necessitate the need to examine the steady state calculation standards in such expected future scenarios in order to assess the mismatch between the dynamic simulations and the steady state calculations and to propose solutions if any problem exists.

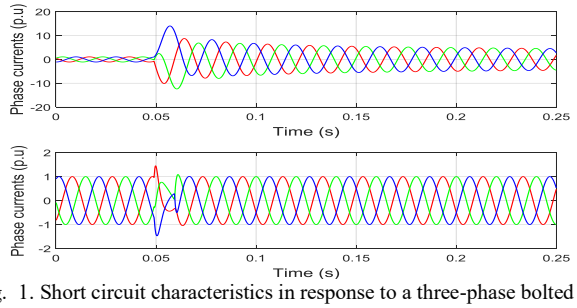

Fig. 1. Short circuit characteristics in response to a three-phase bolted fault: a) SG current, and b) RES utilizing FRC

II. Calculation Methods

TABLE I
UTILIZED METHODS FOR STEADY STATE CALCULATIONS

Method	Description
IEC1	IEC standards with no contribution from the converter
IEC2	IEC standards using static converter-fed drive
Complete 1	Complete method (dynamic voltage support) with 0 MVA sub-transient
Complete 2	Complete method (dynamic voltage support) with rating MVA sub-transient

III. Case Study and Results

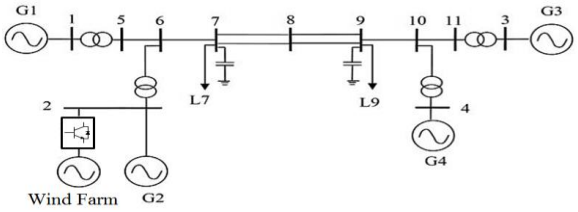

Fig. 2. Adjusted two-area test system with a RES penetration on Bus 2

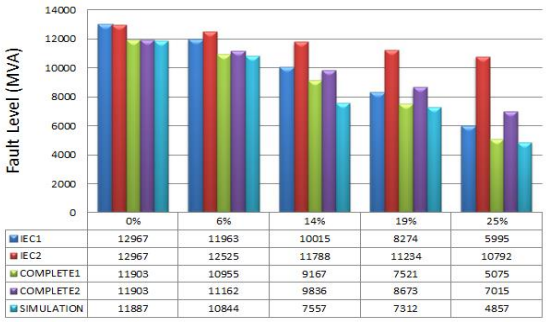

	0%	6%	14%	19%	25%
IEC1	12967	11963	10015	8274	5995
IEC2	12967	12525	11788	11234	10792
COMPLETE1	11903	10955	9167	7521	5075
COMPLETE2	11903	11162	9836	8673	7015
SIMULATION	11887	10844	7557	7312	4857

Fig. 3. Results of dynamic simulation versus steady state calculation methods at bus 6

References

[1] N. D. Tleis, *Power Systems Modelling and Fault Analysis: Theory and Practice*: Newnes, 2008.

[2] R. Teodorescu, M. Liserre, and P. Rodriguez, *Grid converters for photovoltaic and wind power systems*: John Wiley & Sons, 2011.

[3] L. Freris, and D. Infield, *Renewable energy in power systems*: John Wiley & Sons, 2008.

Stability Analysis of Microgrids under Disturbances via Reachable Sets

Yan Li*, Peng Zhang†
Department of Electrical and Computer Engineering
University of Connecticut, Storrs, Connecticut 06269–4157
Emails: *yan.7.li@uconn.edu, †peng.zhang@uconn.edu

***Abstract*—A stability assessment approach via reachable set calculation is presented to efficiently evaluate the dynamics of microgrids. Through the reachable set-based method, the bounds of all possible trajectories of a microgrid under a series of disturbances can be directly obtained, which makes repeated traditional time-domain simulations unnecessary. Moreover, a zonotope is used to better quantify these uncertainties and is integrated into the reachable sets calculation procedure. Extensive testing shows that reachable set calculations enable an efficient analysis of disturbances impacts on a microgrids dynamics, as well as offer a potent tool for evaluating how far the system is from its stability margins and what actions should be taken by system operators.**

I. Methodology Description

Reachable set calculation aims at finding the bounds of all possible system trajectories under various disturbances. The calculation process can be presented as follows: First, the original nonlinear DAEs of a dynamic system are abstracted into linear differential inclusions at each time step, obtaining a finite-dimensional state matrix $\mathbf{A} = [a_{ij}] \in \mathbb{R}^{n\times n}$. Its reachability model can then be expressed as follows:

$$\Delta\dot{\mathbf{x}} \in \mathbf{A}\Delta\mathbf{x} \oplus \mathbf{P}, \tag{1}$$

Second, a reachable set can be obtained at each time step via a closed-form solution:

$$\mathcal{R}^e(t_{k+1}) = \phi(\mathbf{A}, r)\mathcal{R}^e(t_k) \oplus \Psi(\mathbf{A}, r, \mathbf{p_0}) \oplus I_p^e(\mathbf{p_\Delta}, r), \tag{2}$$

$$\mathcal{R}^e(\tau_k) = C(\mathcal{R}^e(t_k), \phi(\mathbf{A}, r)\mathcal{R}^e(t_k) \oplus \Psi(\mathbf{A}, r, \mathbf{p_0})) \oplus I_p^e(\mathbf{p_\Delta}, r) \oplus I_\xi^e, \tag{3}$$

II. Test Cases

A typical microgrid system that is deeply integrated with distributed renewables and DC power loads is used to test and validate the reachable set approach. Fig. 1 shows the reachable sets of control signals in DER under disturbances. Fig. 2 shows the corresponding simulation verification. Fig. 3 shows the stability margin obtained via reachable sets. From Fig. 1 to Fig. 3, it can be seen that:

- The sizes of zonotopes along reachtubes increase as the uncertainty level increases.
- The time domain trajectories are fully enclosed by reachable sets, which validates the over-approximation capability of reachable set.

This material is based upon work supported by the National Science Foundation under Grant No. 1611095, and UConn Academic Plan Level 1 under Award No. 2806600.

- The stability margin can be efficiently obtained, which verifies reachable set is able to identify stability margins.

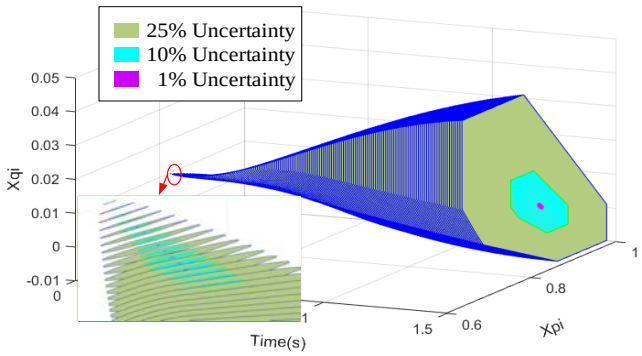

Fig. 1 3-D reachable set of DER

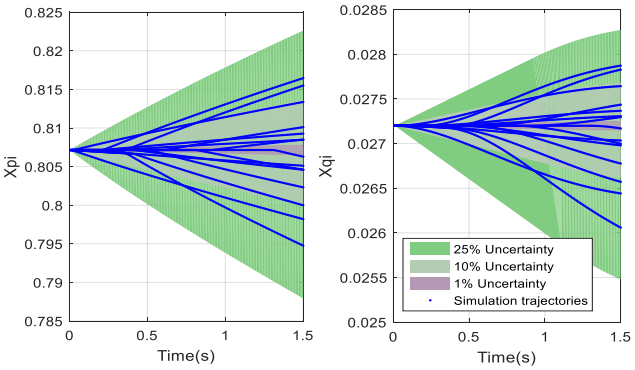

Fig. 2 Time domain simulation verification

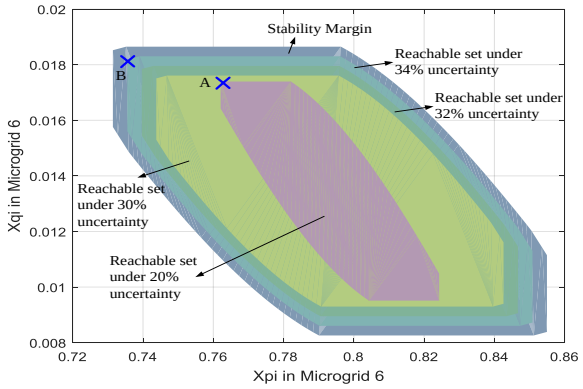

Fig. 3 Stability margin of Microgrid

An in-depth analysis of grid-connected solar plant feasibility and technology selection

Greg Stephens, Chris Dieterle, Eklas Hossain, Senior Member, IEEE
Oregon Tech, and Portland General Electric
Greg.Stephens@oit.edu; Chris.Dieterle@pgn.com; eklas.hossain@oit.edu

***Abstract*—** Energy storages appeared as the equipment of choice to overcome the problems arising from the different time-periods of peak renewable generation and peak demand. In this work, the possibilities to increase a proposed solar plant's peak-shaving efficiency using a MW-scale energy storage system is discussed; along with an algorithm for storage system control, and a study into the suitable storage systems available commercially.

***Keywords*–** *Feasibility study, Grid connected energy storage, Solar plant, Peak shaving.*

I. Grid Support by Energy Storage

In this work, a feasibility study of a grid connected solar plant is conducted. The site selection factors are reviewed along with the construction of an intuitive mathematical model. Based on the modeling, a feasibility analysis, selection of proper storage, and its control algorithm are demonstrated.

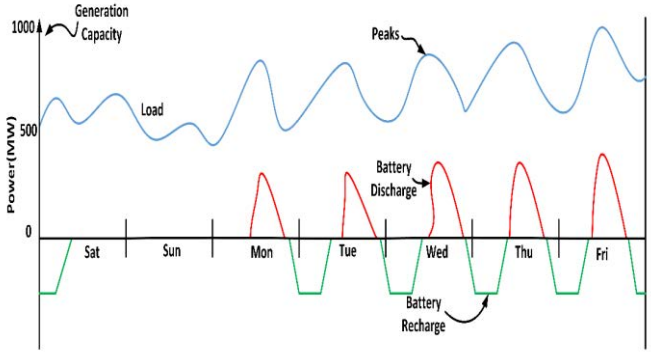

Fig. 1. Energy storage discharging during peak hours and charging during peak generation to increase the efficiency of renewable energy [1].

II. Storage System Control Algorithm

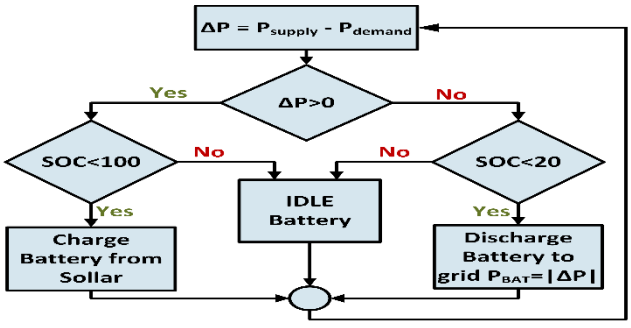

Fig. 2. Flow chart of battery storage control algorithm by checking the state of power difference and state of charge.

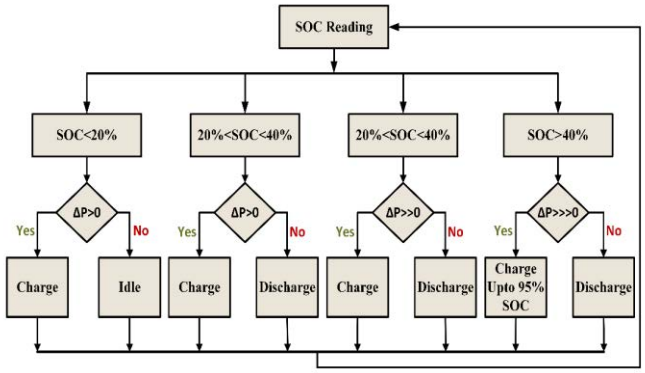

Fig. 3: SOC control algorithm with an altered sequence than the previous one. SOC status is checked first here.

III. Comparison of Available Energy Storages

Table 1. Comparison of possible storage technologies [2].

Technology	Duration (hrs)	Efficiency (%)	Lifetime (cycles)	Cost ($/kWh)
Pumped Hydro (small)	6-8	80-82	>13,000	420-430
CAES (aboveground)	5	Varies by plant	>10,000	390-430
Flywheel	0.25	85-87	>100,000	7,800-8,800
Lead Acid Batteries (advanced, demonstration)	3.2-4	75-90	4,500	625-1,150
Lithium Ion Batteries	2-4	90-94	4,500	900-1,700
Sodium Sulfur Batteries	7.2	75	4,500	445-555
Flow Batteries (vanadium)	4	65-70	>10,000	780-830

Proper site selection and the right technology can go a long way in improving solar plant performance.

References

[1] Cleverson Takiguchi "Energy storage for solar PV generation integration" *EE Publishers* May 13th, 2015.

[2] D. Rastler., "Electric Energy Storage Technology Options: A White Paper Primer on Applications, Costs, and Benefits," EPRI, Palo Alto, CA, 2010. 10206

An LMI Based Stability Margin Analysis for Active PV Power Control of Distribution Networks with Time-Invariant Delays

Chang Fu, Caisheng Wang, Saeed Alyami
Department of Electrical and Computer Engineering, Wayne State University, Detroit, Michigan USA
chang.fu@wayne.edu; cwang@wayne.edu; saeed.alyami2@wayne.edu

***Abstract*—High penetration of photovoltaic (PV) generators can lead to voltage issues in distribution networks. Various approaches including the real power control through PV inverters have been proposed to address voltage issues. However, among different control strategies, communication delays are inevitably involved and they need to be carefully considered in the control loop. Those delays can significantly deteriorate the system performance with undesired voltage quality, and may also cause system instability. In this paper, according to the inverter based active power control strategy, a linearized state space model with communication delay is presented. A delay dependent stability criterion using linear matrix inequality (LMI) approach is used to rigorously obtain the delay margins based on different system parameters. The method can handle multiple PVs in the distribution network as well.**

***Index Terms*—active power curtailment, communication delay, LMI, modeling, photovoltaic generators.**

I. Introduction

As one of the most important clean renewable sources for sustainable energy development, PV generation has been rapidly increased for more than two decades worldwide. The majority of the PV systems has been and will be installed in distribution networks. As a result, the PV penetration level will become unprecedentedly high (e.g. well over 50%) and continue to grow around the world. A poor voltage profile in a distribution network may lead to issues of power quality, equipment safety, system reliability and stability, and thus can raise system losses and cause equipment damages. Overvoltage is one of the most significant concerns among the above mentioned challenges, and limits the capacity of PV accommodation.

Linear matrix inequality (LMI) based stability methods have been studied extensively in recent decades. For distribution networks with high penetration of PVs, it is necessary to have a controller that can guarantee the systems' stability and performance while the systems are subject to various disturbances (load and solar irradiance variations) and communication delays. Therefore, in this paper, in addition to control the voltage in the distributed network via active power, an LMI based stability criterion will also be studied according to the state space model considering communication delays.

II. Key Formulas

Assume that an uncertain time-invariant time delay in [0, τ_d], i.e., $\tau \in [0, \tau_d]$. Then if there exists $P > 0$, $Q > 0$, $V > 0$ and W such that

$$\begin{bmatrix} (1,1) & -W^T A_d & A^T A_d^T V & (1,4) \\ -A_d^T W & -Q & A_d^T A_d^T V & 0 \\ V A_d A & V A_d A_d & -V & 0 \\ (1,4)^T & 0 & 0 & -V \end{bmatrix} < 0 \qquad (1)$$

where

$$(1,1) \triangleq (A + A_d)^T P + P(A + A_d) + W^T A_d + A_d^T W + Q$$

$$(1,4) \triangleq \tau_d [W^T + P]$$

then the system is asymptotically stable.

III. Key Results

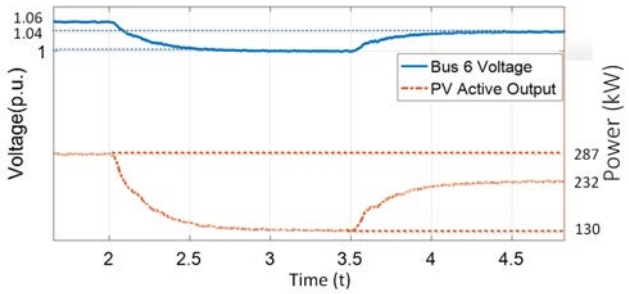

Fig. 1. Voltage and PV active power output at Node 6.

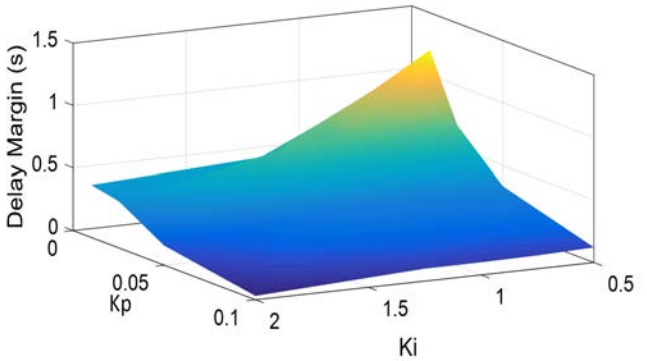

Fig. 2. Relationships among τ_d, K_{P4} & K_{I4}.

A Framework to Utilize DERs' VAR Resources to Support the Grid in an Integrated T-D System

Ankit Singhal
Department of Electrical and Computer Engineering
Iowa State University
Ames, Iowa 50010
Email: ankit@iastate.edu

Venkataramana Ajjarapu
Department of Electrical and Computer Engineering
Iowa State University
Ames, Iowa 50010
Email: vajjarap@iastate.edu

***Abstract*—Increasing penetration of inverter-based distributed energy resources (DERs) opens up interesting opportunities for the transmission systems. We present a hypothesis that the numerous DERs in var control mode can be seen as geographically distributed var devices (mini-SVCs) and if controlled properly, can be exploited to increase system flexibility by providing local var support to the grid as an ancillary service. Based on this premise, a var support framework is proposed in this paper. It utilizes a novel D-OPF formulation for unbalanced three-phase feeders enabling the estimation of the maximum var support that can be provided by the DERs to the grid at different operating points without compromising the distribution network performance. Further, a co-simulation method is developed to investigate the true impact of the proposed DER var support on the grid in an integrated Transmission-Distribution (T-D) system.**

***Index Terms*—Distributed Energy Resources, Transmission System, Solar Integration, VAR Support.**

I. Introduction

The conducive environment for distributed energy resources (DER) growth is pushing its penetration to as high as 100% . While the DER integration can impact the grid both adversely and positively, the purpose of this paper is to explore the opportunities offered by the DERs to improve transmission system performance. In particular, we present a hypothesis that, from the grid perspective, thousands of DER devices with volt/var control capability can be seen as the geographically distributed var resources (*'mini- static voltage compensators*) to improve system performance. It is known that the bulk transmission system needs to install its own reactive power devices such as SVC and capacitors at certain locations to enhance the system flexibility and voltage stability. Usually, these devices are very costly whereas due to the distributed nature, DERs can provide more flexible and localized var support to the bulk system at less economic cost, if controlled properly. Based on this premise, we propose a DER var support framework that utilizes the DERs volt/var capability for the benefits of the grid and verifies its impact in an integrated transmission-distribution (T-D) network.

Overall, the objective of this work is to investigate the var support opportunities provided by the DERs for the grid benefits by proposing a DER var support framework. The support framework has two main novel aspects i.e. distributed optimal power flow (D-OPF) and the T-D co-simulation which intend to provide following unique contributions: 1) To estimate the *'day ahead maximum var support curve'* for the grid while enforcing distribution system operating limits; 2) To verify the true impact of var support on the gridusing an integrated T-D co-simulation; 3) To confirm our proposition that the DERs can be exploited as mini-SVCs to provide flexibility and ancillary services to the grid; and 4) To provide a general framework which enables further investigation of the DERs utilization for various grid support applications in an integrated T-D environment.

II. Proposed VAR Support Framework

Fig.1 depicts the overall framework of providing var support to the grid from DERs in an integrated T-D system, proposed in this work. The objective of this framework is to estimate the *maximum var support capacity curve* and send it to the transmission system operator (TSO). This is achieved through a D-OPF module which estimates the maximum available var support at the feeder substation at different operating points throughout the day while ensuring the distribution system is within its operational limits. This capability works as an potential ancillary service to TSO which can be utilized when needed. The results will be presented and discussed in the poster.

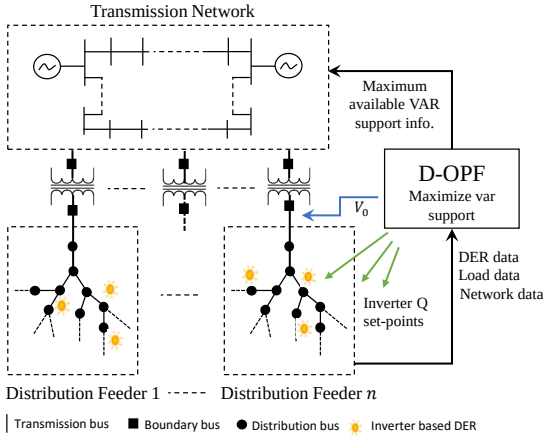

Fig. 1. The DER var support framework for an integrated T-D system

Quantitative Control Approach for Wind Turbine Generators to Provide Fast Frequency Response With Guaranteed Rotor Security

Siqi Wang
Dept. of Electrical Engineering and Computer Science
The University of Tennessee
Knoxville, TN, USA
swang31@utk.edu

Kevin Tomsovic
Dept. of Electrical Engineering and Computer Science
The University of Tennessee
Knoxville, TN, USA
tomsovic@utk.edu

***Abstract*— The high penetration of wind generation reduces the inertial response of the system. This can be compensated by enabling the double-fed induction generator (DFIG) to provide fast frequency response. This paper proposes a quantitative control approach for DFIG to deliver fast frequency response in the inertial response time scale with guaranteed rotor security based on estimation of maximum extricable energy. The proposed approach not only provides adequate inertial response but also ensures the rotor speed is kept within a specified operating range.**

***Index Terms*— Active power control; DFIG; high wind penetration; inertial response; kinetic energy**

I. INTRODUCTION

With more synchronous generators being replaced by wind turbine generators, the system overall inertial response is reduced [1]. DFIG is able to provide fast frequency response similar as conventional generators. A general approach is to introduce a support function as a supplementary control loop, adding to the active power reference of DFIG. This paper proposed a quantitative control approach for DFIG to provide fast frequency response with guaranteed rotor security to answer the following two questions: 1) How to quantitatively design the power surge function to maximize a DFIG's contribution without stalling the rotor? 2) How to coordinate multiple DFIGs under different operating conditions to provide fast and adequate system response?

II. PROPOSED DFIG FFR APPROACH

The maximum extricable energy for DFIG during inertial response period can be expressed as follows:

$$\Delta E_{del} = (\frac{\eta}{12} K V_w^2 \frac{\partial C_p}{\partial \lambda}|_{t=0} - J\frac{\omega_r(0)}{\omega_s^2} T_{del})\Delta\omega_r + (\frac{\eta}{36} K V_w^2 \frac{\partial C_p}{\partial \lambda}|_{t=0} + \frac{\eta}{216} K V_w \frac{\partial^2 C_p}{\partial \lambda^2}|_{t=0} - \frac{J}{2\omega_s^2} T_{del})\Delta\omega_r^2 \quad (1)$$

Considering a delivery time T_{del} , the maximum active power injection can be calculated as:

$$\Delta P_{del} = \frac{\Delta E_{del}}{T_{del}} \quad (2)$$

Considering converter overload limit $P^{\lim} = 1.2\text{p.u}$.

$$\Delta P_{del}^{tpi}|_{\max}(V_w, T_{del}) = \min(\Delta P_{del}, P^{\lim} - P_0(V_w)) \quad (3)$$

The sensitivity of active power injection change to frequency nadir incremental can be expressed as:

$$S = \partial f_{na}^{\min} / \partial \Delta P \quad (4)$$

Figure 1 shows the flow chat of the proposed approach.

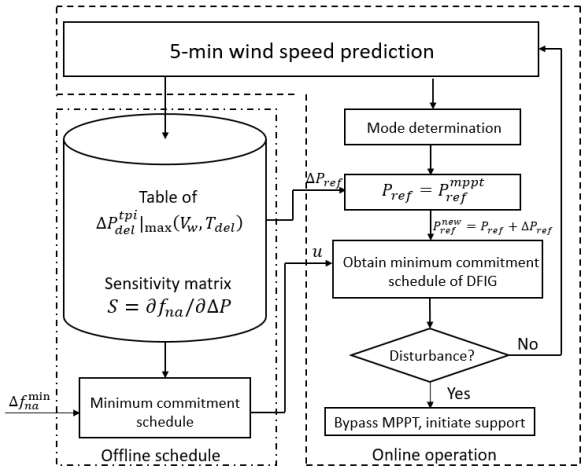

Figure 1. Flow chat of proposed approach

III. CONCLUSIONS AND FUTURE WORK

This paper presents a quantitative control approach for DIFG to provide fast frequency response by incorporating a supplementary power injection to the existing DFIG active power reference. The active power injection is calculated with consideration of maximum extricable energy and converter overload limits. The proposed approach not only improves the overall frequency response but also ensures the rotor speed is kept within a safe range.

REFERENCES

[1] J. Conto. Grid challenges on high penetration levels of wind power. In Proc. IEEE Power Energy Soc. Gen. Meeting (PES GM), pages 1–3, July 2012.

Optimal Corrective Control for Bipolar Multi-terminal HVDC Grid

Jiahong Li, Hua Ye, Yutian Liu
Key Laboratory of Power System Intelligent Dispatch and Control of Ministry of Education (Shandong University)
17923 Jingshi Road, Ji'nan 250061, China
lijiahongjhh@163.com, {yehua, liuyt}@sdu.edu.cn

Yanling Du, Haitao Liu,
State Grid Jibei Electric Power Company
Beijing 100053, China
liuhaitaob@126.com

***Abstract*—An outage of DC transmission lines or converters occurs in bipolar multi-terminal HVDC grid (MTDC) may result in security violation. Corrective control strategies are therefore needed to ensure the operational security of the system. For MTDC grid following N-1 contingencies, a power shift-based optimal corrective control method is presented in this paper. Certain power are shifted from the faulty pole to the normal pole or among different converter stations within a pole, so that the amount of renewable energy accommodation of the MTDC is maximized. The method is intensively studied on a modified New England 10-machine 39-bus test system with inclusion of a four-terminal bipolar DC grid.**

***Index Terms*—Corrective control, multi-terminal HVDC, power shift, renewable energy integration, security analysis.**

I. Introduction

Like the AC power grid, after an outage of DC transmission line in the bipolar MTDC grid, power will immediately transfer to the parallel paths. In this case, an intractable problem is the possible overloads on DC transmission lines caused by outage of stressed DC lines and converters. To deal with such critical DC N-1 contingencies and to eliminate the resultant overloads, an optimal corrective control method is presented in this paper by using the power shift capability of the bipolar MTDC grid. First, two types of power shifts, including pole-to-pole and station-to-station power shifts are introduced. Then, corrective control strategies are obtained by intensively analyzing different load level of converters and different type of outages. Third, a mixed-integer non-linear programming model is established to address all these corrective control strategies.

II. Power Shift in the Bipole MTDC Grid

Without loss of generality, the symmetric bipolar four-terminal HVDC grid illustrated in Fig. 1 is used to address the corrective control problem in MTDC grid.

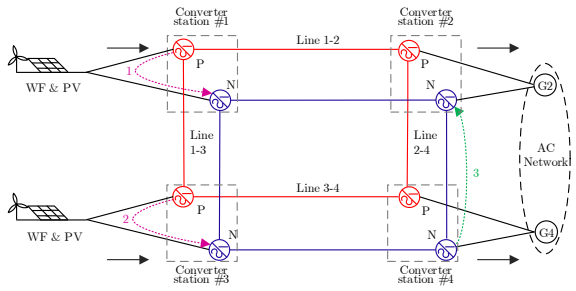

Fig. 1. Schematic of pole-to-pole and station-to-station power shift

The bipolar MTDC grid may violate the security constraints when an outage of stressed DC transmission lines or converters occurs. Since the positive and negative poles of the MTDC grid are operated independently, it is a promising way to guarantee the operational security of MTDC grid by shifting certain power from the faulty pole to the normal pole (i.e., pole-to-pole power shift, pink dotted lines 1 and 2 shown in the Fig. 1) or by shifting power among different converter stations within a pole (i.e. station-to-station power shift, the green dotted line 3 in Fig. 1).

III. Optimal Corrective Control for MTDC Grid

The aim of corrective control is to ensure the security of the power system with bipolar MTDC grid embedded when N-1 contingency of DC grid occurs. The cheapest and the most effective control measure is the power shift. In some cases that the wind and solar energy is abundant, the least amount of renewable energy should be curtailed and the smallest number of generators in the AC grid should be rescheduled to balance the hybrid grid. To address this, a mixed integer programming model is established.

$$\min_{u} \left(P_{\text{trans1}} + P_{\text{trans3}} + P_{\text{inc2}}\right) + w_1 \sum_{i \in S_G} u_i \left(\Delta P_{Gi}\right)^2 + w_2 \sum_{i \in S_G} u_i + w_3 \left(P_{\text{cut1}} + P_{\text{cut3}}\right) \tag{1}$$

IV. Key Results

Cases 1 and 2 are used to verify the correctness of the optimal corrective control for the outage of DC line in the positive pole (faulty pole).

TABLE I Power Flows on the DC Lines before and after the Corrective Contorl (p.u.)

		Case 1		Case 2	
		Pre-control	Post-control	Pre-control	Post-control
Faulty Pole	$P_{\text{dc42-43}}$	0	0	0	0
	$P_{\text{dc42-44}}$	1.1886	1.1751	1.1886	0.8935
	$P_{\text{dc43-45}}$	-1.2118	-1.2118	-1.2118	-1.2118
	$P_{\text{dc44-45}}$	**1.5847**	**1.5000**	**1.8830**	**1.5000**
Normal Pole	$P_{\text{dc42-43}}$	1.1322	1.1392	1.1572	1.4324
	$P_{\text{dc42-44}}$	0.0650	0.0579	0.0400	0.0630
	$P_{\text{dc43-45}}$	-0.0687	-0.0616	-0.0437	-0.0614
	$P_{\text{dc44-45}}$	0.4646	0.5425	0.7389	0.8117

TABLE II Power Transfer Optimal Reaults in Cases 1 and 2 (p.u.)

Case	P_{trans1}	P_{trans3}	P_{inc2}	P_{cut1}	P_{cut3}
1	0	0.0852	0	0	0
2	0.3	0.0500	0.2926	0	0.04

Bi-Level Arbitrage Potential Evaluation for Grid-Scale Energy Storage Considering Wind Power and LMP Smoothing Effect

Hantao Cui, *Student Member, IEEE*; Fangxing Li, *Fellow, IEEE*;
Xin Fang, *Member, IEEE*; Hao Chen, Honggang Wang

***Abstract*—This paper deals with extended-term energy storage (ES) arbitrage problems to maximize the annual revenue in deregulated power systems with high penetration wind power. The conventional ES arbitrage model takes the locational marginal prices (LMP) as an input and is unable to account for the impacts of ES operations on system LMPs. This paper proposes a bi-level ES arbitrage model, where the upper level maximizes the ES arbitrage revenue and the lower level simulates the market clearing process considering wind power and ES. The bi-level model is formulated as a mathematical program with equilibrium constraints (MPEC) and then recast into a mixed-integer linear programming (MILP) using strong duality theory. Wind power fluctuations are characterized by the GARCH forecast model and the forecast error is modeled by forecast-bin based Beta distributions. Case studies are performed on a modified PJM 5-bus system and an IEEE 118-bus system with a weekly time horizon over an annual term to show the validity of the proposed bi-level model. The results from the conventional model and the bi-level model are compared under different ES power and energy ratings, and also various load and wind penetration levels.**

I. Summary

In this paper [1], we focus on the extended-term arbitrage revenue study, which can be used to evaluate existing ES systems or incorporated into cost-benefit analysis for planning. To consider the price changes due to arbitrage activities, a bi-level model is proposed by maximizing the arbitrage potential in the upper-level model and simulating the market-clearing process in the lower level. Instead of relying on price inputs or price forecasts, the upper-level model uses the prices generated on the lower level and adjusts the ES outputs, which, in turn, affects the price in the lower level. Linear transformation techniques are applied to reformulate it as a single level mathematical programming with equilibrium constraints (MPEC) and then a mixed-integer linear programming (MILP).

Comparing with the conventional model, the proposed bi-level ES arbitrage model incorporates the LMP information from the market clearing process in the lower level problem. By using appropriate information such as wind forecast and estimated generation bids, this method can yield more accurate LMP forecasts and arbitrage potential evaluations.

Fig. 1 (b) compares the LMP at bus D obtained from the two models in a time horizon of 168 hours (7 days), where some LMP bottoms are driven up but more LMP peaks are reduced in the bi-level model. The LMP changes show a verification of the LMP smoothing effect as the discharging operation of ES during higher LMP hours, as well as the charging of ES during the low LMP hours, affects the clearing price. Fig. 1 (c) and (d) shows the comparison of ES power output and SOC from the conventional and the bi-level models. The positive values of the ES power indicate ES discharging activities, while the negative ones indicate ES is charging. It is important to note that the power is seen from the power grid side so that the round-trip efficiency has been included. Therefore, the maximum power the ES can supply is smaller than the 50 MW power rating due to self-discharging, and the charging power is greater than 50 MW to compensate for the motor losses.

In conclusion, the proposed bi-level can reflect the ES operations and wind power fluctuations on the LMPs; in contrast, the conventional model must rely on historical or pre-computed LMP data as inputs. Based the system operating condition, the conventional model would either over-estimate or underestimate the annual arbitrage revenue using static price inputs when considering line flow limits.

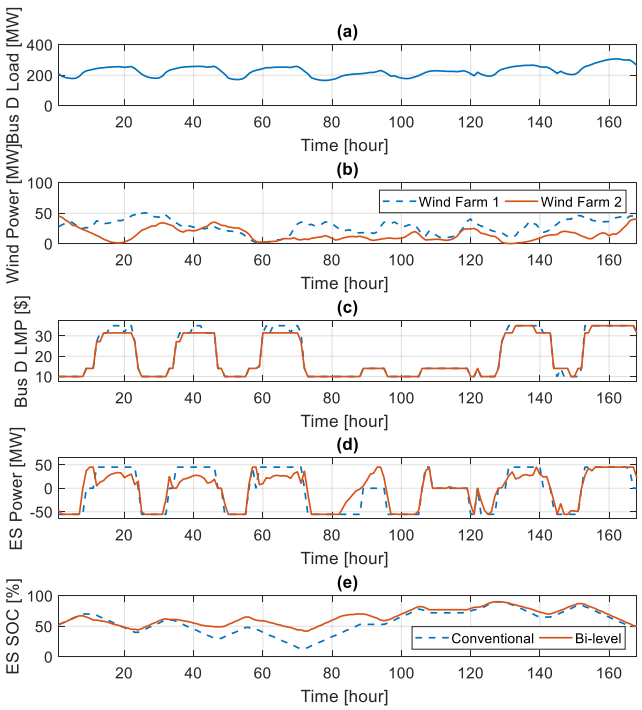

Fig. 1. Comparisons of (a) Bus D load, (b) Wind farm outputs, (c) Bus D LMP, (d) ES Power and (e) ES SOC from the two models

[1] H. Cui, F. Li, X. Fang, H. Chen, H. Wang. Bilevel Arbitrage Potential Evaluation for Grid-Scale Energy Storage Considering Wind Power and LMP Smoothing Effect. *IEEE Transactions on Sustainable Energy*, 2018, 9(2), 707-718.

State Space Model of Electric Vehicle Aggregator for Frequency Control

Mingshen Wang, Fangxing Li

Department of Electrical Engineering and Computer Science, the University of Tennessee, Knoxville, TN 37996, USA.
mwang38@utk.edu, fli6@utk.edu

***Abstract*—With the obvious power imbalance caused by the renewable energy in the power system, the electric vehicles (EVs) are suggested to be an alternative for the frequency control. The existing models that managed a large quantity of EVs for centralized control achieved high accuracy at the expense of the heavy calculation workload and the high requirement for real-time communication. This paper develops a state space model (SSM) that provides a probability to realize the real-time power control of EV aggregator (EVA) with the high accuracy and calculation efficiency but the low requirement for real-time communication. The SSM, a reduced model based on the state space method, accurately describes the EVA with different connecting states and various state of charge (SOC) states. Considering the charging characteristics and the travelling behaviors of EVs, the SSM realizes the state transition prediction and the regulation capacity estimation with the Markov chain method, which has much higher calculation efficiency than the existing models. The SSM is used for the frequency control, and the SOC adaptive coefficient is used to derive the identical control signal (ICS) and improve the prediction accuracy. The SSM lowers the requirement for real-time communication by replacing some real-time process with offline process. The ICS is much suitable for real-time dispatching by transmitting the same control signal to each EV. The simulation results validate the effectiveness of the SSM of EVA for the frequency control.**

I. Modeling Framework

A. State Model of an Individual EV

$$S_i(k+1)=\begin{cases} S_i(k)-P_i(k)\cdot\eta_{c,i}\cdot T/Q_i, & P_i(k)<0,\ \text{CS} \\ S_i(k), & P_i(k)=0,\ \text{IS} \\ S_i(k)-P_i(k)/\eta_{d,i}\cdot T/Q_i, & P_i(k)>0,\ \text{DS} \end{cases} \quad (1)$$

where k is the time step; S_i is the SOC of EV i; P_i is the charging power; CS/IS/DS is abbreviation of Charging State/Idle State/Discharging State; S_i is the battery capacity.

B. State Transition of EVA

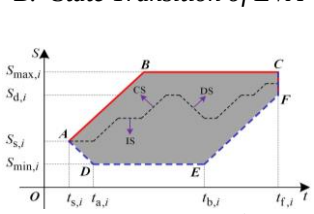

Fig. 1. Operation area of an EV.

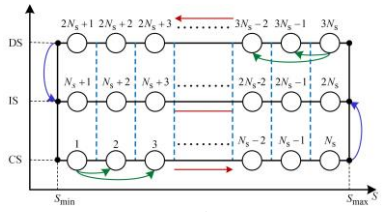

Fig. 2. State space of aggregated EVs.

The state transition of EVs in one time step:

$$\boldsymbol{x}(k+1)=\boldsymbol{A}\boldsymbol{x}(k) \quad (2)$$

where $\boldsymbol{A}$ is a ($3N_s$×$3N_s$) matrix and is derived to describe the transition of the EVs from one state interval to another; $\boldsymbol{x}$ is ($3N_s$×1) state vector.

Markov estimation method and analytical method can be used to obtain the A (State Transition Matrix).

C. State Space Model of EVA

$$\begin{cases} \boldsymbol{x}(k+1)=\boldsymbol{A}\boldsymbol{x}(k)+\boldsymbol{B}\boldsymbol{u}(k)+\boldsymbol{C}\boldsymbol{v}(k) \\ y(k)=\boldsymbol{D}\boldsymbol{x}(k) \end{cases} \quad (3)$$

where $\boldsymbol{u}$/$\boldsymbol{v}$ is the (N_s×1) input vector that indicates responding modes; y is a (1×1) output vector; $\boldsymbol{B}$/$\boldsymbol{C}$/$\boldsymbol{D}$ is constant matrixes.

II. Frequency Control with State Space Model

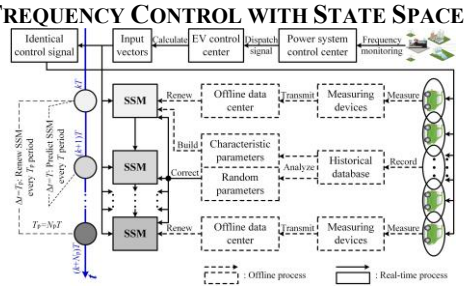

Fig. 3. Frequency regulation with SSM of aggregated EVs.

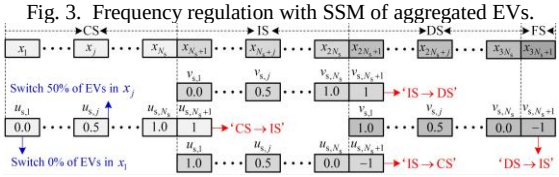

Fig. 4. Structure of identical control signal.

III. Study Results

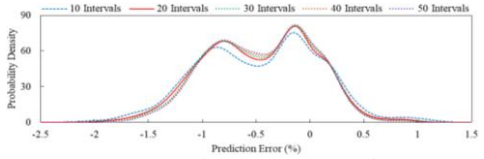

Fig. 5. Probability density of prediction errors of EVA (T_D=5 min).

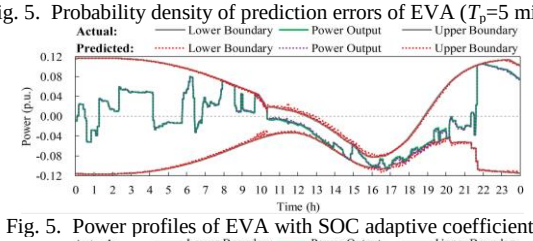

Fig. 5. Power profiles of EVA with SOC adaptive coefficient.

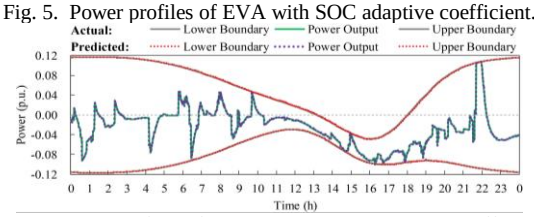

Fig. 6. Power profiles of EVA without SOC adaptive coefficient.

The SSM realize the real-time power control of EVA with the high accuracy and calculation efficiency with ICS.

Stochastic market clearing for integrated energy systems considering CHP and power-to-gas technology

Haibing Wang, *Student Member, IEEE,* Fangxing Li, *Fellow, IEEE*
Dept. of Electrical Engineering and Computer Science
University of Tennessee
Knoxville, USA
{hwang104, fli6}@utk.edu

***Abstract*—This paper utilizes natural gas-fired power plant (NGFPP), combined heat and power (CHP) and power-to-gas (P2G) technology as energy conversion approaches to construct integrated power, natural gas and heat system, aimed at increasing the energy utilization efficiency. A two-stage stochastic market clearing model for the integrated energy system is proposed to analyze the impact of P2G on the wind curtailment rate and operation cost.**

Keywords—integrated energy systems; stochastic programming; CHP; P2G; market clearing

I. INTRODUCTION

Multi energy integration is beneficial to increase the energy utilization efficiency. Power system and natural gas system integration was studied in the previous literature. This paper contains CHP units to cover the heat load and introduces the P2G technology to prevent the curtailment of renewable energy. The integrated power, natural gas and heat system is described in Fig.1, where NGFPPs and P2G process couple the natural network and power network, and CHP units couple the natural gas network, power network and district heat network. A scenario-based market clearing model is proposed to analyze the impact of CHP and P2G on the operation of integrated energy system.

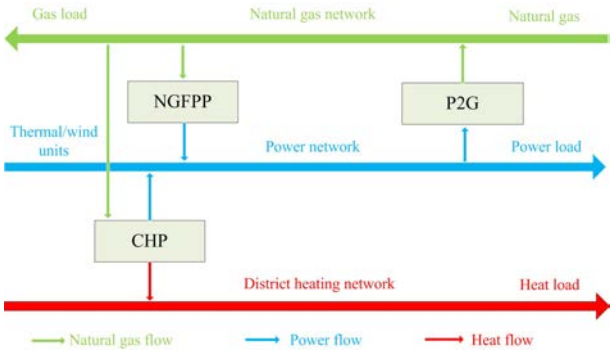

Fig.1. Description of integrated energy systems containing CHP and P2G

This work was supported by the China Scholarship Council.

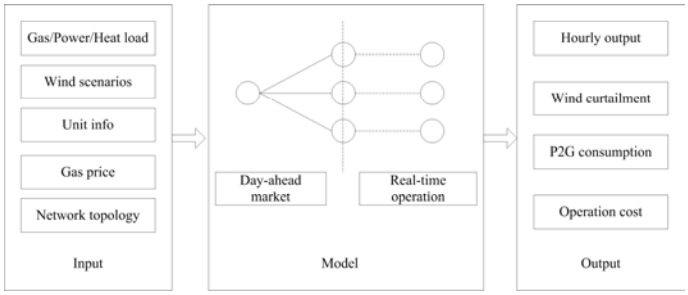

Fig.2. Framework of two-stage stochastic market clearing model of integrated energy systems

II. MODEL FRAMEWORK AND SIMULATION

The model framework is described in Fig.2. Day-ahead market and real-time operation are optimized simultaneously. Day-ahead dispatch decisions are made before the realization of wind scenarios, while real-time operation depends on wind scenarios. The input includes hourly gas/power/heat load, wind scenarios, units information, gas price and network topology. The output includes hourly output of units and gas wells, wind curtailment, power-to-gas conversion and operation cost. Simulation was made on a six nodes system and seven nodes natural gas system, depicted in Fig.3, to verify the effectiveness of the proposed model and investigate the benefits of P2G process.

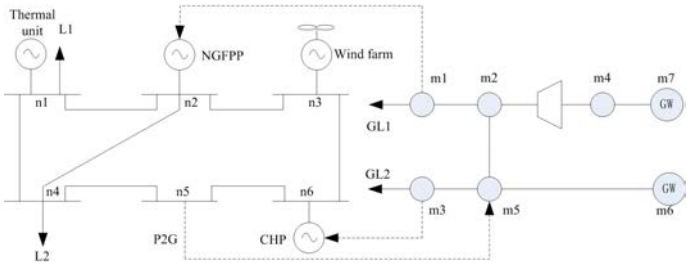

Fig.3. Case study of six nodes power system and seven nodes natural gas system

Optimal Placement of Grid-connected Solar Generation using Geographical Information System

Ana M. Ospina, *Student Member, IEEE,* Milad Soleimani, *Student Member, IEEE,*
Mladen Kezunovic, *Life Fellow, IEEE*

***Abstract*—This work presents a decision making approach for selecting an optimal placement of the grid-connected solar generation using Geographical Information System (GIS) as the decision making tool. Terrain analysis for assessment of solar radiation, as well as buildings and vegetation spatial data is analyzed in order to determine the shadow impact that can be anticipated for medium or large-scale PV installation. In addition, different historical weather conditions are considered and integrated into the model to show the impact of this variable on the solar generation output. Some details of the methodology and initial results related to selection of potential sites for PV installation are presented. To illustrate the process and proposed methodology, an example using large scale synthetic networks is implemented.**

***Index Terms*—PV Generation, Power System, Geographical Information System, Decision Making, Optimal Placement.**

I. Introduction

THE high penetration of PV generation being installed in the transmission and distribution grid may be causing severe problems in power systems operation such as line overload, voltage instability, power quality deterioration, among others. In order to perform a detailed analysis that leads to the decision about the optimal placement, the realistic models of the grid and PV integration options allowing consideration of maximum number of constraint that are crucial for planning and operational purposes is necessary. We propose a methodology to create an input layer using GIS that assists the decision-making process for the optimal location of PV generation based on solar radiation, vegetation location, placement of supporting structures, historical weather patterns and grid operating regimes.

II. Geographical Information System as a Decision Making Support Tool

A. Terrain Analysis

The terrain analysis using GIS is an accurate and adequate approach to determining the potential advantages or disadvantages of integration of solar generation into the distribution and transmission systems [1]. Using different public sources of information, it is possible to determine the optimal location for PV generation under different conditions as illustrated in Fig. 1.

B. Decision Making Process

Multi-criteria decision analysis is frequently used in the decision making process for power system planning and operation. In this case, using the results of the terrain analysis, it is possible to evaluate the impacts that PV generation can have on the current distribution power system [2]. Fig. 2 shows the decision making process applied to a synthetic network.

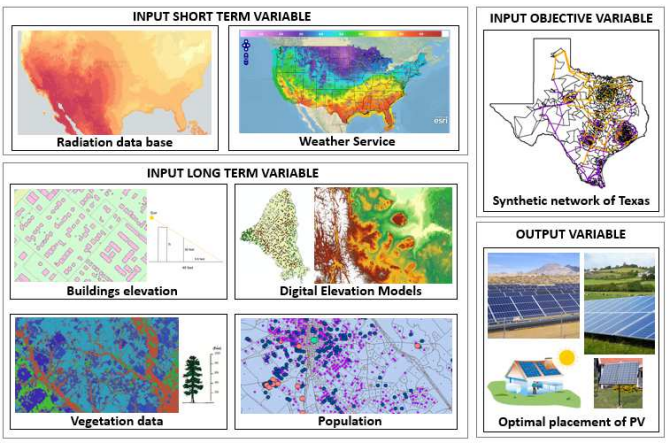

Fig. 1. Terrain analysis using Geographical Information System.

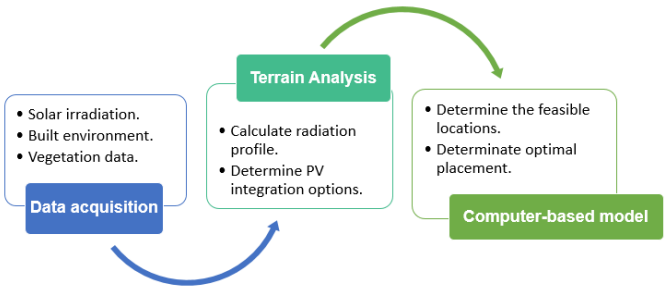

Fig. 2. Decision-Making process for optimal location of PV generation.

III. Conclusion

This poster presents a systematic, practical and easily implementable methodology to optimally locate PV generation from GIS information using public data. These type of models are crucial to carry out planning and operation studies required to assess the impacts of the integration of non-conventional energy sources, such as solar or wind generation, into the grid in order to improve power systems reliability and resiliency.

References

[1] P. Quesada, A. Arguello, J. Quiros-Tortos and G. Valverde, *Distribution Network Model Builder for OpenDSS in Open Source GIS Software*, 2016 IEEE T&D PES Latin America. Morelia, Mexico.

[2] Y. Kakumoto, Y. Koyamatsu, A. Shiota, Y. Qudaih and Y. Mitani *Application of Geographic Information System to Power Distribution System Analysis*, 3rd ed CPESE 2016. Kitakyushu, Japan.

A. Ospina (ana.ospina@tamu.edu), M. Soleimani and M. Kezunovic are with the Department of Electrical and Computer Engineering, Texas A&M University, College Station, TX, 77840 USA.

Frequency Support of DFIG by Using Improved Inertial Control

Tang Fei[1], Xiao Gucheng[1*], Liu Dichen[1], Liao Qingfen[1], He Zhijuan[2], Liu Yu[3], Liu jiale[1],Wang Chenxu[1]

[1]School of Electrical Engineering Wuhan University Wuhan, China

[2]Computer school, Wuhan University Wuhan, China

[3]School of Foreign language, South-Central University for Nationalities Wuhan, China

Email: xiaogucheng@whu.edu.cn

***Abstract*—This paper proposes a modified temporary over-production inertial control. It consists of two parts: the deceleration phase and the acceleration phase. In the deceleration phase, the reference active power maintains constant first. Then it starts to decrease linearly with the decreasing of the rotor speed when the DFIG has released half of the available energy stored in the rotating masses. In the acceleration phase, the reference active power switches to the mean value of mechanical power and electromagnetic power under maximum power point tracking control. Compared with the temporary over-production inertial control, the modified temporary over-production inertial control is simplified with one parameter and there is no over-speed. Moreover, the performance of the second frequency dip is improved with less power reduction. The simulation results show that the modified temporary over-production inertial control has the same ability to arrest the frequency nadir as temporary over-production inertial control while improving the performance of the second frequency dip.**

***Index Terms*—temporary over-production inertial control; over-speed; second power dip; frequency nadir**

I. INTRODUCTION

Doubly fed induction generator (DFIG) almost makes no contribution to the power system inertia for the rotor of the DFIG is connected to power grid through the converters. To provide inertial response, temporary over-production inertial control (TOPC) [1] are applied in DFIG. TOPC could provide constant additional power support in a period which significantly help arrest the frequency nadir (FN). If parameters are not set properly, over-speed will occur. Moreover, the power reduction between the deceleration and acceleration phase will cause a serious second frequency dip (SFD). This paper proposes a modified temporary over-production inertial control (MTOPC) to arrest the FN while causing a small SFD.

II. METHODOLOGY

The proposed MTOPC scheme consists of two parts: the deceleration phase and the acceleration phase. The whole inertial response process of the MTOPC is summarized in Fig. 1.

III. KEY RESULTS

The performance of the MTOPC is verified in a modified WSCC 9-bus system. The results are compared with no inertial control and the conventional TOPC. The parameters of the MTOPC and TOPC are shown in TABLE I. The simulation results are shown in Fig. 2.

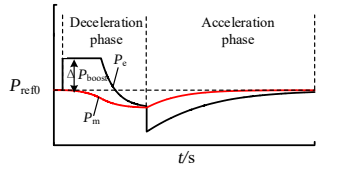

(a) Reference power function

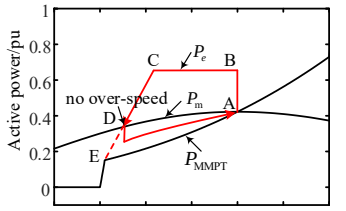

(b) Power-speed trajectory

Fig. 1 Operational characteristics of the MTOPC scheme

TABLE I. PARAMETERS OF THE MTOPC AND TOPC

Controllers	Parameters			
	ΔP_{boost} (pu)	T_{boost} (s)	ΔP_{rec} (pu)	T_{rec} (s)
MTOPC	0.1	/	/	/
TOPC	0.1	20	0.1	27

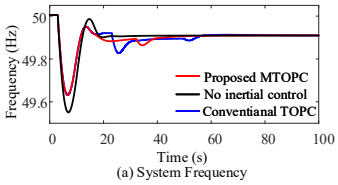

(a) System Frequency

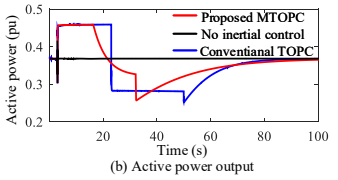

(b) Active power output

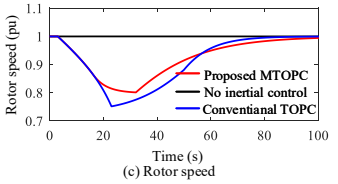

(c) Rotor speed

Fig. 2 Results of providing frequency support by DFIG

REFERENCES

[1] Ullah, Nayeem Rahmat, T. Thiringer, and D. Karlsson. "Temporary Primary Frequency Control Support by Variable Speed Wind Turbines— Potential and Applications." IEEE Transactions on Power Systems, vol. 23, no. 2, pp. 601-612, 2008.

Combined Heat and Power Dispatch Based on Integrated Demand Response and Heat Transmi ssion for Wind Power Accommodation

Yeyan Xu, Qingfen Liao, Fei Tang*, Dichen Liu, Deping Ke, Sicheng Peng, Zheng Yang
Department of Electrical Engineering Wuhan University Wuhan, China
Email: tangfei@whu.edu.cn

***Abstract*—The fixed heat-power ratio has limited the flexibility of CHP(combined heat and power) units for wind power accommodation. Multi-energy end-users possess electrical load and heat load. The complementation between the two kinds of load enables the end-users to participate in IDR(integrated demand response), which makes the CHP units more flexible. The heat transmission can decouple the real-time balance between the heat supply and the heat load. This paper integrates IDR with heat transmission to promote wind power accommodation in IEGM. Firstly we formulate a simplified linear model of the complementation between different kinds of load in the end-user. Then the annular heat transmission network is formulated by the quasi dynamics model of the pipeline temperature. An IDR bi-level optimal dispatch model is proposed to gain a "win-win" situation between the IEGM operator and end users. The simulation results verify that the proposed dispatch can improve wind power accommodation and operational economy.**

***Index Terms*—combined power and heat dispatch; integrated demand response; heat transmission; bi-level optimal dispatch; integrated energy micro-grid**

I. INTRODUCTION

The IEGM is a combined heat and power micro-grid, containing end-users, CHP units and wind turbines.

A. Linear Model of the complementation between different kinds of load in the end-user

The energy conversions inside an end-user is shown as Fig.1. The Linear model is shown as (1). The heat load is linearly decreased with the rise of electrical load.

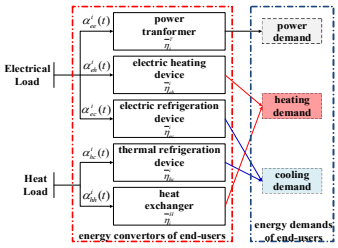

Fig.1 The energy conversions inside an end-user

$$P_h^i(t) = -\frac{\bar{\eta}_{ec}^i}{\bar{\eta}_i^i}\frac{\bar{\eta}_{ec}^i}{\eta_{hc}} P_e^i(t) + \frac{1}{\bar{\eta}_i^i}\frac{1}{\eta_{hc}}[p_c^i(t) + \frac{\bar{\eta}_{ec}^i}{\bar{\eta}_T^i}\frac{\bar{\eta}_{ec}^i}{\eta_i} p_e^i(t) + \frac{\bar{\eta}_{hc}^i}{\bar{\eta}_H^i}\frac{\bar{\eta}_{hc}^i}{\eta_i} p_h^i(t)] \quad (1)$$

B. Quasi-Dynamics model of the pipeline temperaturte in the annular pipeline network

For the heat balance, the quasi-dynamics model of the annular pipeline temperature is established as (2). It shows that $\tau_i(t)$ is the mixing temperature of the flow masses injected by the uptstream nodes before period *t*.

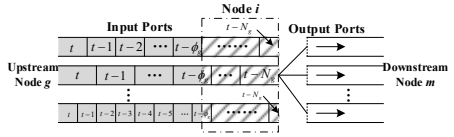

Fig.2 Vertical section of a node in the supply network

$$\tau_i(t) = \frac{\sum_{g\in\Gamma_g}\sum_{k=0}^{N_{gi}} G_{gi}\tau_g(t-k\Delta t)\alpha_g(t-k\Delta t)}{\sum_{m\in\Gamma_m} G_{im}} \quad (2)$$

C. *Bi-level optimal dispatch for IDR*

Price-based IDR is utilized and the end-users schedule load curves in response to the price signals. The lower level optimal dispatch is to minimize the total cost of the customer side; The upper level is to maximize the profit of the IEGM operator.

$$C_1 = \min\sum_{t=1}^{T}\sum_{i=1}^{n}\left[c_e^t P_e^i(t) + \alpha_t c_e^t P_h^i(t)\right]\Delta t \quad (3)$$

$$C_2 = \max[C_1 - \sum_{t=1}^{T}(c_g^t\sum_{j=1}^{J} F_{MT,t}^j + c_{gr}^t P_t)\Delta t] \quad (4)$$

II. SIMULATION RESULTS

III. Table 3 The set of simulation scenes

Scene	IDR	annular pipeline network
1	×	×
2	✓	×
3	×	✓
4	✓	✓

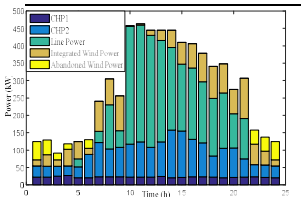

Fig.7 Generation curves in Scene1

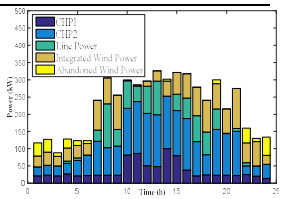

Fig.8 Generation curves in Scene2

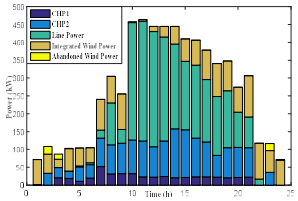

Fig.9 Generation curves in Scene3

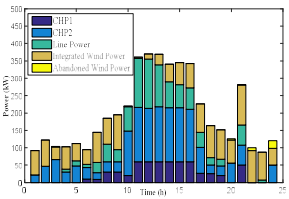

Fig.10 Generation curves in Scene4

VSG Control for DFIG-based Islanded Wind Farm with LCC-HVDC Integration

Xiuqiang He, Hua Geng, Geng Yang
Department of Automation
Tsinghua University, Beijing, China

Xin Zou
State Power Economic Research Institute
Beijing, China

***Abstract*—Doubly-fed induction generator (DFIG)-based islanded wind farms (WFs) cannot be directly integrated by line-commutated converter (LCC)-HVDC through conventional vector control algorithms, due to the lack of a voltage source support on the sending-end bus (SEB) of HVDC. This paper proposes a novel system topology and a virtual synchronous generator (VSG) based control algorithm for islanded DFIG-based WFs with LCC-HVDC integration. In the system topology, batteries are installed at the back-to-back converters of wind turbines (WTs) to generate the terminal voltage and then supply energy for rotor excitation, therefore to provide a prerequisite of the system startup. After the startup, synchronous generator characteristics are exhibited by the DFIGs via the VSG control algorithm. Moreover, a frequency control algorithm is applied into the rectifier of HVDC to achieve active power balance and frequency stability of the SEB. Simulations performed on PSCAD/EMTDC verify the proposed control algorithm.**

***Index Terms*—DFIG, LCC-HVDC, startup, VSG, wind farm.**

I. Introduction

Transmitting electricity from islanded WFs (e.g., offshore WFs) into the main grid through LCC-HVDC (HVDC for short hereinafter) is a critical issue from the operation principle point of view: 1) conventional vector controls are incompetent); 2) Startup of DFIG requires external power sources to supply energy for rotor excitation. This paper proposes a battery based system topology to realize its black startup, and a VSG control algorithm to mimic the operational characteristics of SGs with HVDC connection.

II. Proposed Control Algorithm

The proposed system topology is shown in Fig. 1 (right part). The battery cannot only help generate the SEB voltage through grid side converters (GSCs), but also provides energy to start DFIGs through rotor side converters (RSCs). System startup process is summarized as follows:

Step 1: The back-to-back converter dc-bus capacitor of WT is charged (close s_4 in Fig. 1); The SEB voltage is generated through the GSC based on the constant-alternating-voltage control (set s_5 ~ s_7 to positon 2);
Step 2: The pre-synchronization of DFIG is achieved based on the VSG pre-sync control (open s_0, set s_1 ~ s_3 to positon 2);
Step 3: Close s_0, and the RSC is switched to VSG normal (vs. pre-sync) control (set s_1 ~ s_3 to positon 1). Later, the GSC is switched to the unity power factor control (set s_5 ~ s_7 to positon 1).
Step 4: Unlock HVDC and the corresponding frequency control (set s_8 to positon 1) once active power starts to increase.

III. Results and Conclusions

The WF is equivalent to two single-machine DFIG-based WTs (300 and 500MVA). The simulation results shown in Fig. 2 can verify the effectiveness of the proposed control algorithm. Based on the batteries, the constant-alternating-voltage control of GSCs generates the initial ac voltage as a reference for the system startup. Later, the proposed VSG control algorithm of RSCs of islanded DFIGs makes the DFIGs mimic the operational characteristics of SGs, such as inertia simulation, excitation and regulate voltage. The proposed frequency control algorithm in the rectifier of HVDC achieves the active power balance of the SEB and the SEB frequency stability.

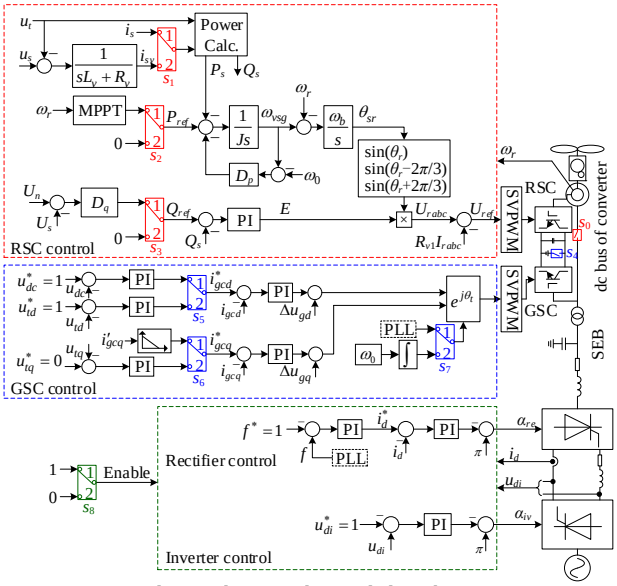

Fig. 1. System topology and proposed control algorithm.

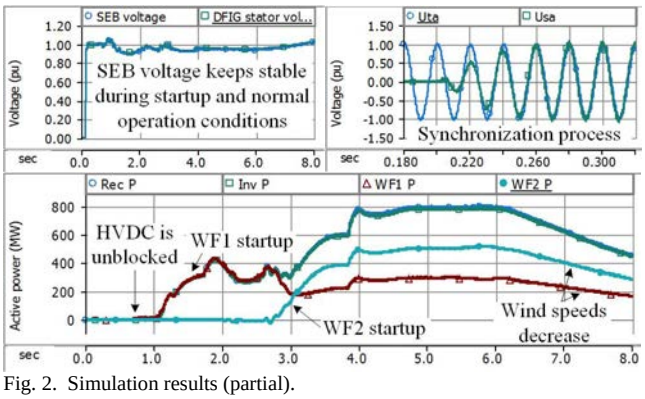

Fig. 2. Simulation results (partial).

Voltage Sensitivity Matrix-Based Volt-Var Control for Unbalanced Distribution Systems using DERs

Catie McEntee, David Mulcahy, Jiyu Wang, Ning Lu
FREEDM Systems Center
North Carolina State University
Raleigh, NC, USA
cmmcente@ncsu.edu

***Abstract*— This study explores a control strategy that optimizes the use of utility control devices as well as distributed customer-owned resources to control voltage and power factor on a distribution feeder. Control actions include voltage regulator tap changes, shunt capacitor switching, reactive power injection and absorption by smart inverters, PV curtailment, and customer demand response. This strategy uses a Voltage Sensitivity Matrix (VSM) in a mixed-integer linear program to choose the least-cost combination of control actions that successfully brings all voltages within desired voltage limits, maintains an acceptable power factor at the top of the feeder and minimizes changes in voltage between time periods.**

I. Introduction

Increased DER penetration can exacerbate voltage issues on distribution feeders, but also offers opportunities for distribution system operators to more precisely and efficiently control voltage. In this control scheme, five types of control actions are coordinated to find an acceptable voltage solution at the least cost. Each possible control action is assigned a cost: voltage regulators have a cost per tap change; capacitors have a cost per switching operation; customer loads have a piecewise linear per-kWh cost function; and PV plants have a per-kWh curtailment cost as well as a per-kVAR reactive power cost (which applies for both injection and absorption). Each of these control actions is limited by the respective resource availability. The effect of each control action is estimated using a Voltage Sensitivity Matrix (VSM). The VSM and control costs are used in a mixed integer linear program to find the optimal control actions for each 5-minute time period for a given distribution feeder or substation.

II. Objective Function

$$\min \quad C_P^{PV}\sum_{j\in S_{PV}}\left(\Delta P_j^{PV}\right)+C_Q^{PV}\sum_{j\in S_{PV}}\left(Q_j^{PV,inj}+Q_j^{PV,abs}\right) \\ +\sum_{k=1}^{K}\sum_{j\in S_{Load}}\left(C_k^{DR}\cdot\Delta P_{j,k}^{Load+}+C_k^{DR}\cdot\Delta P_{j,k}^{Load-}\right)+\varpi\sum_{i\in S_V}\left(\Delta V_i^{up}+\Delta V_i^{down}\right) \quad (1)$$

Where

$$\Delta V_i^{up,t}-\Delta V_i^{down,t}=V_i^{1,t}-V_i^{1,t-1} \quad (2)$$

$$V_i^1=V_i^0+\sum_{j\in S_{PV}\cup S_{Load}}VLSM_{i,j}^{P}\cdot\Delta P_j^{Total}+\sum_{j\in S_{PV}\cup S_{Load}}VLSM_{i,j}^{Q}\cdot\Delta Q_j^{Total} \\ +\sum_{j\in S_{cap}}VLSM_{i,j}^{cap}\cdot\Delta s_j^{cap}+\sum_{j\in S_{reg}}VLSM_{i,j}^{reg}\cdot\Delta s_j^{reg} \quad (3)$$

Subject to:

$$V^{\min}<V_i^1<V^{\max} \quad (4)$$

III. Key Results

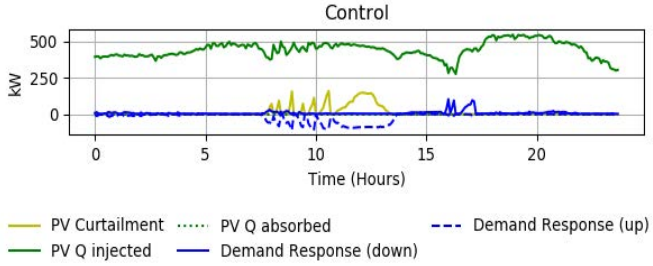

Fig. 1. Total reactive power injection, PV curtailment and demand response for one day simulation

	Existing Control	VSM Control
Capacitor Switches	0	0
Tap Changes	79	13
PV Curtailment	0	310.95 kWh
Smart Inverter Q injection	0	10516.06 kVARh
Smart Inverter Q absorption	0	0.00 kVARh
Demand Response	0	605.40 kWh

Table 1. Comparison of conventional control and VSM volt-VAR control actions for one day simulation

IV. Conclusion

This control strategy allows utilities to take advantage of controllable customer-owned loads and generators to assist or replace voltage regulators and capacitors for voltage control. The algorithm effectively keeps voltages within desired limits, smooths the voltage variation throughout the day, and reduces the number of tap changes and capacitor switching operations. This reduction can contribute to lower maintenance costs for the utility especially where PV variability would cause excessive tap changes under traditional control strategies.

This work is funded by the U.S. Department of Energy SunShot Initiative.

Minimizing Wind Power Curtailments Using OPF Considering Voltage Stability

Elis Nycander and Lennart Söder
Department of Electric Power and Energy Systems
KTH Royal Institute of Technology Stockholm, Sweden
Email: {elisn,lsod}@kth.se

Robert Eriksson and Camille Hamon
Svenska Krafnät, Stockholm, Sweden
Email: {Robert.Eriksson,Camille.Hamon}@svk.se

***Abstract*—As the amount of wind power in power systems has increased it has become necessary to curtail wind power in some high-penetration situations. In order to assess the need for curtailment arising from voltage stability considerations we develop a security constrained optimal power flow for minimizing the expected curtailment. We find that with a very high wind penetration and wind farms operating at unity power factor curtailment becomes necessary to satisfy voltage limits. In this case the optimal solution is to curtail at a single bus rather than curtailing by a smaller amount at several buses. However, allowing for reactive power production from wind farms reduces the need for curtailments.**

***Index Terms*—Wind power, Curtailment, Voltage stability, OPF**

I. Introduction

We develop an optimal power flow to minimize the expected curtailments of wind power, subject to security constraints under contingencies and different wind power scenarios. The objective is to investigate under what situations voltage stability may limit transmission from an area with high wind penetration and the curtailments arising as a result.

II. Problem formulation

A. Problem

$$\min \mathbb{E}\left(\sum_{j\in\mathcal{W}} P_{w,j}\beta_j\right) = \sum_{s\in\mathcal{S}} p^s \sum_{j\in\mathcal{W}} P^s_{w,j}\beta^s_j \qquad (1)$$
$$g(\mathbf{x}) = 0$$
$$h(\mathbf{x}) \leq 0$$

Table I: Summary of load flow for original Nordic 32 system

Area	Generation (MW)	Load (MW)	Losses (MW)
North	4630	1180	266
Central	2850	6070	150
Southwest	1590	1390	14
External	2300	2300	0
Total	11370	10940	430

B. Power factor constraints

$$|Q^s_{w,j}| \leq \kappa_w P^s_{w,j}\left(1-\beta^s_j\right),\ j\in\mathcal{W} \qquad (2)$$
$$|Q^s_{g,j}| \leq \kappa_g P^s_{g,j},\ j\in\tilde{\mathcal{G}} \qquad (3)$$
$$|Q^s_{g,j}| \leq \kappa_g P_{g,j},\ j\in\mathcal{G}\setminus\tilde{\mathcal{G}} \qquad (4)$$

III. Results

For high wind power penetration in exporting area (North) there is insufficient reactive power capability which requires curtailment (Figure 1) to keep voltage limits. Curtailment occurs at a single bus (Figure 2). When allowing wind farms to operate at variable PF there is no need for curtailment.

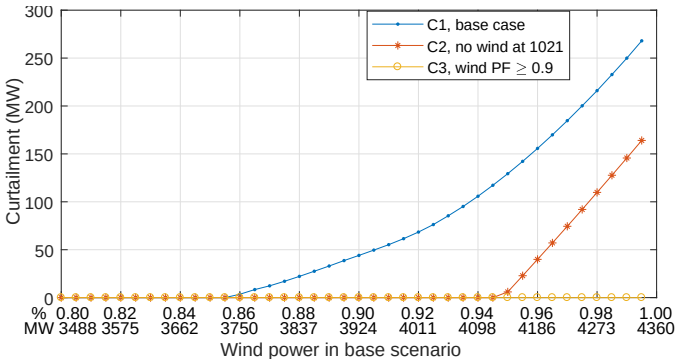

Figure 1: Curtailment for increasing wind penetration.

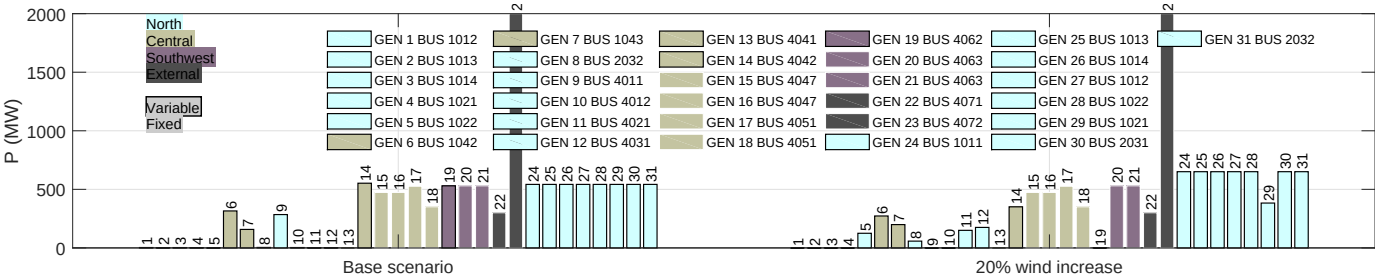

Figure 2: Active power of generators for 99.5% penetration in North for case C1.

The Value of Reactive Power for Voltage Control in Lossy Networks

Matthew Deakin, Thomas Morstyn, Malcolm McCulloch
Department of Engineering Science
University of Oxford, Oxford, UK

Dimitra Apostolopoulou
Department of Electrical & Electronic Engienering
City, University of London, London, UK

***Abstract*—Reactive power has been proposed as a method of voltage control for distribution networks. The value of reactive power can therefore be measured according to an increase in *transferred* energy, where the transferred energy is defined as the total generated energy, less the total network losses. If network losses are ignored, an error in the valuation of a given amount of reactive power will be observed. The non-linear closed-form solution of a two-bus network is studied, and non-trivial upper and lower bounds are determined for this 'valuation error'. The properties predicted by this two-bus network are demonstrated to hold on a three-phase unbalanced distribution test feeder.**

I. Introduction

Reactive power is one of a number of technologies that can be used as a method of increasing the amount of distributed generation (DG) connected to distribution networks, by reducing the voltage at generators that is seen (for a given real power generation). Sinking reactive power changes the network losses. Without taking into account the changes in losses, we cannot fairly assess the value of the reactive power.

II. Reactive Power Valuation

We study the closed-form solution of the two bus network shown in Fig. 1 to study network losses P_l (using notation $S_{(\cdot)} = P_{(\cdot)} + \mathrm{j}Q_{(\cdot)}$ as apparent, real, reactive powers respectively). These losses come about due to the network impedance Z, representing an equivalent positive sequence impedance from generator to source. For a given load S_0 and generation profile P_S, we can calculate the generated and transferred energy as

$$E_g = \int_0^T P_g(\tau, \hat{Q}_g)\, d\tau\,, \quad E_t = \int_0^T P_t(\tau, \hat{Q}_g)\, d\tau\,,$$

for a given time period T, given reactive power limit $\hat{Q}_g$, grid voltage V_t, and maximum generator voltage V_g. The increase in energy generated and transferred, as 'approximate' and 'true' reactive power valuations ($\Delta E_g, \Delta E_t$ respectively, as E_t includes changes to network losses), are thus

$$\Delta E_g = E_g(\hat{Q}_g) - E_g(0)\,, \quad \Delta E_t = E_t(\hat{Q}_g) - E_t(0)\,.$$

As such, we can define both energy and instantaneous (power) *valuation errors* respectively as

$$\epsilon_E(\hat{Q}_g) = \frac{\Delta E_g - \Delta E_t}{\Delta E_t}\,, \quad \epsilon_P(\hat{Q}_g) = \frac{\Delta P_g - \Delta P_t}{\Delta P_t}\,.$$

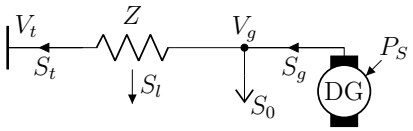

Fig. 1. Two bus power flow model.

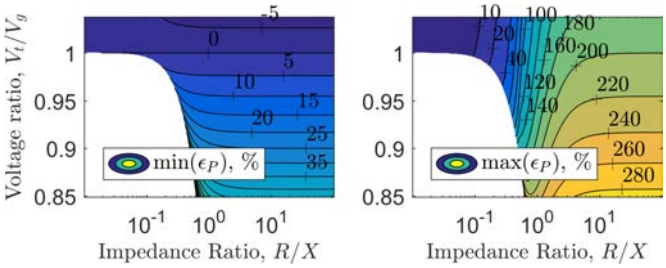

Fig. 2. Lower (l) and upper (r) bounds on valuation error ϵ_E.

III. Results & Conclusions

The power valuation error ϵ_P bounds the energy valuation error ϵ_E. We therefore calculate ϵ_P as $\hat{Q}_g$ tends to zero, and at a maximum power transfer (MPT) point, to bound ϵ_E (see Fig. 2). These bounds are irrespective of the generation profile.

Three case studies were run (on the IEEE 34 bus distribution test feeder) with 2.7, 4.8 and 6.7 MWp distributed generation, using the generation profile of Fig. 3. The two-bus model is reasonably accurate, slightly over-estimating ϵ_E. This is caused by the voltage dependency of reactive power loads.

We conclude that the significance of these losses is modelled accurately using the two bus model. The model can be used to show when losses can (and cannot) justifiably be ignored.

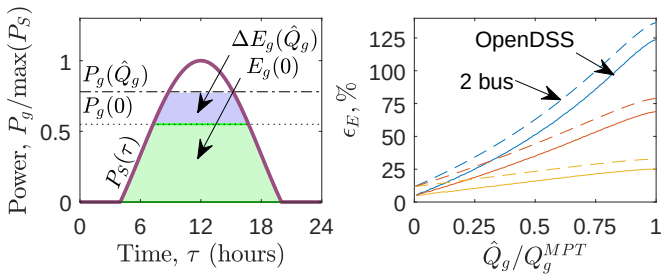

Fig. 3. Generation profile (l), and case study results (r).

Study and Comparison of Wind Power Correlation Using Two Types of Dataset

Yurong Wang, *Member*, *IEEE*, Yannan Luo
School of Electrical Engineering, Southeast University
Nanjing 210096, China
Email: wangyurong@seu.edu.cn

Zeyu Dai
State Grid Taizhou Power Supply Company
Taizhou 225300, China

***Abstract*—With the integration of large-scale wind farms, stability and economy of power grid are greatly challenged. Considering the stochastic characteristics of wind and the coupling relationship of geographically distributed wind farms, this paper presents the comparison of analysis methods and results when using wind speed dataset and wind power output dataset in wind power spatial correlation research based on copula. Combined with several revised criteria, a novel method is proposed to select copula type and judge goodness of fit. In the case study, copula models and typical scenarios using the two datasets are highlighted and compared. Study results clarified the advantages and disadvantages of using different datasets.**

***Index Terms*—Copula, evaluation index, wind power correlation, typical scenario, wind power.**

I. Introduction

With the access of multiple large-scale wind farms, power grid faces serious problems in system operation, especially the generation scheduling and unit commitment problems. Researchers found that there is some type of correlation between geographically distributed wind farms. Copula theory is used to study the output correlations of multiple wind farms based on wind speed dataset and wind power output dataset in this paper, and a novel method to select copula model is proposed based on three revised indices in order to evaluate the accuracy of modeling.

II. Key Equations

A. Relationship of Wind Speed and Wind Power Output

$$P_{WTG}=\begin{cases}0, 0\le V\le V_{ci}\ or\ V\ge V_{co}\\ P_{WTG,r}\dfrac{V-V_{ci}}{V_r-V_{ci}},\ V_{ci}\le V\le V_r\\ P_{WTG,r}, V_r\le V\le V_{co}\end{cases} \quad (1)$$

B. Copula Theory

$$F(x_1,x_2,\cdots,x_N)=C\big(F_1(x_1),F_2(x_2),\cdots,F_N(x_N)\big) \quad (2)$$

C. Mixed-Copula Theory

$$C=\omega_1C_1+\omega_2C_2+\omega_3C_3 \quad (3)$$

$$C=\pi C_1+(1-\pi)C_2 \quad (4)$$

III. Case Study

A. Binary Frequency Histograms

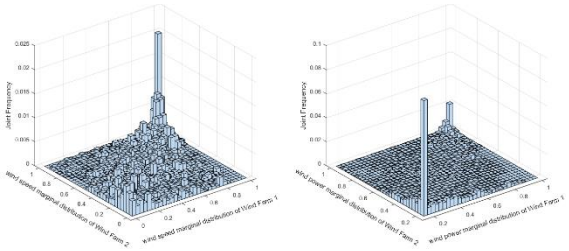

(a) Result using wind speed dataset (b) Result using wind power dataset

Fig. 1. Binary frequency histogram using two different datasets.

B. A Novel Method for the Selection of Copula Function

TABLE I. Copula Selection Using Wind Speed Dataset

Type / Criterion	normal-Copula	t-Copula	Clayton Copula	Frank Copula	Gumbel Copula
Euclidean			×		√
Kendall			×	√	
Spearman	×		×		○
AIC			×		√

TABLE II. Copula Selection Using Wind Power Dataset

Type / Criterion	normal-Copula	t-Copula	Clayton Copula	Frank Copula	Gumbel Copula
Euclidean	○		×		×
Kendall	√				×
Spearman				×	○
AIC	○		×		×

IV. Conclusions

This paper finally come to conclusions as follow:

1) Under the same research method, copula model can describe the correlation of wind speed better than wind power output in this case study.

2) The results of clustering using wind power is better for further research, but incorporating copula method to describe the correlation of wind power output produces larger error.

Application of Solid State Transformers in Hybrid Residential Energy Delivery

Manisha Maharjan and Rajesh Kavasseri
Department of Electrical Engineering and Computer Science
North Dakota State University
Fargo, North Dakota
Email: manisha.maharjan@ndus.edu

***Abstract*—The integration of renewable energy sources like solar and wind, has been continuously increasing in the residential distribution system. These require improved controllability to maintain proper coordination between stochastic renewable sources and load. Solid state transformers (SSTs) are power electronic devices which consist of the converter models that can reduce the conversion stages in hybrid AC/DC residential distribution systems. This work presents the preliminary results of integrating this simplified model of SST in an example model of residential distribution system, comprised of a residential house with AC, DC loads, solar panel and battery system. This will create a baseline for using these simplified models to compare the performance of such hybrid system in the residential distribution systems. Traditional transformers replaced with these SSTs solve the purpose of bi-directional power flow and provide integration of renewable energy sources and DC loads,without add-on power electronic components, reducing complexity.**

I. Introduction

Renewable energy sources like residential photovoltaics (PV) in low voltage distribution feeders help in addressing energy demand without adding large generation and transmission units [1]. Due to the decrease in installation cost of PV, the residential PV market has been growing rapidly. Increase in the use of modern DC appliances render the prospect of energizing these DC devices from renewable energy sources directly. The key idea of this work is to explore the use of simplified solid state transformer (SST) [2] in the residential distribution system, which incorporates DC power sources like PV and battery with residential AC as well as DC loads.

II. Key Figure

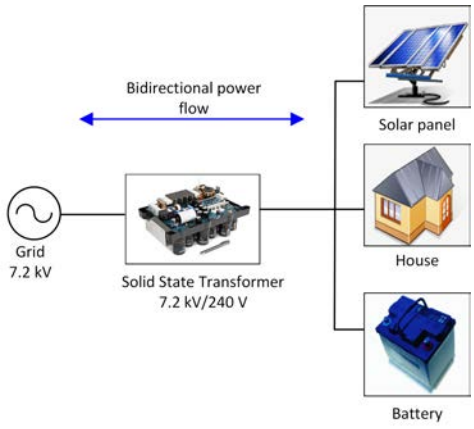

Fig. 1. A example model for residential distribution system.

III. Key Result

The preliminary results show that the load is being supplied by solar power and battery primarily. When there is deficiency in solar power and battery is undercharged or off, the load power consumption is fulfilled through the utility. SST supports the bi-directional power flow as surplus power is fed back to the utility, when battery charging is not required.

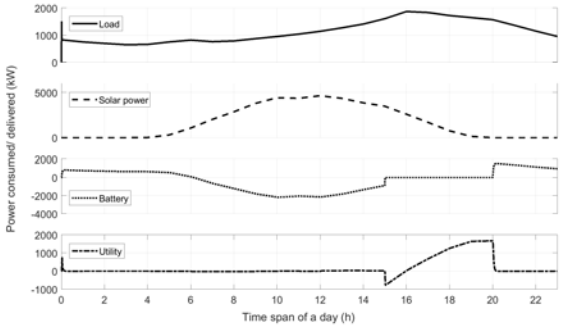

Fig. 2. Power consumed and delivered by load, solar, battery and utility in a 24.hour period.

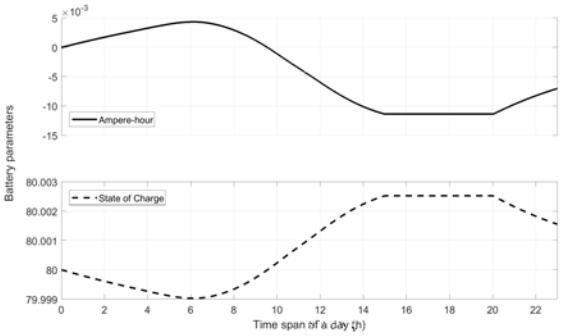

Fig. 3. Battery ampere-hour and state of charge for 24 hour period.

References

[1] Solar Energy Industries Associations. (2016) *Solar Market Insight Report 2016 Q4*. [Online]. Available: http://www.seia.org/research-resources/solar-market-insight-report-2016-q4

[2] M. Maharjan, U. Tamrakar, S. Bajagain, T. M. Hansen, and R. Tonkoski, "A steady-state equivalent model of solid state transformers for voltage regulation studies," in *2017 IEEE Power Energy Society General Meeting*, July 2017, pp. 1–5.

Comparing Capacity Value Metrics of Energy-Limited Resources

Sarah Awara
Department of Electrical and Computer Engineering
University of Calgary
Calgary, Canada
saawara@ucalgary.ca

Hamidreza Zareipour
Department of Electrical and Computer Engineering
University of Calgary
Calgary, Canada
hzareipo@ucalgary.ca

Andy Knight
Department of Electrical and Computer Engineering
University of Calgary
Calgary, Canada
aknigh@ucalgary.ca

***Summary*— Capacity value, or capacity credit, measures the contribution of an added generation resource to meet the demand in a power system. Unlike conventional generators, whose available capacity depends on the mechanical availability, energy-limited resources have limiting factors that affect their ability to operate continuously on a daily basis. Examples of energy-limited resources are renewable and energy storage resources. With the increase in energy-limited resources in power systems, it is critical to accurately determine their capacity value during generation planning to maintain system reliability. This poster will focus on comparing the capacity value of wind computed by different capacity value methods for different locations in Alberta.**

I. Introduction

The reliability of supply is a major concern in electric power systems. This reliability will increase when more renewables and energy storage resources are added to the current electric power system. However, when energy-limited resources replace dispatchable generators, there is a concern about the reliability of the system [1]. Higher amounts of reserve capacity are needed to maintain the system's adequacy. Therefore, it is important to determine the capacity value (CV) of generation resources to ensure that the reliabitiy of the system is met during power generation planning.

The CV of a generator resource depends on the risk model characteristics used to calculate the CV. The risk model for solar is different than the risk model used to calculate the CV of storage. Based on the literature, the CV of a renewable facility can have a wide range between 5% and 95% of the nameplate capacity and some of the factors that contribute to this range are related to geography, penetration levels of the technology and the correlation of generation and demand [2].

II. Research & Methodology

When calculating the CV of a specific technology, the literature includes several different risk models with different assumptions. Also, when comparing the capacity value studies of the same system using different methodologies, it is critical to pay attention to the details of the method [3].

There are two classes for quantifying capacity value: probabilistic-based and approximation-based methods. Most system operators use the approximation-based method (capacity factor methodology) to calculate the CV of renewables. This methodology calculates the CV based on the capacity factor of renewables during a set number of hours.

The probabilistic-based method uses extensive data from all hours of the day to compute the CV with a higher resolution. The probabilistic-based methodology is illustrated in Fig. 1. In this approach, the generation model only considers conventional generation and is developed by computing the Capacity Outage Probability Table (COPT). Wind power time series are included by means of a net load model. For a specified period under investigation, the wind time series is treated as negative load and subtracted from the load time series. The generation model and the net load model are convolved to compute the Loss of Load Expectation (LOLE) and Expected Unserved Energy (EUE).

Alberta is currently designing a capacity market. One of the major topics discussed by the Alberta Electric System Operator (AESO) is capacity value determination. Therefore, this poster will compare the capacity value of wind using different probabilistic-based and approximation-based methods using historical data.

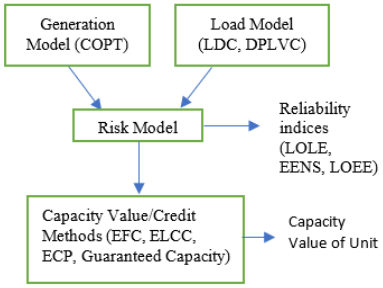

Fig. 1. Capacity Credit Determination Methodology

III. References

[1] M. Amelin and L. Söder, "Taking Credit: The Impact of Wind Power on Supply Adequacy- Experience from the Swedish Market," *IEEE Power and Energy Magazine*, vol. 8, no. 5, pp. 47-52, 2010.

[2] D. Gami, R. Sioshansi and P. Denholm, "Data Challenges in Estimating the Capacity Value of Solar Photovoltaics," *IEEE Journal of Photovoltaics* , vol. 7, no. 4, pp. 1065-1073, July 2017.

[3] P. O. Aguirre, C. J. Dent and G. P. Harrison, "Realistic Calculation of Wind Generation Capacity Credits," in *CIGRE*, Calgary, 2009.

We acknowledge the support of the Natural Sciences and Engineering Research Council of Canada (NSERC), CRDPJ 477323 – 14 (Cette recherche a été financée par le Conseil de recherches en sciences naturelles et en génie du Canada (CRSNG), CRDPJ 477323 – 14). This project was funded in part by Alberta Innovates, which supports and accelerates research, innovation and entrepreneurship. This project is also supported by Rocky Mountain Power.

Energy Storage Integration in an Islanded Wave Energy System

Eric Wu, Andrew M. Knight

Department of Electrical and Computer Engineering, University of Calgary

***Abstract*— Energy storage systems are vital for integrating renewable energy resources into the existing power system in a reliable and sustainable manner. In particular, an islanded microgrid should be able to rely on renewable energy systems when grid faults occur. This research will endeavor to determine an energy storage control system capable of ensuring the reliable operation of an islanded microgrid heavily populated by renewable energy sources.**

I. Introduction

Microgrids combine distributed energy resources, energy storage and loads together. The ability to operate during grid faults and support remote communities have made microgrids a popular topic among fellow researchers. Renewable energy represents one of the distributed energy resources commonly implemented in microgrids. Similar to microgrids, renewable energy is experiencing prominent growth as a result of its promise to supply clean and limitless energy. However, power intermittency is a well-known issue associated with renewable energy that can compromise the reliability and resiliency that microgrids promise. Power intermittency refers to the varying and fluctuant nature of renewable resources. To mitigate power intermittency, energy storage can be used. The control strategy for energy storage systems depends on whether the microgrid is operating in grid-connected or in islanded operation. In this research, the control strategies needed for a microgrid operating in islanded operation will be explored. Furthermore, the microgrid of interest will consist of a wave energy system, a battery energy storage system and a constant power load. In the model, three different wave energy systems will be considered. The first wave energy system will consist of a single Wave Energy Converter (WEC). A second WEC will be added to form the second wave energy system. Finally, the third wave energy system will contain a total of three WECs. For each of these systems, an arbitrary, but reasonably sized, battery storage system and load will be connected at the system's Point of Common Coupling (PCC). The objective of exploring wave energy systems with varying sizes is to evaluate the flexibility of the battery storage's control system. By analyzing the power waveforms generated at the PCC of each system, the effectiveness of the battery storage's control system can be assessed.

II. Methodology and Results

A. *Islanded Wave Energy System*

Figure 1 illustrates the generic islanded wave energy system investigated in this research.

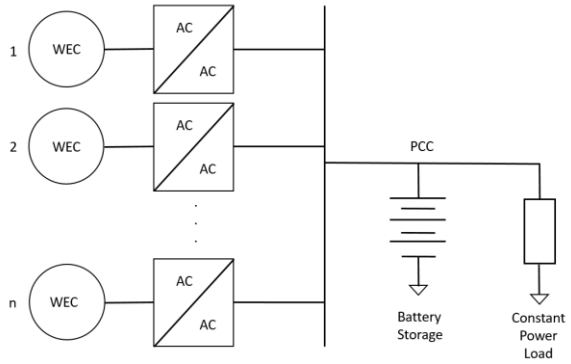

Fig 1. Islanded Wave Energy System with Battery Storage and a Constant Power Load

As shown in Fig. 1, each WEC contains a back-to-back converter for active and reactive power control. By appropriately controlling an adequately sized battery storage system, a constant power flow can be guaranteed for the constant power load, regardless of the power supplied by the wave energy system. Initially, a single WEC with battery storage is connected at the PCC in Figure 1. A 120Ω resistor is used in place of the constant power load and the system is modelled in a simulation software. In the simulation, the battery is controlled as a voltage source by setting its d-axis voltage equal to one.

B. *Power Flows Measured at the PCC*

Figure 2 shows the power flowing through each of the three sources considered in Figure 1 for a system with one WEC.

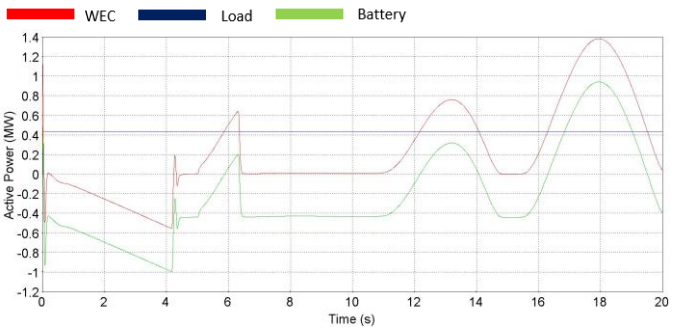

Fig 2. Power Flow at PCC measured out of WEC and into Load and Battery

As observed in Figure 2, the battery storage system is able to accommodate the power required by the load by supplying the deficit or absorbing the excess power generated by the WEC.

Life Cycle Testing of Vanadium Redox Flow Battery and Lithium Ion Energy Storage Systems

Muhammad Rashid, Andy Knight
Department of Electrical and Computer Engineering
University of Calgary
Calgary, AB, Canada
Email: muhammad.rashid2@ucalgary.ca, andy.kinght@ucalgary.ca

I. INTRODUCTION

The integration of energy storage systems in power grids has gained vast interest in recent years. Energy storage systems can take many forms with sizes varying from few kilowatt-hours to many gigawatt-hours. Such systems can resolve some of the challenges faced by the different segments of power grids. They can also aid in the integration of renewable energy generation.

II. METHODOLOGY

This abstract focuses the performance of Battery Energy Storage Systems (BESS). Life cycle testing is being performed on two types of BESS. The first is a vanadium redox flow battery and the other is a Lithium-Ion backup power system. The main objective of the test is to measure the performance of the BESS in terms of round trip efficiency and how it correlate to operational conditions such ambient temperature. The test also measures the degradation in efficiency caused by the continuous cycling.

A. *Vanadium redox flow battery*

A Vanadium Redox Flow Battery (VRFB) employs vanadium electrolytes as the energy storage element. It also includes all the necessary hardware such as flow pumps and ion exchange membrane. The life cycle testing on the VRFB is carried out by commercially available DC battery testing equipment that charges and discharges the battery at rates that are specified by the user, also called C rate.

The maximum allowable continuous C rate as per the manufacturer's specifications is used for this testing work. At the time of writing this abstract, a total of 165 cycles have been performed on the VRFB.

An important metric of evaluating the performance of flow batteries is the electrolyte temperature. This metric is directly correlated to the round trip efficiency of the VRFB. Figure **1** clearly shows such correlation.

B. *Lithium-Ion energy storage system*

The second BESS that is also being tested in this work is a fully integrated lithium-ion energy storage system. It is a commercially available backup power system intended for use in residential dwellings. In contrast to the VRFB, this system comes fully integrated with a battery management system and inverter. The user does not have direct access to the lithium-ion battery; neither can they specify the settings needed for the life cycle testing since the system is designed for autonomous operation.

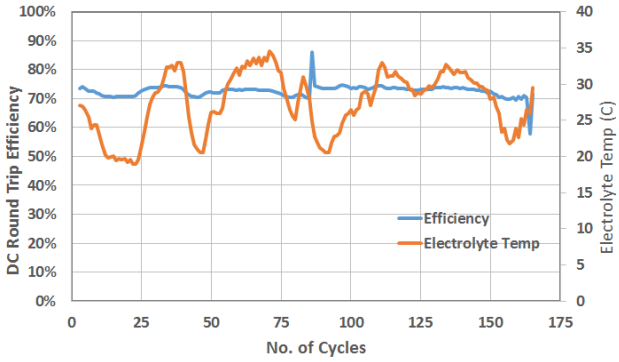

Figure 1: VRFB efficiency and electrolyte temperature

In order to perform the intended testing procedures, a testing setup had to be implemented in order to force the system to perpetually charge and discharge the battery to full capacity. The diagram in Figure **2** shows how the testing setup was implemented.

The setup incorporates measurement and control devices as well a space heater to serve as a constant power load. The measurement devices are one potential transformer (PT) two current transformers (CT-1 & CT-2). The control devices are two solid-state relays (SW-1 & SW-2). In order to force the system to go into charging or discharging modes, the readings from CT's are monitored and as per a user defined control sequence, the relays are actuated accordingly. The voltage and current measurements are used to calculate the system round trip efficiency and capacity degradation.

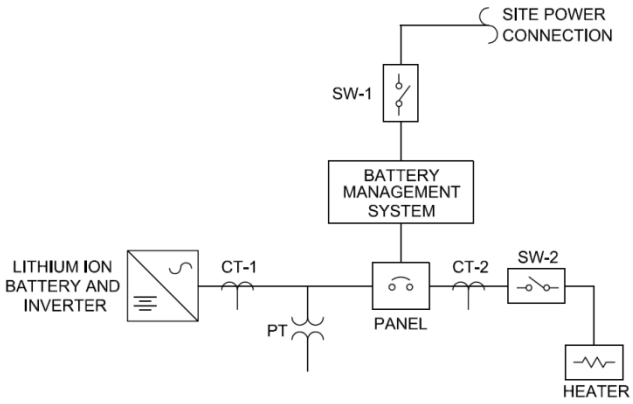

Figure 2: Li-Ion energy storage system testing setup

Modeling and Control of an Integrated Wind Power Generation and Modular Multilevel Converter with Energy Storage System

[1]Jaesik Kang, *Member*, *IEEE*, [1]Sangmin Kim, *Member*, *IEEE*, [1]Wooyoung Shin, *Member*, *IEEE*, [1]Sehwan Lim, *Member*, *IEEE*, [1]Jae Woong Shim, *Member*, *IEEE* and [1]Kyeon Hur, *Senior Member, IEEE*
[1]School of Electrical and Electronic Engineering, Yonsei University, Seoul, Korea
Email: jaesikkang84@gmail.com, tkdminn@gmail.com, shinwoo0514@naver.com, bulls92@hanmail.net, khur@yonsei.ac.kr

***Abstract*—This paper analyzes the internal dynamics of modular multilevel converter (MMC) for exploiting sub-modules (SM) as an energy storage system for smoothing the fluctuating output power of wind power generation. The fluctuating output power of the wind generation may cause an oscillatory impact on an interconnected grid, and it thus aggravates the grid stability. In conventional method for achieving the stability enhancement, energy storage system (ESS) is a key role of maintaining the changes in renewable generation system, which might be considered as slightly unnecessary solution in high-voltage direct current (HVDC) transmission system for the wind power generation due to the controllability of the converter for HVDC. In this paper, the MMC system and controller with energy storage management is modeled and developed by investigating the internal dynamics of the MMC, and a simple system with a synchronous generator (SG) and wind power plant (WPP) based on PSCAD/EMTDC is simulated to demonstrate the efficacy of the proposed control scheme for establishing a role of the ESS in the MMC, and it requires that the system be stabilized by the ESS based MMC system to avoid the oscillatory mode from the fluctuating output power of the wind generation system.**

***Index Terms*—Modular multilevel converter (MMC), high voltage direct current (HVDC), wind power generation, PSCAD/EMTDC, energy storage system (ESS), synchronous generator (SG).**

I. KEY FIGURES

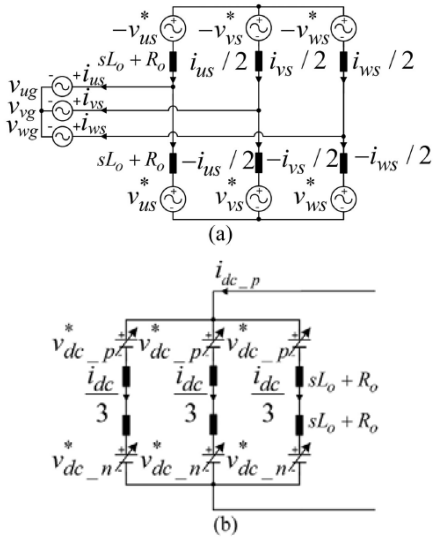

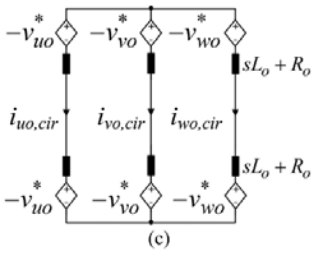

Fig. 1. Internal dynamics of MMC with a decoupled control of ESS for an integrated wind generation system: (a) behavior for AC current, (b) DC current and (c) circulating current.

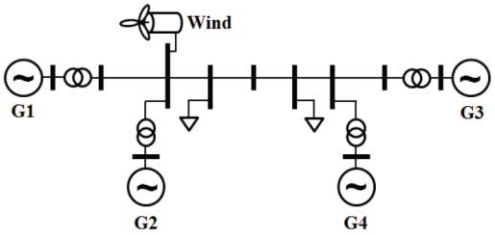

Fig. 2. Two area test system.

II. KEY RESULTS

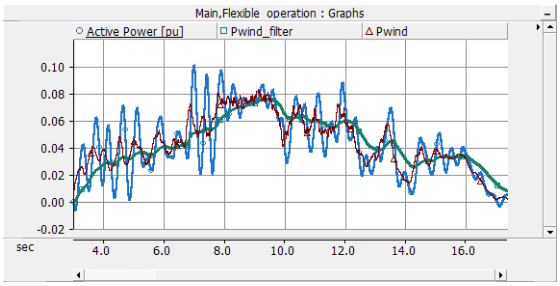

Fig. 3. The fluctuating and mitigated output power of the wind generation with and without ESS operation in the MMC.

III. REFERENCE

[1] Jae Woong Shim, *et. al.*, "Impact Analysis of Variable Generation on Small Signal Stability", in *Proc. Australian Universities Power Engineering Conf., Perth, Austrailia*, Oct 2014.

[2] Shenghui Cui and Seung-Ki Sul, "A Comprehensive DC Short-Circuit Fault Ride Through Strategy of Hybrid Modular Multilevel Converters (MMCs) for Overhead Line Transmission", *IEEE Trans. on Power Electronics*, Vol. 31, No. 11, pp. 7780-7796. Nov. 2016.

[3] Zhenhua Jiang, *et. al.*, "Modeling and Control of an Integrated Wind Power Generation and Energy Storage System", in *Proc. IEEE Power and Energy Soc. General Meeting*, 2009.

Indirect Mechanism Design for Efficient and Stable Renewable Energy Aggregation

Hossein Khazaei
Dept. of Electrical and Computer Engineering
Stony Brook University
Stony Brook, NY, 11794 USA
Email: hossein.khazaei@stonybrook.edu

Yue Zhao
Dept. of Electrical and Computer Engineering
Stony Brook University
Stony Brook, NY, 11794 USA
Email: yue.zhao.2@stonybrook.edu

***Abstract*—Mechanism design is studied for aggregating renewable power producers (RPPs) in a two-settlement power market. Employing an indirect mechanism design framework, a payoff allocation mechanism (PAM) is derived from the competitive equilibrium (CE) of a specially formulated market with transferrable payoff. Given the designed mechanism, the strategic behaviors of the participating RPPs entail a non-cooperative game: It is proven that a unique Nash equilibrium (NE) exists among the RPPs, for which a closed form expression is found. Moreover, it is proven that the designed mechanism achieves a number of key desirable properties at the NE: these include efficiency (i.e., an ideal "Price of Anarchy" of one), stability (i.e., "in the core" from a coalitional game theoretic perspective), and no collusion. In addition, it is shown that a set of desirable "ex-post" properties are also achieved by the designed mechanism. Extensive simulations are conducted and corroborate the theoretical results.**

I. Introduction

Renewable energies play a central role in achieving a sustainable energy future. However, renewable energies such as wind and solar power are inherently non-dispatchable, and yet highly uncertain and variable. Aggregation of statistically diverse renewable energy sources can decrease the uncertainty of the renewable power producers (RPPs). A key question in aggregating RPPs is how to allocate the total payoff of an aggregation among its member RPPs. In this paper, we propose a *mechanism* to address this question.

II. Problem Formulation

We consider the case where an aggregator represents a set of N RPPs (denoted by $\mathcal{N}$) in the DA-RT market. In the DA market, aggregator asks the RPPs to submit their DA commitments $\{c_i\}$ to it. Aggregator then commits $c_{\mathcal{N}} = \sum_{i\in\mathcal{N}} c_i$ in the DA market. In the RT market, the aggregator collects all the realized generations from the RPPs, denoted by $x_{\mathcal{N}} = \sum_{i\in\mathcal{N}} x_i$. The realized payoff of the aggregator is

$$\mathcal{P}_{\mathcal{N}} = p^f c_{\mathcal{N}} - p^{r,b}\left(c_{\mathcal{N}} - x_{\mathcal{N}}\right)_+ + p^{r,s}\left(x_{\mathcal{N}} - c_{\mathcal{N}}\right)_+ \quad (1)$$

We denote the expected payoff of the aggregator in the DA market by $\pi_{\mathcal{N}} = \mathbb{E}\left[\mathcal{P}_{\mathcal{N}}\right]$.

We use the following payment allocation mechanism (PAM) to allocate the realized payoff of the aggregator in (1) among the RPPs. The realized payoff of RPP i in the aggregation is

$$\mathcal{P}_i = \begin{cases} p^f c_i + p^{r,b}\left(x_i - c_i\right) & \text{if } x_{\mathcal{N}} - c_{\mathcal{N}} < 0 \\ p^f c_i + p^{*}\left(x_i - c_i\right) & \text{if } x_{\mathcal{N}} - c_{\mathcal{N}} = 0 \\ p^f c_i + p^{r,s}\left(x_i - c_i\right) & \text{if } x_{\mathcal{N}} - c_{\mathcal{N}} > 0 \end{cases}, \quad (2)$$

where p^* can arbitrary be chosen within the range $p^{r,s} \le p^* \le p^{r,b}$. The expected payoff of the RPP i in the aggregation is denoted by $\pi_i = \mathbb{E}\left[\mathcal{P}_i\right]$.

III. Contract Game

Within the aggregation, each RPP tries to maximize its expected payoff. This competitive behavior is modeled using a non-cooperative game termed the *contract game*, where the players are the RPPs forming the aggregation, the strategy of each RPP is its DA commitment, i.e. c_i, and the payoff of each RPP is π_i.

It is proved that, under mild assumptions, the contract game always possesses an unique pure Nash equilibrium (NE) with a closed form formula: The strategy of RPP i at this NE is

$$c_i^{\star,ne} = \mathbb{E}\left[X_i \middle| X_{\mathcal{N}} = c_{\mathcal{N}}^{\star,o}\right], \quad (3)$$

where X_i is the random generation of the RPP i, and the $X_{\mathcal{N}} = \sum_{i\in\mathcal{N}} X_i$ is the total random generation of the aggregator. $c_{\mathcal{N}}^{\star,o}$ is the optimal commitment of the aggregator which maximizes the $\pi_{\mathcal{N}}$.

Some of the properties of this mechanism are:

- *Existence of an unique pure Nash equilibrium with closed form formula to compute it*.
- *Optimality of the coalition*.
- *Ex-ante in the core*: Being in the core in an "ex-ante" sense means that the RPPs' expected payoffs satisfy the following condition: if any subset $\mathcal{T}$ of the RPPs leave the aggregation, separately form their own aggregation, and then participate in the market and get their highest possible expected payoff, they will get an expected payoff no higher than the sum of their expected payoffs originally from the aggregator at the unique pure NE of the contract game.

Power-frequency Response Model Identification for Adaptive Virtual Inertia Algorithms

Ujjwol Tamrakar, *Student Member, IEEE*, Reinaldo Tonkoski, *Member, IEEE*
Department of Electrical Engineering and Computer Science
South Dakota State University
Brookings, South Dakota 57007
Email: ujjwol.tamrakar@sdstate.edu

***Abstract*—The rapid growth in renewable energy systems (RESs) has transformed the power system to an inverter dominated system. Virtual inertia systems are being integrated into the power system to improve the frequency stability either through energy storage systems and/or RESs. The total inertia of a power system is thus no longer constant as with the conventional generator dominated system. Hence, the power-frequency response of a system changes continuously over-time based on the number of virtual inertia units that are online. This make it difficult to tune the controllers so that the system can emulate inertia optimally. So, for optimal tuning of these virtual inertia algorithms, an online model of the power-frequency response is needed. This poster presents some preliminary results on identifying the power-frequency response of model based on real-time measurement data.**

I. Key Equations

The integration of components such as photovoltaics (PV), wind and energy storage systems has resulted in significant decrease in the power system inertia. Furthermore, the inertia is time-varying and dependent on the system operating conditions. Virtual inertia systems are proposed in the literature to counteract this reduction in inertia. To optimally tune a controller an online modeling technique which can model the time-varying, dynamic of the relationship between the active power and frequency is needed. A linear least-square estimation method is presented in this poster which can identify the dynamic system based on input and output measurements. In general, an estimated dynamic system can be represented as:

$$\hat{y}(t|\theta) = \phi^T \theta \tag{1}$$

where ϕ is a vector of of input and output data and θ is the poles and zeros that represent the system dynamics. For a known set of measured input-output data, Z^N, defined as:

$$Z^N = \{u(1), y(1), ..., u(N), y(N)\} \tag{2}$$

The unknown of parameter of the model, θ, can be estimated by minimizing:

$$V_N(\theta) = \frac{1}{N} \sum \|y(t) - \hat{y}(t|\theta)\|^2 \tag{3}$$

II. Key Figures

The simulation setup used for power-frequency response identification is shown in Fig. 1. A 13 KVA hydro system is modeled along with the governor and the excitation systems. The inertia constant is set to 2 s. Step load changes of 250 W are applied and the corresponding change in frequency and input power is logged at a sampling rate of 10 Hz. Random Gaussian noise (mean =0, variance = 0.001) is also added to the frequency measurements to make the measurements more realistic.

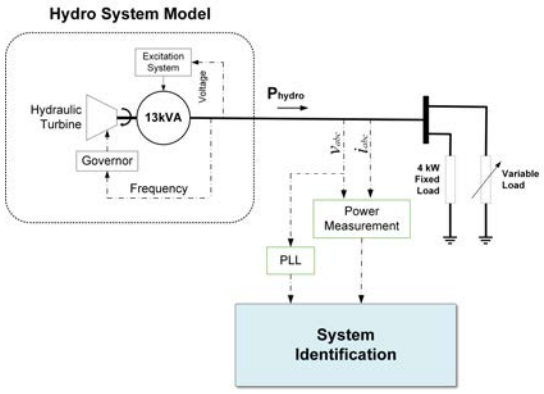

Fig. 1. Simulation setup used for model identification.

III. Key Results

A transfer function with 2 poles and 1 zero provided a good fit of 77.44% with the testing dataset. The fitted model along with the original measured data is illustrated in Figure 2. The dotted-lines around the fitted response represents the 95% confidence interval. Higher order models were also tested but it did not provide any significant improvement in the fit of the model.

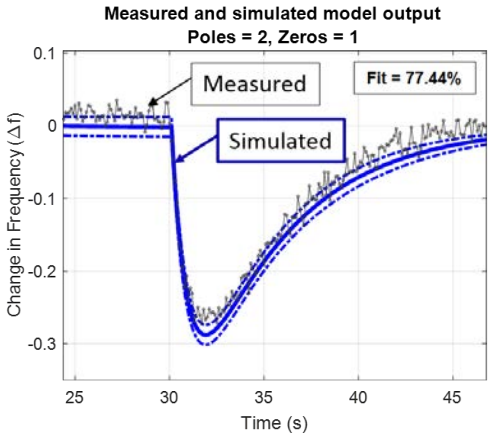

Fig. 2. Identified power-frequency response model and its verification.

IV. Conclusions and Future Work

A linear least-square estimation technique can effectively predict the frequency response of a power system. A online recursive algorithm which can be updated based on system measurements will be developed in the future to account for the inertia variability.

Enhancement of Grid Connected PV Arrays Fault Ride Through and Post Fault Recovery Performance

Aslan Mojallal, *Student Member, IEEE*, and Saeed Lotfifard, *Member, IEEE*

***Abstract*—The proposed control scheme is composed of two controllers: Finite-Time Sliding Mode Control (FTSMC) and Proxy-Based Sliding Mode Control (PBSMC). The FTSMC, which assures the finite time convergence of the tracking error, controls the DC/DC converter of GCPA during voltage sags to assure the DC-link capacitor voltage does not exceed its limits. PBSMC controls the DC/AC inverter. PBSMC provides accurate and fast tracking feature during normal condition (similar to PID controller) and is capable of very smooth resuming to the desired reference value/trajectory after large disturbances that may lead the control signal to exceed the limits. Therefore, during post-fault voltage recovery period, PBSMC exits saturation faster which significantly enhances the recovery performance of GCPA.**

***Index Terms*—Low Voltage Ride Through (LVRT), Nonlinear Control, Photovoltaic (PV), Recovery enhancement.**

I. Introduction

In this research effort, a Finite Time Sliding Mode Control (FTSMC) method is used to assure fast and stable operation of DC/DC converter during voltage sags. FTSMC guarantees the tracking error reaches the sliding surface in finite time. As nonlinear FTSMC is used in the proposed method, the controller can operate effectively in wide range of operation condition. A (Proxy Based Sliding Mode Control) PBSMC-based controller is also proposed for the DC/AC inverter to enhance the post-fault recovery performance of the Grid Connected PV Array (GCPA). PBSMC provide fast response during normal operation of the system while provides smooth resuming to the desired value after large disturbances.

II. Key Equations

A. FTSMC Equations:

(a) Control law:

$$u = \frac{1}{2}(1 + sgn(S_{FTSMC})) \tag{1}$$

where:

$$S_{FTSMC} = \dot{e}_1 + \alpha_1 e_1 + \alpha_2 . |e_1|^{\alpha_3} . sgn(e_1) \tag{2}$$

$$\dot{e}_1 = \frac{v_{dc}}{L}\bar{u} - \frac{v_{pv}}{L} \tag{3}$$

$$\ddot{e}_1 = -\frac{\bar{u}.e_1}{LC} - \frac{dG(i_{pv})}{di_{pv}}\dot{e}_1 + \frac{\bar{u}.i_{pv}^*}{LC} - \frac{\bar{u}.i_{dc}}{LC} \tag{4}$$

(b) Condition for Stability:

$$\frac{1}{LC}e_1 - \frac{i_{pv}^*}{LC} + \frac{i_{dc}}{LC} < \left(-\frac{dG(i_{pv})}{di_{pv}} + \alpha_1 + \alpha_2.\alpha_3.|e_1|^{\alpha_3 - 1} \right)\dot{e}_1 < 0 \tag{5}$$

B. PBSMC Equations:

The following control law is obtained for PBSMC:

$$f = F.sat\left(\frac{k_d}{F}.\left(\frac{\sigma - \frac{d\rho}{dt}}{K} + \frac{k_i.\rho + k_p.\frac{d\rho}{dt}}{k_d} \right) \right) \tag{6}$$

III. Key Results:

TABLE I
Control Parameters

DC/AC Inverter, current regulator		*DC/AC Inverter, DC voltage regulator*	
k_p	0.3	k_p	7
k_i	20	ki	800
k_d	10^{-7}	k_d	10^{-4}
Voltage Limit	2 p.u.	Current Limit	1.25 p.u.
DC/DC Converter		***FTSMC***	
Switching Frequency	5000 Hz	α_1	2.05
PBSMC		α_2	50
K, F	0.01, 1.25	α_3	0.85

Case (a): Conventional Control System
Case (b): FTSMC-controller and PID:
Case (c): FTSMC-controller and PID controller with anti-windup scheme
Case (d): Conventional control for DC/DC converter and PBSMC controller for DC/AC inverter
Case (e): FTSMC and PBSMC-controller

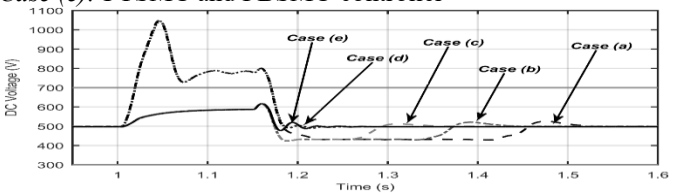

Fig. 1. DC-Link Voltages of GCPA for 3-phase voltage sag to 0.2p.u.

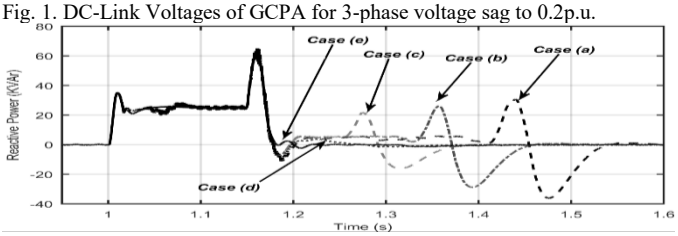

Fig. 2. Injected reactive power by GCPA for 3-phase voltage sag to 0.2p.u.

Real-Time Modeling and Battery-in-the-Loop Characterization of an Energy Storage System

Ali Arzani[1] and Ganesh K. Venayagamoorthy[1,2]
[1]Real-Time Power and Intelligent System Laboratory, Clemson University, SC, USA
[2]School of Engineering, University of KwaZulu–Natal, Durban, South Africa
aarzani@g.clemson.edu and gkumar@ieee.org

I. Introduction

The quest towards inertia less Distributed Energy Systems (DES) dispatchability at higher penetration levels (>25%) in the grid demands incorporation of Battery Energy Storage Systems (BESS). In this study, development of a battery hardware-in-the-loop (BIL) simulation platform for testing BESS under different operating conditions. It consists of an actual battery interfaced with a real-time simulation model of the system in RSCAD as seen in Fig. 1b. Battery electrical equivalent circuit models are developed for estimation of State of Charge (SOC) and its comparison with hardware battery SOC measurements for verification of accuracy.

The initial platform consists of testing three BESS SOC in RSCAD, where: (a) Charge/discharge is through a hardware amplifier source/sink feature. (b) High power residential load is the hardware interfaced to RTDS, (c) Li-ion battery is the HIL with RTDS simulation. The implementation of the power hardware in the loop (PHIL) is based on the ideal transformer method (ITM) interface algorithm. ITM is widely used due to its higher accuracy and low processor burden. The real time digital simulator (RTDS) simulation environment (RSCAD) generates reference current for VSI based on measured HuT feedback voltage. This procedure is not straightforward as the time-delay introduced in the closed loop can lead to instability and also deteriorates the accuracy of the experiment. Therefore, a stability analysis (theoretic or/and dynamic simulation) is necessary before performing the PHIL experiment and appropriate protection schemes are applied (software and hardware). The testing of BIL of Fig. 1b provide means to analyze different operational issues of the battery such as: charge/discharge cycling operation effect on the battery cells, modules and the entire system; charge/discharge controller issues taking into account interaction with battery cells and VSI.

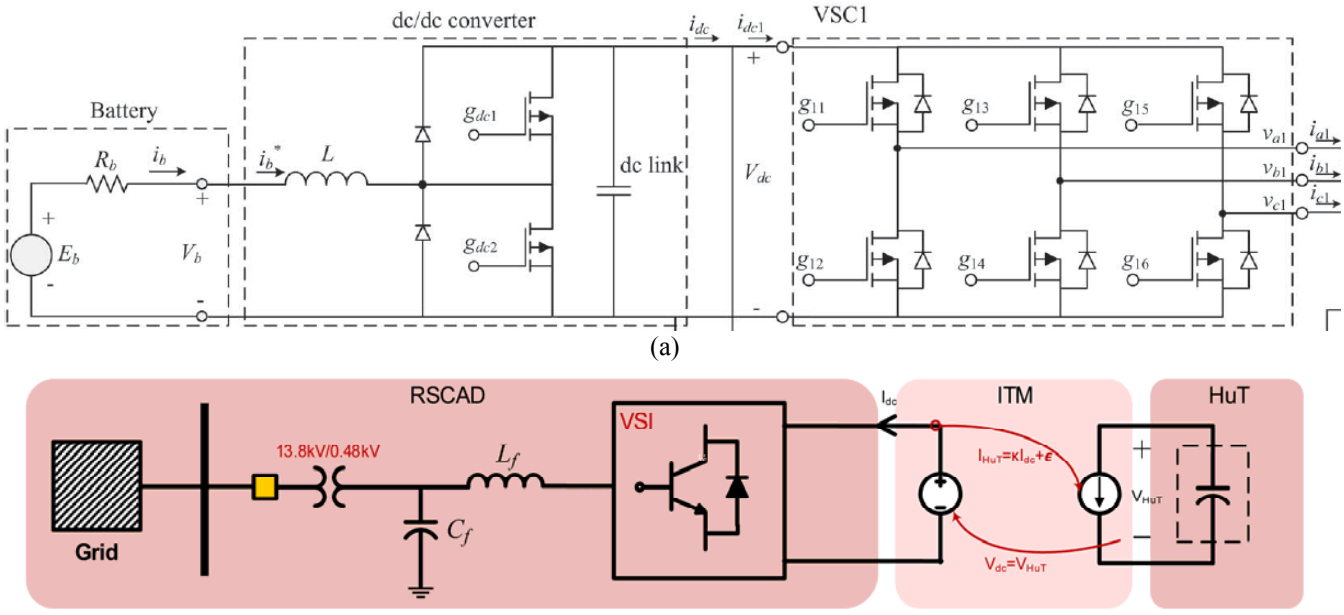

Fig 1. (a) BESS components for vehicle to-grid support, (b) BIL Testing Platform

This work is supported by US National Science Foundation (NSF) under grants IIP #1312260, IIP #1308192, and ECCS #1408141. Any opinions, findings, and conclusions or recommendations expressed in this material are those of the author(s) and do not necessarily reflect the views of NSF.

Robust Microgrid Economic Dispatch Considering Renewable Uncertainty using Interval Optimization

Cody Rooks, *Student Member*, *IEEE*, Xiao Kou, *Student Member, IEEE*, and Fangxing Li, *Fellow*, *IEEE*
Department of Electrical Engineering and Computer Science
The University of Tennessee
Knoxville, TN 37996
{crooks2, fli6}@utk.edu

***Abstract*—Renewable energy systems create a challenging problem for microgrid operators to balance supply and demand in an economically efficient way. The intermittent nature of renewable generators result in dispatch cost fluctuations depending on their power output, requiring a robust solution approach. Interval analysis and optimization is used to formulate and solve the economic dispatch problem of a microgrid system given renewable generator uncertainties.**

Keywords—microgrids, economic dispatch, interval optimization, electricity markets

1. Background

Similar to the challenges faced by an Independent System Operator (ISO), a microgrid operator will attempt to balance a portion or all of its load in an economically optimized way. In other words, it will attempt to solve the economic dispatch problem in its own domain. A microgrid operator has several different types of distributed energy resources (DERs) at its disposal. These DERs will take the form of both dispatchable generators, e.g. fuel cells and microturbines, and non-dispatchable generators, e.g. solar PV and small wind turbines. The intermittent nature of renewable generators creates an optimization problem of a stochastic nature, as the output of these systems can never be determined exactly. Therefore, robust methods must be employed that can account for this uncertainty. Interval analysis and optimization is a promising approach to solve this problem for a variety of reasons: it does not require probabilistic models (only upper and lower bounds of uncertain variables), it is computationally efficient, and results in a range of solutions that can serve as a meaningful reference for operators.

2. Microgrid System Modelling

A microgrid can operate in either islanded or grid-connected mode. In grid-connected mode, the microgrid can import energy from the transmission system at the locational marginal price (LMP) of the point of common coupling (PCC). Linearized DistFlow [1] equations have been commonly used and justified in distribution system modelling. The equations developed for this work model real and reactive branch flows and node voltages.

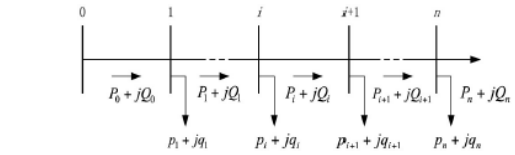

$$P_{i+1} = P_i - r_i(P_i^2 + Q_i^2)/V_i^2 - p_{i+1} \qquad P_{i+1} = P_i - p_{i+1}$$
$$Q_{i+1} = Q_i - x_i(P_i^2 + Q_i^2)/V_i^2 - q_{i+1} \qquad Q_{i+1} = Q_i - q_{i+1}$$
$$V_{i+1}^2 = V_i^2 - 2(r_iP_i + x_iQ_i) + (r_i^2 + x_i^2)(P_i^2 + Q_i^2)/V_i^2 \qquad V_{i+1} = V_i - (r_iP_i + x_iQ_i)/V_i^2$$
$$p_i = p_i^D - p_i^g \qquad q_i = q_i^D - q_i^g$$

Figure 1. Linearized DistFlow Equations

3. Interval Problem Formulation & Algorithm

In the interval optimization method, an upper, optimistic (Z_{min}) and lower, pessimistic (Z_{max}) boundary is solved, resulting in an interval solution.

$$\begin{aligned} Z_{min} &= \min_x c_i^T x_i \\ \text{s.t.}\quad & \underline{b_i} \le A_i x_i \le \overline{b_i} \\ & E_i x_i \le \overline{d_i} \\ & L_i \le x_i \le U_i \end{aligned} \qquad \begin{aligned} Z_{max} &= max \min_x c_i^T x_i \\ \text{s.t.}\quad & (Ax)_i = \underline{b_i} \; or \; \overline{b_i} : \lambda_i, \delta_i \\ & E_i x_i \le \underline{d_i} : \nu_i \\ & L_i \le x_i \le U_i : \gamma_i^L, \gamma_i^U \end{aligned}$$

In the algorithm, the combinatorial max-min problem is transformed into a single maximization problem using strong duality theory as well as the Big-M method [2].

4. Results

The approach was tested on an IEEE 13-bus distribution system, modified with solar PV injections, microturbines and a fuel cell.

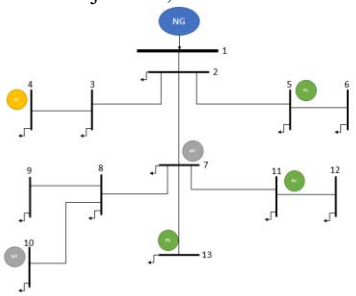

Figure 2. Modified IEEE 13-bus system

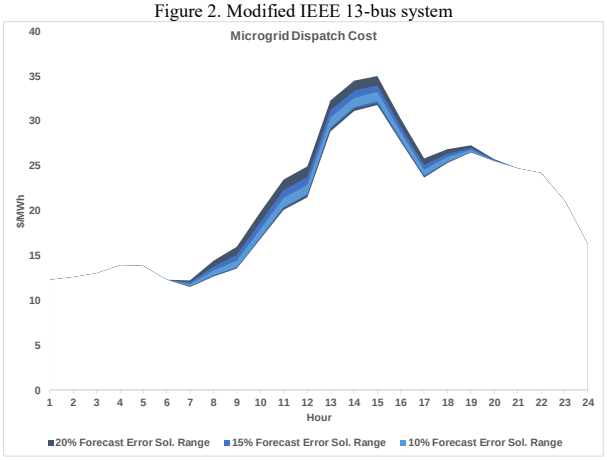

Figure 3. Microgrid Dispatch Cost Intervals

The solution range shows the interval of dispatch costs for different forecast levels of solar generator output. The range of costs increases as the interval of solar output increases.

References

[1] Wu, F.F., "Network reconfiguration in a distribution system for loss reduction and load balancing," *IEEE Transactions on Power Delivery*, 1989, 4, 1401-1407.
[2] X. Kou, F. Li, W. Feng, "Transmission Constrained Economic Dispatch via Interval Optimization Considering Wind Uncertainty," (unpublished).

This work was supported by the Engineering Research Center Program of the National Science Foundation and the Dept. of Energy of USA under NSF Award Number EEC-1041877 and the CURENT Industry Partnership Program.

Benefits of Short-term PV Forecasting in a Remote Area Standalone Off-grid Power Supply System

Taskin Jamal, GM Shafiullah, Craig Carter, SM Ferdous, Md. Moktadir Rahman
School of Engineering & Information Technology
Murdoch University
Perth, WA, Australia

***Abstract*—The application of short-term PV forecasting in standalone off-grid power supply (SOPS) systems in remote electricity networks is an approach to enable higher levels of PV penetration without hampering the network stability. In this study, a diesel run remote electricity network has been considered where high levels of PV penetration has been found techno-economically feasible. Some certain common scenarios, for example, maximum PV variability and abrupt load change have been considered in analyzing system performance and system stability. The application of short-term PV forecasting shows favorable outcomes when accommodating high PV variability and abrupt load fluctuation compared to the same system conditions when PV forecasting is not considered. The study contributes to the ongoing research of developing smart and efficient control mechanisms that enable higher levels of PV penetration in remote electricity networks worldwide.**

***Index Terms*—Remote Electricity Networks, Short-term PV Forecasting, Higher PV Penetration, System Stability**

I. Introduction

PV systems have also been introduced into standalone off-grid power supply (SOPS) systems in remote areas all around the world as a sustainable power generation source. Though PV systems offer an economically viable solution in the long term to provide electricity in remote networks, the issue of PV output variability and other technical challenges have been identified as the primary challenges for integration of higher amounts of PV power in SOPS systems. PV power variability requires the system dispatchable generators to follow not only load changes but also accommodate PV power variations. Experts believe that an adequate mechanism is still not available to combat the short-term power fluctuations on power systems due to PV output variability. Study shows, higher PV penetration could be facilitated if PV power variability could be forecast, to maintain acceptable performance of the power system.

Prediction of cloud locations greatly increases the accuracy of PV output forecasts, when used in conjunction with regional meteorological and historical data. Higher forecasting accuracy ensures lower costs related to control of spinning reserve and flexible generator operation and maintenance. The introduction of PV forecasting can reduce the system operation and maintenance costs and associated risks due to better planning and management of the whole system.

This study analyses the system performance and stability of a remote SOPS system while addressing the impact of abrupt load fluctuations and high PV variability, both before and after applying the short-term PV power forecasting, facilitated by sky camera technology. Power system impacts arising from PV variability are shown in Table I. Table II presents the fundamental differences between three primary forecasting methods. Table III shows the application areas of PV forecasting for different entities.

TABLE I: Power system impacts from PV variability

Timescale of Variability	Potential Impact on Power System
Seconds	Power Quality
Minutes	Regulation Reserves
Minutes to Hours	Load Following
Hours to Days	Unit Commitment

TABLE II: Different methods of PV forecasting

Method	Sky Imagery	Satellite Imagery	NWP
Sampling Rate	30 Sec	15 Min	1 Hour
Spatial Resolution	10-100 metres	1km	2-50km
Spatial Coverage	3-8km radius	65°S-65°N	Worldwide
Forecast Horizon (Max)	10s to Minutes	5 hours	10 days
Application Area	Ramps, Regulation	Load following	Unit commitment, Regional power estimation
Approach	Statistical	Statistical	Physical

TABLE III: PV forecasting application area and advantages

Entity	Role / Usage
Consumer	o Behavioral attitude on using solar PV system o Decision making on system design o Decision making on increasing system size
Third Party	o Managerial issues o Handling load aggregation issues o Decision making on services needed to provide
Utility Company	o Predict generator capacity scheduling o Fossil fuel arrangement decision o Network management and planning o Operation and maintenance of supply system

II. Conclusion

Introduction of sky camera based short-term PV forecasting predicts PV output variability well ahead of time, which in the long run enables higher levels of PV penetration into SOPS systems in remote areas. This study has successfully identified the effectiveness of the short-term PV forecasting in a SOPS system considering several worst case scenarios.

A Comparison Study of Dispatching Various Battery Technologies in a Hybrid PV and Wind Power Plant

Yuqing Yang
School of Photovoltaic & Renewable Energy Engineering, UNSW.

Chris Menictas
School of School of Mechanical and Manufacturing Engineering, UNSW.

Stephen Bremner
School of Photovoltaic & Renewable Energy Engineering, UNSW.

Merlinde Kay
School of Photovoltaic & Renewable Energy Engineering, UNSW.

***Abstract*— This paper presents a comparison study for various types of battery technologies using selected BESS parameters in a hybrid PV and wind power plant (HPP), taking the aging of the batteries into account. The optimization problem was reformulated as a Mixed Integer Linear Programming (MILP) problem, with the aim being to minimize the overall operating cost. IBM CPLEX was used to solve the problem. For forecasting, two techniques, i.e., the persistence and Elman Neural Network, were applied for both day-ahead and hour-ahead forecasting. Moreover, four case studies were performed, including the scenario without battery, day-ahead dispatch, day-ahead dispatch with a rolling horizon and hour-ahead dispatch. The simulation results showed that hour-ahead dispatch demonstrated the highest profitability. Furthermore, among different battery technologies, lithium-ion batteries resulted in the highest operating profits, whereas lead-acid batteries had the shortest payback period and vanadium redox flow batteries demonstrated the least degradation from cycling.**

Keywords -- Battery Energy Storage System, Battery Scheduling, Forecasting Errors, Hybrid PV and Wind Power Plant.

I. INTRODUCTION

Battery energy storage systems (BESS) have been playing increasingly important roles in the modern power network. There are a wide range of battery technologies that have been used for demonstrations or in commercial applications. These include the Lead Acid Battery (LAB) , Lithium-ion Battery (LIB), Sodium Sulfur Battery (NAS) and Vanadium Redox Flow Battery (VRB). It is noted that many research articles concentrate on battery energy storage system applications without clarifying the type of storage system technology by using a generic model. Therefore, the generic model for battery energy storage systems is the most commonly used in a wide range of studies.

The contributions of this work include: 1) providing a comprehensive comparison study by analyzing the performances of four different battery technologies, namely LAB, LIB, NAS and VRB, in the operation of a hybrid PV and Wind Power Plant (HPP), using the reported battery parameters from previous and technical reports. 2) adopting a generic battery model for four different technologies and an aging process linearized by using a degradation rate. 3) implementing three different dispatch strategies, i.e. day-ahead dispatch, day-ahead dispatch with a rolling horizon and hour-ahead dispatch, to evaluate the performance of different battery technologies.

II. KEY RESULTS AND CONCLUSION

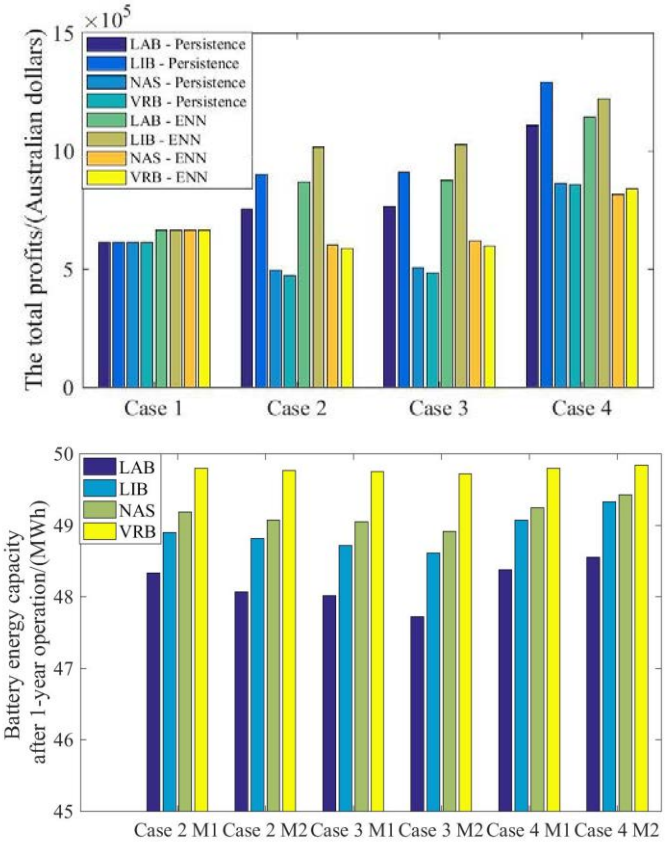

In this work, four different types of batteries were optimally dispatched for a hybrid power plant, aiming at minimizing the overall operating cost of the hybrid power plant. Moreover, two forecasting techniques and three dispatch strategies were implemented to evaluate the performances of different battery technologies. From the simulation results, it is noticeable that hour-ahead dispatch in Case 4 achieves the highest profits. However, among the four battery technologies, lithium-ion batteries demonstrated the best performance in terms of the operating profitability, whereas lead-acid batteries had the shortest payback period when the capital costs of battery technologies were taken into account. Besides that, from the perspective of battery aging, vanadium redox flow batteries demonstrated the least degradation from cycling.

Monitoring the Voltage Stability Margin Using Norton Current Distribution Relationship

Qi Wang[1], Yufeng Guo[1,2], Jilai Yu[1,*], Dongrui Zhang[1], Jie Wan[1],Jin Zhong[2]
1. School of Electrical Engineering and automation, Harbin Institute of Technology, Harbin, China
2. Department of Electrical and Electronic Engineering, HKU, Hong Kong, China

***Abstract*—The impedance matching condition has been a fundamental assumption of many existing studies on voltage stability assessment. In this paper, it has been proven that the Norton current distribution law is equivalent to the impedance matching condition. Based on this law, a new voltage stability index is proposed, which can be further divided into bus voltage stability index and line voltage stability index. These indexes of the focused load bus can be calculated by phasor measurement units data. Then, the voltage stability margin can be assessed by computing the difference between the index value and 1. The effectiveness of the proposed on-line voltage stability index are verified from simulation results perform in a 10-bus system and 39-bus system. Moreover, practical operating constraints such as the generator power limits are taken into account for practical assessment of the proposed method. *Index Terms*-- impedance matching condition; Norton current distribution law; voltage stability index; phasor measurement units; voltage stability margin**

I. INTRODUCTION

This paper discuss the corresponding law between Norton current distribution and the maximum power transfer. Based on this law, a new voltage stability index is proposed. The proposed index is calculated with voltage and current magnitude provided by on-line PMU data. In addition, the index can be extended to dispersion indexes, each offering the voltage stability information of specified line.

II. KEY EQUATIONS

A. *new voltage stability index*

$$H_{(k+1)} \approx \left|1-\frac{I_{L_{(k)}}}{I_{L_{(k+1)}}}\right| \Big/ \left|1-\frac{U_{L_{(k)}}}{U_{L_{(k+1)}}}\right| \qquad (1)$$

The index shown in (1) means that:

(1) System is within the limits of transmission capacity when $H_{(k+1)} > 1.0$;

(2) System is beyond the limits of transmission capacity when $H_{(k+1)} < 1.0$;

(3) System is in critical state when $H_{(k+1)} = 1.0$;

B. *extend the index to dispersion indexes*

$$H_{l\to n}^{(k+1)} = \left|1-\frac{I_{L_{l\to n}}^{(k)}}{I_{L_{l\to n}}^{(k+1)}}\right| \Big/ \left|1-\frac{U_{L_{l\to n}}^{(k)}}{U_{L_{l\to n}}^{(k+1)}}\right| \qquad (l=1,\cdots m) \quad (2)$$

Where, $I_{L_{l\to n}}^{(k)}$ is the current flow into bus n from line l at the k th point.

As can be seen from (18), a higher value of $H_{l\to n}^{(k+1)}$ indicates a higher ability of maintaining bus voltage stability by line l. Furthermore, a negative value of $H_{l\to n}^{(k+1)}$ means line l do not provide any power for maintaining bus voltage stability.

III. KEY RESULTS

The proposed method is tested on the 10-bus system and 39-bus system.

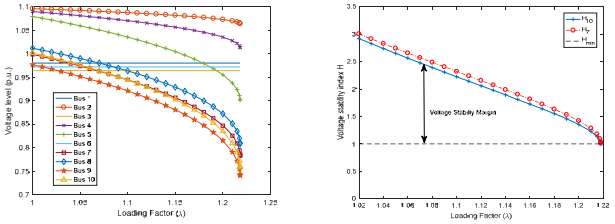

Fig. 1. Bus voltage and Voltage stability indexes corresponding to loading factor increasing at Bus 7 and 10 (10-bus system)

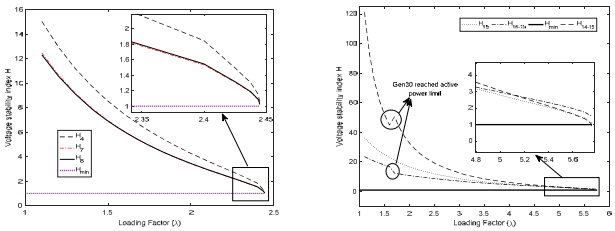

Fig. 2. Voltage stability indexes corresponding to loading factor increasing at Bus 4, 7 and 10 (39-bus system)

IV. CONCLUSIONS

This paper proposed a new online voltage stability index based on the Norton current distribution relationship. It is mathematically proven that the Norton current distribution law is equivalent to the impedance matching condition. With this new method, both bus voltage stability and the ability of lines to maintain bus voltage stability can be calculated on-line. Simulations results in 10-bus system and 39-bus system show that the voltage stability indexes are effective at different scenario. Moreover, the proposed new index uses only voltage and current amplitude information from PMU measurements, which reduces the communication complexity.

Fault Classification and Location Identification in a Smart Distribution Network Using ANN

Muhammad Usama Usman*, Juan Ospina, Md. Omar Faruque
Electrical and Computer Engineering and Center for Advanced Power Systems, Florida State University
2000 Levy Avenue, Tallahassee, FL., USA. Email: *musman@fsu.edu

***Abstract*—This paper presents a novel approach to classify and locate different types of faults in a smart distribution network (DN). The proposed method is able to classify all types of faults that can occur in a DN and then based on fault type, it can identify the approximate fault location (FL) with a high accuracy. The method is based on artificial neural networks pattern recognition which uses data from μPMUs/smart meters placed at different locations in a DN. The proposed technique needs fault-on voltages of all the nodes connected to the end of line/branches in order to classify and locate different types of faults. The method is tested on a modified IEEE-37 bus system with distributed generation along with dynamic loading conditions and varying fault resistances.**

I. Methodology

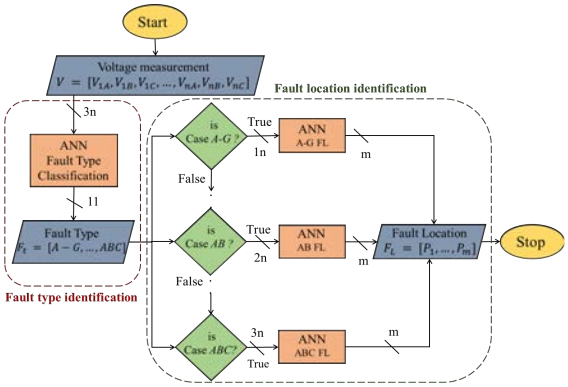

Fig. 1: Flowchart of fault location identification procedure

II. Case Study and Verification

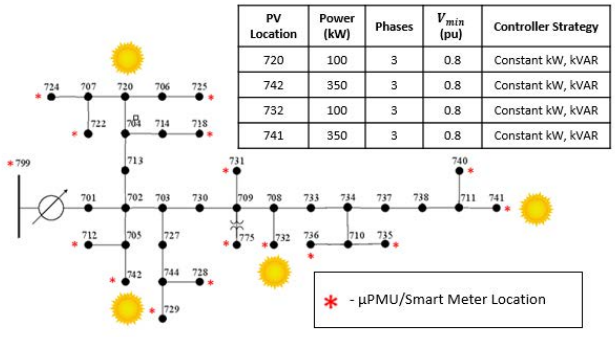

PV Location	Power (kW)	Phases	V_{min} (pu)	Controller Strategy
720	100	3	0.8	Constant kW, kVAR
742	350	3	0.8	Constant kW, kVAR
732	100	3	0.8	Constant kW, kVAR
741	350	3	0.8	Constant kW, kVAR

Fig. 2: IEEE-37 Bus Test Feeder with PV

A. Fault Type Classification

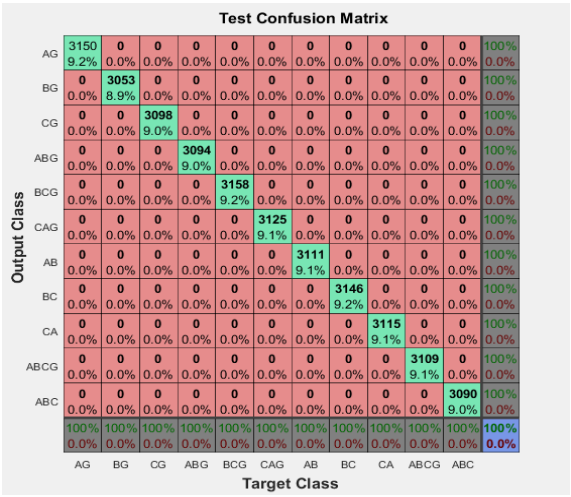

Fig. 3: Confusion Matrix for Fault Classification

B. Fault Location Identification

TABLE I: FL Identification Results for faults on the nodes

Fault Type	Fault Placement	Fault Resistance (ohm)	Accuracy for faults on the nodes
ABC-G	All 37 nodes	0-5	100%
ABC	All 37 nodes	0-5	99.5%
AB-G	All 37 nodes	0-5	100%
BC-G	All 37 nodes	0-5	100%
CA-G	All 37 nodes	0-5	100%
AB	All 37 nodes	0-5	100%
BC	All 37 nodes	0-5	100%
CA	All 37 nodes	0-5	100%
A-G, B-G, C-G	All 37 nodes	0-5	99.7%

TABLE II: FL Identification Results for faults on the lines

Line Type	Line Length	Fault Placement	Fault Resistance (ohm)	Faulted Nodes
702-703	1320ft	Every 200ft	0.5, 1.5, 2.5	702 and 703
738-711	400ft	Every 50ft	0, 1, 2	738 and 711
734-710	520ft	Every 50ft	2, 3, 4	734 and 710
720-707	920ft	Every 100ft	0.3, 1.3. 2.6	720 and 707
744-728	200ft	Every 30ft	0.001, 0.1, 0.8	744 and 728
733-734	560ft	Every 50ft	0.05, 2.5, 5	733 and 734
714-718	520ft	Every 50ft	1, 2, 3	714 and 718

Sub-Synchronous Resonance Detection in Series Compensated DFIG-Based Windfarms

Bo Gao
Department of Electrical and Computer Engineering, University of Alberta

***Abstract*—Series compensated DFIG-Based wind farms are vulnerable to sub-synchronous resonance (SSR). The SSR components need to be detected at early stage to provide early warning. The SSR frequency is uncertain and the components are always very small at the early stage. Hence, it needs long sampling period for transitional FFT algorithm. In this paper, voltage and current waveforms are used to exactly compute the SSR frequency and the magnitude. The results show that the new algorithm is fast and accurate for the early stage SSR components measurements.**

***Index Terms*—DFIG, Windfarm, SSR, Detection, Waveform,**

I. Introduction

Series compensated DFIG-based windfarms are vulnerable to SSR. SSR has been widely investigated and lots of paper presented mathematical analysis and simulation work. For SSR detection, the traditional method is to conduct the FFT to give the information of the frequency and the magnitude of SSR components. However, this may be some issues as the frequency of SSR components is uncertain, which means the sampling window need to vary for different SSR frequencies. This may lead to long time to obtain the SSR frequency and magnitude. In addition, FFT is steady-state concept, and if the amplitude of SSR components vary, FFT results about the magnitude will have a large error.

Other mathematic based method has also been introduced to get the frequency and magnitude of the SSR components. Prony, Recursive Least Square (RLS) algorithms, Kalman Filter algorithm have been used to compute the SSR and these methods can track the SSR components exactly. However, these algorithms require lot of computation and the complexity make them unsuitable for on-line calculation.

With the Waveform Measurement Unit (WMU) available in power system, SSR components can be computed by waveforms with less computation work. The waveform-based algorithms use both the voltage and current waveforms. The results show that the waveform-based algorithm can calculate the frequency and the magnitude fast even when the magnitude of SSR components is relative low to the fundamental frequency components.

II. Key Steps

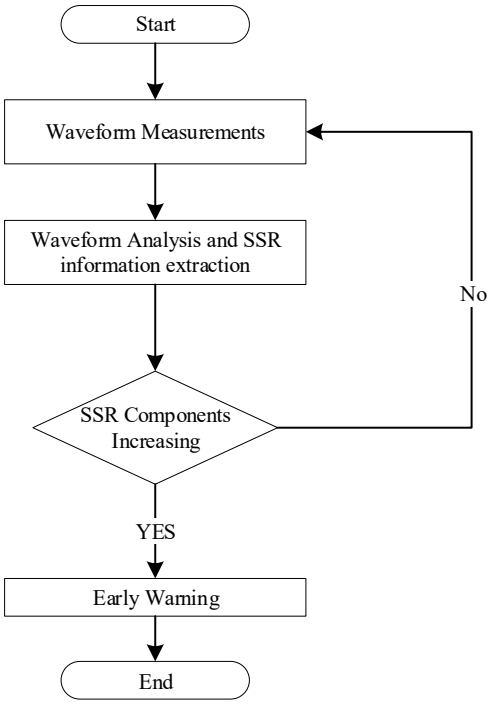

Fig.1 SSR computation steps

III. Simulation Results

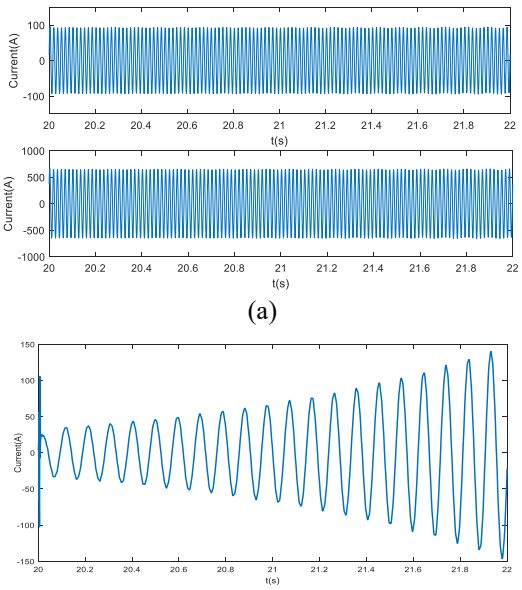

Fig.2 SSR extraction. (a) current waveform, (b) SSR components

An Distributed Event Diagnosis Solution for Protection Operation in IEC 61850

M. Touhiduzzaman, *Student Member, IEEE,* and A. Hahn, *Member, IEEE*, and S. Lotfifard, *Member, IEEE,*

***Abstract*—This poster presents a novel distributed event-based diagnosis solution (DDS) for substation automation system (SAS), based on the backward reachability graph analysis (B-W) of behavioral Petri-net (BPN). We develop a hierarchical model and propose a distributed event diagnoser for SAS that focuses on the IEC 61850 communication protocol. This distributed diagnoser produces a local diagnosis result which is consistent and correct without the use of centralized diagnosis scheme. A case study on substation automation system is discussed to verify our proposed distributed diagnoser scheme. The result highlighted different scenarios that successfully identified different protection (distance or differential fault), cyber (cyber-attack) and system mul-function events.**

I. Introduction

Due to the complexity of cyber-physical SAS, It become more difficult for the substation intelligent electronic device(IED) to detect unknown failure modes and cyberattack. Also, traditional IED diagnosis solution is centralized which required a large number of agents to analyze to detect the fault. In this work, we design an agent based DDS that guarantees that local diagnosers provide correct diagnosis result during the identification of events in the SAS.

A. Stage 1: Modeling substation automation using BPN

In SAS, each physical device is divided into logical nodes(LN) according to IEC 61850 protocol where each LN has their own naming convention and communicate each other through GOOSE messages. In order to construct the substation automation accordance with real system, we use the hierarchical BPN approach [1] where the entire SAS model of one substation is divided into five blocks(Fig. 1).

B. Stage 2: Distributed diagnosis solution (DDS)

In the DDS, the centralized system is divided into a set of n subsystem (single substation IED). Each of the subsystem interacting each other by passing the token through bordered places. The BPN distributed diagnosis solution (DSS) for a subsystem i is defined as:

$$DSS_i = \{N_i, B_i, Ft_i, (\gamma_i^+, \gamma_i^-), \zeta\}$$

where, $N = (P, T_N, T_{OR}, F)$ is the behavioral petrinet model, $B = (B_{in}, B_{out}, B_x)$ is the set of bordered places, Ft is the set of possible fault initiating from subsystem i, (γ_i^+, γ_i^-) is the initial local observation originated from subsystem i and ζ represents the final local observation which only take the information from B and Ft. In this DDS, ζ will decide what type of events(e.g. fault, cyber-attack, system mal-function) occur to the subsystem, and also decide whether those events occur inside the subsystem or outside the subsystem. Once the initial places have been identified that contain token, then those token will be continually analyzed using B-W reachability graph to identify events.

II. Key Figures and Result

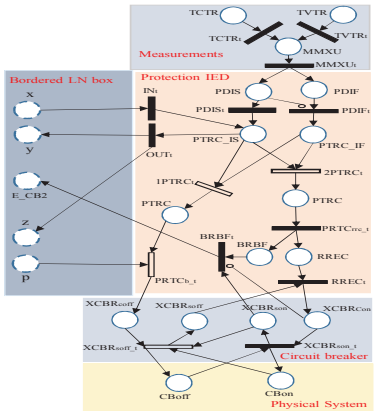

Fig. 1: BPN model for substation IED

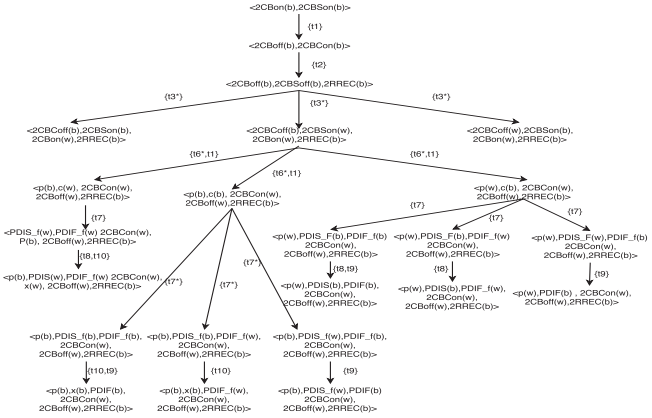

Fig. 2: B-W reachability analysis of simple case study

Scenarios for CB2 open and status signal on	<p, x, >	<PDIS, PDIF>	state
<2CBC$_{on}$(b),2CBS$_{on}$(b), 2CB$_{on}$(w), 2RREC(b)>	<∅, ∅>	<∅, ∅>	Inconsistency (cyber-attack)
<2CBC$_{on}$(w),2CBS$_{on}$(b), 2CB$_{on}$(w),2RREC(b)>	<∅, ∅>	<∅, ∅>	Inconsistency(cyber-attack)
<p(b), PDIS(w), PDIF_f(w) 2CBC$_{on}$(w), x(w), 2CB$_{on}$(w),2RREC(b)>	<b, w>	<w, ∅>	System malfunction
<p(w), PDIS(b), PDIF(b), 2CBC$_{on}$(w) 2CB$_{on}$(w),2RREC(b)>	<w, ∅>	<b, b>	Bus 2 and line fault (z1 for sub2)
<p(w), PDIS(b), PDIF_f(w), 2CBC$_{on}$(w), 2CB$_{on}$(w),2RREC(b)>	<w, ∅>	<b, ∅>	Line fault
<p(w), PDIF(b), 2CBC$_{on}$(w), 2CB$_{on}$(w),2RREC(b)>	<w, ∅>	<∅, b>	Bus 2 fault
<p(b), x(b), PDIF(b), 2CBC$_{on}$(w), 2CB$_{on}$(w),2RREC(b)>	<b, b>	<∅, ∅>	Bus 2 fault and line fault (z2 for sub2)
<p(b), x(b), PDIF_f(w), 2CBC$_{on}$(w), 2CB$_{on}$(w),2RREC(b)>	<b, b>	<∅, ∅>	Line fault (z2 for sub2)
<p(b), PDIS, f(w), PDIF(b), 2CBC$_{on}$(w), 2CB$_{on}$(w),2RREC(b)>	<b, ∅>	<∅, ∅>	System malfunction

Fig. 3: Event identification by analyzing DDS

References

[1] L. Portinale, "Behavioral petri nets: A model for diagnostic knowledge representation and reasoning", *IEEE Trans. Syst., Man Cybern. B,* vol. 27, no. 2, pp. 184-195, Apr. 1997.

Toward a Synthetic Model for Distribution System Restoration and Crew Dispatch

Bo Chen, *Member IEEE*, Zhigang Ye, *Student Member IEEE*, Chen Chen, *Member IEEE*, Jianhui Wang, *Senior Member,* IEEE and Kai Wu, *Senior Member IEEE*
Argonne National Laboratory and Xi'an Jiaotong University

***Abstract*— In this paper, we introduce a synthetic model that integrates service restoration model and crew dispatch model based on a universal routing model. The proposed model can provide the estimated time of restoration (ETR) for each load, switching sequence for safely operating remotely/manually operated switches, and dispatch solutions for crew with different skill sets. The proposed models are formulated as a mixed-integer linear programming model (MILP), and their effectiveness is evaluated via the IEEE 123 node test feeder.**

Keywords— Distribution service restoration, crew dispatch, mixed-integer linear programming, repair, switching sequence management.

I. Introduction

Natural disasters are increasingly reported during the recent years to have caused wide-spread social and economic effects, including large-scale power outages that normally take utilities companies several weeks to completely restore the electricity services [1-2]. In case of extreme weather events that can cause multiple power outages within a short period of time and leave a large region of utility service territories without power, seamless coordination among OMS modules is the key to maximize the restoration effort. The work proposed in this paper is motivated by the fact that a synthetic model that can effectively integrate DSR and crew dispatch models is still lacking in the literature. This paper introduces a synthetic model for DSR and crew dispatch model.

II. Key Tables and Figures

TABLE I. Interdependence between DSR and Crew Dispatch

Domain			Interdependence Description
DSR	*Crew for Operation*	*Crew for Repair*	
√	√		A crew operates a manually operated switch to energize components.
	√	√	A switch can be operated only after the lock status, if any, is removed.
√		√	A faulted component can be energized only after being repaired. The crew can operate the switch right after the repair.
√	√	√	To repair a faulted component, the component should be isolated by opening upstream/downstream switches to ensure crew safety. A switch cannot be energized when an operation crew is in the process of operating it.

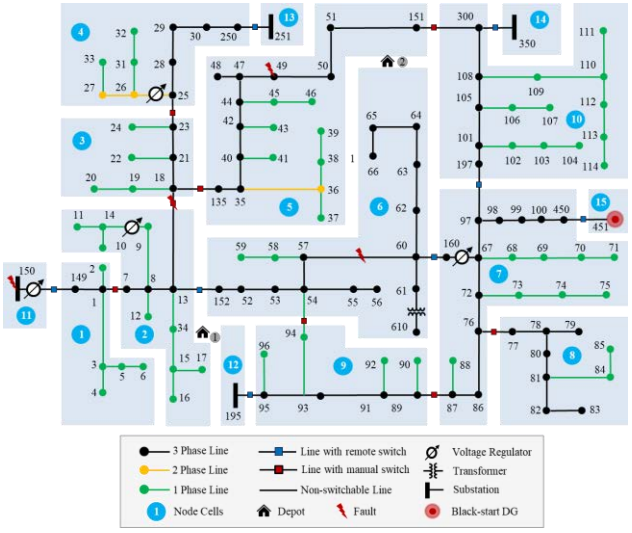

Fig. 2. Modified IEEE 123 node test feeder partitioned into 15 node cells by 16 switches.

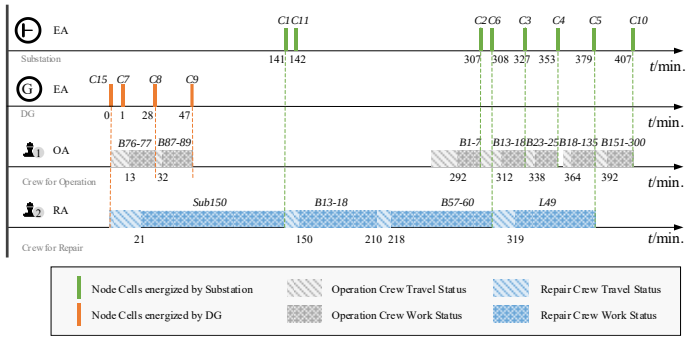

Fig. 3. Repair and Restoration Sequence for EA/OA/RA

References

[1] Y. Wang, C. Chen, J. Wang, and R. Baldick, "Research on Resilience of Power Systems Under Natural Disasters-A Review," *IEEE Transactions on Power Systems,* vol. 31, no. 2, pp. 1604-1613, 2016.

[2] "Hurricanes Nate, Maria, Irma, and Harvey Situation Reports," https://www.energy.gov/oe/downloads/hurricanes-nate-maria-irma-and-harvey-situation-reports.

Enabling Resiliency Through Outage Management and Real Time Data-Driven Aggregated DERs

Matteo Menazzi, *Student Member, IEEE*
Washington State University, matteo.menazzi@wsu.edu

Anurag K. Srivastava, *Senior Member, IEEE*
Washington State University, asrivast@eecs.wsu.edu

***Abstract*—This project aims to enhance distribution system resiliency by effectively controlling and utilizing Distributed Energy Resources (DERs) for outage management and restoration under hazard scenarios, leveraging available measurements from smart meters and micro-PMUs. To achieve this, the current industry practice of just using an aggregate statistical model for the whole secondary network is not sufficient. A novel secondary distribution network equivalent model is proposed, composed of an Equivalent Controllable DER (ECDER), an Equivalent Controllable Load (ECL), and the Residual Power Injection (RPI), comprising, in turn, losses, uncontrollable loads and DERs power, necessary to ensure total power injection equivalency. The model features 3 decision variables: ECDER, ECL, and a binary variable which allows to shed specific loads using respective smart meters. The model is meant to allow an optimal power restoration algorithm, running at primary distribution system level, to determine the optimal value of ECDER, ECL, and the loads to be shed, without having to consider either a detailed secondary network or each controllable DER and load individually. Uncontrollable loads and DERs power is modeled as a parameter, which is determined feeding available measurements into Nonlinear Autoregressive Neural Networks (NARnet), whose output is subsequently adjusted considering cold load pick-up phenomena. System losses and, therefore, RPI change in function of the decision variables in order to maintain total power injection equivalency, so that, as seen from the primary network, the same total power is injected into the secondary system.**

I. Key facts

Fig. 1 depicts the utilized secondary distribution test system and the proposed equivalent model. ECDER and ECL values are distributed to single DERs and loads according to their individual power limits. Six models, differing in system losses estimation techniques, have been studied. Models 1-4 are algorithm based, while Models 5-6 are analytic, meaning RPI is expressed as an explicit function of the state variables, allowing deterministic optimization techniques to be used.

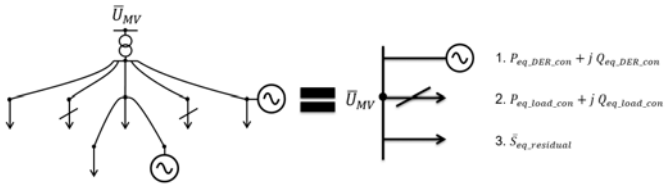

Fig. 1. Secondary distribution test system and proposed equivalent model.

II. Key Results

The secondary test system has been completely modeled in GridLAB-D and compared with the relative equivalent models, implemented in MATLAB. Total active power injection, relative percentage error and rms error versus execution time are shown in Fig. 2, 3, 4 for all the six models.

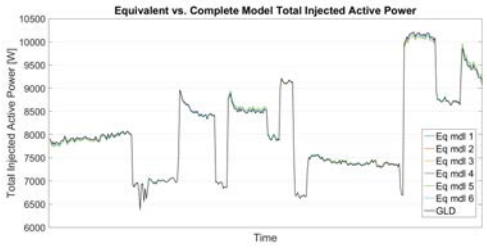

Fig. 2. Total injected power from complete GridLab-D and equivalent models.

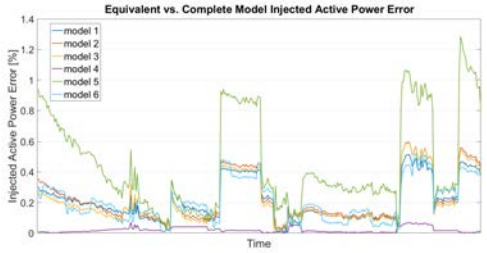

Fig. 3. Total injected active power percentage error.

Fig. 4. Active and reactive power rms percentage error versus execution time.

Acknowledgment

This project is supported by the DOE under award number DE-OE0000878. Project partners include Argonne National Lab, Commonwealth Edison, GE Grid Solutions, Massachusetts Institute of Technology, Seattle City Light, Virginia Polytechnic Institute and State University, and NRECA.

Building Energy Scheduling with Transactive Approach Having Autonomous Temperature Setting

Ashim Basnet
The University of Hong Kong
Student Member, IEEE
Hong Kong, HKSAR
ashim@eee.hku.hk

***Abstract*— Residential buildings consume significant share of the total energy, yet the efficient building energy scheduling is hardly considered. These buildings can operate flexibly in response to the change in the energy markets and environment conditions to gain financial benefits. In this poster, scheduling of energy consuming devices in a building has been proposed, where the building has three virtual transactive energy markets, namely heat, gas and electricity markets. Each market is supposed to have multiple suppliers and demands and clears their marginal energy prices. Autonomous temperature setting of the heating system is based on the interpolation of extreme day ahead market prices and temperature settings input by end-user. Case studies demonstrate that the transactive control of heating devices for the building can autonomously operate the heating system in a flexible way providing the optimal scheduling of heating devices.**

Keywords—Transactive Market, Building Energy Management

I. Introduction

The residential buildings utilizes mainly three energy resources: heat, natural gas and electricity. Heating loads can provide significant amount of operational flexibility in response to the changes in market prices and ambient temperature. As heat demand can be fulfilled from multiple energy vectors, flexibility is further enhanced. A building can economically schedule the energy intensive devices without compromising the user defined comfort level. In this poster, a building has been envisaged as a virtual energy market having electricity, gas and heat market as shown in Fig. 1. These energy markets are interconnected by combined heat and power (CHP) plant, gas boiler heater, power-to-gas converter (P2G) and Electric Heater (EH). In each energy market, there are sets of suppliers and demands. P, G, H denotes the electricity, gas and heat quantity respectively in Fig. 1, while subscripts S and D indicates whether they are supply or demand quantity. User sets the desired maximum and minimum temperature, which is then used to interpolate linear relationship against minimum and maximum day-ahead electricity price obtained from the utility. Based on the interpolation relation, hourly day-ahead prices and ambient temperature condition, the autonomous temperature setting is obtained and hence the value of the heating load demand bid in the virtual heat market. The proposed framework has been modelled as linear program having minimization of total energy cost with three energy balance equality constraints for electricity, natural gas and heat energy. From the equality constraints, the dual variables are generated which act as the virtual transactive energy prices inside the building. The optimization solves for the supply quantities within the proposed framework having few fixed energy loads. This concept of virtual transactive energy prices can be useful for scheduling of distributed energy resources in future applications.

This work was supported by the National Key R&D Project of China under Grant 2016YFB0901903.

II. Key Results

Results from the case studies suggest that the scheduling of the heating devices are obtained from the proposed framework as shown in Fig. 2. CHP has been found to be turned off during low electricity price period in contrast to EH which is only turned on in this period. Gas boiler remains the major source of heating energy for the building. P2G is never used accounting to high virtual building electricity price when compared to virtual building gas price. During the hours when the gas grid supply is congested, the building gas price becomes higher than grid gas price as shown in Fig. 3. The virtual heat price is high during the morning period when ambient temperature is low and virtual energy prices of gas and electricity are higher, while at afternoon, heat price becomes lower. The autonomous temperature setting saved the operation costs for building rather than having a fixed temperature.

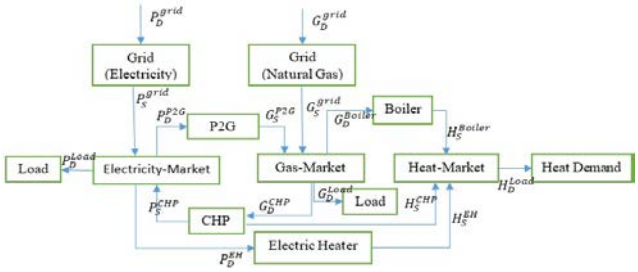

Fig 1. Virtual Building transactive Market

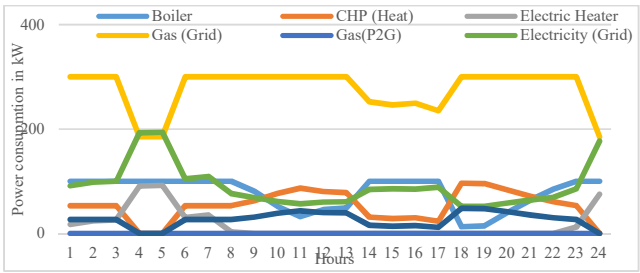

Fig 2. Scheduling of Energy Suppliers

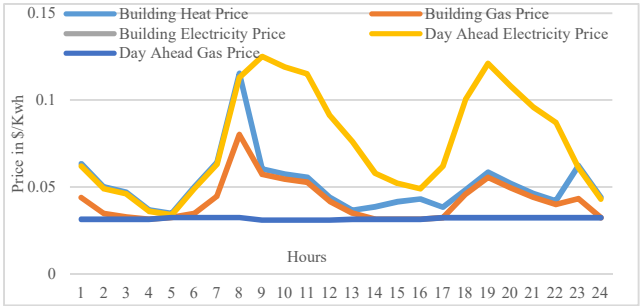

Fig 3. Transactive Market Prices in the Building

Cooperative Game Theory for Allocating Cost Savings from Coalitional Energy Management

Liyang Han, Thomas Morstyn, Malcolm McCulloch
Department of Engineering Science
University of Oxford
Oxford, UK
{Liyang.Han, Thomas.Morstyn, Malcolm.McCulloch}@eng.ox.ac.uk

***Abstract*—Distributed energy storage (ES) is widely regarded as a tool to mitigate the supply-demand imbalance caused by intermittent generation and variable loads in a distribution network. Because a retail supplier generally offers a lower electricity sell price (e.g. feed-in tariff) than its buy price, ES owners are monetarily incentivized to store excess generation for later usage. However, because each ES system tends to be operated only to minimize the energy cost of its direct owner, the joint load balancing effect of multiple ES systems becomes insignificant. A centralized ES control strategy can be used to provide local energy services such as peak shaving and energy shifting to increase the utilization of local renewable generation, but how to encourage ES owners to participate in such a scheme remains a challenge. This paper proposes the novel use of cooperative game theory to incentivize optimized ES system control for a prosumer[1] grand coalition. The optimization objective is to gain the highest joint monetary benefit for the participants through collaborative operation of multiple ES systems, and cooperative game theory is used to allocate this profit to each individual prosumer in a way that ensures the grand coalition providing the best economic outcome for every participant.**

***Index Terms*—Cooperative game theory, energy management, nucleolus, prosumers**

I. Framework

Let a group of N prosumers form a *grand coalition* $\mathcal{N}$ indexed by $i \in \mathcal{N} := \{1, 2, ..., N\}$. For each prosumer i we assume a noncontrollable load, and/or a generation source, and no more than one ES system, which operation is constrained by its energy capacity, charging and discharging power limits, and the requirement to restore its original state of charge (SoC) at the end of each analysis period.

For each analysis period, we consider K timesteps ($t = 1, 2, ..., K$) with a time interval of Δt, and we define:

$\mathbf{p}^b \in \mathbb{R}^{1\times K}$: Electricity *buy price*, in $[\$/kW_{AC}\Delta t]$
$\mathbf{p}^s \in \mathbb{R}^{1\times K}$: Electricity *sell price*, in $[\$/kW_{AC}\Delta t]$
where $p^b_t > p^s_t, \forall t \in [1, K]$.

A. Coalitional Energy Cost

For each prosumer i, we define:

$\mathbf{q}_i \in \mathbb{R}^{1\times K}$: *net energy load without ES*, $[kW_{AC}\Delta t]$
$\mathbf{b}_i \in \mathbb{R}^{1\times K}$: *ES operation variables*, $[kW_{AC}\Delta t]$

The energy cost for any *coalition* $\mathcal{S} \subseteq \mathcal{N}$ is defined as

$$\mathrm{C}(\mathcal{S}) = \min_{\mathbf{b}_i, \forall i \in \mathcal{S}} \left\{ \mathbf{p}^b [\sum_{i\in\mathcal{S}} (\mathbf{b}_i^\intercal + \mathbf{q}_i^\intercal)]^+ + \mathbf{p}^s [\sum_{i\in\mathcal{S}} (\mathbf{b}_i^\intercal + \mathbf{q}_i^\intercal)]^- \right\}$$

where $[\mathbf{z}]^{+(-)} = \max(\min)\{\mathbf{z}, \mathbf{0}\}$, and $\mathbf{b}_i$ s.t. ES constraints.

[1]proactive-consumers with distributed energy resources that actively manage their consumption and production of energy

B. Cooperative Game Formulation

The *value function* v is defined as the coalitional energy cost savings: $v(\mathcal{S}) = \sum_{i\in\mathcal{S}} \mathrm{C}(\{i\}) - \mathrm{C}(\mathcal{S}), \forall \mathcal{S} \subseteq \mathcal{N}$.

We use vector $\mathbf{x} \in \mathbb{R}^N$ as the *payoff allocation* whose entry x_i represents the payment to member $i \in \mathcal{N}$. $\mathbf{x}$ is an *imputation* if $\sum_{i\in\mathcal{N}} x_i = v(\mathcal{N})$, and $x_i \geq v(\{i\}), \forall i \in \mathcal{N}$. We test two important *imputations*: the *Shapley value* and the *nucleolus*, and show that both imputations guarantee savings for all players, but only the *nucleolus* $\mathbf{u}$ is stabilizing: $\sum_{i\in\mathcal{S}} u_i \geq v(\mathcal{S}), \forall \mathcal{S} \subset \mathcal{N}$.

II. Key Results and Discussion

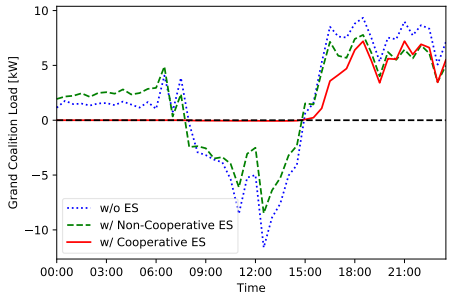

Fig. 1: 12-prosumer energy coalition example: 24-hour load profiles

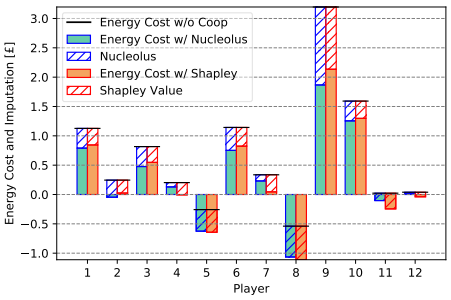

Fig. 2: 12-prosumer coalitional energy costs and cost savings (24 hrs)

We test our model using load and PV data from the Customer-Led Network Revolution trials. Fig. 1 shows that the cooperative ES operation, simply with the objective to minimize the coalitional energy cost, is significantly more effective in load balancing than the non-cooperative ES operation. Fig. 2 confirms that all players can financially benefit from participating in the *grand coalition*. Further analysis shows that the nucleolus is stabilizing, meaning it guarantees that no groups of players could achieve higher savings by leaving the *grand coalition* to form smaller coalitions.

Game-theory-based Real-Time Inter-Microgrid Market Design Using Hierarchical Optimization Algorithm

Mohammad Mahmoudian Esfahani, Abla Hariri, *Student Members IEEE* and Osama A. Mohammed, *Fellow, IEEE*
Florida International University.

***Abstract*—This paper proposes a Game-theory-based real-time reverse auction model for inter-microgrid market in a multi-microgrid system using a hierarchical optimization algorithm to address the optimal operation of microgrids in distribution systems. This market is organized to optimally assign the net power mismatch inside an area to microgrids' market agents aiming at minimizing both the dependency on the utility and the market clearing cost. To implement the proposed framework in a Multi-Agent System (MAS), a fast and reliable communication middleware is required. Therefore, a data-centric communications middleware based on the real-time publish-subscribe protocol is deployed for this purpose, where each agent is developed as a domain participant combining a publisher and subscriber. To validate the effectiveness of the proposed market framework, it is applied on the modified 37-bus IEEE distribution test feeder system, and the numerical results are obtained and presented.**

Index terms— Multi-agent system; Inter-microgrid market; Game theory; Hierarchical optimization; Data distribution service; Demand response.

I. Introduction

In this paper, a game-theory-based inter-microgrid market algorithm is proposed for the real-time energy management in a multi-microgrid system, where all market players (DGs, DESSs and Loads' DR) can participate in this market. Real-time in this work is defined as a 5-minutes-ahead market. It means that this market is executed in 5 minutes before the actual operation interval to minimize the forecasted energy mismatch in a multi-microgrid area in order to determine energy transactions between microgrids. It is anticipated to increase the accuracy significantly compared with running the real-time market one hour before the operation interval. Since this algorithm needs to be solved very fast, a hierarchical optimization algorithm is developed and utilized for this purpose to distribute the optimization between several agents aiming at decreasing the solution time compared with solving an overall optimization problem in the upper layer agent. All agents' calculations and optimization process are developed using the programming language of DIgSILENT PowerFactory 2017 and the Dynamic Data Exchange (DDE) is deployed to transfer data between agents through the DDS to meet the communication requirements of the proposed MAS framework [11]. Fig. 1 shows the structure of each agent and the interface used for communication.

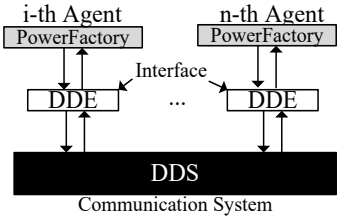

Fig. 1: Data exchange between agents through the DDS

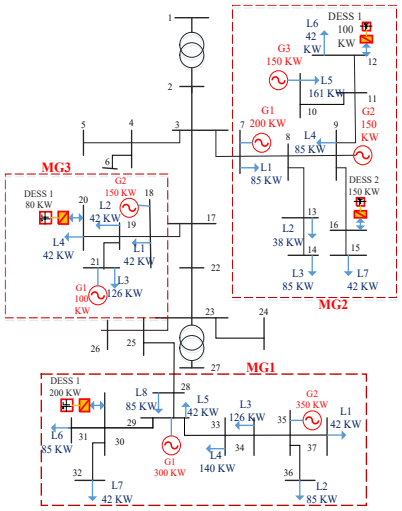

Fig 2: The modified IEEE 37-bus distributed network

II. Numerical Results

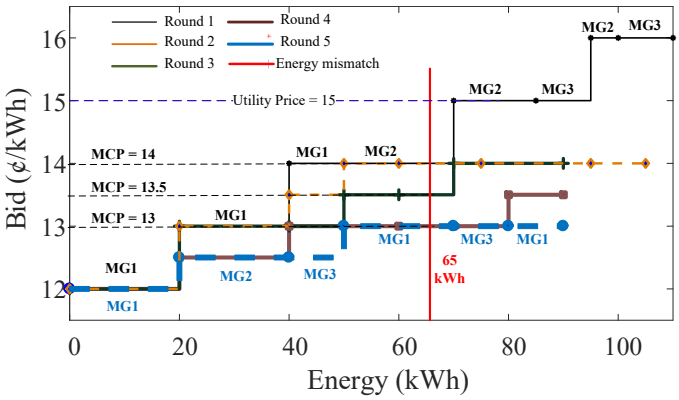

Fig. 3: Results of the game-theory-based reverse auction

Reference Bus Independent Components of LMP through a Non-Marginal Choice of its Energy Component

Deep Kiran, *Student Member, IEEE*, A R Abhyankar, *Member, IEEE* and B K Panigrahi, *Senior Member, IEEE*
Department of Electrical Engineering, Indian Institute of Technology Delhi, New Delhi, India 110016
Email: dkiran5@gmail.com, abhyankar@ee.iitd.ac.in, bkpanigrahi@ee.iitd.ac.in

***Abstract*—In the loss compensated direct current optimal power flow (LCDCOPF) markets, the reference bus plays a crucial role in the decomposition of locational marginal price (LMP) components. For the correct valuation and settlement of financial instruments in these markets, it is important to rationally decompose the LMP into its components. Therefore, this paper proposes a simple non-marginal method for calculating reference bus independent components of LMP. The efficacy of the proposed method is supported by numerical results.**

***Index Terms*—Locational marginal prices, energy component, loss component, congestion component and reference bus independent.**

I. Loss Compensated DCOPF Model

In LMP markets, surplus (S) is accumulated with the independent system operator (ISO) in market settlement which corresponds to both loss and congestion. A well-defined components of LMP for effective congestion management and loss allocation at each bus location is one of the pre-requisite for these hedging instruments [1], [2]. The typical LCDCOPF model is shown below in (1)-(5) [1], [2].

$$\underset{G_i,L}{\text{Min.}} \quad \sum_i f_i(G_i) \tag{1}$$

$$[\lambda] : \sum_i (G_i - D_i) = L \tag{2}$$

$$[\gamma] : L = \sum_i LF_i(G_i - D_i) - \omega \tag{3}$$

$$[\underline{\mu_l}, \overline{\mu_l}] : -\overline{P_l} \leq \sum_i SF_i^l(G_i - D_i - DF_iL) \leq \overline{P_l} \ \ \forall l \tag{4}$$

$$[\underline{\alpha_i}, \overline{\alpha_i}] : \underline{G_i} \leq G_i \leq \overline{G_i} \ \ \forall i \tag{5}$$

In above model, LF, ω and DF are calculated based on the optimal solution of DCOPF model (which is a pre-requisite in [1]). On the contrary, in [2], these terms are updated based on an AC power flow solution in an iterative manner.

II. Proposed Method

LMP (Λ_i) is defined by the partial derivative of Lagrange function with respect to D as,

$$\Lambda_i = \underbrace{\gamma - LF_i\gamma}_{\text{(a)}} + \underbrace{\sum_l SF_i^l\mu_l - \sum_l \sum_i SF_i^l DF_i\mu_l}_{\text{(b)}} \ \ \forall i \tag{6}$$

In (6), the terms in (a) correspond to energy (Λ_i^E) and loss (Λ_i^L) component of LMP and the terms in (b) correspond to congestion (Λ_i^C) component of LMP. The dependency of Λ_i^E on reference bus can be eliminated as

$$\sum_i \Lambda_i D_i - S = \sum_i \Lambda_i G_i = \sum_i \Lambda_i^E D_i \tag{7}$$

It is assumed that Λ_i^E is same across the network [1], [2], therefore, from (7),

$$\Rightarrow \sum_i \Lambda_i G_i = \Lambda_i^E \sum_i D_i \tag{8}$$

$$\Rightarrow \Lambda_i^E = \frac{\sum_i \Lambda_i G_i}{\sum_i D_i} \tag{9}$$

Using the fact that dispatch and LMP remains same, to make a non-marginal choice for Λ_i^E in (9) leads to its reference bus independency. Thus, Λ_i^L can be written as

$$\Lambda_i^L = (a) - \Lambda_i^E \tag{10}$$

III. Numerical Results

The proposed method derive the components of LMP based on the LCDCOPF model in [1], [2]. The results are shown for 5-bus [2] system.

A. 5-Bus System

TABLE I
Clearing result of 5-bus system when compared with [1]

		Proposed method			[1] with Reference @ A			[1] with Reference @ D		
Bus	Λ_i	Λ_i^E	Λ_i^L	Λ_i^C	Λ_i^E	Λ_i^L	Λ_i^C	Λ_i^E	Λ_i^L	Λ_i^C
A	15.85	14.87	13.42	-12.43	28.28	0.00	-12.43	28.57	-0.29	-12.43
B	24.18	14.87	14.02	-4.70	28.28	0.60	-4.70	28.57	0.32	-4.70
C	27.20	14.87	14.07	-1.73	28.28	0.65	-1.73	28.57	0.37	-1.73
D	35.00	14.87	13.70	6.44	28.28	0.28	6.44	28.57	0.00	6.43
E	10.00	14.87	13.30	-18.16	28.28	-0.12	-18.16	28.57	-0.41	-18.16

TABLE II
Clearing result of 5-bus system when compared with [2]

		Proposed method			[2] with Reference @ A			[2] with Reference @ D		
Bus	Λ_i	Λ_i^E	Λ_i^L	Λ_i^C	Λ_i^E	Λ_i^L	Λ_i^C	Λ_i^E	Λ_i^L	Λ_i^C
A	15.85	14.81	7.32	-6.29	22.14	0.00	-6.29	22.36	-0.23	-6.29
B	24.09	14.81	7.82	1.46	22.14	0.49	1.46	22.36	0.27	1.46
C	27.11	14.81	7.86	4.44	22.14	0.53	4.44	22.36	0.31	4.44
D	35.00	14.81	7.55	12.64	22.14	0.23	12.64	22.36	0.00	12.64
E	10.00	14.81	7.23	-12.04	22.14	-0.10	-12.04	22.36	-0.32	-12.04

References

[1] E. Litvinov, T. Zheng, G. Rosenwald, and P. Shamsollahi, "Marginal loss modeling in lmp calculation," *IEEE Trans. Power Syst.*, vol. 19, no. 2, pp. 880–888, 2004.

[2] Z. Hu, H. Cheng, Z. Yan, and F. Li, "An iterative lmp calculation method considering loss distributions," *IEEE Trans. Power Syst.*, vol. 25, no. 3, pp. 1469–1477, Aug 2010.

Who has an incentive to improve the renewable day-ahead forecast?

Evangelia Spyrou, *Student Member, IEEE*, Benjamin F. Hobbs, *Fellow, IEEE*

***Abstract*—Improving forecasts of renewable generation is one way to improve the efficiency of grid operation with high renewable penetration ([1],[2]). Ideal market incentives would enable participants to capture the economic benefits of improved forecasts. But in practice, market failures might discourage market participants from providing better renewable forecasts or methods. We consider how Residual Unit Commitment (RUC) market processes might introduce such a failure by enabling wind plants to take advantage of inaccurate/imprecise ISO forecasts.**

I. Introduction

MULTIPLE agents use renewable forecasts in electricity markets: generators, traders, load, and independent system operators (ISO). ISOs use the forecasts for many purposes but here we focus on RUC. ISOs utilize RUC to ensure that adequate capacity is committed for next day's demand in case the financial day-ahead (DA) market commits inadequate capacity, which can occur for several reasons. For instance, net virtual supply can displace the commitment of physical resources, lower than forecasted demand might clear, or renewable offers might be overly optimistic. RUC procurement and associated costs significantly increased in California in 2016.

Most ISOs use their own DA forecasts of renewable generation in RUC (e.g., CAISO, ERCOT, SPP). We investigate if use of ISO forecasts in RUC provides market participants a disincentive to integrate better forecasts.

II. Motivating Example

We assume a simple one-bus, one-time period, energy-only market with identical granularity for DA and real-time markets. Our system consists of three generators (see Table 1) and has a perfectly forecasted demand of 660 MW. We assume that the ISO forecasts 250 MW of wind day-ahead, and has a 50% chance of -20 MW error, and 50% chance of +20MW error.

Table 1. Capacity and costs of generators in the example

Plant	Capacity (probability) / Pmin	Start-up / Variable cost
Gen 1	400 MW (p=1) / 100 MW	\$0 / \$5.47/MWh
Gen 2	60 MW (p=1) / 12 MW	\$437 /\$26.11/MWh
Wind	230 (p=0.5) / 270(p=0.5)	\$0 / \$0/MWh

We compare the average settlement ("avg. settl.") for wind bidders and load under two wind bidding strategies: (a) wind bidders offer the perfect forecast in DA market, (b) wind bidders offer the lesser of their perfect forecast and the ISO forecast. We provide the market clearing results for both wind realizations (i.e., 230 MW/270 MW) under each strategy in Tables 2 and 3. We assume that the DA uplift costs are paid by load and the RUC uplift costs are paid by the party whose schedule differs from the ISO forecast (here wind). Uplift credits are equal to unit's market shortfall.

Table 2. Market clearing under (a): wind offers perfect forecast

(low / hi wind)	DA	RUC	RT	Avg Settl.
Gen 1	400MW/390MW	-	-/(-12MW)	\$6,256
Gen 2	30MW/0MW	-/commit	-/(+12MW)	\$985*
Wind	230MW/270MW	-	-	\$3,399*
Load	660MW/660MW	-	-	\$10,640*
Price(\$/MWh)	26.11/5.47	-	26.11/5.47	-
Start-up costs	\$437/\$0	-/\$437	-	-

Table 3. Market clearing under (b): wind bids strategically

(low / hi wind)	DA	RUC	RT	Avg Settl.
Gen 1	400MW/398MW	-	-/(-20MW)	\$6,256
Gen 2	30MW/12MW	-	-/-	\$985*
Wind	230MW/250MW	-	-/+20MW	\$3,741
Load	660MW/660MW	-	-	\$10,982*
Price(\$/MWh)	26.11/5.47	-	26.11/5.47	-
Start-up costs	\$437/\$437	-	-	-

* Adjusted for uplift for unrecovered start-up & energy costs

The real-time dispatch and commitment is identical for both strategies but the cost allocation among participants is different. Wind generators would prefer strategy (b) whereas load would prefer strategy (a). Thus, if wind bidders had access to a perfect forecast and were strategic, they would prefer to offer based on the perfect forecast only when it was lower compared to the ISO's to avoid any costs incurred by RUC.

Under both bidding strategies, the total system cost is \$3,113, which is inefficient. If RUC used the perfect forecast, then Gen 2 would never be committed under high wind conditions, saving in expectation \$342—so the quality of forecast used in RUC might affect the system cost.

III. Conclusions and Future Work

Our example demonstrates a simple case in which RUC might increase system costs if (i) the quality of ISO forecast is systematically inferior to market participants' forecasts and (ii) RUC leads to commitment of additional units. According to our example, RUC costs might discourage strategic renewable bidders from providing better forecasts to the system. In the poster, we will provide more motivating examples, present simulation results, and discuss alternative market designs.

IV. References

[1] B. Kroposki *et al*., "Achieving a 100% Renewable Grid: Operating Electric Power Systems with Extremely High Levels of Variable Renewable Energy," *IEEE Power and Energy Mag*., *15*(2), 61-73, Mar.-Apr. 2017.

[2] Q..Wang *et al.*, "The value of improved wind power forecasting: Grid flexibility quantification, ramp capability analysis, and impacts of electricity market operation timescales," *Appl. Energy*, *184*, 696-713, 2016.

Acknowledgments. E. Spyrou is an Onassis Foundation Scholar and would like to thank the Foundation for the support of her research. B. Hobbs is supported by the National Science Foundation.

A Bi-Level Optimization Formulation of Priority Service Pricing

Yuting Mou
Center for Operations Research and Econometrics
Université catholique de Louvain
Email: yuting.mou@uclouvain.be

Anthony Papavasiliou
Center for Operations Research and Econometrics
Université catholique de Louvain
Email: anthony.papavasiliou@uclouvain.be

Philippe Chevalier
Center for Operations Research and Econometrics
Université catholique de Louvain
Email: philippe.chevalier@uclouvain.be

***Abstract*—Priority service pricing is a promising approach for mobilizing residential demand response, by offering electricity as a service with various levels of reliability. Higher levels of reliability correspond to higher prices. The proper pricing guarantees that consumers self-select a level of reliability that corresponds to the reliability that the system can offer. However, traditional theory for menu design is based on numerous stringent assumptions, which may not be respected in practice, such as a well-behaved (convex) cost functions. In addition, the objective of the menu design is to maximize social welfare, while the profit requirement of the aggregator is not accounted for. Moreover, no guidelines are provided regarding how to discretize the menu into finite options. In this study, we design a priority service menu as the equilibrium solution to a Stackelberg game where an aggregator moves first with a menu offering, and residential consumers react by selecting menu options and revealing their valuation. The Stackelberg game is modelled as a bi-level optimization problem involving the aggregator and consumers, and then reformulated as a mixed-integer problem. As a consequence of this approach, the menu design problem can be integrated within a day-ahead unit commitment model, and profit requirements of the aggregator can be modeled explicitly. The approach is illustrated on a toy numerical example as well as a large-scale model of the Belgian power market.**

I. Introduction

The operation of power systems has become increasingly challenging due to the large-scale integration of renewable energy sources. Demand-side management is a promising approach for overcoming this challenge The LINEAR project in Belgium unveils substantial demand response potential in the residential sector [1]. In the domain of demand-side management, researchers have focused on price-based control and direct load control. The former method is based on price signals provided to consumers, whereby consumers react to the price signal by adjusting their electricity consumption. However, if the price is too volatile, consumers face substantial price uncertainty, which is politically objectionable. In direct load control, household appliances, such as electric vehicles and air conditioners, would be controlled directly by aggregators. Nevertheless, this method is criticized as being too intrusive and ideally control is imposed behind the meter.

Another paradigm based on priority service is proposed in [5], with the underlying economic theory dating back to [6]. In this paradigm, electricity supply is perceived as a service that can be offered with various degrees of quality. Specifically, the authors describe contracts whereby power is offered to consumers with various degrees of reliability. Higher degrees of reliability correspond to higher prices. The proper pricing of the contracts guarantees that consumers self-select a level of reliability that corresponds to the reliability that the system can actually offer, and indirectly reveal their valuation for power. However, traditional theory for menu design is based on numerous stringent assumptions. We aim to relax these assumptions in this paper.

II. Methodology

In this study, we design a priority service menu as the equilibrium solution to a Stackelberg game where an aggregator moves first with a menu offering, and residential consumers react by selecting menu options and revealing their valuation. The Stackelberg game is modelled as a bi-level optimization problem involving the aggregator and consumers, and then reformulated as a mixed-integer problem. Numerical simulations are also carried out.

References

[1] R. Dhulst, W. Labeeuw, B. Beusen, S. Claessens, G. Deconinck, and K. Vanthournout, "Demand response flexibility and flexibility potential of residential smart appliances: Experiences from large pilot test in belgium," *Applied Energy*, vol. 155, pp. 79–90, 2015.

[2] Y. Mou, H. Xing, Z. Lin, and M. Fu, "Decentralized optimal demand-side management for phev charging in a smart grid," *IEEE Transactions on Smart Grid*, vol. 6, no. 2, pp. 726–736, 2015.

[3] H. Xing, Y. Mou, M. Fu, and Z. Lin, "Distributed bisection method for economic power dispatch in smart grid," *IEEE Transactions on power systems*, vol. 30, no. 6, pp. 3024–3035, 2015.

[4] H. Xing, M. Fu, Z. Lin, and Y. Mou, "Decentralized optimal scheduling for charging and discharging of plug-in electric vehicles in smart grids," *IEEE Transactions on Power Systems*, vol. 31, no. 5, pp. 4118–4127, 2016.

[5] S. S. Oren, "A historical perspective and business model for load response aggregation based on priority service," in *System Sciences (HICSS), 2013 46th Hawaii International Conference on*. IEEE, 2013, pp. 2206–2214.

[6] H.-p. Chao and R. Wilson, "Priority service: Pricing, investment, and market organization," *The American Economic Review*, pp. 899–916, 1987.

[7] A. Papalexopoulos, J. Beal, and S. Florek, "Precise mass-market energy demand management through stochastic distributed computing," *IEEE Transactions on Smart Grid*, vol. 4, no. 4, pp. 2017–2027, 2013.

[8] K. Margellos and S. Oren, "Capacity controlled demand side management: A stochastic pricing analysis," *IEEE Transactions on Power Systems*, vol. 31, no. 1, pp. 706–717, 2016.

Transactive Energy Based Multi-microgrids System Operation

[†*] Chirath Pathiravasam, *Student Member*, IEEE, [*‡] Ganesh Venayagamoorthy, *Senior Member*, IEEE
[*]Real-Time Power and Intelligent Systems Laboratory
Holcombe Department of Electrical and Computer Engineering, Clemson University, Clemson, SC, 29634, USA
[†]Department of Electrical Engineering, University of Moratuwa, Katubedda, Sri Lanka
[‡]School of Engineering, University of KwaZulu-Natal, Durban, South Africa
{chirath.d.pathiravasam, gkumar}@ieee.org

***Abstract*—High proliferation of distributed energy resources (DER) demands controllability in the distribution system. Microgrid is one of the solutions to mitigate variability of the distribution system. However, complete independent operation of microgrids may not be cost effective. To overcome this challenge, predictive and prescriptive analytics based transactive retail energy framework is proposed to optimize the dispatch in a multi-microgrid system. A transactive distribution system operator (TDSO) will act as the aggregator of the microgrids and other prosumers. TDSO will also perform system parameter predictions to optimize future energy dispatches. Dispatch of the microgrids are done using decision trees based on the microgrid priorities. The transactive operation enables microgrids to increase reliability with lower energy storage capacities.**

***Index Terms*—Transactive energy; dynamic energy management system decision tree; predictive analytics; micro-grids; renewable energy**

I. Introduction

The increasing penetration of DER and prosumers will add to requirements of reliability of the system. Prosumers willingness to participate in energy markets will need to be satisfied by either the distribution utility or distribution system operator: TDSO. TDSO will aggregate generation and demand of the multi-microgrid distribution system. A real-time price based transactions with microgrids and among microgrids are performed by the transactive energy framework of TDSO which in turn participate in the bulk energy market. Participation in energy markets by TDSO and prosumers such as microgrids can be viewed as a nested market.

In this project, each microgrid 1 consist of wind and solar pv power generation, battery energy storage, backup diesel generator, critical loads and controllable loads is considered. Individual microgrids are managed by Dynamic Energy Management Systems (DEMS) [1].

The predictive analytics platform of the TDSO utilizes individual microgrid parameters such as wind speed and solar irradiance to predict the future variable renewable energy generation. The predictions are performed in a cellular computational networks framework [2].The forecast renewable energy will be used by the microgrid DEMS to dispatch resources and TDSO to transact energy with microgrids and the main grid (ISOs).

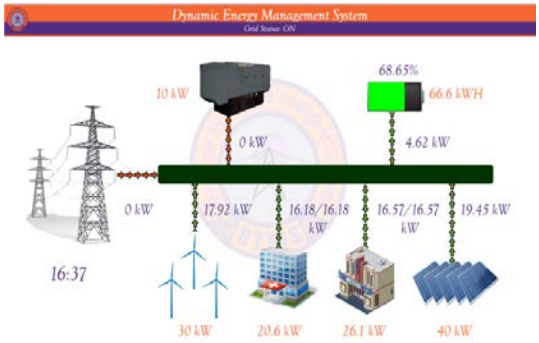

Fig. 1: Microgrid system with Dynamic Energy Management System

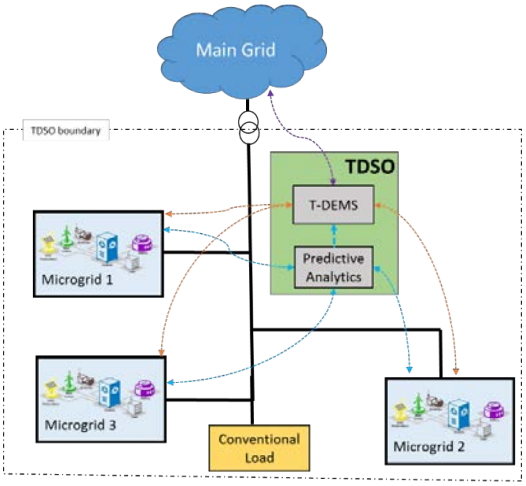

Fig. 2: Transactive energy framework of TDSO

References

[1] G. K. Venayagamoorthy, R. K. Sharma, P. K. Gautam, and A. Ahmadi, "Dynamic energy management system for a smart microgrid," *IEEE transactions on neural networks and learning systems*, vol. 27, no. 8, pp. 1643–1656, 2016.

[2] C. Pathiravasam and G. K. Venayagamorthy, "Spatio-temporal characteristics based wind speed predictions," in *2016 IEEE International Conference on Information and Automation for Sustainability (ICIAfS)*, Dec 2016, pp. 1–6.

Generator Contingency Modelling in ISOs: Pricing Implications

Karthik Saikumar, *Student Member, IEEE*, and Kory W. Hedman, *Member, IEEE*

***Abstract*—Electric Energy Market clearing models rely on solving bid-based security constrained energy and ancillary co-optimization problem. Security constraints need to be modelled in the optimization model to ensure that the market solution is secure, and the system can survive a N-1 event. Typically, market clearing models have been using a deterministic approach to deal with generator contingencies by enforcing a quantitative procurement constraint that would procure a specific amount of reserves either zonally or system wide to ensure sufficient reserves are available after a generator contingency event. However, recent industry initiatives suggest there is a movement to explicitly modelling uncertainty in market models. The California Independent System Operator (CAISO) has proposed the explicit modelling of critical generator contingencies to capture the post contingency flow constraints in the optimization models. Meanwhile, the Midcontinent ISO has implemented the incorporation of zonal reserve deployment transmission constraints for post generator contingency scenarios. However, the inclusion of stochastic scenario-based modelling into market models can have an impact on pricing and settlements. This work aims at analyzing the pricing impacts such stochastic modelling by leveraging concepts from duality theory.**

***Keywords* – Electric Energy Markets, Generator Contingency, Duality Theory, Pricing**

I. Introduction

Modelling of various contingencies in market models is critical in ensuring that the market solution respects the security constraints that the system operator needs to conform to and to also ensure that the economic signals from the pricing that comes out of the security constrained market model accurately reflects the cost of respecting the security constraints. One of the crucial barriers to applying scenario based stochastic modelling to market models with respect to generator and transmission contingencies has been the impact stochastic modelling can have on pricing.

II. PRICING IMPACTS

The impact of stochastic modelling on pricing is mainly duet the presence of a second stage recourse decision variable. The loss of a transmission element does not mandate a change in generation set points post contingency as only the system topology has changed and as a result, line flows. This change can be captured using a Line Outage Distribution Factor (LODF). However, for the loss a generator, there is a need to change dispatch set points of all or some of the remaining generation fleet after the loss of a single generator.

The typical constraint for a transmission security modelling is:

$$F_{k,c} = F_{k0} + LODF_{k,c} * F_{c0}$$
$$F_{k,c} \leq P_{kmax}^{Rate\,C}$$

Since the generator has no second stage recourse action, the only major impact on the pricing is that the LMP will now capture a new post contingency congestion component. However, for generator contingencies, there needs to be a second stage decision variable. One possible way to capture the response of the remaining generation fleet to the loss of a single generating fleet is the Generation Distribution Factor (GDF). The change in generation and the corresponding impact on transmission line flows is captured as shown below:

$$P_{g,c} = P_g + GDF_{g,c} * P_{g=c}$$
$$\sum_n PTDF_{k,n}^R * (P_{g,c} - l_{nc}) \leq P_{kmax}^{Rate\,C}$$

The link between the second stage dispatch in the post generator contingency scenario and the first stage decision variable of the pre-contingency dispatch is masked by a static term called the GDF for certain critical generator contingencies. This linkage has a direct impact on the way the dual for the given primal problem is formed. By leveraging duality theory, we can observe the impact on generation rent and locational marginal pricing.

III. REFERENCES

[1] CAISO, "Draft final proposal: Generator contingency and remedial action scheme modeling," Jul. 2017[Online]. Available: https://www.caiso.com/Documents/DraftFinalProposal-GeneratorContingencyandRemedialActionSchemeModeling_updatedjul252017.pdf

[2] Y. Chen, P. Gribik, and J. Gardner, "Incorporating post zonal reserve deployment transmission constraints into energy and ancillary service co-optimization," IEEE Trans. Power Syst., vol. 29, no. 2, pp. 537–549, Mar. 2014.

Optimal Energy Management for the Integrated Power and Gas Systems via Real-time Pricing

KangAn Shu, Xiaomeng Ai, Jinyu Wen
Huazhong University of Science and Technology
Wuhan, China

Jiakun Fang, Zhe Chen
Aalborg University
Aalborg, Denmark

Cheng Luo
Northern Indiana Public Service Company
Merrillville, USA

***Abstract*— This work proposed a bi-level formulation for energy management in the integrated power and natural gas system via real-time price signals. The upper-level problem minimizes the operational cost, in which dynamic electricity price and dynamic gas tariff are proposed. The lower level problem is the arbitrage model of gas-fired plants and P2Gs stations, in which the transient gas flow is introduced. This bi-level model is relaxed to a mixed-integer quadratic programming problem using the Karush-Kuhn-Tucker optimality conditions. Results show that the dynamic price and tariff can make gas-fired units and P2Gs plants follow the system operator's preferences such as wind power accommodation, mitigation of unsupplied load and relieving the network congestion.**

***Index Terms*—integrated energy system, bi-level programming, equilibrium constraints.**

I. METHODOLOGY

The optimal energy management via dynamic pricing in the integrated power and gas system is formulated using the following bi-level model as shown in Fig. 1.

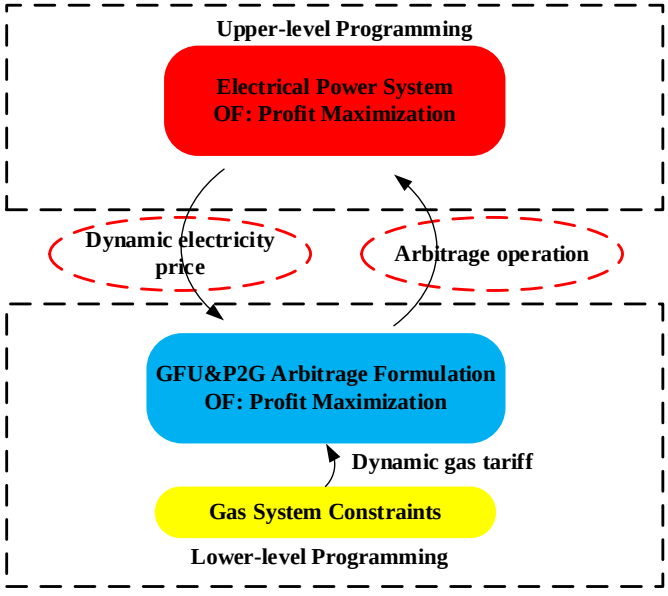

Fig. 1. The framework of bi-level energy management

The bi-level problem can be transferred into mix-integer quadratic programming using the KKT optimality conditions

II. RESULTS

The Graver 6-bus system and the 12-node natural gas system are used as the test case.

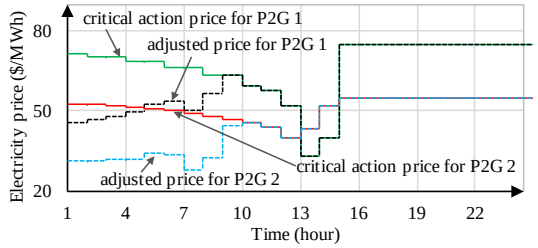

Fig. 2. The electricity price relevance for P2Gs

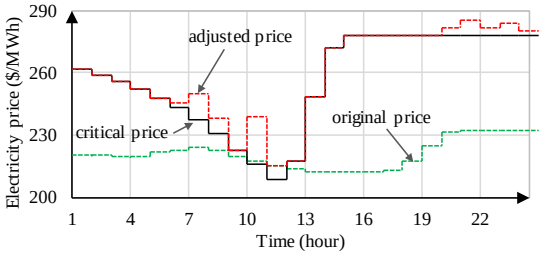

Fig. 3. The electricity price relevance for gas-fired unit

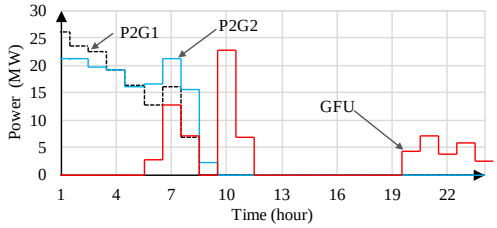

Fig. 4. The arbitrage operation of P2Gs.

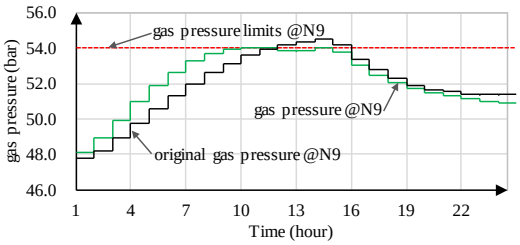

Fig. 5. The gas pressure at node 9.

III. CONCLUSION

The price signals are proposed to guide the operation of the GFU and P2G stations according to the upper-level system operator's preference. Simulation results demonstrate that the real-time pricing can successfully mobilize the arbitrage operation of GFU and P2Gs to accommodate wind power, satisfy load shortage and relieve gas state variables off-limit.

Cost Benefit Analysis of Technology Options for Enabling High PV Penetration

Lisha Sun, David Lubkeman, Mesut Baran
Dept. of Electrical and Computer Engineering
North Carolina State University
Raleigh, USA

Jeffrey Thomas, Joe DeCarolis
Dept. of Civil, Construction, and Environmental Engineering
North Carolina State University
Raleigh, USA

***Abstract*—This paper provides an economic comparison of three technologies that enable high PV penetration on the distribution system: Medium voltage solid state transformer (SST), grid edge regulator and smart inverter. In order to compare these three technologies, simulations are performed on a representative utility feeder using OpenDSS. Quasi-static time series analysis over a year is used to predict the effectiveness of high PV penetration and more aggressive conservation voltage reduction enabled by each technology. Comprehensive cost benefit analyses are conducted based on these simulation results. The cost benefit analysis results indicate that the medium voltage solid state transformer (MV SST) is the most cost effective option with a 3 year payback period for utilities that are trying to accommodate high PV penetration in the distribution grid.**

***Index Terms*--Cost benefit analysis, Grid edge regulator, High PV penetration, Smart inverter, Solid state transformer.**

I. HIGH PV PENETRATION OVERVOLTAGE MITIGATION TECHNOLOGIES

Many technologies have been developed to address overvoltage issues in order to enable higher PV penetration. The MV SST addresses the overvoltage issue by regulating the voltage on the customer side and isolating the customer from seeing overvoltage on the distribution primary. The grid edge regulator can be used as a mitigation method by regulating the voltage on the customer side of the distribution transformer. The smart inverter is being promoted for use in new PV interconnections. The smart inverter does not regulate voltage directly. Instead, it controls the reactive power injection to impact the local customer voltage.

TABLE I. TECHNICAL COMPARISON OF MV SST, GRID EDGE REGULATOR AND SMART INVERTER

Product	MV SST	Grid Edge	Smart Inverter
Power Rating	0-100 kVA	50 kVA	12 kW - 30 kW
Input Voltage	3.6 kV Vac	240 Vac	1000 Vdc
Output Voltage	120Vac/200Vdc	240 Vac	480/277 Vac
Volt. Regulation	Any	± 10%	-
VAR Compensation	Any	10% of rating (lead. Or lag.)	0-1power factor (lead. Or lag.)
Efficiency	97%	≥ 99%	98.30%
DC Port	Yes	No	No

II. SIMULATION AND RESULT

In order to quantify the benefits of the MV SST, grid edge regulator and smart inverter, OpenDSS quasi-static time series simulation are performed based on a representative utility feeder.

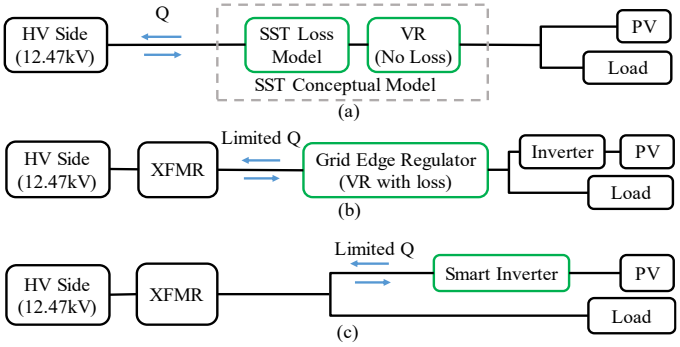

Figure 5. (a) FREEDM SST (b) Grid edge regulator (c) Smart Inverter

TABLE II. SIMULATION RESULTS

Diff Δ to Base	MV SST (32 used)		Grid Edge (32 Used)		Smart Inverter (133 used)	
	Energy MWh-yr.	*Peak kW*	*Energy MWh-yr.*	*Peak kW*	*Energy MWh-yr.*	*Peak kW*
DER	-1,187	-2	-1,110	-3	-1,082	-11
CVR	-534	-146	-534	-146	-153	-36
Total	-1,721	-147	-1,644	-149	-1,236	-46

III. COST BENEFIT ANALYSIS

This session describes the cost and benefits estimation and also discusses the cost benefit analysis results. A comprehensive cost estimation is performed and the benefits quantified by the quasi-static circuit simulation discussed in the previous section are monetized.

TABLE III. COMPARISON OF FINANCIAL METRIS

Technology	Estimated Utility Investment Cost	Estimated Annual Benefits	Estimated Net Present Value	Discounted Payback Period
MV SST	$160k	$91k	$665k	3.0 years
Grid Edge	$163k	$82k	$590k	3.5 years
Smart Inverter	$148k	$53k	$330k	4.8 years

Transmission Constrained Economic Dispatch via Interval Optimization Considering Wind Uncertainty

Xiao Kou, *Student Member*, *IEEE*, Wei Feng, *Student Member*, *IEEE*, and Fangxing Li, *Fellow*, *IEEE*

***Abstract*— High penetration renewable energy integration can negatively affect the secure operations of power grids. In this work, an interval optimization based algorithm is presented to solve the transmission-constrained economic dispatch problem considering wind uncertainty. The aim of introducing interval optimization is to determine the possible generation cost range, which consists of a lower (optimistic) boundary and an upper (pessimistic) boundary. The optimistic value is obtained by solving a trivial LP problem. However, the pessimistic model is a combinatorial max-min problem. To solve the pessimistic model, the strong duality theory is first applied to transfer the max-min problem into a minimization problem. Then the big-M method is employed to manage the combinatorial equality constraints for efficient calculation. The proposed algorithm is solved by interfacing GAMS with MATLAB. Simulation results on a modified IEEE 30 bus system validate the effectiveness of the proposed methodology.**

***Index terms*—economic dispatch, interval optimization, renewable energy integration, strong duality, wind uncertainty.**

I. Introduction

Large-scale wind integration can reduce the fuel costs and carbon emissions. However, the stochastic and intermittency natures of renewables presents substantial challenges for the generation scheduling of committed units. In this context, it is imperative to study the optimization techniques that can manage uncertainties to guarantee the safe and economic operations of the bulk power system.

The conventional method to schedule generators' power outputs is to formulate a fuel cost optimization problem with deterministic parameters, subjecting to power balance and other reliability requirements. In this framework, all the parameters are viewed as fixed values. The deterministic methods are effective tools for analyzing those cases where the fluctuation is small. However, the wind disturbance may cause significant difference on the optimization solutions. Moreover, wind fluctuation can cause generation-demand imbalance, transmission violations, and frequency deviation. At that time, the deterministic model would fail to handle the large deviations between the forecasted and actual wind power generations. To solve this problem, growing attention has been paid to probabilistic methods, such as stochastic programming. However, the disadvantage is that these approaches heavily relies on the accuracy of wind power probability distribution function. Since the current wind power forecasting technology is still immature, this may lead to considerable prediction errors and further affects the optimality of the generation schedule.

It's based on the above concerns that in this work we propose an interval optimization based economic dispatch model to address the wind power uncertainty. The most prominent advantage of interval optimization is that it only focuses on the boundaries of the uncertain variables, i.e. wind power, which can be derived from historical data fairly precisely, and does not require their accurate PDF formulation. As a consequence, interval optimization can provide a more robust generation schedule range under real-time scenarios by avoiding the forecast errors.

The main contributions of this work are summarized as follows: firstly, interval optimization is applied to get the possible generation cost range; secondly, strong duality theory is introduced to transform the max-min problem into a single level maximization problem; and thirdly, big-M is employed to convert the combinatorial problem into a MILP problem, which ensures the global optimal solution can be obtained within a short time.

II. Test System

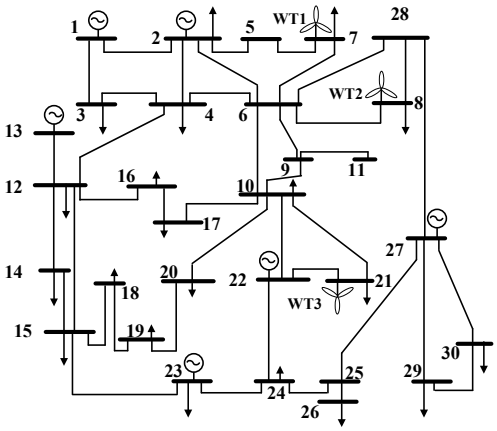

Figure 1. Configuration of the modified IEEE 30 bus system.

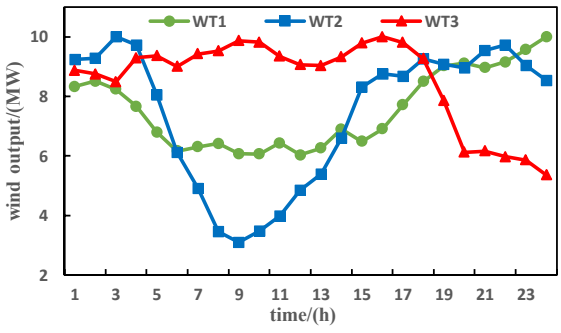

Figure 2. Wind power output.

Analytical Method to Aggregate Multi-Machine SFR Model with Applications in Power System Dynamic Studies

Qingxin Shi, Fangxing Li
University of Tennessee, Knoxville
Dept. of Electrical Engineering and Computer Science
Knoxville, TN, United States

***Abstract*— The system frequency response (SFR) model describes the average network frequency response after a disturbance and has been applied to a wide variety of dynamic studies. However, the traditional literature does not provide a generic, analytical method for obtaining the SFR model parameters when the system contains multiple generators. In this project, an analytical method is proposed for aggregating the multi-machine SFR model into a single-machine model. The verification study indicates that the proposed aggregated SFR model can accurately represent the multi-machine SFR model. The results show the method is promising with broad potential applications.**

***Index Terms*-- System frequency response (SFR), multi-machine, frequency control, model reduction.**

I. Analytical Method to Aggregate SFR Model

The SFR model is shown in Fig. 1. The droop value R_i is correlated to S_i (after reaching the steady state, $\Delta P_{mi}=S_i\cdot\Delta f/R_i$). Also, the multiple turbine governors are summed up with a constant gain $K_{mi}=S_i/S_{sys}$, which represents the portion of rated power of machine i w.r.t. the whole system. The equivalent droop value R is given by (1):

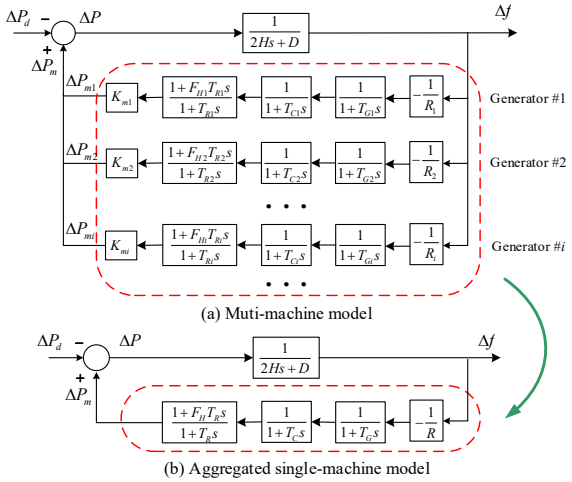

Fig. 1. Aggregation of SFR model.

$$\frac{1}{R}=\sum_{i=1}^{N}\frac{K_{mi}}{R_i}=\sum_{i=1}^{N}\kappa_i \tag{1}$$

where the equivalent gain is defined as $\kappa_i=K_{mi}/R_i$. In the aggregated SFR (ASFR) model (shown in Fig. 1 (b)), the four equivalent parameters $X=\{T_G,\ T_C,\ T_R$ and $F_H\}$ represent the combined effect of N turbine governors. We define the normalized gain λ_i of each branch in Fig. 1 (a).

$$\lambda_i=\kappa_i\Big/\sum_{i=1}^{N}\kappa_i\ ,\ \sum_{i=1}^{N}\lambda_i=1 \tag{2}$$

Since a larger λ_i value means that generator #i has a larger rated power and more sensitive frequency droop, it has a larger impact on the equivalent X. Therefore, we guess that the ASFR model parameters equal to the weighted average of those of each machine.

$$X=\sum_{i=1}^{N}\lambda_i X_i \tag{3}$$

Then, it is proved by *Mathematical Induction Method*.

II. Serification Study

The performance of the proposed model is by time-domain simulation of a six-machine system. The parameters of each machine are in a wide range, as listed in Table I. The frequency response of a step disturbance ΔP is shown in Fig. 2. It can be concluded that the ASFR model can accurately represent the bus frequency response of a small-scale system. This model can be applied to load-frequency control studies.

Table I. Parameters of 6-machine SFR model.

Gen. No.	K_m	T_G (s)	T_C (s)	T_R (s)	F_H (pu)	$1/R$	λ
1	0.14	0.20	0.37	10.5	0.28	13.33	0.113
2	0.18	0.12	0.24	9	0.17	10	0.109
3	0.19	0.27	0.41	6	0.23	20	0.230
4	0.22	0.30	0.48	14	0.32	16.67	0.222
5	0.14	0.22	0.36	12	0.39	20	0.169
6	0.13	0.19	0.21	8.5	0.24	20	0.157
Equ.	1.00	0.231	0.363	10.0	0.278	16.5	1.00

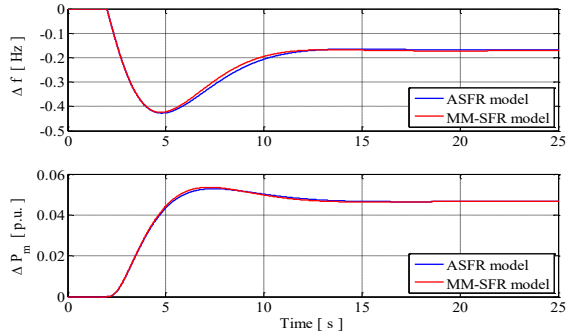

Fig. 2. Frequency & generation response of ASFR model.

Matlab Simulation Framework for Integration of Battery Storage and Solar Generation in Distribution Systems

Milad Soleimani, Student Member, IEEE, Ana M. Ospina, Student Member, IEEE,
Mladen Kezunovic, Life Fellow, IEEE.

***Abstract*—This poster presents a microgrid model including battery storage, photovoltaic (PV) generation, and the converters which connected them into the grid. The goal of the proposed model is to provide a realistic simulation framework in which an optimum interaction of electric vehicle (EV) chargers and PV generation is achieved using an energy battery storage. The model is divided in two parts: power system and power electronics model. Different scenarios are considered in a sub-hourly time frame. The optimum scenario for the next steps is calculated and the charging/discharging order is given to the battery. Some details and results of the implemented model are demonstrated in this poster.**

***Index Terms*—Electric Energy Storage, PV Generation, Modelling, Simulation Framework.**

I. Power System Model

The optimum decision for the charging/discharging of the batteries in the microgrid is being made every five minutes and the order will be sent to the battery charger to store energy in the battery or discharge it back to the grid. The schematic of the model used for the system part is shown in Figure 1.

II. Power Electronics Model

When the decision is made by the power system model, the converters will start to charge or discharge the batteries based on the received order.

III. Algorithm for Simulation Integration

Providing such a model has a considerably heavy calculation burden and requires a huge capacity of random access memory (RAM). In the flowchart shown in Figure 2, an algorithm is proposed to make such a modelling possible using ordinary computers.

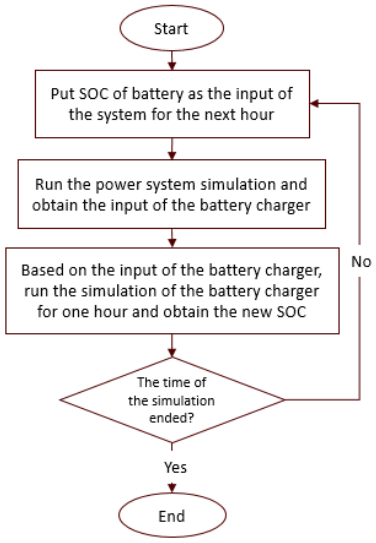

Figure 2. Flowchart of the implemented algorithm.

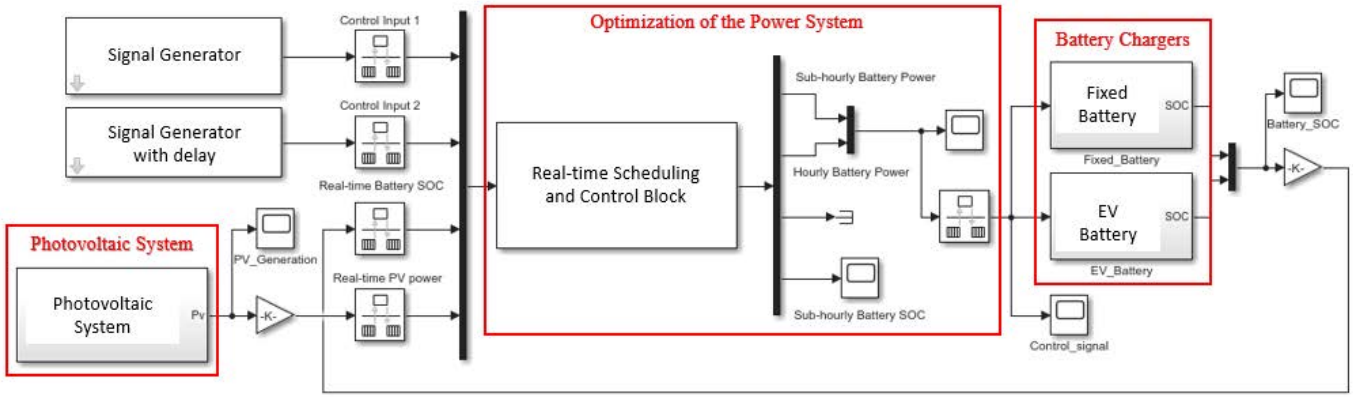

Figure 1. Matlab implemented simulation framework.

The Work is supported by Qatar National Research Fund Project "Integration of Solar Generation and Electrical Vehicles in the Smart Grid".

Global Sensitivity Analysis of Islanded Microgrid Power Flow

Kun He, Xiaoyuan Xu, Han Wang, and Zheng Yan
Department of Electrical Engineering
Shanghai Jiao Tong University, Shanghai, China

***Abstract*—With the increasing penetration of renewable energies into microgrids (MGs), the uncertainties of MG operation are more remarkable. Therefore it is necessary to evaluate the influence of random input variables on the state of systems. In this paper, a global sensitivity analysis (GSA) based on the Sobol method is proposed to evaluate the influences of uncertainties on islanded MG (IMG) power flow. First, considering the droop control of distributed generations and uncertainties of renewables and loads, an IMG probabilistic power flow model is established. Then, the Sobol method based on Monte Carlo simulation (MCS) is used to perform GSA and the Levenberg-Marquardt (LM) method is used to solve power flow. Finally, the proposed method is tested using a 33-bus IMG system, and the influences of renewable generation on power flow and frequencies are analyzed.**

***Index Terms*—Droop control, global sensitivity analysis, Levenberg-Marquardt method, microgrid, Sobol method**

I. Introduction

The uncertainty of distributed generation (DG) output is important for islanded microgrid (IMG) system operation. Sobol GSA method considers system nonlinearities and interactions of variables, and evaluates the influences of input variables based on the fractions of the output variance. The influences of renewable-based DG (RDGs) on the IMG frequency and power flow are analyzed under different droop control strategies.

II. Key Equations

A. Power flow equation of IMG

$$\begin{cases} P_{Gi} = (U_{1i} - U_i)/m_i \\ Q_{Gi} = -(\omega_1 - \omega)/n_i \end{cases}$$

$$\begin{cases} P_{Li} = P_{0i} U_i^{\alpha} \left[1 + h_{pf,i}(\omega - \omega_3)\right] \\ Q_{Li} = Q_{0i} U_i^{\beta} \left[1 + h_{qf,i}(\omega - \omega_3)\right] \end{cases} \tag{1}$$

$$\boldsymbol{F}(\boldsymbol{x}) = 0, \quad \boldsymbol{x} = (\omega, \boldsymbol{U}, \boldsymbol{\theta}) \tag{2}$$

B. High-dimensional Model Representation (HDMR)

$$f(\boldsymbol{x}) = f_0 + \sum_{i=1}^{k} f_i + \sum_{1 \le i < j \le k} f_{ij} + \ldots + f_{12\ldots k} \tag{3}$$

$$\begin{aligned} &\int_0^1 f_{m\ldots n} \mathrm{d}x_w = 0, \; m \le w \le n \\ &\int f_{i_1 \ldots i_s} f_{j_1 \ldots j_l} \mathrm{d}\boldsymbol{x} = 0, \quad (i_1, i_2, \ldots, i_s) \ne (j_1, j_2, \ldots, j_l) \end{aligned} \tag{4}$$

C. Sobol sensitivity coefficients

$$\int f^2(\boldsymbol{x}) \mathrm{d}\boldsymbol{x} - f_0^2 = \sum_{i=1}^{k} \int f_i^2 \mathrm{d}x_i + \sum_{1 \le i < j \le k} \int f_{ij}^2 \mathrm{d}x_i \mathrm{d}x_j + \ldots + \int f_{12\ldots k}^2 \mathrm{d}\boldsymbol{x} \tag{5}$$

$$\begin{aligned} &D = \int f^2(\boldsymbol{x}) \mathrm{d}\boldsymbol{x} - f_0^2, \quad D_{m\ldots n} = \int f_{m\ldots n}^2 \mathrm{d}x_m \ldots \mathrm{d}x_n \\ &S_i = D_i / D \\ &S_{Ti} = S_i + \sum_{j \ne i}^{k} S_{ij} + \ldots + S_{1\ldots i\ldots k} \end{aligned} \tag{6}$$

III. Case Studies

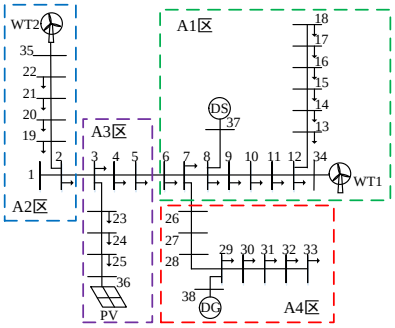

Fig. 1 Structure of the 33-bus IMG.

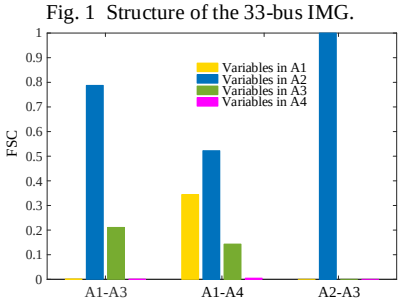

Fig. 2 FSCs of random variables with respect to power flow between different zones.

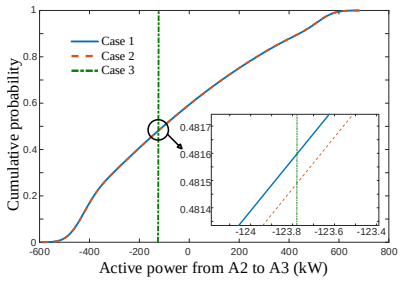

Fig. 3 Cumulative distributions of power flow for different cases.

Simultaneous Global Identification of Dynamic and Network Parameters in Transient Stability Studies

Mark K. Transtrum, Benjamin L. Francis
Dept. of Physics and Astronomy
Brigham Young University, UT, USA
mktranstrum@byu.edu

Andrija T. Sarić [1], Aleksandar M. Stanković [2]
[1] Dept. of Power, Electronics and Com. Engineering
[1] University of Novi Sad, Faculty of Technical Sciences, Serbia
[2] Dept. of Electrical and Computer Engineering
[2] Tufts University, Medford, MA, USA
[1] asaric@uns.ac.rs; [2] astankov@ece.tufts.edu

***Abstract*—This paper describes a global identification procedure for dynamic power system models in the form of differential and algebraic equations. Power system models have a number of features that makes their improvement challenging – they are multi-level, multi-user and multi-physics. Not surprisingly, they are nonlinear and time varying, both in terms of states (memory variables) and parameters; and discrete structures, such as graphs, are strongly blended with continuous dynamics, resulting in network dynamics. Transient stability models are used as a prototypical example. Our method is based on information geometry, and uses advances in computational differential geometry to characterize high-dimensional manifolds in the space of measurements. The results are illustrated on the case of a IEEE 14-bus test system with 58 parameters in our realization.**

***Index Terms*— System Identification, Global Optimization, Parameter Estimation.**

I. Introduction

We use an IEEE 14-bus test system as our dynamical model. The system is initially in steady state and is perturbed at $t = 0$, and the subsequent transient is observed with measurements from all generators and buses in the system. We use a global system identification procedure known as the Manifold Boundary Approximation Method (MBAM) to simultaneously reduce the dynamical model and estimate network and component parameters, given these observations. In addition, we use sensitivity analysis to examine the possibility of additional reduction using partial response matching.

TABLE I. Reduction Steps.

Step	Number of parameters	Reduced parameter	Reduced element	Type
1	57	$x''_d \to x'_d$	Bus 6	
2	56	$T''_{d0} \to 0$	Bus 6	Singular Limit
3	55	$B_{2,5} \to 0$	Line 2-5	Network Reduction
4	54	$x''_q \to x'_q$	Bus 8	
5	53	$T''_{q0} \to 0$	Bus 8	Singular Limit
6	52	$x''_q \to x'_q$	Bus 6	
7	51	$T''_{q0} \to 0$	Bus 6	Singular Limit
8	50	$x'_d \to x_d$	Bus 1	
9	49	$B_{6,13} \to 0$	Line 6-13	Network Reduction
10	48	$x''_d \to x'_d$	Bus 8	
11	47	$T''_{d0} \to 0$	Bus 8	Singular Limit
12	46	$x'_d \to x_d$	Bus 6	
13	45	$T'_{d0} \to 0$	Bus 6	Singular Limit

I. Key Figures

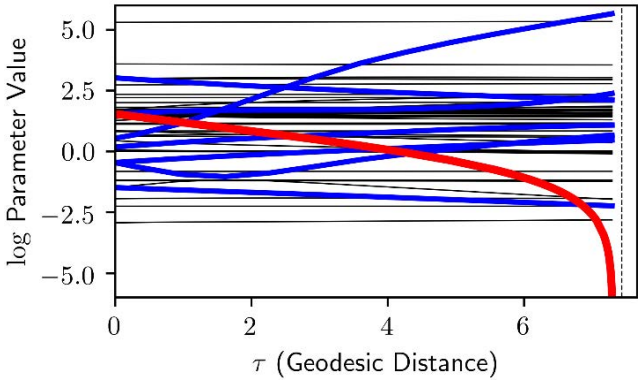

Figure 1. Parameter values along a geodesic in step 2. Here, $T''_{d0} \to 0$ in Bus 6 (i.e., its log value goes to negative infinity in red) corresponding to a singular perturbation that removes the d-axis subtransient. In order to compensate for this approximation, several other parameter values change (blue lines), while most other parameter values are constant (black curves).

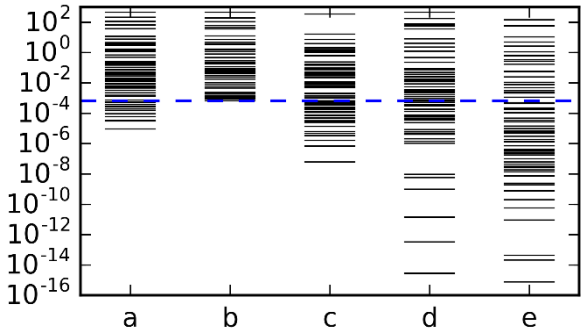

Figure 2. Eigenvalue spectra of the FIM, shown for (a) the full model with all observations, (b) the reduced model with all observations, (c)-(e) the full model with three types of partial observations. The dashed line marks the smallest eigenvalue of the reduced model.

II. Key Results

Reduction from 58 to 45 parameters was achieved for the full set of system observations. The 13 parameters removed from the model cannot be identified using these observations. Conversely, these parameters are unimportant for the observed system behavior. Fig. 2 shows that additional reduction of the model could be achieved by observing only part of the system.

Comparative Analysis of Hybrid Bipolar HVDC and FACTS Performance for Improving Commutation Failure Immunity

Zicong Zhang, Kisuk Kim, Gilsoo Jang
Department of Electrical Engineering, Korea University, Seoul, Korea
zicongyouyou@korea.ac.kr, kks1213@korea.ac.kr, gjang@korea.ac.kr

***Abstract*— This article will discuss a new transmission method that is different from traditional high-voltage direct current(HVDC) transmission. The new way will use Hybrid bipolar HVDC to compare with the flexible AC transmission systems (FACTS) which based on Real Time Digital simulator(RTDS). An interconnected power system includes generators, hybrid bipolar HVDC, FACTS and variable loads. Experiments are needed to compare the commutation failure immunity index(CFII) of the system under different conditions and to make a delicate analysis of the commutation failure and the change of the extinction angle at the time of the faults. Single phase inductive ground fault will be used respectively on the rectifier side and the inverter side. At the same time, its comparative analysis of the transient states and fault recovery time of each line for faults. Further analysis of the hybrid bipolar HVDC and FACTS for evaluating the performance of the transmission lines.**

Keywords— HVDC; Hybrid bipolar HVDC; FACTS; Commutation failure immunity index(CFII); RTDS

I. INTRODUCTION

This paper will compare the hybrid bipolar HVDC with bipolar LCC-HVDC which connect with FACTS. In the past, the LCC-HVDC transmission mode needs to take into account the commutation failure. FACTS and VSC-HVDC will be used separately to connect with LCC-HVDC which specific composition shown in Figure 1. VSC-HVDC will effectively provide the required commutation voltage for LCC-HVDC commutation, and when a fault occurs, it can shorten the fault recovery time by using the black start. FACTS can effectively reduce the impedance of AC system and improve the robustness of AC system. CFII is a brand new important indicator for evaluating that LCC-HVDC can avoid commutation failure during operation. CFII represents the transient characteristics of robustness of LCC-HVDC significantly and more directly than calculates the changing of voltage drop(ΔV) when the mathematical models of the power system become more complex than before. The larger value of CFII meant the lager level of the fault that can be sustained without the commutation failure. CFII equation is shown as (1):

$$\text{CFII} = \frac{Critical\ Fault\ MVA}{P_{dc}} \times 100 = \frac{V_{ac}^2}{\omega L_{min} P_{dc}} \times 100 \quad (1)$$

where, L_{min} is the lowest inductive fault impedance. Therefore, the CFII is the critical fault level that does not cause a commutation failure, expressed as a percentage of the HVDC rated power. Because of the time step of RTDS is very shorter(about 2us), they can provide better performance when analyzing system transient states.

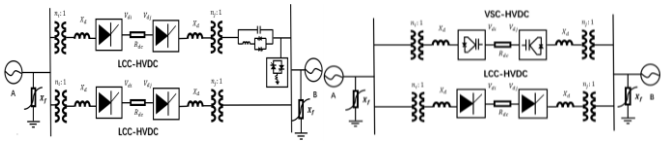

(a) (b)

Figure 1. (a)Traditional HVDC System with FACTS (b) Hybrid Bipolar HVDC System

II. KEY RESULT

A. Traditional HVDC System with FACTS

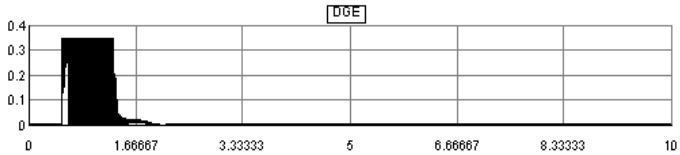

Figure2. Traditional HVDC with FACTS extinction angle when the fault occurs at the rectifier side, which the SCR of the rectifier is 1.77

B. Hybrid Bipolar HVDC System

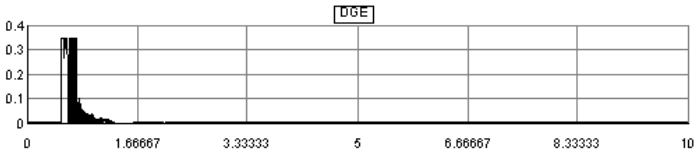

Figure3. Hybrid Bipolar HVDC extinction angle when the fault occurs at the rectifier side, which the SCR of the rectifier is 1.77

C. Talbe of Cases

Case	CFII(%)	Recovery Time
Hybrid HVDC	47.51	0.1667s
HVDC with FACTS	38.62	0.3114s

Impact of Dynamic Load Model on Short-Term Voltage Stability of Korea Power System

Jaemin Moon, *Student Member*, *IEEE*, Jae-kyeung Kim, *Member*, *IEEE*, Kyeon Hur, *Senior Member*, *IEEE*
School of Electrical and Electronic Engineering
Yonsei University
Seoul, Korea
Email: yonseimoon@gmail.com, JK.Kim@yonsei.ac.kr, khur@yonsei.ac.kr

***Abstract*—This paper study structural and regional impact of dynamic load model on short-term voltage stability. Analyses imply the needs of developed models structure changed from ZIP load model which Korea power system operator conventionally use and precise modeling of loads near the accident during contingency analysis. For analyzing structural impact of load model, we apply complex load model and ZIP load model in Korea power system, and then compare those results. Also, we analyze regional impact of load model by comparing results which apply complex load model for different region of Korea power system in each simulation.**

Keywords—dynamic load model, structural impact, regional impact

I. KEY FIGURE

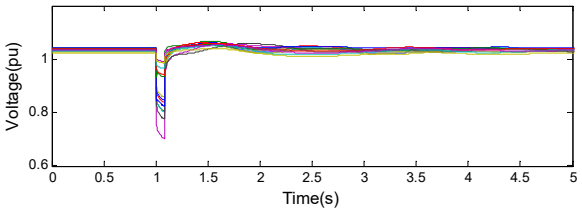

(a) ZIP load model

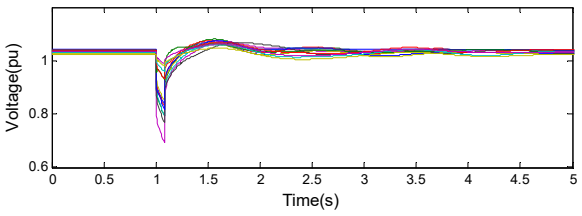

(b) Large motor: 10%, Small motor: 40%, Exponential: 50%

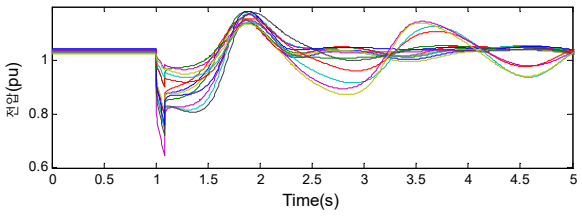

(c) Large motor: 20%, Small motor: 80%

Figure 1. Bus voltage with different load model structure

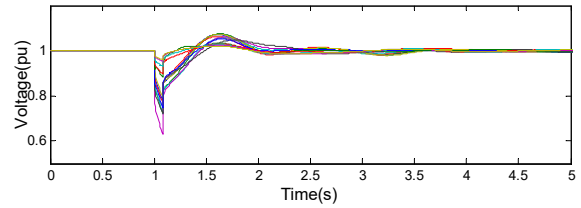

(a) Region 1

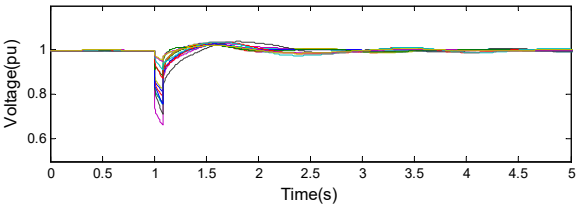

(b) Region 2

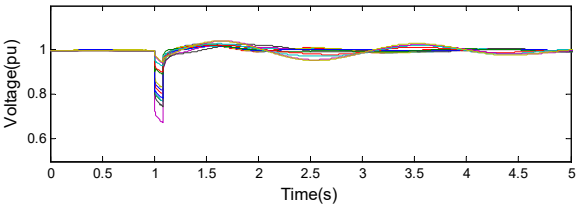

(c) Region 3

Figure 2. Bus voltage with different region applied complex load model

Impact of Load Step Change on Thermal and Voltage Stability Limits of Overhead Transmission Lines

Mahbubur Rahman, *Student Member, IEEE*; Valentina Cecchi, *Member, IEEE*
Energy Production & Infrastructure Center
University of North Carolina at Charlotte

***Abstract*– The power handling capability of a transmission line is mainly constrained by thermal and voltage stability limits. When there is a change in system load, the line reaches a new steady-state conductor temperature after a certain period of time unless it violates the thermal and voltage stability limits. This paper investigates the impact of a step change in system load on both limiting factors and proposes an approach to determine the critical limiting factor and corresponding time during that change. For higher accuracy, the change in line current and resultant conductor temperature, as well as the effect that a variation in conductor temperature has on line resistance are taken into account. Noticeable differences were found on the line's power transfer limiting factor under different levels of load step change. Moreover, the impact line length on the power transfer limiting factors with respect to load changes is also studied in this work.**

I. Poster Overview

The motivation of the work comes from the fact that variation of system load affects both thermal and voltage stability conditions of a transmission line. Given a change in system load, the line current changes due to two factors: 1. the change in load itself, and 2. the change in line impedance due to the change in conductor temperature (T_c) caused by the change in load. The step change in line current introduces a gradual change in line T_c, which in impacts the line impedance. This variation in line impedance effects the current flowing through the line to serve the new system load. This continuous variation in line impedance and current have a direct effect on thermal and voltage stability limits of transmission lines.

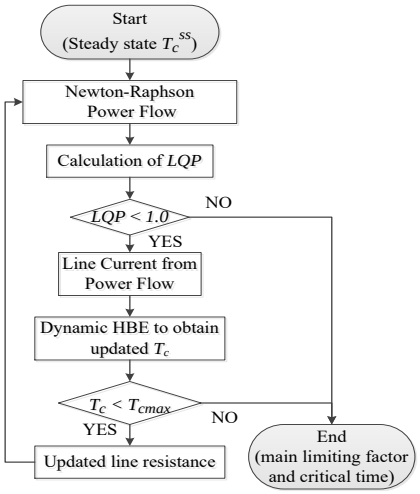

Figure 1: Flowchart to determine critical factor and critical time

This work was supported in part by the National Science Foundation award #1509681 "A Novel Electric Power Line Modeling Approach: Coupling of Dynamic Line Ratings with Temperature-Dependent Line Model Structures."

In this paper, a methodology, as in Fig. 1, is proposed to determine the critical limiting factor and the corresponding time to reach it during a load step change. Line stability factor, *LQP* [1] is used to determine the voltage stability index of different lines of a system. The iterative process continues until the line under consideration reaches: i. the maximum allowable T_c, ii) a new steady state T_c, with $LQP < 1.0$, iii) the *LQP* index of 1.0.

The proposed method was applied on a two bus system with a 200 mi long line under specific ambient conditions. When the system load was increased by three different percentages from the steady state, three different outcomes are observed as in Fig. 2. Fig. 3 shows the impact of the line lengths on the power transfer limiting factors of the transmission line.

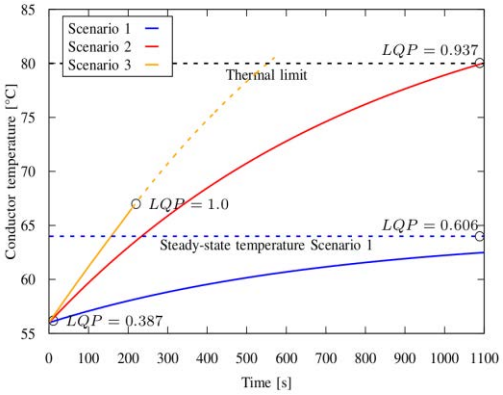

Figure 2: Conductor temperature and voltage stability index (LQP) over time for different scenerios

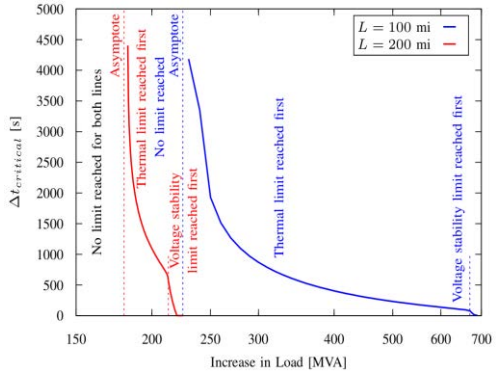

Figure 3: Critical time over increase in load for two different line lengths for Hawk conductor

References

[1] A. Mohamed and G. B. Jasmon, "A new clustering technique for power system voltage stability analysis," *Electric Machines & Power Systems*, vol. 23, no. 4, pp. 389–403, 1995.

A Dynamic Inverse-Time Overcurrent Relay Model for Overload Analysis with Varying Overcurrents

Jianan Liu
Department of Electrical & Computer Engineering
University of Nebraska-Lincoln
Lincoln, NE 68588-0511 USA
jianan1991@huskers.unl.edu

Wei Qiao
Department of Electrical & Computer Engineering
University of Nebraska-Lincoln
Lincoln, NE 68588-0511 USA
wqiao3@unl.edu

***Abstract*—Most of the past overload cascading failure analyses either ignored the effect of inverse-time overcurrent relays with the assumption that transmission/distribution lines will trip once overloaded, or assumed static inverse-time characteristics of the inverse-time overcurrent relays even under varying overcurrent conditions. This work presents a dynamic inverse-time overcurrent relay model. The inverse-time characteristics of overcurrent relays corresponding to the current overload states are derived according to the proposed dynamic inverse-time overcurrent relay model. The proposed dynamic inverse-time overcurrent relay model can be applied to analyze overload cascading failures in power systems, such as determining the trip sequence of transmission/distribution lines when an overload cascading failure occurs.**

I. Introduction

Inverse-time overcurrent relays have been widely installed in North America in the form of electromechanical relays and then microprocessor relays. In 1996, an IEEE standard [1] was issued, which defined the inverse-time characteristics for overcurrent relays and provided an integral equation for microprocessor overcurrent relays to emulate their dynamics. However, most of the overload cascading failure analysis did not take inverse-time overcurrent relays into consideration, thus assuming that transmission/distribution lines will trip once overloaded [2]. The static inverse-time overcurrent relay model, which reveals the reciprocal characteristics between the relay operating time and input overcurrent, has been adopted in a few papers [3]. However, the static model is not accurate to calculate the relay operating time under varying input overcurrent conditions. In an overload cascading failure procedure, contingencies will occur continuously, which will result in redistribution of power flows and, thus, variation of the relay input overcurrent. A dynamic inverse-time overcurrent relay model can be used to predict the relay operating time under varying overcurrent conditions. Furthermore, it can be used to determine the trip sequence of transmission/distribution lines, which reveals how the cascading failure spreads along with time.

II. Key Equations and Case Study

A. Static Inverse-time Overcurrent Relay Model

$$t = TD(\frac{A}{M^p - 1} + B) \tag{1}$$

where TD is the time dial setting, A is a constant to determine the inverse type, B is a constant to simulate saturation, M is the ratio of the input current to the pickup current, p is a constant to simulate specific characteristics, and t is the time delay for relay contacts to close when $M > 1$.

B. Dynamic Inverse-time Overcurrent Relay Model

$$t_n = TD(\frac{A_n}{M^p - 1} + B_n) \tag{2}$$

$$A_n = A\prod_{i=1}^{n-1}(1 - \frac{t_i}{t_i^{max}}) \tag{3}$$

$$B_n = B\prod_{i=1}^{n-1}(1 - \frac{t_i}{t_i^{max}}) \tag{4}$$

where A_n and B_n are the coefficients in the n_{th} overcurrent states which depend on the previous states, t_i is the actual time elapsed during the i_{th} state, t_i^{max} and t_n are the time delays for relay contacts to close during the i_{th} and n_{th} state, respectively.

C. Case Study

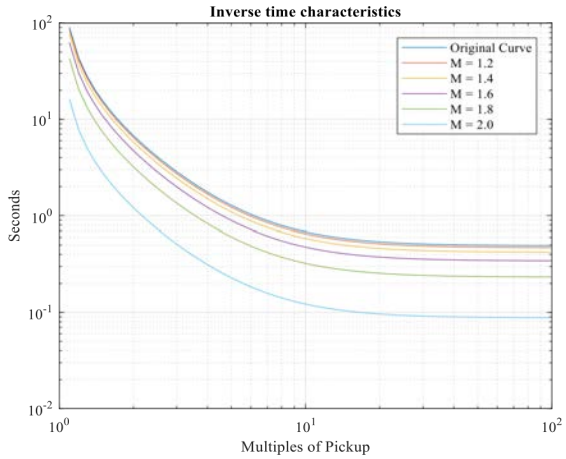

Fig. 1. Dynamic inverse time characteristics of an overcurrent relay when M increases from 1 to 2 with a step of 0.2 every two seconds.

In Fig. 1, the curves with $M = 1.2$ and $M = 1.4$ correspond to the characteristics after the input overcurrent has held 1.2 times of the pickup value for two seconds and 1.4 times for another two seconds, respectively. The last curve with $M = 2.0$ corresponds to the present overcurrent state. By using the $M = 2.0$ curve, it is easy to predict the relay's operating time after five varying overcurrents.

References

[1] *IEEE Standard Inverse-Time Characteristic Equations for Overcurrent Relays*, IEEE Standard C37.112, 1996.
[2] B.A. Carreras, V.E. Lynch, and M.L. Sachtjen, "Modeling blackout dynamics in power transmission networks with simple structure," *Proc. IEEE International Conference on System Sciences*, Jan. 2001, pp. 1-9.
[3] Y. Cai, Y. Cao, Y. Li, T. Huang, and B. Zhou, "Cascading failure analysis considering interaction between power grids and communication networks," *IEEE Trans. Smart Grid*, vol. 7, no. 1, pp. 530-538, Jan. 2016.

A Novel MILP-Based Method of Optimal Energy Flow in Gas -electricity System

Tianhao Liu [1], *Student Member, IEEE*
1. Department of Electrical and Electronic Engineering
The University of Hong Kong, Hong Kong, China

Yufeng Guo [2], *Member, IEEE*
2. School of electrical engineering and automation,
Harbin Institute of Technology, China

Abstract—This poster proposes a novel method to calculate the optimal energy flow of gas-electricity system. Because of nonconvex and nonlinear properties of gas transmission lines, the optimal problem of gas-electricity system is difficult to solve. To tackle with this problem, one-dimensional piecewise linear approximation method is proposed to reformulate natural gas transmission constraints. Accordingly, the optimal model of gas - electricity system is reformed as a mixed integer linear programming (MILP) problem. Compared with the nonlinear method, the proposed method can be solved by existing optimization techniques, which can be easily applied in optimal operation and planning of multiple energy system. The proposed method is verified by a six-bus power system with a seven-node gas system and a 118-bus power system with a fourteen-node gas system. The tests show that the proposed method can reduce computation time with a relatively precise result.

Keywords—MILP; gas-electricity system; optimal operation; piecewise linear approximation method

I. INTRODUCTION

The fast and accurate calculation of gas-electricity model is essential for optimal operation and planning of gas-electricity system. Previous works provided nonlinear programming method or mixed integer nonlinear programming method. These methods don't have the general technique and the optimum solution can't be guaranteed, which can only be effective in small scale model. When considering nonlinear and nonconvex characteristics of large-scale gas-electricity system, the method is not useful. The contribution of this paper is providing a one-dimensional piecewise linear approximation method, which can compute fast as well as accurate. The proposed method is effective in large-scale system.

II. THE PROPOSED METHODS

The objective function of gas-electricity model:

$$TC = \sum_{g,t}(b_g P_{g,t} + c_g)\lambda_g + \sum_{n,t} sd_{n,t}\lambda_n + \sum_{i,t} VOLL * l_{shi,t} \quad (1)$$

Where, $P_{g,t}$ is power generation at bus g and time t. $sd_{n,t}$ is gas demand at node n and time t. $l_{shi,t}$ is Load shedding at bus i and time t. b_g and c_g are the coefficients of power generation function. λ_g is contract gas or coal price at bus g. λ_n is contract gas price at node n. $VOLL$ is the price of load shedding.

a) Power transmission constraints

$$\sum_{g\in\Omega_G^i} P_{g,t} + l_{shi,t} - L_{i,t} = \sum_{j\in\Omega_l^i} P_{ij,t} \quad (2)$$

$$P_{ij,t} = (\delta_{i,t} - \delta_{j,t}) / X \quad (3)$$

$$-P_{ij}^{\max} \le P_{ij,t} \le P_{ij}^{\max}, P_g^{\min} \le P_{g,t} \le P_g^{\max}, 0 \le l_{shi,t} \le L_{i,t} \quad (4)$$

$$P_{g,t} - P_{g,t-1} \le RU_g, P_{g,t-1} - P_{g,t} \le RD_g \quad (5)$$

Where, $\delta_{i,t}$ is the angle of bus i and time t. $L_{i,t}$ is electricity load at bus i. RU_g / RU_d is ramp up/down limit of generation g.

b) Gas transmission constraints:

$$\sum_{m\in\Omega_i^n} f_{mn,t} = sg_{n,t} - sd_{n,t} - \sum_{g\in\Omega_n^{gas}} (b_g P_{g,t} + c_g) \quad (6)$$

$$\mathrm{sgn}(p_{m,t}, p_{n,t}) f_{mn,t}^2 = C_{mn}(p_{m,t} - p_{n,t}) \quad (7)$$

The left side of Eq (7). can be reformulated as:

$$f_{mn,1,t}^2 + \sum_{k=1}^{N-1}(f_{mn,k+1,t}^2 - f_{mn,k,t}^2)\delta_{mn,k,t} = C_{mn}(p_{m,t} - p_{n,t}) \quad (8)$$

$$f_{mn,t} = f_{mn,1,t} + \sum_{k=1}^{N-1}(f_{mn,k+1,t} - f_{mn,k,t})\delta_{mn,k,t} \quad (9)$$

$$0 \le \delta_{k,t} \le 1, \delta_{k+1,t} \le \eta_{k,t}, \eta_{k,t} \le \delta_{k,t} \quad (10)$$

Compressor model: $p_{m,t} \le R_c p_{n,t}$, $0 \le f_c \le F_c^{\max}$ (11)

$$sg_{n,t}^{\min} \le sg_{n,t} \le sg_{n,t}^{\max}, p_n^{\min} \le p_{n,t} \le p_n^{\max} \quad (12)$$

Where, Ω_n^{gas} is set of gas fired generation connect to node n. $sg_{n,t}$ is the gas supply. $p_{n,t}$ is the square of pressure at node n and time t. C_{mn} is gas flow transmission parameter. $\delta_{mn,k,t}$ is position in the segment of transmission mn at time t. η_k is binary variable. f_c is gas flow through the compressor. R_c is the square of ratio of compressor, $F_c^{\max}$ is the upper limitation transmission of the compressor. By using reformation method mentioned in Eq (7). The NLP model is changed to MILP model. A typical six-bus power system with seven-node gas transmission system and a IEEE 118-bus power system with a fourteen-node gas system [1] are taken as examples. We calculate the model by using nonlinear method and one-dimensional piecewise linear approximation method. The proposed method is solved by MILP solver CPLEX and NLP model is solved by the NLP solvers CONOPT on GAMS, respectively.

III. KEY RESULTS

The segments of MILP model is 20. From the table, it can be seen that in *a)*, the proposed method use 60% computation time with the same accuracy. In *b)*, the proposed method can solve the problem in 3.372s, while NLP can't solve.

a) A typical six-bus power system with seven-node gas transmission system

Models	Methods	Times (s)	TC ($)
NLP	CONOPT	0.325	$1369744.54
MILP	CPLEX	0.187	$1369744.54

b) A IEEE 118-bus power system with a fourteen-node gas system

Models	Methods	Times (s)	TC ($)
NLP	CONOPT	NA	NA
MILP	CPLEX	3.372	$7472695.2457

This work was supported by the Key R&D Project of China under grant number: 2016YFB0901903.

Reference

[1] http://motor.ece.iit.edu/data/OPF_MCES/

Modeling of Geomagnetically Induced Currents in the Power Grid Using Time-Domain Simulation

Hemanth Kumar Vemprala, Student Member, IEEE and Dr. Bruce A. Mork, Fellow, IEEE
Dept of Electrical and Computer Engineering, Michigan Technological University, Houghton, MI.
Email: hvempral@mtu.edu, bamork@mtu.edu

***Abstract*— A GIC/GMD event could produce a large scale disturbance in the power network and is categorized as high-impact, low-frequency (HILF) event. With long and crowded HV transmission corridors and unavoidable solar storms impending, a wide-spread flow of GIC could produce undesirable effects. GIC has the ability to knock the system out of normal operating conditions and has occurred in the past. At present the system impact and equipment impact assessments due to GMD are analyzed largely by a steady-state phasor analysis which uses a snapshot of geomagnetic storm at a particular event and a modified load-flow engine to emulate GIC at the neutrals. These ill-effects are not completely captured in phasor domain simulation due to absence of nonlinearity, frequency dependency, and partly also due to over-simplified models.**

The time-domain simulation mitigates all these problems and provides a scope for user-defined modeling depth based on the study requirements. In this work, the time series of geoelectric field values are dynamically computed in ATP MODELS using GMD event data and using piecewise-layered earth model. The proposed modeling approach of GIC aids in studying the GMD vulnerability assessment in the time domain. Further, this poster illustrates the modeling approaches and presents a simulation case using a benchmark of 1989 GMD event (TPL-007-1) that caused the Hydro Quebec blackout. The system impact assessment, mainly in the increased transformer VAr losses and half-cycle saturations, are researched and presented. As a path forward, this modeling approach shall be extended to a real-time simulation tool envisioned to monitor the GMD event and effects on the network.

I. Proposed Framework

The overview of the geomagnetic induced current calculation in ATP is demonstrated in Fig. 1. Fig. 2 presents the 20 bus IEEE benchmark case modeled in ATP.

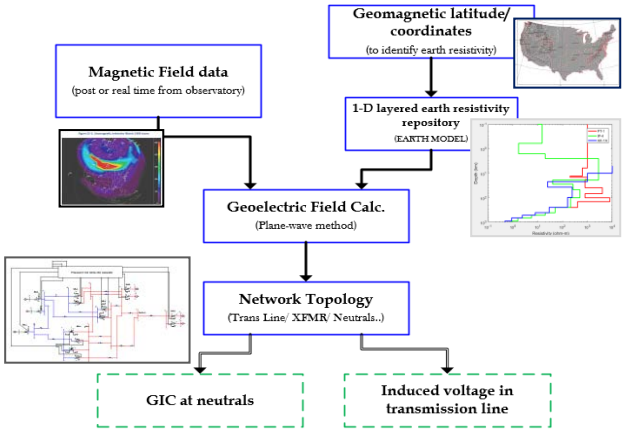

Fig. 1. Concept of GIC calculation

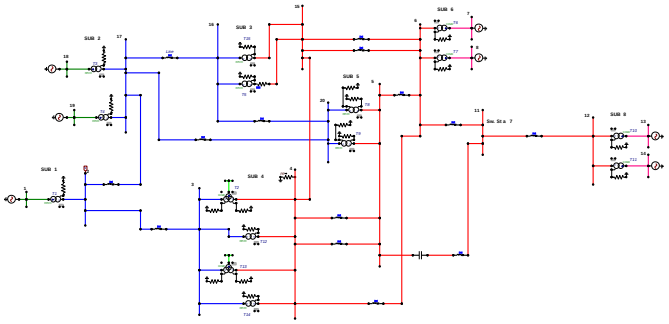

Fig. 2. IEEE 20-bus benchmark case for GIC study modeled in EMTP-ATP

II. Key Simulation Results

The Fig. 3 presents the typical half-cycle saturation effect and a quasi-dc current flow.

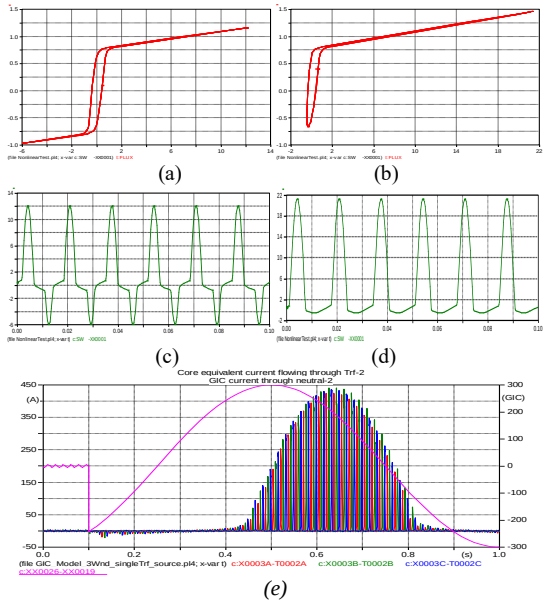

(e)

Fig. 3. Typical half-cycle saturation on power transformers (a) flux vs I characteristics for a power transformer with GIC = 33.33 amps/ph. (b) transformer characteristics for GIC current of 67 amps/ph. (c) & (d) half-cycle saturation currents with GIC of 100 and 200 amps through its neutral respectively. (e) Line current flows into transformer with GIC of time varying 0.01 Hz, 100 A (Ipeak) through its neutrals

References

[1] North American Electric Reliability Council (NERC), Application Guide, "Computing Geomagnetically-Induced Current in the Bulk-Power system," Dec. 2013.

[2] R. Horton, D. Boteler, T. J. Overbye, R. Pirjola and R. C. Dugan, "A Test Case for the Calculation of Geomagnetically Induced Currents," in IEEE Transactions on Power Delivery, vol. 27, no. 4, pp. 2368-2373, Oct. 2012.

Optimization of Electric Vehicle Aggregation in Energy and Balancing Markets in the Nordics

Lars Herre, *Student Member, IEEE,* Jacob Dalton, and Lennart Söder, *Member, IEEE*

***Abstract*—Aggregators of flexible residential loads, such as electric vehicles can enter the electricity market and bid in both energy and ancillary services markets. This research provides an optimal bidding strategy for an aggregator of electric vehicles that places bids in the energy market and in the ancillary services market. In this analysis we model the bidding strategy of a risk averse aggregator and include uncertainty from prices and vehicle availability. The results show the separated profits from ancillary services and costs from the energy market. We conclude with an estimation of the value of aggregation and the potential in the Nordic electricity market.**

***Index Terms*—electricity market, stochastic optimization, electric vehicle aggregation.**

I. Key Issues

THE electrification of private transport is a technology of growing interest that can provide flexibility to the power system if adequately utilized. Electric vehicles (EV) are can be considered as temporary energy storages with availability constraints. If aggregated in sufficient numbers or combined with other assets they can fulfill the minimum bid size of specific markets.

An aggregator of EVs can enter the electricity market and bid in both energy and balancing markets. This research provides an optimal bidding strategy for an aggregator of electric vehicles that places bids in the energy and balancing markets in the Nordic countries. In this analysis we consider uncertainty ($\omega \in \Omega$) from prices and vehicle utilization and model risk averse aggregator that aims to maximize its profits in Eq. (1).

$$\max. \quad (1-\beta)\cdot E\left[\mathbf{\Pi}_\omega\right] + \beta \cdot \text{CVaR} \tag{1}$$

$$\text{s.t.} \quad \mathbf{\Pi}_\omega = \pi_\omega \sum_\omega \sum_t \Pi_t^R - \Pi_t^E - \Pi_{t,\omega}^C - \Pi_{t,\omega}^P \quad \forall t,\omega \tag{2}$$

$$\Pi_t^R = \sum_t [\lambda_t^{DA,R} R_t^{DA}] \quad \forall t \tag{3}$$

$$\Pi_t^E = \sum_t [\lambda_t^{DA,E} E_t^{DA}] \quad \forall t \tag{4}$$

$$\Pi_{t,\omega}^C = \pi_\omega \sum_\omega \sum_t [\lambda_{t,\omega}^{RT,E} \triangle E_{t,\omega}] \quad \forall t,\omega \tag{5}$$

$$\Pi_{t,\omega}^P = \pi_\omega \sum_\omega \sum_t M \cdot \triangle E_{t,\omega} \quad \forall t,\omega \tag{6}$$

$$\triangle E_{t,\omega} = E_{t,\omega}^{RT} - E_t^{DA} \quad \forall t,\omega \tag{7}$$

$$\text{EV fleet power/energy constraintss on } E_{t,\omega}^{RT} \quad \forall t,\omega \tag{8}$$

L. Herre, J. Dalton and L. Söder are with the Department of Electrical Power & Energy Systems, KTH Royal Institute of Technology, Stockholm, Sweden (e-mail: see http://www.kth.se/profile/lherre).

The constraints are summarized in Eq. (2) - (8). The profit ($\mathbf{\Pi}$) is comprised of the revenue in the day-ahead (DA) balancing market (Π^R), cost from day-ahead energy purchase (Π^E), cost from real-time (RT) energy consumption (Π^C) and cost penalties for deviation of the RT consumption from the DA purchase (Π^E) in hour t and scenario ω.

The DA balancing price is $\lambda_t^{DA,R}$, the energy prices are $\lambda_t^{DA,E}$ and $\lambda_{t,\omega}^{RT,E}$, and the penalty is M. The probability of scenario ω is given by π_ω.

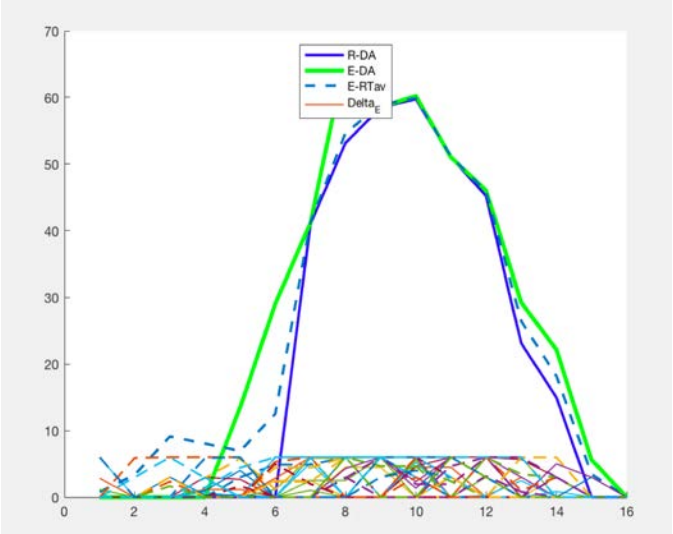

Fig. 1. DA energy bid E^{DA}, real-time energy consumption E^{RT} averaged over all scenarios and DA regulation bid R^{DA} over a 16 hour period. ΔE is the deviation between DA energy bid and real-time consumption in different scenarios.

An illustration the EV aggregator's bidding strategy for a winter day is shown in Fig. 1. It can be seen that the consumption is largely shifted towards the hours where the balancing market prices and the respective bids are high.

II. Key Findings

We present a portfolio optimization model for an aggregator of electric vehicles, that is bidding in two markets: an energy market (day-ahead and real-time) and a balancing market (FCR: frequency containment reserves). We apply this model to a risk averse aggregator of 1000 electric vehicles in the Nordic electricity market.

The results demonstrate the applicability of the proposed optimization problem formulation. We also explore the economic potential for an aggregator in the Nordic electricity market. Further, we investigate the value of aggregation and the conditional value at risk CVaR.

Building Very Large Synthetic Power Grids

Adam B. Birchfield, *Student Member, IEEE* and, Thomas J. Overbye, *Fellow, IEEE*
Department of Electrical and Computer Engineering
Texas A&M University
College Station, TX, USA

***Abstract*—Power systems research can benefit from non-confidential, fictitious power systems datasets that match characteristics and statistics of real grids. This poster introduces the scaling of the grid synthesis approach to a 70,000 bus system. The approach extends previous work in placing substations with load and generation, dispatching the system economically, and iteratively building the dc-solvable power system with a transmission planning algorithm. Then the system can be augmented with reactive power compensation devices, using an iterative reactive power planning algorithm, to obtain a solvable ac power flow solution. The resulting 70,000 bus case is able to be fully shared.**

Keywords—synthetic power grids, power system analysis

I. Scaling the Synthetic Creation Algorithms to Very Large Grids

For creating fictitious realistic power system cases, previous work including [1]-[3] describe a methodology that starts with public data on population and generators. A synthetic transmission system is designed using an automated approach by first clustering substations and connecting them internally, then iteratively adding and removing transmission lines to meet a variety of statistical metrics. Geographic constraints are key, as the algorithms use the Delaunay triangulation, geographic length, and geographic feature matching to capture realistic constraints [1]-[2]. In addition, power flow constraints are met in avoiding overloading lines in base and contingency conditions.

Once the transmission network is in place, an iterative reactive power planning algorithm builds on [3]. This process augments the system with voltage control devices such as shunt capacitors and reactors to obtain a feasible ac power flow solution with acceptable voltage characteristics.

II. Example 70,000 bus case

The above processes are demonstrated in at 70,000 bus example case. This case has the geographic footprint of the U.S. portion of the eastern interconnect, a region covering all or part of 39 states, serving about 600 GW of peak load with over 10,000 generating units. Nominal voltage levels of 69 kV through 765 kV are modeled in the system, with the approach to handling the multiple overlapping networks based on [2]. The single-line diagram of the case is shown in Fig. 1.

A major impact of this work is that publicly available test cases can be used to spur power systems research and innovation. As one of the largest realistic power system test cases published, this 70,000 bus system is particularly useful for testing scalability of research algorithms and the suitability of ideas for large-scale actual power system models. Because the systems are geographically-based, they are useful for visualization research, research on geomagnetically induced current, and coupling with actual geographically-based data. A variety of engineering design and practice is found in this system, with a diversity of voltage levels, modeling assumptions, generation mixes, and load density patterns across a wide geographic footprint. With much actual power system data subject to strict confidentiality concerns, synthetic grids offer researchers and innovators additional platforms for testing and demonstration.

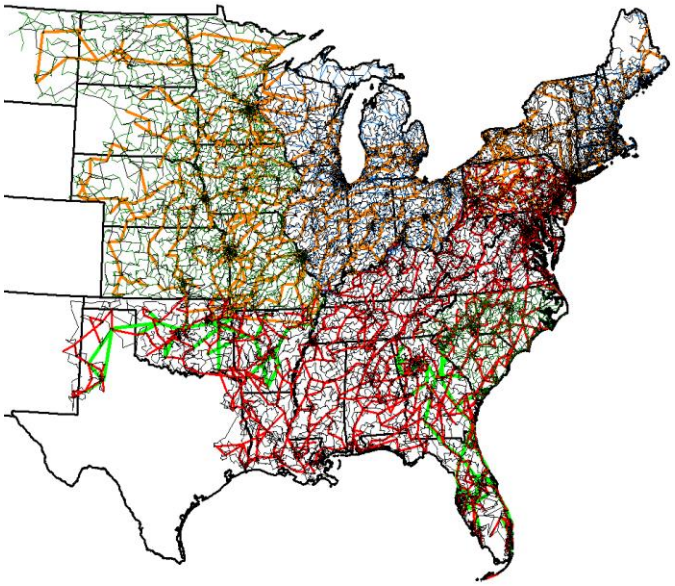

Fig. 1. One-line diagram of the 70,000-bus test case. This system was built with as synthetic methodology, is fictitious, and does not represent the actual power grid in this location.

References

[1] A. B. Birchfield, T. Xu, K. M. Gegner, K. S. Shetye and T. J. Overbye, "Grid structural characteristics as validation criteria for synthetic networks," *IEEE Transactions on Power Systems*, vol. 32, no. 4, pp. 3258-3265, July 2017.

[2] A. B. Birchfield, T. Xu, K. S. Shetye, and T. J. Overbye, "Building synthetic power transmission networks of many voltage levels, spanning multiple areas," *2018 51st Hawaii International Conference on System Sciences,* January 2018.

[3] A. B. Birchfield, T. Xu, and T. J. Overbye, "Power flow convergence and reactive power planning in the creation of large synthetic power grids," *IEEE Transactions on Power Systems,* to be published, 2018.

Initial Work on Formalizing the Multiple-Time Scale Structure of Power System Models

Matthew Hin
Center for Applied Mathematics
Cornell University
Ithaca, NY, USA
mfh72@cornell.edu

***Abstract*—Power system models are incorporating more and more quantities that evolve on vastly different time-scales. A common approach is to perform a hybrid simulation of a transient stability model and an electromagnetic model. The work here proposes a multiple time-scale formalism for interfacing these two models and analyzes the framework numerically using two power systems: a 3-bus test grid and the 2224-bus Great Britain transmission network.**

***Index Terms*—multiple time scales, power system dynamics, electromagnetic transients**

I. Formal Model

To illustrate the hierarchy of subsystems, we can make explicit the time scale separation between mechanical, electromechanical, and electromagnetic states form a 3-time scale system:

$$\dot{x} = \epsilon f(x, y, z), \tag{1}$$
$$\dot{y} = g(x, y, z), \tag{2}$$
$$\eta \dot{z} = h(x, y, z). \tag{3}$$

In this full system, we have written the model with respect to the time scale relevant to electromechanical states and introduce two parameters ϵ and $0 < \eta < 1$. The former represents the time-scale separation between the slow mechanical states x and fast electromechanical states y, while the latter represents the separation between y and the electromagnetic transient states z. We also derive a corresponding hierarchy of slow, fast, and transient subsystems. We obtain the slow subsystem by rescaling time to the slowest time-scale $\tau = \epsilon t$ and considering the limit $\epsilon \to 0$:

$$x' = f(x, y, z), \tag{4}$$
$$0 = g(x, y, z), \tag{5}$$
$$0 = h(x, y, z). \tag{6}$$

This slow subsystem has many similarities to simple swing equations, but does not suffer from excessive model reductions as the electromechanical states are still constraining the evolution of the mechanical states. We obtain the fast subsystem by returning to (**??**) and considering the limit $\epsilon \to 0$:

$$\dot{x} = 0, \tag{7}$$
$$\dot{y} = g(x, y, z), \tag{8}$$
$$0 = h(x, y, z). \tag{9}$$

This subsystem serves as an electromechanical correction to the slow subsystem. We obtain the transient subsystem by rescaling time ($\tau = \eta t$) and considering the limit $\epsilon \to 0$:

$$x' = 0, \tag{10}$$
$$y' = 0, \tag{11}$$
$$z' = h(x, y, z). \tag{12}$$

Here, all slower states are treated as constant parameters while the transient states are allowed to evolve under little to no algebraic constraints.

II. Case Studies

We test this formalism using two power systems: a small-scale 3-bus system shown in Fig. 1 and the 2224-bus Great Britain transmission network [1]. These power systems are populated by generators with third order synchronous machines regulated by a nonlinear voltage exciter [2] and loads with constant power demand and first order induction motors. The electromagnetic states are low-pass time-varying phasors [3].

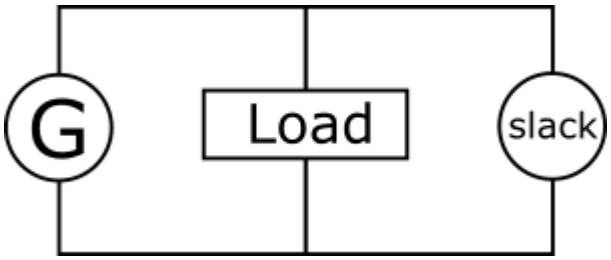

Fig. 1. A simple 3-bus power system.

References

References

[1] "Power Systems Test Case Archive." Internet: http://www.maths.ed.ac.uk/optenergy/NetworkData/index.html, Mar. 31, 2013 [Apr. 20, 2018].

[2] C. Chu, & H.D. Chiang, "Constructing Analytical Energy Functions for Network-Preserving Power System Models". *Circuits Syst Signal Process* vol. 24, pp.363-383, 2005.

[3] V. Venkatasubramanian, H. Schättler, & J. Zaborszky, "Fast Time-Varying Phasor Analysis in the Balanced Three-Phase Large Electric Power System". *IEEE Trans. Automat. Contr.*, vol. 40, pp. 1975-1982, Nov. 1995.

Convex Relaxations and Approximations of Chance-Constrained AC-OPF Problems

Lejla Halilbašić, Pierre Pinson, and Spyros Chatzivasileiadis
Technical University of Denmark (DTU)
{lhal, ppin, spchatz}@elektro.dtu.dk

***Abstract*—This paper deals with the impact of linear approximations for the unknown nonconvex confidence region of chance-constrained AC optimal power flow problems. Such approximations are required for the formulation of tractable chance constraints. In this context, we introduce the first formulation of a chance-constrained second-order cone (SOC) OPF. The proposed formulation provides convergence guarantees due to its convexity, while it demonstrates high computational efficiency. Combined with an AC feasibility recovery, it is able to identify better solutions than chance-constrained nonconvex AC-OPF formulations. To the best of our knowledge, this paper is the first to perform a rigorous analysis of the AC feasibility recovery procedures for robust SOC-OPF problems. We identify the issues that arise from the linear approximations, and by using a reformulation of the quadratic chance constraints, we introduce new parameters able to reshape the approximation of the confidence region. We demonstrate our methods on the IEEE 118-bus system.**

I. Introduction

While power system operations are increasingly relying on the AC Optimal Power Flow (OPF) to identify optimal decisions, higher shares of intermittent renewable generation add an additional layer of complexity, calling for modeling approaches which account for uncertainty. Literature considers uncertainty either in the form of stochastic formulations, which optimizes over several possible realizations, or in the form of robust formulations, where chance constraints are incorporated in the optimization problem accounting for a continuous range of uncertainty. This work focuses on chance-constrained optimization.

As the AC-OPF is a nonlinear and nonconvex problem, it is impossible to formulate tractable chance constraints able to cover the whole continuous uncertainty space. Instead, literature has proposed tractable approximations. Chance constraints define the maximum allowable violation probability ϵ of inequality constraints and reduce the nonconvex feasible space of the AC-OPF to a desired confidence region (CR), which is also nonconvex. The main challenge of the chance-constrained AC-OPF lies in approximating the unknown nonconvex CR. In this work, we propose the first formulation of a chance-constrained second-order cone optimal power flow (CC-SOC-OPF), which (a) coupled with an AC feasibility recovery is able to identify solutions within the CR (i.e., solutions feasible to the original chance-constrained AC-OPF), (b) finds more cost-efficient solutions than the alternative nonconvex approach based on the full power flow equations, (c) leverages the benefits of iterative convex programming to provide convergence guarantees and a high computational efficiency, and (d) introduces new parameters which allow to reshape the convex approximation of the CR offering a high degree of flexibility w.r.t. the robustness of the solution. We perform a rigorous investigation of how the approximation of the quadratic chance constraints impacts the CC-SOC-OPF and its recovered solution.

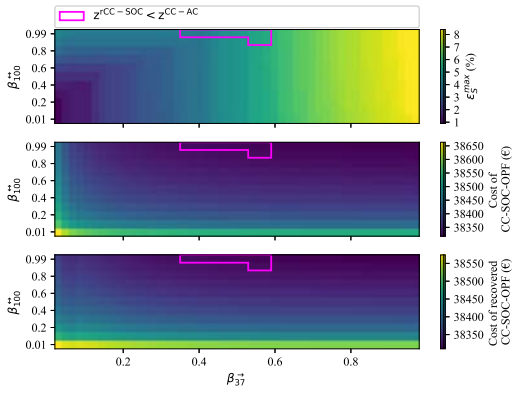

Fig. 1. Maximum violation probability of apparent branch flows ϵ_S^{max}, generation cost of the CC-SOC-OPF ($z^{\text{CC-SOC}}$) and the recovered CC-SOC-OPF solution ($z^{\text{rCC-SOC}}$) as functions of $\beta^{\rightarrow}_{37}$ and $\beta^{\leftrightarrow}_{100}$.

II. Case Study

We evaluate the performance of the proposed CC-SOC-OPF on the IEEE 118 bus test system with two wind farms. The wind power output is assumed to follow a Gaussian distribution. The constraint violation probabilities of the CC-SOC-OPF solutions are evaluated empirically using 10'000 Monte Carlo simulations.

We use the solution of the CC-SOC-OPF as an input to an AC power flow analysis to recover the feasibility of the solution. We investigate the impact of the approximation of the quadratic chance constraints through a sensitivity analysis of the input parameters β. Our results depicted in Fig. 1 show that higher values of β increase the level of conservatism and thus, reduce the maximum allowable violation probability increasing the generation cost of both the CC-SOC-OPF and its recovered solution. We identify 18 operating points, highlighted in the pink box, which are AC feasible, fulfill the original chance constraints and are still cheaper than the nonconvex CC-AC-OPF. This highlights the potential of convex relaxations to determine the boundaries of the CR and the true optimal of nonconvex problems. Despite the required tuning, β provides the flexibility to vary the shape of the convex approximation and direct the solution from a true lower bound back into the original feasible space and the CR.

Analysis of Transformers Thermal Response to Geomagnetic Disturbances

Pooria Dehghanian, *Student Member, IEEE*, Thomas J. Overbye, *Fellow, IEEE*, and Katherine R. Davis, *Member, IEEE*

***Abstract*—Solar geomagnetic storm releases a burst of plasma carrying intense magnetic field to flow into the magnetosphere. This results in a sudden change in the earth's magnetic field which induces currents in long conductors such as power transmission lines on the earth's surface. The geomagnetically induced currents (GICs) are a potentially catastrophic threat to large-scale power system operations especially the bulk transformers, possibly leading to severe outages. This poster aims to conduct a hotspot temperature analysis of transformer heating due to a GICs-caused half-cycle saturation. A sensitivity analysis is accomplished to realize the effect of GICs on transformer temperature response. The proposed approach is applied to the 20-bus and 500-bus test systems facing a geomagnetic disturbance (GMD) event and the temperature responses are estimated in both normal and contingency scenarios.**

Keywords—geomagnetic disturbances; hotspot temperature; transformer; geomagnetic induced current

I. Introduction

GICs are injected into the grounding points of the electric power grid. Power transformers are the most common gateway for GICs resulting in an offset of the alternative current sinusoidal flux in the transformer cores. As a result, transformers may face asymmetric or half-cycle saturations imposing additional eddy current in various segments of the core, winding, and metallic parts. Such induced overcurrent leads to an intensified temperature of windings and metallic plates. Motivated by procedure given in [1], Figure 1 illustrates the suggested architecture for power system analysis impacted by GICs. The developed GIC model is based on the effective GIC current characterized by uniform earth conductivity. The corresponding temperature impacts are studied through a sensitivity analysis approach implemented in two different case studies.

II. Transformer Thermal Assessment Impacted by GICs

A. Approximate Transformer Heating Model

In order to find the transformer heating response, an asymptotic thermal behavior is considered using the available NERC metallic hotspot thermal data to a DC-step injected current [1]. The impulse response of the transformer heating is found from the step unit function. The benchmark GMD E-field data from the case in 1989 is utilized to assess the corresponding GIC values as the input to the heating function. The heating function is closely dependent on transformer characteristics such as cooling constant.

B. Case study

The proposed heating model will be demonstrated on the 20-bus and 500 bus test cases. The results of the heating function for the time series input GIC, shown in Fig. 2, are applied in different scenarios. For instance, Fig. 3 demonstrates the transformer thermal behavior during the system normal operating condition for 20-bus test case.

A precise determination of the transformer thermal behavior is generally difficult due to its sensitivity to many factors such as ambient temperature, materials, core type, cooling constant, etc. However, the proposed approach offers actionable information to operators to approximately predict the thermal behavior of transformers facing GMD events.

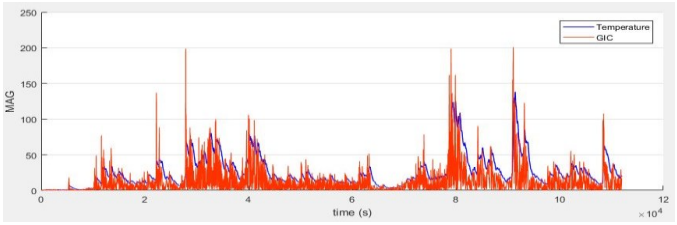

Figure 2. Real-time time series of GIC/temperature for the studied transformer

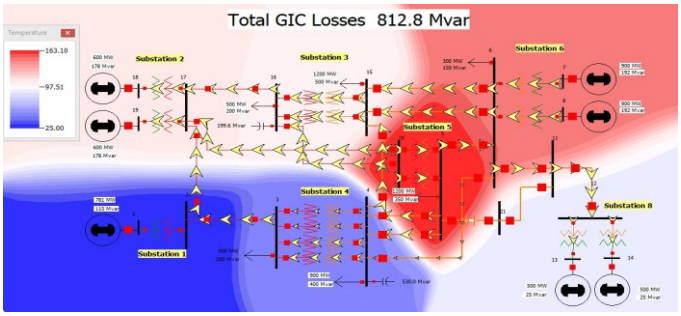

Figure 3. Temperature heat map of all transformers in the 20-bus test case when the simulated GMD event hits the grid.

References

[1] "Screening criterion for transformer thermal impact assessment". Developed by the NERC project 2013-03.

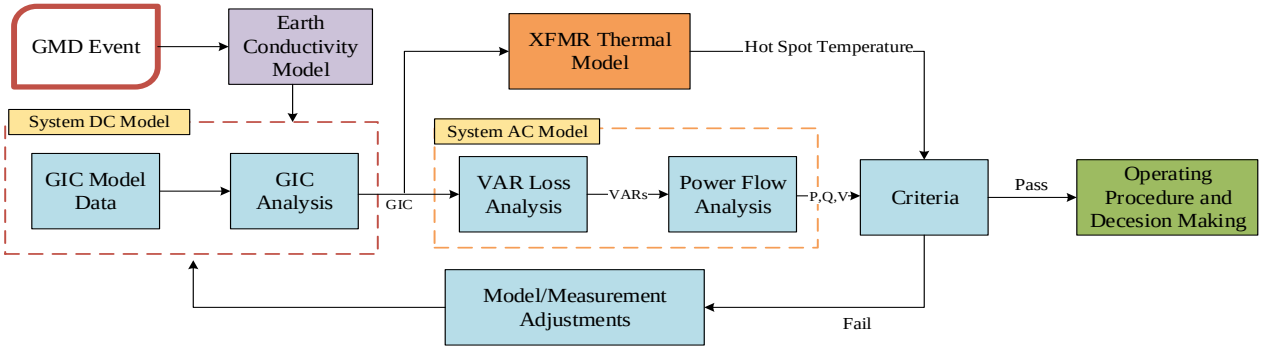

Figure 1. Overall architecture suggested for analysis of power grids impacted by GICs.

A Hybrid Simulator for the Study of EP Project Multi-Terminal DC in South Korea Gird

Jeehoon Lee, *Student Member, IEEE*
School of Electrical andelectronic Enginnering
Yonsei University
Seoul, Korea
Jeehun87@yonsei.ac.kr

Kyeon Hur, *Senior Member, IEEE*
School of Electrical andelectronic Enginnering
Yonsei University
Seoul, Korea
khur@yonsei.ac.kr

***Abstract*—This poster introduces a hybrid simulator that is used to study on the impacts of MMC tap to LCC-HVDC (MTDC) operation in South Korea Grid. Main reason for MTDC study is to demonstrate that the MTDC operation is beneficial in terms of better system stability compared to Double Bi-pole LCC-HVDC in South Korea grid. However, as the increase in HVDC and FACTS device complicate the grid operation, precise analysis of grid is required. Conventional simulation has challenges that focus on either detailed models in small system or simplified models in large system. Hybrid simulator approach addresses these challenges by using both EMT and phasor-domain simulation methods. Using the Hybrid simulator in this situation, it is possible to perform the integrated simulation considering the reaction and characteristics of the Korea AC system, away from the limited EMT study. Simulation Studies were conducted for the stipulated fault scenarios. The objective of this study is to prove that MTDC configuration has effect on reducing the number of east generator to be tripped for stability in case of 765kV double line contingency.**

Keywords—Hybrid Simulator, MTDC, MMC, LCC-HVDC, Tap, RTDS, TSAT, South Korea grid

I. KEY FIGURE

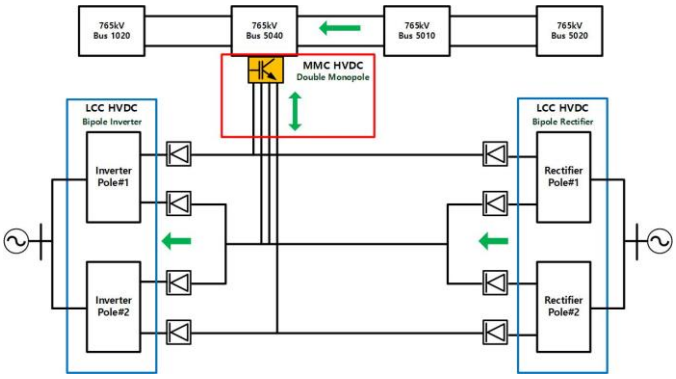

Figure 1 MMC tap to LCC HVDC

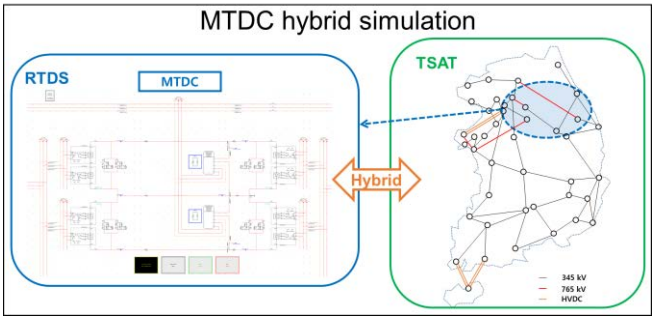

Figure 2 MTDC hybrid Simulation (RTDS & TSAT)

II. KEY RESULT

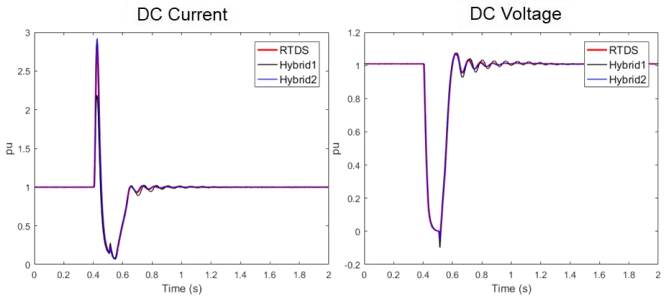

REFERENCES

[1] Lin, X., Gole, A. M. and Yu, M. "A Wide-Band Multi-Port System Equivalent for Real-Time Digital PowerSystem Simulators." Power Systems, IEEE Transactionson, 24, 237-249.

[2] Liang, Y., Lin, X., Gole, A. M. and Yu, M. "Improved Coherency-Based Wide-Band Equivalents for Real-Time Digital Simulators." Power Systems, IEEE Transactions on, 26, 1410-1417

Design of Scalable and Flexible Distributed Islanded Microgrid for Rural Electrification

Rabia Khan and Noel N. Schulz
School of Electrical Engineering and Computer Science
Washington State University
Pullman, WA

Abstract—DC microgrids are a viable solution to provide electricity to off-grid communities in developing countries. The microgrids designed for rural areas mostly constitute centralized generation and storage that lack scalability and flexibility. This paper aims to describe a design and model distributed scalable DC islanded microgrid for rural electrification. The modified Newton Raphson Power flow is solved for the designed system. The performance of the designed system is evaluated by computing distribution efficiency, line losses, and maximum voltage drop for distributed microgrid and comparing with the centralized microgrid. The adaptation of the distributed DC microgrid to scalability and flexibility is validated by adding new power generation sources and increasing the demand. Additionally the designed model is optimized in Hybrid Optimization Model for Electric Renewables (HOMER) based on the cost of energy for the top three energy stricken locations, i.e., Uganda, Ethiopia, and Brazil. The low cost of energy, low power losses, and high efficiency show that the distributed scalable DC microgrid serves as an optimal design for rural electrification which can be extended in future based on the increased power demand.

I. Introduction

The fossil fuels used for the generation of electricity have been depleting for decades because of their high consumption. The

Renewable energy resources have played a vital role to provide electricity since 2000. More than one billion people live around the world without electricity [2]. The locally available renewable energy resources can be used to enlighten the lives of millions of people living in countries where electricity is not available or is highly intermittent. DC microgrids are a viable solution to provide electricity to the off-grid communities in developing countries. The distributed scalable DC islanded microgrid is designed and modeled in this paper. The cost of electricity is a major factor in energy-deprived countries, so the cost of energy for the designed system is calculated using HOMER for three different locations that have the highest energy needs, i.e., Uganda, Ethiopia, and Brazil. The solar and wind data for the locations are taken from National Solar Radiation Database and NREL Wind Prospector respectively.

A. Proposed Benchmark

The block diagram of the proposed scalable and flexible system is shown in Fig. 1. The proposed configuration has distributed generation and distributed storage. To validate the flexibility of the system, three different type of sources and loads are added.

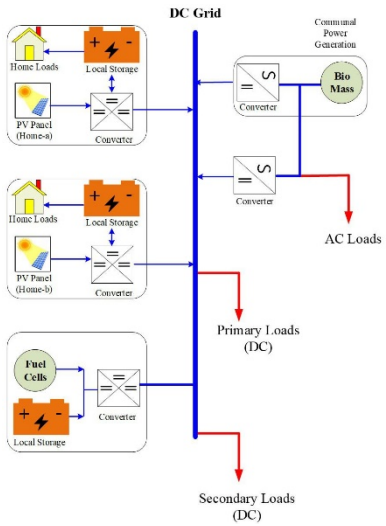

Fig. 1. Proposed design of the distributed microgrid.

II. Case Studies

The three different case studies are implemented which are described below.

Case Study 1: Modeling of the proposed system with different sources and loads

Case Study 2: Implementation of the designed system in HOMER.

III. Conclusion

This paper focuses on the design of a scalable and flexible DC islanded microgrid for rural electrification. The results of power flow and the optimized cost of energy for the designed system shows its effective implementation in rural areas with future growth perspective.

References

[1] Nasir, M., Khan, H.A., Hussain, A., Mateen, L. and Zaffar, N.A., 2018. Solar PV-Based Scalable DC Microgrid for Rural Electrification in Developing Regions. IEEE Transactions on Sustainable Energy, 9(1), pp.390-399.

[2] World Bank Group, Ahmed, A., Portale, E., Azuela, G., Liu, J., de Wit, J., Sinton, J., Bazilian, M., Angelou, N., Banergee, S. and Foster, V., 2015. Sustainable Energy for All 2015: Progress Toward Sustainable Energy. World Bank.

[3] Patel, A.M. and Singal, S.K., 2016, November. Off grid rural elec-trification using integrated renewable energy system. In Power India International Conference (PIICON), 2016 IEEE 7th (pp. 1-5). IEEE.

Synthetic Residential Load Models for Analysis of Energy Management Impact on Smart Cities

Fernando B. dos Reis†, Timothy M. Hansen
Electrical Engineering and Computer Science Department
South Dakota State University
Brookings, South Dakota 57007
Email: †fernando.beretadosreis@sdstate.edu

***Abstract*—Demand response (DR), shifting load in response to system conditions, can achieve defined goals, e.g., reducing cost, losses, and curtailment of renewable resources. There are considerable challenges in obtaining customer load curves to be able to perform residential DR due to privacy concerns, lack of data, daily/seasonal variability, etc. This work focuses on the generation of synthetic load curves for residential customers made of individual appliance and thermal loads. The aggregated load of the individual customer synthetic load curves sum to a known system load curve that is now made of millions of individual appliances and thermal loads for city-sized DR studies. Additionally, the synthetic load curves incorporate the ZIP load model, allowing for realistic variations in active and reactive power of loads in response to changes in voltage. As a first DR study, large-scale DR considering distribution system limitations in the presence of distributed generation, e.g., photovoltaic solar, is studied.**

***Keywords*—Residential load model, ZIP parameters, demand response, home energy management systems, distributed generation.**

I. Introduction

The current work significantly expands the queuing load models presented in [1], which intrinsically considers the time-varying characteristics of load and makes use of only openly available aggregated load data from electric utilities and system operators. The queue model synthetically generates individual appliances being turned on by customers with a defined power rating and time duration, such that when summed together equal a known system load curve.

Let $\lambda(t)$ be the time-varying appliance rate into the system described by a Poisson process, D and P be random variables describing the duration and power rating of the set of appliances, respectively, and $m(t)$ be the average number of appliances running at time t. Making use of the linear-with-time-shift (LIN-S) approximation from [2], $\lambda(t)$ is expressed as

$$\lambda\left(t\right) = \frac{m\left(t + \mathbb{E}\left[D\right]\right)}{\mathbb{E}\left[D\right]}. \tag{1}$$

Let $l(t)$ be the expected aggregated household load at time t so that the average number of ruining appliances is

$$m\left(t\right) = \frac{l\left(t\right)}{\mathbb{E}\left[P\right]}. \tag{2}$$

Substituting (2) into (1), the time-varying appliance rate into the system with a Poisson process is described as

$$\lambda\left(t\right) = \frac{l\left(t + \mathbb{E}\left[D\right]\right)}{\mathbb{E}\left[P\right]\mathbb{E}\left[D\right]}. \tag{3}$$

The expected home load $l(t)$ is an input from the utility data which contains residential, commercial, and industrial costumers. Thus, it does not represent the behavior of a typical residential load, presented in Fig. 1. The distinct behavior of residential customers, having its nadir near midday, is crucial for studies with distributed photovoltaic generation, i.e., at/near maximum generation during low load periods. The ZIP appliance parameters are presented in [3] with their respect contribution in average residential costumers.

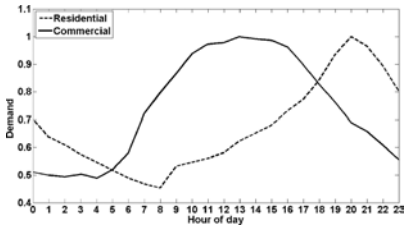

Fig. 1: Daily expected behavior of residential and commercial customers [3].

References

[1] T. M. Hansen, E. K. P. Chong, S. Suryanarayanan, A. A. Maciejewski, and H. J. Siegel, "A partially observable markov decision process approach to residential home energy management," *IEEE Transactions on Smart Grid*, vol. 9, no. 2, pp. 1271–1281, March 2018.

[2] S. G. E. Eick, A. M. William, and W. Whitt, "Mt/G/\infinity Queues with sinusoidal arrival rates," *Management Science*, vol. 39, no. 2, pp. 241–252, 1993.

[3] M. Diaz-aguiló, J. Sandraz, R. Macwan, F. D. León, S. Member, C. Comack, and D. Wang, "Field Validated Load Model for the Analysis of CVR in Distribution Secondary Networks : Energy Conservation," *IEEE Transactions on Power Delivery*, vol. 28, no. 4, pp. 2428 – 2436, 2013.

Finite Element Analysis of Transformers in Subterranean Vaults

Jaime Kolln, Robert B. Bass
Dept. of Electrical and Computer Engineering
Portland State University
Portland, Oregon, USA
kolln@pdx.edu

I. Introduction

Portland's local utility, Portland General Electric (PGE) installs transformers below grade in vaults in the downtown area. When a transformer is under electrical load, its temperature tends to rise due to thermal losses caused by the circulation of electric current and magnetic flux. When installed in a vault, a lack of sufficient ventilation may cause the transformer temperature to rise above the transformer's rated operating temperature. Extended operation beyond this limit could lead to thermal damage, shortened asset lifetime, and possibly interruption in service.

All vaults have a removable lid for maintenance access, and often these lids are vented to facilitate convective heat transfer out of the vault. Vault lids with top-vent grates often require a lifting force greater than 55 lbs and must be fitted with a lift-assist mechanism which reduces the amount of ventilation through the grate. Further, grated lids eventually get filled with leaves and debris, blocking the air passage and making the lid even heavier. Regular clearing of debris from the grates also adds a maintenance cost.

In order to alleviate these concerns, PGE asked the Power Engineering Group at Portland State University to simulate how various vault-mounted transformers behave within different climate conditions. The purpose of this work is to study these models to determine under what conditions solid lids may be used without endangering the transformer or causing the vault lid to become too hot to step on.

II. Thermal Modeling

Finite element analysis (FEA) is used to analyze the fluid and thermal behavior of our vault-mounted transformer models. The transformers, vaults, lids, soil and air conditions are represented as reasonably as possible without excessive detail. A typical electrical load profile was used, with a focus on warmer climate conditions, and only a handful of transformer/vault combinations were examined. Doing so allows for the ability to concisely convey a set of results without an excess of scenario details.

Over the course of this project several improvements have been made to the models. The most successful modification was to include radiation, with smaller improvements including a realistic ambient temperature profile and a 50% average load profile.

III. Results

Five transformer sizes were analyzed in a typical 660-PGE vault from Oldcastle Precast. It was found the transformers do not result in excessive transformer top oil temperatures or lid temperatures under average mid-summer conditions when the vaults feature a vented or solid lid. In the model, the transformers generally produce temperatures just less than 20 °F higher with the solid lid. The models show lid surface temperatures as high as 141 °F on the larger transformer vaults with solid lids under summer conditions

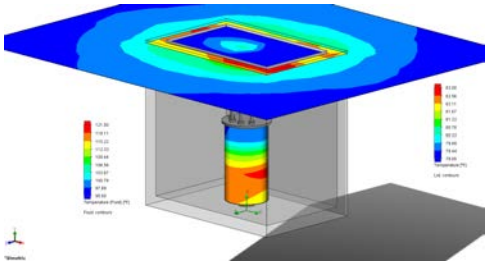

Fig. 1. 25 kVA Transformer, PGE-660 Vented Lid Vault Temp Profile.

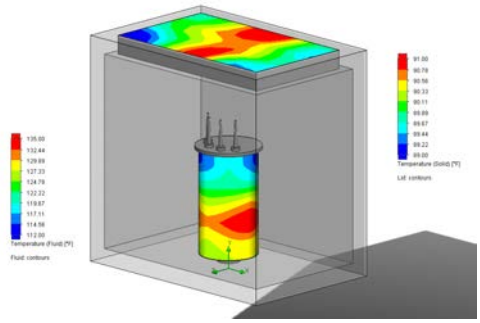

Fig. 2. 25 kVA Transformer, PGE-660 Solid Lid Vault Temp Profile.

IV. Validation

Portland State University's research continues and is currently in the validation stage. As real world temperatures, load profiles, and weather data is compared to the simulation results the models can be improved. These results should be available at the time of the conference and shall be presented then.

An Object Oriented Matlab Toolbox for Power Distribution System Analysis

Hasala Dharmawardena, *Student Member, IEEE* *
Ganesh K. Venayagamoorthy, *Senior Member, IEEE* * †
*Real-Time Power and Intelligent System Laboratory
Clemson University, South Carolina, USA
†School of Engineering, University of KwaZulu-Natal, Durban, South Africa
hasala@ieee.org and gkumar@ieee.org

***Abstract*—This study describes a new Matlab based object-oriented simulation tool for power system analysis. It is applicable to any unbalanced condition, be it single phase loads, un-transposed lines or single phase switching. The program constructs the Bus admittance matrix by using the primitive admittance matrices of the power system components. The complexities associated with three-phase power flow are minimized by applying the Object Oriented Programming framework. The toolbox supports studies related to three-phase power flow solvers and short circuit analysis. It is also useful for classroom education.**

***Index Terms*—Bus Admittance Matrix, Distribution Power Flow, Object Oriented Programming, Software, Three Phase Distribution.**

I. Introduction

The modern power system, at the distribution level, is presently undergoing a transformation in topology and dynamics. Given the complexity of the connected models and system specific temporal dynamics, it is important to precisely model the distribution system to ensure safe, reliable and economical operation of the system.

Modeling and simulation of the power system in the phase reference frame is much more complicated and time-consuming than modeling in the balanced positive sequence reference frame. This is because of the size of the problem, at minimum increases by a magnitude of three. As a result, three-phase analysis requires more input data and computation resources. The computational tools applied in the analysis need to be extremely efficient and robust. Whereas in a balanced system analysis, the system states are much closer to the nominal value, in the unbalanced system, the system states have a larger possibility to stray away from the nominal value.

The existing commercial tools for distribution analysis requires a significant investment in resources, to learn the operational idiosyncrasies, which is better invested in mastering the computation engine. Additionally, on the educational front, there is a need for an easily understood, accessible, well developed and maintained three power system toolbox.

Many free toolboxes such as MatPower are available for balanced system analysis. However, the options for three-phase system analysis are limited. The available Free and Open Source (FOSS) software in this domain are written in programming languages that are not widely used by the power engineering community. Students and researchers are already well versed in Matlab and have access to it. Though many existing power system toolboxes are based on Matlab, none of them support three-phase unbalanced system studies. This could partly be attributed to the difficulty in using a procedure-oriented programming framework to encapsulate the complexities inherent to modeling the distribution system.

II. Discussion

The typical Kron reduced primitive impedance matrix of the unbalanced transmission line is given by (1).

$$Z_{abc} = \begin{bmatrix} Z_{aa} & Z_{ab} & Z_{ac} \\ Z_{ba} & Z_{bb} & Z_{bc} \\ Z_{ca} & Z_{cb} & Z_{cc} \end{bmatrix} \tag{1}$$

The modeling of the transformer is even more complicated and dependent upon the connection type as well as the ground impedance. Based on [1] the simplest model that can be presented is in the form given by (2). Each of the four matrix elements refers to a different 3x3 submatrix based on the type of primary and secondary connections.

$$\begin{bmatrix} I_p \\ I_s \end{bmatrix} = \begin{bmatrix} Y_{pp} & Y_{ps} \\ Y_{sp} & Y_{ss} \end{bmatrix} = \begin{bmatrix} V_p \\ V_s \end{bmatrix} \tag{2}$$

The Matlab toolbox presented in this study addresses all these complexities using the object-oriented programming framework. It is a useful place to start developing new computational methods for power distribution system analysis.

This study is supported by the National Science Foundation (NSF) of the United States, under grants IIP #1312260, #1408141 and #1638321, and the Duke Energy Distinguished Professorship Endowment Fund. Any opinions, findings and conclusions or recommendations expressed in this material are those of author(s) and do not necessarily reflect the views of National Science Foundation and Duke Energy.

References

[1] J. Arrillage, C. Arnold, and B. Harker, "Computer modelling of electrical power systems," 1983.

Big Data: Application to Transmission and Distribution Co-Simulation for the Future Grid

Yaswanth "Nag" Velaga, P.K. Sen
Colorado School of Mines, Golden, CO

***Abstract*—Renewable energy is growing rapidly and is already a significant source of electricity in many states in the United States. Rapid integration of these sources is expected to change the notions of power delivery in the near future. With current research efforts for the future grid focused heavily towards Co-Simulation model, time has come to devise a practical way to implement. This project aims at using big data to create a replica of the actual model for the distribution. Reliability Coordinators (RC), Independent System Operators (ISO) and Regional Transmission Organizations (RTO) can use these models to maintain the reliability of the system.**

Keywords—Big Data, Co-Simulation, ISO, RTO, RC, Utilities

I. Introduction

As the grid becomes less centralized with the resource mix integrates distributed energy resources (DERs), new tools are required to study the interactions between T&D. Co-Simulation is widely accepted by the industry as the future of grid simulation. There are seven ISO/RTOs and eleven RCs in the United States that coordinate the reliable power grid operations. They run the transmission systems without distribution grid. This model has been working because the penetration level of DERs is low. With the reverse power flows, they need a distribution model to prepare for the unexpected events. Therefore, in order to create a virtual model, big data can be used.

II. Co-Simulation

The traditional T&D systems are decoupled at the operational level and solved separately using the legacy software's. In Co-Simulation approach T&D networks are solved separately and the interactions are captured by interchanging the solutions obtained for the two models. They converge at every time step of the power flow and move forward to the next (Fig. 1).

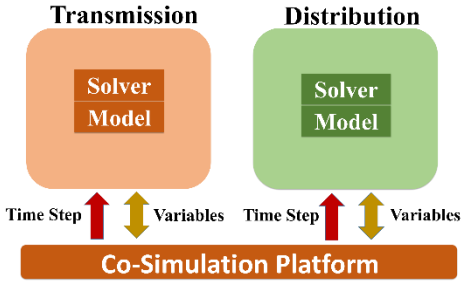

Fig. 1. Co-Simulation Overview

III. System Model

Approximately two-thirds of country's transmission system is operated by ISO/RTOs and Balancing Authorities. Reliability coordinators keep oversight of bulk transmission system to meet regulation standards. Models with these operators cover upto 69kV with no visibility into distribution grid. Transmission system is very accurately modeled and reflects the current state. Distribution system consists of thousands of nodes and also not accurately modeled down to the load. In order to co-simulate the T&D systems, ISO/RTO/RCs need a model which can give the accurate results and still capture all the characteristics of the system. Either utilities need to share the model with the operators or establish a communication platform to link the T&D systems. These are not practical solutions because the model needs constant updates and communication systems are not dependable every time. It is virtually impossible to integrate T&D systems in the present framework. Only other way is to model the system based on constant data from field (Fig. 2). Utilities often collect numerous amount of data from advanced metering infrastructure (AMI) and sensors but not used properly. This data needs to be processed by big data algorithms and change it to the way it can be used to build a model. Current setup will relieve the utilities from the constant communication with operators. The idea was inspired from the IEEE T&D conference student poster contest feedback.

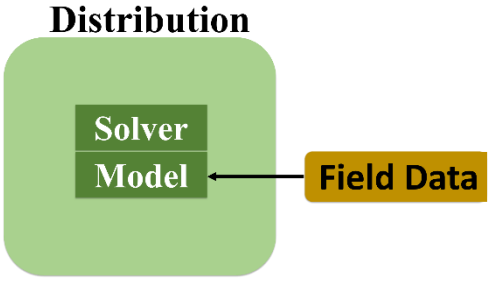

Fig. 2. Distribution System Model

Interdependent Electric and Water Infrastructure Modeling, Optimization and Control: System Simulations for Severe Contingencies and Drought Conditions

Scott Zuloaga, *Student Member*, *IEEE*, Vijay Vittal, *Fellow*, IEEE

School of Electrical, Computer and Energy Engineering, Arizona State University, Tempe, AZ, USA

***Abstract*— The water-energy nexus is a phrase commonly used to describe the inherent and critical interdependencies between the electric power system and the water delivery system (WDS). In the work presented here, the analytical framework capturing the key interactions between these two critical infrastructures is explained and a summary of the mathematical model used to describe the associated power and water system dynamics is shown. The time scales for the system parameters of interest are known to be large, so the electric network behavior is represented using time-series power flows with inputs of generator status determined from a short-term unit commitment model and real power set-points given from a modified optimal power flow solution. The WDS is represented within the EPANET software with optimization of the systems' operation implemented via a genetic algorithm. The simulation engine which integrates the different software used for modeling and optimizing the operation of the interdependent infrastructure systems will also be described. Results of the system responses to an overall WDS water shortage and severe power outages at a pumping station are shown for a one-month long simulation.**

Keywords— Critical Interdependent Infrastructures, Combined Economic and Environmental Dispatch, Water Delivery and Treatment System, Time-Domain Simulations, Water-Energy Nexus.

I. Introduction

The electric power system and the water distribution system (WDS) are an example of critical infrastructure systems which have interdependencies that arise in normal system operation. These major interdependencies which exist have been recognized and studied at a high level for some time. The main dependency of the electric system on the water infrastructure results from the fact that thermoelectric power plants require water for the cooling cycle. Water usage for power plants is defined in terms of water withdrawal and water consumption rates where the consumption is defined as the difference between the water withdrawn and the water returned to a water source. The rates of these factors for modern power plants are dependent on many factors such as whether an open or closed-loop cooling cycle is used, the type of emission control schemes implemented and, of course, the plant's physical location. The water system dependency on the electric infrastructure is clearly seen by the fact that water from its source will most likely require electricity for pumping and/or treatment before its final delivery to the end user.

II. Methodology and Initial Simulation Results

Because the interdependent simulation which has been implemented has parameters of interest which can change slowly with respect to time, long-term time-domain simulations are considered here. For instance, since thermoelectric power plants in the area of interest are usually supplied with two or more independent sources for cooling water and each plant typically has about two-weeks of water storage onsite, the rate of change of this parameter can be small. Since fast acting phenomena of the power system do not need to be considered here, only time-series power flows are used for the network solution. The power system operation is optimized with both a short-term unit commitment model implementation as well as a modified version of an optimal power flow which takes environmental factors into consideration. Economic dispatch formulations that take environmental constraints into account are sometimes referred to as a combined economic and environmental dispatch (CEED). The CEED objective function contains in it an operational water cost which is adjusted according to the rate of change of a given power plant's onsite water storage tank level. Under severe drought and heat conditions, it has been noted historically that some plants will have their maximum output limited. Along these lines, two models have been developed and are presented here as a method of de-rating plants under extreme drought conditions.

Initial results for a one month-long simulation which had an overall, system-wide shortage of water as well as a pumping station power outage are shown below. A modified version of the IEEE 14-bus test case and a test case representative of a typical city's WDS were used for network modeling.

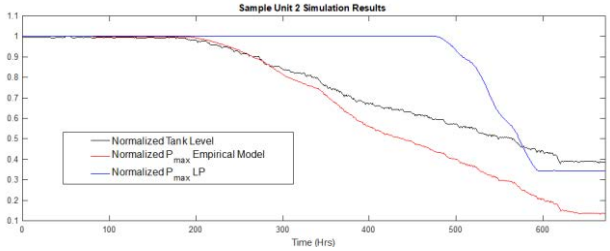

Fig. 1. Simulation Results for Normalized Tank Level and De-Rating Schemes

Online Identification of Generator Participation Factors using Cellular Computational Networks

[1,3]U. A. Abu, *Student Member, IEEE*, [1]P. Arunagirinathan, *Student Member, IEEE*,
[1,2]G. K. Venayagamoorthy, *Senior Member, IEEE*, [3]K. A. Folly, *Senior Member*, IEEE
[1]Real-Time Power and Intelligent System Laboratory, Clemson University, SC, USA
[2]School of Engineering, University of KwaZulu–Natal, Durban, South Africa
[3]Department of Electrical Engineering, University of Cape Town, South Africa
uabu@clemson.edu, parani@ieee.org, gkumar@ieee.org and komla.folly@uct.ac.za

***Abstract*—Electromechanical oscillation modes are exhibited by synchronous generators following a system disturbance. Identifying the generator participation factors is important in designing effective oscillation damping controller for the power system. A cellular computation network (CCN) based online identification of generator participation factors is studied. IEEE 68 bus 16 generator New England-New York benchmark power system has been simulated on a real-time digital simulator. Remote power system measurements are available at control centers with synchrophasor devices installed. Synchrophasor data driven online identification of generator participation factors can be used in selective tuning of power system stabilizers for different operating conditions of the power system.**

***Index Terms*—: Cellular computational network, generator participation factors, power system stabilizer, synchrophasor data.**

I. Introduction

The complexity of the power system increases with limited generation options and increasing interconnections in the transmission network, etc. Following a system disturbance inter-area oscillation modes are present in the system. Power system becomes vulnerable when these oscillations are poorly damped. A new methodology is presented for online prediction of generator participation factors. The participation factors give the information about the contribution of generators to the electromechanical oscillation modes in a power system. IEEE 68 bus 16 generator power system shown in Fig. 1 has been studied. The deployment of synchrophasor devices brings the remote measurements to the electric utility's control center hundred times faster rate compared to existing SCADA technologies.

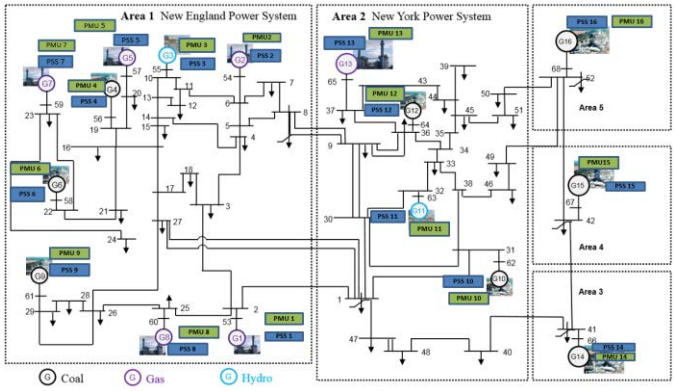

Fig. 1 IEEE 68 bus 16 generator five area power system

A synchrophasor data driven online identification of generator participation factors using a cellular computational network (CCN) [1] is studied. CCN is a highly nonlinear, scalable computer architecture for learning the dynamics of large networked system. CCN based frequency prediction on a multi machine power system is presented in [2]. The CCN diagram for the test power system used for this study is shown in Fig. 2. The test power system and controllers are simulated on a real-time digital simulator (RTDS), which is capable of simulating power system in a 50µs time step. The synchrophasor devices are receiving measurements from the simulated power system at RTPIS laboratory, Clemson University. Power system oscillation damping devices such as power system stabilizers can be selectively tuned for changing operating conditions based on the generator participation factors identified online using CCN.

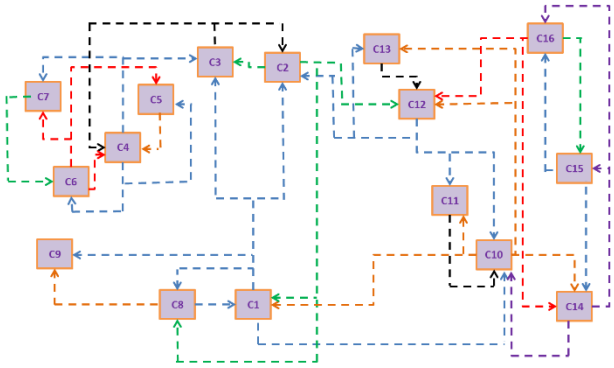

Fig. 2 CCN diagram

References

[1] B. Luitel and G. K. Venayagamoorthy, "Cellular computational networks - A scalable architecture for learning the dynamics of large networked systems," *Neural Networks*, vol. 50, pp. 120-123, February 2014.

[2] Y. Wei and G. K. Venayagamoorthy, "Cellular Computational Genaralized Neuron Network for Frequency Situational Intelligence in a Multi-machine Power System," *Neural Networks*, vol. 93, pp. 21-35, Sept., 2017.

A Real-Time Hardware-in-the-Loop Simulation of Sampled Value based Differential Protection

Jaya R A K Yellajosula, Sumit Paudyal, and Bruce A. Mork
Department of Electrical and Computer Engineering, Michigan Technological University, Houghton, USA
Email: jyellajo@mtu.edu, sumitp@mtu.edu, bamork@mtu.edu

***Abstract*—This work examines the transfer of sampled value measurement data between different substations in a wide-area network and utilize them for phasor estimation and transmission protection. The main goal of this work is to develop an IEC61850 based Intelligent Electronic Device (IED), which can be utilized in wide-area protection. This IED is designed to subscribe sampled value measurement data from remote and local terminal, and estimate the required phasors, which will be used for protective application. In case of fault, the IED executes the predefined protection logic and outputs trip signal in the form of Generic Object Oriented System Event (GOOSE) message. In relation towards protection application, this work focuses on developing adaptive alpha plane algorithm for transmission line differential protection, with a focus on estimating phasors from sampled value measurements using kalman filter. In summary, this work is intended to develop an IEC61850 based IED and perform real-time hardware in the loop simulation to test the effectiveness of the designed board and also protection algorithm for transmission line differential protection in a wide-area network.**

I. Key Figures

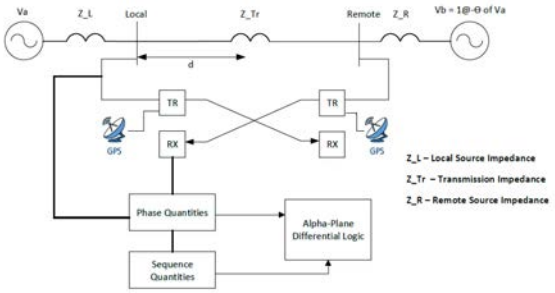

Fig. 1. System Level Schematics

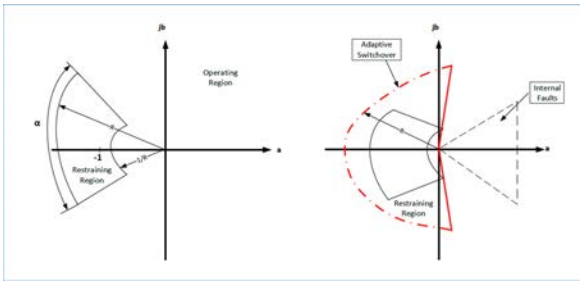

Fig. 2. Adaptive Alpha-Plane Algorithm

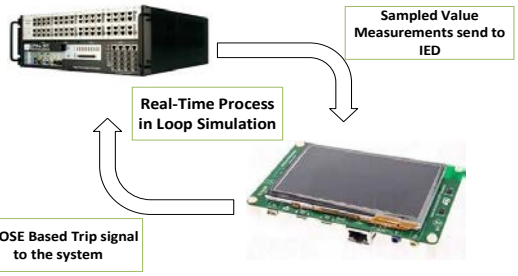

Fig. 3. HIL lab setup

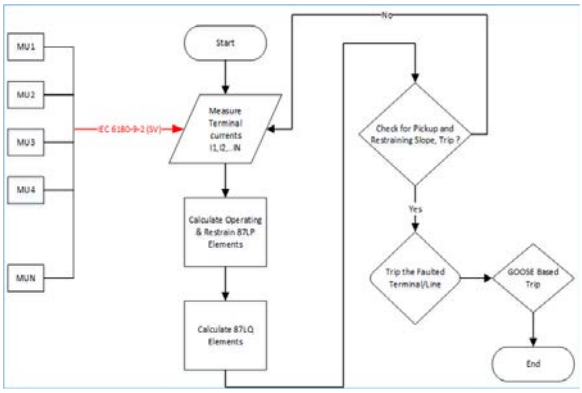

Fig. 4. Line differential protection logic execution.

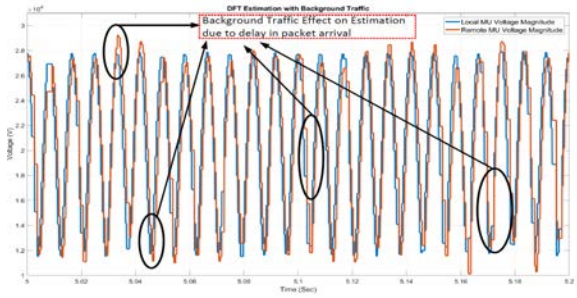

Fig. 5. Estimation algorithm output with some needed corrections to compensate the effect of network traffic

Optimal Routing and Charging of an Electric Vehicle Fleet for High-Efficiency Dynamic Transit Systems

Tao Chen, *Student Member, IEEE,* Bowen Zhang, *Student Member, IEEE,* Hajir Pourbabak, *Student Member, IEEE,* Abdollah Kavousi-Fard, *Member, IEEE,* and Wencong Su, *Member, IEEE*

***Abstract*—This paper proposes a framework and its mathematical model for optimal routing and charging of an electric vehicle fleet for high-efficiency dynamic transit systems, while taking into account energy efficiency and charging price. Based on an extended pickup and delivery problem, an optimization model is formulated from the transit service providers' perspective and is applied to an electric vehicle fleet with economically efficient but small batteries in very urbanized areas.**

I. Introduction

WE live in an increasingly urban world with abundant transport and electricity infrastructure. Today, 54% of the world's population lives in urban areas, a proportion that is expected to increase to 66% by 2050. This poses unprecedented environmental, economic and social challenges to transportation systems that move the people, goods and services of society [1]. Recently, advances in intelligent transportation systems and smart grid technologies offer great promise to widely popularize electric vehicles (EVs), and have the potential to revolutionize urban transportation systems and power systems [2]. Besides, increased occupancy is another high-potential method for decreasing transportation energy consumption, emissions and congestion. Urban mobility has traditionally been restricted to privately owned vehicles or public transport. Innovative dynamic transit services are radically changing the traditional views of the transportation industry, the social environment, and the business world.

On top of these services, this paper will take dynamic commuter transit services a step further with its special focus on high-efficiency EV fleet. Our proposed framework builds upon the similar business model of an emerging commuter service named "*MagicBus*", in San Francisco, California. "MagicBus" offers unique services such as "Book from your phone ahead of time", "Choose when your ride will arrive" and "Pick up near home, drop off near work". This paper implements a similar idea and also considers an optimal EV charging strategy and its potential impact on the average load in the power distribution system, as illustrated in Figure 1.

The conventional traffic network Sioux Falls scenario with static origin-destination matrices is used for simulation purposes. The altered scenario aims at keeping the topological structure, in which the length ratio between different routes is not in proportion to the ones in the real map. The routing results are shown in Figure 2.

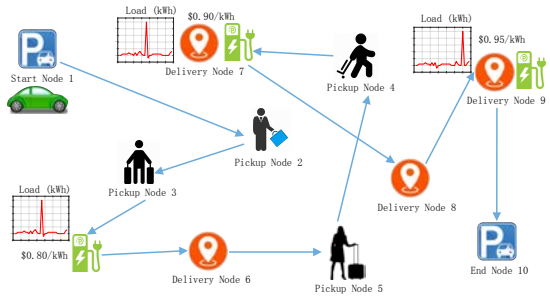

Fig. 1. The optimal routing and charging decision for a single EV in an fleet

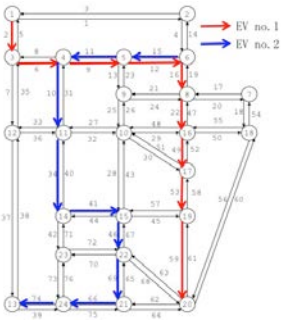

(a) EV No. 1 and No. 2

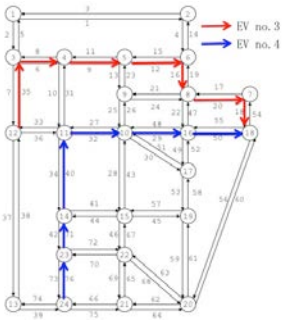

(b) EV No. 3 and No. 4

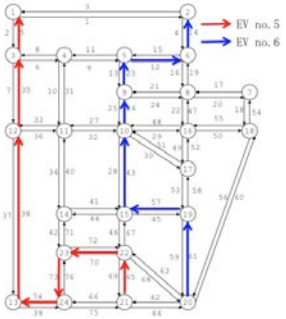

(c) EV No. 5 and No. 6

Fig. 2. Optimal routing solutions for different EVs

References

[1] W. Su, J. Wang, and Z. Hu, "Planning, Control, and Management Strategies for Parking Lots for PEVs," *Plug In Electric Vehicles in Smart Grids*, pp. 61-98. Springer Singapore, 2015.

[2] W. Su, H. Rahimi-Eichi, W. Zeng, and M.-Y. Chow, "A Survey on the Electrification of Transportation in a Smart Grid Environment," IEEE Trans. on Industrial Informatics, vol.8, no. 1, pp.1-10, February 2012.

Analysis of "8·15" Blackout in Taiwan and the Improvement Method of Contingency Reserve Capacity Through Direct Load Control

Hongxun Hui, *Student Member, IEEE*, Yi Ding, *Member, IEEE*, Kaining Luan, Daoqiang Xu

***Abstract*—Electric power has been one of the most important energy for modern cities. Therefore, blackouts always have great impacts on our modern societies. This paper reviews the process of the large-area blackout in Taiwan on August 15th, 2017. The direct cause of the accident is the incompetence of an employee in the natural gas company, while the fundamental cause is the shortage of the contingency reserve capacity (CRC). Faced with the insufficient installed capacity in Taiwan, this paper proposes an improvement method of CRC through direct load control. A control framework, on account of the system frequency and the gas pipeline pressure, is developed to regulate the power consumption of demand side resources (DSRs). Besides, a droop controller is also proposed to determine the regulation capacity of DSRs. The effectiveness of the proposed control strategy is verified by the numerical studies.**

***Index Terms*—blackout; contingency reserve; direct load control; demand side resource.**

I. Improvement Method of Contingency Reserve Capacity Through Direct Load Control

This paper proposes the improvement method of CRC through direct load control (DLC), as shown in Fig. 1. Both the system frequency and the pressure of the gas pipeline are monitored by the controller, which can send signals to the demand side resources (DSRs). When the system frequency drops or the gas pipeline pressure decreases abnormally, the controller will reduce the power consumption of DSRs to provide CRC for the system.

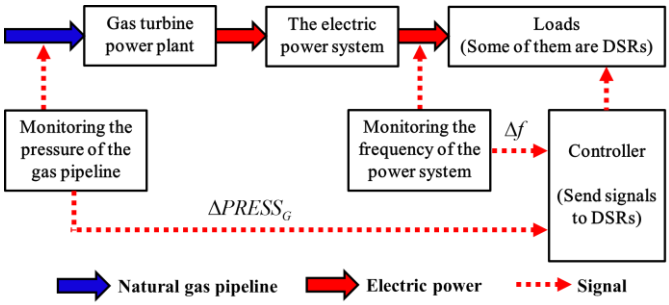

Fig. 1. The framework of DLC considering the gas pipeline pressure.

The controller is designed as the droop control theory, which is described as:

$$\Delta P_{DLC} = \gamma_0 \Delta f + \int \beta_0 \Delta f dt + \sum_{j=1}^{m} \int \beta_j \Delta PRESS_{Gj} dt \qquad (1)$$

II. Case Studies

The test system (Fig. 2) is set to simulate an electric power system, which has a low level of operating reserve capacity, just as the power system in Taiwan.

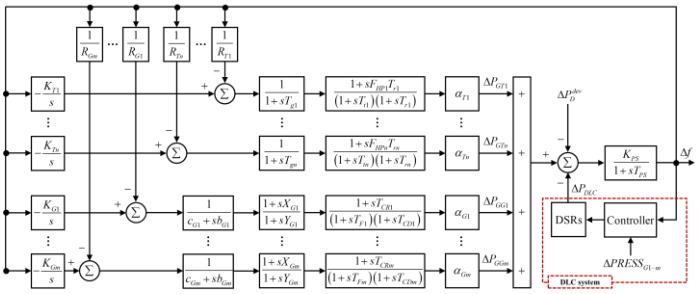

Fig. 2. Transfer function model of multi-sources single area system [12].

No loads provide CRC in Case 1. 10% loads can be controlled to provide CRC by only monitoring the system frequency. 10% loads can be controlled to provide CRC by monitoring both the system frequency and the pressure of the natural gas pipeline. Fig. 3 shows the simulation results.

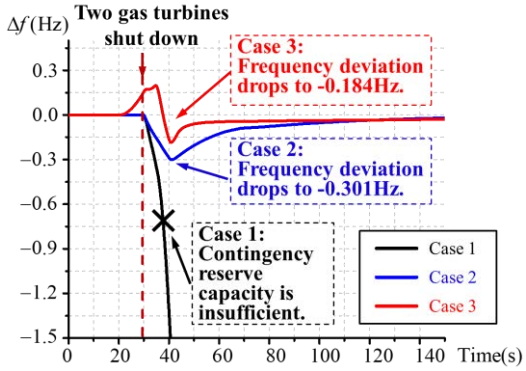

Fig. 3. Simulation results of the system frequency in the three cases.

III. Conclusions

The abnormal gas pressure can be detected earlier than the abnormal system frequency, when the accident is caused by the supply of primary energies. Simulation results show that the frequency deviation can decline 38.87% than another case, which only monitors the system frequency.

A Hierarchical Control Structure for Residential Community Energy Optimization

Priti Paudyal, Prateek Munankarmi, Zhen Ni, and Timothy M. Hansen
Department of Electrical Engineering and Computer Science
South Dakota State University, Brookings, SD 57006
United States
Email: {priti.paudyal, zhen.ni}@sdstate.edu

***Abstract*—Demand response, change in energy consumption pattern of the consumer in response to system conditions, can help to provide economic benefits to the utility. Residential sector is one of the major sectors for electricity consumption in the U.S. Thus, there is potential of energy management systems in residential communities. However, there should be some motivating factors such as financial incentives for the residential consumers to participate in the energy optimization programs. Moreover, ensuring the residents' comfort will encourage the long-term participation in such programs. This work presents a hierarchical control structure for residential community energy optimization with reward for the participating consumers. The framework is designed from utility's perspective which seeks to fulfill the demand reduction while minimizing the reward. Meanwhile, the framework also considers the residents' comfort.**

I. Key Figures

The proposed hierarchical control structure is shown in Fig. 1. In case of the demand response (DR) event, central controller (CC) in the upper level sends the demand reduction request signal to the local controllers (LCs). Each LC performs optimization, keeping its total power within different limits, and calculates the corresponding rewards. A reward corresponding to a demand limit comprises a bid. Then, each LC submits its different bids to the CC. Finally, the CC selects the optimal bids for each LC and the LCs issue the control signals to the houses based on the selected bids. Home appliances model adopted from [1].

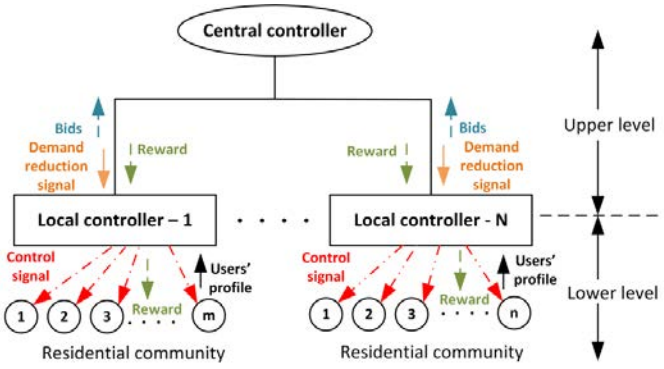

Fig. 1. System block diagram of the proposed hierarchical control structure for residential community energy optimization.

II. Key Equations

Each LC performs optimization to generate several bids. Each bid is generated by calculating the reward ($RW_{i,b}$) for the corresponding power limit ($P_{i,b}$). The objective function for the LC is to minimize the reward which is expressed mathematically as:

$$\min \quad RW_{i,b} = \sum_t \sum_a Reward_{a,t} \tag{1}$$

subject to

$$\sum_a P_a \cdot \delta_{a,t} \leq P_{i,b} \tag{2}$$

and the appliances constraints.

The CC selects the optimal bid (R_i) of each LC 'i' for maintaining the total power within its limit (P_{limit}).

$$\min \quad \sum_{i=1}^{N} R_i \tag{3}$$

subject to

$$\sum_{i=1}^{N} P_i \leq P_{limit} \tag{4}$$

and constraints to ensure only 1 bid is selected from each LC.

III. Key Results

Considering two LCs with 12 and 20 houses, the bids sent by the LCs are presented in Table I. The bids selected by the utility for 150 kW total demand limit are presented in Table II. The CC selects the bids which provide the minimum reward thereby satisfying the total demand limit.

TABLE I
Bids generated by local controllers

Local controller-1		Local controller-2	
Demand limit (kW)	Reward ($)	Demand limit (kW)	Reward ($)
65	1.95	120	6.67
60	3.14	115	7.02
55	5.07	110	9.84
50	26.14	105	123.05
45	210.46	100	28.02

TABLE II
Central controller's decision

	Local controller	Reward ($)	Power limit (kW)
Total demand limit = 150 kW	1	210.46	45
	2	123.05	105

IV. Conclusion

The proposed hierarchical framework achieves the demand reduction by allocating demand limits to each LCs while providing minimum reward and considering consumer comfort.

References

[1] M. Pipattanasomporn, M. Kuzlu, and S. Rahman, "An algorithm for intelligent home energy management and demand response analysis," *IEEE Transactions on Smart Grid*, vol. 3, no. 4, pp. 2166–2173, Dec 2012.

Home Energy Management System in Co-Simulation Framework

Prateek Munankarmi, Robert Fourney, and Timothy M. Hansen
Department of Electrical Engineering and Computer Science
South Dakota State University, Brookings, SD 57006
United States
Email: {prateek.munankarmi, robert.fourney, timothy.hansen}@sdstate.edu

***Abstract*—A home energy management system (HEMS) changes the energy consumption pattern of the consumer based on dynamic pricing programs or incentives. HEMS can utilize building energy simulator such as EnergyPlus to accurately model the energy consumption of the residential house considering finer details of building geometry and orientation, internal heat gain of the appliances, and weather. As internal heat gain of appliances and people have significant effect in the HVAC energy consumption, an integrated HVAC and appliance scheduling is necessary to properly evaluate HEMS. This work presents the formulation of HEMS considering detailed house model in EnergyPlus, and combined scheduling of HVAC and appliances in time-varying tariff. The proposed HEMS also considers the consumer comfort while minimizing the electricity cost.**

I. Key Figures

The system block diagram of the proposed home energy management system (HEMS) is shown in Fig. 1. The detailed model of the residential house is modeled in EnergyPlus. HEMS optimization calculates the optimized HVAC setpoint and the appliances schedules based on the price and consumer preferences. HEMS+ represents a co-simulation framework between HEMS and EnergyPlus. Consumer preferences, price, and weather data are provided to HEMS optimization.

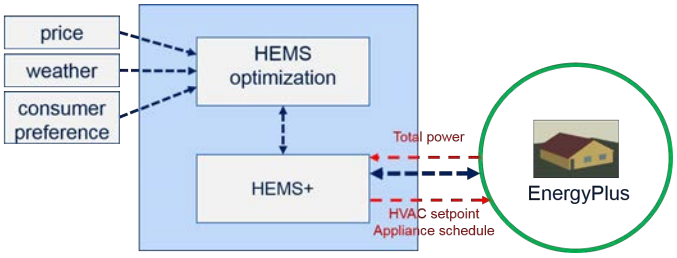

Fig. 1. System block diagram of the proposed HEMS.

II. Key Equations

The objective of the proposed HEMS is to minimize the electricity bill as shown in (1). Here, λ_t represents the time-varying tariff rate such as real-time price (RTP), $p_{hvac,t}$ represents HVAC power (kW), p_a represents rated appliance power (kW), and $\delta_{a,t}$ is the on/off status of appliance a at time t.

$$\min \quad C = \sum_{t=1}^{N_T} \lambda_t \cdot T \cdot (p_{hvac,t} + \sum_{a=1}^{n} (p_a \cdot \delta_{a,t})) \qquad (1)$$

subject to power limit, HVAC, and appliance constraints.

III. Key Results

Different cases which are considered to evaluate HEMS are as follows.

1) Base Case: No optimization performed.
2) Case-I (upper bound): Optimization with perfect future price information.
3) Case-II: Optimization with imperfect knowledge of future price.

The total energy consumption of a house in all three cases are comparable as shown in Table I.

TABLE I
Total Energy Consumption for Jan-2014 in Different Cases

	Base	Case-I	Case-II
HVAC energy (kWh)	1488.72	1407.45	1460.45
Appliance energy (kWh)	1691.40	1691.99	1655.31
Total energy (kWh)	3180.12	3099.45	3115.76

The HEMS reduces the energy consumption during high price and vice-versa to reduce the total electricity bill as shown in Fig 2. HEMS with imperfect price information (presented in Case-II in Table II) saves 11.36% over status quo whereas the upper bound (Case-I) of saving is 16.05%.

TABLE II
Total Electricity Energy Cost for Jan-2014 in Different Cases

	Base	Case-I	Case-II
HVAC cost ($)	134.59	145.25	143.6
Appliance cost ($)	125.98	73.49	87.35
Total cost ($)	260.57	218.74	230.95
Saving (%)	-	16.05	11.36

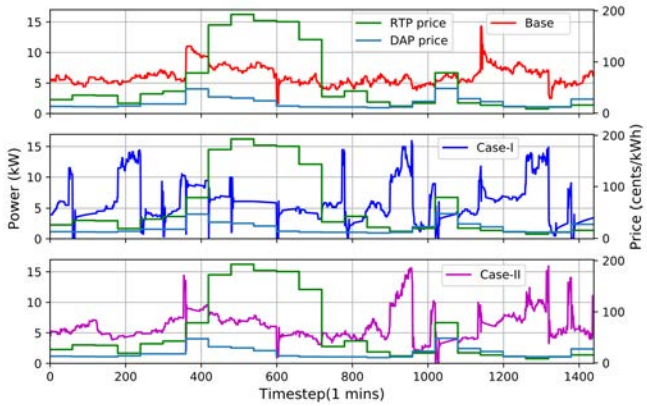

Fig. 2. Total house power for Jan-7, 2014

Distributed Locational Marginal Pricing based of Smart Home Management

Amin Mohsenzadeh
Department of Electrical and Computer Engineering
Wichita State University
Wichita, USA
Axmohenzadeh@wichita.edu

Chengzong Pang
Department of Electrical and Computer Engineering
Wichita State University
Wichita, USA
Chengzong.pang@wichita.edu

Abstract— **This paper proposes the application of Distributed Locational Marginal Pricing (DLMP) concept as a price signal to improve economic efficiency and system operations at both power distribution system and end user levels. Results demonstrate the advantage of DLMP over existing distribution pricing schemes.**

***Index Terms*— Distributed energy resources, DLMP, Scheduling, Smart grid, Smart home.**

I. INTRODUCTION

Demand response can play a significant role to modify the consumption patterns of customers by demand-side resources considering technical and financial issues [1]. The utilization of DR for residential consumers can affect approximately 40% of energy consumption in the world[2]. In this paper, DLMP is proposed as a price signal for end users instead of traditional scheme such as TOU or RTP. It reflects the marginal cost of delivering incremental energy to a specific location in a distribution grid and has effect on congestion and system losses. The superiority of using DLMP is providing a fair allocation of power loss among nodes and connected customers. To the best knowledge of aouthors, this is the first study in the literature considering PV, EV with capability of two-way energy trading, residential scale of ESS, and smart appliances in a single SHMS and distribution network in order to decrease energy bill and power loss simultaneously.

II. DLMP CALCULATION IN POWER DISTRIBUTION SYSTEM

The DLMP is similar to LMP in transmission system in which the cost for one additional unit of energy to be served at a particular bus is obtained. DLMP of a node depends on load level, transmission LMP, circuit diagram, and location of the node which is given in (8)

$$DLMP_{i,t} = LMP_t\ (1 + \frac{Tploss_{i,t}}{PLOSS}) \quad (8)$$

III. OBJECTIVE FUNCTION

The goal of this paper is minimizing total daily cost of electricity usage of a customer. In addition, smart homes are able to sell back energy to grid and gain revenue.

$$Total\ \cos t = \sum_{t=1}^{24} [P_t^{grid}.DLMP_t^{node,i} - P_t^{sell}.\lambda_t^{sellback}] \quad (21)$$

IV. NUMERICAL RESULTS

Fig. 1 shows decomposition of smart home power demand via proposed SHMS strategy. The negative part represents the amount of injected energy to house or grid. The green line shows how much energy should be bought from grid.

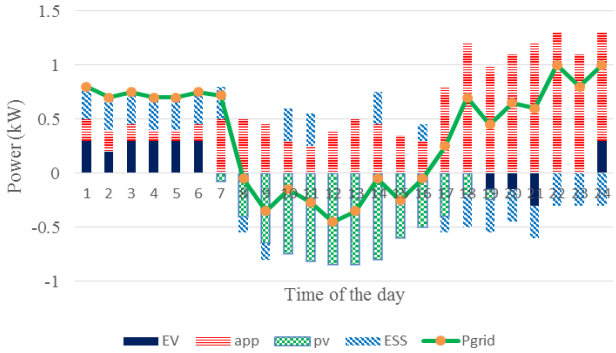

Figure 1. Decomposition of smart house power demand

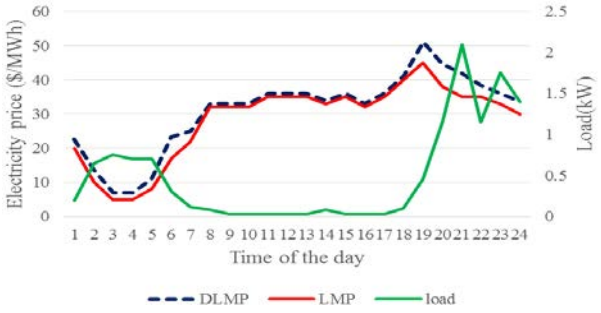

Figure 2. Correlation between energy bough from gridt and DLMP

V. CONCLUSION

Based on simulations conducted, despite the extensive and non-linear mathematical models, the proposed approach proved to be computationally efficient.

Impacts of Smart Inverters on Microgrids' Controls and Protections

Husam S. Samkari and Brian K. Johnson
University of Idaho
Department of Electrical and Computer Engineering
Moscow, Idaho USA
samk6783@vandals.uidaho.edu, bjohnson@uidaho.edu

***Abstract*— This project investigates the impacts of using smart inverters in microgrid systems. The impacts on protection and control systems are evaluated. An EMTP-RV model is used to represent the power system and the control system of a smart inverter. Analysis of several types of smart inverters' controllers, and different possible connections to power system are investigated during symmetrical and unsymmetrical faults.**

***Index Terms*— Distribution System, Microgrid, Photovoltaic, Smart Inverter, Power System.**

I. INTRODUCTION

In literature, microgrids may use more renewable energy resources, which are inverter based. In this work, the focus is on the inverter units, and the use of smart inverters. High penetration of photovoltaic (PV) systems are causing reverse power flow and voltage rise [1]. Several authors show benefits of using smart inverters on controlling the voltage profile at the distribution level such as [2]. However, having smart inverters on a microgrid during island mode requires more investigations [1].

Smart inverters, basically, have the capability to control both active and reactive power to improve their terminal voltage. Inverters have several control schemes such as: fixed reactive power, voltage-dependent reactive power, fixed power factor, fixed power factor in terms of injected active power, and volt/var control (terminal voltage regulation). Additionally, papers show that having multi control modes during different events can improve the voltage further [3].

In this project, a full smart inverter, and power system are modeled using EMTP-RV program. Switch and averaged inverter models are tested and compared to another model on a different EMTP-type program for validation. Different control schemes are tested to characterize the impact of each control type on the microgrid protection and control system. Additionally, there are several ways to connect an inverter to a distribution system. It can be connected directly to the power system, or through a power transform with different configurations. These variations of connections and configurations are tested since they can impact the protection scheme. The next step is testing the system during island mode because the impact can be more severe. Moreover, the percentage of penetration of inverter based sources will be investigated. Finally, suggestions for choosing the appropriate control scheme, and protection will be provided. The results in this paper show only one scenario.

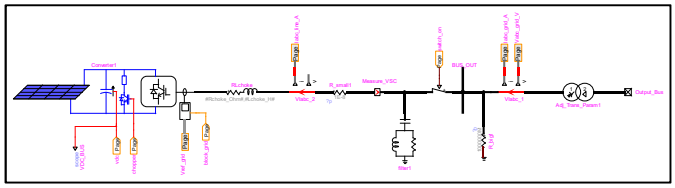

Fig. 1 Simplified one-line diagram of the smart inverter system

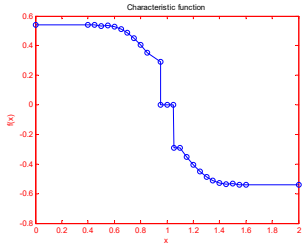

Fig. 2 Voltage-dependent reactive power characteristic (x is voltage in pu)

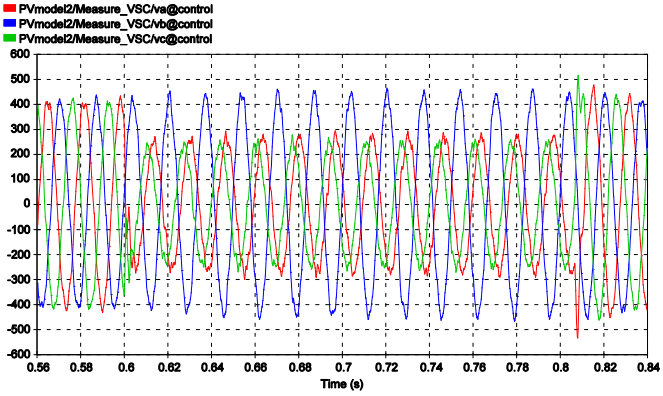

Fig. 3 Three phase voltage measured at the inverter's terminal during a SLG phase A fault beyond a Y-grounded/Δ transformer

[1] F. Katiraei, C. Sun, and B. Enayati, "No Inverter Left Behind: Protection, Controls, and Testing for High Penetrations of PV Inverters on Distribution Systems," *IEEE Power Energy Mag.,* vol. 13, no. 2, pp. 43–49, 2015.
[2] P. Jahangiri and D. C. Aliprantis, "Distributed Volt/VAr control by PV inverters," *IEEE Trans. Power Syst.,* vol. 28, no. 3, pp. 3429–3439, 2013.
[3] A. R. Malekpour and A. Pahwa, "A Dynamic Operational Scheme for Residential PV Smart Inverters," *IEEE Trans. Smart Grid,* vol. 8, no. 5, pp. 2258–2267, 2016.

Multi-parameter Intelligent Energy Forecasting: From Insight to Impact

Nazmus Sakib[1], Eklas Hossain[2], Sheikh Iqbal Ahamed[1]
[1]Department of Mathematics, Statistics and Computer Science, Marqutte University, Milwaukee, WI-53233
[2]Department of Electrical Engineering and Renewable Energy, Oregon Institute Technology, Klamath Falls, OR 97601
nazmus.sakib@marquette.edu, eklas.hossain@oit.edu, sheikh.ahamed@mu.edu

***Abstract*– This work is aimed at employing data science to develop insights on demand-side management at Oregon Institute of Technology (OIT) by exploring historical load data, load profiles, electricity consumption data, load demand data, time-of-use rates data, critical-peak pricing data, and user behavior data obtained from Oregon Renewable Energy Center. To achieve this, different techniques of data science are compared and evaluated according to their influence on different parameters of forecasting. The final outcome of this work is a framework based on the data-driven insights for intelligent decision-making and real-time interaction for the OIT system. Along the course of this work, the state-of-the-art Big Data collection, storage, and management techniques for energy systems, along with their mining and analysis techniques are explored.**

***Keywords*–** *Big Data, Multi-parameter Intelligent Forecasting, Machine learning, Demand-side management, Energy Forecasting.*

I. Research Objectives

In this work, we seek to answer the following three research questions: 1) how can we design advanced computational sciences techniques in collecting, storing, and managing large-scale noisy energy data streams after exploring the start-of-the-art techniques in this regard? 2) How can we improve data computation, mining, and analysis in dealing with the real-time, dynamic energy data addressing the salient features and limitation of the start-of-the-art computation techniques for the existing system at OIT? 3) How can we come up with the valid decisions, insights, and values for the existing system at OIT, and test its efficacy, particularly by working with collaborators in the energy domain? The scope of this research- for both the theoretical study and analytics- will be limited to the specific area requirement from the Oregon Renewable Energy Center for demand-side management.

II. Data Science Intervention in Energy Systems

In a popular conceptualization, Big Data is defined by its "3V" characteristics: Variety, Volume, and velocity. In the era of Big Data, as Data Scientists, it is our onus to extract significant "Value" from the large "Volume" of wide "Variety," and high "Velocity" captured data. This "Value" can be characterized by a "3E" model: Energy, Exchange, and Empathy. Here, the "energy" refers to the energy saving achieved from the analytics, "exchange" to the integration of other data sources for better realization, and " empathy" to the better energy services and the consequent satisfaction of the consumers. In this project, our step-by-step research plan is aligned to meet "3E" of energy science domain leveraging the "Value" of "3V" of Data Science (Fig.1.). The primary initial result of our analytics is depicted below in Fig. 2. It endeavors to find out a pattern in energy consumption in different meters as well as in different time of two different years (2013 and 2014). From the pattern, we aim to predict and compare the consumption for 2015.

Fig. 1. Data science intervention in energy system: from insight to impact.

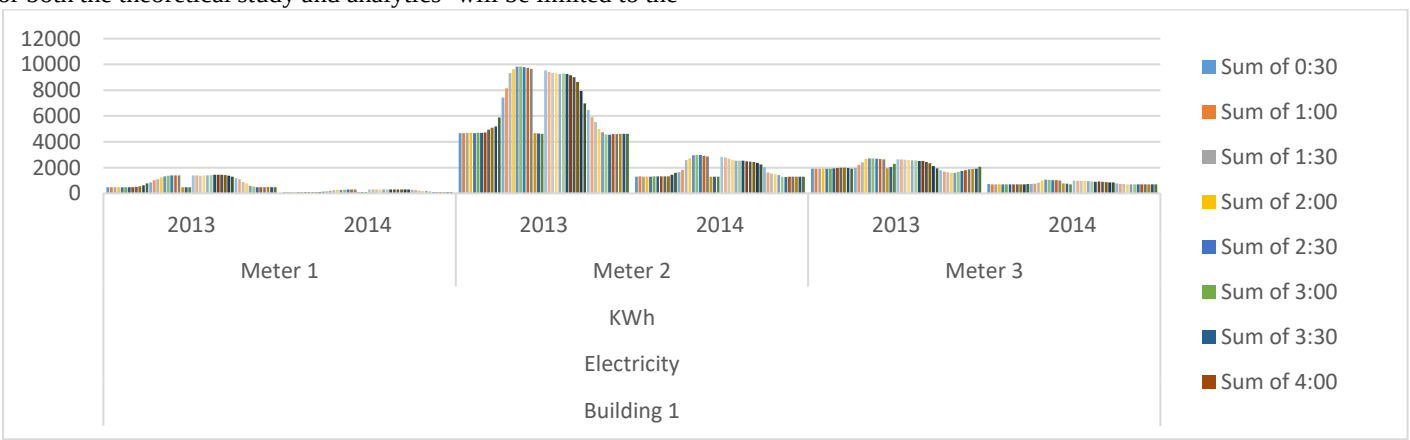

Fig. 2. Energy consumption as recorded by three different meters at different times of the day over two years.

Adaptive Phasor Estimation Algorithm Using Improved KFs under Steady-State/Dynamic Conditions

Yinfeng Wang, Chao Lu
Department of Electrical Engineering
Tsinghua University
Beijing, China
Email: luchao@tsinghua.edu.cn

Chen Fang, Ping Ling
Shanghai Electric Power Research Institute
State Grid Corporation of China
Shanghai, China

***Abstract*—Devoted to balancing the performance of phasor estimation under steady-state and dynamic conditions, this paper proposes an adaptive phasor estimation algorithm based on two improved Kalman filters (KF). A moving average method is adopted to increase the signal to noise ratio (SNR) of measurements in traditional Kalman filter. Besides, a real-valued operations based Taylor-Kalman filter (RTKF) is developed to reduce the computational complexity of traditional TKF. Then, the two KFs are initialized by rough frequency estimates and updated by precise ones sequentially. The appropriate results corresponding to the current conditions are adaptively selected by a fast change detector based on residuals. Tests under steady-state and dynamic conditions demonstrate the effectiveness of the whole algorithm.**

***Index Terms*—Phasor estimation, improved Kalman filter, moving average, computational complexity, fast change detector.**

I. Introduction

Recently, some researches have designed several algorithms that attempts to simultaneously meet the requirements of both P-class and M-class PMUs. However, this potential superiority is achieved at expense of more complex structure and extra computation burden.

In this paper, we continue the efforts to integrate the M-class and P-class PMUs, and design an adaptive phasor estimation algorithm via two improved KF and TKF methods. This algorithm is focused on the accuracy improvement of the traditional KF and the computational reduction of the traditional TKF.

II. Proposed Algorithm

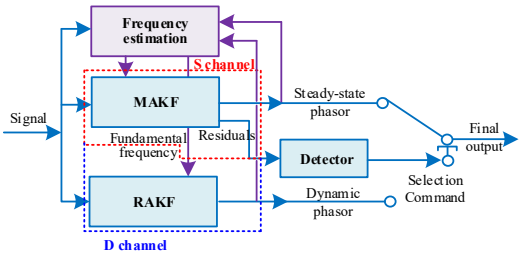

Fig. 1 Framework of the proposed algorithm

A. The S channel based on MAKF

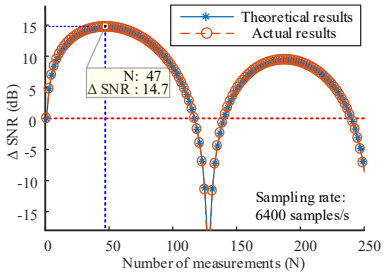

Fig. 2 Comparison of the theoretical and actual ΔSNR

Process model: $\mathbf{X}(k)=\mathbf{A}\mathbf{X}(k-1)+w_k$ (1)

Measurement model: $\bar{s}_N(k)=\mathbf{H}\mathbf{X}(k)+\bar{v}_k$ (2)

B. The D channel based on RTKF

$$\mathbf{x}_i(t)=\begin{bmatrix}\mathbf{R}_i(t)\\ \mathbf{I}_i(t)\end{bmatrix}=\begin{bmatrix}\mathbf{F}(\tau)\cos(2\pi f\tau_i) & -\mathbf{F}(\tau)\sin(2\pi f\tau_i)\\ \mathbf{F}(\tau)\sin(2\pi f\tau_i) & \mathbf{F}(\tau)\cos(2\pi f\tau_i)\end{bmatrix}\begin{bmatrix}\mathbf{R}_i(t_0)\\ \mathbf{I}_i(t_0)\end{bmatrix}=\mathbf{\Phi}_i(\tau)\mathbf{x}_i(t_0) \quad (3)$$

where $\mathbf{R}_i(t)=\left[R_i(t),\dot{R}_i(t),\cdots R_i^{(K)}(t)\right]^T$, $\mathbf{I}_i(t)=\left[I_i(t),\dot{I}_i(t),\cdots I_i^{(K)}(t)\right]^T$.

C. Fast Change Detector

$$d^2{}_n=\hat{v}_k{}^T\left(\mathbf{H}\mathbf{P}(k\,|\,k-1)\mathbf{H}^T+R\right)^{-1}\hat{v}_k \quad (4)$$

with $\hat{v}_k=\left(\bar{s}_N(k)-\mathbf{H}\mathbf{X}(k)\right)$ is the residual vector based on the steady-state results. $d^2{}_n$ is the detection factor.

D. Frequency estimation module

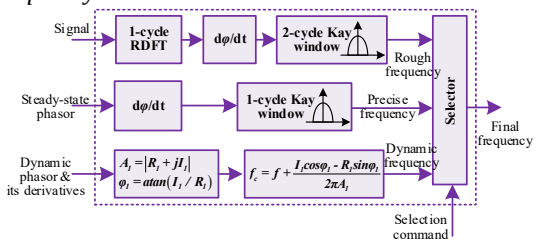

Fig. 3 Structure of the frequency estimation module

III. Performance Evaluation

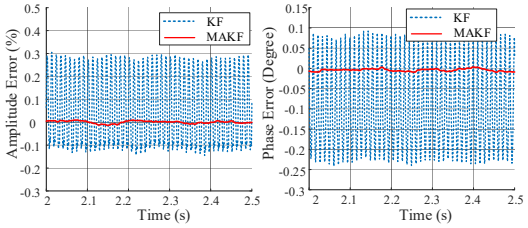

Fig. 4 Test results based on the steady-state signal

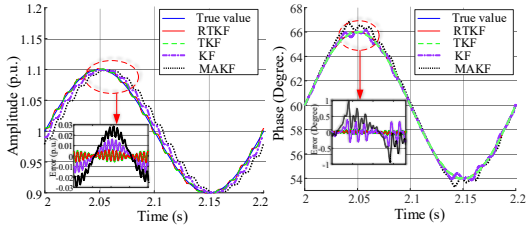

Fig. 5 Test results of the amplitude and phase modulation.

TABLE I. Computation Complexityies of the TKF and RTKF

Complexity	Number of real addition	Number of real multiplication	Time for 1 min estimations
TKF	$M_k\times(5K^2+11K+5)$	$M_k\times(4K^2+12K+5)$	1.38 s
RTKF	$M_k\times(2K^2+2K+1)$	$M_k\times(2K^2+4K)$	0.54 s

Frequency Ramp Test: To test the frequency tracki

IV. Conclusion

This paper designs a KF based phasor estimation algorithm to balance the dynamic and steady-state requirements.

Robust Unit Commitment and Dispatch Considering with Atmospheric Pollutant Concentration Constraints

Yongcan Wang, Suhua Lou, Yaowu Wu, Mengxuan Lv
State Key Laboratory of Advanced Electromagnetic Engineering and Technology
Huazhong University of Science and Technology, Wuhan, 430074, China
Email: wangyc@hust.edu.cn

***Abstract*—With the increasing problem of air pollution, improving atmospheric quality has been attracting more attentions in the worldwide, especially in coal-burning areas. As an important emission source of atmospheric pollutant, the scheduling strategy of coal-fired power plants has a significant impact on atmospheric quality. It should be worthy to note that the relationship between atmospheric quality and the total amount of pollutant emissions is non-linear. The pollutant concentration in atmosphere, not only depends on pollutant emissions, but also depends on meteorological conditions, i.e. the ability of atmospheric diffusion. In this paper, a day-ahead unit commitment and dispatch model of power system considering with pollutant concentration constraints is developed to improve atmospheric quality. In addition, robust optimization is adopted to ensure the robustness of pollutant concentration constraints.**

Keywords—Atmospheric diffusion model, Environmental dispatch, Robust optimization, Pollutant concentration constraints.

I. KEY EQUATIONS

A. Gaussian Puff Model

Pollutant released into the atmosphere is transported by the wind, and mixed into the surrounding air by turbulent eddies and molecular diffusion. The Gaussian puff model is an analytical model to describe atmospheric pollutant transfer and diffusion of non-continuous and no-constant pollutant source.

$$C(x,y,z,t)=\sum_{t_0=-\infty}^{t_0=t}\frac{C_xC_yC_zQ\Delta t}{(2\pi)^{3/2}\sigma_x\sigma_y\sigma_z}=C_{pollu}(x,y,z,t)\times Q \tag{1}$$

$$C_x=\exp[-\frac{(x-x_0-X)^2}{2\sigma_x^2}] \tag{2}$$

$$C_y=\exp[-\frac{(y-y_0-Y)^2}{2\sigma_y^2}] \tag{3}$$

$$C_z=\exp[-\frac{(z-z_0-Z)^2}{2\sigma_z^2}]+\exp[-\frac{(z+z_0-Z)^2}{2\sigma_z^2}] \tag{4}$$

B. Robust Unit Commitment and Dispatch Model

The proposed model aims to minimize total fuel cost in the worst-case, and immunize against all realizations of net load uncertainty. The ground level pollutant concentration near populated regions is considered as a particular constraint.

$$\max_{P_t^L}\min_{u,P}\quad\sum_{i=1}^{N}\sum_{t=1}^{T}(F_{i,t}+ST_{i,t}) \tag{5}$$

$$\sum_{i=1}^{N}\{C_{pollu,i}(x,y,2,t)\times[Q'_{i,t}+Q''_{i,t}]\}\le C^{\max} \tag{6}$$

$$Q'_{i,t}=\xi_iP_{i,t}+\gamma_iu_{i,t} \tag{7}$$

$$Q''_{i,t}=q_{i,t}EU_i/T_{\text{stup},i} \tag{8}$$

$$q_{i,t}=\max\{r_{i,t+1},\ r_{i,t+2},\ \ldots,\ r_{i,t+T_{\text{stup},i}}\} \tag{9}$$

II. KEY RESULTS

Based on a three-unit power system, two cases (case 1 with 500μg/m^3 pollutant concentration constraint, case 2 without pollutant concentration constraint) are simulated. Fig. 1 and Fig.2 depict the hourly pollutant concentration and power outputs of three units for two different cases, respectively. Results show that the proposed mole is effective to control the pollutant concentration of concerned regions by changing power outputs strategically.

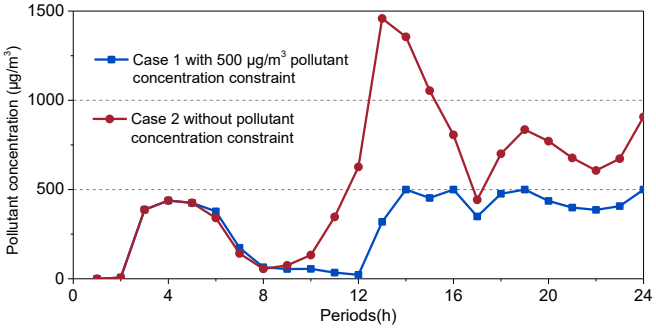

Fig. 1 The hourly pollutant concentration of controlled location

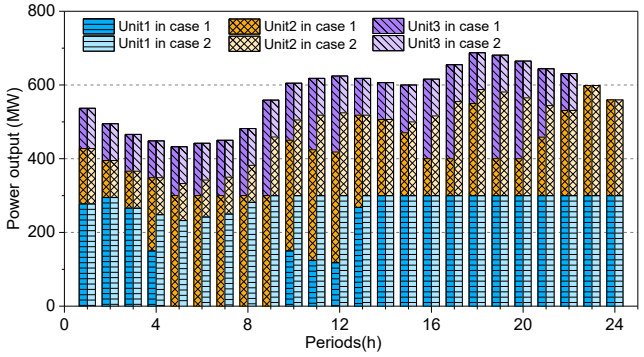

Fig. 2 The hourly power outputs of three units

Coordinated Power Allocation and Robust DC Voltage Control of UPQC with Energy Storage Unit During Source Voltage Sag

Ziwen Liu, Shihong Miao, Zhihua Fan, Kaiyun Chao, Yilong Kang

***Abstract*—Reasonable power allocation and robust DC voltage response are essential requirements of unified power quality conditioner (UPQC) during source voltage sag. Motivated by this objective, this paper presents a control scheme for UPQC based on an improved UPQC-Q power allocation strategy and sliding mode control of DC side voltage. The prominent features of the proposed scheme are: 1) The active power needed for compensating the voltage sag is eliminated and the feeder current is reduced during the source voltage sag; 2) The VA loading of the series and shunt converters are controlled to be maintained within the rated capacity range; 3) The sliding mode control of DC voltage can effectively suppress the external disturbance and improve the robustness of UPQC during source voltage sag. Simulations are presented to validate the effectiveness of the proposed control.**

***Index Terms*—Unified power quality conditioner; Energy storage unit; Coordinated power allocation; Robust control**

I. Introduction

A coordinated power allocation scheme and an improved sliding mode DC voltage control of UPQC are proposed. With the power allocation scheme, the active power needed for compensating the voltage sag is eliminated and the feeder current is reduced. Meanwhile, the VA loading of the series and shunt converters can be maintained within the rated capacity range. In addition, the improved sliding mode DC voltage control can suppress external disturbance without any chattering.

II. Key Equations and Schematic Diagram

A. The series compensation voltage

$$\begin{cases} \left|V'_{sr}\right| = \sqrt{V'^2_L - V'^2_S} = V\sqrt{1-k^2} \\ \angle\varphi_{sr} = 90° \end{cases} \tag{1}$$

B. The shunt compensation current

$$\begin{cases} \left|I'_{sh}\right| = I\sin\varphi_L \\ \angle\varphi_{sh} = 180° - \sin^{-1}\left(\dfrac{\sin\beta}{\sin\varphi_L}\right) \end{cases} \tag{2}$$

C. Power control schematic diagram

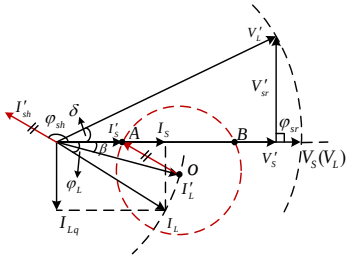

Fig. 1. Power control strategy of the improved UPQC-Q

D. The disturbance observation

$$\begin{cases} \dot{\hat{x}}_1 = u_e x_2 / C - \hat{w} \\ \hat{w} = -k_{DO}\left(x_1 - \hat{x}_1\right) \end{cases} \tag{3}$$

E. The proposed sliding-mode control

$$u = -\frac{a}{b} + \frac{C}{bu_e}\left(-k_1\frac{u_e}{C}x_2 - k_2 e - k_{tr}\,\mathrm{sgn}(s)\right) + \frac{C}{bu_e}\cdot k_1\hat{w} \tag{4}$$

III. Key Results

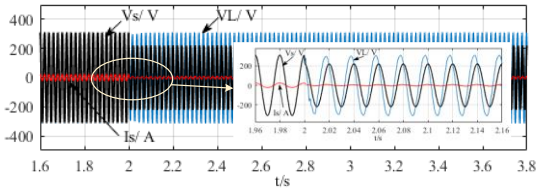

(a) Source voltage, load voltage and feeder current

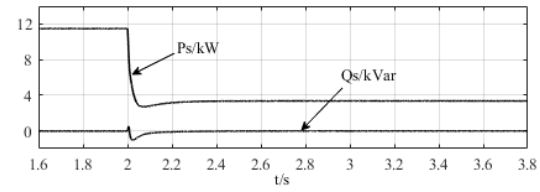

(b) Active and reactive power of the source

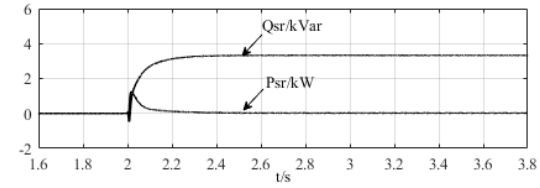

(c) Active and reactive power of the series converter

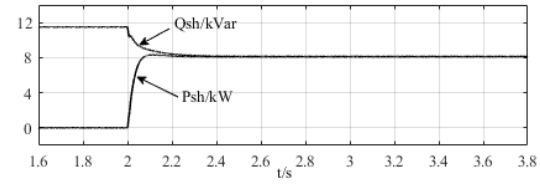

(d) Active and reactive power of the shunt converter

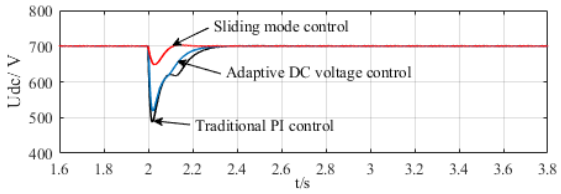

(e) DC voltage with different controls

Fig. 2. Simulation results of case 1

During source voltage sag, the coordinated power allocation among UPQC units is realized and the DC voltage with the proposed control can be restored to normal state with improved transient performance.

Distributed Voltage Control for Demand Response

Jinrui Guo, Balarko Chaudhuri
Imperial College London, United Kingdom
j.guo16@imperial.ac.uk
b.chaudhuri@imperial.ac.uk

Shu Yuen Ron Hui
The University of Hong Kong, Hong Kong, China
Imperial College London, United Kingdom
ronhui@eee.hku.hk

***Abstract*—Distributed voltage control (DVC) at the points of connection of individual loads could provide larger demand flexibility compared with voltage control at substations (VCS). This is especially true during high loading conditions as the allowable voltage reduction would be largely limited. This paper quantifies the demand reduction capability through DVC and compared with that of VCS using a 24 hour high-resolution stochastic demand model. Implementing DVC would require voltage compensators, the cost of which is carefully evaluated to weigh the benefits. The results are firstly shown through a synthesized low voltage network with random distribution of clusters of domestic customers and random length of feeder sections. Then, conclusions are further justified using a Cigre benchmark medium- and low-voltage (MV/LV) network. A case study on an islanded microgrid shows that DVC produces better frequency control with wind power fluctuations.**

***Index Terms*—Demand response, voltage control, demand reduction, microgrid**

I. Methodology and Key Equations

Distributed voltage control (DVC) could be realized using a power electronic compensator (PEC) which decouples a cluster of domestic customers (CDC) from the low voltage (LV) feeder. The supply voltage to each CDC could be reduced independently to its stipulated limit which would offer more flexibility for demand reduction (DR). The total DR through DVC is given by (1) and compared against that from VCS.

$$DR = \sum_{i=1}^{N_b} P_{i0}\left[V_{Bi}^{n_{pi}} - V_{min}^{n_{pi}}\right] - \Delta P_{LL} - \sum_{i=1}^{N_b} P_{LCi} \quad (1)$$

where, N_b is the total number of CDC, ΔP_{LL} is the change in network power loss and P_{LCi} is the total loss of PECs.

Improved DR capability through DVC comes at the expense of requirement of PECs at each CDC. To exercise maximum reduction in CDC voltage, the voltage injected by PEC is designed in phase with the feeder-side voltage. The apparent power processed by the PEC at ith CDC can be given as:

$$S_{Ci} = (V'_{Bi} - V_{min})\sqrt{P_{i0}^2 V_{min}^{2(n_{pi}-1)} + Q_{i0}^2 V_{min}^{2(n_{qi}-1)}}\,(1 + pf'_i) \quad (2)$$

where, V'_{Bi} and pf'_i are the modified feeder-side voltage and power factor due to reduction in voltage of the ith CDC.

The 24 hour high-resolution demand and power exponent profile of individual domestic customers, which would be aggregated to form CDCs at each LV feeder during DR capability calculation, is generated using a demand model developed by the Centre for Renewable Energy Systems Technology.

II. Key Results

Index ΔDR indicates the DR capability of VCS compared with that through DVC. The investment in PECs could be recovered by utilizing the DR capability from DVC to cut down the necessity for conventional operating reserve.

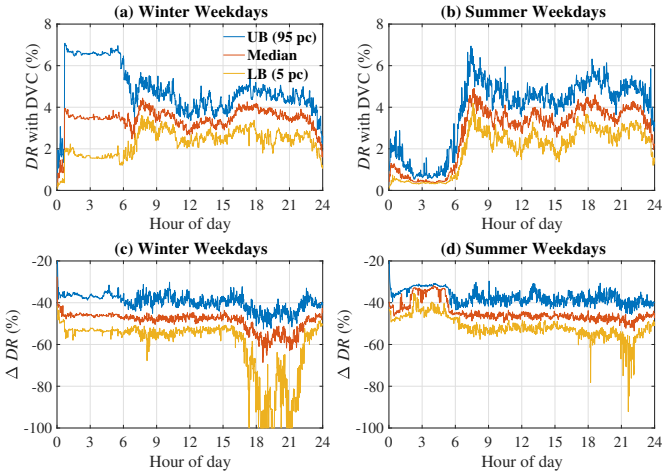

Fig. 1. Results through a synthesized LV network (a) ΔDR and (b) DR Capability through DVC for winter weekdays; (c) ΔDR and (d) DR Capability through DVC for summer weekdays

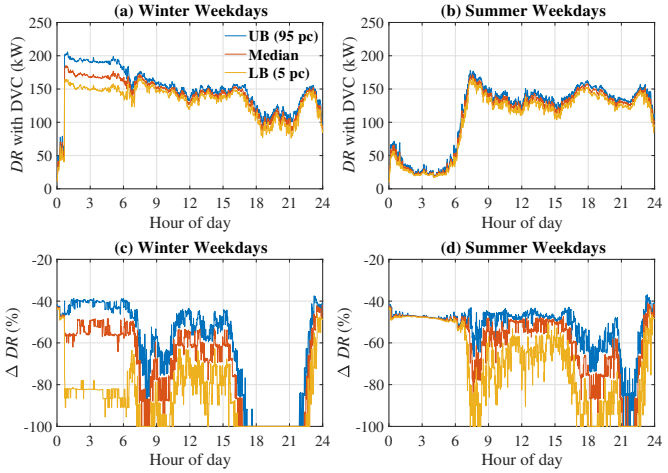

Fig. 2. DR capability from DVC and comparison with that of VCS (ΔDR) through a Cigre benchmark MV/LV network for winter and summer weekdays

Progressive Time-differentiated Peak Pricing (PTPP) for Aggregated Air-conditioning Load in Demand Response Programs

Yunwei Shen, Fangxing Li

Department of Electrical Engineering and Computer Science, the University of Tennessee, Knoxville, TN 37996, USA;
yshen26@utk.edu, fli6@utk.edu

***Abstract*—The continuous increase of peak load in China has posed a significant challenge to the safety and stability of the power grid. By reasonable control of the air-conditioning (AC) load, peak load could be reduced and balance could be achieved between supply and demand at lower cost without affecting customers' comfort. In this paper, a baseline model of the aggregated AC load is introduced and simplified to describe the relationship between temperature setpoint and AC power and the relationship between the electricity price and the temperature setpoint of AC is described based on the consumer psychology theory. Then, a new demand response (DR) project called Progressive Time-differentiated Peak Pricing (PTPP) for the AC load is designed. Finally, case study proves the feasibility of the optimal price mechanism proposed in this paper. The influence of different price shapes and different compositions of consumers on simulation results is analyzed, providing a theoretical basis and reference data for the practical implementation of PTPP.**

***Keywords*—Demand response, Critical peak pricing, Time-differentiated peak pricing, Air-conditioning**

I. MODELING METHODOLOGIES

A. Thermal Dynamic models of a single AC

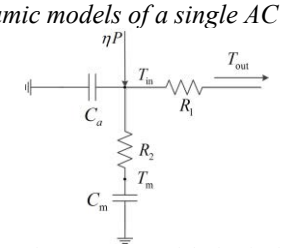

Fig. 1. Equivalent thermal parameters model of a single air-conditioning unit.

$$T_{\mathrm{i}}^{t+1} = T_{\mathrm{o}}^{t+1} - (T_{\mathrm{o}}^{t+1} - T_{\mathrm{i}}^{t})\mathrm{e}^{-\frac{\Delta t}{RC}}, \quad s=0 \quad \forall t \in [1,\cdots,\Gamma-1] \quad (1)$$

$$T_{\mathrm{i}}^{t+1} = T_{\mathrm{o}}^{t+1} - \eta PR - (T_{\mathrm{o}}^{t+1} - \eta PR - T_{\mathrm{i}}^{t})\mathrm{e}^{-\frac{\Delta t}{RC}}, \quad s=1 \quad \forall t \in [1,\cdots,\Gamma-1] \quad (2)$$

Where T_o is the ambient temperature, °C; T_i is the air temperature inside the house, °C; C and R are the equivalent heat capacity, J/°C and the equivalent thermal resistance, °C/W respectively; P is the cooling/heating power of the AC unit, kW; η is coefficient of performance (COP); s is the AC on/off state variable, and 1 means on while 0 means off. Furthermore, the aggregated power consumption of N ACs can be obtained without intentional interference such as manual control and price signal:

$$L_{AC,t}^{uncontrolled} = \sum_{n=1}^{N} P_n \times s_{n,t} \quad \forall t \in [1,\cdots,\Gamma] \quad (3)$$

Assume Tset represents the temperature setpoint and δ denotes temperature deadbands. The indoor temperature limits [Tmin, Tmax] could be calculated by (4) and (5).

$$T_{\min} = T_{set} - \delta/2 \quad (4)$$

$$T_{\max} = T_{set} + \delta/2 \quad (5)$$

B. Consumer psychology theory

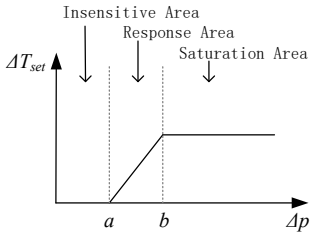

Fig. 2. Relationship between Δp and $\Delta Tset$

C. Simplified method to calculate AC load variation

$$L_{ACcut,t} = \sum_{i=1}^{N_{agg}} \alpha_i \times \Delta T_{i,t}^{\ 2} + \beta_i \times \Delta T_{i,t} + \gamma_i \quad \forall i \in [1,\cdots,N_{agg}], \forall t \in [1,\cdots,\Gamma] \quad (6)$$

$$L_{ACrebound,t} = x_1 L_{ACcut,t-1} + x_2 L_{ACcut,t-2} + x_3 L_{ACcut,t-3} \quad \forall t \in [4,\cdots,\Gamma] \quad (7)$$

$$L_{AC,t} = L_{ACbase,t} - L_{ACcut,t} + L_{ACrebound,t} \quad \forall t \in [1,\cdots,\Gamma] \quad (8)$$

II. PTPP OPTIMIZATION MODEL

The objective function of the PTPP optimization model is set to minimize the difference between the response load reduction and the target load reduction.

$$Min \sum_{t=1}^{\Gamma} (L_{AC,t} - L_{ACbase,t} - L_{target,t})^2 \quad (9)$$

subject to:

Equations (1)-(8)

$$\Delta T_{i,t} = \begin{cases} 0 & 0 \le \Delta p_{i,t} \le a_i \\ K_i \times (\Delta p_{i,t} - a_i) & a_i \le \Delta p_{i,t} \le b_i \\ \Delta T_{i,\max} & \Delta p_{i,t} \ge b_i \end{cases} \quad \forall i \in [1,\cdots,N_{agg}], \forall t \in [1,\cdots,\Gamma] \quad (10)$$

$$(u_{i,t} - u_{i,t-1}) + (u_{i,t+\tau-1} - u_{i,t+\tau}) \le 1 \quad \forall t \in [2,\cdots,\Gamma-1], \forall \tau \in [1,\cdots,N_{CPP}-1] \quad (11)$$

$$\sum_{t=1}^{\Gamma} u_{i,t} = N_{CPP} \quad \forall i \in [1,\cdots,N_{agg}] \quad (12)$$

$$p_{CPP,\min} \le \Delta p_{i,t} * p_{base} \le p_{CPP,\max} \quad \forall i \in [1,\cdots,N_{agg}], \forall t \in [1,\cdots,\Gamma] \quad (13)$$

$$\max(L + L_{AC} - L_{ACbase}) \le \max(L + L_{target}) \quad (14)$$

III. SIMULATION AND DISCUSSIONS

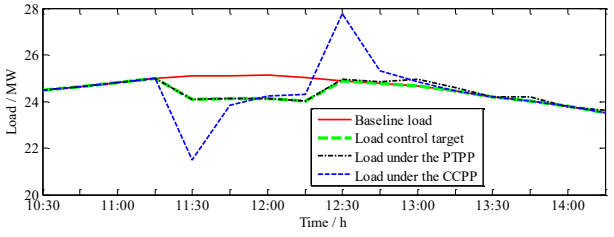

Fig. 3. Aggregated AC load under different pricing mechanisms

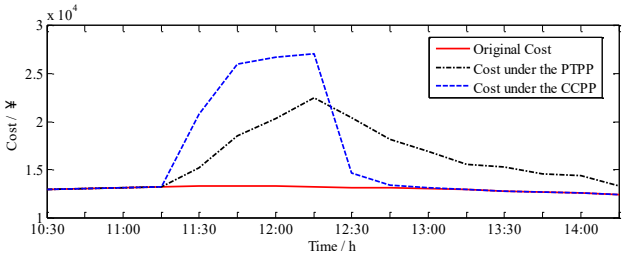

Fig. 4. Total electricity cost under different pricing mechanisms

A Multilevel Dual Converter fed Open end Transformer Configuration for Hybrid AC-DC Microgrid

Krishna Chaithanya Bandla, Student Member IEEE, Narayana Prasad Padhy, Senior Member IEEE
Department of Electrical Engineering, Indian Institute of Technology Roorkee, India

***Abstract*— Recent trends in renewable source integration and advancements in electric loads led to the emerging of local DC microgrids. However, due to majority of AC loads hybrid AC-DC microgrids are formed, incorporating feasible power converters as medium of power flow. Instead of conventional bidirectional AC-DC and DC-DC converters as interlinking converters in hybrid AC-DC microgrid, an open-end transformer based multilevel converter configuration is proposed as interlinking converter in this paper. The converter configuration includes two converters concatenated with primary of transformer, is a unique substitution for conventional multiple converters utilized. The salient features of the configuration include reduced control complexity, inherent isolation from AC grid, and able to provide inter-grid bidirectional power flow. A modified control scheme is proposed for precise power flow control in the system. Real time simulation of the proposed configuration of hybrid AC-DC microgrid is implemented in RSCAD/RTDS and experimented on a scaled hardware prototype. The outcomes depict the potency of control scheme in inter-grid power flow control.**

***Index Terms*—Multilevel Inverter, Open-end winding transformer, Power flow control, Hybrid AC-DC microgrid.**

I. INTRODUCTION

In this paper, Multi-level converter configuration for Hybrid AC-DC microgrids is proposed. Further, a modified power flow control scheme to synthesize accurate power flow among hybrid AC-DC microgrid is proposed. The converter topology acts as interfacing converter between AC and DC micro-grids as shown in Fig.1. This includes two 3-phase voltage source converter (VSC) modules connected differentially to both the ends of primary winding of the transformer. The VSC modules utilized are easily available, thus reducing the effort of designing new circuitry for prototype design. The secondary of transformer is connected to AC grid. The key feature of the converter configuration is its ability to interface dissimilar voltage rated DCMGs to AC grid simultaneously with multilevel output voltage. The advantages of transformer in this configuration are suppression of DC component in current fed to grid, isolation of DCMGs from AC grid and acts as filter inductance at primary side.

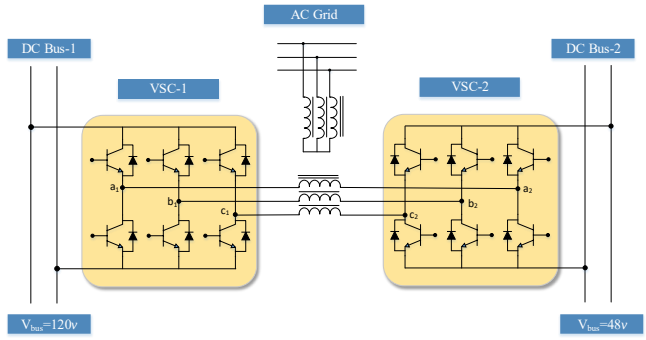

Fig. 1. Open end transformer-based converter configuration for hybrid micro-grid.

II. POWER FLOW CONTROL SCHEME

The modified control scheme utilizes a primary and secondary control of which primary control is a centralized control for both VSCs and secondary control is a localized control for each VSC. Primary control involves regulating the active and reactive power flow to AC grid form the DCMGs. The secondary control modifies the output of primary control such that required response is achieved from the DCMGs.

III. EXPERIMENTAL RESULTS

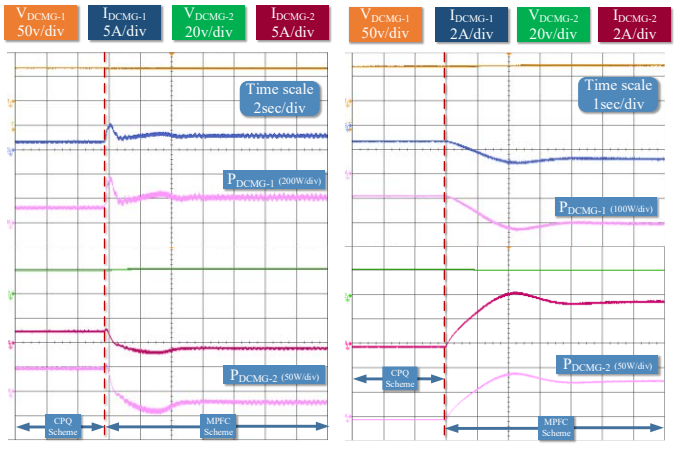

Fig. 2. Experimental results of Hybrid AC-DC microgrid for different power flow scenarios.

Reactive Power Support from EVs for Distribution Grid Voltage Management

Jingyuan Wang, *Student Member, IEEE,* and Sumit Paudyal, *Member, IEEE,*
Michigan Technological University, USA
Email: jwang11@mtu.edu, sumitp@mtu.edu

***Abstract*—In this paper, we first developed optimal distribution power flow and optimal EV charging models, which utilize reactive power injection capability of the EVs to support the grid. We demonstrated the benefits of dispatching reactive power from EVs to the grid operation and also to the EV owners. Reactive power dispatch from EVs could help manage distribution grid constraints, e.g., undervoltage issues caused by the active power consumption during the EV charging. We have shown that in coordinated charging scheme, if EVs agree to inject reactive power into the grid, it benefits EVs by reducing the costs of charging the EVs in dynamic energy pricing schemes. We have also demonstrated that the reactive power injection from EVs can be coordinated with the load shifting and load curtailment in demand response applications to help accommodate increased number of EVs on constrained grids.**

***Index Terms*—Electric vehicles, optimization, distribution grid, demand response, reactive power control.**

I. Key Equations

The optimization objective of this model is to minimize the total power loss on the distribution grid as well as the active power shifting and curtailment of EV loads.

$$\Omega_2 = P^{loss} + \sum_{m,k}(\lambda_1 P^{sh}_{m,k} + \lambda_2 P^{ct}_{m,k}) \tag{1}$$

where P^{sh} stands for active power shifting and P^{ct} stands for active power curtailment.

EVs can provide reactive support back to distribution grid. There are lower and upper limits for reactive power which EVs could provide, which can be mathematically modeled as following,

$$Q^{min}_{m,k} \leq Q_{m,k} \leq Q^{max}_{m,k} \tag{2}$$

where

$$Q^{min}_{m,k} = -\sum_{e}\sqrt{R^2_{m,e} - P^{ev^2}_{m,k,e}} \tag{3}$$

$$Q^{max}_{m,k} = \sum_{e}\sqrt{R^2_{m,e} - P^{ev^2}_{m,k,e}} \tag{4}$$

II. Key Figures

Figure 1-a) shows a high-level schematic of the proposed coordinated EV charging, where EVs support reactive power to the grid while charging the EVs at lowest possible costs. In this work, we consider EVs operating on the first and fourth P-Q quadrants to demonstrate the concept, i.e., EVs can inject/withdraw reactive power while charging.

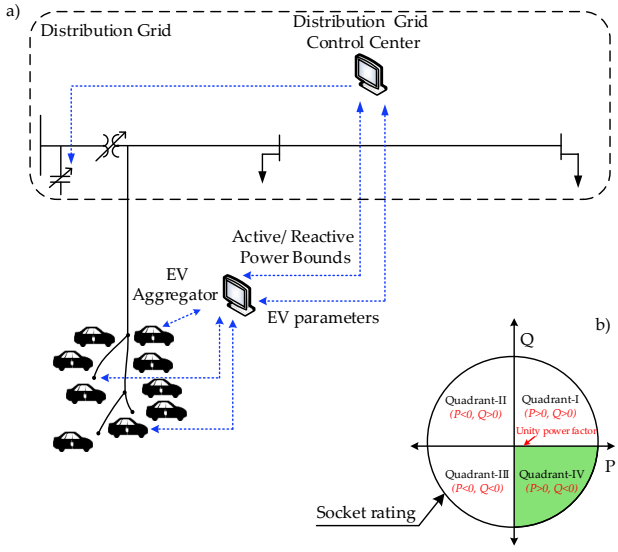

Fig. 1. a) High-level overview of the proposed active/reactive power scheduling of EVs, and b) Charging region of EVs.

III. Key Results

Voltage profile of node-18 is shown in Fig. 2. Voltages at node-18 are within the limit from 0.95 p.u to 1.05 p.u. when EVs operate in non-unity power factor mode. When EVs operate at unity power factor mode, voltages at node-18 (and other nodes) are below 0.95 p.u. at some of the time intervals.

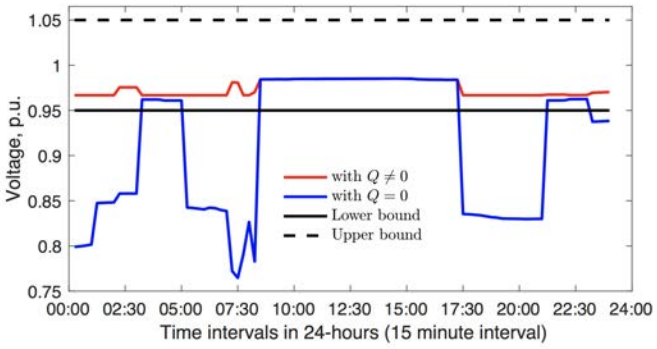

Fig. 2. Voltage profile at node-18 with and without reactive power support.

2018 IEEE PES General Meeting, Portland, OR USA
5-9 August 2018

Joint Planning of BESS and DR for industrial consumers participating in peak-shaving

Xiao, Hu
Shanghai Jiao Tong University
Shanghai, China

Li, Wang
Guangzhou Power Supply
Guangzhou, China

Introduction

In this paper, a joint planning method of battery energy storage systems (BESS) and demand response (DR) designed for exploring the feasibility of industrial consumers participating in the peak-load shaving in IPs distribution system is proposed. This bi-level optimization method considering both planning and operation provides a systemic solution which determines the optimal installed capacity of BESS, layout of BESS and joint economic dispatching of BESS and DR, concurrently. An 11-buses IP distribution system located in Guangdong Province in the south of China is utilized as the study case to verify the validity of proposed method.

Problem Formulation

● *Joint peak-shaving strategy of BESS and D*

Since the production of industrial enterprises will be adversely affected by *DR*, we propose an equivalent cost C_{DR} to represent the reduction loss. A reasonable assumption is that C_{DR} is in proportion to E_{DR}, and then E_{DR} is more suitable to shave the shadow area between L_{max} and L_{div} with a relatively small area.

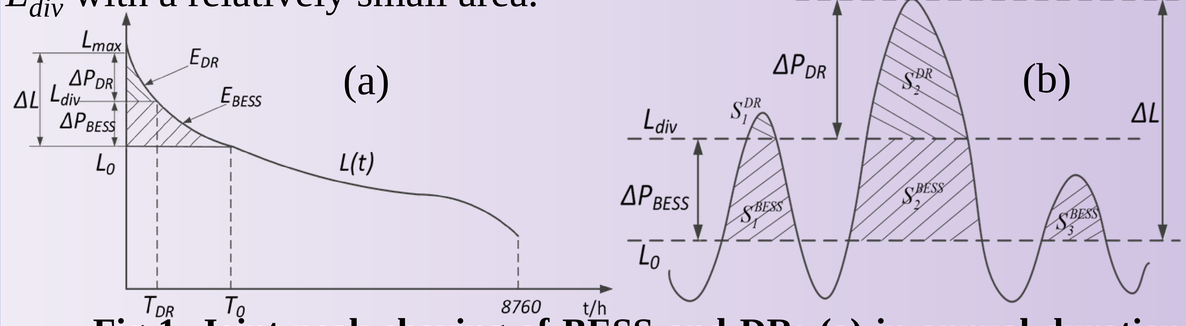

Fig 1. Joint peak shaving of BESS and DR: (a) in annual duration load curve; (b) in annual time-series load curve.

● *Optimization Model*

Total objective:

$$\max f = B_{base} + B_{watt} + B_{PSC} + B_{sub} - C_{BESS\_i} - C_{BESS\_m} - C_{DR} - C_{loss}$$

Level-1 objective:

$$\min \quad f_1 = C_{BESS\_i} + C_{BESS\_m}$$

Level-2 objective:

$$\max \quad f_2 = B_{base} + B_{watt} + B_{PSC} + B_{gov} - C_{DR} - C_{loss}$$

Case Study

An industrial park distribution system containing 11 industrial enterprise consumers is utilized to evaluate the performance of the proposed method.

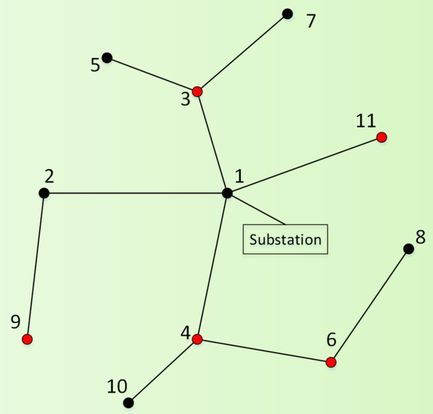

Fig 2. Layout of an 11-buses industrial park distribution system.

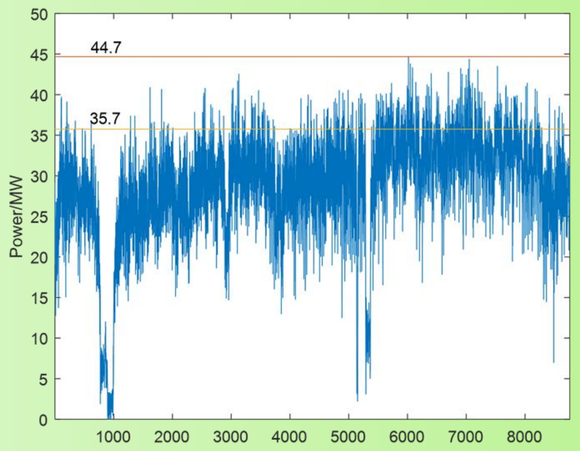

Fig 3. Primary load curve.

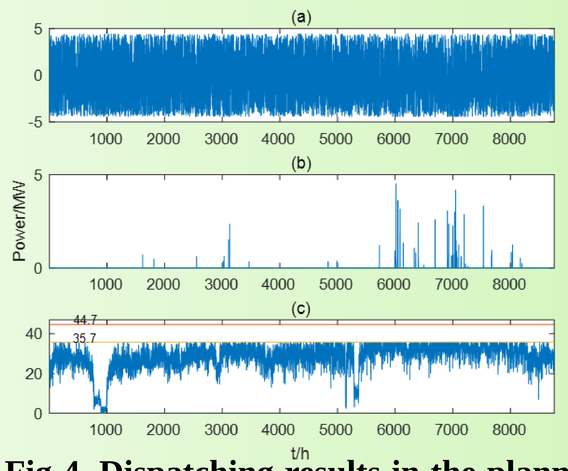

Fig 4. Dispatching results in the planning target year: (a) BESS output; (b) DR output; (c) load curve after peak-shaving

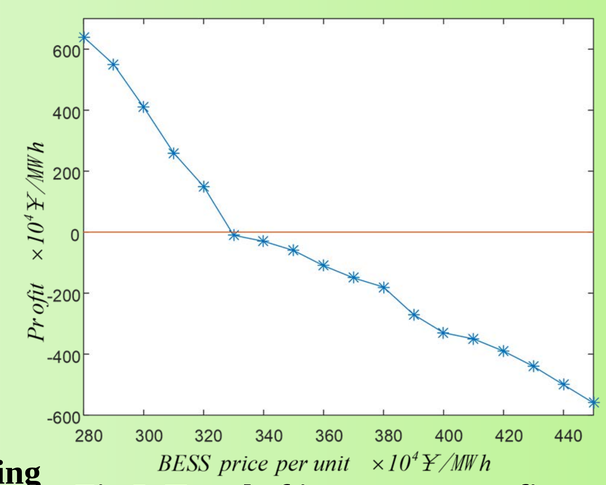

Fig 5. Trend of investment profit varying with BESS price per unit

Conclusion

In our method, the annual time-series and duration load curve are applied to ensure the accuracy of optimization results instead of a typical scenario, because the peak-load periods in IPs present stronger randomness and uncertainty than that in residential districts.At present, industrial consumers participating in peak-load shaving via the joint investment of BESS and DR are unable to get a profit in the investment cycle because of the high price of BESS. But a good prospect for the investment of BESS is indicated.

Stochastic Optimal Transmission Switching Considering N-1 Security Constraints

Heng Zhang
Haozhong Cheng
Department of Electrical Engineering
Shanghai Jiao Tong University
Shanghai, China
hengzhang_ee@163.com

Jianping Zhang
Jianzhong Lu
East China Grid Company Limited
Shanghai, China

Cong Li
State Grid Beijing Electric Power Company
Beijing, China

***Abstract*—A novel multi-scenario based two-level stochastic optimal transmission switching model incorporating economic and N-1 security constraints is presented considering wind farms integration in this paper. The optimal strategy of switching lines is obtained in the upper level, and N-1 security check is carried out in the lower level to test whether the scheme meets the security requirements. Corridor load rate (CLR) is used as index to add new constraints to upper level to accelerate solving process. The Affinity Propagation (AP) clustering algorithm is used to construct different operation scenarios for the sake of handling the short-term fluctuation of load and the intermittence of wind power. The modified IEEE-RTS system is introduced to test the model.**

***Index Terms*—optimal transmission switching, AP clustering algorithm, N-1 security constraints, corridor load rate.**

I. MATHEMATIC MODEL

A. Upper Level

Aiming to minimize the generators fuel cost and load shedding, the OTS model can be presented as follows (In order to avoid isolated island, some lines are forbidden to be switched off.):

$$Min \quad Op = \sum_{\omega \in N} LD_{\omega} * (\sum_{k \in \Xi} OC_k * P_{G,k}^{\omega} + \sum_{b \in \Psi} SC_b * R_{sh,b}^{\omega})$$

$$\text{s.t.} \quad \sum_{k \in \Xi_b} P_{G,k}^{\omega,c} + \sum_{s \in \Xi_b} P_{Re,s}^{\omega,c} + \sum_{\forall m,n \in \Xi_b} f_{mn(i)}^{\omega,c} = P_b^{\omega,c} - R_{sh,b}^{\omega,c} \quad (1)$$

$$\left| f_{mn(i)}^{\omega,c} - r_{mn(i)}^{c} (\theta_m^{\omega,c} - \theta_n^{\omega,c}) \right| \le M * (1 - \alpha_i l_i) \ (i \in \Omega^+) \quad (2)$$

$$\alpha_i * PL_{i,\max} \le f_{mn(i)}^{\omega,c} \le \alpha_i * PL_{i,\max} (i \in \Omega^-) \quad (3)$$

$$\left| f_{mn(i)}^{\omega,c} \right| \le PL_{i,\max} * (\alpha_i l_{ti}) \quad (i \in \Omega^+) \quad (4)$$

$$P_{G,k\min} \le P_{G,k}^{\omega,c} \le P_{G,k\max} \quad (k \in \Xi^-) \quad (5)$$

$$0 \le R_{sh,b}^{\omega,c} \le \lambda_b P_b^{\omega,c} \quad (b \in \Psi) \quad (6)$$

B. Lower Level

In order to reduce solving time, the N-1 security could be realized by adding lines one by one according to corridor load rate (CLR) index until the model converges.The CLR can be obtained by (7):

$$\text{CLR} = \left| f_{mn(i)}^{\omega} / PL_{i,\max} \right| \quad (7)$$

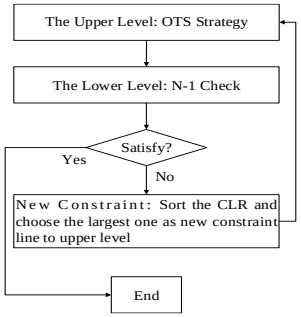

Fig.1 Flow chart of iterative process

II. NUMERCIAL EXAMPLES

TABLE I. OTS RESULTS OF DIFFERENT SWITCHABLE LINES

Number of disconnected lines	Lines disconnected	Generator fuel cost (M$)	Load shedding cost(k$)	AC feasible check
0	-	15.96	0	feasible
1	10-11	14.79	0	feasible
2	9-11,10-11	13.84	617.6	feasible
3	9-11,10-11,17-18	13.73	534.5	feasible
4	1-2,9-11 10-11,17-18	13.71	586.8	feasible

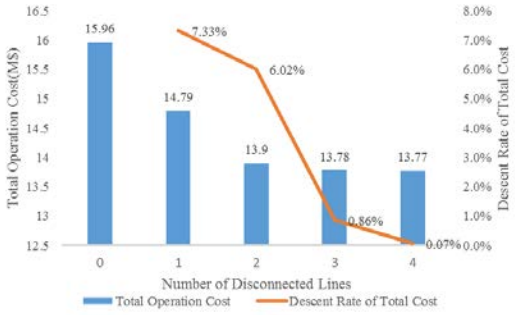

Fig.2. Total operation cost and ratio change with different switchable lines

TABLE II. SOLVING TIME OF SINGLE AND TWO LEVEL MODEL

Number of disconnected lines	1	2	3
Single Level	3682s	11756s	21382s
Two Level	120s	544s	3885s

Peak Energy Management using Renewable Integrated DC Microgrid

P Sanjeev, Student Member IEEE, Narayana Prasad Padhy, Senior Member IEEE
Department of Electrical Engineering, Indian Institute of Technology Roorkee, India

***Abstract*— Thirst for energy is increasing significantly with increase in economy around the world which burdens conventional grid (CG) due to peak demand, energy deficit and carbon emission, but major part of continents has plentiful wind and solar energy which can be harnessed locally to minimize it. Major objective of this research is to reduce the peak power deficit present in CG system and to provide a reliable power supply even in case of grid failure or during blackout. In this paper, development and evaluation of a small-scale grid interactive DC microgrid (DCMG) for residential houses, telecommunication systems and data center has been proposed. The objective is being achieved by designing a comprehensive power flow control strategy and explored for different practical scenarios through real time simulation in RSCAD/RTDS platform. A Prototype is developed to validate the simulation results presented during grid connected and isolated mode.**

Index Terms*— DC Microgrid, energy management, peak energy, power flow control strategy, real time simulation.

I. INTRODUCTION

In this paper, to eliminate the communication link between AC and DC buses, a modified droop control strategy is used for power transfer between AC and DC bus with simple relation between voltage of DC bus and AC bus frequency in order to compensate any power fluctuations on one side by using power on other side. But it considers the synchronous generators and DC voltage sources as renewable sources inside microgrids which unable to mimic intermittency and low inertia characteristics of renewable sources. A simplified power flow control strategy (PFCS) is proposed to mitigate above demerits by considering all cases of grid interactive DCMG along with depreciation of peak energy and energy deficit which ultimately yields to releasing the stress on CG and low carbon foot print.

II. SYSTEM ARCHITECTURE & POWER FLOW CONTROL STRATEGY

Using a DC distribution network, it makes easier to include local renewable energy sources and storage devices. Since modern electronic loads can be supplied with dc without modifying the load itself, it would save the losses incurred during conversions from AC to DC if they are fed directly from AC grid. Grid interactive DCMG system contemplated in this paper which is shown in Fig. 1.

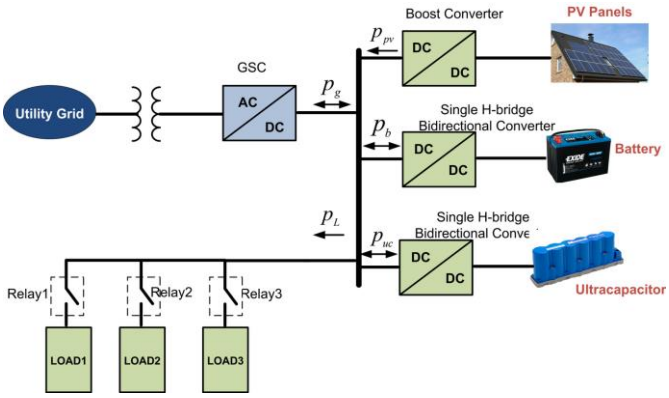

Fig. 1. Grid interactive DCMG structure

III. EXPERIMENTAL RESULTS

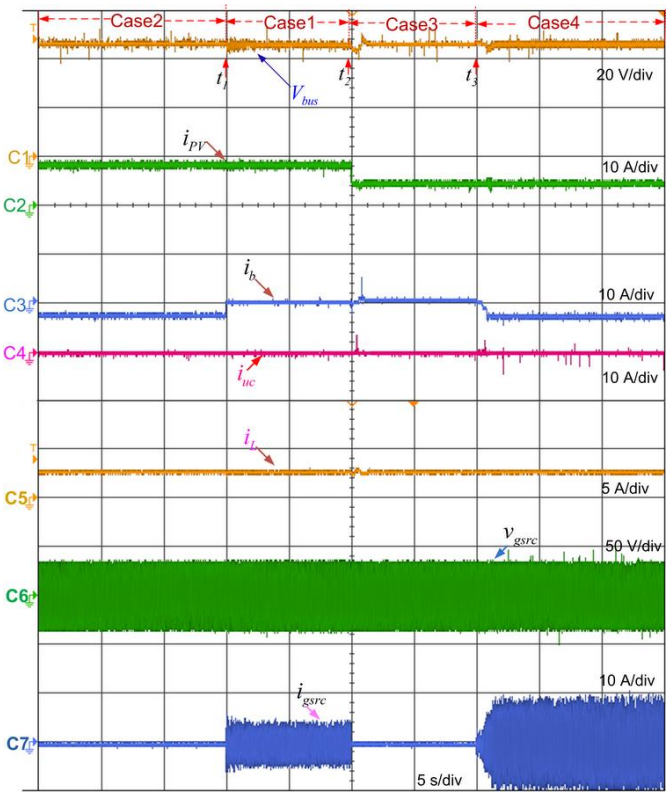

Fig. 2.Experimental waveforms during off peak mode: DC bus voltage (V_{bus}), input currents (i_{pv}, i_b, i_{uc}), load current (i_L), grid side quantities (V_{gsrc}, i_{gsrc}).

A Two-Step Load Disaggregation Algorithm for Quasi-static Time-series Analysis on Actual Distribution Feeders

Jiyu Wang, Xiangqi Zhu, David Mulcahy, Catie McEntee, David Lubkeman, and Ning Lu
Electrical & Computer Engineering Department
FREEDM Systems Center
North Carolina State University, Raleigh, NC
jwang49@ncsu.edu

Nader Samaan
Pacific Northwest National Laboratory
Richland, WA

Brant Werts and Andrew Kling
Duke Energy Carolinas
Charlotte, NC

***Abstract*—This paper focuses on developing a two-step load disaggregation method for conducting quasi-static time-series analysis using actual distribution feeder data. This can help utilities conduct power flow studies using smart meter measurements to assess the impact of high penetration of distributed energy resources. In the first step, load profiles of residential and commercial buildings obtained from smart meter data are used to match the load profile at the feeder head. This step will determine the number of residential and commercial loads on the feeder. The second step is to allocate the selected load profiles to each load node based on its transformer rating. This allows each load node to have its own load profile and the aggregation of those nodal load profiles matches closely to the metered feeder load shape at the substation. This algorithm is validated using smart meter data and the SCADA data of a real feeder. We compared the performance of the proposed method with the traditional load allocation method (i.e. use the feeder load shape for all subsequent load nodes scaling by the transformer capacities) when conducting quasi-static power flow studies. Results show that the proposed algorithm matches the utility data well and the obtained voltage profiles reveal more voltage dynamics than using the conventional load allocation method.**

***Index Terms*—Load disaggregation, load shape, quasi-static time-series analysis, distribution feeder, voltage profile**

I. Introduction

Quasi-static time-series simulation [9] is now widely used to assess the operational characteristics (e.g. voltage profiles, overloading conditions, etc.) of an electricity distribution system. A critical step in the Quasi-static time-series simulation is the allocation of nodal load profiles. In the past, the shape of the feeder head load profile is used for each subsequent load nodes and the load shape is scaled by letting its peak load be scaled based on the distribution transformer capacity at the node [13].

In [16-17], we proposed a load disaggregation method using a load profile database containing hundreds of load profiles. In this paper, we further developed the methodology. The paper has two major contributions. First, because we obtained a yearly utility feeder head load profile with the corresponding yearly smart meter data of all the residential and commercial buildings in the area, we are able to validate the performance of the algorithm by comparing the calculated number of houses and load types with the actual utility information. Second, we reformulated our load disaggregation algorithm into a 2-step algorithm that reflects the two main processes: load profile selection and allocation.

II. Key Figures

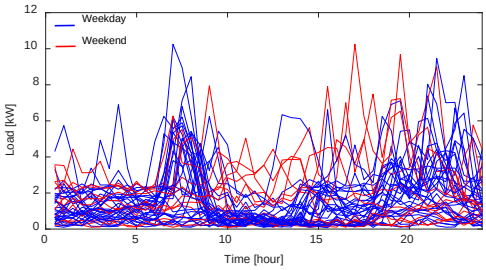

Fig. 1. Monthly energy consumption for a residential house

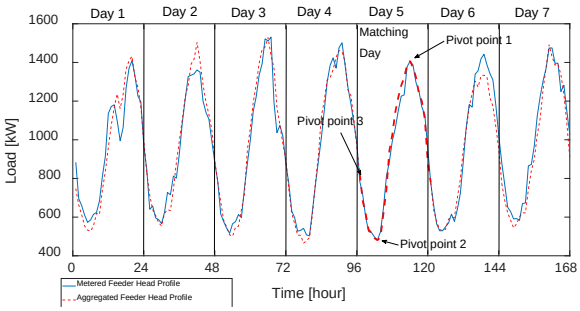

Fig. 2. Feeder head profile comparison

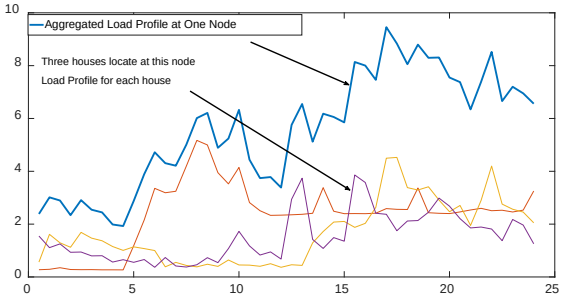

Fig. 3. An example of load allocation disaggregation at a load node

Optimal Water-Power Flow Problem: Formulation and Distributed Optimal Solution

Ahmed S. Zamzam, *Student Member, IEEE*, Emiliano Dall'Anese, *Member, IEEE*, Changhong Zhao, *Member, IEEE*, Josh A. Taylor, *Member, IEEE*, and Nicholas D. Sidiropoulos, *Fellow, IEEE*

***Abstract*—This paper formalizes an optimal water-power flow (OWPF) problem to optimize the use of controllable assets across power and water systems while accounting for the couplings between the two infrastructures. Tanks and pumps are optimally managed to satisfy water demand while improving power grid operations; for the power network, an AC optimal power flow formulation is augmented to accommodate the controllability of water pumps. Unfortunately, the physics governing the operation of the two infrastructures and coupling constraints lead to a nonconvex (and, in fact, NP-hard) problem; however, after reformulating OWPF as a nonconvex, quadratically-constrained quadratic problem, a feasible point pursuit-successive convex approximation approach is used to identify feasible and optimal solutions. In addition, a distributed solver based on the alternating direction method of multipliers enables water and power operators to pursue individual objectives while respecting the couplings between the two networks. The merits of the proposed approach are demonstrated for the case of a distribution feeder coupled with a municipal water distribution network.**

I. Introduction

Power and water networks are critical infrastructures. These systems are predominantly planned and operated independently, although their operation is intrinsically coupled at multiple spatial and temporal scales. For example, in the United States the overall operation of drinking and wastewater networks represents 4% of the total electricity consumption [1]. Optimizing water pump operation has therefore significant potential to save energy, reduce emissions, and enhance the reliability and efficiency of the power grid.

It is increasingly recognized that a *joint* optimization of power and water infrastructures can bring significant benefits from operational and economical standpoints [2]. Controllable assets of water utilities can provide valuable services to power systems to enhance reliability and efficiency, as well as to cope with the volatility of distributed renewable generation.

This paper formulates an optimal water-power flow (OWPF) problem to minimize the (sum of the) cost functions associated with water and power operators while respecting relevant engineering and operational constraints of the two systems as well as pertinent intra-system coupling constraints. The problem is tailored to coupled power distribution feeders and municipal water distribution networks, and it addresses the controllability of distributed energy resources (DERs) and water pumps.

II. The OWPF Problem

Water and power networks are coupled because the power consumed by a pump is proportional to the pump's pressure gain times its flow rate. Let $\mathbf{x}_p$ and $\mathbf{x}_w$ denote the control variables of the power and water networks, respectively. Then, the *Optimal Water Power Flow* problem can be formalized as

$$\min_{\mathbf{x}_p,\mathbf{x}_w} \quad \sum_{t=1}^{T} \left(C_p^t(\mathbf{x}_p) + C_w^t(\mathbf{x}_w) \right)$$
$$\text{s.t.} \quad \mathbf{x}_p \in \mathbf{\Omega}_p, \qquad \mathbf{x}_w \in \mathbf{\Omega}_w, \qquad \mathbf{A}_p\mathbf{x}_p - \mathbf{A}_w\mathbf{x}_w = \mathbf{0}$$

where $\mathbf{\Omega}_p$ and $\mathbf{\Omega}_w$ are the nonconvex operational sets of the power and the water systems, respectively. The last constraint represent the coupling (consensus) constraint.

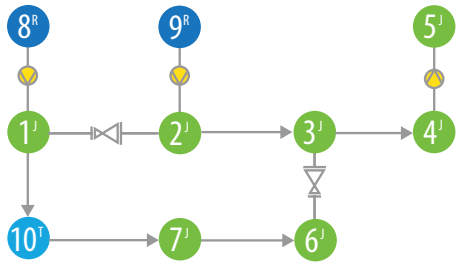

Fig. 1: Municipal water network

III. Distributed Algorithm

Algorithm 1: Distributed OWPF algorithm

Initialization: *Systems use feasible points to initializes their variables.*
repeat
- [S1a] Update power-related variables
- [S1b] Update water-related variables
- [S2] Update dual variables
- [S3] Update restriction points

until *convergence criterion is met*

IV. Experimental Results

The proposed approach is tested in a setting where the IEEE 13-node test feeder is coupled with a municipal water distribution network in Fig. 1 which has three pumps.

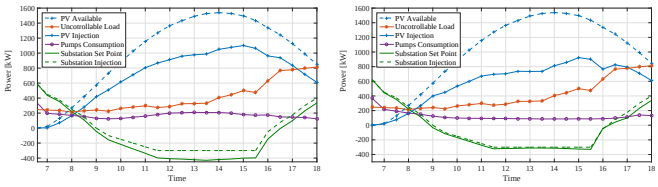

(a) OWPF Solution (b) Decoupled Solution

References

[1] D. Denig-Chakroff, "Reducing electricity used for water production: Questions state commissions should ask regulated utilities," *Water Research and Policy*, 2008.

[2] E. Dall'Anese, P. Mancarella, and A. Monti, "Unlocking flexibility: Integrated optimization and control of multi-energy systems," *IEEE Power and Energy Magazine*, vol. 15, no. 1, pp. 43–52, Jan 2017.

Real Time Tool to Characterize Power System Communication Delays

Christoph Lackner
Rensselaer Polytechnic Institute
Troy, NY
lacknc@rpi.edu

Felipe Wilches-Bernal
Sandia National Laboratories
Albuquerque, NM
fwilche@sandia.gov

Brian J. Pierre
Sandia National Laboratories
Albuquerque, NM
bjpierr@sandia.gov

David A. Schoenwald
Sandia National Laboratories
Albuquerque, NM
daschoe@sandia.gov

I. Communication Delays in Synchrophasor Measurements

Synchrophasor Measurement Units (PMUs) allow high resolution monitoring of power systems spanning large geographical areas [2]. One Advantage of PMU measurements is that they include a time tag according to a common and highly accurate time reference. The IEEE C37.118 standard defines the requirements for the transmission of PMU data across communication networks and specifies the accuracy of the UTC time reference [1].

While a considerable amount of work has been done on how to measure delays in general communication networks [3], very little work has been done specifically looking at delays of PMU data. Because PMU data already has a very accurate Timestamp it can be leveraged to determine delays with a much higher accuracy.

Nowadays, PMU data is used in a number of real time control and monitoring applications such as RT state estimation [4], HVDC modulation [5] and inter-area oscillation damping [6]. The performance of these applications is affected by delays of the incoming data, i.e. PMU data, if not properly addressed [7]. Hence, understanding the nature of the delays in the PMU data is critical to ensure the performance of PMU based real time applications.

This work describes the implementation of a Real Time Tool to measure the delays of PMU data with extreme accuracy. The tool is named network characterizer (NC).

II. Tool Implementation

The NC consists of two parts:

1) A sychnronous part, which is implemented on a National instrument RT-PXI.
2) An asynchronous part which is implemented on a PC connected to the RT-PXI.

The synchronous part records all PMU data packages received and records the delay associated with each packet by recording a GPS time-stamp. The asynchronous part processes the PMU data and record any anomalies such as packets that were received out of order or lost in the communication network. Fig. 1 shows the setup of these two parts.

Sandia National Laboratories is a multimission laboratory managed and operated by National Technology and Engineering Solutions of Sandia, LLC., a wholly owned subsidiary of Honeywell International, Inc., for the U.S. Department of Energys National Nuclear Security Administration under contract DE-NA0003525.

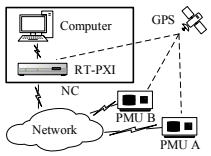

Fig. 1. Setup of the NC including the RT-PXI and the PC

III. Results

Fig. 2 shows the delays of a PMU connected to the tool through a small dedicated local area network. The figure also shows the measurement obtained by using Wireshark (WS), a traditional network analysis tool. In this test UDP was used by the PMU to send the phasor measurements taken every 33 ms. The full poster will contain a more detailed section on some of the results obtained using this tool.

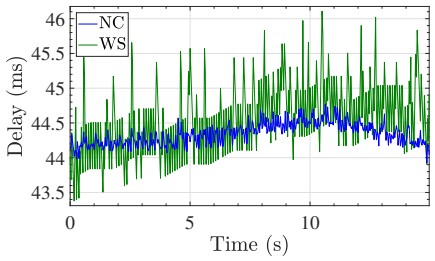

Fig. 2. Delays of a PMU measurement as determined by the NC and WS

References

[1] IEEE Standard for Synchrophasor Data Transfer for Power Systems, IEEE Std C37.118.2-2011 (Revision of IEEE Std C37.118-2005), pp. 153, Dec 2011.
[2] A. G. Phadke, Synchronized phasor measurements in power systems, IEEE Computer Applications in Power, vol. 6, no. 2, pp. 1015, April 1993.
[3] R. Kay, Pragmatic network latency engineering fundamental facts and analysis, cPacket Networks, White Paper, pp. 131, 2009.
[4] C. Lackner, Q. Zhang and J. H. Chow, "Real-Time phasor-only state estimation with topology processing as OpenPDC adapter," 2017 IEEE Power & Energy Society General Meeting, Chicago, IL, 2017, pp. 1-5
[5] D. Trudnowski, et al, Initial closed-loop testing results for the Pacific DC Intertie wide area damping controller, in Power and Energy Soc. General Meeting, 2017. IEEE, Chicago, IL, 2017, pp. 15.
[6] F. Wilches-Bernal, et al, Effect of time delay asymmetries in power system damping control, in 2017 IEEE Power Energy Society General Meeting, July 2017, pp. 15.
[7] H. Ali and D. Dasgupta, Effects of Time Delays in the Electric Power Grid. Berlin, Heidelberg: Springer Berlin Heidelberg, 2012, pp. 139154.

Diagonal Quadratic Approximation for Decentralized Collaborative TSO+DSO Optimal Power Flow

Ali Mohammadi, *Student Member, IEEE,* Mahdi Mehrtash, *Student Member, IEEE,* and Amin Kargarian, *Member, IEEE*

***Abstract*- Collaborative operation of electricity transmission and distribution systems improves the economy and reliability of the entire power system. However, this is a challenging problem given that transmission system operators (TSOs) and distribution system operators (DSOs) are autonomous entities that are unwilling to reveal their commercially sensitive information. This paper presents a decentralized decision-making algorithm for collaborative TSO+DSO optimal power flow (OPF) implementation. The proposed algorithm is based on analytical target cascading (ATC) for multilevel hierarchical optimization in complex engineering systems. A local OPF is formulated for each TSO/DSO taking into consideration interactions between the transmission and distribution systems while respecting autonomy and information privacy of TSO and DSOs. The local OPF of TSO is solved in the upper-level of hierarchy, and the local OPFs of DSOs are handled in the lower-level. A diagonal quadratic approximation (DQA) and a truncated diagonal quadratic approximation (TDQA) are presented to develop iterative coordination strategies in which all local OPFs are solved in a parallel manner with no need for a central coordinator. This parallel implementation significantly enhances computations efficiency of the algorithm. The proposed collaborative TSO+DSO OPF is evaluated using a 6-bus and the IEEE 118-bus test systems, and promising results are obtained.**

***Index Terms*- Collaborative transmission and distribution operation, analytical target cascading, diagonal quadratic approximation, decentralized optimization, parallel algorithm.**

I. Introduction

The transmission system is operated by a transmission system operator (TSO), and the distribution system is controlled by a distribution system operator (DSO). Since the transmission and distribution grids are parts of an interconnected system, any decisions made by TSO (DSOs) affects the DSOs' (TSO's) operation and decisions. On the other hand, TSO and DSOs are autonomous control entities with their own rules, policies, and objectives. While one entity aims at minimizing its own costs, the objective of another entity might be reliability maximization with respect to its local operational constraints. Furthermore, TSO and DSOs might compete with each other to achieve their objectives. Thus, although TSO and DSOs are parts of an interconnected system, they are unwilling to share their commercially sensitive data with each other.

In this paper, we present a decentralized collaborative two-level TSO+DSO optimal power flow solution. The proposed algorithm is based on analytical target cascading (ATC) method and allows a *fully parallel* implementation TSO+DSO OPF. A local OPF problem is formulated for TSO and each DSO which accounts for interactions between the transmission and distribution systems. A limited amount of information is exchanged among TSO and DSOs which is in line with respecting the information privacy of the autonomous control entities. While the transmission OPF problem is formulated and solved in the upper-level of hierarchy, the distribution OPF is handled in the lower-level. Two coordination strategies, namely diagonal quadratic approximation (DQA) and truncated diagonal quadratic approximation (TDQA), are presented to coordinate the local OPF problems in a parallel manner.

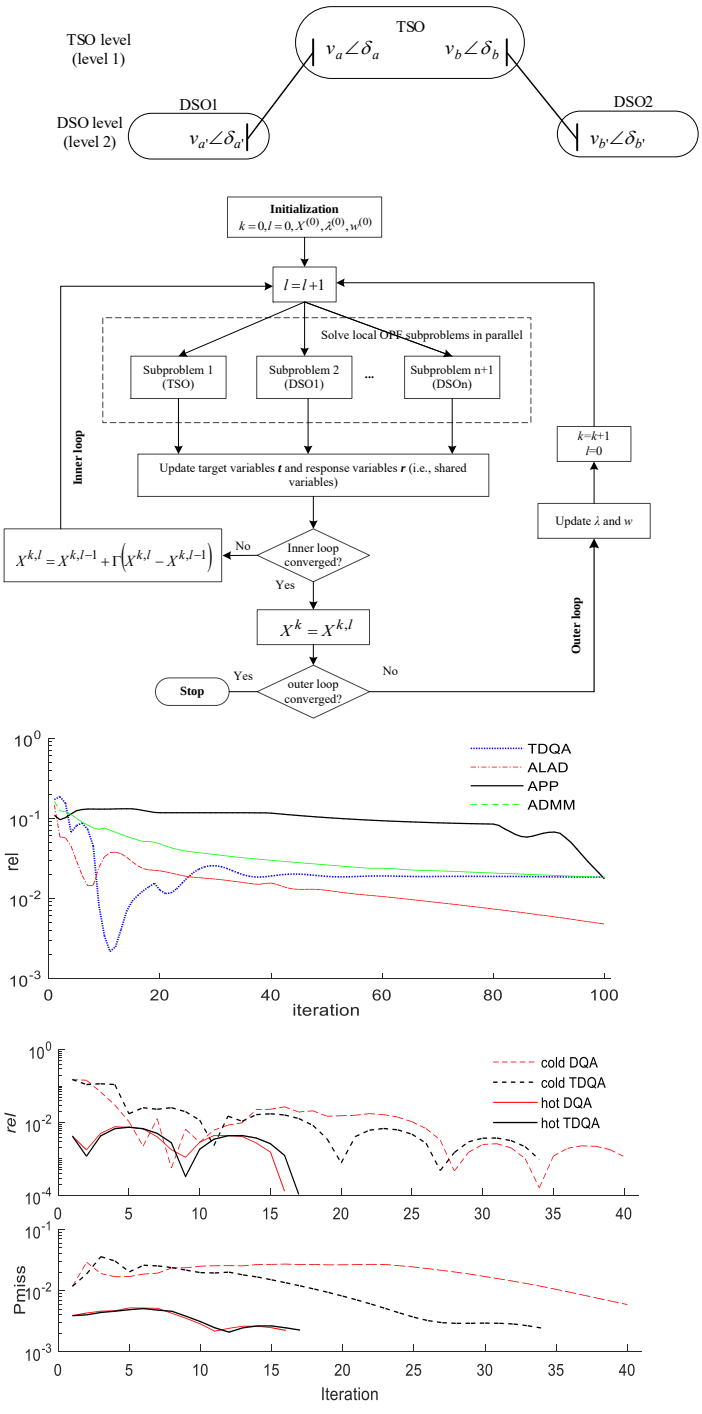

A Data-driven Voltage Control Framework for Power Distribution Systems

Hanchen Xu, Alejandro D. Domínguez-García, and Peter W. Sauer
Department of Electrical and Computer Engineering, University of Illinois at Urbana-Champaign
Email: {hxu45, aledan, psauer}@illinois.edu

***Abstract*—In this paper, we address the problem of coordinating a set of distributed energy resources (DERs) to regulate voltage in power distribution systems to desired levels. To this end, we formulate the voltage control problem as an optimization problem, the objective of which is to determine the optimal DER power injections that minimize the voltage deviations from desirable voltage levels subject to a set of constraints. The nonlinear relationship between the voltage magnitudes and the nodal power injections is approximated by a linear model, the parameters of which can be estimated in real-time efficiently using measurements. In particular, the parameter estimation requires much fewer data by exploiting the structural characteristics of the power distribution system. As such, the voltage control framework is intrinsically adaptive to parameter changes. Numerical studies on the IEEE 37-bus power distribution test feeder validated the effectiveness of the propose framework.**

I. Voltage Control Framework

A. Framework Overview

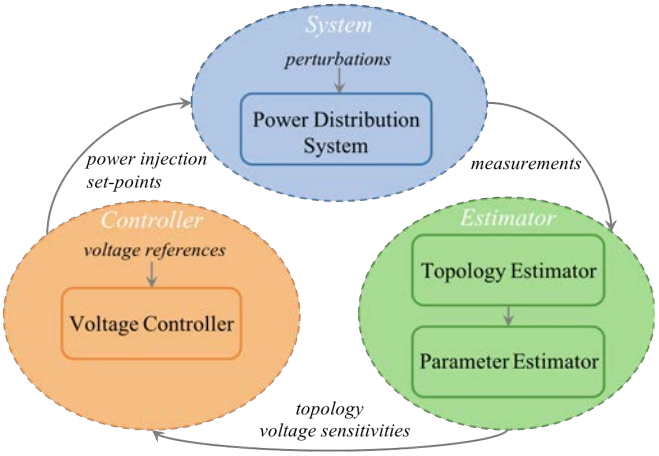

Fig. 1. Data-driven voltage control framework.

B. Voltage Sensitivity Estimator

The sensitivity estimation problem is formulated as follows:

$$\underset{\boldsymbol{r},\boldsymbol{x}}{\text{minimize}} \sum_{k} \left\| \boldsymbol{R}\boldsymbol{p}^{(k)} + \boldsymbol{X}\boldsymbol{q}^{(k)} - \tilde{\boldsymbol{u}}^{(k)} \right\|_2^2, \tag{1}$$

where $\tilde{\boldsymbol{u}} = \boldsymbol{V}^2 - V_0^2 \mathbf{1}_N$. Define $\boldsymbol{\Gamma}_i = 2(\boldsymbol{M}^{-1})^\top \boldsymbol{e}_i \boldsymbol{e}_i^\top \boldsymbol{M}^{-1}$, where $\boldsymbol{e}_i$ is the i^{th} basis vector in $\mathbb{R}^L$. Then, $\boldsymbol{X}\boldsymbol{q}^{(k)} = \sum_{i=1}^{L} \boldsymbol{\Gamma}_i \boldsymbol{q}^{(k)} x_i$, and $\boldsymbol{R}\boldsymbol{p}^{(k)} = \sum_{i=1}^{L} \boldsymbol{\Gamma}_i \boldsymbol{p}^{(k)} r_i$, where $r_i = \alpha_i x_i$. Define $\boldsymbol{\phi} = [(\tilde{\boldsymbol{u}}^{(k_1)})^\top, \cdots, (\tilde{\boldsymbol{u}}^{(k_m)})^\top]^\top$, and

$$\boldsymbol{\Phi} = \begin{bmatrix} \boldsymbol{\Gamma}_1(\alpha_1 \boldsymbol{p}^{(k_1)} + \boldsymbol{q}^{(k_1)}) & \cdots & \boldsymbol{\Gamma}_L(\alpha_L \boldsymbol{p}^{(k_1)} + \boldsymbol{q}^{(k_1)}) \\ \vdots & \vdots & \vdots \\ \boldsymbol{\Gamma}_1(\alpha_1 \boldsymbol{p}^{(k_m)} + \boldsymbol{q}^{(k_m)}) & \cdots & \boldsymbol{\Gamma}_L(\alpha_L \boldsymbol{p}^{(k_m)} + \boldsymbol{q}^{(k_m)}) \end{bmatrix}.$$

Then (1) is equivalent to the following:

$$\underset{\boldsymbol{x}}{\text{minimize}} \, \|\boldsymbol{\Phi}\boldsymbol{x} - \boldsymbol{\phi}\|_2^2, \tag{2}$$

the solution of which is given by $\hat{\boldsymbol{x}} = (\boldsymbol{\Phi}^\top \boldsymbol{\Phi})^{-1} \boldsymbol{\Phi}^\top \boldsymbol{\phi}$.

C. Voltage Controller

The voltage control problem is formulated as follows:

$$\underset{\boldsymbol{p}^g \in [\underline{\boldsymbol{p}}^g, \overline{\boldsymbol{p}}^g], \boldsymbol{q}^g \in [\underline{\boldsymbol{q}}^g, \overline{\boldsymbol{q}}^g]}{\text{minimize}} \quad c(\boldsymbol{p}^g, \boldsymbol{q}^g, \boldsymbol{u})$$

$$\text{s.t. } \boldsymbol{u} - u_0 \mathbf{1}_N = \hat{\boldsymbol{R}}(\boldsymbol{p}^g - \boldsymbol{p}^d) + \hat{\boldsymbol{X}}(\boldsymbol{q}^g - \boldsymbol{q}^d).$$

where $c(\boldsymbol{p}^g, \boldsymbol{q}^g, \boldsymbol{u}) = \mathbf{1}_N^\top (\boldsymbol{p}^g + \boldsymbol{q}^g) + \gamma([\underline{\boldsymbol{u}} - \boldsymbol{u}]_+ + [\boldsymbol{u} - \overline{\boldsymbol{u}}]_+)$.

II. Numerical Simulations

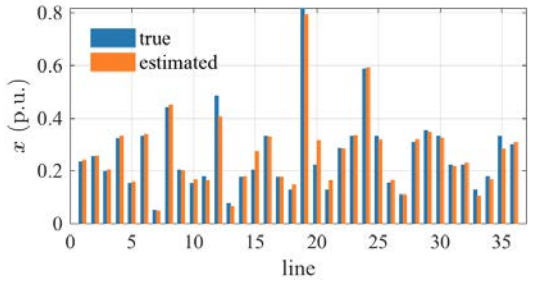

Fig. 2. Line parameter estimation results.

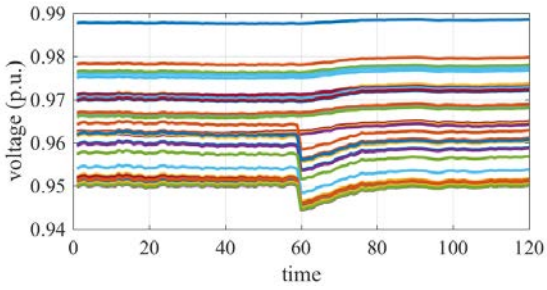

Fig. 3. Voltage profiles under proposed control. (Disturbance at time 60.)

A Machine Learning Approach for Residential Load Extraction using Low-resolution Smart Meter Data

Yao Meng, *Student Member, IEEE*, Ming Liang, *Student Member, IEEE*, Ning Lu, *Senior Member, IEEE*

***Abstract*— This paper presents a data-driven approach for load disaggregation. A 3-step machine learning algorithm is developed to perform load disaggregation 15-minute, 30-minute, and hourly smart meter data. In the first step, a shared-learning method is used to identify baseload days so that the baseline load consumption of each customer (defined as the electricity consumption without or with very little heating or cooling loads) can be extracted. In the second step, the cooling and heating loads are extracted for each out-door temperature cluster using an averaging method followed by a trimming procedure. In the final step, energy signatures are derived from the energy disaggregation results for conducting energy disaggregation for feeders without smart meter data. The method is developed, tested, and validated using minute-by-minute sub-metered energy consumption data collected from 145 household in the PECAN street project.**

Keywords-load modeling, load disaggregation, machine learning, smart meter, data-driven methods, unsupervised learning.

I. INTRODUCTION

A common goal of the Load Disaggregation algorithms is to extract time series load profiles of end use electricity consumptions from measured total load consumptions. There are two types of load disaggregation algorithms: power and energy. The time series of the power consumptions of a disaggregated end use load can be used to develop load models for power management programs such as peak shaving and load shifting. The sampling rates of the meter data required for power disaggregation algorithms are high. Normally, data collected by power quality meters (usually higher than 60 Hz) are used. At the very minimum, minute-by-minute measurements are needed to identify the operation characteristics of an end use load. The time series of the energy consumptions of a disaggregated end use load can be used to derive load composition, which is a critical piece of information required for power grid operation and planning. The sampling rates of the meter data required for energy disaggregation algorithms can be much lower than those for the power ones. Traditionally, utilities use hourly, daily or even monthly energy measurements to perform load disaggregation to extract the load composition data from a very high level (i.e. commercial, residential, agricultural, and industrial). The deployment of the smart meters allows utilities to have access to a large amount of intra-hour meter measurements. This creates an emerging need for accurate, robust, and computationally efficient energy disaggregation methods so that low-resolution smart meter data can be used to derive energy related signatures. Thus, in this paper, we will focus on the energy disaggregation algorithms for deriving energy signatures using 15-minute, 30-minute, and hourly smart meter measurements.

II. KEY EQUATIONS

Estimate the house cooling consumption

$$P_{cooling} = P_{hotday}^{ave} - P_{mildday}^{ave} \quad (1)$$

In mild days (transition seasons), HVAC system is not operating, so that the smart meter data in this period does not include HVAC energy consumption, only non-temperature sensitive load, which is regarded as base load.

$$P_{heating} = P_{colday}^{ave} - P_{mildday}^{ave} \quad (2)$$

Variations in the electricity usage of different day can lead to very different calculation results. So this method is applied to daily average electricity load profiles.

$$r_t^i = {HVAC_t^i}/{total_t^i} \quad (3)$$

Using a trimming method based on HVAC usage ratio is simple and effective.

III. KEY SIMULATION RESULTS

Unit in following tables is kWh.

Table I Cooling and Heating Load Estimation Accuracy

	Overall RMSE	MAE	Best RMSE
Cooling Load	0.2971	0.6601	0.0849
Heating Load	0.7559	1.8350	0.1524

Table II Cooling load accuracy comparison before and after trimming

	Overall RMSE	MAE	Best RMSE
Before trimming	0.2971	0.6601	0.0849
After trimming	0.2190	0.5511	0.0542

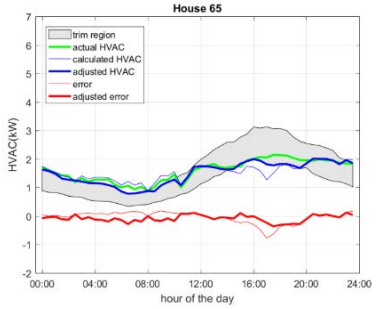

Fig. 1 HVAC load before and after trimming for House 65

Nonparametric User Behavior Prediction for Distributed EV Charging Scheduling

Behnam Khaki*, Yu-Wei Chung†, Chicheng Chu‡, and Rajit Gadh§
Smart Grid Energy Research Center (SMERC), University of California, Los Angeles
Los Angeles, USA
Email:{ *behnamkhaki, †ywchung, ‡peterchu, §gadh}@ucla.edu

***Abstract*—Electric vehicles (EVs) are controllable loads which can participate in demand response and load shaping in the distribution grids. Their charging scheduling (CS) is, however, challenging due to the uncertainty in EV user behavior. To address this issue, we use nonparametric diffusion-based kernel density estimator (DKDE) to model the stochasticity of EV charging load. DKDE is based on smoothing properties of linear diffusion process which is more adaptive to the training dataset and results in optimal bandwidth selection comparing to Gaussian kernel density estimator (GKDE). Using predicted EV user behavior, we propose a distributed CS to flatten total load profile and to reduce charging cost which is formulated as *sharing problem* and solved by alternating direction method of multipliers (ADMM). Using numerical simulation with real data, we evaluate DKDE prediction accuracy and verify the proposed CS performance.**

***Index Terms*—EV charging scheduling, nonparametric density estimator, alternating direction method of multipliers.**

I. Motivation and Proposed Approach

EVs are receiving more attention due to rising environmental concerns and government-related driven policy. As in California, it is expected to have 1 million zero-emission EVs on the road by 2020. Although EVs reduce greenhouse gas emission in the transportation sector, they can degrade power quality and jeopardize the stability of electrical grids. Management of EV charging load can decrease the negative effects of EVs on a distribution system. Nonetheless, the uncertainty of EV charging behavior including start time, stay duration and energy demand is challenging.

To address the challenges of stochastic EV user behavior and EV integration in the grid in this poster, diffusion-based kernel density estimator (DKDE) is used to predict EV users behavior, and EV load demand is scheduled by a distributed optimization method. Although Gaussian kernel density estimator (GKDE) can provide a promising solution to EV user behavior prediction based on a historical charging data, its optimal bandwidth determined by the normal reference rule leads to an oversmoothed distribution density function which in some cases is not realistic. Inspired by the adaptive KDE method, we use DKDE to improve the prediction accuracy owing to its optimal bandwidth selection which is adaptive to the training dataset (Fig. 1). Afterwards, we formulate optimal charging scheduling as a *sharing problem* and solve it in a distributed manner by ADMM through an iterative procedure between a central entity (CE), located in distribution grid operator, and EV chargers. The proposed distributed approach is scalable in terms of EV population and preserves EV owners' privacy as they do not need to share their private information (arrival/departure time as well as required charging energy) with CE.

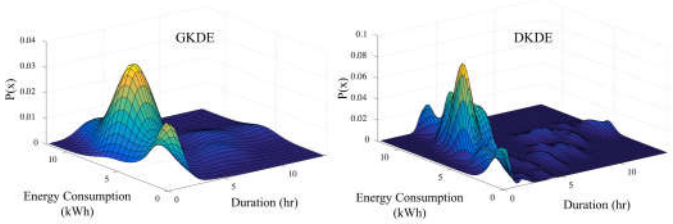

Fig. 1. Probability density distribution of stay duration vs. energy consumption

II. Simulation Results

To compare GKDE with DKDE and to evaluate the performance of the proposed distributed charging scheduling, real data of 80 EVs collected on UCLA campus is used for numerical simulation, and the prediction accuracy is evaluated using mean estimation deviation (MED) in Fig. 2. Using the estimated user behavior for 80 EVs and real net-load data, CS is optimized using *sharing problem* and ADMM. The objective function of CS is twofold: charging cost reduction (CCR) and load variance minimization (LVM). As Fig. 3 shows, the proposed coordinated CS (CC) results in CCR and LVM in comparison to uncoordinated charging (uCC).

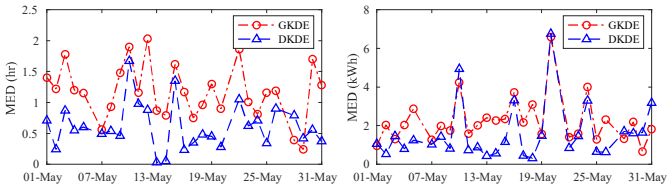

Fig. 2. Stay duration MED (left) and energy consumption MED (right)

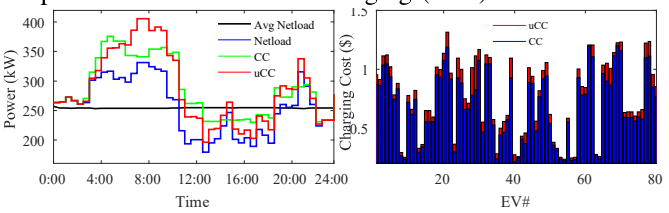

Fig. 3. LVM (left) and CCR (right) using the proposed distributed CS.

Detection of PMU Time Error Sources Using Phase Angle Measurement Data

Ikponmwosa Idehen, *Student Member, IEEE* and Thomas J. Overbye, *Fellow, IEEE*

***Abstract*—In the event of data corruption or loss which invalidates time and message quality bits in IEEE C37.118 protocol, measurement data from phasor measurement units (PMUs) could be rendered incomprehensible. In this work, we describe four time-based errors in PMU device operation, while observing the unique characteristic patterns formed. As a data post-processing tool, a subsequence dynamic time warping technique is utilized in a similarity-based, time-series pattern query to identify instances of time-related errors in reported PMU data. Results are demonstrated using transient stability data from a 2000-bus synthetic case and actual utility PMU data.**

***Index Terms*—phasor measurement unit, error analysis, error prototype, pattern similarity, pattern recognition, time-errors**

I. Introduction

Fast-paced deployment of phasor measurement units (PMUs) is considerably increasing operator situational awareness of the power grid. Generated data are transmitted to control centers where they are used in short-term control schemes and long-term future planning. However, the unique operation of these devices makes them vulnerable to a new paradigm of errors increasing the spectra of data quality issues tackled by control centers.

Some of the synchronization and time-related issues associated with PMU devices are attributed to intermittency in global positioning system (GPS) signals, total GPS signal loss (GSL), drifting PMU internal clocks and signal spoofing [1]. Often, these translate to phase angle errors and manifest as sporadic or periodic jumps in angles. Figures (1) and (2) show voltage angles (VA) observed in four different prototype PMU error simulations for a duration of 30 seconds.

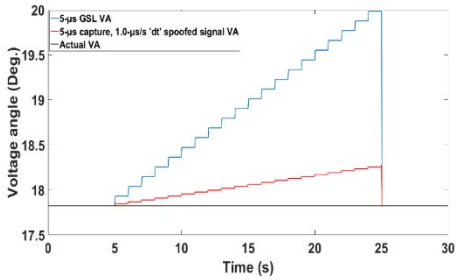

Fig.1. Prototyped PMU voltage angles due to GSL and time signal spoofing

In Fig. (1), the black horizontal line represents the original, steady state condition while the staircase-like VA profiles are typical of continous drifting angles attributed to GSL and signal spoofing events. For the same 5 μs time error, the blue curve, which is a result of GSL, shows a larger VA deviation than the red curve, which is a result of signal spoofing. Fig. (2) shows different patterns in the VA profiles observed for a drifting PMU clock. One pattern is due to an internal time offset (green curve), and the other is a result of intermittent GPS signals (pink curve). Two key features are the non-divergence of the VA measurements, and the short segment error duration prior to the next data error.

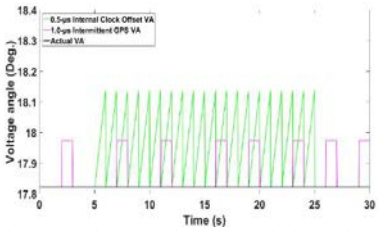

Fig.2. Prototyped PMU voltage angles due to drifung clock and intermittent GPS

In order to provide details on device time synchronization and quality of measured data, the IEEE C37.118.2 protocol [2] utilizes flag bits to encode time and message quality information in data frames. In the data lifecycle and archival process involving data compression, migration and storage activities, reported PMU data are vulnerable to possible data loss, corruption or modification of flag bits, which in turn affects intelligibility of the stored data. As part of a post-processing stage, engineers can lose sight of the presence and cause of logical inconsistencies in the data, and result in a reduced grid awareness level.

The purpose of this work is to provide a post-processing technique for the source identification of PMU time-related errors based on the sole use of reported phasor measurements. It leverages on defined PMU error mechanisms to generate prototype data error patterns, which are then used as training sets in the error analysis and source error identification in synthetic and actual PMU data. A subsequence dynamic time warping technique is employed in the search for distinct patterns in PMU data error measurements.

References

[1] Y, Wenxuan, Yong Liu, D. Zhou, Z. Pan, J. Zhao, M. Till, L. Zhu, L. Zhan, Q. Tang, and Yilu Liu. "Impact of GPS signal loss and its mitigation in power system synchronized measurement devices." Smart Grid, IEEE Transactions on, vol. PP, no.99, pp.1-1, 2016.

[2] Q. Zhang, V. Vittal, G. Heydt, Y. Chakhchoukh, N. Logic and S. Sturgill, "The time skew problem in PMU measurements," *2012 IEEE Power and Energy Society General Meeting*, San Diego, CA, 2012, pp. 1-6.

[3] NASPI and PNNL. (2017). NASPI-2016-TR-002 A Framework for the Attributes of PMU Data Quality and a Methodology for Examining Data Quality Impacts upon Synchrophasor Applications. [Online]. Available: https://ws680.nist.gov/publication/get_pdf.cfm?pub_id=920627

Stability Robustness for Secondary Voltage Control in Autonomous Microgrids With Consideration of Communication Delays

Guannan Lou, Wei Gu
Department of Electrical Engineering
Southeast University
210096, Nanjing, Jiangsu, China
Guannan_lou@seu.edu.cn

Yinliang Xu
Shenzhen Environmental Science and New Energy Technology Engineering Laboratory
Tsinghua-Berkeley Shenzhen Institute
518055, Shenzhen, China

***Abstract*—The extensive usage of open communication networks for secondary voltage control in autonomous microgrids (MGs) inherently introduce time delays, which would degrade the system performance. This paper proposes an analytical method to determine the stability robustness of secondary voltage control in MGs by taking into account the communication latency. A closed loop small-signal model of a MG installed with PI secondary voltage controllers is derived to include time delays between the MG centralized and local controllers. Delay stability criterions based on tracing critical eigenvalue and cluster treatment of characteristic roots are thus formulated to deliver delay margins for single and multiple delays. By a series of trial declarations, the qualitative impact of controller gains on delay-dependent stability can be uncovered, to guide the controller design. The effectiveness of the proposed methodology is verified by a simulation study.**

I. Introduction

The microgrid (MG) is emerging as a promising means of distributed generations (DGs), loads and storages. The most attractive advantage of MG concept is to island itself from the main grid and to provide an uninterrupted power supply, where droop algorithm attracts attention to facilitate power sharing among DGs. Typically, voltage droop exhibits a poor reactive power sharing due to the inconformity of output impendences, and secondary voltage control (SVC) is introduced to generate control signals for individual local controllers (LCs) shown in Fig. 1. With the increasing usage of open communication networks, the time delays between SVC and LCs are expected to degrade system performance and even cause instability, which consequently cannot be simply ignored. Therefore, secondary voltage control with consideration of communication delays during control signal transmission is addressed in this paper.

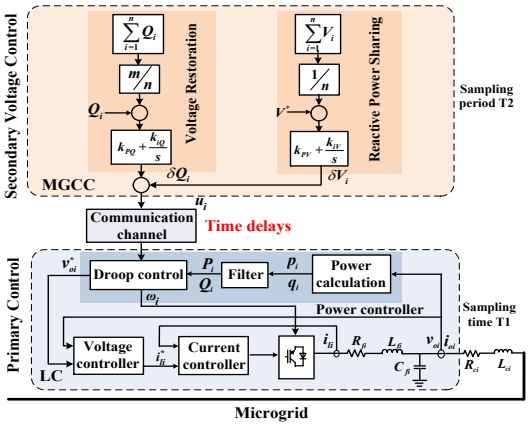

Fig. 1. Hierarchical control scheme for an inverter-based DG

II. Delay-Dependent Stability Analysis

In the view of above analysis, the implementation of the proposed approach includes the following steps:

Step 1: Establish an overall small-signal model of MG including inverters, network and loads, with consideration of time-delayed secondary voltage controller.

Step 2: Select sets of feasible PI controller parameters.

Step 3: For each set of PI control gains, obtain the characteristic equation. Furthermore, the delay-dependent stability robustness is determined in the forms of delay margin and stability regions, respectively.

Step 4: Investigate the qualitative impact of controller gains on system stability robustness against time delays.

Step 5: Simulation is utilized to verify the accuracy of the theoretical results by increasing the delay gradually while observing the system stability.

III. Analysis Results\

The stability robustness analysis of secondary voltage control is performed by a typical MG in the presence of both single and independent multiple delays.

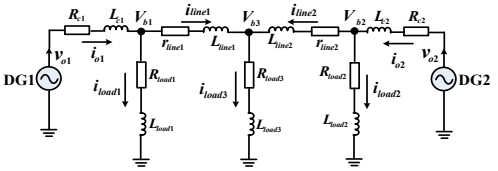

Fig. 2. Diagram of the MG test system.

A. Single time delay

The delay margin τ_d using different controller gains is calculated for MG with a single delay. The root loci related to critical stability with k_{iQ}=0.02, k_{iV}=20 is depicted in Fig. 3 and τ_d for different sets of controllers is shown in Fig. 4.

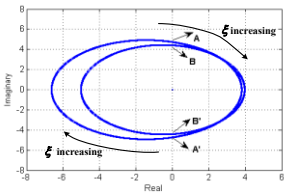

Fig. 3. Root loci of $CE_\xi(s, \xi)$ related to critical stability with k_{iQ}= 0.02, k_{iV}= 20.

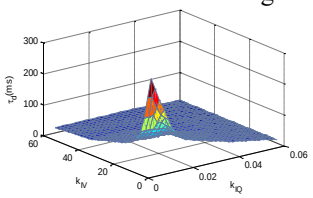

Fig. 4. Single delay margins for different sets of controller gain

B. Independent multiple communication delays

The stability posture over the delay domain for unrelated multiple delays τ_1 and τ_2 are investigated, where Kernel curve in building block and the relationship among critical ω, τ_1 and τ_2 are shown in Fig. 5 and Fig. 6, respectively.

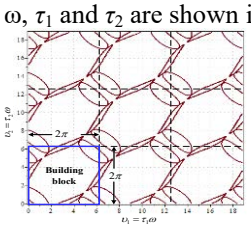

Fig. 5. Kernel curve in building block and its offspring for an MG with unrelated delays (k_{iQ}= 0.02, k_{iV}= 20).

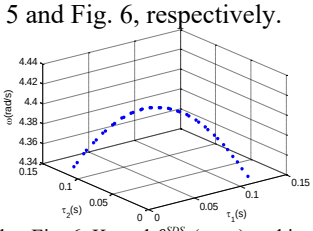

Fig. 6. Kernel ϑ_0^{SDS} (τ_1, τ_2) and its corresponding ω variations (k_{iQ}= 0.02, k_{iV}= 20).

A Novel Consensus-based Distributed Algorithm for Economic Dispatch Based on Local Estimation of Power Mismatch

Hajir Pourbabak, *Student Member, IEEE,* Jingwei Luo, *Student Member, IEEE,* Tao Chen, *Student Member, IEEE* and Wencong Su, *Member, IEEE*

***Abstract*—This paper proposes a novel consensus-based distributed control algorithm for solving the economic dispatch problem of distributed generators. A legacy central controller can be eliminated in order to avoid a single point of failure, relieve computational burden, maintain data privacy, and support plug-and-play functionalities. The optimal economic dispatch is achieved by allowing the iterative coordination of local agents (consumers and distributed generators). As coordination information, the local estimation of power mismatch is shared among distributed generators through communication networks and does not contain any private information, ultimately contributing to a fair electricity market. Additionally, the proposed distributed algorithm is particularly designed for easy implementation and configuration of a large number of agents in which the distributed decision making can be implemented in a simple proportional-integral (PI) or integral (I) controller. In MATLAB/Simulink simulation, the accuracy of the proposed distributed algorithm is demonstrated in a 29-node system in comparison with the centralized algorithm. Scalability and a fast convergence rate are also demonstrated in a 1400-node case study. Further, the experimental test demonstrates the practical performance of the proposed distributed algorithm using the VOLTTRON™ platform and a cluster of low-cost credit-card-size single-board PCs.**

***Index Terms*—Economic Dispatch, Distributed Control, Consensus Algorithm, Distributed Generator.**

I. Introduction

Future power systems are equipped with a great number of distributed generators (DGs), distributed energy storage devices, dispatchable loads and advanced communication networks, which increases the customer participation in the electricity market. As a result, the optimal economic dispatch (ED) of future power systems is becoming much more challenging. A sophisticated control is needed to fully address the increasing customer participation at the edge of the electric power system and the inability of existing practices to accommodate these changes [1–4].

In a centralized ED, all participants (DGs and consumers) must release their information to the central controller. As the market penetration of DGs and consumers is continuously growing, the centralized algorithms are no longer suitable due to the heavy computational burden [5]. Moreover, the centralized algorithms are not designed to support plug-and-play functionalities of a large number of participants.

Consensus-based distributed approaches have been found to be practical in many multi-agent applications, such as industrial systems, automated high way systems, and computer networks [6]. Consensus-based distributed approaches are to find the global optimal decision by allowing local agents to iteratively share information through two-way communication links. All agents reach a consensus when they agree upon the value of the information state [7–11]. The information state can be physical quantities or control signals such as voltage, frequency, output power, incremental cost, and estimated power mismatches [12]. Figure 1 compares the centralized and distributed methods for solving the ED problem in power systems [13]. The major advantages of distributed methods are summarized as follows:

Scalability and Interoperability: As the number of agents increases to hundreds of thousands, the legacy centralized method faces certain challenges such as computational burden. As more DGs are integrated into power systems, the centralized methods are not suitable for such heterogeneous systems [12, 14].

Monopoly and Monopsony: A central organization usually has a kind of monopoly over the consumers and a monopsony toward the electrical energy DGs. However, as it is discussed in various research papers and academic notes, consumers have a much more apathetic role than DGs do in electrical energy markets under centralized control [15, 16].

Privacy and Stealth Protection: One of the essential and notable features of every competitive system is the equal opportunity for competition for all players. Therefore, it should be ensured that no private information is released by a third-party and no preferences are given to one or more DGs in a competitive market [1].

Computational Cost: Heavy computational load is imposed on the central controller when dealing with a large multi-agent network [12, 17]. However, the computational load can be shared among agents using distributed approaches.

Single Point of Failure: A distributed approach is robust to the single point of failure because there is no need for a center for the supervisory of the entire system [14, 18].

Network Topology: In future power systems, the communication network and power network are subject to frequent change [19]. Accordingly, there are serious doubts about the ability of centralized methods to handle the variable topology.

The literature review shows a growing interest in distributed algorithms in the field of power systems. A distributed algorithm for solving the ED problem that considered thermal generation and random wind power was discussed in [20]

Automated Distribution System Restoration with the Multiagent Q-Learning Based Algorithm

Inalvis Alvarez-Fernandez, Jungseok Hong, and Wei Sun
Department of Electrical and Computer Engineering
University of Central Florida
Orlando, Florida, United States
alvarezfernandez@knights.ucf.edu, jasonhong@knights.ucf.edu, sun@ucf.edu

***Abstract*—This paper proposed using Q-Learning, multiagent system (MAS), combination and battery algorithm for power system restoration considering the system's operation constraints in order to adapt to quick changes. The developed algorithm considers voltage and current constraints, while finding system switching configuration to maximize the load pick-up after faults happen to the given system. The algorithm consists of three parts. First, it finds switching configurations using Q-learning. Second, the combination algorithm works as a back-up plan in case of the solution from Q-learning violates system constraints. Third, the battery algorithm is applied to determine the charging or discharging schedule of battery systems. The obtained switching configuration provides restoration solutions without violating system constraints. Furthermore, the algorithm can adjust switching configurations after the restoration. For example, when renewable output changes, the algorithm provides an adjusted solution to avoid violating system constraints. Simulation results demonstrate that the algorithm offers an efficient and effective restoration strategy for resilient distribution system operation.**

Keywords—Restoration, Q-Learning, MAS, Renewables

I. Proposed Restoration Algorithm

Q-learning is one of the popular methods in reinforcement learning. However, the simplest form of Q-learning has limited applications to power system since every state needs to be defined prior to the implementation. Therefore, Q-learning without states is necessary to decrease the computational burden and increase the efficiency of the algorithm. Modified Q-learning from [1] is applied to power systems restoration.

From the experiment, it was found that Q-learning does not always provide the solutions free from violating the constraints. Therefore, it is necessary to have supplementary algorithms to provide solutions in case of failure of Q-learning. This algorithm utilizes a combination approach to find the best solution to restore the given distribution system. However, it only considers a reduced number of switch configuration combinations to decrease the computational load of the restoration algorithm.

The goal of the battery algorithm is to use the most surplus power from the given distribution system.

II. Results

The proposed algorithm is tested on the testbed. The testbed is built based on the IEEE 9-Bus system. The model should have a generator, load, switch, PV, and battery. There is no limit to the number of components to run the proposed algorithm. The testbed has two DGs, one battery, one PV, and three loads. Each load has its own priority between 0 and 1. If a load has higher priority than other loads, it is restored first. Typically, the voltage of distribution system ranges from 120V to 35kV. The voltage of substation is 24.9kV, and the voltage of remaining network is 4.16kV in the testbed.

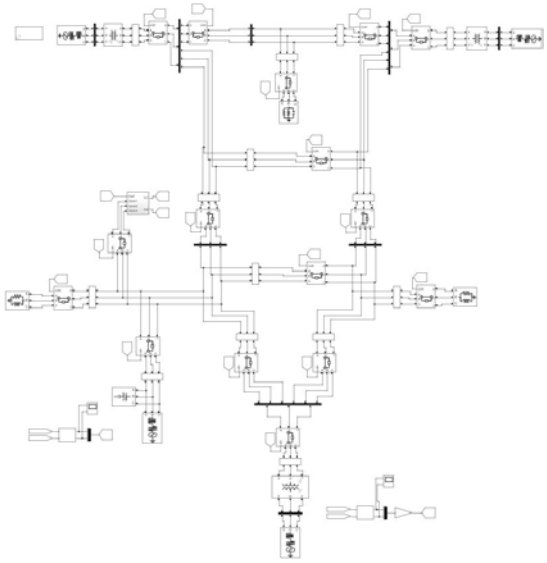

Fig.1. Overview of IEEE 9-Bus System

III. References

[1] D. Ye, M. Zhang and D. Sutanto, "A Hybrid Multiagent Framework With Q-Learning for Power Grid Systems Restoration," in IEEE Transactions on Power Systems, vol. 26, no. 4, pp. 2434-2441, Nov. 2011

Modelling and evaluation of flexible multi-energy systems for low carbon environment

Ninoslav Holjevac, *Student member, IEEE*, Tomislav Capuder, *Member, IEEE*, Igor Kuzle, *Senior Member, IEEE*
Faculty of Electrical Engineering and Computing
University of Zagreb
Zagreb, Croatia
ninoslav.holjevac@fer.hr, tomislav.capuder@fer.hr, igor.kuzle@fer.hr

***Abstract*—With the increasing penetration of variable renewable energy sources (RES) and distributed generation it is becoming increasingly harder to maintain the optimal operation of the power system distribution networks. The paper presents a corrective receding horizon mixed integer linear programming (MILP) model of multi-energy microgrid (MEM) in which the operational behavior of local, aggregated generating units, renewable energy sources and customers is investigated through different modelling assumptions and multiple MEM system configurations/layouts. This paper elaborates how these assumptions affect MEM behavior in market driven environment and demonstrates MEM capability to respond to intra-day disturbances caused by variability and uncertainty inherent to the production of the renewable energy sources (RES) when controlled by means of the proposed optimization model.**

Keywords—multi-energy systems; power system flexibility; reeceding horizon corrective scheduling

I. Introduction and Contributions

Aggregating groups of consumers of different energy vectors and generating units at the same location with centralized control is known as the concept of multi-energy microgrid. However, if those potentially flexible producers and consumers do not have the ability to balance the variability and uncertainty of renewable energy sources production within them, from the system perspective, they are seen as a source of imbalances The work will present a MILP model expanded with corrective receding horizon scheduling approach in order to capture the value of integrating multiple energy vectors, their optimal operation and their flexibility potential.

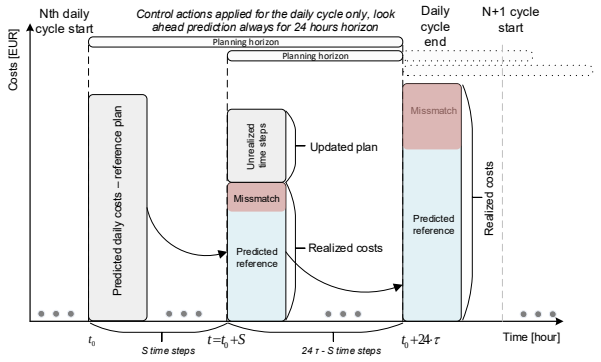

Fig. 1. Illustration of the developed receding horizon corrective scheduling algorithm

II. Core Equation Set

At its core the corrective scheduling algorithm is guided by the following equation set:

$$COST = \sum_{t=1}^{24\cdot\tau+1-S} \left\{ \left[\text{predicted (PRE)} \right] + \left[\text{missmatch (MIS)} \right] \right\} + \\ + \sum_{t=24\cdot\tau+1-S}^{24\cdot\tau} \left[\text{"updated" predicted costs (UPD)} \right] \quad (1)$$

$$PRE = \sum_{t=1}^{24\cdot\tau+1-S} \begin{bmatrix} (F_t^{ng}\cdot c^{ng} + F_t^{CCHP}\cdot c^{f} + F_t^{D}\cdot c^{d}) + (E_t^{imp0}\cdot c_t^{mcp} - E_t^{\exp 0}\cdot c_t^{mcp}) \\ +(P\cdot E_t^{w-cur} + P\cdot H_t^{waste}) + (H_t^{binCCHP}\cdot c_{const}^{CCHP} + H_t^{suCCHP}\cdot c_{start}^{CCHP}) \\ +(E_t^{binD}\cdot c_{const}^{D} + E_t^{suD}\cdot c_{start}^{D}) + (emiss_t\cdot c^{emiss}) \end{bmatrix} \quad (2)$$

$$MIS = \sum_{t=1}^{24\cdot\tau+1-S} \begin{bmatrix} (-)short_t^{imp}\cdot \mathrm{M}^{sell}\cdot c_t^{mcp} + long_t^{imp}\cdot M^{buy}\cdot c_t^{mcp} + \\ short_t^{\exp}\cdot \mathrm{M}^{buy}\cdot c_t^{mcp} - long_t^{\exp}\cdot \mathrm{M}^{sell}\cdot c_t^{mcp} \end{bmatrix} \quad (3)$$

$$UPD = \sum_{t=24\cdot\tau+1-S}^{24\cdot\tau} \begin{bmatrix} F_t^{ng}\cdot c^{ng} + F_t^{CCHP}\cdot c^{f} + F_t^{D}\cdot c^{d} + E_t^{imp}\cdot c_t^{imp} - E_t^{\exp}\cdot c_t^{\exp} \\ +P\cdot E_t^{w-cur} + P\cdot H_t^{waste} + H_t^{binCCHP}\cdot c_{const}^{CCHP} + H_t^{suCCHP}\cdot c_{start}^{CCHP} \\ +E_t^{binD}\cdot c_{const}^{D} + E_t^{suD}\cdot c_{start}^{D} + emiss_t\cdot c^{emiss} \end{bmatrix} \quad (4)$$

III. Key Results

In addition to fact that MEM governed by the proposed control strategy is achieving better cost and emission indicators compared to traditional control strategies the proposed optimization framework can be used to extract valuable insights and information of the available flexibility resources since this will present a key future of the modern distribution system networks.

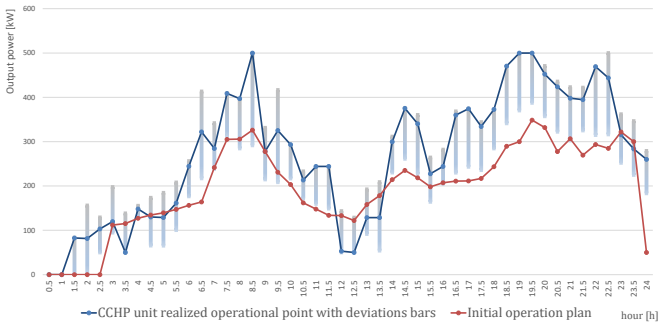

Fig. 2. The operational point of the CCHP unit through out the whole daily cycle (with deviation range bars) compared to the initial operation plan

Adoption of IoT framework for DER aggregation and control

Tylor Slay, Crystal Eppinger, Robert B. Bass
Dept. of Electrical and Computer Engineering
Portland State University
Portland, Oregon, USA
tslay@pdx.edu

I. Introduction

The PSU team has worked with utility partner Portland General Electric over the past five years to develop an ad-hoc grid management system for DER Aggregation. The Distributed Energy Resources (DER) Aggregation System (DERAS) is a bi-level control system that utilizes an IoT framework designed to aggregate resources, optimize scheduling and provide utility ancillary services. Figure 1 The multi-agent platform hosts two tiers, the energy management system (EMS) and the distributed management system (DMS). This provides the security of a distributed network and the coordination of a central control paradigm. The EMS aggregates DER and can optimize dispatch to provide ancillary services, prioritize renewable energy dispatch and ensure grid stability. The EMS will use cloud-based asset models and characteristic asset groupings to provide an alternative to previously-proposed, low-latency, high-transfer systems.

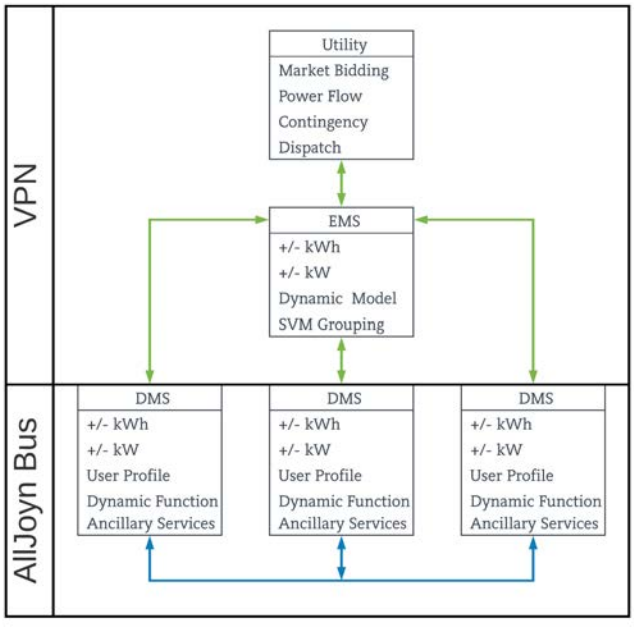

Fig. 1. DERAS Architecture

The DMS facilitates peer-to-peer interaction between assets, forming a distributed network that can participate in grid recovery and form power hubs following a potential large-scale grid disturbance. The DMS can communicates with neighboring devices via a wi-fi mesh network to schedule regional participation, effectively minimizing the data transfer between each tier.

II. Key Components

This research uses PJM's "Reg D" regulating resource signal to confirm aggregated DER can participate in ancillary services. The performance criteria is expressed in Equations 1-2 [1] and must result in 75% or greater to enroll in regulation services. Once accepted the resource must maintain a performance level greater than 40%, else it will have to re-apply to participate in the regulatory market. This effectively sets the the bounds for DERAS testing.

$$\begin{aligned} Performance(t) = max_{i=0-5_{min}} \\ [A * Delay(t+i) \\ + B * (Correlation(t+i)] \\ + C * Precision(t) \end{aligned} \tag{1}$$

where,

$$\begin{aligned} CorrelationScore &= r_{signal}(\delta, \delta + 5_{minutes}) \\ DelayScore &= |\frac{\delta - 5_{minutes}}{5_{minutes}}| \\ Error &= |\frac{response - signal}{signal_{hourly}}| \\ PrecisionScore &= 1 - \frac{1}{n}\sum |Error| \end{aligned} \tag{2}$$

A. Results

At present, the DERAS system is in testing. Results will be presented at the conference. Current tests include: simulated DER model validation, communication resource requirements, and PJM performance testing and validation.

References

[1] PJM. Pjm manual 12: Balancing operations. Technical report, November 2017.

A Distributed Energy Resource Aggregated System for Providing Ancillary Services

Manasseh Obi, Kevin Marnell, Robert B. Bass
Dept. of Electrical and Computer Engineering
Portland State University
Portland, Oregon, USA
marnell@pdx.edu

***Abstract*—Stochastic renewable generation, like solar and wind, presents a new challenge to the electrical grid. These generation assets can change rapidly due to clouds or a lull in wind. To maintain grid stability, fossil fuel generation assets like combustion turbines and combined cycle gas turbines are used to balance the differences between generation and load. Fossil generation corrects these problems, but frequently must operate inefficiently to do so. Distributed energy resources (DER) offer a solution to traditional generation, especially when aggregated as part of a distributed energy resource aggregation system (DERAS). A DERAS utilizes a vast number of DER assets including solar generation, wind generation, battery storage, and customer loads to compensate for stochastic renewable generation. DERAS provide ancillary services to compensate for grid events. The presenters introduce a resource estimator located at the aggregator which combines emulated asset data from DER agents using an Internet of Things architecture. This resource estimator can predict the availability of fast acting DER assets and use these to correct problems in the power grid by offering ancillary services.**

I. Introduction

DERs include a wide range of small devices that may be aggregated for use by the utility. DER includes small generation assets like solar generators and diesel reserve generators, which can be used to produce additional power. DER includes demand response assets like water heaters, commercial refrigerators, and heat pumps, which can be used to absorb excess power. DER also includes small storage assets like batteries and electric vehicle chargers which can be used to both discharge power to the grid or absorb power from the grid. The availability of these resources depends on both the physical state of the device (a full battery cannot charge) and its decision to be available for grid applications (owner preferences).

By combining DER devices, an aggregator can provide grid ancillary services that have previously been provided by fossil fuel generation. These services include load following by adding and subtracting load to match generation, frequency regulation by absorbing or discharging power in short bursts, and reserve service by having additional generation available. Aggregating many DER assets allows for the availability of these ancillary services.

II. Key Components

For aggregating these DER, the presenters propose the DERAS architecture outlined in Figure 1. Using the AllJoyn IoT Framework DERAS can discover and aggregate tens of thousands of DER assets. DER assets that choose to be managed by an aggregator will be connected into the DERAS as agents. The physical DER assets will report their states, both phyical states and availability states, to DERAS. The agent hub continually reports and updates these states to the emulated asset models, also known as "digital twins."

The digital twins are used to assess megawatt and megawatt-hour capacities, so the resource estimator can determine which ancillary services can be offered. The resource estimator determines a percentage of certainty with which ancillary services will be available. For instance, the resource estimator may predict a 75% chance of having 400 kW available for reserve service and a 99% chance of 300 kW available for reserve service. The resource estimator will employ optimization techniques to determine the ideal allocation of DER assets to provide ancillary services. The aggregator or utility can then use this information to bid into power markets.

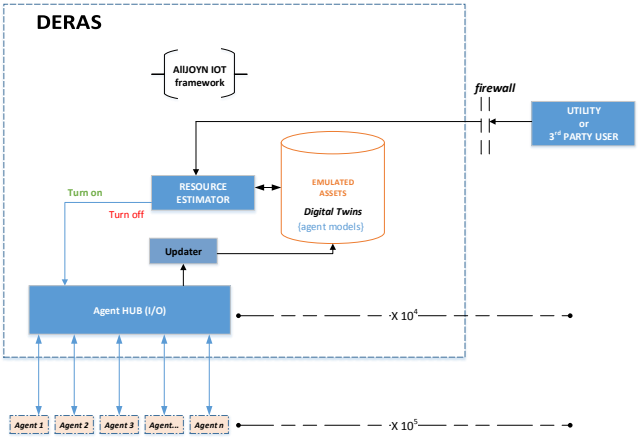

Fig. 1. DERAS system architecture.

Online Identification of Power System Electromechanical Modes

[1]P. Arunagirinathan, *Student Member, IEEE*, [1,2]G. K. Venayagamoorthy, *Senior Member, IEEE*
[1]Real-Time Power and Intelligent System Laboratory, Clemson University, SC, USA
[2]School of Engineering, University of KwaZulu–Natal, Durban, South Africa
parani@ieee.org and gkumar@ieee.org

***Abstract*—Poorly damped electromechanical oscillations exhibited by synchronous generators have caused wide spread blackouts in the past. The oscillation frequencies including the inter-area and intra area modes in the range from 0.3Hz to 2.0Hz are studied carefully. The increasing penetration levels of renewable energy generation sources produce more oscillations due to its uncertainty. Therefore online identification of power system electromechanical modes is required in mitigating these oscillations. Data driven techniques are commonly used for power system stability analysis and stochastic subspace identification (SSI) is used in this study. Synchrophasor devices are installed in the electric power grid and streaming data to the control centers. SSI based online identification of power system electromechanical modes using synchrophasor data is studied. An IEEE 68 bus New England-New York benchmark power system has been simulated on a real-time digital simulator (RTDS) for this study.**

***Index Terms*—Electromechanical modes, power system, RTDS, stochastic subspace identification, synchrophasors**

I. Introduction

The power system operation is challenged by low frequency electromechanical mode oscillations exhibited by synchronous generators for system disturbances. Poorly damped inter area oscillations have caused wide spread blackouts of the system in the past. Therefore identification of critical low frequency electromechanical oscillation modes and mitigation of those is important for secure power system operation. The low frequency oscillation modes in the range from 0.3 Hz to 2.0 Hz are considered for system stability analysis. In order to design an effective adaptive controller it is required to have an online model of the power system. Despite the power system is highly complex and non-linear, the representation of power system through linear state space has been widely used for stability analysis and control. This is because, first, although individual generators can only be best modeled by nonlinear differential equations, modal analysis based on the linearization of interconnected power system near a nominal operating point can effectively uncover the characteristics of oscillation modes; second, although power systems are subject to changes of operating conditions, these variations are comparatively small comparing to the major systematic topology and generator parameters that remain unchanged; thus, the modal analysis results can be well applied to a range of operating points.

This work is supported in part by US National Science Foundation (NSF) under grants #1312260, # 1408141 and #1232070 and the Duke Energy Distinguished Professor Endowment Fund. Any opinions, findings and conclusions or recommendations expressed in this material are those of the author(s) and do not necessarily reflect the views of National Science Foundation and Duke Energy.

State space representation of power system has been used in various studies. Considering the stochastic nature of the power system, a stochastic subspace identification (SSI) [1] method is used for online power system electromechanical oscillation mode identification. SSI is a data driven system identification technique and it has already been used in power system applications [2]. SSI can be applied to an input/output based model or an output based model of the power system.

Synchrophasors deployed in the power system are streaming remote measurements at a very fast rate to utility control centers [3]. Power system model validation tools with synchrophasor measurements are already available. Synchrophasor measurement based adaptive controller designs are proposed to damp the critical low frequency electromechanical oscillations modes. Therefore, synchrophasor data driven SSI method for power system electromechanical modes has been studied. IEEE 68 bus New England-New York benchmark power system shown in Fig.1 has been simulated on a real-time digital simulator and the synchrophasor devices are configure to receive measurements from RTDS using GTAO cards.

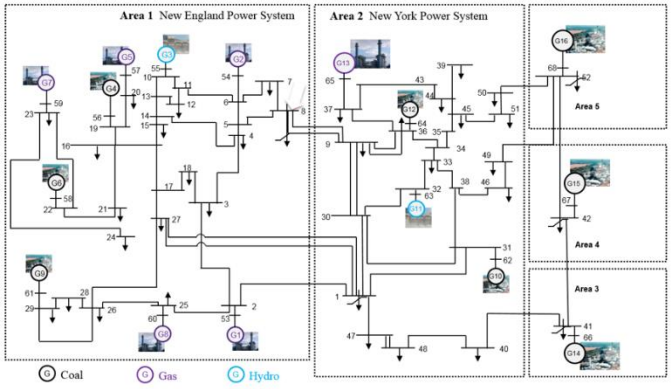

Fig. 1 IEEE 68 bus 16 generator five area power system

References

[1] N. J. Bershad, J. C. M. Bermudez and J. Y. Tourneret, "Stochastic analysis of the LMS algorithm for system identification with subspace," *IEEE Transactions on Signal Processing,* vol. 56, no. 3, pp. 1018-1027, 2008.

[2] K. Tang and G. K. Venayagamoorthy, "Damping inter-area oscillations using virtual generator based power system stabilizer," *Electric Power Systems Research,* vol. 129, pp. 126-141, 2015.

[3] I. Kamwa and R. Grondin, "PMU configuration for system dynamic performance measurement in large multiarea power systems," *IEEE Transactions on Power Systems,* vol. 17, no. 2, pp. 385-394, May 2002.

A Power Waveform Classification Method for Adaptive Synchrophasor Estimation

Cheng Qian, *Graduate Student Member, IEEE*, Mladen Kezunovic, *Life Fellow, IEEE*
Dept. of Electrical and Computer Engineering
Texas A&M University, College Station, TX
peterqiancheng@tamu.edu, kezunov@ece.tamu.edu

***Abstract*—An input waveform classification scheme is proposed, which is used to facilitate synchrophasor estimation. The classification is achieved by scrutinizing the temporal trajectories of input waveform frequency and amplitude features, which are extracted by a uniquely designed multiresolution time-frequency analysis technique using "pseudo-wavelet". Such time-frequency waveform features are further exploited to classify input waveform types. Contrary to traditional approaches for synchrophasor estimation, where a single algorithm is designed for all types of input signal, a new framework is discussed where an adaptive switching of algorithms is enabled, so that the most suitable algorithm can be used for the specific type of waveform. The efficacy and efficiency of proposed methods are validated with standardized PMU testing waveforms, and simulated power system waveforms. Detailed work has been published in IEEE Transactions on Instrumentation and Measurement.**

***Index Terms*—Correlation, multiresolution analysis, power system measurements, spectral analysis, synchronized phasor measurement**

I. Methodology and Key Equations

The proposed method essentially utilizes a single cosine wave as the mother wavelet in classic continuous wavelet transform (CWT) definition, shown in (1).

$$\gamma(x;a,b)=\int_{-\infty}^{\infty}\hat{x}(t)\vartheta(\frac{t-b}{a})\mathrm{d}t \tag{1}$$

where $\gamma(x;a,b)$ is the correlation coefficient between $\hat{x}(t)$ and $\vartheta(t)$ for selected pair of a and b, $\hat{x}(t)\coloneqq[x(t)-\bar{x}]/\max[x(t)]$is the centered and normalized input signal, $\vartheta(t)$ is a proposed pseudo-wavelet, which are unit cosine waves.

The resultant transform is able to reveal the time-frequency composition of waveform on a multiresolution level. $\gamma(x;a,b)$ shows zero intensities when the instant waveform frequency ω_1 satisfies:

$$\omega_1=k\omega_{\mathrm{pw}},k=0,2,3,4,\dots$$
$$\omega_{\mathrm{pw}}\geq\omega_{\mathrm{pw,min}}\equiv\frac{2\pi}{T_{\mathrm{window}}} \tag{2}$$

where T_{window} is the length of data observation window in seconds.

This property can be leveraged to track the time-frequency trajectory of input waveform, which can be further used to identify and classify input waveform types.

This work was supported by the Power Systems Engineering Research Center (PSERC) Project T-57HI "Life-cycle management of mission-critical systems through certification, commissioning, in-service maintenance, remote testing, and risk assessment"

II. Key Figures

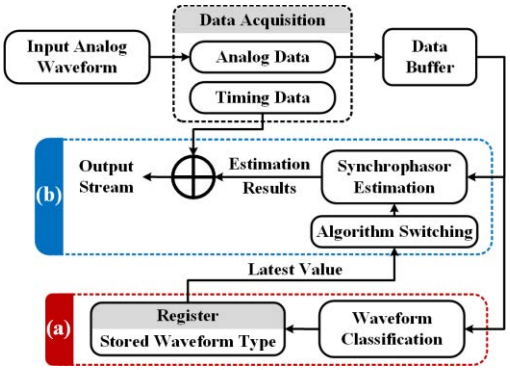

Fig. 1. Framework for synchrophasor estimation utilizing proposed waveform classification procedure.

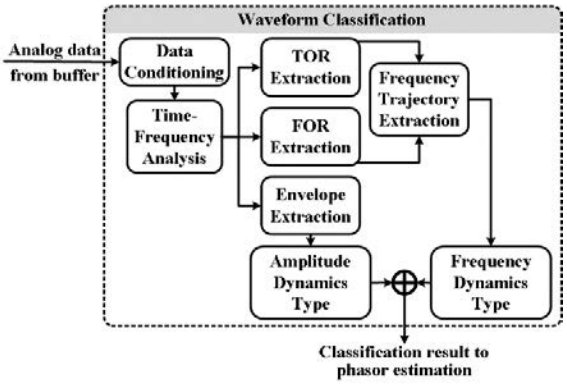

Fig. 2. Overall structure of proposed waveform classification method employing the proposed PW time-frequency multiresolution analysis.

III. Key Results

The proposed methods are implemented in NI CompactRIO and SEL-3355, where the performances are tested. The efficacy and efficiency of proposed methods are verified.

TABLE I. Summary of Computation Time

Procedure \ Platform	MATLAB (SEL-3355)	LabVIEW (NI cRIO-9082)
Sampling Rate	1kHz	1kHz
Data Length	10 cycles	10 cycles
Time-Frequency Analysis	11ms	4ms
Freq. Trajectory Extraction	11ms	11ms
Total	22ms	16ms

Non-Invasive System Impedance Estimation Based on Data Selection

Ori Zhang
Department of Electrical and Computer Engineering
University of Alberta
Edmonton, Canada
Shijia2@ualberta.ca

Frank Wang
Department of Electrical and Computer Engineering
University of Alberta
Edmonton, Canada
Yang5@ualberta.ca

***Abstract*—Distribution network fault levels or equivalent circuit impedances are important data for both utility companies and their customers. The data has many uses, such as specifying equipment rating, establishing protective relay setting, and determining the power quality impact of motor starting. In this poster, a novel and practical method has been developed for non-intrusive measurement of network impedances using the waveform data collected by power quality monitors. The method has been verified using simulation studies and field cases. The results show that the proposed method can serve as a useful tool to support the impedance measurement task of utility companies.**

Keywords— Power quality, fault level, impedance measurement

I. INTRODUCTION

Distribution network fault levels are important data for both utility companies and their customers. The data has many uses, such as specifying equipment rating, establishing protective relay setting, and determining the power quality impact of motor starting. The fault level data are typically obtained using model based short-circuit calculations. The accuracy of the results is highly dependent on the quality of input data and the status of equipment used by the model. Over the past many years, utility companies have been looking for methods that can measure the actual fault level at a given point of a power system. In recent years, the need to measure network fault levels has become more evident due to the concerns on power quality and the proliferation of distributed generators.

Determining the fault level of a network is equivalent to determining the Thevenin circuit impedance of the network or the supply system impedance. After many years' research efforts, two broad approaches to estimating the equivalent circuit impedance of a network have been proposed: invasive and noninvasive methods. The first methods are usually operated by injecting disturbances into the network in order to cause variations in the voltage and current and then determine the impedance. Although these methods could provide reliable results, the disturbances may cause negative impacts on the grid operation. Furthermore, the devices used to generate the disturbances can be quite expensive.

In contrast, noninvasive methods use natural voltage and current variations to obtain the impedance information without any extra devices and negative impact.

This poster shows an appropriate method for non-intrusive measurement of equivalent circuit impedance using the waveform data collected by power quality monitors. It been tested using various field data and its performance has been found acceptable for industry applications. The basic frame work is shown as follows:

II. KEY EQUATIONS

$$\min f(Rs, Xs, E, \delta) = \sum_{i=1}^{N} \left\| V \right| \angle \alpha - (R_s + jX_s) \times \left| I \right| \angle \beta - \left| E \right| \angle \delta \right|^2$$

$$\begin{bmatrix} Rs + jXs \\ \left| E \right| \angle \delta \end{bmatrix} = (X^T X)^{-1} X^T Y, \quad \text{where } X = \begin{bmatrix} \left| I_1 \right| \angle \beta_1 & 1 \\ \left| I_2 \right| \angle \beta_2 & 1 \\ \vdots & 1 \\ \left| I_N \right| \angle \beta_N & 1 \end{bmatrix}, Y = \begin{bmatrix} \left| V_1 \right| \angle \alpha_1 \\ \left| V_2 \right| \angle \alpha_2 \\ \vdots \\ \left| V_N \right| \angle \alpha_N \end{bmatrix}$$

V and I are measured data, $-(Rs + jXs)$ is the estimated system impedance

III. KEY FIGURES

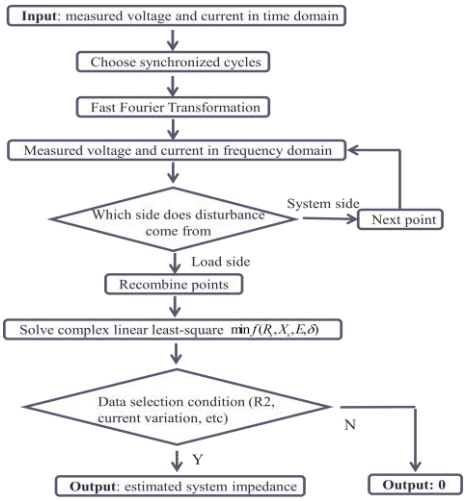

An advanced maximum power point capturing technique with supercapacitor for PV system

Lijun Zhang, *Student Member, IEEE,* Samson Shenglong Yu, *Member, IEEE,*
Herbert H.C. Iu, *Senior Member, IEEE,* Tyrone Fernando, *Senior Member, IEEE,*
Department of Electrical, Electronic and Computer Engineering. University of Western Australia

***Abstract*—In this paper, the characteristic curves considering complete Current-Voltage (I-V) and Power-Voltage (P-V) relations for PV system are presented. Based on the I-V characteristic curve, a novel Maximum Power Point Capturing (MPPC) technique is proposed to overcome the steady-state oscillation and slow dynamic response problems existing in the conventional Maximum Power Point Tracking (MPPT) technique. In order to further mitigate the fluctuations for PV system, an appropriate supercapacitor (SuperC) is selected to be connected in parallel with the PV system. The simulation results demonstrate the designed MPPC-superC structure has a better performance than the conventional MPPT method and MPPC method in both steady-state and dynamic responses.**

I. Key Contributions

(1) Wrong perturbation under dynamic state is eliminated. The proposed MPPC technique is designed on both steady and dynamic characteristics of PV system, respectively shown in Fig. 1 and Fig. 2, instead of the conventional MPPT technique only considering the steady characteristics of PV system. The combination of Fig. 1(a) and Fig. 2(a) is defined as the complete I-V curves and the combination of Fig. 1(b) and Fig. 2(b) is defined as the complete P-V curves.

(2) The trade-off for duty ratio step size does not exist. MPPC technique is based on above complete I-V curves and a practical PV model with following equations:

$$I = I_{sc}[1 - C_1[e^{(\frac{V}{C_2 V_{oc}})} - 1]], \tag{1}$$

where C_1 and C_2 are the relevant coefficients.

Through solving (1), MPP can be captured online in Fig. 3. Therefore, its control strategy is designed a steady area ϵ:

$$\epsilon = |(V(k) - V_m)/(V_m)|. \tag{2}$$

When $\epsilon \leq \epsilon_{\text{th}}$ (ϵ_{th} is error threshold), duty cycle stops varying. When $\epsilon > \epsilon_{\text{th}}$, MPPC is triggered and V_m will be updated.

(3) The flicker is better prevented when SuperC is connected in parallel with the PV system in Fig. 4. When $RC/\Delta t >> 1$,

$$\Delta V/V \leq ((P_{PV2} - P_{PV1})\Delta t)/(2CV^2). \tag{3}$$

II. Key figures

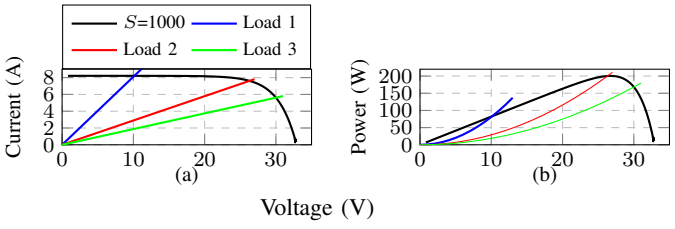

Fig. 1: I-V and P-V curves under a constant solar irradiance

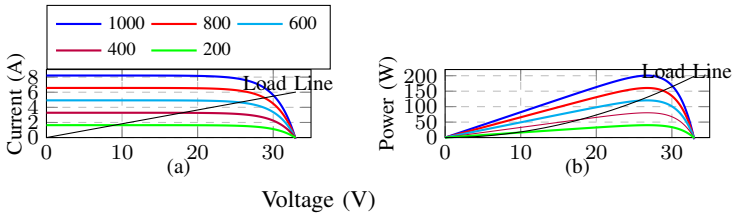

Fig. 2: I-V and P-V curves under changing solar irradiance

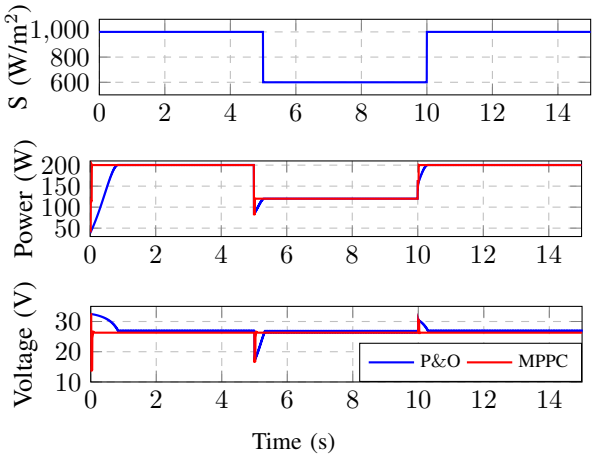

Fig. 3: Solar irradiance S has a rapid change.

In Fig. 4, the power provided by SuperC shown in green line is a transient power. Specifically, this power has an ability to stabilize output voltage of PV array.

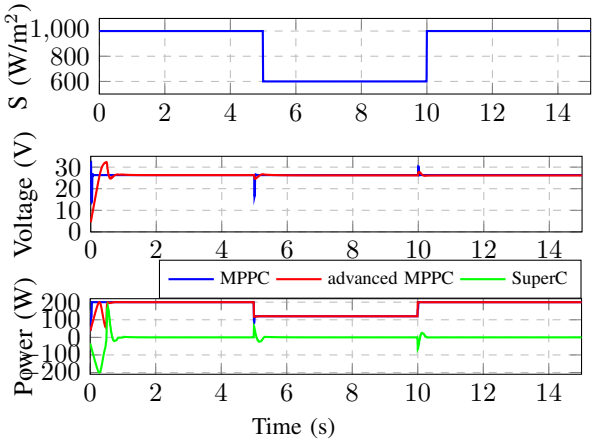

Fig. 4: Comparison with a step change solar irradiance S.

Comparative Analysis of Demand Response and Load Management Algorithms

Divya T. Vedullapalli, *Student Member, IEEE*
Ramtin Hadidi, *Member, IEEE*
The Holcombe Dept. of ECE
Clemson University, SC, USA
dvedull@clemson.edu, rhadidi@clemson.edu

Bill Schroeder, Ryan Baumgartner
Johnson Controls, Inc.
507 E. Michigan St., P.O. Box 423
Milwaukee, WI, USA

***Abstract* —The objective of this project is to quantify the efficacy of the Model Predictive Control (MPC) demand charge management algorithm developed by Johnson Controls Inc. (JCI) against the existing demand side management strategies. Clemson and JCI are working together to develop industry benchmarks and define metrics that effectively evaluate the performance of these algorithms in real world limitations. These algorithms are to be tested on a 50kW, 165kWh energy storage system installed behind the meter at a Clemson University academic building. The next phase of this work involves augmenting the most advantageous algorithms for the energy storage system with the building management system to realize greater opportunities to the end users.**

***Index Terms*— Battery energy storage system (BESS), Demand charge management, Load forecasting, Model Predictive Control (MPC), Optimization**

I. INTRODUCTION

To avoid installation of capacity with increasing demand of electricity, utilities employ Time-of-Use (TOU) pricing schemes for energy and/or include demand charges during peak hours. A battery can be utilized to shift the load partially during peak to off-peak time and reduce the electricity cost. The schematic of the system is shown in Fig. 1, in which arrows represent directions of power flows in the system.

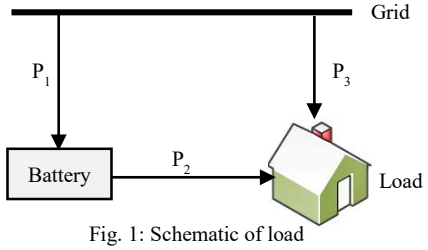

Fig. 1: Schematic of load management with battery

The goal of the demand side management algorithm is to determine the optimal schedule of battery for minimizing electricity cost while satisfying customers' load and battery operating conditions.

II. OPTIMIZATION FORMULATION

$$\underset{P_1,P_2,P_{Shave}}{\text{Minimize}}\ J=\sum_{t=1}^{N}\left[\left(P_1(t)+P_L(t)-P_2(t)\right)*\Delta t*\rho_E(t)\right]$$
$$+\max\left(P_1(t)+P_L(t)-P_2(t)\right)*\rho_D(t)$$

s. to :

$$SOC(t)=SOC(0)+\frac{\eta_C\sum_{\tau=0}^{t-1}P_1(\tau)\Delta t-\frac{1}{\eta_D}\sum_{\tau=0}^{t-1}P_2(\tau)\Delta t}{B_{Cap}}$$

$$0\le P_1(t)+P_L(t)-P_2(t)\le P_{Shave}$$

$$SOC^{\min}\le SOC(t)\le SOC^{\max}$$

$$0\le P_i(t)\le P_{i,\max};i=1,2$$

III. MPC FRAMEWORK

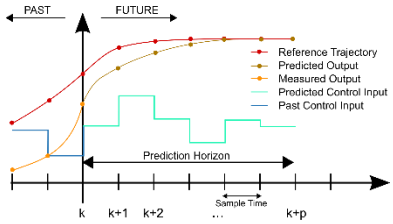

Fig. 2 MPC Strategy
(Courtesy of Wikipedia)

IV. SAMPLE RESULTS

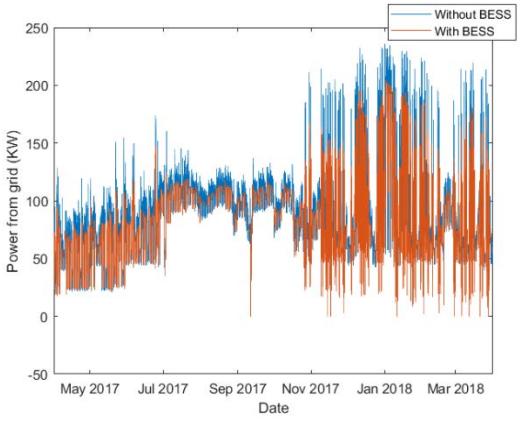

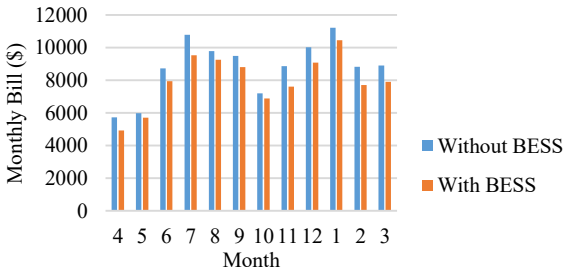

Fig. 4 Grid demand and Electricity bill

A Non-Contact Method for Real-Time Monitoring of Conductor Sag

Monish Mukherjee and Robert G. Olsen
School of Electrical Engineering and Computer Science
Washington State University, Pullman WA

***Abstract*—In this work a simple non-contact method to inexpensively and accurately measure conductor sag is validated. The method involves measurement of the space potential (amplitude and relative phase) near the transmission line conductors. The key to the new idea is make the measurement of space potential much more sensitive to sag by placing a pair of space potential probes at two points symmetric with respect to the centerline so that the difference in phase between the two points is 180°. It has been validated that the net current induced on the probes is very sensitive to conductor sag.**

I. Introduction

The amount of power carried by a high voltage transmission line is limited by the current that can flow through the conductors since the voltage is relatively fixed. Excessive current produces excessive heating of the wires that may result in annealing, premature aging of components such as splices and/or excessive sag that may result in violations of safety standards. Existing devices (tension monitor, video sago-meter, power donut) used for measuring power-line conductor sag are expensive, require shielding and/or require de-energizing of the power lines.

II. Differential Space Potential Probes

The amplitude and phase of the space potential for a horizontal 230 kV transmission line are shown in Figure 1 and 2 respectively.

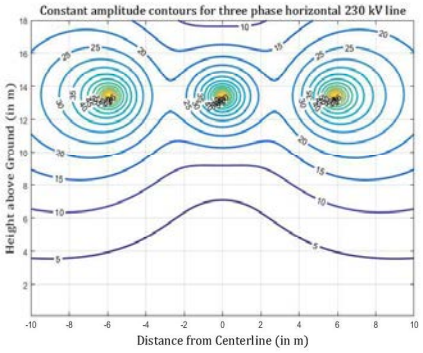

Fig. 1. Constant amplitude contours for the three phase horizontal 230 kV transmission line

As shown in Fig. 2 a pair of space potential probes are placed at two symmetric points so that the phase difference between the two points is 180° (-90°/90° contours). The superimposed short circuit current from the two probes is zero for the particular geometry of the arrangement and changes rapidly with sag. Since the transmission line voltage is constant, the arrangement measures only conductor sag.

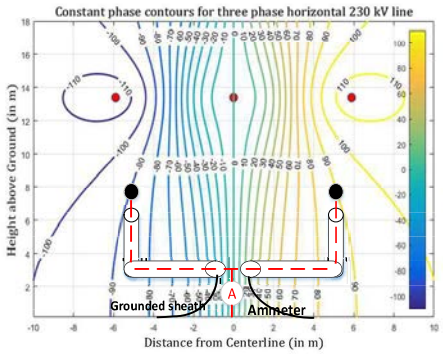

Fig. 2. Constant phase contours for the three phase horizontal 230 kV transmission line with the sag measurement arrangment (differential probe).

III. Experimental Validation

In order to validate the idea, the probes were moved horizontally and the net induced current recorded.

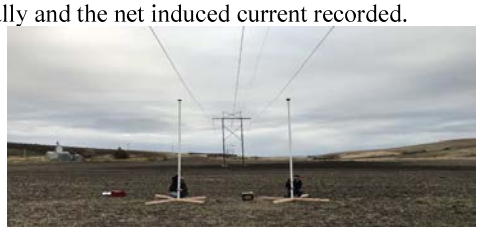

Fig. 3. Photograph of the site with the space potential probe arrangement.

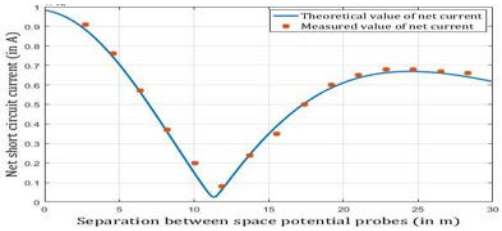

Fig. 4. Measured and Theoretical values of neet current for different horizontal position of the space potential probe arrangment.

The measured values of net current matches closely with the theoretical values. The dip in the net current curve indicates that the probes are at -90°/90° phase contours.

The differential probe arrangement increases the sensitivity of the sag measurement. The method has been experimentally validated on an asymmetric real life 230 kV transmission system. The sensitivity to sag can be further improved by orienting the space potential probes along the more sensitive constant phase contours (-100°/100° contours) and using phase shifting circuitry.

Smart Grid-enabled CVR: An advanced application for Distribution Management System

Shailendra Singh[1,2], S. P. Singh[1], *Senior IEEE Member*
Department of Electrical Engineering[1]
Indian Institute of Technology (BHU)
Varanasi, U. P., India

Santosh Veda[2], Murali Baggu[2] *Senior IEEE Member*
Power System Engineering Centre[2]
National Renewable Energy Laboratory
Golden, Colorado, USA

***Abstract*—In this paper, a multi-level multi-tasking smart grid enabled conservation of voltage reduction (CVR) control and optimization methodology has been proposed for advance distribution management system (ADMS) application. First level deals with centralized optimization of Volt/VAr optimization (VVO) devices and second one is voltage control in local domain or decentralized control. The assessment of proposed method in terms of energy saved and CVR factor has been analyzed in third level. The problem has been solved through particle swarm optimization (PSO) and droop control method. The simulation results reveal that enabling of CVR during presence of high photovoltaic (PV) penetration is not only produces significant power saving also mitigates the over/under voltage problem.**

I. SMART GRID ENABLED CVR AND OPTIMIZATION

Figure 1 shows the proposed framework that will fit into the existing distribution grid. The ADMS is fed back through advance metering infrastructure and supervisory control and data acquisition (SCADA) points which update the field monitored measurements at regular intervals. The fundamental task of VVO processor is to optimize the settings of VVO devices according to CVR server. The range of CVR duration and CVR voltage are set by control centre operator in CVR server block according to requirement.

II. MATHEMATICAL FORMULATION AND SOLUTION

The formulation of proposed CVR control is formulated in three layers as delineated under:

A. First layer: Centralized control and optimization

In this layer, CVR is enabled using below objective functions.

$$f_1 = \min\left\{\sum_{a,b,c}\sum_{k}^{n-1}\left(V_{CVR,h}-V_{k,h}\right)^2_{a,b,c}\right\} \quad (1)$$

$$f_2 = \min\left\{\sum_{a,b,c}\left(P^{a,b,c}_{loss,h}+jQ^{a,b,c}_{loss,h}\right)\right\} \quad (2)$$

where, $V_{k,h}$, $V_{CVR,h}$, $P^{a,b,c}_{loss,h}$ and $Q^{a,b,c}_{loss,h}$ is the node voltage (p,u.) at k^{th} node, expected CVR voltage (p,u.) , active power loss and reactive power loss with a,b,c as phase notation respectively and n is number of nodes.

The above problem has been solved through multi objective PSO with system constraints.

Supported by Indo-US Science & Technology Forum, India under the Bhaskara Advance Solar Energy Fellowship-2018

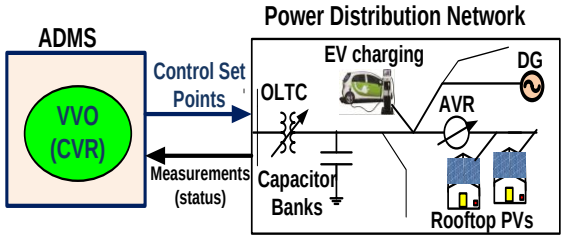

Fig.1 Closed loop framework for CVR operation

B. Second Layer: Local voltage control

If the voltage violation occurs in with defined time horizon of first layer, then this layer operates and provides additional reactive power compensation through PV inverters. The compensation value is determined using Volt/VAR droop control characteristics.

C. Third Layer: Calculation of Savings and CVR factor

$$CVR\ factor = \frac{\Delta W\%}{\Delta V\%} \quad (3)$$

where $\Delta W\%$ is the percentage of reduction in quantity and $\Delta V\%$ is the percentage of voltage reduction.

III. SIMULATIONS AND RESULTS

The proposed method has validated on modified IEEE 123 distribution test feeder in the presence of three PVs during peak demand hour. Fig. 2 and Fig. 3 shows some key results using OpenDSS and MATLAB environment.

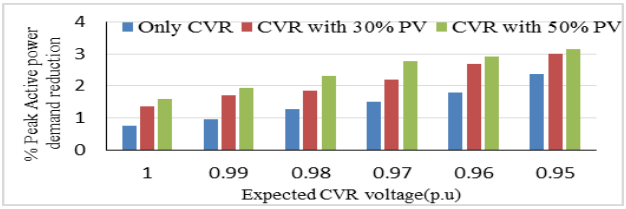

Fig.2 % peak active power demanad reduction w.r. to different CVR voltages

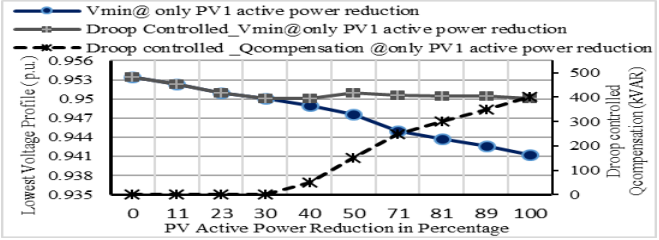

Fig.3 Lowest voltage profile during different % PV active power reduction

D^{2}NDZ: Evaluating Unintentional Islanding Risks in Distribution Grids with Deep Integration of Distributed Energy Resources

Yan Li[1], Peng Zhang[1], Joseph N. Debs[2], David A. Ferrante[2],
Donald J. Kane[2], Samuel N. Woolard[2], Roderick S. Kalbfleisch[2], and Kenneth B. Bowes[2]
[1]Dept. of Electrical and Computer Engineering, University of Connecticut, Storrs, CT 06269-4157, USA
[2]Eversource Energy, Berlin, CT 06037, USA

***Abstract*—Efficiently calculating non-detection zones (NDZ) becomes increasingly important when evaluating unintentional islanding risks of distribution grids that are highly integrated with distributed energy resources (DER). A rigorous theoretical method, the learning-based DER-Driven Non-Detection Zone (D^{2}NDZ), is presented to estimate NDZ for any given distribution feeders. Numerical examples indicate that by using D^{2}NDZ, NDZ can be quickly and effectively obtained while avoiding numerous and time-consuming electromagnetic transient simulations.**

I. Methodology of D^{2}NDZ

The basic idea of D^{2}NDZ is to efficiently figure out an operation boundary by combining a theoretical analysis of the steady state of a generic system with the learning-based dynamic impact of DERs on a system. Specifically, it includes that (1) a primary NDZ considering different types of loads is analytically determined based on the steady state of a system after islanding and (2) the dynamic impact of DERs on the boundary of a primary NDZ is then analyzed and integrated into the primary NDZ to obtain the desired result.

- Active power steady-state analysis

$$\left.\frac{P_{DER}}{P_L}\right|^{S} = \frac{(1+\mu)^2(P_I P_C + P_I P_P + P_P P_C)}{(1+\mu)^2 P_I P_C + (1+\mu) P_I P_P + P_P P_C} \quad (1)$$

- Reactive power steady-state analysis

$$\left.\frac{Q_{DER}}{Q_L}\right|^{S} = (1+\mu)^2(1+\rho) \quad (2)$$

- Exponential impact of DER dynamics on NDZ

$$\phi_{PV,L} = \beta_{PV,L}(1-\alpha_{PV,L}\mathrm{e}^{-N_{PV}}), \quad (3)$$

$$\phi_{PV,H} = \beta_{PV,H}(1-\alpha_{PV,H}\mathrm{e}^{-N_{PV}}), \quad (4)$$

As an estimation method, the performance of D^{2}NDZ mainly depends on the parameters in each formula. A learning-based method is established to optimize these parameters from the experiments' data.

$$\min f = \sum_{i=1}^{N_C} m_i \Big(\left.\frac{P_{DER}}{P_L}\right|_{min,i} (\beta_{PV,L}, \alpha_{PV,L}) - \left.\frac{P_{DER}}{P_L}\right|_{min,i}^{E} \Big)^2 \quad (5)$$

This material is based upon work supported by the National Science Foundation under Grant No. 1611095, Eversource Energy Center under Grant No. 6367940, and UConn Academic Plan Level 1 under Award No. 2806600.

II. Test Cases

A typical distribution feeder in Eversource Energy's service territory is used to validate D^{2}NDZ. Corresponding results are shown in Fig. 1 and Fig. 2.

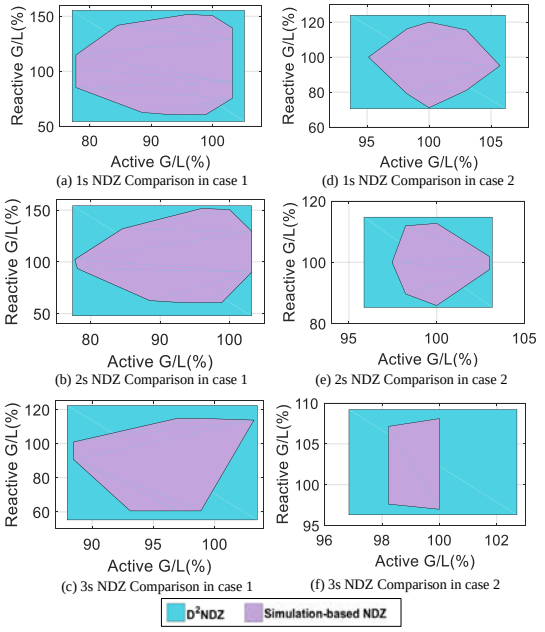

Fig. 1 Comparisons between D^{2}NDZ and simulation-based method

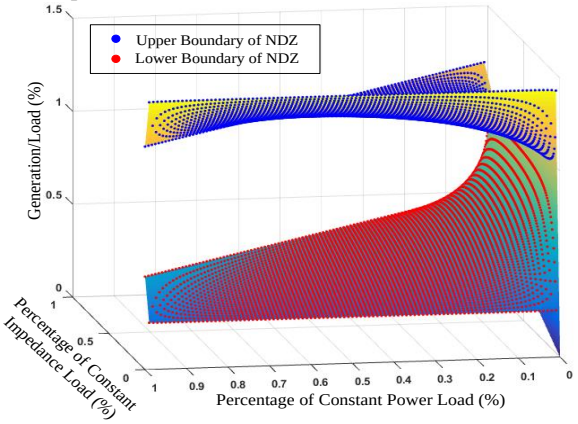

Fig. 2 Impacts of loads on baseline NDZ

Real-time Operation Pattern Detection using Measurements from a Network of PMUs

Ming Liang, *Student Member, IEEE*, Yao Meng, *Student Member, IEEE*, Ning Lu, *Senior Member, IEEE*

***Abstract*—This paper presents data-driven approach for real-time, operational pattern detection using measurements from a network of PMUs. Real-time 3-phase PMU data from a network of PMUs are used to derive multi-dimensional signatures that benchmark the operational signatures of frequency, voltage, and power flow at different location of the transmission grid. Those signatures dynamically baseline the operation patterns of a given system and can be used for detecting anomalies that are caused by equipment malfunctions, intentional and unintentional man-made errors, or cyber-attacks. Because the existing of inherent operational patterns between system nodes, we demonstrated that using a combination of 1-dimensional threshold-based identifiers and 2-dimensional correlation-based operational regions, one can quickly establish a database that can be continuously updated and trained using new data set. The method provides system operators model- and topology-free approach to monitor and detect anomaly in grid operation.**

Keywords-data driven approach, PMU, operation patterns, anomaly detection, fluctuation, longest common subsequence.

I. INTRODUCTION

In the past, researchers rely mainly on synthetic PMU data for deriving operational patterns and signatures because actual data from a network of PMUs are not available to them. Because of the lack of access to actual PMU data, especially data from a network of PMUs in actual power grid, IEEE test systems are often used for generating the synthetic PMU data sets for signature detection and validation. For example, in [1], events via simulation are carried out on an IEEE 39-bus system. In [2], the authors present a data-driven real-time cyber-physical detection and defense strategy with distributed control using real-time data from PMUs. Their strategy is tested on a modified IEEE 118-bus test system.

Because synthetic data lacks of actual system dynamics as well as the true correlation between generation and load (i.e. the power flow changes), it is sometime impossible for researchers to derive and validate methods for real-time, operational pattern detection using measurements from a network of PMUs. The true value of PMU data collected from a network of PMUs lies in the fact that it provides the grid operator close to real-time snapshots of values from inherently correlated system variables, i.e. the system frequency, power flow (real and reactive), system voltage (angle and magnitude). Therefore, investigating the data to reveal the characteristics of each variable or among variables can reveal the inherent system operational patterns that are native to the system only. This makes it possible for grid operators to develop a knowledge database that can be dynamically updated and fine-tuned based on new datasets.

In this paper, we present our preliminary results on real-time operation pattern detection using measurements from a network of PMUs located in a regional power grid.

II. KEY EQUATIONS

Remove the DC offset of the original signal

$$y(k) = \sum_{i=1}^{30}(x_i - \bar{x}) \quad (1)$$

Conduct a linear regression for all the $y(k)$ data points during the modelling period. The regression value at each time k is called as the trend and marked as $yn(k)$. Calculate the error between the signal *y(k)* and the trend $yn(k)$.

$$e(k) = y(k) - yn(k) \quad (2)$$

Finally, calculate fluctuation value, this process of detrending followed by fluctuation measurement is repeated over a range of different sizes n.

$$F(n) = \sqrt{\frac{1}{n}\sum_{k=1}^{n}[e(k)]^2} \quad (3)$$

III. KEY FIGURES

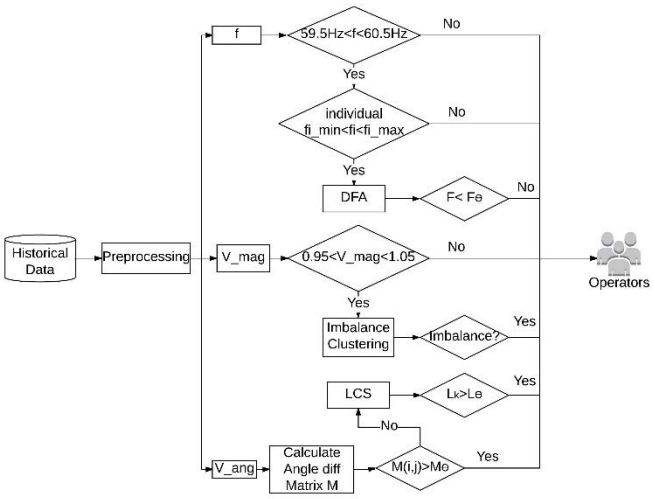

Fig. 1 The flow chart to build up operation patterns and events detection

REFERENCES

[1] Yufei Tang, Jun Yang. Dynamic Event Monitoring Using Unsupervised Feature Learning Towards Smart Grid Big Data. 2017 International Joint Conference on Neural Networks (IJCNN), p 1480-1487.

[2] Jin Wei. A Data-Driven Cyber-Physical Detection and Defense Strategy Against Data Integrity Attacks in Smart Grid Systems. 2015 IEEE Global Conference on Signal and Information Processing (GlobalSIP), p 667-671.

Nonlinear Dynamics Based On-line Detection of Oscillation Using Power System Measurement Data

Hwanhee Cho and Byongjun Lee*
School of Electric Engineering
Korea University
Seoul, Republic of Korea
leeb@korea.ac.kr

Suchul Nam
Power Transmission Laboratory
Korea Electric Power Research Institute(KEPRI)
Daejeon, Republic of Korea
suchul.nam@kepco.co.kr

***Abstract*—This study proposes a time-series analysis approach and a nonlinear dynamics originated method to detect sub-synchronous oscillation in power systems. Mathematical expressions of the fundamental instantaneous signal and sample discrete signal of peak values are derived to examine the phenomenon of interaction between power system components. The results of the circulating trajectory are shown in a two-dimensional map of the calculated rms value and estimated Floquet multiplier when two signals of different modes are mixed. Without applying a digital filter or frequency decomposition, nonlinear oscillation detection is possible by monitoring a nonlinear oscillatory index based on the maximum Lyapunov exponent.**

***Index Terms*—Phasor measurement units, Power system measurements, Series compensation, Subsynchronous resonance, Time series analysis.**

I. Key Concepts

The proposed method introduces the Floquet multiplier and provides another perspective to analyze measured values. Rate of change(RoC) of data indirectly gives information of power system dynamics by linearizing Poincaré map. And then by mapping RoC and magnitude in the same plane, power system status can be monitored by using MLE. So that the proposed method detects the abnormal nonlinear behavior of power systems.

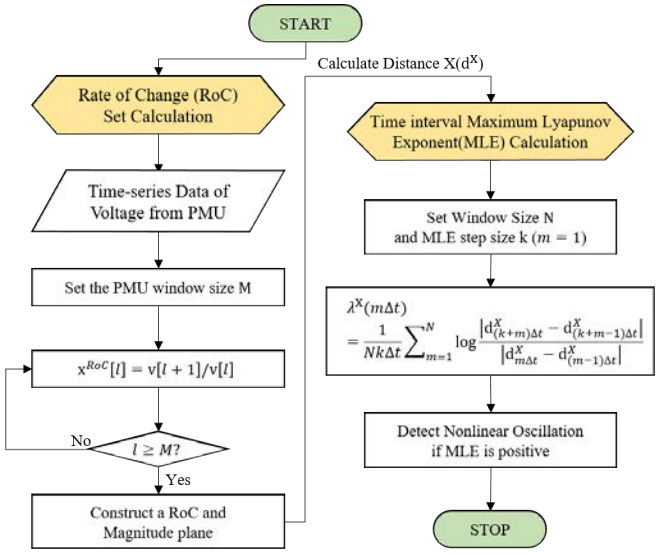

Fig. 1. Flowchart describing conceptual principle of the proposed algorithm.

II. Key Results

Figures below shows important results applying the proposed method of comprehensive application of nonlinear time series analysis.

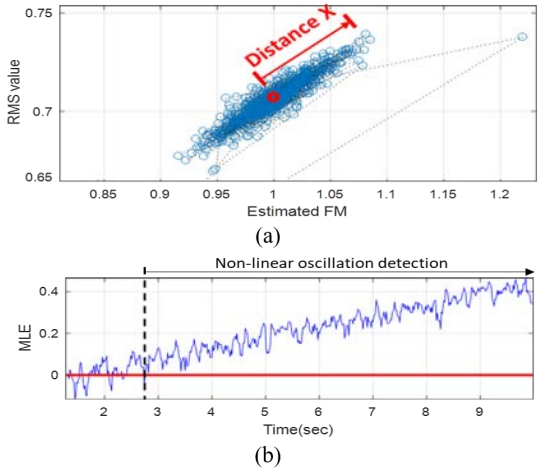

Fig. 2. Nonlinear oscillation detecting index based on the MLE (result of +0.3450).

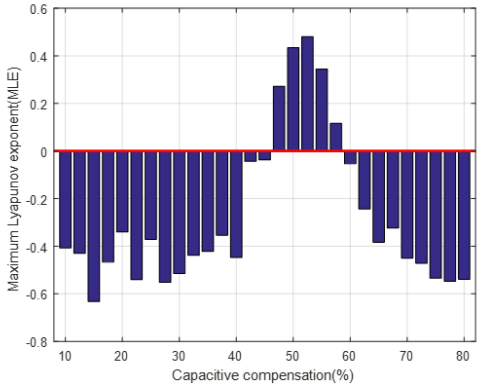

Fig. 3. Nonlinear oscillation detection index for a compensation range from 10 to 80%.

This novel index is capable to express the unique phenomenon in power systems such as SSR, SSTI, and SSCI. And its computation cost is relatively less and higher accuracy comparing other digital filter based decomposing methods.

Frequency Response Estimation Following Large Disturbances using Synchrophasors

Lucas Lugnani, Daniel Dotta
UNICAMP
Campinas, Brazil
Email: lugnani@dsee.fee.unicamp.br
dottad@unicamp.br

Joao M. F. Ferreira
ONS
Rio de Janeiro, Brazil
Email: jmarco@ons.org.br

Ildemar C. Decker
UFSC
Florianópolis, Brazil
Email: ildemar.decker@ufsc.br

Joe H. Chow
RPI
Troy, NY
Email: chowj@rpi.edu

***Abstract*—One new challenge, with the massive penetration of renewable generation (wind and solar), is the decline of the Electrical Power System's (EPS) frequency response. In order to deal with this new scenario, the development of tools to estimate key valuable parameters for frequency response is imperative. The Wide Area Measurement Systems (WAMS) signals can be useful to estimate the EPS frequency response after large disturbances. The paper main goal is to estimate the frequency response of the Brazilian Interconnected Power System (BIPS) after large disturbances using synchrophasors. These events were recorded at outlet voltage by a synchronized phasor measurement prototype, the LVS (low voltage synchrophasor), with PMUs (Phasor Measurement Units) installed in 26 universities throughout Brazil. The results show that high penetration of wind generation contributes to change the inertial EPS response.**

***Index Terms*—Inertial Response, Frequency Response, Electrical Power Systems, Phasor Measurement Units.**

I. Key Concepts

The Frequency Response of a Generator to a power imbalance (here referred as disturbance) can be described as:

$$s\Delta f = \frac{1}{2H}(-\Delta G + (\frac{1}{R_D}\frac{1}{1+sT_G} + D)\Delta f) \quad (1)$$

During the first moments after the disturbance, the Frequency disturbance can be resumed to the Inertial Frequency Response:

$$\Delta \dot{f} = -\frac{\Delta G}{2H} \quad (2)$$

In steady state, when $P_{acc} = 0$, the frequency deviation will be given as:

$$\Delta f = \frac{1}{D + \frac{1}{R_D}}\Delta G \quad (3)$$

Where $D + \frac{1}{R_D} = \beta$ is the frequency response. Equations 2 and (3) compose the response prior to nominal frequency reestablishment and will be used to estimate the BIPS frequency response using PMU data.

II. Key Results

Two real large disturbances are considered in this work: Under-Frequency and Over-Frequency (high wind penetration) Disturbances.

It becomes evident a relevant variation of H_{eq} for the Ne region between the First and Second Event. However, an analysis of power generation source for both events shows that First Event had a 2.25/2.5 GW hydro/wind regional generation and the Second Event had a 1.57/5.8 GW hydro/wind regional generation.

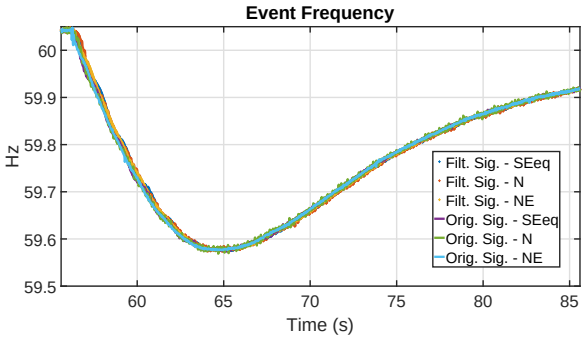

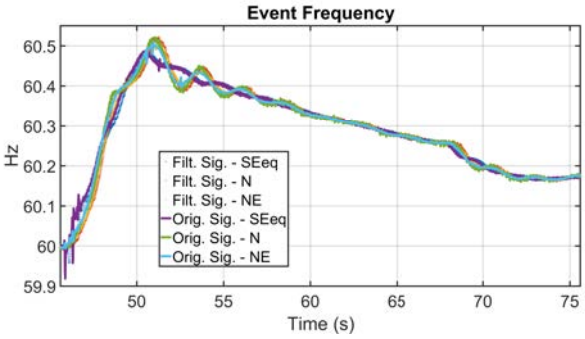

Fig. 1: Original and Filtered Frequencies - Under and Over-Frequency Events.

TABLE I: Estimated Parameters

	ROCOF (Hz/s)		H_{eq} (s)	β (MW/0.1Hz)
First Event				
	avg	*max*	*avg*	*avg*
SEeq	-0.0603	-0.0759	6.473	978
N	-0.0989	-0.0651	2.289	992
NE	-0.0404	-0.1027	7.137	980
Second Event				
SEeq	0.0833	0.0924	5.716	1,251
N	0.0921	0.0927	2.016	1,236
NE	0.1155	0.1196	5.691	1,189

A Hybrid Approach towards Event Detection in Multi-machine Power Systems

Abhishek Banerjee, *Student Member, IEEE*, and Rajesh Kavasseri, *Senior Member, IEEE*

***Abstract*—This paper presents a hybrid approach to determine the type of fault occurrence in a large scale power system by exploiting the underlying information of events in the structure preserving energy function (SPEF) components. A sliding window based method is proposed to determine the maximum singular values of these components. The resulting stacked up indices provide a metric for determining sensitivity of the energy function components. The proposed approach encapsulates a two stage process, i.e, firstly, a physical overview with a Sliding Window Prediction (SWP) is presented and in the second stage a validation is done by performing Principal component analysis (PCA) on the SPEF components.**

***Index Terms*—energy functions, event detection, singular value decomposition, principal component analysis.**

I. Introduction

REAL time detection of events in a large scale power system requires the knowledge of the the entire dynamics of the system. Analysis of fault in real time is a challenge in case of a contingency, when the approach is completely based on statistical methods applied on end data, collected post events. Such statistical approaches pose a huge computational burden as well it considers the entire system properties as a "black-box" problem. This data driven method is prone to failure with the loss of data and does not provide an insight into the physics of the problem. On the contrary, Structure Preserving Energy Functions (SPEF's) provide a way to derive every component of the energy terms in a multi-machine power system [1], [2], giving us complete knowledge of the system properties. Thus, motivated, our goal is provide a hybrid approach where there can be a one-to-one mapping between properties of energy function components and the occurrence of the type of fault in the system.

II. Sliding Window Prediction for Analyzing Sampled Dynamic Response

A sliding window based approach is used to determine the intrinsic properties of the SPEF's subject to different faulted scenarios. From [1], we know that the different types of faults will leave different signatures on the wide area measurement system. The sliding window approach is designed to detect the sensitivity of the different energy function components to various types of faults. After the energy function components are calculated, the total length of individual component is used to determine the number of sliding windows. An appropriate selection of window width needs to be done in order to capture

A. Banerjee and R. Kavasseri are with Department of Electrical & Computer Engineering, North Dakota State University, Fargo, ND, USA (e-mail: *abhishek.banerjee@ndus.edu, rajesh.kavasseri@ndus.edu*).

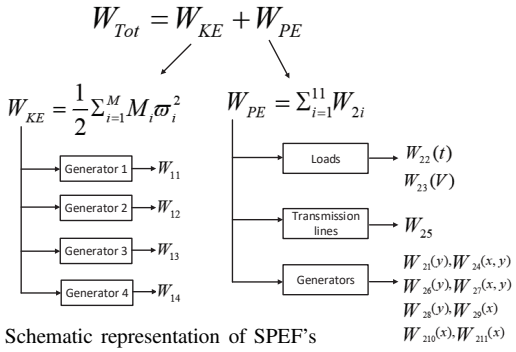

Fig. 1. Schematic representation of SPEF's

maximum information from the trajectories of the individual energy function components. The total number of windows (n_w) is calculated as

$$n_w = \frac{l_w - \varepsilon}{\Delta} \tag{1}$$

where,

l_w = length of each component of $W_{\mathbf{1}}$, $\sum_{i=\mathbf{1}}^{\mathbf{11}} W_{\mathbf{2}i}$

ε = window width, Δ = slide increment

After the total number of windows are determined, the window span is calculated using

$$\sum_{j=\mathbf{1}}^{n_w} j : (j + \varepsilon) \tag{2}$$

In each window span, each energy component is subjected to a singular value decomposition, $\Phi_W = U\Sigma V^T$, where maximum singular values ($\overline{\sigma}_k$) are stacked up in a vector for each window span. The sensitivity of the energy components are evaluated by analyzing the stacked up maximum singular values.

III. Feature Extraction using PCA

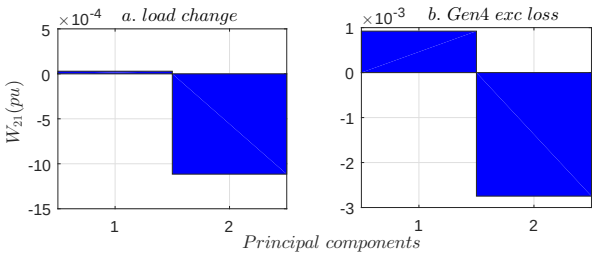

Fig. 2. PCA plots of W_{21} subject to a) sudden change in load, b) generator 4 excitation failure

It can be seen from Fig. 2, generator 4 excitation affects the $W_{\mathbf{21}}$ component more than sudden load change.

References

[1] R. G. Kavasseri, Y. Cui and S. M. Brahma, "A new approach for event detection based on energy functions," 2014 IEEE PES General Meeting, National Harbor, MD, 2014, pp. 1-5.

[2] K. R. Padiyar, *Structure Preserving Energy Functions in Power Systems* CRC Press, 2013.

Security versus Computation Time in IV-ACOPF with SOCP Initialization

Sayed Abdullah Sadat, David Haralson, and Mostafa Sahraei-Ardakani
Department of Electrical and Computer Engineering, University of Utah
email: sayed_abdullah@ieee.org

***Abstract*—Achieving the optimal solution to the security constrained AC optimal power flow (SCACOPF) problem in real-time is a computationally challenging task. Successive linear programming (SLP) with a near optimal initialization has shown promising potential for solving the problem. It is, however, essential to improve the computational performance of the algorithm by only choosing the most critical contingencies, instead of modeling the extensive list of all the possible contingencies. This work examines the trade-off between different levels of reliability, i.e., post-contingency network violations, and computation time in the SCACOPF problem. It is shown that a similar level of reliability can be obtained by only modeling the most critical contingencies, while substantially improving the computation time. The work uses a combination of second order conic programming (SOCP) relaxation of the ACOPF and fast decoupled power flow to initialize the SLP algorithm for solving the SCACOPF. The method is tested on a range of test systems, using off-the-shelf solvers, i.e., Gurobi and CPLEX, and the results are presented and compared.**

Keywords*—*AC optimal power flow (ACOPF), computational complexity, contingency constraints, second order conic programming (SOCP), security constraints, stress metrics, successive linear programming (SLP).

I. Introduction

Power system operators in the United States are required to comply with North American Electric Reliability Corporation (NERC)'s standards. NERC N-1 reliability standard requires uninterrupted delivery of power even after a major disturbance (single outage of a line, transformer, or generator). To guarantee N-1 reliability, security-constraints can be added to the OPF problem, used for bulk power system operation [10]. Identifying the globally optimal solution to the security constrained ACOPF (SCACOPF) problem within the limited available computational time remains an open problem. This work investigates a method to reduce the computational time by employing a successive linear programming (SLP) method, initialized through a combination of second order conic programming (SOCP) and decoupled power flow. The SLP method is developed upon the voltage and current in the rectangular coordinate, "IV" formulation, rather than the common active and reactive power representation, P and Q.

Additionally, this work seeks to further reduce the computational time required for solving the SLP IV-ACOPF by only selecting the most critical contingencies. System stress metrics are used to guide the contingency selection procedure by filtering out the contingencies that are inconsequential as shown in Fig.1. The resulting algorithm is more apt for large systems, and will pave the way for potential employment of SCACOPF in real-time operations. The contribution of this work is the development of an algorithm to reduce the overall SCACOPF computation time, through (i) smart initialization of the SLP method and (ii) appropriate selection of the contingencies.

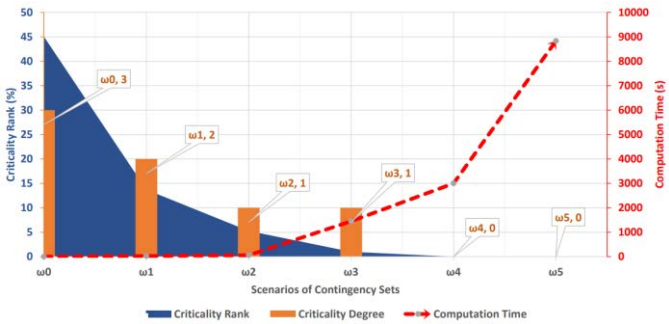

Fig. 1 Stress metrics and computation time, presented for the IEEE 118-bus test case, with different number of contingencies modeled within the SCACOPF problem

II. Results and Conclusions

Finding the optimal solution to the security-constrained AC optimal power flow in real-time is an extremely challenging task, due to its heavy computational burden. Successive linear programming with a near optimal initialization has shown promising potential for solving this problem. This work employs a combination of SOCP and decoupled power flow to initialize SLP in an attempt to reduce the solution time, required for solving the SLP-SCACOPF. To further improve the computational performance, this work develops a contingency selection method, based on system stress metrics, and only models the most critical contingencies. Thus, a large number of possible N-1 contingencies are eliminated from the security constraints. This work shows that a trade-off exists between different levels of reliability, measured in stress metrics, and the computation time for the SCACOPF model. The work further shows that the reliability saturates at some system-specific point and further inclusion of additional security constraints will only increase the computation time, without providing any reliability improvement. Thus, careful selection of the contingency set represented in the SCACOPF problem can play a significant role in reducing the computational burden of the problem.

Advanced Situational Awareness: Identification of Localized and Widespread Events

Paroma Chatterjee, *Student Member*, IEEE, and Mojdeh Khorsand, *Member*, IEEE
School of Electrical, Computer and Energy Engineering, Arizona State University, Tempe, AZ, USA
pchatte6@asu.edu and mojdeh.khorsand@asu.edu

***Abstract*—Power system disturbances are initiated by aging equipment, weather, cyber-attack, human error, and/or relay mis-operation. After major disturbances, power system response is highly dependent on protection schemes and system dynamics. Improving situational awareness requires proper and simultaneous assessment of protection scheme behavior and dynamic characteristics. This paper proposes a novel approach to enhance online situational awareness during disturbances by: 1) fast detection of critical protective relays prone to operation and 2) real-time generator coherency identification. The proposed algorithm is tested using an equivalent Western Electricity Coordinating Council (WECC) system.**

I. Introduction

A single initiating event combined with an inappropriate or lack of action of essential control and protective systems can result in major blackouts. Prior analysis confirms the significant role of protection and control schemes during blackouts [1]-[2]. Hidden failures of control and protection schemes are often leading factors of widespread blackouts. The ultimate goal of online dynamic security assessment is to improve situational awareness and to provide observability over system behavior after critical contingencies. However, this goal cannot be achieved without properly capturing the responses of protective and control schemes: one of the underlying factors of most blackouts. Most prior approaches of online dynamic security assessment do not account for either protection systems behavior or critical, automated and manual control actions. To overcome these challenges, two methods for online dynamic security assessment have been proposed, to be able to ultimately hedge against cascades.

II. Proposed Methodology

A. Minimum Voltage Evaluation (MVE)

This paper proposes to evaluate voltage dips across transmission assets, as an attribute to identify whether the impact of the initial event has spread through the system or is local to the disturbance. A low voltage (without an actual fault) is a flag for a local or widespread power swing and the location of the electrical center. Such detection is of critical importance in order to identify whether protection systems may mis-operate, as this is one primary cause of uncontrolled islanding. Using PMU data, the minimum voltage magnitude through a line is calculated at each time interval using the optimization problem, (1)-(2).

$$\text{Minimize: } |V_a| = \sqrt{\left(V_x - aRI_x + aXI_y\right)^2 + \left(V_y - aXI_x - aRI_y\right)^2} \quad (1)$$

$$\text{Subject to: } 0 \le a \le 1 \quad (2)$$

In (1), I_x, I_y, V_x, and V_y are the real and imaginary parts of the line current and bus voltage at either end bus. R and X are the resistance and reactance of the line respectively and a is the fraction of the line length. $|V_a|$ is voltage magnitude at a.

Given the special structure of this optimization problem, the optimal solution can be calculated at the rate of PMU data collection. MVE via a pre-established threshold (ε) is shown in (3). If (3) holds for a very small value of ε, the contingency would lead to an unstable power swing and the related transmission line would be located along the electrical center.

$$|V_{a^{min}}| \le \varepsilon \quad (3)$$

In (3), $|V_{a^{min}}|$ is the minimum voltage magnitude through the line, which occurs at a^{min} fraction of the line length.

B. Real-time Generator Coherency

In today's power systems, system response based corrective actions are an absolute necessity. One way of determining the need of such an action is by observing generator coherency. For this purpose, the method of Dynamic Time Warping (DTW) has been employed here [3]. At every cycle, minimum DTW distance (d_{DTW}) between generator's relative rotor angles are evaluated. The rate of change of d_{DTW} is used to identify coherent group of generators. Limited variation in rate of change of d_{DTW} for two generators identifies coherency of these generators. This information can be leveraged to enable essential corrective actions in case of loss of synchronism.

C. Identifying Critical Areas

The aforementioned methods can be used as parallel metrics to combine the results and identify areas that are critical and need to be monitored. For the purpose of illustration, the WECC-179 bus system is used. A contingency (*N-3*) case was simulated which could be depicted as the equivalent of the outage of the California-Oregon corridor. Use of the methodologies described in this paper ensue in the identification of critical areas shown in fig. 1, for the case being investigated.

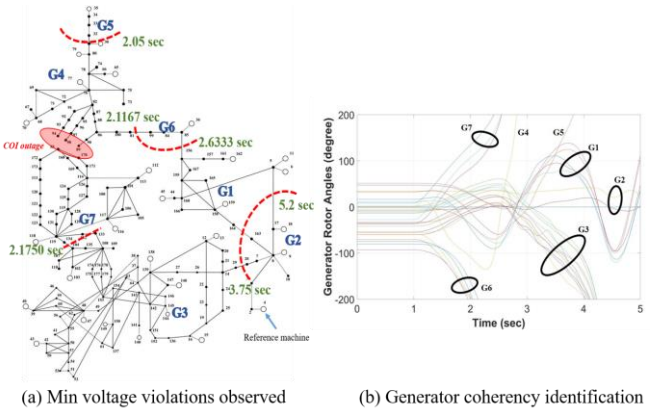

(a) Min voltage violations observed across multiple lines at certain times

(b) Generator coherency identification based on the DTW method

Fig. 1. An N-3 contingency case simulated in the WECC-179 bus system for identifying critical areas to be monitored

References

[1] P. Pourbeik, P. S. Kundur, and C. W. Taylor, "The anatomy of a power grid blackout," *IEEE Power and Energy Magazine*, September 2006

[2] M. K. Hedman, "Analytical Approaches for Identification and Representation of Critical Protection Systems in Transient Stability Studies," Ph.D. dissertation, School of Elect. Comput. & Energy Eng., Arizona State Univ., Tempe, AZ, USA, May 2017

[3] M. Muller, "Dynamic Time Warping" in *Information Retrieval for Music and Motion*, Springer, 2007, pp. 69-84

Measurement-Based Voltage Stability Indicator for Voltage Dependent and Induction Motor Loads

Mariana Kamel
Department of Electrical Engineering and Computer Science
University of Tennessee
Knoxville, Tennessee
kvf552@vols.utk.edu

Fangxing Li
Department of Electrical Engineering and Computer Science
University of Tennessee
Knoxville, Tennessee
fli6@vols.utk.edu

***Abstract*— This work presents a new voltage stability index which takes into account the voltage dependency of system loads in particular ZIP, exponential and induction motor loads. This index is based on the idea that at the collapsing point, the system PV curve and the load curve share the same tangent line. The proposed index is evaluated based on local bus measurements of voltage and current which makes it suitable for real-time assessment of the system stability. The performance of the proposed index is to be tested on both the IEEE 14-bus system and the 181-bus WECC system developed by the CURENT center.**

***Keywords*— induction motor, voltage collapse, voltage instability**

I. Introduction

Voltage instability and voltage collapse are identified as the main reason behind several major blackouts worldwide. The severity of these blackout events has prompted significant research effort in the area of monitoring and control of system voltage stability. However, assessing the system stability and predicting reliable security margins proves to be a challenge. This is due to the complexity of the involved dynamics that leads the system to eventually collapse. In order to simplify the assessment process several assumption are made. One of these assumptions is to ignore load dynamics and assume a constant PQ load model. For voltage dependent loads (ZIP and exponential loads), such assumption works fine if the load bus voltage is close to nominal. However, when the system is operating close to its limit, such assumption does not hold well and will eventually lead to a more conservative and pessimistic security margin. On the other hand, if the system load includes a large percentage of induction motors then such assumption will lead to highly optimistic and unreliable margins. Therefore, in this work a novel voltage stability index which accounts for load characteristics is proposed. Such index will help provide a practical and a more accurate assessment of system voltage security.

II. Voltage Stability Index Formualtion

The index is based on the idea that at the collapsing point, the sensitivity dP/dV from the system PV curve is equal to dP/dV from the load characteristic curve. The normalized system dP/dV at a given load bus i can be evaluated based on the Thevenin equivalence at that bus as follows:

$$\overline{\frac{dP_i}{dV_i}} = \frac{V_i}{P_i}\frac{dP_i}{dV_i} = V_i^2\left(\frac{E_{TH,i}^2 - 2\left(V_i^2 + R_{TH,i}P_i + X_{TH,i}Q_i\right)}{Z_{TH,i}^2 S_i^2 + V_i^2\left(R_{TH,i}P_i + X_{TH,i}Q_i\right)}\right)$$

Where $E_{TH,i}$ $R_{TH,i}$, and $X_{TH,i}$ are the equivalent Thevenin parameters at bus i (voltage, resistance and reactance respectively). The power of ZIP and exponential loads can be expressed mathematically as follows.

$$P_{ZIP,i} = P_{Z,i} + P_{I,i} + P_{P,i} = aV_i^2 + bV_i + c$$

$$P_{exp,i} = V_i^{\propto_p}$$

Where $a, b,$ and c are the ZIP load parameters. $\propto_p$ is the exponential load parameter. Therefore, the normalized load dP/dV can be calculated as:

$$\overline{\frac{dP_i}{dV_i}} = \frac{V_i}{P_{ZIP,i}}\frac{dP_{ZIP,i}}{dV_i} = \frac{2P_{Z,i} + P_{I,i}}{P_{ZIP,i}}$$

$$\overline{\frac{dP_i}{dV_i}} = \frac{V_i}{P_{exp,i}}\frac{dP_{exp,i}}{dV_i} = \propto_p$$

For an induction motor load, as it can be seen from its equivalent circuit, the motor load is equivalent to a constant P load behind a transmission line. Therefore, when obtaining the Thevenin equivalent at load bus i, the induction motor is to be considered as part of the system rather than a load connected to bus i

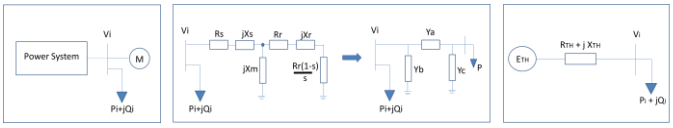

(a) (b) (c)

Fig. 1: (a) load bus i (b) Induction Motor Equivalent Circuit (c) Thevenin Equivalent at load bus i

The voltage stability index is defined as

$$VSI_i = \tan^{-1}\left(\frac{dP_i}{dV_i}\Big|_{Load}\right) - \tan^{-1}\left(\frac{dP_i}{dV_i}\Big|_{System}\right)$$

III. Results and Conclusion

The performance of the proposed index is to be tested on both the IEEE 14-bus system and the 181-bus WECC system developed by the CURENT center.

Advanced Situational Awareness: Identification of Localized and Widespread Events

Paroma Chatterjee, *Student Member*, IEEE, and Mojdeh Khorsand, *Member*, IEEE
School of Electrical, Computer and Energy Engineering, Arizona State University, Tempe, AZ, USA
pchatte6@asu.edu and mojdeh.khorsand@asu.edu

***Abstract*—Power system disturbances are initiated by aging equipment, weather, cyber-attack, human error, and/or relay mis-operation. After major disturbances, power system response is highly dependent on protection schemes and system dynamics. Improving situational awareness requires proper and simultaneous assessment of protection scheme behavior and dynamic characteristics. This paper proposes a novel approach to enhance online situational awareness during disturbances by: 1) fast detection of critical protective relays prone to operation and 2) real-time generator coherency identification. The proposed algorithm is tested using an equivalent Western Electricity Coordinating Council (WECC) system.**

I. Introduction

A single initiating event combined with an inappropriate or lack of action of essential control and protective systems can result in major blackouts. Prior analysis confirms the significant role of protection and control schemes during blackouts [1]-[2]. Hidden failures of control and protection schemes are often leading factors of widespread blackouts. The ultimate goal of online dynamic security assessment is to improve situational awareness and to provide observability over system behavior after critical contingencies. However, this goal cannot be achieved without properly capturing the responses of protective and control schemes: one of the underlying factors of most blackouts. Most prior approaches of online dynamic security assessment do not account for either protection systems behavior or critical, automated and manual control actions. To overcome these challenges, two methods for online dynamic security assessment have been proposed, to be able to ultimately hedge against cascades.

II. Proposed Methodology

A. Minimum Voltage Evaluation (MVE)

This paper proposes to evaluate voltage dips across transmission assets, as an attribute to identify whether the impact of the initial event has spread through the system or is local to the disturbance. A low voltage (without an actual fault) is a flag for a local or widespread power swing and the location of the electrical center. Such detection is of critical importance in order to identify whether protection systems may mis-operate, as this is one primary cause of uncontrolled islanding. Using PMU data, the minimum voltage magnitude through a line is calculated at each time interval using the optimization problem, (1)-(2).

$$\text{Minimize: } |V_a| = \sqrt{\left(V_x - aRI_x + aXI_y\right)^2 + \left(V_y - aXI_x - aRI_y\right)^2} \quad (1)$$

$$\text{Subject to: } 0 \le a \le 1 \quad (2)$$

In (1), I_x, I_y, V_x, and V_y are the real and imaginary parts of the line current and bus voltage at either end bus. R and X are the resistance and reactance of the line respectively and a is the fraction of the line length. $|V_a|$ is voltage magnitude at a.

Given the special structure of this optimization problem, the optimal solution can be calculated at the rate of PMU data collection. MVE via a pre-established threshold (ε) is shown in (3). If (3) holds for a very small value of ε, the contingency would lead to an unstable power swing and the related transmission line would be located along the electrical center.

$$|V_{a^{min}}| \le \varepsilon \quad (3)$$

In (3), $|V_{a^{min}}|$ is the minimum voltage magnitude through the line, which occurs at a^{min} fraction of the line length.

B. Real-time Generator Coherency

In today's power systems, system response based corrective actions are an absolute necessity. One way of determining the need of such an action is by observing generator coherency. For this purpose, the method of Dynamic Time Warping (DTW) has been employed here [3]. At every cycle, minimum DTW distance (d_{DTW}) between generator's relative rotor angles are evaluated. The rate of change of d_{DTW} is used to identify coherent group of generators. Limited variation in rate of change of d_{DTW} for two generators identifies coherency of these generators. This information can be leveraged to enable essential corrective actions in case of loss of synchronism.

C. Identifying Critical Areas

The aforementioned methods can be used as parallel metrics to combine the results and identify areas that are critical and need to be monitored. For the purpose of illustration, the WECC-179 bus system is used. A contingency (*N-3*) case was simulated which could be depicted as the equivalent of the outage of the California-Oregon corridor. Use of the methodologies described in this paper ensue in the identification of critical areas shown in fig. 1, for the case being investigated.

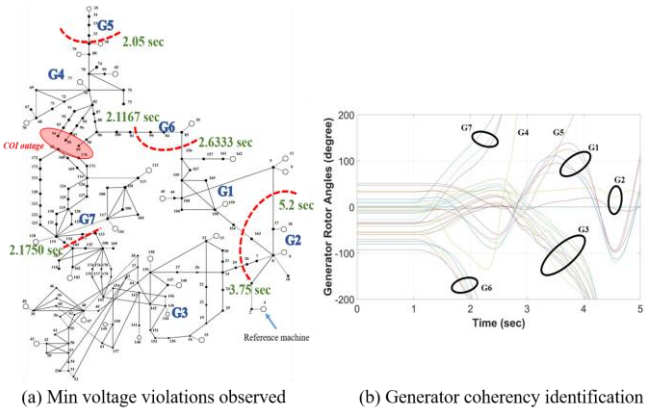

(a) Min voltage violations observed across multiple lines at certain times

(b) Generator coherency identification based on the DTW method

Fig. 1. An N-3 contingency case simulated in the WECC-179 bus system for identifying critical areas to be monitored

References

[1] P. Pourbeik, P. S. Kundur, and C. W. Taylor, "The anatomy of a power grid blackout," *IEEE Power and Energy Magazine*, September 2006

[2] M. K. Hedman, "Analytical Approaches for Identification and Representation of Critical Protection Systems in Transient Stability Studies," Ph.D. dissertation, School of Elect. Comput. & Energy Eng., Arizona State Univ., Tempe, AZ, USA, May 2017

[3] M. Muller, "Dynamic Time Warping" in *Information Retrieval for Music and Motion*, Springer, 2007, pp. 69-84